01 Feb 1980

The strength of cold-formed steel columns

Du Thinh Dat

Teoman Peköz

Department of Structural Engineering

School of Civil and Environemental Engineering

Cornell University

Report No. 80-4

— DRAFT —

THE STRENGTH OF COLD-FORMED STEEL COLUMNS

F

by

Du Thinh Dat

Teoman Peköz, Project Director

A Research Project Sponsored by the

American Iron and Steel Institute

Ithaca, New York

February 1980

PREFACE

This report is based on a thesis presented to the faculty of the Graduate School of Cornell University for the degree of Doctor of Philosophy.

The sponsorship of the American Iron and Steel Institute and the cooperation of the committees of the Institute are gratefully acknowledged.

TABLE OF CONTENTS

CHAPTER		PAGE
1	INTRODUCTION	1
2	THE BUCKLING OF COLUMNS	3
	2.1 Introduction	3
	2.2 Elastic Buckling	3
	2.3 Elastic-Plastic Buckling	4
	2.3.1 Engesser	4
	2.3.2 Von Karman	5
	2.3.3 Shanley	6
	2.3.4 Residual Stresses	9
	2.3.5 Residual Stresses and Initial Deflections	12
	2.4 Plastic Buckling	13
	2.5 Buckling In The Strain-Hardening Range	15
	2.6 Conclusion	18
3	COLD-FORMING EFFECTS	20
	3.1 Introduction	20
	3.2 Literature Review	20
	3.3 Cross-sectional Geometry	25
	3.4 Tensile Coupon Tests	27
	3.5 Compressive Coupon Tests	30
	3.6 Results of Tensile and Compressive Coupon Tests	32
4	RESIDUAL STRESSES DUE TO COLD-FORMING: THEORY	114
	4.1 Introduction	114

CHAPTER PAGE

4.2 Literature Review 115

4.3 Theory of Sheet Bending 118

4.3.1 Yield Criterion 118

4.3.2 Equilibrium 119

4.3.3 Plastic Loading 119

4.3.4 Elastic Unloading 121

4.3.5 Residual Stresses 122

4.4 Approximate Stresses 123

4.4.1 Plastic Loading 123

4.4.2 Elastic Pressure Unloading 123

4.4.3 Elastic Bending Unloading 124

4.5 Theory of Sheet Bending with Inelastic Bending 124

4.5.1 Case 1 126

4.5.2 Case 2 128

4.5.3 Case 3 131

4.5.4 Case 4 135

4.6 Springback 139

4.7 Elastic Relaxation of the Longitudinal Residual Stresses 139

4.8 Results and Discussion 140

4.9 Summary 143

5 RESIDUAL STRESSES DUE TO COLD-FORMING: EXPERIMENTS 175

5.1 Introduction 175

5.2 Literature Survey 175

5.2.1 Non-Destructive Techniques 175

CHAPTER PAGE

5.2.2 Semi-Destructive Techniques 176

5.2.3 Destructive Techniques 176

5.2.4 The Method of Sectioning 177

5.2.5 Effect of Cutting on Residual Stresses 179

5.2.6 Accuracy of Measurements 180

5.3 Residual Strain Measurements 181

5.3.1 Description of Experiments 181

5.3.2 Results and Discussion 182

5.4 Sectioning of Annealed Specimens 186

5.5 Closure 187

6 COLUMN STRENGTH: THEORY 224

6.1 Literature Survey 224

6.1.1 Deflection Methods 224

6.1.1.1 Exact Approach: Jezek's Method 225

6.1.1.2 Numerical Approach: The Column Deflection Curve Method 225

6.1.1.3 Approximate Approach: Jezek's Method 227

6.1.2 The Modified Deflection Method 228

6.1.3 The Curvature Method 229

6.1.4 The Moment Method 230

6.1.5 The Finite Difference Method 231

6.1.6 The Finite Element Method 231

6.1.7 Newmark's Integration Method 232

6.2 Approximate Determination of Column Strength Using Jezek's Method 232

CHAPTER PAGE

6.2.1 Equilibrium 233

6.2.2 Strain-Displacement Relationship 234

6.2.3 Computational Scheme 234

6.2.4 Discretization 235

6.2.5 Residual Strains 236

6.2.6 Experimental Input 237

6.2.7 Equilibrium Corrections 239

6.2.8 Determination of the Extent of Yield 241

6.3 Implementation. Effect of Initial Deflection and Direction of Buckling 242

6.4 Effect of Residual Stresses 244

6.5 Closure 246

7 STUB COLUMN TESTS 258

7.1 Purpose 258

7.2 Length 258

7.3 Testing Procedure 259

7.4 Effects of Annealing 260

7.5 Results and Discussion 263

8 INITIAL DEFLECTIONS AND COLUMN CENTERING 278

8.1 Literature Survey 278

8.2 Measurement of Initial Deflections 281

8.2.1 Method 1 282

8.2.2 Method 2 282

8.2.3 Method 3 283

CHAPTER PAGE

8.3 Computations 284

8.4 Results 286

8.5 Errors 286

8.5.1 Relative Error of Measurement of Initial Deflections 286

8.6 Column Centering 287

8.6.1 Curved Column Under Eccentric Load 288

8.6.2 Generalization 291

8.7 Summary 291

9 COLUMN TESTS 306

9.1 Review of Various Procedures 306

9.1.1 Dynamic Method 306

9.1.2 Modified Dynamic Method 306

9.1.3 Static Method 307

9.1.4 Boundary Conditions 307

9.2 Description of Procedure 308

9.3 Results and Discussion 311

9.4 Column Curves 314

9.5 Effect of Transverse Residual Stresses 319

9.6 Closure 322

10 CONCLUSIONS 430

10.1 Contributions 430

10.2 Conclusions 431

10.3 Future Work 433

REFERENCES 435

LIST OF APPENDICES

APPENDIX		PAGE
A	COMPUTATION OF FORCES AND MOMENTS IN CHAPTER 4	442
	Case 1	442
	Case 2	444
	Case 3	446
B	EFFECT OF RESIDUAL STRESSES ON COLUMN STRENGTH	449
	B.1 Elemental Force and Moment for Assumed Residual Strain Distributions	449
	B.1.1 Linear Strain Distribution, Straight Element	449
	B.1.2 Linear Strain Distribution, Curved Element	449
	B.1.3 Rectangular Strain Distribution, Straight Element	450
	B.1.4 Rectangular Strain Distribution, Curved Element	451
	B.2 Relation of Experimental Results to Assumed Rectangular Distribution	452
	B.2.1 Straight Element	452
	B.2.2 Curved Element	453
C	ANALYSIS OF VARIANCE	455
D	ALTERNATIVE BUCKLING MODES FOR C14	457
E	INPUT FOR PROGRAM COLUMN	464
	EXAMPLE OF PARTS i,j and k OF INPUT	466
F	PROGRAM COLUMN	468
G	PROGRAM SHEET BENDING	496

LIST OF TABLES

TABLE		PAGE
	CHAPTER 3	
3.1	Cross-sectional properties	35
3.2a	Channel section properties	36
3.2b	Hat section properties	38
3.3	Cross-sectional area from weight and linear dimensions	40
3.4	Corner yield strength: actual, Karren's formula and 5t formula	41
3.5	PBC 14 tensile coupon tests	44
3.6	PBC 14 compressive coupon tests	46
3.7	Comparison between coupon area by weight and dimension for PBC 14	47
3.8	RFC 14 tensile coupon tests	48
3.9	RFC 14 compressive coupon tests	50
3.10	Comparison of area from weight and from dimensions	51
3.11	PBC 13 tensile coupon tests	52
3.12	PBC 13 compressive coupon tests	53
3.13	PBC 13 tensile coupon tests	54
3.14	RFC 13 compressive coupon tests	55
3.15	H11 tensile coupon tests	56
3.16	H11 compressive coupon tests	57
3.17	H7 tensile coupon tests	58
3.18	H7 compressive coupon tests	59
3.19	HT tensile coupon tests	60
3.20	HT compressive coupon tests	61

TABLE		PAGE
3.21	HT compressive coupon tests (strain gages)	62
3.22	List of tables and figures for tensile and compressive tests	63
	CHAPTER 4	
4.1	Relaxation of z residual stresses: axial and bending components	144
4.2	Location and extent of yield zone: a = 10., b = 12	146
4.3	Location and extent of yield zone: a = 3.0, b = 4.0	147
4.4	Location and extent of yield zone: a = 10., b = 18	148
4.5	Location and extent of yield zone: a = 10., b = 22	149
4.6	Location and extent of yield zone: a = 10., b = 30	150
4.7	Loading stresses: c = 3.0	151
4.8	Loading stresses: c = 3.1	151
4.9	Loading stresses: c = 3.2	152
4.10	Loading stresses: c = 3.3	152
4.11	Loading stresses: c = 3.4	153
4.12	Loading stresses: c = 3.464	153
4.13	Residual stresses: c = 3.0	154
4.14	Residual stresses: c = 3.1	155
4.15	Residual stresses: c = 3.2	156
4.16	Residual stresses: c = 3.3	157
4.17	Residual stresses: c = 3.4	158
4.18	Residual stresses: c = 3.464	159
	CHAPTER 5	
5.1	PBC 14 Residual strains	188

TABLE		PAGE
5.2	RFC 14 Residual strains	189
5.3	PBC 13 Residual strains: specimen a	190
5.4	PBC 13 Residual strains: specimen b	191
5.5	RFC 13 Residual strains	191
5.6	H11 Residual strains	192
5.7	H7 Residual strains: specimen a	192
5.8	H7 Residual strains: specimen b	193
5.9	HT Residual strains	193
5.10	Residual strains due to milling; annealed specimens	194
5.11	Residual strains due to milling; annealed specimens	194
5.12	PBC 14 Residual strains: detail	195
5.13	RFC 14 Residual strains: detail	197
5.14	PBC 13 Residual strains: detail	199
5.15	RFC 13 Residual strains: detail	201
5.16	H11 Residual strains: detail	203
5.17	H7 Residual strains: detail	204
5.18	H7 Residual strains: detail	206
5.19	HT Residual strains: detail	208
5.20	Residual strains of annealed specimens	209
5.21	Relaxation of z residual stresses: theory and experiment	210
5.22	List of tables and figures for residual strain measurements	211
	CHAPTER 6	
6.1	Effect of initial imperfection and direction of buckling on column strength	247

TABLE		PAGE

6.2 Southwell plot 248

6.3 Effect of magnitude and distribution of residual stresses on column strength 249

6.4 Effect of models of residual stresses and direction of buckling on column strength 250

CHAPTER 7

7.1 Stub column tests 265

7.2 Stub column tests: non-dimensionalized results 266

CHAPTER 8

8.1 PBC 14, group 1: initial deflections 292

8.2 PBC 14, group 2: initial deflections 293

8.3 RFC 14, group 1: initial deflections 294

8.4 RFC 14, group 2: initial deflections 295

8.5 PBC 13, group 1: initial deflections 296

8.6 PBC 13, group 2: initial deflections 297

8.7 RFC 13, group 2: initial deflections 297

8.8 H11, group 1: initial deflections 298

8.9 H11, group 2: initial deflections 298

8.10 H7: initial deflections 299

8.11 HT: initial deflections 300

CHAPTER 9

9.1a PBC 14, group 1: column test results 323

9.1b PBC 14, group 1: non-dimensionalized column test results 323

9.2 PBC 14, group 2: column test results 324

TABLE		PAGE

9.3a	RFC 14, group 1: column test results	325
9.3b	RFC 14, group 1: non-dimensionalized column test results	325
9.4	RFC 14, group 2: column test results	326
9.5a	PBC 13, group 1: column test results	326
9.5b	PBC 13, group 1: non-dimensionalized column test results	327
9.6	PBC 13, group 2: column test results	327
9.7a	RFC 13, group 1: column test results	328
9.7b	RFC 13, group 1: non-dimensionalized column test results	328
9.8	RFC 13, group 2: column test results	329
9.9a	H11, group 1: column test results	329
9.9b	H11, group 1: non-dimensionalized column test results	330
9.10	H11, group 2: column test results	330
9.11a	H7 column test results	331
9.11b	H7 non-dimensionalized column test results	331
9.12a	HT column test results	332
9.12b	HT non-dimensionalized column test results	332
9.13	Least square regression on column data	333
9.14	ANOVA using average yield strength: Dat's 80 data points	334
9.15	ANOVA using average yield strength: Dat's 75 data points (all except C1,D1,D2,D3,D5)	335
9.16	ANOVA using average yield strength: 55 data points (Dat's 75 - Stubs)	336
9.17	ANOVA using average yield strength: 92 data points (Dat's 75 + Karren's 17)	337

TABLE PAGE

9.18 ANOVA using average yield strength: 70 data points (Dat's 55 + Karren's 15. No stub) 338

9.19 Weighted least squares and ANOVA using average yield strength. 92 data points (Dat's 75 + Karren's 17)... 339

9.20 ANOVA using yield strength of flat: Dat's 80 data points 340

9.21 ANOVA using yield strength of flat: Dat's 75 data points (all except C1,D1,D2,D3,D5) 341

9.22 ANOVA using yield strength of flat: 55 data points (Dat's 75 - stubs) 342

9.23 ANOVA using yield strength of flat: 92 data points (Dat's 75 + Karren's 17) 343

9.24 ANOVA using yield strength of flat: 70 data points. (Dat's 55 + Karren's 15. No stub)....................... 344

9.25 Weighted least square and ANOVA using yield strength of flat. 92 data points (Dat's 75 + Karren's 17) 345

9.26 Karren's column test results 346

APPENDIX D

D.1 Buckling loads for C14 463

LIST OF FIGURES

FIGURE PAGE

CHAPTER 2

2.1 Stress-strain curve for gradually yielding steel 19

2.2 Column curve for steel 19

CHAPTER 3

3.1 Effects of strain-hardening and strain-aging on stress-strain characteristics of structural steel 67

3.2 Cold-stretching of a sheet 67

3.3 Cold-forming of a corner 67

3.4 Cross-sections 68

3.4a Measurement of corner thickness 69

3.5 PBC 14 tensile and compressive coupon tests 70

3.6 PBC 14 tensile coupons 71

3.7a PBC 14 tensile coupon tests 72

3.7b PBC 14 tensile coupon tests 73

3.7c PBC 14 tensile coupon tests 74

3.7d PBC 14 tensile coupon tests 75

3.8a PBC 14 compressive coupon tests 76

3.8b PBC 14 compressive coupon tests 77

3.9 RFC 14 tensile and compressive coupon tests 78

3.10 Tensile coupons for RFC 14, RFC 13 and PBC 13 79

3.11 Compressive coupons for RFC 14, RFC 13, PBC 14 and PBC 13 .. 79

3.12a RFC 14 tensile coupon tests 80

3.12b RFC 14 tensile coupon tests 81

FIGURE		PAGE
3.12c	RFC 14 tensile coupon tests	82
3.13a	RFC 14 compressive coupon tests	83
3.13b	RFC 14 compressive coupon tests	84
3.14	PBC 13 tensile and compressive coupon tests	85
3.15a	PBC 13 tensile coupon tests	86
3.15b	PBC 13 tensile coupon tests	87
3.16a	PBC 13 compressive coupon tests	88
3.16b	PBC 13 compressive coupon tests	89
3.17	RFC 13 tensile and compressive tests	90
3.18a	RFC 13 tensile coupon tests	91
3.18b	RFC 13 tensile coupon tests	92
3.19a	RFC 13 compressive coupon tests	93
3.19b	RFC 13 compressive coupon tests	94
3.20	H11 tensile and compressive coupon tests	95
3.21	H11 tensile and compressive coupons	96
3.22	H11 tensile coupon tests	97
3.23a	H11 compressive coupon tests	98
3.23b	H11 compressive coupon tests	99
3.24	H7 tensile and compressive coupon tests	100
3.25	H7 tensile and compressive coupons	101
3.26a	H7 tensile coupon tests	102
3.26b	H7 tensile coupon tests	103
3.27a	H7 compressive coupon tests	104
3.27b	H7 compressive coupon tests	105
3.28	HT tensile and compressive tests	106

FIGURE		PAGE
3.29	HT tensile and compressive coupons	107
3.30	HT tensile coupon tests	108
3.31a	HT compressive coupon tests	109
3.31b	HT compressive coupon tests	110
3.32a	HT compressive coupon tests with strain gages	111
3.32b	HT compressive coupon tests with strain gages	112
3.32c	HT compressive coupon tests with strain gages	113
	CHAPTER 4	
4.1	Yielded zone after unloading (case 1)	160
4.2	Yielded zone after unloading (case 3)	160
4.3	Location and extent of yield zones	161
4.4	Some radii of interest for the case b/a = 1.33	162
4.5a	Loading and residual stresses: c = 3.00	163
4.5b	Loading and residual stresses: c = 3.00	164
4.6a	Loading and residual stresses: c = 3.10	165
4.6b	Loading and residual stresses: c = 3.10	166
4.7a	Loading and residual stresses: c = 3.20	167
4.7b	Loading and residual stresses: c = 3.20	168
4.8a	Loading and residual stresses: c = 3.30	169
4.8b	Loading and residual stresses: c = 3.30	170
4.9a	Loading and residual stresses: c = 3.40	171
4.9b	Loading and residual stresses: c = 3.40	172
4.10a	Loading and residual stresses: c = 3.464	173
4.10b	Loading and residual stresses: c = 3.50	174

FIGURE PAGE

CHAPTER 5

5.1 PBC 14 residual strains 214

5.2 RFC 14 residual strains 215

5.3a PBC 13 residual strains 216

5.3b PBC 13 specimen for residual strains 217

5.4 RFC 13 residual strains 218

5.5 H11 residual strains 219

5.6 H7 residual strains 220

5.7 HT residual strains 221

5.8 Annealed specimens: residual strains due to milling 222

5.9 Residual strains due to milling; annealed PBC 14 223

CHAPTER 6

6.1 Imperfect column under central load 251

6.2 Sign convention for cross-section 251

6.3 Flowchart 252

6.4 Corner element 251

6.5 Extent of plastification 253

6.6 Load-strain curves 254

6.7 Load-deflection curves 255

6.8 Effect of initial deflection on maximum load 256

6.9 Southwell plot 257

CHAPTER 7

7.1 Stub column test set-up 268

7.2a PBC 14 Stub column tests 269

FIGURE		PAGE

7.2b	PBC 14 Stub column tests	270
7.3a	RFC 14 Stub column tests	271
7.3b	RFC 14 Stub column tests	272
7.4	PBC 13 Stub column tests	273
7.5	RFC 13 Stub column tests	274
7.6	H11 Stub column tests	275
7.7	H7 Stub column tests	276
7.8	HT Stub column tests	277
	CHAPTER 8	
8.1	Measurement of initial deflections: method 1	301
8.2	Measurement of initial deflections: method 2	301
8.3	Measurement of initial deflections: method 3	302
8.4	Imperfect column under eccentric load	303
8.5	Deflected column shapes	303
8.6	Elastic curve of initially deflected column loaded eccentrically	304
8.7	Column deflections	305
	CHAPTER 9	
9.1	End fixture for column tests	348
9.2	PBC 14 Column A1, L = 18.0"	349
9.3	PBC 14 Column A2, L = 27.0"	350
9.4	PBC 14 Column A3, L = 27.0"	351
9.5	PBC 14 Column A4, L = 33.0"	352
9.6	PBC 14 Column A5, L = 39.0"	353

FIGURE PAGE

9.7 PBC 14 Column A6, L = 39.0" 354

9.8 PBC 14 Column A7, L = 45.0" 355

9.9 PBC 14 Column A8, L = 51.0" 356

9.10 PBC 14 Column A9, L = 57.0" 357

9.11 PBC 14 Column A10, L = 63.0" 358

9.12 PBC 14 Column A11, L = 69.0" 359

9.13 PBC 14 Column A12 L = 75.0" 360

9.14 PBC 14 Column A13, L = 78.0" 361

9.15 PBC 14 Column A14, L = 89.0" 362

9.16 PBC 14 Column tests; average yield strength 363

9.17 PBC 14 Column tests; yield strength of flat 364

9.18 RFC 14 Column B1, L = 27.0" 365

9.19 RFC 14 Column B2, L = 27.0" 366

9.20 RFC 14 Column B3, L = 39.0" 367

9.21 RFC 14 Column B4, L = 39.0" 368

9.22 RFC 14 Column B5, L = 51.0" 369

9.23 RFC 14 Column B6, L = 51.0" 370

9.24 RFC 14 Column B7, L = 51.0" 371

9.25 RFC 14 Column B8, L = 63.0" 372

9.26 RFC 14 Column B9, L = 80.5" 373

9.27 RFC 14 Column B10, L = 80.5" 374

9.28 RFC 14 Column B11, L = 84.9" 375

9.29 RFC 14 Column tests; average yield strength 376

9.30 RFC 14 Column tests; yield strength of flat 377

9.31 PBC 13 Column C1, L = 27.0" 378

FIGURE PAGE

9.32 PBC 13 Column C2, L = 27.0" 379

9.33 PBC 13 Column C3, L = 39.0" 380

9.34 PBC 13 Column C4, L = 51.0" 381

9.35 PBC 13 Column C5, L = 63.0" 382

9.36 PBC 13 Column C6, L = 82.0" 383

9.37 PBC 13 Column C7, L = 100.0" 384

9.38 PBC 13 Column tests; average yield strength 385

9.39 PBC 13 Column tests; yield strength of flat 386

9.40 RFC 13 Column D1, L = 19.25" 387

9.41 RFC 13 Column D2, L = 21.0" 388

9.42 RFC 13 Column D3, L = 27.0" 389

9.43 RFC 13 Column D4, L = 27.0" 390

9.44 RFC 13 Column D5, L = 33.0" 391

9.45 RFC 13 Column D6, L = 39.0" 392

9.46 RFC 13 Column D7, L = 45.0" 393

9.47 RFC 13 Column D8, L = 51.0" 394

9.48 RFC 13 Column D9, L = 57.0" 395

9.49 RFC 13 Column D10, L = 63.0" 396

9.50 RFC 13 Column D11, L = 69.0" 397

9.51 RFC 13 Column D12, L = 75.0" 398

9.52 RFC 13 Column D13, L = 87.0" 399

9.53 RFC 13 Column tests; average yield strength 400

9.54 RFC 13 Column tests; yield strength of flat 401

9.55 H11 Column E1, L = 19.4" 402

9.56 H11 Column E2, L = 23.0" 403

FIGURE		PAGE
9.57	H11 Column E3, L = 28.0"	404
9.58	H11 Column E4, L = 39.0"	405
9.59	H11 Column E5, L = 51.0"	406
9.60	H11 Column tests; average yield strength	407
9.61	H11 Column tests; yield strength of flat	408
9.62	H7 Column F1, L = 31.0"	409
9.63	H7 Column F2, L = 39.0"	410
9.64	H7 Column F3, L = 42.4"	411
9.65	H7 Column F4, L = 45.0"	412
9.66	H7 Column F5, L = 51.0"	413
9.67	H7 Column tests; average yield strength	414
9.68	H7 Column tests; yield strength of flat	415
9.69	HT Column G1, L = 27.9"	416
9.70	HT Column G2, L = 39.0"	417
9.71	HT Column G3, L = 51.0"	418
9.72	HT Column G4, L = 65.4"	419
9.73	HT Column G5, L = 71.0"	420
9.74	HT Column tests; average yield strength	421
9.75	HT Column tests; yield strength of flat	422
9.76	Column tests; average yield strength (Dat)	423
9.77	Column tests; yield strength of flat (Dat)	424
9.78	Column tests; average yield strength (Dat and Karren)..	425
9.79	Column tests; yield strength of flat (Dat and Karren)..	426
9.80	Column curves	427
9.81	Longitudinal and transverse residual stresses	428

FIGURE PAGE

APPENDIX B

B.1 Straight element with linear strain distribution 454

B.2 Curved element with linear strain distribution 454

B.3 Straight element with rectangular strain distribution .. 454

B.4 Curved element with rectangular strain distribution ... 454

LIST OF PHOTOGRAPHS

PHOTO		PAGE
3.1,3.2 3.3,3.4	Compressometer, compression jig for corners and flat coupons	65 66
5.1,5.2 5.3	Residual strain measurement: channel section ready for sectioning	212 213
5.4	Residual strain measurement: sectioning	213
7.1	Stub column test: general setup	267
7.2	Stub column test: use of compressometer	267
9.1	Long column test: general setup	347
9.2	Long column test: detail	347

NOMENCLATURE

Numbers and letters in ( ) refer to Chapters and Appendices unless otherwise indicated. Distance is in inch, load in kip, coupon weight in gram.

A	Area
A	Integration constant (4,8)
A_d	Area computed from dimensions (3)
A_e	Elastic area (6)
A_p	Plastic area (6)
A_w	Area computed from weight (3)
a	Internal corner radius (3,4)
a	Specimen designation (3)
a	Coefficient in Eq. (6.4)
a_1	Internal radius of corner between web and flange (3)
a_2	Internal radius of corner between flange and lip (3)
B	Width of rectangular section (2)
B	Flange flat width (3)
B	Integration constant (4,8)
B	Element width (6)
b	External corner radius (3,4)
b	Specimen designation (3)
b	Coefficient in Eq. (6.4)
b_o	Intercept of linear regression line (9)
b_1	Slope of linear regression line (9)

C	Empirical coefficient (2)
C	Lip flat width (3)
C	Integration constant (4,8)
C_w	Warping constant (D)
c	Specimen designation (3)
c	Radius of neutral axis (4)
c	Coefficient in Eq. (6.4)
c	Radius of centroidal axis of curved element (6)
c_i, c_o	Radius of centroidal axis of inside, outside part of curved element (Rectangular residual stress distribution) (6)
c_o	Maximum radius of neutral axis (4)
D	Section depth (2,6)
D	Integration constant (4)
D_s	Unstiffened flat width of stiffener plus corner radius (D)
d	Empirical coefficient (3)
d	Coupon width (3)
d	Specimen designation (3)
d	Coefficient in Eq. (6.4)
E	Young's modulus
E_{eff}	Effective modulus (2)
E_r	Reduced modulus (2)
E_t	Tangent modulus (2)
e	Specimen designation (3)
e	Load eccentricity (6,8)
e_n	Fourier coefficient in expansion of e (6,8)

F	Unbalance force (6)
$\bar{F}$	Resultant of z residual forces (4)
f	Specimen designation (3)
f_j	Element force (6)
$f(\Phi,P)$	Function (6)
G	Shear modulus (4,D)
g	Function (6)
$\bar{g}$	Function (6)
$2H$	Web flat width (3)
H	Integration constant (4)
h^2	P/EI (6)
$2h$	Yield strain in two-dimensional space (9)
I	Moment of inertia
I	Iteration index (Fig. 6.3)
I_e	Moment of inertia of elastic part (2)
I_s	Moment of inertia of stiffener (D)
I_x	Moment of inertia about the x-axis (2)
I_y	Moment of inertia about the y-axis (2)
J	St.Venant torsion constant (D)
j	Element number (6)
K	Effective length coefficient (2,D)

K	Plate buckling coefficient (D)
K^2	P/P_{cr} = Load parameter (8)
k	Empirical coefficient (3)
$2\bar{k}$	Yield stress in two-dimensional space (4,9)
$(k_w)_{a.s.}$	Buckling coefficient for adequately stiffened flange (D)
L	Column length
l	Coupon length (3)
l	Empirical coefficient (3)
M	$\bar{M}/2\bar{k}$ = Moment (4)
M	Moment (6)
$\bar{M}$	Moment (4)
M_{in}	Internal moment (6)
M_m	Maximum moment (4,6)
M_u	Unbalance moment (6)
M_y	Yield moment (6)
$\bar{M}_z$	Moment of z-residual stresses about center of curvature (4)
$\bar{M}_z^{rel}$	Relaxation moment of z-residual stresses (4)
MS_R	Mean square due to regression (9)
m	Empirical coefficient (2)
m	M/M_y = Normalized moment (6)
m_j	Unbalance moment for element j (6)
m_{pc}	Coefficient in Eq. (6.4)
m_1	Limiting moment between elastic and primary plastic states (6)
m_2	Limiting moment between primary and secondary plastic states (6)

N	Distance between centroidal axis and web midthickness (3)
N	Geometric constant (4)
N	Number of computation points on equilibrium path (Fig. 6.3)
n	Empirical coefficient (3)
n	Mode number (6)
n	Total number of elements (6)
P	Load
P_{cr}	Critical load
P_{crx}	Flexural buckling load about the x-axis (2)
P_{cry}	Flexural buckling load about the y-axis (2)
P_{in}	Internal load (6)
P_{pa}	Proportional limit load for annealed stub columns (7)
P_{pn}	Proportional limit load for non-annealed stub columns (7)
P_r	Reduced-modulus load (2)
P_t	Tangent-modulus load (2)
P_T	Torsional buckling load (D)
P_{TF}	Torsional-flexural buckling load (D)
P_{TFO}	Elastic torsional-flexural buckling load (D)
P_{th}	Theoretical column strength (9)
P_u	Ultimate load, column strength (9)
P_{ua}	Ultimate load for annealed stub columns (7)
P_{un}	Ultimate load for non-annealed stub columns (7)
P_y	Yield load
P_{ya}	Average yield load (9)
P_{yf}	Yield load based on yield strength of flat (9)
p	$\bar{p}/2\bar{k}$ = Pressure (4)

p_a — p at which $r_y = a$ (4)

p_ℓ — p at which $c = a$ (4)

p_m — Maximum pressure at which $M = 0$ (4)

p_t — p at which $t_o = a$ (4)

$\bar{p}$ — Pressure (4)

$\tilde{p}$ — P/P_y = Normalized load (6)

Q — Defined in Eq. (4.74)

$q(z)$ — Lateral load (6)

$\bar{q}(z)$ — q/M_y (6)

$\tilde{q}(z)$ — $q/(h^2 M_y)$ (6)

R — Radius of gyration (2,3,6,8)

R — Mean corner radius (6)

R — Correlation coefficient (9)

R^2 — Multiple correlation coefficient (9)

R_i — Mean radius of inside part (rectangular distribution of residual stresses) (6)

R_o — Mean radius of outside part (rectangular distribution of residual stresses) (6)

r — Radial coordinate (4,6)

r_o — Polar radius of gyration about shear center (D)

r_1, r_3 — Mean radius of web-flange juncture (3)

r_2, r_4 — Mean radius of flange-lip juncture (3)

r_y — Yield radius (4)

S — Section modulus (6)

S — Amplitude of sinusoidal fit to dead load deflection (8)

$s(\xi)$	Sinusoidal fit to dead load deflection (8)
s^2	Mean square about regression (9)
T	$\bar{T}/2\bar{k}$ = Tension (4)
$\bar{T}$	Tension (4)
t	Thickness
t_c	Thickness of corner (3)
t_{c1}	Thickness of corner between web and flange (3)
t_{c2}	Thickness of corner between flange and lip (3)
t_f	Thickness of flat (3)
t_i	Radius of concave edge yield zone (4)
t_o	Radius of internal yield zone (4)
t_y	Thickness of yielded zone (6)
u	$\varepsilon_o + \varepsilon_i$ (6)
$\bar{u}$	$\bar{\varepsilon}_o + \bar{\varepsilon}_i$ (6)
V	Additional midheight column deflection (2,6,8)
V_o	Maximum initial deflection (6)
V_o	Amplitude of sinusoidal fit to actual initial deflection (8,9)
V_{on}	Fourier coefficient in expansion of v_o (6)
V_n	Fourier coefficient in expansion of v (6)
V_t	Maximum assumed initial deflection (6,9)
v	Additional column deflection (6)
v	Additional deflection due to eccentrically applied load (8)
v_o	Initial deflection (6)

v_o	Sinusoidal fit to actual initial deflection (8)
v_o	Initial deflection of eccentric column (8)
$\bar{v}_o$	Experimental measurements of initial deflections (8)
$\tilde{v}_o$	Elevation at z (8)
W	Maximum lateral deflection of column due to central load (8)
W_o	Maximum w_o (8)
w	Coupon weight (3)
w	$\varepsilon_o - \varepsilon_i$ (6)
w	Width (D)
w_o	Initial deflection of centrally loaded column (8)
$\bar{w}$	$\bar{\varepsilon}_o - \bar{\varepsilon}_i$ (6)
X	$\bar{\lambda}$ = Abcissa of data points in regression analysis (9)
x	Coordinate axis
x_o	Abcissa of section centroid (6)
x_o	Distance between centroid and shear center (D)
x_{cj}	Abcissa of centroid of element j (6)
x_{dj}	Abcissa of middle (midthickness, bisector) of element j (6)
Y	P_u/P_y = Ordinate of data points in regression analysis (9)
$\bar{Y}$	Mean of Y (9)
$\hat{Y}$	Linear model of data (9)
y	Coordinate axis
z	Longitudinal coordinate axis
z_I, z_F	Locations of end measurements of initial deflection (8)

2α	Corner angle
$2\alpha_1, (2\alpha)_1$	Angle of corner between web and flange (3)
$2\alpha_2, (2\alpha)_2$	Angle of corner between flange and lip (3)
β	t/B = ratio of element thickness to width (6)
β	$1 - x_o^2/r_o^2$ = shape factor (D)
γ	b/a = ratio of external to internal radius of corner (4)
Δ_j	Denominator (6)
Δ	Error in measuring initial deflections (8)
δ	Eq. (4.26)
ΔF	Increase in corner yield load (3)
ε	Strain
ε_a	Axial strain (6)
ε_b	Bending strain (6)
ε_{ij}	Value of residual longitudinal strain at inside (concave) face of element j (6)
ε_{oj}	Value of residual longitudinal strain at outside (convex) face of element j (6)
ε^{res}	Residual strain (6)
ε_{st}	Hardening strain (2)
ε_y	Yield strain
ε_1	Force equilibrium correction (6)
ε_2	Moment equilibrium correction (6)
$\bar{\varepsilon}$	Equivalent strain (3)
$\bar{\varepsilon}_{ij}$	Experimental values of ε^{res} at inside face of element j (6)

$\bar{\varepsilon}_{oj}$	Experimental values of ε^{res} at outside face of element j (6)
ε'	$\ln(1 + \varepsilon)$ = Natural strain
$\varepsilon_1', \varepsilon_2', \varepsilon_3'$	Principal natural strains
ζ	$2\rho_n/t$
η	a^2p/M = relative importance of cold-forming actions (4)
θ	Angular coordinate
θ	Curvature angle (4)
λ	Slenderness ratio (2)
λ_{el}	Elastic slenderness ratio (2)
λ_o	Slenderness ratio at which $\sigma_{Euler} = \sigma_y$ (9)
λ_{red}	Reduced slenderness ratio (2)
λ_{rev}	Reversal slenderness ratio (2)
$\bar{\lambda}$	λ/λ_o = Normalized slenderness ratio (2,7)
$\bar{\lambda}_a$	$\bar{\lambda}$ based on average yield strength of section (6,9)
$\bar{\lambda}_f$	$\bar{\lambda}$ based on yield strength of flat (6,9)
μ	V_o/e = Ratio of maximum initial deflection to eccentricity for eccentrically loaded column (8)
μ_n	V_{on}/e = Ratio of Fourier coefficient of maximum initial deflection to eccentricity (8)
$\bar{\mu}$	W_o/e = Ratio of maximum initial deflection of centrally loaded column to eccentricity of equivalent eccentric column (8)

ρ	Radial coordinate (from midthickness outward) (6)
ρ_y	Radial coordinate at which $\varepsilon = \varepsilon_y$ (6)
ρ_n	Radial coordinate of neutral axis (6)
σ	Stress
σ	$\bar{\sigma}/2\bar{k}$ = normalized stress (4)
$\bar{\sigma}$	Stress (4,5)
$\bar{\sigma}$	Equivalent stress (3)

Subscripts on σ

a	Axial (4), applied (6) or average (9)
b	Bending (5)
c	Compressive (3)
co	Corner (3)
cr	Critical (2,D)
e	Elastic (4)
f	Flat (3)
max	Maximum (3)
p	Proportional limit (3)
p	Plastic (4)
p+	Plastic in tension (4)
p-	Plastic in compression (4)
r	Radial (4)
t	Tensile (3)
u	Ultimate (3)
y	Yield

z	Longitudinal (4)
1,2,3	Principal (3)
θ	Tangential (4)

Superscripts on σ

bu	Bending unloading (4)
pu	Pressure unloading (4)
rel	Relaxation (4,5)
res	Residual (4)
o rel	Relaxation assuming elasto-plastic unloading (4)
* rel	Relaxation assuming elastic unloading (4)
τ	E_t/E = Ratio of tangent modulus to Young's modulus (D)
ν	Poisson's ratio (4)
ξ	z/L = Length coordinate (8)
Φ	Curvature (6)
Φ_y	Yield curvature (6)
ϕ	Φ/Φ_y = Normalized curvature (6)
ϕ_{io}	Initial curvature at i (6)
ϕ_m	Midspan curvature (6)
ϕ_1	Limiting curvature between elastic and primary plastic states (6)
ϕ_2	Limiting curvature between primary and secondary plastic states (6)
ω	Density of steel (8)

"In this temple they were desirous of using columns; but, being ignorant of their symmetry, and of the proportions necessary to enable them to sustain the weight, and give them a handsome appearance, they measured the (human) foot of a man to be the sixth part of his height, they gave that proportion to their columns, making the thickness of the shaft at the base equal to the sixth part of the height, including the capital. Thus the Doric column, having the proportions, firmness and beauty of the human body, first began to be used in buildings."

Vitruvius Pollio - De Architectura

CHAPTER I

INTRODUCTION

The flexural buckling of columns is a fundamental problem whose solution was found by Euler more than 200 years ago. Since then, refinements have extended the solution to the inelastic range and clarified the influence of initial deflections and residual stresses. Most of these advances were made by studying hot-rolled steel columns, which are widely used.

Cold-formed sections are coming into greater and greater use, thanks to the great variety of geometries available, which make them suitable for specific needs, and the significant advances made in the last four decades in understanding the behavior of cold-formed steel and in developing simple design methods.

Previous works on the behavior and strength of cold-formed members in compression have concentrated on phenomena associated with, but not specific to thin-walled structures, such as local and torsional buckling. For flexural buckling, only a few tests have been performed on cold-formed sections, and use has been made of results developed for hot-rolled sections, although cold-forming affects the mechanical properties of steel differently than hot-rolling; in particular, cold work increases the yield strength at the expense of ductility and introduces residual stresses which are completely different from the thermal residual stresses in hot-rolled sections.

The need for the present study, the flexural buckling strength of cold-formed columns, is thus clear. It is, of course, impossible to investigate all types of cross-sections; only the stiffened channel and the hat sections are studied here, mainly because of their availability and many structural uses. The extension to other shapes must be done by theory.

This work starts with a review of the column problem (Chapter 2) and measurements of the effects of cold-forming (Chapter 3). Next, residual stresses due to cold-forming are investigated, both theoretically (Chapter 4) and experimentally (Chapter 5). Chapter 6 develops a numerical scheme for determining column strength. Chapter 7 shows the results of stub column tests. Chapter 8 examines the effects of initial out-of-straightness and the process of load alignment. Chapter 9 covers the procedure for testing long columns and discusses the results. Finally, the conclusions of this study and recommendations for future work are presented in Chapter 10.

CHAPTER 2

THE BUCKLING OF COLUMNS

2.1 Introduction

The history of the theory of columns has been lively and controversial, probably more so than any other branch of mechanics. This history is covered very well in a number of publications (Hoff [1954], Tall et al [1964], Johnston [1976], Bleich [1952]) which also give a rather complete list of references and original sources. For completeness, the main events, dates and concepts are summarized below, together with more recent developments.

Van Musschenbroek is reported to be the first one (1729) to have obtained a column formula of the form:

$$P_{cr} = KBD^2/L^2 \tag{2.1}$$

where P_{cr} is the column buckling load, K is an empirical factor, D and B are the depth and width of the rectangular section and L is the column length. This formula is really not too different from present day formulas.

2.2 Elastic Buckling

In 1744, Euler derived an analytical solution to the problem and gained fundamental insight into its nature, a stability problem. Euler established the differential equation governing the equilibrium of columns and solved for the eigenvalues and eigenfunctions, thus determining the loads at which bifurcation of the equilibrium path of centrally loaded columns occurs. He obtained the famous formula:

$$P_{cr} = \pi^2 EI/(KL)^2 \tag{2.2a}$$

where EI is the column stiffness and K is a constant that depends on the boundary conditions. Only pin-ended columns will be considered here, so K = 1 and Euler's formula becomes:

$$P_{cr} = \pi^2 EI/L^2 \tag{2.2b}$$

The limitations of Euler's theory has been misunderstood in the past, but it remains to this day the cornerstone of column theory. Euler's formula is, of course, only valid in the elastic range.

2.3 Elastic-plastic Buckling

2.3.1 Engesser

Development of inelastic buckling theories came in 1889 with Considere and independently, Engesser. To extend the validity of Euler's formula to the inelastic range, Considere* advocated the substitution of an effective modulus E_{eff}, whose value would be between Young's modulus E and the tangent modulus E_t (Fig. 2.1) for E in (2.2b)

$$P_{cr} = \pi^2 E_{eff}\ I/L^2 \tag{2.3}$$

Engesser, on the other hand, suggested it was only necessary to substitute E_t for E in (2.2b):

$$P_{cr} = \pi^2\ E_t I/L^2 \tag{2.4}$$

*Considere is also credited with establishing the foundations of modern column testing techniques. He tested 32 columns using adjustable knife-edge fittings and centered the load by measuring midheight deflection at half the buckling load and adjusting the end fittings accordingly.

Engesser's tangent modulus formula was criticized in 1895 by Jasinski, who was also aware of Considere's work. Subsequently and that same year, Engesser published a correction to his theory and noted that the effective modulus E_{eff} depended not only on E and E_t but also on the shape of the cross-section.

Although Engesser, in his final formulation, had derived the correct formula for figuring out E_{eff} for an arbitrary cross-section, his work and the controversy that led to it did not attract much attention. Hoff [1954] noted the surprising fact that Tetmajer, in his comprehensive book on buckling, "Die Gesetze Der Knickungs Und Der Zusammengesetsten Druckfestigkeit Der Technisch Wichtigsten Baustoffe" (The Laws Of Buckling and Combined Compressive Strength Of The Technologically Most Important Construction Materials) published in 1903, only mentioned Euler's theory. Being a professor at the Federal Polytechnic Institute in Zurich, Tetmajer had easy access to the "Schweizerische Bauzeitung", where Jasinski's criticism and Engesser's final formulation were published.

2.3.2 Von Karman

The effective modulus theory, otherwise known as the reduced modulus or double modulus theory, was revived by Theodore von Karman in 1910 in his doctoral dissertation. He derived the expressions for the reduced moduli of rectangular and wide-flange sections and performed a series of careful column tests. In addition, he computed the strength of eccentrically loaded columns by using the actual stress-strain diagram of the material and finding the actual deflected shape.

He showed that the failure of eccentrically loaded or initially curved columns is due to a loss of stability and thus, proved that formulas which establish column strength as the load at which the maximum stress reaches yield are not theoretically justified. The term buckling can thus be applied to initially crooked or eccentrically loaded columns as well as initially perfectly straight ones.

2.3.3 Shanley

In contradiction to Karman's theory, test points tend to fall closer to the tangent modulus load than to the reduced modulus load. (For very short columns, where the tangent modulus approaches a constant value, the opposite is often true (Shanley [1947]). Also, for short columns and where the yield point is pronounced, test points lie close to the yield load (Timoshenko and Gere [1961] p. 189)). In 1947 Shanley came up with the observation, genial in its simplicity, that a column is "free to try to bend at any time" (Shanley [1947]). Thus, he rejected the classical stability concept, whereby a perfect column is assumed to remain straight until the critical load is reached, at which point bending occurs with no change in load. This concept is the same that has been used successfully in elastic buckling. According to Shanley, a perfect column begins to bend upon attainment of the tangent modulus load, at which point bending and load increase proceed simultaneously. Thus, Shanley generalized the question "what is the load at which equilibrium of a straight column becomes unstable under the same load" to "what is the smallest load at which bifurcation of the equilibrium positions can occur regardless of whether or not the transition to the bent position requires an increase of the axial load" (from Von Karman's discussion of Shanley's paper).

It must be emphasized that Shanley's contribution is <u>not</u> a return to Engesser's original concept although both are called the tangent modulus theory. According to Engesser, there is no unloading of any sort; increases in stress are therefore governed by the tangent modulus. Shanley proved that, although there is no unloading at the inception of bending, strain reversal must occur on the convex side of the column as soon as deflection becomes finite. In fact, the region of strain reversal grows continuously from the convex to the concave side.

Duberg and Wilder [1952] investigated the behavior of inelastic columns with a Shanley column in which the flexible midheight cell consists of two springs. As the initial imperfection of the column approaches zero, the departure from the straight configuration occurs precisely at the tangent modulus load, rather than anywhere between the tangent modulus load and the Euler load. For columns with vanishing initial lack of straightness, the maximum load may be significantly above the tangent modulus load or only slightly above it, depending on whether the stress-strain curve of the material departs gradually or abruptly from the initial elastic slope.

More recently, Shanley's concept was confirmed with the use of computer technology (Johnston [1963]). A column model similar to Shanley's except that the flexible cell is now a solid cube (rather than just two legs) made of continuously strain-hardening aluminum was investigated using a computer program that increases deflections gradually. Shanley's conclusions regarding the maximum load and strain reversal were verified quantitatively. In the same paper, Johnston also remarked that, for real material whose tangent modulus decreases with increasing strains, equilibrium paths obtained by restraining a column to remain straight until a load between the tangent modulus load P_t and the reduced modulus load P_r is reached, do not tend asymtotically to P_r. Johnston showed that the assumption of a constant tangent modulus leads to a reduced modulus load that may be grossly in error. (This is in response to von Karman's discussion of Shanley's paper, where von Karman stated that there is an infinity of equilibrium paths and not just the two corresponding to bending beginning at P_t and P_r. All such paths, according to Von Karman, tend asymptotically to P_r provided E_t remains constant. The non-uniqueness of equilibrium paths is characteristic of plastic phenomena).

For singly-symmetric sections buckling in the plane of the axis of symmetry, the reduced modulus load not only depends on E, E_t and the shape of the cross-section but also on the direction of buckling. In fact, the value of the slope, dP/dV, of the curve of the load P versus the maximum lateral deflection V at $P = P_t$ (at which value V ceases to be 0), called the inelastic buckling gradient by Johnston [1964], also depends on the direction of buckling. A negative inelastic buckling gradient is characteristic of an imperfection-sensitive structure. The inelastic buckling gradient is smaller for the smaller of the two reduced-modulus loads and the column tends to buckle in the direction from mid-depth toward the center of gravity of the section. Such direction dependence is called trifurcation by Johnston, asymmetric bifurcation by Croll and Walker [1972].

2.3.4 Residual Stresses

Discrepancies between critical loads determined through experiments and those predicted by the tangent modulus formula were attributed solely to initial deflections and load eccentricities. Although these factors do play an important role, it is now known that residual stresses have a determining influence on the buckling load in the elastic-plastic range (Fig. 2.2). This influence was suspected as early as 1908 (Johnston [1976] p. 50), but definite research on the subject was not done until the 1950's. Virtually all the work on the effect of residual stresses on column strength was done at Lehigh University (Huber and Beedle [1954], Beedle and Tall [1960], Tall [1964]). The residual stresses studied at Lehigh were due to cooling or cold-straightening (also referred to as cold-bending, but this is bending of the member in the longitudinal direction, perpendicular to the bending involved in forming the corners of a cross-section).

Residual stresses result in earlier initiation of yield in a column, causing a loss of stiffness, and thus a lower strength as compared to residual stress-free columns. This lowering of strength (up to 30%) is greatest at slenderness ratios corresponding to a critical Euler stress about equal to the yield stress of the material (i.e. for $\bar{\lambda} = \frac{1}{\pi} \sqrt{\frac{\sigma_y}{E}} \frac{L}{R} = 1.0$).

Sherman [1971], however, reported a very slight increase in the strength of tubular members with the introduction of residual tension at the corners. The severity of this effect depends not only on the magnitude and distribution of the residual stresses, but on the axis of buckling as well. Thus, the application of the tangent-modulus formula with the tangent-modulus determined from a stub column test, even if the stub is sufficiently long to include residual stresses, is not correct in general.(This was the practice before 1952; discrepancies with actual test results were attributed to various imperfections, and empirical parameters were chosen for a good fit with experimental data). A stub column does not exhibit any dependence on direction, whereas the effect of residual stresses, unless they are axisymmetric, varies with the axis of buckling. Investigators at Lehigh made the important observation that the buckling load of a column is the same as that of a column consisting of the elastic part of the section only, i.e., at buckling the total external moment is resisted by the moment of the increases of internal stresses:

$$P_{cr} = \pi^2 EI_e/L^2 \tag{2.5}$$

I_e being the moment of inertia of the elastic part of the section.

This is an important discovery, but not a new column formula at the same level as the reduced modulus or tangent modulus formulas. Since strain reversal at buckling increases I_e, the above formula is only valid if used with the Engesser-Shanley concept of column buckling. It should be noted that I_e is the moment of inertia of the elastic part of the section immediately before buckling. After buckling has occurred, the convex and concave sides of the column plastify to different extent and this, of course, contributes to the internal moment.

The directional effect of residual stresses can be illustrated by the simple example of a rectangular section with linearly distributed residual stresses (Chajes [1974] p. 65). If the residual stresses are symmetrical with respect to the x-(strong) axis and are constant in the y-(weak) direction, then formula (2.5) gives

$$P_{cry} = \pi^2 E_t I_y/L^2 \qquad (2.6)$$

but

$$P_{crx} = \pi^2 (E_t/E)^2 E_t I_x/L^2 \qquad (2.7)$$

where I is the moment of inertia of the entire cross-section and the subscripts x and y denote the axes of buckling.

Osgood [1951] applied formula (2.5) to a rectangular section with parabolic residual stress distribution and ended up with a Rankine-type formula.* This was the first theoretical justification of such a formula.

Huber and Ketter [1958] investigated the effects of residual stresses due to cold-straightening (bending in a plane parallel to the flanges) and differential cooling. Frey [1969] showed that cold-straightening has a beneficial effect because it practically wipes out the thermal residual stresses and introduces residual stresses of a more favorable distribution and smaller magnitude (maxima are still at the flange tips when straightening is about the weak axis, but are

---

* $\sigma_{cr} = \dfrac{\sigma_y}{1 + C\lambda^2}$ where C is an empirical coefficient and λ is the slenderness ratio.

tensile on one side, compressive on the other). Alpsten [1972] reported that only a small amount of rotorizing is necessary to achieve a complete and beneficial redistribution of residual stresses.

2.3.5 Residual Stresses and Initial Deflections

In a most important paper, Batterman and Johnston [1967] made a computer study of the combined effect of residual stresses and initial crookedness on the strength of aluminum and steel columns. The presence of residual stresses in steel sections makes the stress-strain curve of a stub column continuously curved beyond the proportional limit so that the same computer program can be used for both aluminum and steel. Cold-straightened aluminum sections were considered free of residual stresses. Once again, Shanley's observations were verified numerically. It was noted, however, that for initially crooked columns, strain regression does not necessarily occur as bending begins and that, for initially straight, wide-flange aluminum columns, the gain of the ultimate load over the tangent modulus load P_t is less than 2.0%. This justifies the use of the tangent modulus load as a basis for column strength. For long steel columns, results showed that the combined effect of initial deflections and residual stresses is greater than the sum of the parts. The longer the column and the higher the steel strength, the less important the effects of initial imperfections are. For slender columns made of high strength steel, residual stresses have almost no effect on column strength, whereas for short columns, the reduction in strength attributable to residual stresses is about the same for various yield strengths. Also, variations of the patterns of residual stresses have much less influence on crooked columns than on perfectly straight ones. The reason for the higher critical load of a wide-flange column buckling about its strong axis, compared to the buckling load about its weak axis, for the same slenderness ratio, is the presence of thermal residual stresses. In the absence of residual stresses, the opposite is true.

Batterman and Johnston concluded that for the same residual stresses, no single design curve is satisfactory for all yield strengths, but that the Structural Stability Research Council (SSRC) curve* is also adequate for high strength steel with nominal residual stresses and initial deflections.

2.4 Plastic Buckling

For the range of slenderness ratio where elastic-plastic buckling occurs, the presence of residual stresses causes gradual yielding of the column. In Fig. 2.2, experimental data fall along the dotted line in the elastic-plastic range rather than along the solid line, which would hold for a perfectly straight, residual stress-free column. After the entire cross-section has yielded, however, the effect of residual stresses is completely wiped out. The question arises then, whether or not it is possible to obtain a critical stress as high as, or higher than the yield stress of a material with a well defined yield plateau.

---

* $\sigma_{cr} = \sigma_y - \frac{\sigma_y^2}{4\pi^2 E} \lambda^2 \quad \text{for} \quad \lambda \leq \sqrt{2}\, \pi \sqrt{\frac{E}{\sigma_y}}$

Classical works on stability acknowledge such possibilities but disregard them. One reads, for example, in Timoshenko and Gere [1961]: "Such values for critical stresses (above the yield stress) can be obtained experimentally only if special precautions are taken against buckling at the yield point stress; thus they have no practical significance in the design of columns." Similarly, Bleich [1952] states: "Such high values for the critical stress (above the yield stress) of very short columns could be observed only in very careful tests on small specimens and cannot be relied upon in the design of columns." Such statements are justified by the tangent modulus formula (2.4) which gives $P_{cr} = 0$ at the yield plateau of the stress-strain diagram of steel (Fig. 2.1), where the tangent modulus E_t is zero. Thus, buckling must occur at P_y, the yield load of the section.

This is, however, not so. Haijer and Thurlimann [1958], among others, reported the attainment of σ_{cr} greater than σ_y without special precautions. The mechanics of plastification offer an explanation to this phenomenon. Yielding occurs in slip bands and starts at points of weakness and stress concentration; although the existence of a yield plateau is observed macroscopically, there is no finite amount of material at a strain between the yield strain ε_y and the strain-hardening strain ε_{st}. The process of yielding entails a discontinuous jump between ε_y and ε_{st}. Therefore, during yielding, part of the material is still elastic while part of it has already reached ε_{st}. When all the material has strain-hardened, the stress rises again. In loose terms, the column jumps right over the yield plateau where $E_t = 0$ and the tangent modulus formula does not apply there.

Haijer and Thurlimann [1958] and Thurlimann [1962] considered two limiting cases. The first column started to yield at the middle and the second at both ends; yielding then progressively spread out to the rest of the column. The columns thus had non-uniform stiffness and were equivalent to columns with varying cross-section, whose strengths could be readily computed. Experimental points fell between these two extreme cases, with yielding starting at the middle as the lower bound. Since the critical stress remains at the yield stress, column curve in the plastic range is expressed as critical strain versus slenderness ratio. For slenderness ratios of about 15 or less, the strain-hardening range is reached. From there on, the buckling load is governed by the tangent-modulus E_t.

Hrenikoff [1966] observed that yielding always initiated at the ends of his annealed steel columns, sometimes only at one end. For longer columns, independent yielding at the middle also occurred and hastened failure. For computational purposes, the plastic parts at the ends were assumed to deflect in a parabolic curve whereas the elastic part followed a sine curve. At the transitions between the two curves the strain jumped from ε_y to ε_{st}. Experimental data provided reasonable support for the analysis, but also fell between the upper and lower bounds established by Thurlimann.

2.5 Buckling in the Strain-Hardening Range

Yanev and Gjelsvik [1977] criticized Thurliman's assumption that yielding in tension and in compression occurs in the same manner, and suggested that an understanding of buckling beyond yield must be sought in the post-buckling behavior of short steel columns. Their study was restricted to an idealized two-flange section with no residual stresses. Local buckling was precluded from happening and strains reached the hardening range.

In the first post-buckling stage, the middle of the column on the concave side has yielded and strain-hardened, while the rest of the column is still elastic. The deflected shape, symmetrical with respect to the middle of the column, consists of three sine curves corresponding to the middle and the ends. As the load increases, yielding spreads to the rest of the concave flange and initiates at the ends of the convex flange: this is the second post-buckling stage. Again, the deflected shape consists of three sine curves corresponding to the middle and the two ends. The middle part has one flange elastic and the other strain-hardening and the ends have both flanges strain-hardening.

A number of experiments were performed. For specimens with slenderness ratios $\lambda \geq 11$ the agreement between theory and experiment is excellent. For $\lambda = 9$ or 10 the lateral displacement tends to be smaller than predicted.

Three slenderness ratios are of importance in determining the behavior of short columns.

By definition, at λ_{el} the critical stress reaches the yield stress:

$$\sigma_{cr} = \sigma_y = \frac{\pi^2 E}{\lambda_{el}^2} \tag{2.8}$$

from which:

$$\lambda_{el} = \pi\sqrt{\frac{E}{\sigma_y}} = \frac{\pi}{\sqrt{\varepsilon_y}} \tag{2.9}$$

By analogy, a reduced slenderness ratio is defined by

$$\lambda_{red} = \pi \sqrt{\frac{E_r}{\sigma_y}} \tag{2.10}$$

where
$$E_r = \frac{2EE_t}{E+E_t} \ . \tag{2.11}$$

Finally a reversal slenderness ratio λ_{rev}, which depends on the tangent modulus, is evaluated numerically. λ_{rev} is the dividing point between two types of behavior in the second post-buckling stage: in one the deflection increases with the load; in the other the column actually straightens as the load increases.

For $\lambda > \lambda_{el}$ the column starts to bend upon reaching the yield load. For $\lambda_{red} \leq \lambda \leq \lambda_{el}$ the column does not regain stability under a load equal to the yield load. After reaching the yield load, the load decreases as the lateral displacement increases. λ_{red} does not depend on the extent or existence of the yield plateau, which only affects the amount of lateral displacement at a given load. For $\lambda_{rev} \leq \lambda \leq \lambda_{red}$, the load decreases upon reaching the yield point, then begins to increase again and regains the value of the yield load by the time the entire concave flange has strain-hardened. The maximum load the column can carry is greater than the yield load. Finally, columns with $\lambda \leq \lambda_{rev}$ develop a straightening process under increasing loads and can sustain loads higher than the yield load.

Sewell [1972] mentioned the effect of transverse shear stiffening on the buckling load. This effect is negligible for purely elastic buckling,but becomes appreciable (up to 20%) in a metal with a rate of hardening small compared to the shear modulus. An extensive bibliography on plastic buckling was presented.

2.6 Conclusion

An understanding of column behavior over the entire range of the stress-strain diagram of the material has thus been achieved. In the elastic range, where the critical stress is less than the proportional limit, Euler's formula applies. In the elastic-plastic range, the tangent-modulus formula governs and residual stresses play an important role. Finally, critical stresses equal to or greater than the yield stress can be achieved without special care for short columns. At all slenderness ratios,initial crookedness reduces column strength.

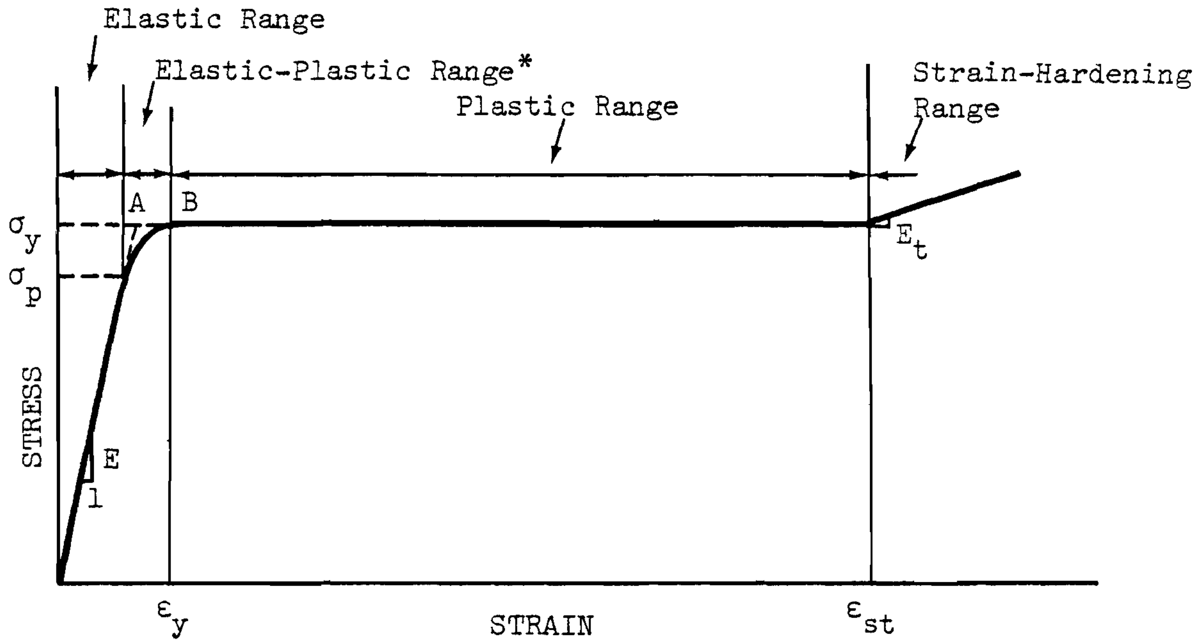

Fig. 2.1 Stress-Strain Curve for Gradually Yielding Steel
*official definition is interval AB

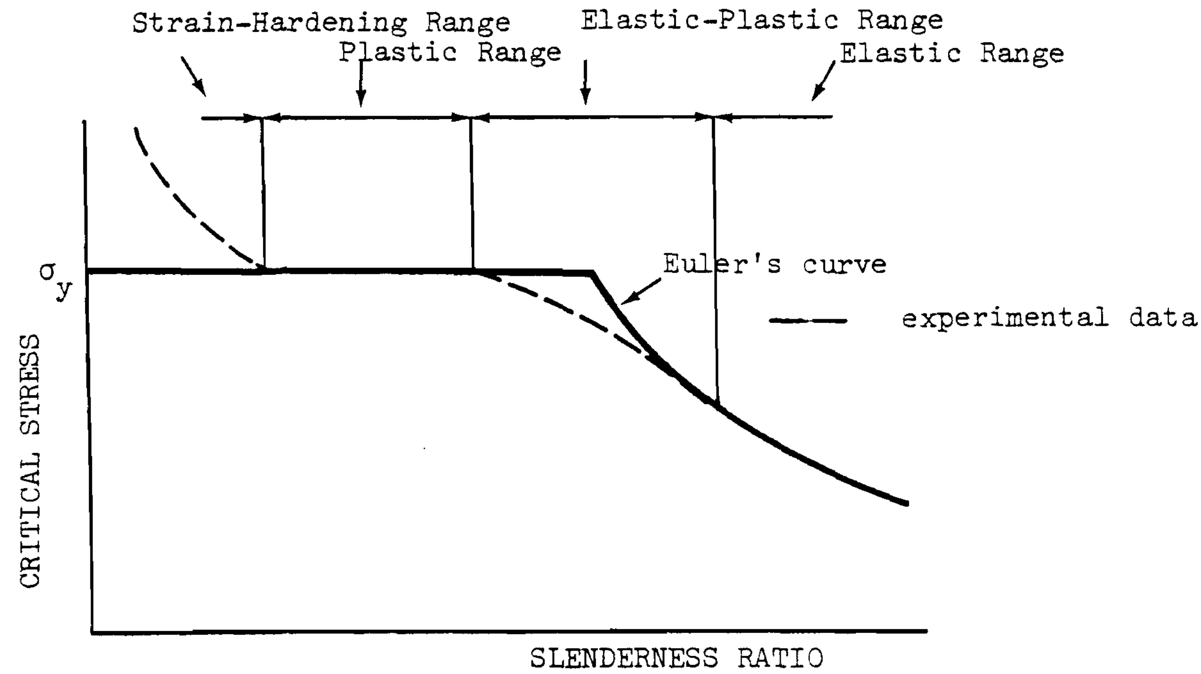

Fig. 2.2 Column Curve for Steel

CHAPTER 3

COLD-FORMING EFFECTS

3.1 Introduction

The previous chapter covers the column problem in general. Since this thesis addresses itself to the problem of determining the strength of cold-formed steel columns, an understanding of the effects of cold-forming is necessary. This is achieved through tensile and compressive coupon tests. Residual stresses due to cold-forming will be covered in subsequent chapters.

3.2 Literature Review

In the 1960's a systematic program of research was conducted at Cornell University under the leadership of Professor G. Winter to investigate the effects of cold-forming on structural steel and members.

Chajes, Britvec and Winter [1963] started by studying the effects of the simplest kind of cold-straining, namely one-dimensional stretching, and attributed these effects to three phenomena: strain-hardening, strain-aging and the Bauschinger effect. Two of these phenomena are illustrated in Fig. 3.1, which is taken from Chajes et al [1963].

Strain-hardening increases the yield strength and decreases the ductility of steel. Strain-aging, obtained by leaving the prestretched and unloaded material for several weeks at room temperature, or accelerated by raising the temperature to 100°C for half an hour, also causes an increase in yield strength and a decrease in ductility. In addition, strain-aging causes an increase in ultimate strength and a regain of the yield plateau. The Bauschinger effect is defined as "the phenomenon that results in an increase in the proportional limit and yield strength by reloading plastically deformed specimens in the same direction, but a decrease by reloading it in the opposite direction" (Chajes et al [1963]).

"Uniform cold stretching in one direction has a pronounced effect on the mechanical properties of the material, not only in the direction of stretching but also in the direction normal to it". "Regardless of the direction of testing, increases in the yield strength and ultimate strength as well as decreases in ductility were always found to be approximately proportional to the amount of prior cold stretching" (Chajes et al [1963]). The Bauschinger effect is observed in the longitudinal direction (i.e. the direction of straining) but an inverse Bauschinger effect exists in the transverse direction (Fig. 3.2). The reason is, in the prestretching operation, extension in one direction causes compression in the direction perpendicular to it. It was also found that, the larger the ratio σ_u/σ_y of the ultimate stress to the yield stress the larger the effect of strain-hardening. In strain-hardened and aged specimens, the increase in yield strength is much larger than the increase in ultimate strength. Finally, strain-aging affects properties in the longitudinal as well as transverse direction.

In general, cold-forming involves states of stress vastly more complicated than uniform tension. The cold-forming of corners out of sheets, for example, involves a combination of radial pressure, end moments and forces (Fig. 3.3). In developing a semi-empirical model of corner strength, Karren [1967] assumed a strain-hardening law of the form

$$\overline{\sigma} = k(\overline{\varepsilon})^n \tag{3.1}$$

where k and n are empirical coefficients expressible in terms of the ultimate stress σ_u and the yield stress σ_y. $\overline{\sigma}$ and $\overline{\varepsilon}$ are the equivalent stress and strain.

$$k = 2.80\ \sigma_u - 1.55\ \sigma_y \tag{3.2}$$

$$n = 0.225\ \sigma_u/\sigma_y - 0.120 \tag{3.3}$$

$$\overline{\sigma} = (1/\sqrt{2})[(\sigma_1 - \sigma_2)^2 + (\sigma_2 - \sigma_3)^2 + (\sigma_3 - \sigma_1)^2]^{1/2} \tag{3.4}$$

$$\overline{\varepsilon} = (\sqrt{2}/3)[\varepsilon_1' - \varepsilon_2')^2 + (\varepsilon_2' - \varepsilon_3')^2 + (\varepsilon_3' - \varepsilon_1')^2]^{1/2} \tag{3.5}$$

Subscripts 1, 2, 3 denote the principal directions and $\varepsilon' = \ln(1+\varepsilon)$ is the natural strain.

Assuming isotropic hardening, Karren found that the yield strength in the longitudinal direction (which is now the direction perpendicular to prior stressing, Fig. 3.3) of a corner can be expressed by

$$\sigma_{yco} = \frac{kd}{(a/t)^{\ell}} \tag{3.6}$$

where a is the internal radius and t the thickness of the corner and d is an empirical coefficient defined below.

In a first model, only pure bending was assumed to be applied in the forming process and there resulted:

$$d = 0.945 - 1.315\ n \tag{3.7}$$

$$\ell = 0.803\ n \tag{3.8}$$

A second model included also radial pressure and provided better agreement with experimental results. For the second model:

$$d = 1.0 - 1.3\,n \tag{3.9}$$

$$\ell = 0.855\,n + 0.035 \tag{3.10}$$

Since forming occurs under plane strain, the plastic strains in the tangential and radial direction are equal, of opposite signs and perpendicular to the final direction of loading, i.e. the longitudinal direction. Thus, the inverse Bauschinger effects of these two plastic strains cancel each other out, a fact that is confirmed experimentally.

Karren was careful to limit the applicability of formulas (3.6 - 3.10) to corners of a/t less than 7.0. Macadam [1967a] found these formulas inapplicable to large a/t typical of round tubing.

The problem was addressed again more recently by Lind and Schroff [1975]. Their elegant work culminated in a very simple formula of wider applicability than Karren's (no restriction on a/t, at least theoretically), called the 5t formula. Assuming linear strain-hardening, the yield strength σ_{yco} of a corner is obtained simply by replacing the yield stress by the ultimate stress over an area $5t^2$ in each 90° corner. For other corner angles, the area is scaled proportionally.

$$\Delta F = (5t)t(\sigma_u - \sigma_y)(2\alpha°)/90° \tag{3.11}$$

$$\sigma_{yco} = \sigma_y + \frac{5t(\sigma_u - \sigma_y)(2\alpha°)/90°}{\pi/2\,(a + t/2)} \tag{3.12}$$

ΔF is the increase in yield load of a corner of angle $2\alpha°$.

If the yield stress is assumed to be a linear function of the work of forming, the increase in yield force, ΔF, is also a linear function of the work of forming. If hardening is further assumed to be linear, then the work of forming, neglecting its elastic part, is independent of the corner radius. Thus, the increase in yield force for a corner is independent of the radius, as Eq. (3.11) shows.

In a paper subsequent to Lind and Schroff's, Karren and Gohil [1975] extended Karren's formulas to large a/t ratios. Equation (3.6) still applies but (3.7) and (3.8) are now replaced by:

$$d = 0.942 - 1.04\ n \tag{3.13}$$

$$\ell = 0.988\ n - 0.0013 \cong n \tag{3.14}$$

Experimental evidence shows the 5t formula to be very good for $a/t > 2$, whereas Karren's formulas show appreciable inaccuracies for $a/t > 10$. However, if k and n in (3.1) are determined from the stress-strain curve of prestrained and aged specimens, Karren's formulas (3.6), (3.2), (3.13) and (3.14) agree well with experimental data for large a/t (> 30), but not for small a/t.

Although no restriction was imposed on a/t in the theoretical development of the 5t rule, Karren's formulas (3.6), (3.13) and (3.14) appear superior for $a/t < 2$, provided k and n (Eq. 3.2 and 3.3) are determined from virgin tensile specimens. For $a/t > 2$, the use of the 5t rule is recommended.

Karren and Winter [1967] found that the pressure of the rolls and aging after stretcher-straightening cause roll-formed members to exhibit significant increase in strength in the flats over virgin yield strength. This is especially true of the flats adjacent to corners, and is confirmed by Macadam [1967b]. This phenomenon is not observed in press-braked members.

Uribe and Winter [1970] investigated the cold-forming effects of thin-walled members. Their work included a statistical study of the as-formed strength of joist chord sections, a study of the strength of flexural members and the buckling of columns of bisymmetrical sections subject to local buckling.

Hlavacek [1968] looked into the effects of cold-waving of a steel sheet. This is sometimes done before press-braking or cold-rolling in order to increase the yield strength, with the sheet flat at the initial and final stages.

Zichy and Moreau [1971] presented test results on angle, channel, welded box and cruciform sections, all of which involve 90° cold-formed corners. Test results confirm the validity of the American Iron and Steel Institute (AISI) specifications [1977].

Grumbach and Prudhomme [1974] studied cold-formed corners and full sections (angle, channel and hat). They confirmed that cold-rolling affects the mechanical properties of a section more than press-braking. Flats that had been bent, then restraightened, showed the usual effects of cold-work. Brittle fracture of corners was studied by impact-flattening them and the sensitivity of a welded material to aging was also examined.

3.3 Cross-sectional Geometry

Sections can be cold-formed to a wide variety of geometrical shapes with relative ease (see, for example, Yu [1973]). At an early stage, it was decided to limit this study to two shapes, the stiffened channel and the hat section. These structural shapes are commonly used as flexural and compression members in racks, space frames, open web joists and so on. The cross-sectional dimensions were selected to preclude local, torsional and torsional-flexural buckling from occurring in the range of slenderness ratio of interest.

The channel and hat sections investigated are shown in Fig. 3.4 and their cross-sectional properties are listed in Tables 3.1, 3.2a and 3.2b. RFC, PBC, H and HT stand for Roll-Formed Channel, Press-Braked Channel, Hat and Thick Hat, respectively. The number following these designations refers to the thickness gage of the steel (there is no number for HT). 2H, B and C designate the flat width of the web, the flange and the lip, a, b, r and 2α the internal, external, mean radius and angle of the corners, N the distance between the centroid of the section and the web midthickness. The juncture between the web and the flange is numbered 1 or 3 and that between the flange and the lip 2 or 4. t_c and t_f refer to the thickness of a corner and that of a flat. Since the thickness of the section is not uniform, the values of t listed in Table 3.1 are only approximate and correspond to the gage thickness. All cross-sectional properties are, however, computed with the actual thickness. The cross-sectional properties of the various specimens tested, with the exception of some of the C14 sections, were found to be within 2% of those listed in Table 3.1. The variations in thickness along the perimeter of the cross-sections and from specimen to specimen are shown in Fig. 3.5, 3.9, 3.14, 3.17, 3.20, 3.24 and 3.28.

The cross-sectional dimensions were determined from the trace of a ground specimen, usually a stub column, precisely cut perpendicular to the longitudinal axis. Corner radii and thicknesses were measured directly from the specimen. Corner thickness was determined with a micrometer and a dowel-pin of known diameter (Fig. 3.4a).

Table 3.3 compares the cross-sectional areas obtained from weighing a specimen (A_w) and from computation based on the measurements described above (A_d). The thickness at any point was obtained by cubic spline interpolation from the local measurements (Shampine and Allen [1973]). The agreement is satisfactory.

3.4 Tensile Coupon Tests

Steels are often designated by their tensile yield strength because tensile tests offer a relatively easy and reliable means of studying the mechanical properties of a material.

Because cold-forming changes the mechanical properties of steel significantly, it was necessary to splice the section of interest into a number of coupons to study the variation of these properties over the cross-section. Tensile coupons cut from the flat portions of the section followed ASTM procedures (Davis et al [1964]). They were about 9.0" long with a middle portion of 2.0" by 1/2", which gradually widened into the ends. These ends were roughened to ensure adequate grip in the testing machine. Corner tensile coupons were usually narrower than 1/2" to avoid inclusion of any of the adjacent flats. The coupons were usually thick enough so flattening of the ends of corner coupons due to the pressure of the grips was only minimal and did not affect the middle portion.

Tensile tests were conducted on a Tinius-Olsen screw-gear type machine and strains were recorded automatically with a 2.00" gage extensometer. Portions of the load-strain curves are shown on Fig. 3.7, 3.12, 3.15, 3.18, 3.22, 3.26 and 3.30. The strain rate was kept constant at 0.015 in/min. until well into the yield plateau, then was gradually increased to 0.10 in/min until final rupture. The pieces were then removed, fitted together and the distance between two lines previously scribed 2.00" apart measured. The percentage elongation is a measure of the ductility of the material.

The total elongation of a ductile metal at the point of rupture is due to plastic elongation, which is more or less uniformly distributed over the gage length, on which is superimposed a localised drawing out or extension of the necked section, which occurs just before rupture. The former is small compared to the latter. The length affected by the final localized drawing out is of the order of 2 or 3 times the thickness of the specimen. It is thus apparent why the gage length must be fixed if comparable elongations are to be obtained and why specifications call for rejection of an elongation measurement if the break is too near the ends (the effect of the localized necking down would extend beyond the gage length).*

Investigations have showed that wide tolerances in loading speed can be permitted without introducing serious error in the results of tests for <u>ductile</u> metals. Davis et al [1964] cite tests of standard specimens of a structural steel in which an eightfold increase in the

---

*Percentage elongation measured over a 2.00" gage length, although accepted ASTM practice (Standard A370-68) presents several disadvantages: it does not account for the specimen cross-sectional area, nor does it separate uniform ductility from local ductility. For a more complete discussion and suggested improvements, the reader is referred to Dhalla and Winter [1974a].

rate of strain increased the yield point by about 4%, the tensile strength by about 2% and decreased the elongation by about 5%. In the machine in which these tests were performed, this change corresponded to a change in idling speed of the head from 0.05 to 0.40 in/min.

It has also been shown that the strength of ductile materials does not appear to be greatly affected by slight eccentricities of load or by bending.

The cross-sectional area of a tensile coupon is, of course, important. For flat coupons, the width and thickness were easily determined with a micrometer after removal of scale or paint. For corner coupons, whose cross-section is not rectangular, the area was determined by weighing the reduced (middle) section. This was done after completion of the tensile test. The two pieces of the ruptured coupon were cut slightly outside of the 2.00" scratches used to determine elongation and the pieces were hand-filed exactly to the marks. The area was obtained by dividing the combined weight of the pieces by the density and the length (determined prior to testing) of 2.00":

$$A_w(\text{in}^2) = \frac{w(\text{grams})}{128.5(\text{g/in}^3) \times \ell(\text{in})} \tag{3.13}$$

Weight can be determined to 0.1 mg and the density is known accurately; thus the only significant source of error was in the cutting and filing process. With proper care, good agreement with the product of width and thickness was obtained (usually less than 1% difference) where the latter two were available (Tables 3.7 and 3.10).

Yield stress was determined by the 0.2 % strain offset method.

3.5 Compressive Coupon Tests

Since columns are compressed, it is desirable to measure the compressive yield strength of the material. Variations in material properties caused by cold-forming necessitates the testing of small compressive coupons cut from various locations of the cross-section. Except for the thickest type of section (HT), all coupons were provided with lateral support in the form of a well-greased jig (Photos 3.1-3.4) to prevent flexural buckling.* Load was applied to the ends of the coupons. A Wiedemann-Baldwin compressometer of 1.00" gage length clamped to the sides of the coupons recorded the strain automatically. Therefore, coupons had to be slightly longer and wider than the 3.00" x 0.50" jig.

As the specimen was compressed, it expanded laterally due to Poisson's effect and friction developed between the specimen on one hand and the lateral support and the machine plates on the other. To minimize this effect, the coupon, the jig, and small areas of the machine bed plate and cross-head were greased prior to the test. In addition, the jig was tightened by hand so it only barely touched the specimen at zero load.

All specimens were tested in a Wiedemann-Baldwin hydraulic press with fixed heads. Although each coupon was machined individually after being cut from a section, so its ends were parallel to within 0.001", and was carefully placed at the center of the machine plate, uniform

*It is, of course, possible to avoid buckling with a short enough coupon. But the effects of end friction would then be important and the use of a compressometer to record strain impossible.

axial straining could never be exactly achieved as seen from the test results for the HT coupons with strain gages (Fig. 3.32).* The reason was a specimen would never be exactly straight because cutting released the longitudinal residual stresses, which were not uniform over the thickness. This phenomenon was, in fact, used to advantage in the "sectioning method" to measure residual stresses.

Strain rate was comparable to that in tensile tests. Cross-sectional area was computed from the dimensions of flat coupons and from the weight of corner coupons. The weighing method was easier here than for tensile coupons, since compressive coupons had a uniform cross-section over their entire length.

For laterally supported coupons, compression was maintained until either the coupon buckled about the strong axis or had shortened so much that the machine plates come close to touching the jig. The stress-strain curve was only used to determine the yield stress by the 0.2% offset method so the portions of the curve involving large plastic strains and possible frictional effects needed not be considered.

One set of HT coupons was tested without lateral supports and with strain gages affixed to both sides of each coupon. Strains were not uniform for reasons mentioned above but an average load-strain curve could be obtained. Coupons buckled shortly after reaching the yield plateau. Yield stress was obtained by the 0.2% offset method and

---

*The HT coupons were thick enough so flexural buckling did not occur before yielding. Lateral support was therefore dispensed with. These coupons were obtained from a previous residual strain measurement test and had strain gages mounted on both faces.

agreed well with that of laterally supported coupons (Tables 3.20, 3.21, Fig. 3.31 and 3.32).

3.6 Results of Tensile and Compressive Coupon Tests

Several specimens were obtained from each type of section and a number of coupons were cut from each specimen. The specimens were designated by the letters a, b, c... or by the length (without end plate) of the column adjacent to which they were cut. Thus, coupon 7a, for example, was coupon 7 of specimen a. There was at least one complete set of tensile and compressive coupons for each section type (complete in the sense it covered the entire cross-section). The compressive coupons were wider than the tensile coupons and thus, fewer of the former were obtained from a specimen. In order to compare compressive test results to tensile test results on the same graph, e.g. Fig. 3.5, equivalent tensile coupon locations were used for the compressive coupons.

Table 3.22 lists the figures and tables where the results of tensile and compressive coupon tests for the various sections are presented. (The strain scale on the load-strain curves may be different from coupon to coupon). The main purpose of these tests was to measure the yield strength to be used subsequently in the determination of column strength.

The 5t formula and Karren's formula predict the yield strength of the corner from the yield and ultimate stresses of the virgin flat and the geometry of the corner. Table 3.4 shows that, if the mechanical properties of the as-formed flat are used instead of the virgin properties, both formulas overestimate corner yield strength. Agreement between predicted and actual values for corner 1 (at the web-flange juncture) of H11 and H7 appears to be coincidental.

The main effects of cold-forming are clear from Fig. 3.5, 3.9, 3.14, 3.17, 3.20, 3.24, and 3.28. Cold forming raises the yield strength, the ultimate stress and decreased ductility. Tables 3.5, 3.8, 3.11, 3.13, 3.15, 3.17, and 3.19 show that elongation remains above 10% and the ratio of the tensile strength to the tensile yield strength is greater than 1.08. Thus, ductility is adequate (Dhalla and Winter [1974b], Winter [1979]). However, the ratio σ_p/σ_y of the proportional limit to the yield strength sometimes dips below 0.70, which is the lower limit of applicability for virgin steel of the AISI Specifications. (Winter [1979]). σ_p/σ_y is lowest at the corners and their vicinity. Measurement of the proportional limit is less reliable than that of the yield or tensile strengths because of its dependence on the shape of the stress-strain curve and, therefore, on the performance of the strain recorder.

Two observations differ from previous works:

1) There is no clear difference between the cold-forming effects due to press-braking and those due to cold-rolling.

2) Although corner yield strengths in compression and in tension appear to be close to one another, the larger size of compression coupons means that the actual corner compressive yield strength is slightly higher than the corner tensile yield strength, since a corner compressive coupon includes a higher proportion of weaker flat area.

Except for the case of RFC 14, the variations in mechanical properties from one specimen to another of the same type are small. It is thus sufficient to take only one set of characteristic values and apply it to all columns of the same type.

The fabrication of tensile coupons by sectioning releases the longitudinal residual stresses (Chapter 5), causing the coupons to shorten or elongate and to bend. Applying tension to the coupons brings them back to straightness and restores the flexural component, but not the axial component of the residual stresses. The presence of these stresses lowers the proportional limit, but does not affect the yield stress in any appreciable way in the vast majority of the coupons. The reason is, the .2% strain offset point lies in the yield plateau, where the effect of residual stresses is wiped out. Unfortunately, there is too much scatter in the proportional limit and other experiments will have to be devised to measure residual stresses.

TABLE 3.1

CROSS-SECTIONAL PROPERTIES

Symbols are explained in Fig. 3.4.

Sections	PBC 14 RFC 14	PBC 13 RFC 13	H11	H7	HT
H (inch)	1.25	1.25	.070	.075	.100
B (inch)	1.20	1.20	.470	.672	.450
C (inch)	.500	.500	.440	.860	1.00
r_1 (inch)	.200	.200	.400	.500	.542
r_2 (inch)	.200	.200	.400	.527	.632
$2\alpha_1$ (degree)	90.0	90.0	70.9	78.0	85.5
$2\alpha_2$ (degree)	90.0	90.0	64.5	68.0	86.0
t (inch)	.073	.090	.120	.179	.300
N (inch)	.634	.636	.585	.952	.992
A (in^2)	.518	.640	.442	.990	1.870
I (in^4)	.217	.269	.0634	.327	.642
R (in)	.647	.648	.379	.575	.586

TABLE 3.2a:

CHANNEL SECTION PROPERTIES

	corner	2	1	3	4	average or typical
	a	3/32	7/64	7/64	7/64	7/64
	t_c	.0732	.0732	.0725	.0715	.0726
	flat locations	(1)	(2)			
PBC 14	t_f	.0750	.0746			.0748
	$a + t_f$					.1842
	$\Delta t/t$ %		min=1.9		max=4.7	
	corner	2	1	3	4	av./typ.
	a	7/64	7/64	3/32	7/64	7/64
	t_c	.0739	.0718	.0710	.0722	.0722
RFC 14	flat locations	(1)	(2)			
	t_f	.0740	.0753			.0746
	$a + t_f$					.1840
	$\Delta t/t$ %	min=.13		max=5.7		

TABLE 3.2a:

CHANNEL SECTION PROPERTIES (continued)

	corner	2	1	3	4	av./typ.
	a	3/32	7/64	7/64	3/32	13/128
	t_c	.0848	.0852	.0854	.0855	.0852
	flat locations	(1)	(2)			
PBC 13	t_f	.0887	.0885			.0886
	$a + t_f$					.1902
	$\Delta t/t$ %	max=4.4			min=3.4	
	corner	2	1	3	4	av./typ.
	a	7/64	3/32	3/32	3/32	3/32
	t_c	.0879	.0874	.0860	.0879	.0873
RFC 13	flat locations	(1)	(2)			
	t_f	.0910	.0920			.0915
	$a + t_f$					.1852
	$\Delta t/t$ %			max=6.5	min=3.4	

TABLE 3.2b:

HAT SECTION PROPERTIES

H 11	flat locations	(1)	(2)			average or typical	$a + t_f$
	t_f	.1250	.1200			.1225	
	corner	2	1	3	4		
	a	12/64			13/64	25/128	.3178
	t_c	.1148			.1142	.1145	
	$\Delta t/t$ %	min=4.3			max=8.6		
	a		14/64	15/64		29/128	.3491
	t_c		.1115	.1174		.1145	
	$\Delta t/t$ %		max=10.8	min=2.2			
H 7	flat locations	(1)	(2)			av./typ.	$a + t_f$
	t_f	.1850	.1777			.1813	
	corner	2	1	3	4		
	a	5/32			5/32	5/32	.3376
	t_c	.1576			.1559	.1567	
	$\Delta t/t$ %	min=11.3			max=15.7		
	a		14/64	15/64		29/128	.4079
	t_c		.1115	.1174		.1145	
	$\Delta t/t$ %		max=39.7	min=33.9			

TABLE 3.2b:

HAT SECTION PROPERTIES (continued)

	flat locations	(1)	(2)			av./typ.	a + t_f
	t_f	.3090	.2971			.3030	
	corner	2	1	3	4		
	a	13/64			13/64	13/64	.5061
H T	t_c	.2625			.2585	.2605	
	$\Delta t/t$ %	min=11.6			max=16.3		
	a		9/32	17/64		35/128	.5764
	t_c		.2639	.2649		.2644	
	$\Delta t/t$ %		max=14.6	min=10.8			

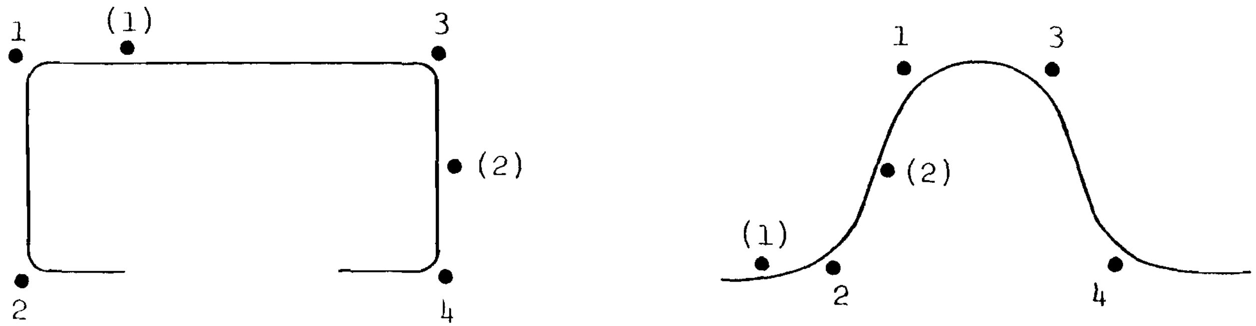

Locations of Flats and Corners

$\Delta t/t$ is the relative change in thickness from corner to flat.

TABLE 3.3

CROSS-SECTIONAL AREA (in^2) FROM

WEIGHT (A_w) and LINEAR DIMENSIONS (A_d)

Section	A_d	A_w	$\frac{A_d - A_w}{.01\,A_d}$
PBC 14	.518	.515	.6
RFC 14	.518	.514	.8
PBC 13	.640	.637	.5
RFC 13	.640	.637	.5
H11	.442	.435	1.6
H7	.990	.985	.5
HT	1.870	1.849	1.1

TABLE 3.4

CORNER YIELD STRENGTH:

ACTUAL, KARREN'S FORMULA AND 5t FORMULA

	PBC 14	
actual	σ_{yf} = 39. KSI σ_{uf} = 58. σ_{yco} = 55.	a = .1094" t_c = .0726" t_f = .0748"
	5t	Karren
t_c	σ_{yco} = 69.1	σ_{yco} = 61.7
t_f	69.8	σ_{yco} = 62.2

	RFC 14	
actual	σ_{yf} = 44. KSI σ_{uf} = 62. KSI σ_{yco} = 59.	a = .1094" t_c = .0722" t_f = .0746"
	5t	Karren
t_c	σ_{yco} = 72.4	σ_{yco} = 66.1
t_f	73.1	66.1

	PBC 13	
actual	σ_{yf} = 38. KSI σ_{uf} = 60.5 σ_{yco} = 57.	a = .1016" t_c = .0852" t_f = .0886"
	5t	Karren
t_c	σ_{yco} = 61.5	σ_{yco} = 67.8
t_f	62.2	σ_{yco} = 68.5

	RFC 13	
actual	σ_{yf} = 38. KSI σ_{uf} = 62. σ_{yco} = 56.	a = .0937" t_c = .0873" t_f = .0915"
	5t	Karren
t_c	σ_{yco} = 66.3	σ_{yco} = 71.2
t_f	67.2	72.2

TABLE 3.4

CORNER YIELD STRENGTH: ACTUAL, KARREN'S FORMULA AND 5t FORMULA (continued)

H 11		
actual	σ_{yf} = 42. KSI	σ_{uf} = 59.5
	σ_{yco} = 60.	t_f = .1225
	a_1 = .1953"	a_2 = .2266
	t_{c1} = .1145	t_{c2} = .1145
	$(2\alpha)_1$ = 70.9°	$(2\alpha)_2$ = 64.5°
	5t	Karren
t_{c1}, t_f	σ_{yco} = 61.9	σ_{yco} = 61.8
	62.9	62.8
t_{c2}, t_f	58.1	59.7
	59.0	60.6

H 7		
actual	σ_{yf} = 45. KSI	σ_{uf} = 63.
	σ_{yco} = 63.	t_f = .1813"
	a_1 = .1563	a_2 = .2266
	t_{c1} = .1567	t_{c2} = .1145
	$(2\alpha)_1$ = 78°	$(2\alpha)_2$ = 68°
	5t	Karren
t_{c1}, t_f	σ_{yco} = 62.5	σ_{yco} = 74.2
	69.7	76.8
t_{c2}, t_f	78.2	63.3
	73.4	70.4

TABLE 3.4

CORNER YIELD STRENGTH: ACTUAL, KARREN'S FORMULA AND 5t FORMULA (continued)

	H T	
actual	σ_{yf} = 52. KSI	σ_{uf} = 65. KSI
	σ_{yco} = 70.	t_f = .3030"
	a_1 = .2031"	a_2 = .2734"
	t_{c1} = .2605"	t_{c2} = .2644"
	$(2\alpha)_1$ = 85.5°	$(2\alpha)_2$ = 86.°
	5t	Karren
t_{c1}	σ_{yco} = 82.7	σ_{yco} = 78.3
t_f	85.6	80.6
t_{c2}	83.7	74.1
t_f	80.2	76.1

σ_{yf} = yield strength of flat, ksi

σ_{uf} = ultimate stress of flat, ksi

σ_{yco} = corner yield strength, ksi

a = corner radius, inch

t_c = thickness of corner, inch

t_f = thickness of flat, inch

2α = corner angle, degrees

Subscripts 1, 2 refer to corner 1 (web-flange) and 2 (flange-lip) respectively.

5t formula (eq. 3.11) and Karren's formulas may be used with $t = t_c$ or $t = t_f$.

Karren's formulation involve equations (3.2), (3.3), (3.6), (3.13) and (3.14).

TABLE 3.5

PBC 14 TENSILE COUPON TEST

Specimen	Coupon	w (gram)	t (in)	d (in)	A (in^2)	σ_p (ksi)	σ_{yt} (ksi)	σ_u (ksi)	% Elong.	$\frac{\sigma_p}{\sigma_{yt}}$	$\frac{\sigma_u}{\sigma_{yt}}$	Int. Radius (in)	Ext. Radius (in)
a	1		.0761	.226	.0172	26.1	44.3	58.4	28.	.59	1.32		
	2	8.096	.0745		.0315	40.6	54.6	65.1	**	.74	1.19	7/64	15/64
	3		.0752	.229	.0173	34.8	41.7	58.2	35.	.83	1.40		
	4		.0756	.227	.0172	26.2	40.7	58.0	31.	.64	1.43		
	5	7.322	.0720		.0285	28.1	54.0	63.8	**	.52	1.18	3/32	7/32
	6		.0762	.229	.0174	28.6	41.3	58.9	27.	.69	1.43		
	7		.0755	.227	.0172	29.1	39.1	58.1	36.	.74	1.49		
	8		.0762	.228	.0174	28.8	39.0	57.6	34.	.74	1.48		
	9		.0800	.227	.0182	33.0	38.8	55.4	34.	.85	1.43		
	10		.0760	.229	.0174	29.3	43.0	58.8	30.	.68	1.37		
	11	7.131	.0730		.0277	23.5	56.0	66.4	**	.42	1.19	7/64	1/4
	12		.0757	.227	.0172	30.2	40.7	58.7	30.	.74	1.44		
	13		.0758	.227	.0172	32.5	40.1	58.7	33.	.81	1.46		
	14	8.151	.0745		.0317	28.4	53.9	65.3	11.	.53	1.21	9/64	17/64
	15		.0760	.227	.0172	24.9	45.9	59.7	23.	.54	1.30		
b	1		.077	.456	.0351	22.8	47.6	59.5	28.	.48	1.25		
	15		.0774	.449	.0347	25.9	45.2	58.4	30.	.57	1.29		
c	8	9.543	.0762	.491	.0374	38.3	40.7	57.6	35.	.94	1.41		
	11	8.007	.0721		.0315	46.1	54.8	64.1	**	.84	1.17		
d	5	7.967	.0716		.0313	42.5	54.6	64.2	18.	.78	1.18		
	8	9.481	.0762	.489	.0373	37.5	40.9	58.4	37 .	.92	1.43		

TABLE 3.5 (continued)

Specimen	Coupon	w gram	t in	d in	A in^2	σ_p ksi	σ_{yt} ksi	σ_u ksi	% Elong.	$\frac{\sigma_p}{\sigma_{yt}}$	$\frac{\sigma_u}{\sigma_{yt}}$	Int. Radius in	Ext. Radius in
75"	8		.0767	.496	.0380	35.5	40.7	56.5	35.	.87	1.39		
column	11		.0720		.0312	36.9	54.9	63.8	**	.67	1.16		
86"	5	6.585	.0725		.0256	39.4	56.2	65.8	**	.70	1.17		
column	8		.0758	.483	.0366	32.7	40.4	57.3	35.	.81	1.42		
99"	8		.0760	.495	.0376	41.3	41.3	57.5	35.	1.00	1.39		
column	11	8.056	.0713		.0313	38.9	54.3	64.5	15.	.72	1.19		

** broke outside of middle 2".

Specimens are sometimes designated by the length of the corresponding column (without end plate).

TABLE 3.6

PBC 14 COMPRESSIVE COUPON TEST

Specimen	Coupon	w gram	t in	d in	A_w in^2	σ_p ksi	σ_{yc} ksi	dt in^2	ℓ in	$\frac{dt-A_w}{.01dt}$	Int. Radius in	Ext. Radius in	$\frac{\sigma_p}{\sigma_{yc}}$
e	1	16.993	.0775		.0430	47.9	53.9		3.075		7/64	7/32	.89
	2	14.501	.0758	.486	.0365	16.2	38.1	.0368	3.089	.8			.43
	3	17.462	.0720		.0442	47.7	52.8		3.077		3/32	7/32	.90
	4	14.512	.0760	.486	.0365	29.9	38.7	.0389	3.090	1.0			.77
	5	14.974	.0760	.502	.0377	28.1	37.9	.0381	3.089	1.1			.74
	6	15.002	.0760	.501	.0378	11.5	37.7	.0381	3.090	.8			.30
	7	17.484	.0730		.0444	35.3	53.4		3.067		3/32	7/32	.66
	8	15.224	.0760	.509	.0383	11.5	39.6	.0387	3.090	.9			.29
	9	17.723	.0740		.0450	45.7	55.1		3.066		9/64	1/4	.83

A_w was used for stress computations.

TABLE 3.7

COMPARISON BETWEEN COUPON AREA BY WEIGHT AND DIMENSION FOR PBC 14

Specimen	Coupon	w (gram)	t (in)	d (in)	ℓ (in)	A_w (in^2)	dt (in^2)	$\frac{A_w - dt}{.01dt}$
c	8	9.543	.0762	.491	2.00	.0371	.0374	
d	8	9.481	.0762	.489	2.00	.0369	.0373	
f	1		.0768	.435	3.0214			
	2	14.254	.0755		3.0080	.0369		
	3	11.710	.0760	.4011	3.0123	.0302	.0305	.8
	4	11.771	.0760	.403	3.019	.0303	.0306	.9
	5	14.055	.0762		3.0156	.0363		
	6	11.761	.0760	.403	3.015	.0304	.0306	.9
	7	13.794	.0760	.4668	3.0377	.0353	.0355	.4
	8	13.969	.0760	.4710	3.0504	.0356	.0358	-.4
	9	13.894	.0760	.467	3.0638	.0353	.0355	.6
	10	11.950	.0761	.4020	3.0573	.0304	.0306	.6
	11	13.490	.0730		3.0597	.0343		
	12	12.082	.0760	.4071	3.0548	.0308	.0309	.5
	13	12.002	.0760	.4020	3.0673	.0304	.0305	.3
	14	15.524	.0760		3.0690	.0394		
	15		.0770	.404	3.0635			

Specimen f was intended for compression tests but was found too narrow.

TABLE 3.8

RFC 14 TENSILE COUPON TEST

Specimen	Coupon	w gram	t in	d in	A in^2	σ_p ksi	σ_{yt} ksi	σ_u ksi	% Elong.	$\frac{\sigma_p}{\sigma_{yt}}$	$\frac{\sigma_u}{\sigma_{yt}}$
a	1		.074	.360	.0266	43.2	49.7	62.9	23.	.87	1.27
	2	5.914	.073		.0230	46.5	59.1	69.5	11.	.79	1.18
	3		.073	.318	.0232	45.2	46.3	62.0	20.	.98	1.34
	4		.074	.311	.0230	32.6	44.1	61.7	**	.74	1.40
	5	8.399	.071		.0327	44.7	56.6	67.2	13.	.79	1.19
	6		.073	.311	.0227	35.2	46.2	61.0	25.	.76	1.32
	7	6.740	.073	.360	.0262	36.2	44.5	60.9	26.	.81	1.37
	8		.072	.335	.0241	36.1	49.7	66.3	26.	.73	1.33
	9		.073	.312	.0228	35.1	45.0	60.2	26.	.78	1.34
	10	8.570	.070		.0333	42.0	54.0	63.6	**	.78	1.18
	11		.073	.311	.0227	37.4	43.0	56.4	25.	.87	1.31
	12		.072	.287	.0207	31.5	40.2	54.0	32.	.78	1.34
	13	7.701	.071		.0230	41.7	50.7	57.4	15.	.82	1.13
	14		.072	.318	.0229	35.8	40.6	53.1	36.	.88	1.31
b	1		.0771	.419	.0323	35.6	48.1	59.4	27.	.74	1.23
	7	9.545	.0740	.499	.0369	36.6	40.1	57.8	36.	.91	1.44
	8		.0760	.438	.0333	34.5	42.1	58.6	33.	.82	1.39
	10	7.613	.0710		.0296	35.5	52.4	63.2	19.	.68	1.21
	14	8.096	.0769		.0315	35.7	47.8	60.3	24.	.75	1.26

TABLE 3.8 (continued)

Specimen	Coupon	w (gram)	t (in)	d (in)	A (in^2)	σ_p (ksi)	σ_{yt} (ksi)	σ_u (ksi)	% Elong.	$\frac{\sigma_p}{\sigma_{yt}}$	$\frac{\sigma_u}{\sigma_{yt}}$
c	2	8.268	.0732		.0322	42.0	55.4	64.5	**	.76	1.16
	3-4		.0754	.424	.0319	37.6	46.0	64.8	35.5	.82	1.41
	5	8.009	.0747		.0311	40.1	54.6	63.4	**	.73	1.16
	6-7	9.228	.0750		.0317	41.9	47.1	66.0	35.5	.89	1.40
	7-8		.0758	.452	.0342	38.7	39.4	54.0	39.	.98	1.37
	8-9	9.754	.0751	.510	.0379	39.6	41.4	58.3	35.	.96	1.41
	11		.0750	.510	.0382	32.7	40.3	58.1	36.5	.81	1.44
d	7-8	9.641	.0750	.499	.0374	36.1	40.1	57.6	39.	.90	1.44
	10	10.261	.0715		.0399	40.1	50.7	61.9	25.	.79	1.22
78" column	5	7.111	.0732		.0276	43.4	60.2	70.3	**	.72	1.17
	6-7	9.199	.0756	.482	.0364	45.3	46.4	62.2	30.	.98	1.34
	8-9	9.479	.0750	.496	.0369	42.0	44.1	59.0	30.	.95	1.34
	10	6.539	.0710		.0254	33.4	58.8	68.2	**	.57	1.16
84" column	5	9.200	.0733		.0358	47.5	57.3	67.4	15.	.83	1.18
	7-8	9.335			.0363	44.1	45.5	60.3	25.	.97	1.32
	10	7.411	.0700		.0288	45.1	58.3	65.9	**	.77	1.13

**broke outside middle 2".

Specimen is identified by the length of the corresponding column (without end plates).

A_w used for all stress computations.

TABLE 3.9

RFC 14 COMPRESSIVE COUPON TEST

Specimen	Coupon	w	t	d	ℓ	A_w	σ_p	σ_{yc}	dt
		gram	in	in	in	in^2	ksi	ksi	in^2
e	1	18.346			3.104	.0460	43.5	55.5	
	2	15.185	.074	.511	3.124	.0378	39.6	42.3	.0378
	3	17.182			3.109	.0430	44.6	56.3	
	4	15.016	.074	.507	3.124	.0374	33.1	40.1	.0375
	5	14.631	.074	.511	3.003	.0379	28.5	37.6	.0378
	6	15.092	.074	.511	3.124	.0376	26.6	38.8	.0378
	7	17.177			3.093	.0432	34.7	51.3	
	8	14.568	.074	.511	3.003	.0377	30.2	38.2	.0378
	9	17.645			3.141	.0437	38.9	50.3	

A_w used for all stress computations.

For tensile coupons ℓ = 2.00".

TABLE 3.10

COMPARISON OF AREA FROM WEIGHT AND FROM DIMENSIONS

	Specimen	Coupon	w	t	d	ℓ	A_w	dt	$\frac{dt-A_w}{.01dt}$
			gram	in	in	in	in^2	in^2	
tension	a	7	6.74	.073	.360	2.00	.0262	.0263	.2
tension	b	7	9.545	.0740	.499	2.00	.0371	.0369	-.6
tension	c	8-9	9.754	.0751	.5102	2.00	.0379	.0383	.9
tension	d	7-8	9.641	.0750	.499	2.00	.0375	.0374	-.2
tension	78" column	6-7	9.199	.0756	.4819	2.00	.0358	.0364	1.7
tension	78" column	8-9	9.479	.0750	.4956	2.00	.0369	.0372	.8
compression	e	2	15.185	.074	.511	3.124	.0378	.0378	0.0
compression	e	4	15.016	.074	.507	3.124	.0374	.0375	.3
compression	e	5	14.631	.074	.511	3.003	.0379	.0378	-.3
compression	e	6	15.092	.074	.511	3.124	.0376	.0378	.6
compression	e	8	14.568	.074	.511	3.003	.0377	.0378	.2

TABLE 3.11

PBC 13 TENSILE COUPON TEST

Specimen	Coupon	w gram	t in	d in	A in^2	σ_p ksi	σ_{yt} ksi	σ_u ksi	% Elong.	dt in^2	$\frac{dt-A_w}{.01dt}$	$\frac{\sigma_p}{\sigma_{yt}}$	$\frac{\sigma_u}{\sigma_{yt}}$
a	1	7.070	.091	.307	.0275	21.8	46.0	63.1	32.	.0279	1.5	.47	1.37
	2	10.358	.090		.0403	17.4	56.1	65.5	30.			.31	1.17
	3	6.900	.091	.298	.0268	22.3	39.1	61.4	30.	.0271	1.0	.57	1.57
	4	6.869	.092	.295	.0267	9.3	39.7	61.7	30.	.0271	1.5	.23	1.55
	5	11.555	.090		.0450	31.1	54.8	64.2	26.			.57	1.17
	6	7.656	.091	.329	.0298	18.5	40.4	61.8	38.	.0299	.5	.46	1.53
	7	10.314	.092	.440	.0401	22.2	37.8	60.5	36.	.0405	.9	.59	1.60
	8	10.328	.092	.440	.0402	21.0	38.3	61.0	35.	.0405	.7	.55	1.59
	9	10.321	.092	.439	.0402	17.3	39.6	61.0	32.	.0404	.6	.44	1.54
	10	10.072	.086		.0392	14.0	52.8	64.8	20.			.27	1.23
	11	6.720	.092	.287	.0261	22.9	39.4	61.2	33.			.58	1.55
	12	6.929	.092	.297	.0270	24.1	37.8	60.3	30.	.0273	1.3	.64	1.60
	13	9.620	.087		.0374	26.7	55.8	64.2	23.			.48	1.15
	14	7.743	.093		.0301	13.3	42.1	61.1	28.			.32	1.45
b	2	10.508	.091		.0409	31.8	59.4	66.0	26.			.54	1.11
c	5	9.451	.0866		.0371	45.8	57.2	63.7	29.			.80	1.11
	7-8	11.426	.0917	.490	.0445	21.1	37.8	60.9	36.	.0449	1.0	.56	1.61
d	10	9.672	.0878		.0380	40.8	56.6	63.5	29.			.72	1.12
	7-8	11.623	.0931	.490	.0452	21.9	37.2	60.7	36.	.0456	.9	.59	1.63

TABLE 3.12

PBC 13 COMPRESSIVE COUPON TEST

Specimen	Coupon	w	t	d	ℓ	A	σ_p	σ_{yc}	dt	$\frac{dt-A_w}{.01dt}$	$\frac{\sigma_p}{\sigma_{yc}}$
		gram	in	in	in	in^2	ksi	ksi	in^2		
e	1	20.765	.088		3.043	.0531	24.0	57.4			.42
	2	18.245	.091	.512	3.085	.0460	21.9	39.5	.0466	1.2	.55
	3	21.256	.085		3.044	.0543	32.4	55.7			.58
	4	18.320	.091	.512	3.087	.0462	27.9	38.5	.0466	.9	.72
	5	18.360	.091	.512	3.095	.0462	24.6	37.9	.0466	.9	.65
	6	18.370	.091	.512	3.092	.0462	28.7	39.6	.0466	.8	.72
	7	21.049	.086		3.042	.0538	49.6	58.9			.84
	8	18.393	.091	.512	3.090	.0463	22.3	38.0	.0466	.6	.59
	9	21.676	.089		3.043	.0554	40.0	56.1			.71

TABLE 3.13

RFC 13 TENSILE COUPON TEST

Specimen	Coupon	w gram	t in	d in	A in^2	σ_p ksi	σ_{yt} ksi	σ_u ksi	% Elong.	$\frac{\sigma_p}{\sigma_{yt}}$	$\frac{\sigma_u}{\sigma_{yt}}$
a	1		.092	.294	.0270	25.9	42.1	61.5	30.	.62	1.46
	2	8.741	.089		.0340	25.0	57.3	65.6	24.	.44	1.14
	3		.090	.310	.0279	19.7	39.4	62.4	36.	.50	1.58
	4		.090	.303	.0273	23.8	38.9	61.8	36.	.61	1.59
	5	10.894	.087		.0424	34.2	55.4	64.9	30.	.62	1.17
	6		.090	.327	.0294	29.7	40.1	62.3	34.	.74	1.55
	7		.090	.329	.0296	28.7	38.2	61.8	30.	.75	1.62
	8		.090	.326	.0293	27.3	38.5	62.0	30.	.71	1.61
	9		.090	.310	.0279	26.9	39.4	62.0	35.	.68	1.57
	10	10.200	.086		.0397	20.2	52.9	65.1	32.	.38	1.23
	11		.090	.295	.0265	26.4	39.7	62.7	34.	.66	1.58
	12		.090	.294	.0265	20.8	39.7	62.2	33.	.52	1.57
	13	9.228	.088		.0359	25.1	56.2	66.5	30.	.45	1.18
	14		.091	.250	.0227	19.8	41.8	61.8	29.	.47	1.48
b	10	9.220	.0860		.0358	40.5	55.9	65.1	26.	.72	1.16
	8		.0910	.498	.0453	30.9	37.5	61.3	40.	.82	1.63
c	5	8.374	.0858		.0326	46.0	59.8	65.2	15.**	.77	1.09
	7		.0900	.500	.0450	29.7	37.4	60.7	36.	.79	1.62

** broke outside of middle 2".

TABLE 3.14

RFC 13 COMPRESSIVE COUPON TEST

Specimen	Coupon	w gram	t in	ℓ in	A_w in^2	σ_p ksi	σ_{yc} ksi	$\frac{\sigma_p}{\sigma_{yc}}$
d	1	21.554	.088	3.111	.0545	22.0	55.3	.40
	2	18.080	.0913	3.051	.0466	23.6	38.4	.61
	3	21.002	.087	3.095	.0533	24.4	56.6	.43
	4	18.075	.0911	3.051	.0466	26.8	38.4	.70
	5	18.049	.0912	3.051	.0465	23.6	37.6	.63
	6	18.015	.0912	3.050	.0464	28.0	39.2	.71
	7	20.040	.086	3.131	.0503	33.8	54.8	.62
	8	17.768	.0908	3.024	.0462	31.2	39.4	.79
	9	20.754	.087	3.089	.0528	24.6	55.8	.44

TABLE 3.15

H 11 TENSILE COUPON TEST

Specimen	Coupon	t in	d in	A in^2	σ_p ksi	σ_{yt} ksi	σ_u ksi	% Elong.	Int. Radius in	Ext. Radius in	$\frac{\sigma_p}{\sigma_{yt}}$	$\frac{\sigma_u}{\sigma_{yt}}$
a	1	.125	.235	.0294	48.0	55.8	71.8	18.			.86	1.29
	2	.112		.0374	36.9	60.1	71.6	11.	15/64	7/16	.61	1.19
	3	.121	.248	.0304	36.2	43.4	59.8	21.			.83	1.38
	4	.123		.0299	30.5	50.9	64.9	14.	9/32	1/2	.60	1.28
	5	.114		.0403	24.8	51.8	65.9	15.			.48	1.27
	6	.111		.0355	28.2	56.3	68.6	11.	9/32	1/2	.50	1.22
	7	.121	.254	.0309	26.6	42.2	59.1	19.			.63	1.40
	8	.112		.0371	35.0	59.2	70.8	12.	15/64	7/16	.59	1.20
	9	.121	.270	.0325	47.7	53.2	65.2	**			.90	1.23
b	3	.1216		.0414	36.2	41.2	59.2	28.5			.88	1.44
	8	.1122		.0369	33.9	61.2	70.9	**			.55	1.16
c	2	.1122		.0373	42.9	60.3	71.2	10.			.71	1.18
	7	.1183	.3141	.0375	31.5	40.7	59.6	24.			.77	1.46

**broke outside middle 2".

TABLE 3.16

H 11 COMPRESSIVE COUPON TEST

Specimen	Coupon	t	d	A	σ_p	σ_{yc}	$\frac{\sigma_p}{\sigma_{yc}}$
		in	in	in^2	ksi	ksi	
d	1	.120		.0601	42.8	56.8	.75
	3	.121	.506	.0612	39.7	45.2	.88
	7	.120	.505	.0605	33.1	44.6	.74
	9	.121		.0618	39.3	52.4	.75
e	2	.110		.0642	30.4	59.7	.51
	4-5	.110		.0633	36.1	55.3	.65
	5-6	.110		.0640	45.4	60.2	.75
	8	.110		.0663	42.4	58.8	.72

TABLE 3.17

H 7 TENSILE COUPON TESTS

Specimen	Coupon	w gram	t in	d in	A in^2	σ_p ksi	σ_{yt} ksi	σ_u ksi	% Elong.	A_w in^2	$\frac{dt-A_w}{.01dt}$	$\frac{\sigma_p}{\sigma_{yt}}$	$\frac{\sigma_u}{\sigma_{yt}}$
a	1	23.568	.181	.513	.0928	36.6	50.2	63.3	27.	.0917	1.2	.73	1.32
	2	22.591	.160		.0892	25.8	62.8	77.0	15.			.41	1.23
	3	11.597	.173	.263	.0455	37.4	45.3	62.7	25.	.0451	.8	.83	1.38
	4	21.847	.160		.0863	44.0	62.8	75.3	14.			.70	1.20
	5	22.801	.162		.0901	42.2	61.1	76.1	15.			.69	1.25
	6	14.466	.174	.328	.0571	40.3	44.1	62.2	25.	.0563	1.4	.91	1.41
	7	18.214	.166		.0719	33.4	66.7	77.2	11.			.50	1.16
	8	21.643	.182	.464	.0844	23.7	48.6	63.4	25.	.0842	.3	.49	1.30
b	1		.1819	.4036	.0734	34.0	50.4	64.3	17.			.67	1.28
	7		.1580		.0573	51.5	68.7	80.5	**			.75	1.17
c	2		.1528		.0634	50.5	66.2	77.0	10.			.76	1.16
	7		.1528		.0414	51.9	67.6	78.4	10.			.77	1.16
	8		.1820	.4021	.0732	32.8	48.5	63.5	20.	.0729		.68	1.31

**broke outside middle 2".

TABLE 3.18

H 7 COMPRESSIVE COUPON TESTS

Specimen	Coupon	t in	d in	A_w in^2	σ_p ksi	σ_y ksi	dt in^2	$\frac{dt-A_w}{.01\,dt}$	$\frac{\sigma_p}{\sigma_{yc}}$
d	1	.182	.505	.0912	43.9	60.0	.0919	.8	.73
	2	.165		.0914	41.7	64.8			.64
	3	.175	.505	.0881	44.6	46.3	.0884	.3	.96
	4	.160		.0884	59.2	65.1			.91
	5	.165		.0882	35.6	63.8			.56
	6	.174	.504	.0880	33.0	45.9	.0877	-.4	.72
	7	.160		.0904	43.5	66.4			.66
	8	.183	.505	.0930	41.5	48.4	.0924	-.6	.86

TABLE 3.19

H T TENSILE COUPON TEST

Specimen	Coupon	w gram	t in	d in	A_w in^2	σ_p ksi	σ_{yt} ksi	σ_u ksi	% elong.	$\frac{\sigma_p}{\sigma_{yt}}$	$\frac{\sigma_u}{\sigma_{yt}}$
a	1	30.771	.309	.400	.120	33.4	56.0	65.0	20.	.60	1.16
	2	29.844	.309	.377	.116	43.1	51.1	64.2	22.	.84	1.26
	3	32.506		.452	.126	23.7	65.2	78.9	15.	.36	1.21
	4	27.788	.291	.305	.0887	39.5	58.0	69.4	8.	.68	1.20
	5	23.659	.263	.329	.0921	41.3	70.6	79.8	10.	.58	1.13
	6	34.916	.303	.446	.136	42.7	60.0	70.6	18.	.71	1.18
	7	20.587			.0801	47.4	71.8	80.8	**	.66	1.13
	8	25.342	.299	.327	.0986		52.8	67.4	18.		1.28
	9	29.514	.252	.425	.115	27.4	71.0	81.9	13.	.39	1.15
	10	28.172	.310	.334	.110	44.7	52.5	66.1	22.	.85	1.26
	11	34.144	.311	.435	.133	45.2	52.1	64.0	24.	.87	1.23
b	9	28.58	.273		.111	42.7	70.9	81.7	**	.60	1.15

** broke outside middle 2".

TABLE 3.20

H T COMPRESSIVE COUPON TEST

Specimen	Coupon	w (gram)	t (in)	d (in)	ℓ (in)	A_w (in^2)	σ_p (ksi)	σ_{yc} (ksi)	$\frac{\sigma_p}{\sigma_{yc}}$
c	1	60.324	.311	.508		.1527	43.2	49.8	.87
	3	54.725	.248		3.098	.1375	46.5	65.8	.71
	5	55.110	.262		3.086	.1390	49.6	70.5	.70
	7	55.742	.264		3.086	.1406	50.5	73.1	.69
	9	56.042	.259		3.098	.1408	46.9	72.6	.65
	11		.294				49.0		
d	2	60.793	.310	.497	3.1455	.1504	53.2	55.2	.96
	6	60.180	.303		3.0976	.1512	52.2	62.7	.83
	10	60.171	.309	.503	3.042	.1539	46.8	52.5	.89
e	4	56.734	.296	.503	3.042	.1451	41.4	57.8	.72
	8	55.949	.297	.493	3.042	.1431	52.4	60.0	.87
	11						49.2		

TABLE 3.21

<u>H T COMPRESSIVE COUPON TEST</u> (strain gages)

Specimen	Coupon	w (gram)	t (in)	d (in)	ℓ (in)	A (in^2)	σ_{max} (ksi)
f	1	64.922	.307	.549	3.062	.165	52.1
	2	52.599	.313	.437	3.078	.133	53.0
	3	58.890	.201	.280	3.078	.149	70.5
	4	60.815	.290	.548	3.078	.154	62.3
	5	57.194	.219		3.078	.145	70.7
	6	97.693	.311	.965	3.078	.247	62.5
	7	67.065	.271		3.078	.170	67.6
	8	53.380	.298		3.078	.135	74.6
	9	53.204	.228	.560	3.078	.134	68.7
	10	50.273	.314	.414	3.078	.127	54.9
	11	60.219	.303	.519	3.078	.152	55.1

TABLE 3.22

LIST OF TABLES AND FIGURES FOR

TENSILE AND COMPRESSIVE TESTS

PBC 14	Fig. 3.5:	$\sigma_p, \sigma_y, \sigma_u$, % elongation , + plots
	3.6:	Tensile coupon locations
	3.7a,b,c,d:	Load-strain curves for tensile tests
	3.8a,b:	Load-strain curve for compressive tests
	Table 3.5:	Tensile coupon tests
	3.6:	Compressive coupon tests
	3.7:	Comparison of area from weight and from dimensions
RFC 14	Fig. 3.9:	$\sigma_p, \sigma_y, \sigma_u$, %elongation, t plots
	3.10:	Tensile coupon locations for RFC 14, RFC 13, PBC 13
	3.11:	Compressive coupon locations for RFC 14, RFC 13, PBC 14, PBC 13.
	3.12a,b,c:	Load-strain curves for tensile tests
	3.13a,b:	Load-strain curves for compressive tests
	Table 3.8:	Tensile coupon tests
	3.9:	Compressive coupon tests
	3.10:	Comparison of area from weight and from dimensions
PBC 13	Fig. 3.14:	$\sigma_p, \sigma_y, \sigma_u$, %elongation, t plots
	3.15a,b:	Load-strain curves for tensile tests
	3.16a,b:	Load-strain curves for compressive tests
	Table 3.11:	Tensile coupon tests
	3.12:	Compressive coupon tests
RFC 13	Fig. 3.17:	$\sigma_p, \sigma_y, \sigma_u$, %elongation, t plots
	3.18a,b:	Load-strain curves for tensile tests
	3.19a,b:	Load-strain curves for compressive tests
	Table 3.13:	Tensile coupon tests
	3.14:	Compressive coupon tests
H11	Fig. 3.20:	$\sigma_p, \sigma_y, \sigma_u$, %elongation, t plots
	3.21:	Location of tensile and compressive coupons
	3.22:	Load-strain curves for tensile tests
	3.23a,b:	Load-strain curves for compressive tests
	Table 3.15:	Tensile coupon test
	3.16:	Compressive coupon test

TABLE 3.22 (continued)

<u>LIST OF TABLES AND FIGURES FOR</u>

<u>TENSILE AND COMPRESSIVE TESTS</u>

<u>H7</u>	Fig. 3.24:	$\sigma_p, \sigma_y, \sigma_u$,% elongation, + plots
	3.25	Location of tensile and compressive coupons
	3.26a,b:	Load-strain curves for tensile tests
	3.27a,b:	Load-strain curves for compressive tests
	Table 3.17:	Tensile coupon test
	3.18:	Compressive coupon test
<u>HT</u>	Fig. 3.28:	$\sigma_p, \sigma_y, \sigma_u$,% elongation, t plots
	3.29:	Location of tensile and compressive coupons
	3.30:	Load-strain curves for tensile tests
	3.31a,b:	Load-strain curves for compressive tests - (compressometer)
	3.32a,b,c:	Load-strain curves for compressive tests (strain gage)
	Table 3.19:	Tensile coupon test
	3.20:	Compressive coupon test (compressometer)
	3.21:	Compressive coupon test (strain gage)

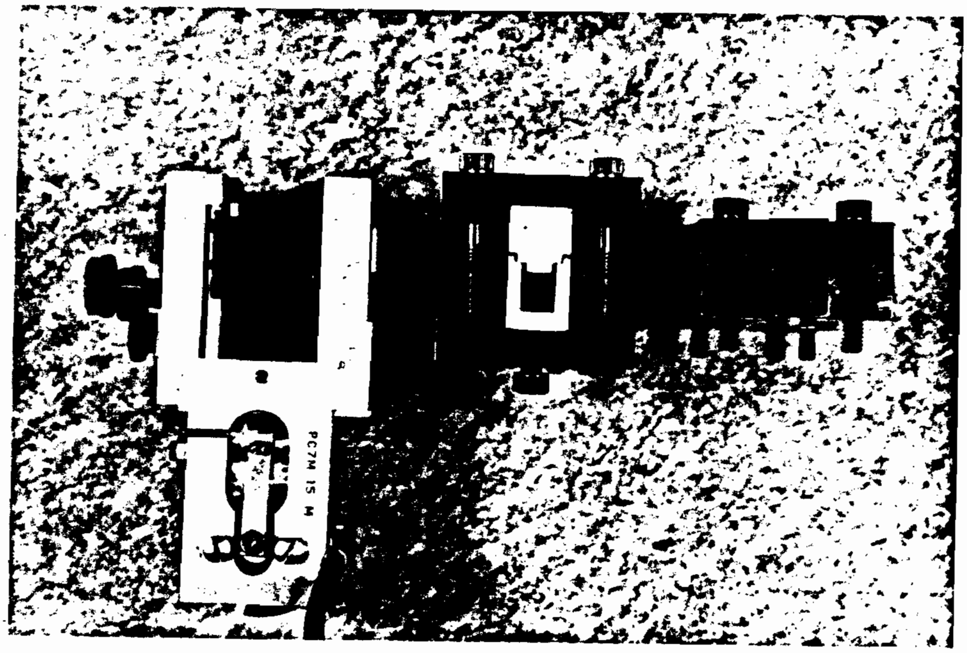

Photo 3.1 Compressometer, Compression Jigs For Corners and Flat Coupons

Photo 3.2 Compressometer, Compression Jigs For Corners and Flat Coupons

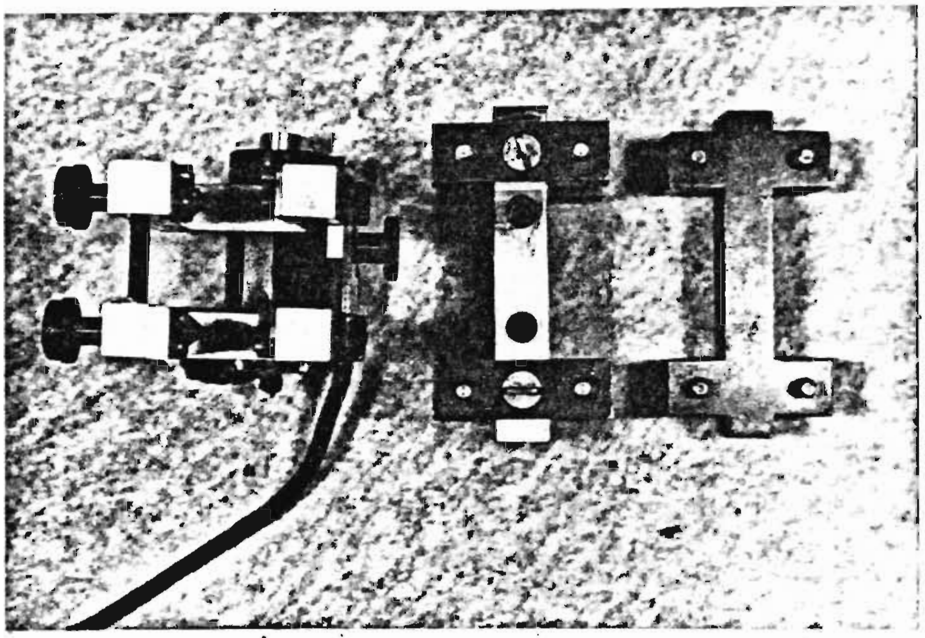

Photo 3.3 Compressometer, Compression Jigs For Corners and Flat Coupons

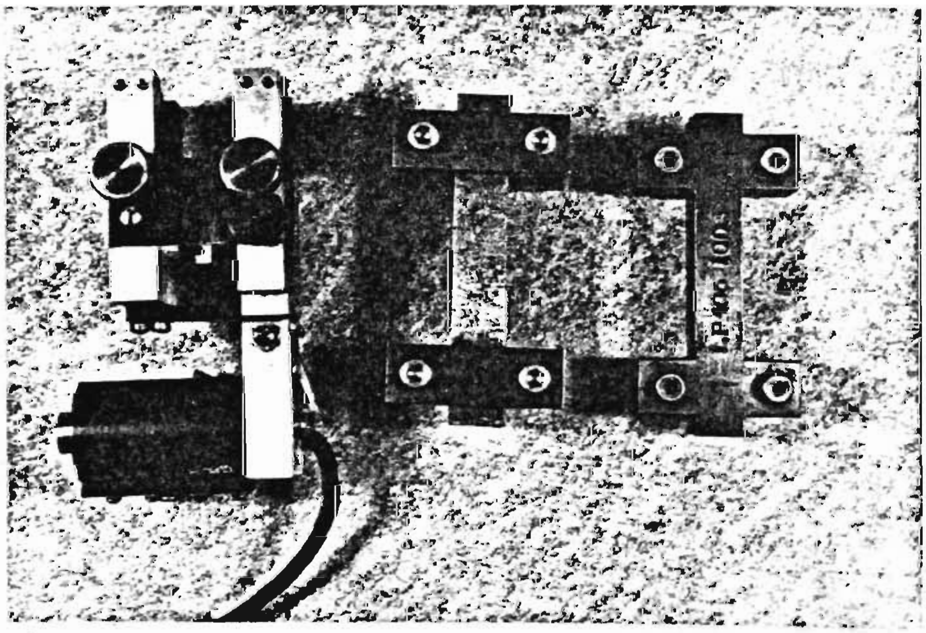

Photo 3.4 Compressometer, Compression Jigs For Corners and Flat Coupons

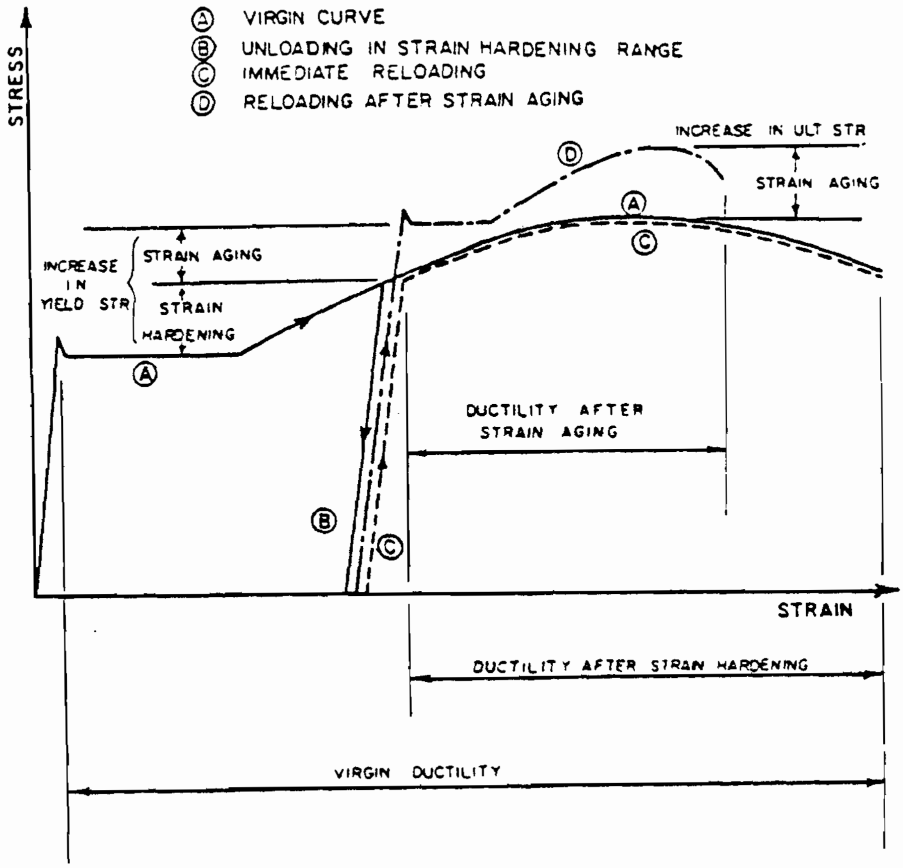

Fig. 3.1 Effects of strain hardening and strain aging on stress-strain characteristics of structural steel (Chajes et al [1963]).

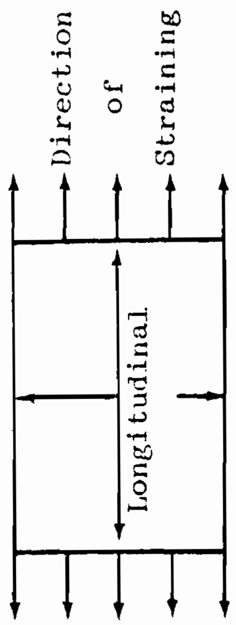

Fig. 3.2 Cold-Stretching of a Sheet.

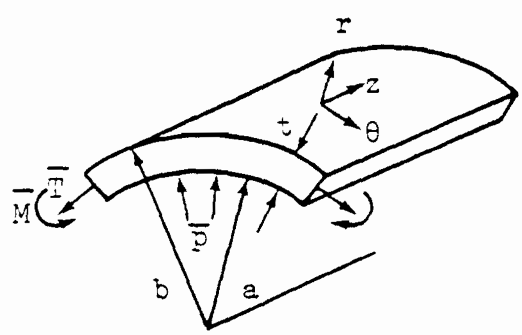

r: radial
z: longitudinal
t: transverse

Fig. 3.3 Cold-Forming of a Corner.

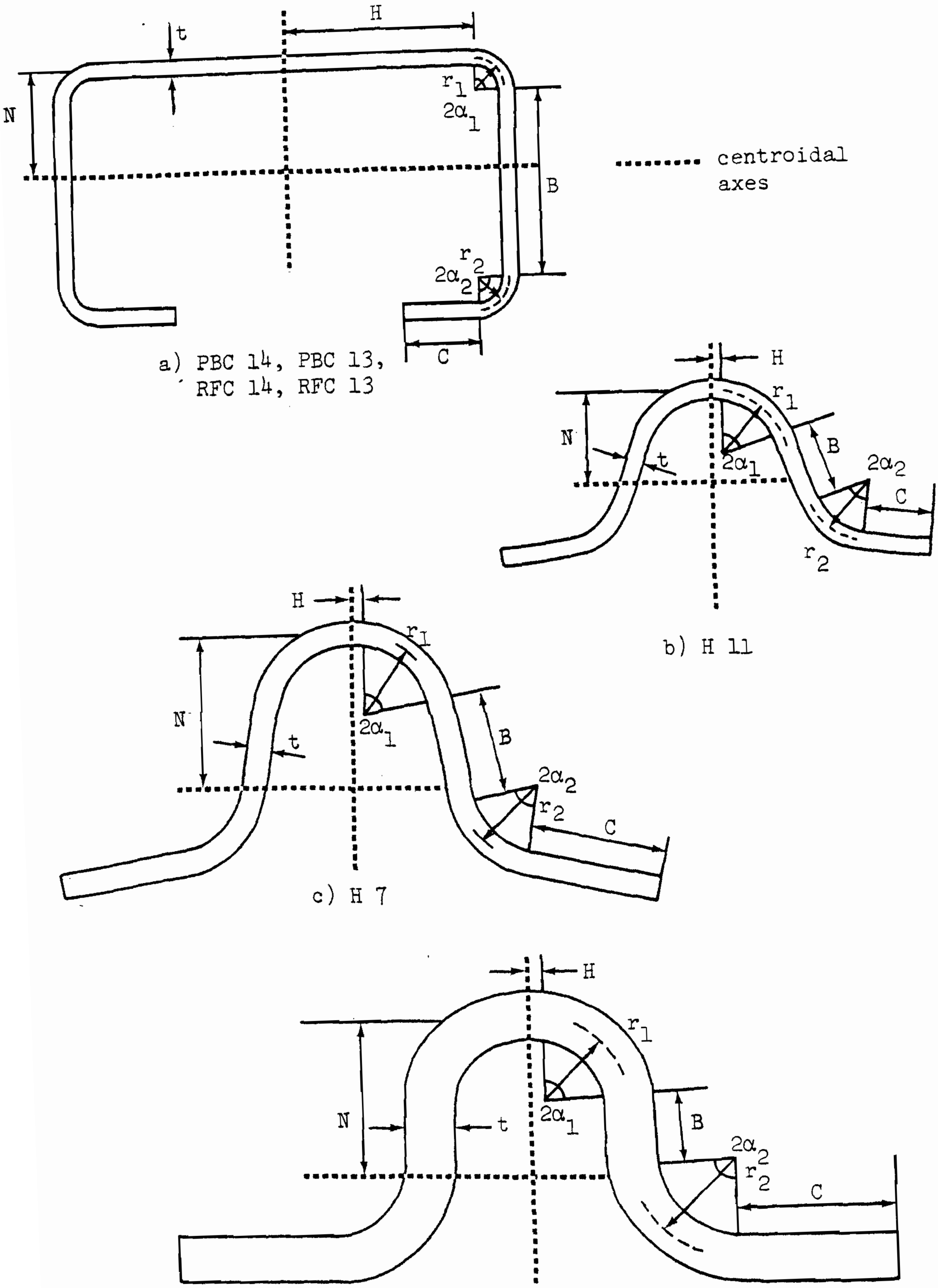

Fig. 3.4 Cross-sections (Properties are listed in Table 3.1).

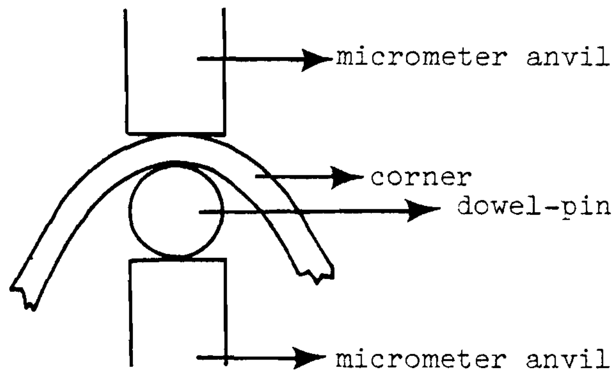

Fig. 3.4a

Measurement of Corner Thickness

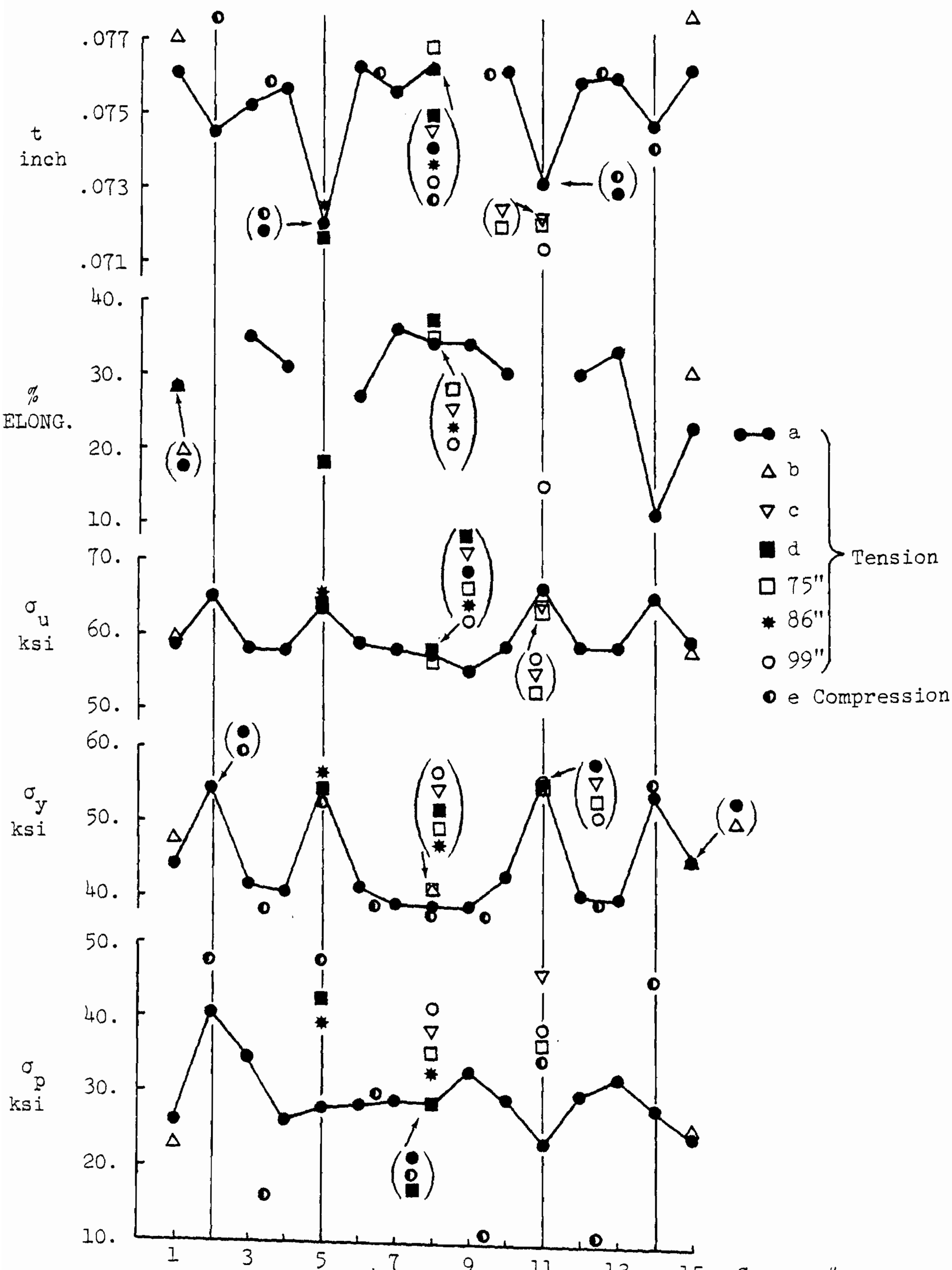

For coupon locations, see Fig. 3.6.

Fig. 3.5 PBC 14 Tensile and Compressive Coupon Tests.

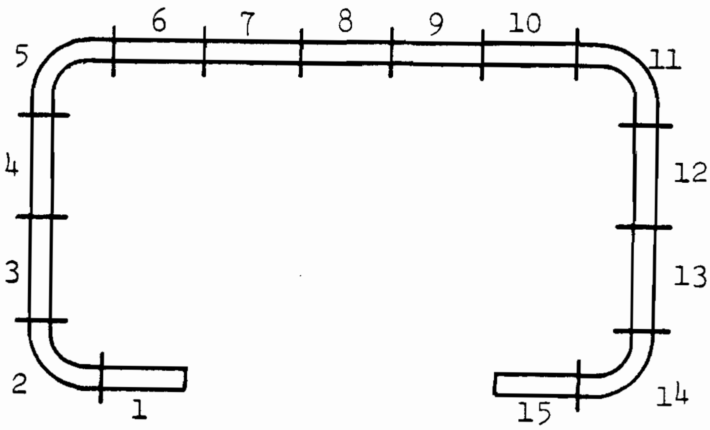

Fig. 3.6 PBC 14 Tensile Coupons. (For compressive coupons, see Fig. 3.11).

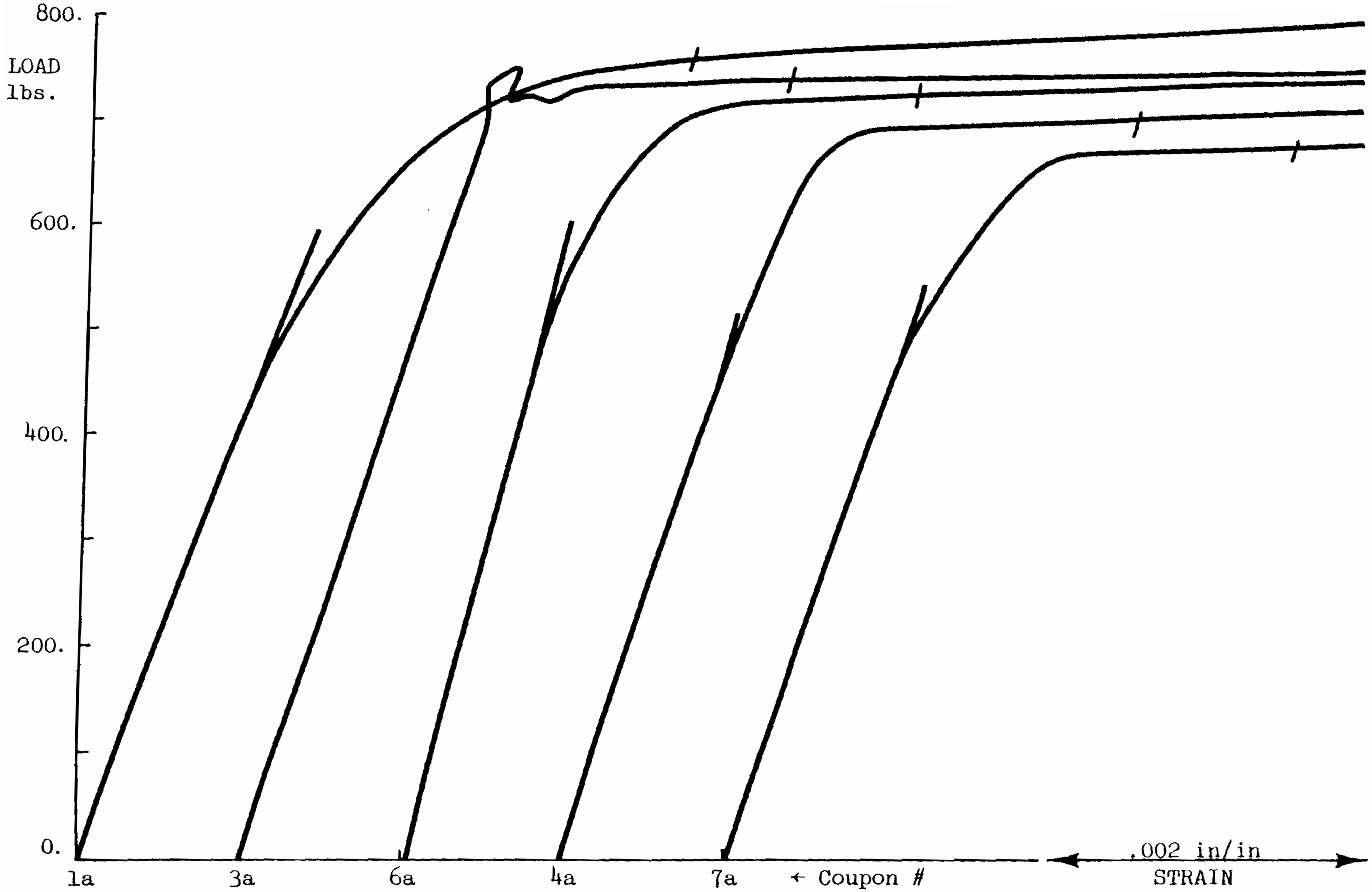

Fig. 3.7a PBC 14 Tensile Coupon Tests (Specimen a).

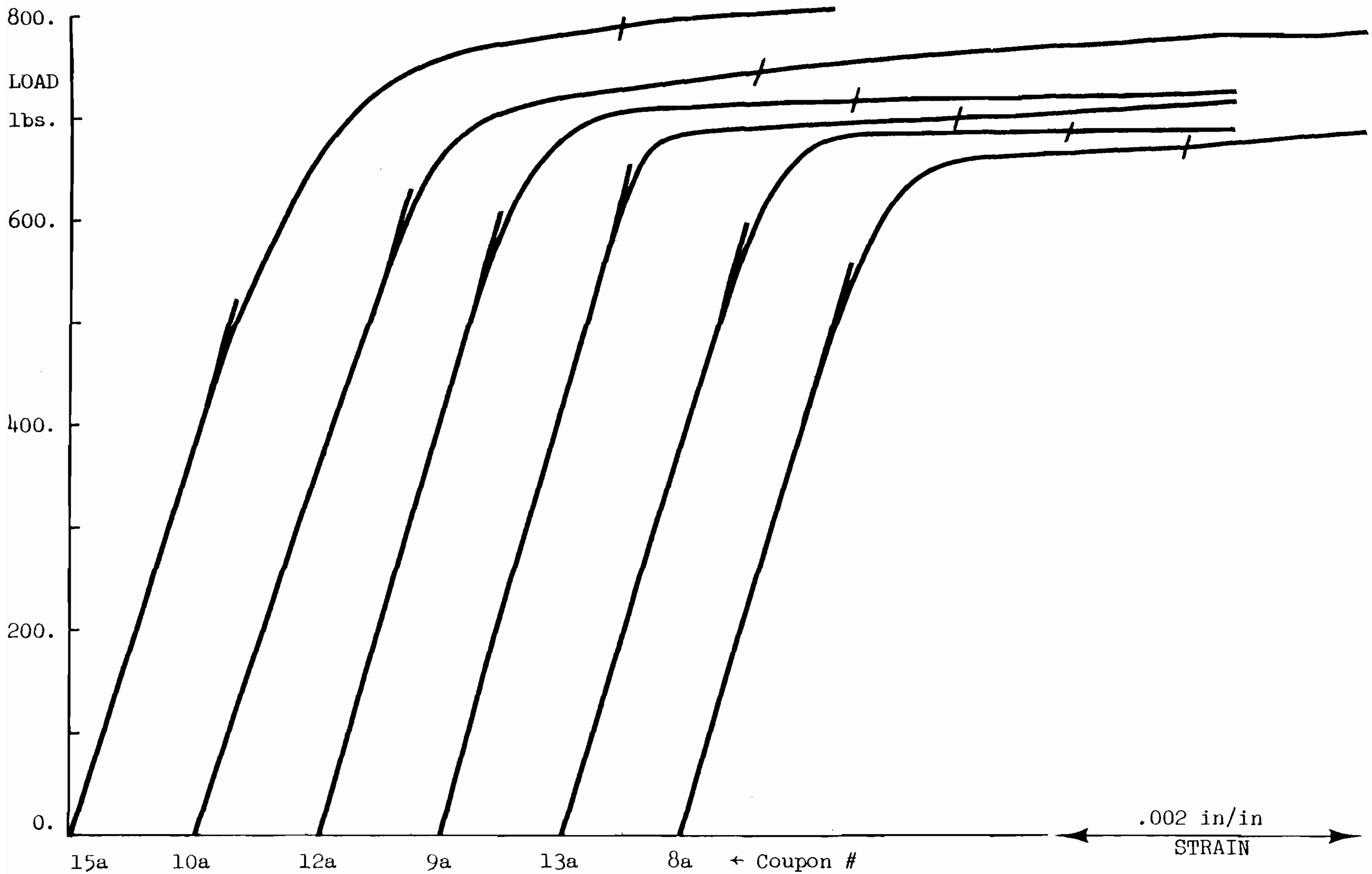

Fig. 3.7b PBC 14 Tensile Coupon Tests (Specimen a).

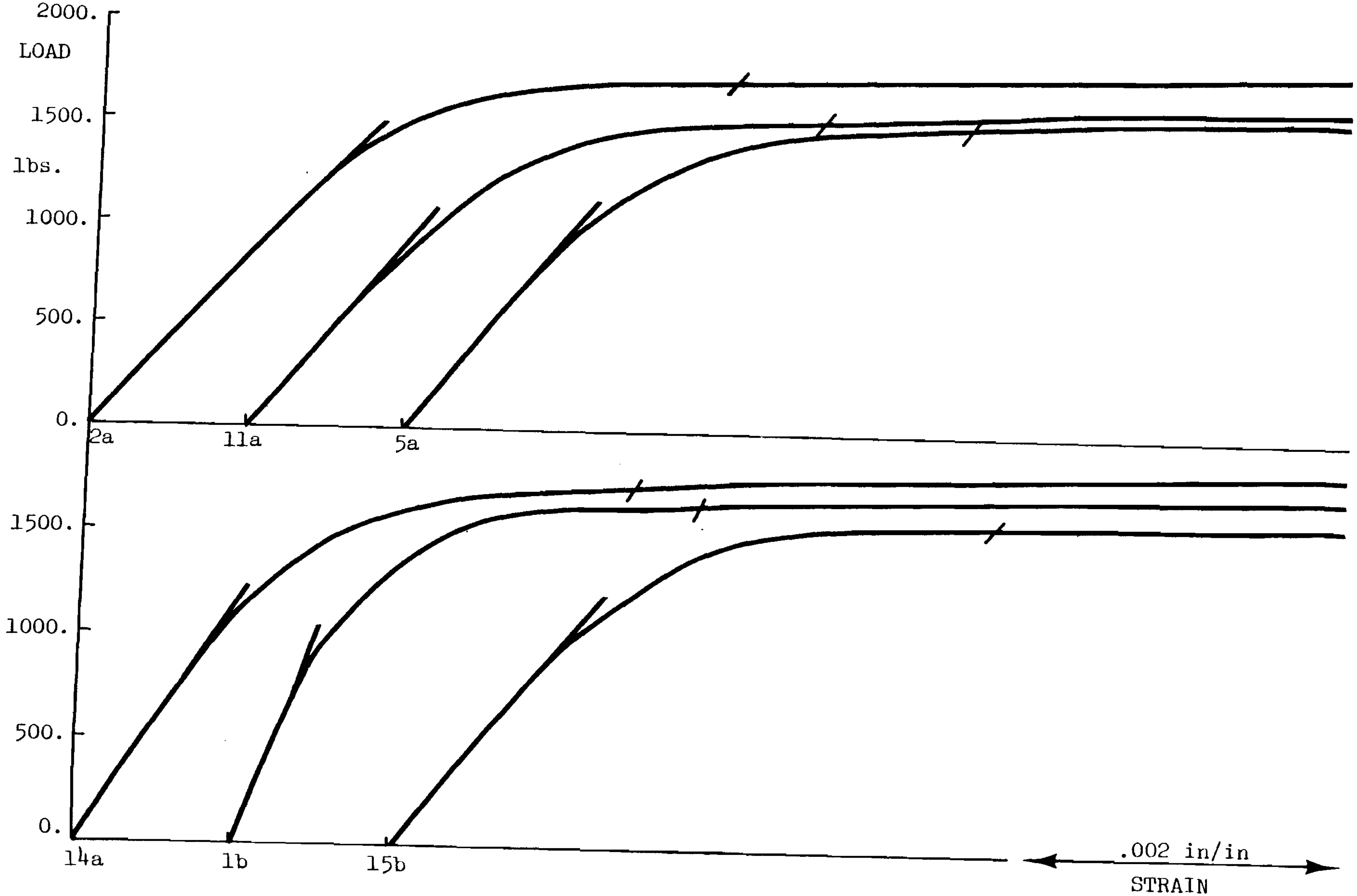

Fig. 3.7c PBC 14 Tensile Coupon Tests (Specimens a and b).

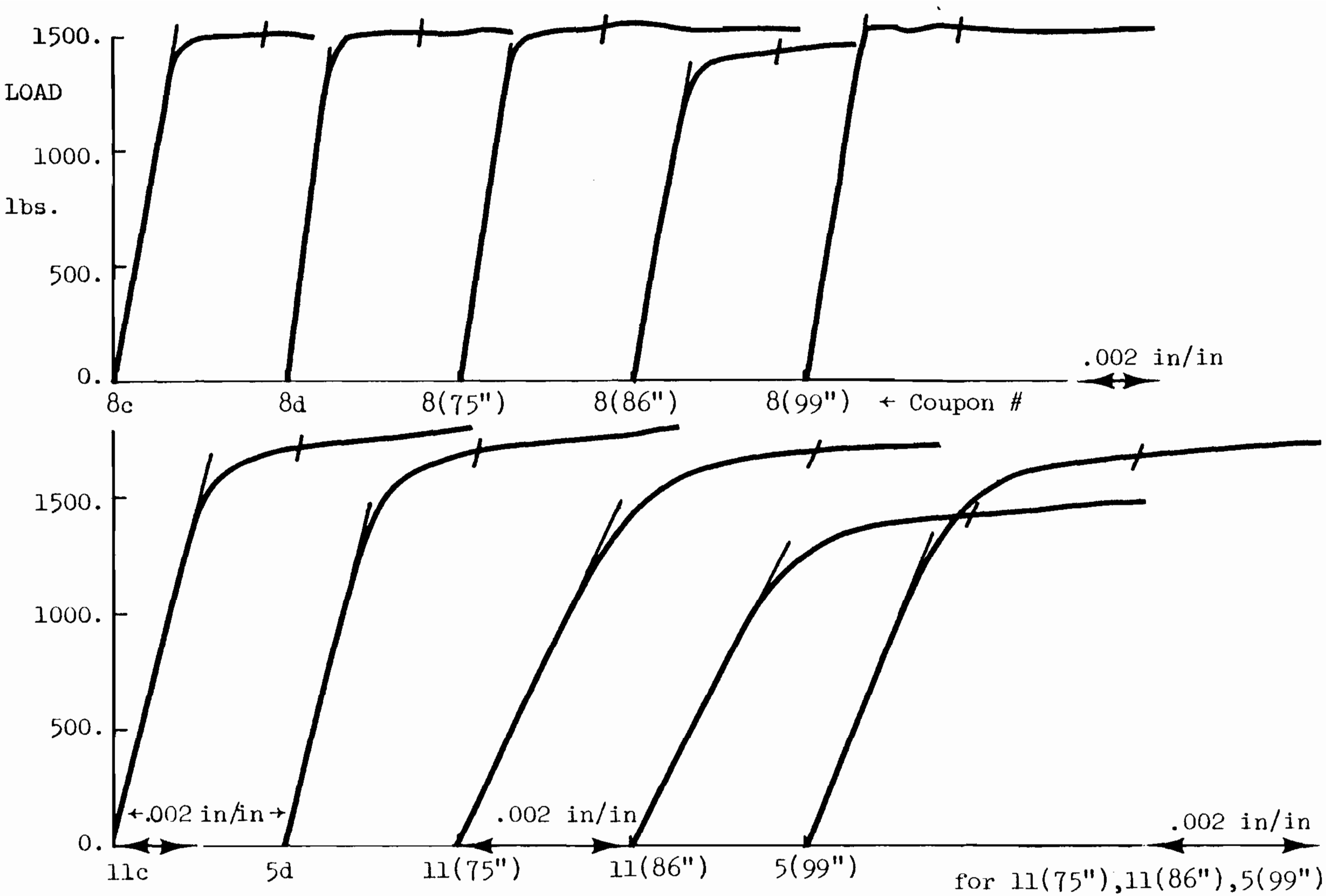

Fig. 3.7d PBC 14 Tensile Coupon Tests.

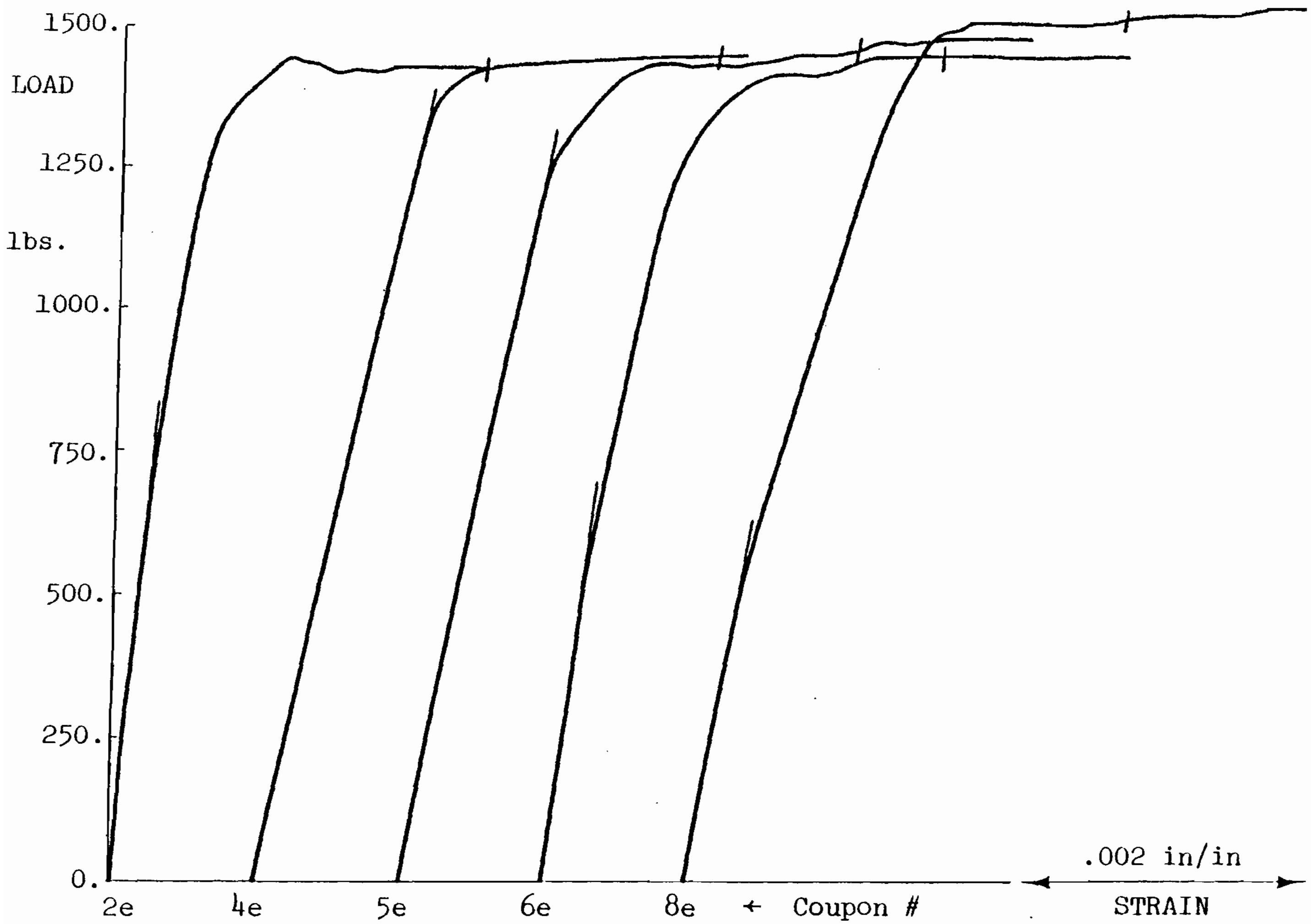

Fig. 3.8a PBC 14 Compressive Coupon Tests.

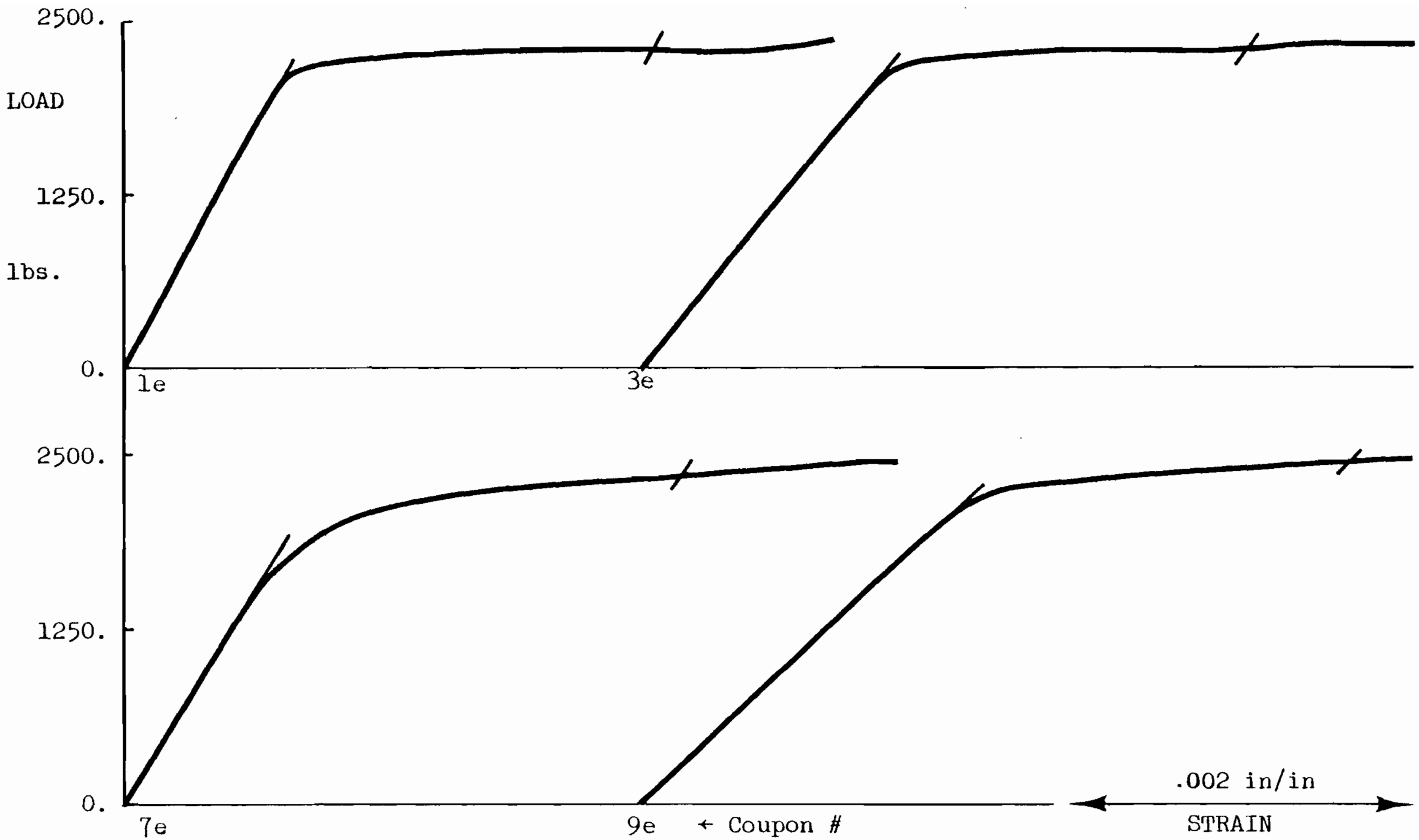

Fig. 3.8b PBC 14 Compressive Coupon Tests.

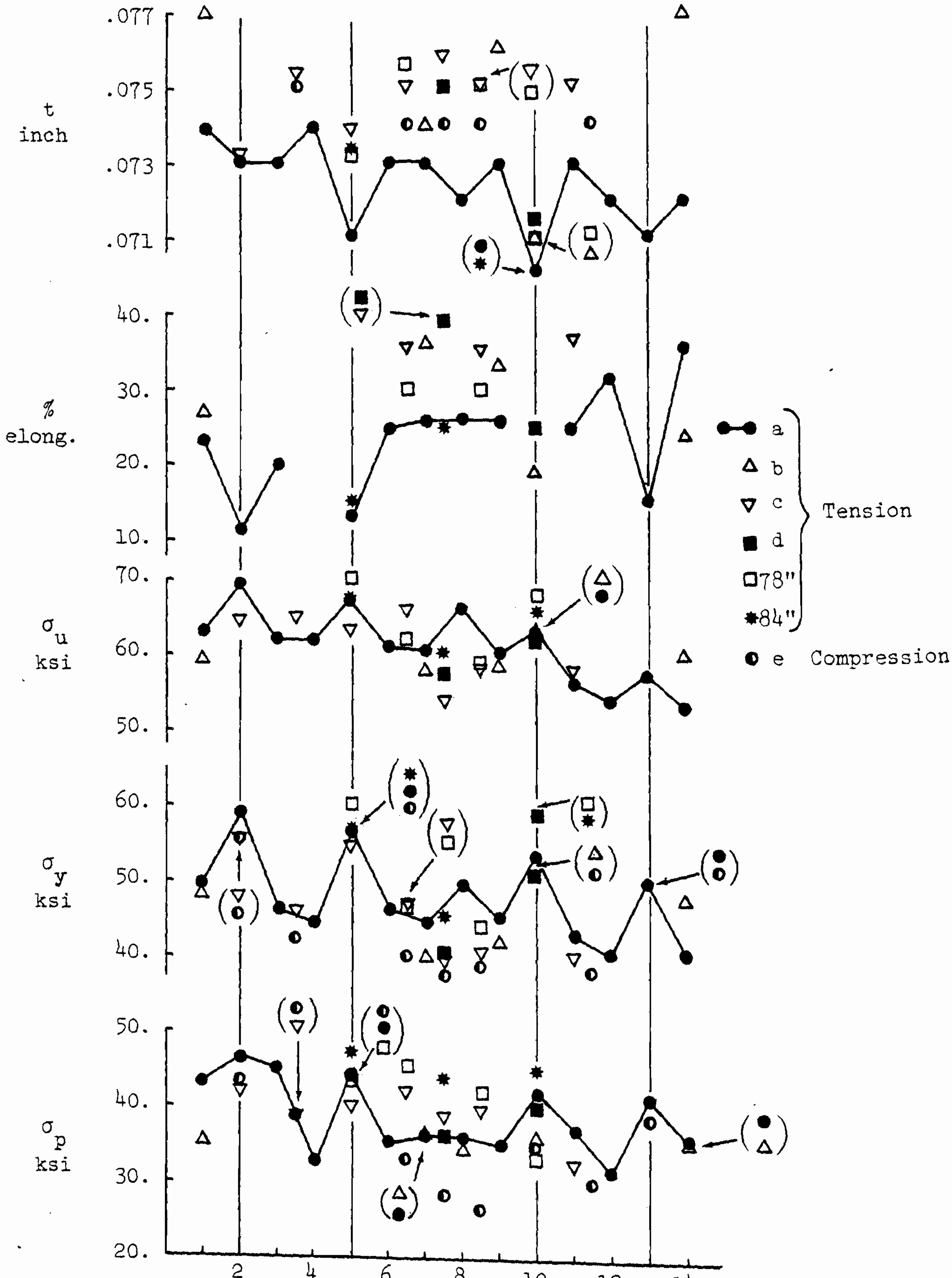

For coupon locations, see Fig. 3.10.

Fig. 3.9 RFC 14 Tensile and Compressive Coupon Tests.

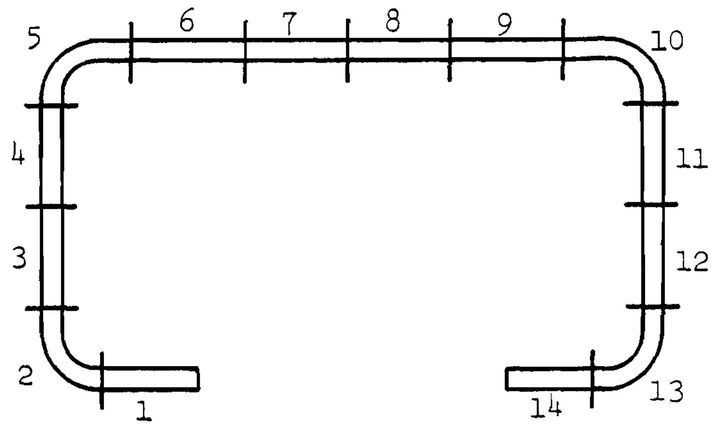

Fig. 3.10 Tensile Coupons for RFC 14, RFC 13 and PBC 13 (also residual strain coupons for RFC 14 and RFC 13).

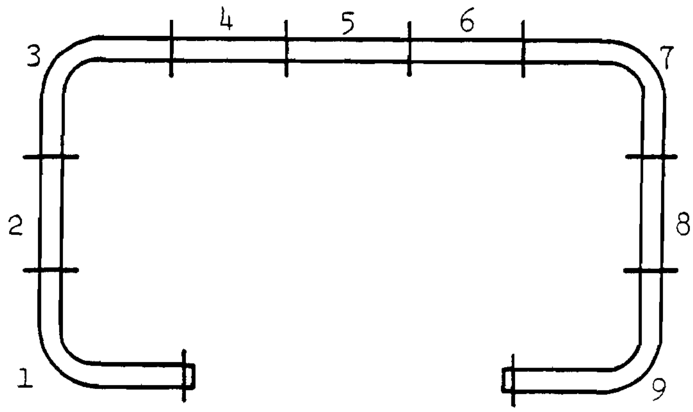

Fig. 3.11 Compressive Coupons for RFC 14, RFC 13, PBC 14 and PBC 13.

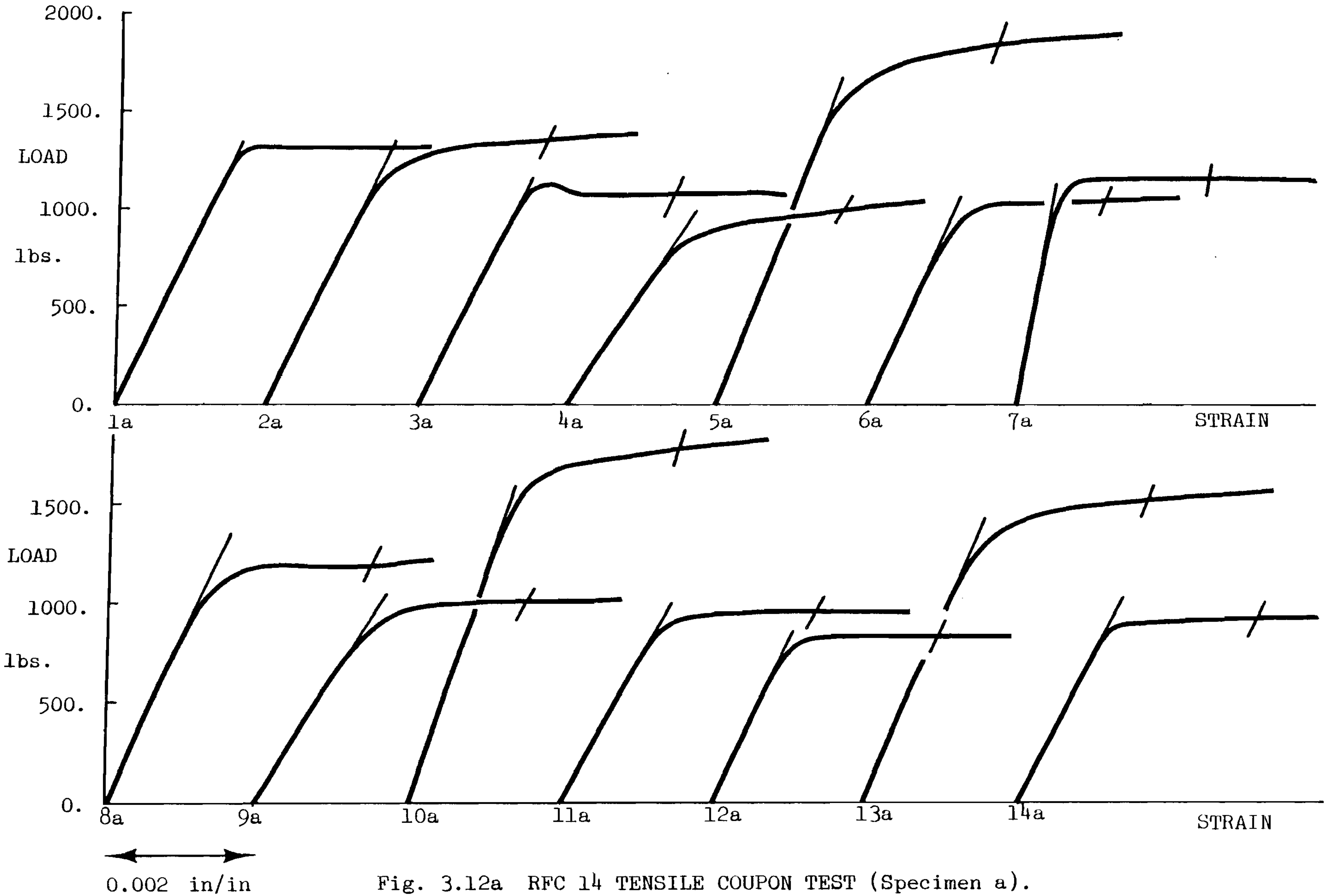

Fig. 3.12a RFC 14 TENSILE COUPON TEST (Specimen a).

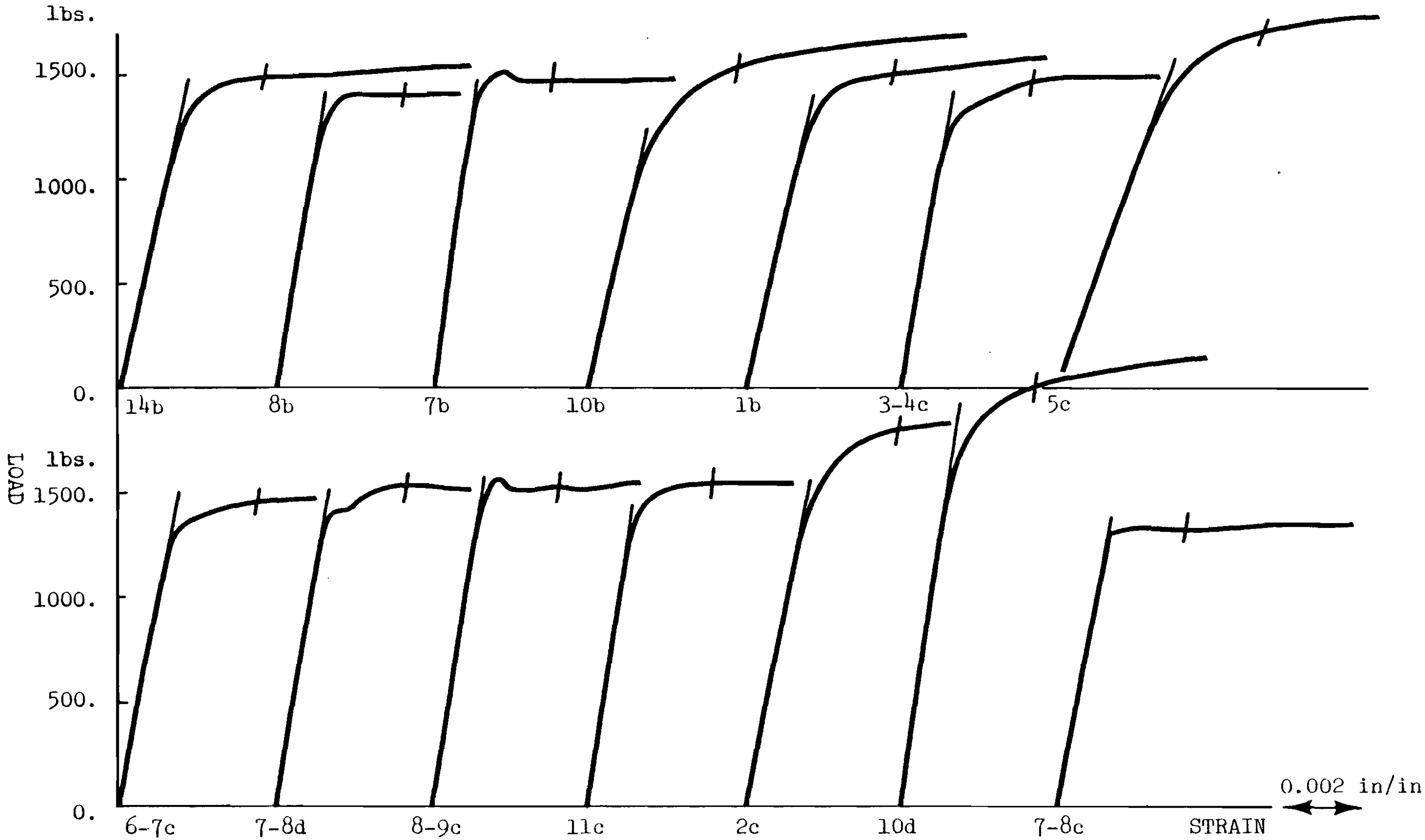

Fig. 3.12b RFC 14 Tensile Coupon Test (Specimens b, c and d).

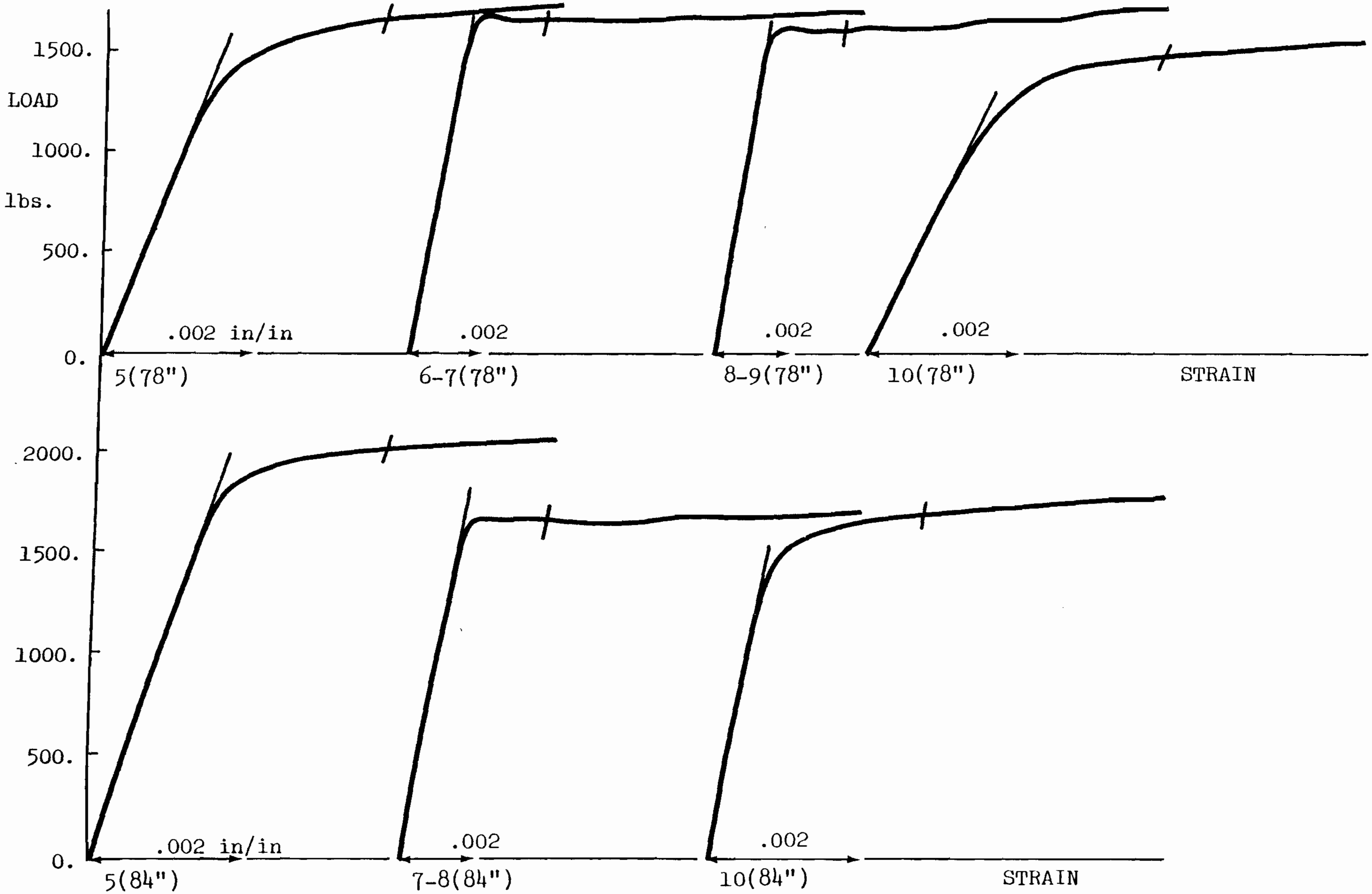

Fig. 3.12c RFC 14 Tensile Coupon Tests.

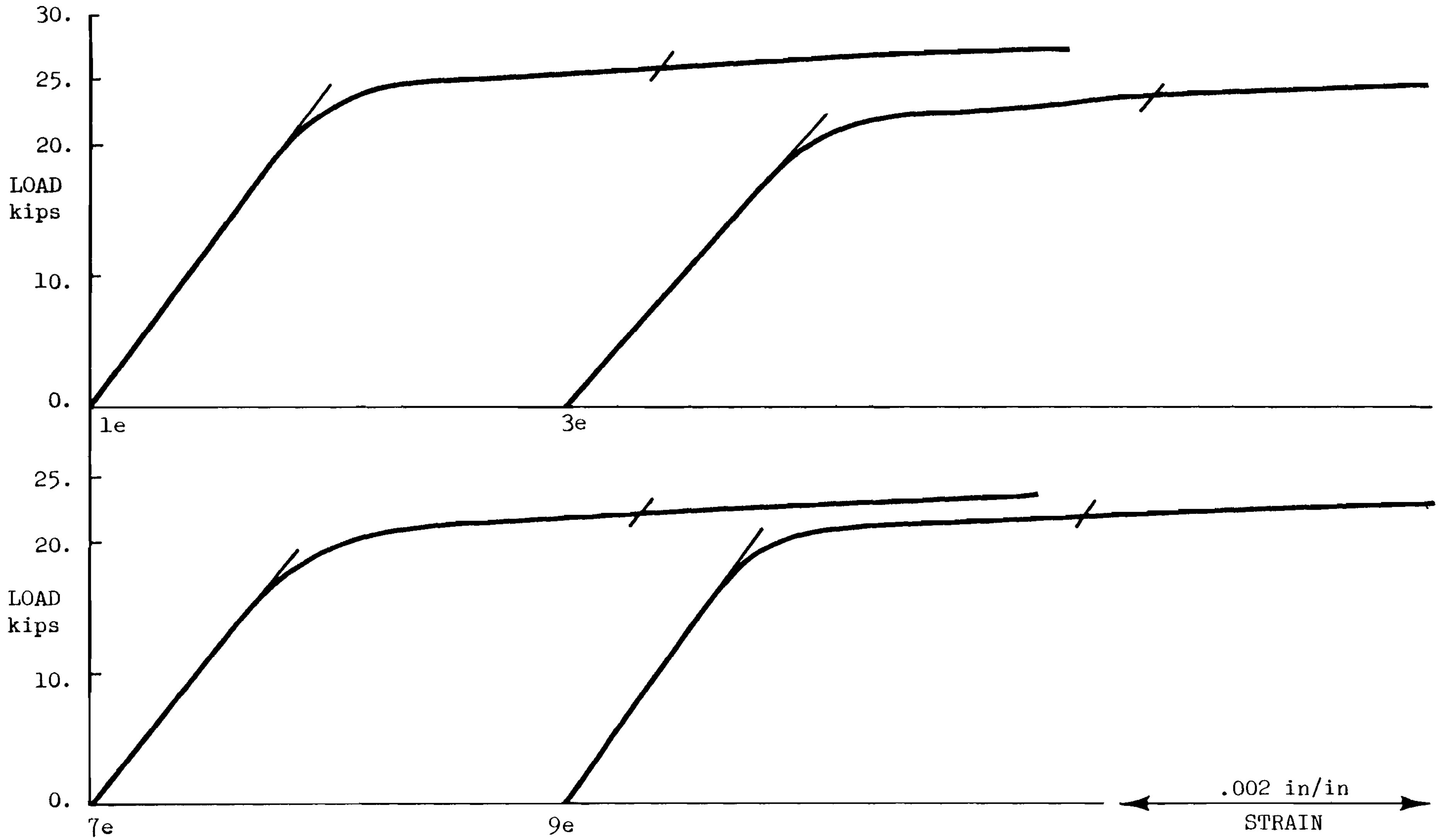

Fig. 3.13a RFC 14 Compressive Coupon Test (Specimen e).

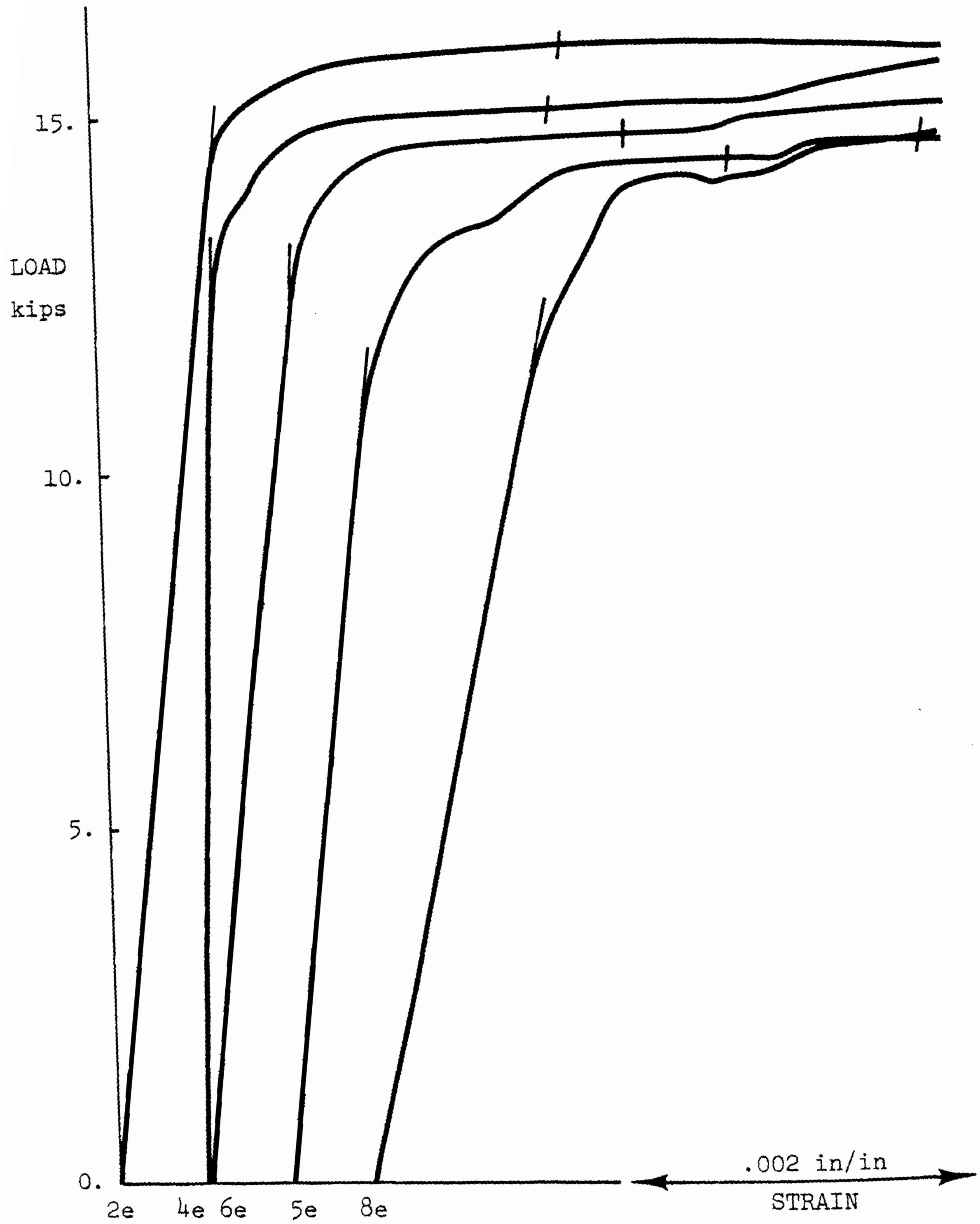

Fig. 3.13b RFC 14 Compressive Coupon Tests (Specimen e).

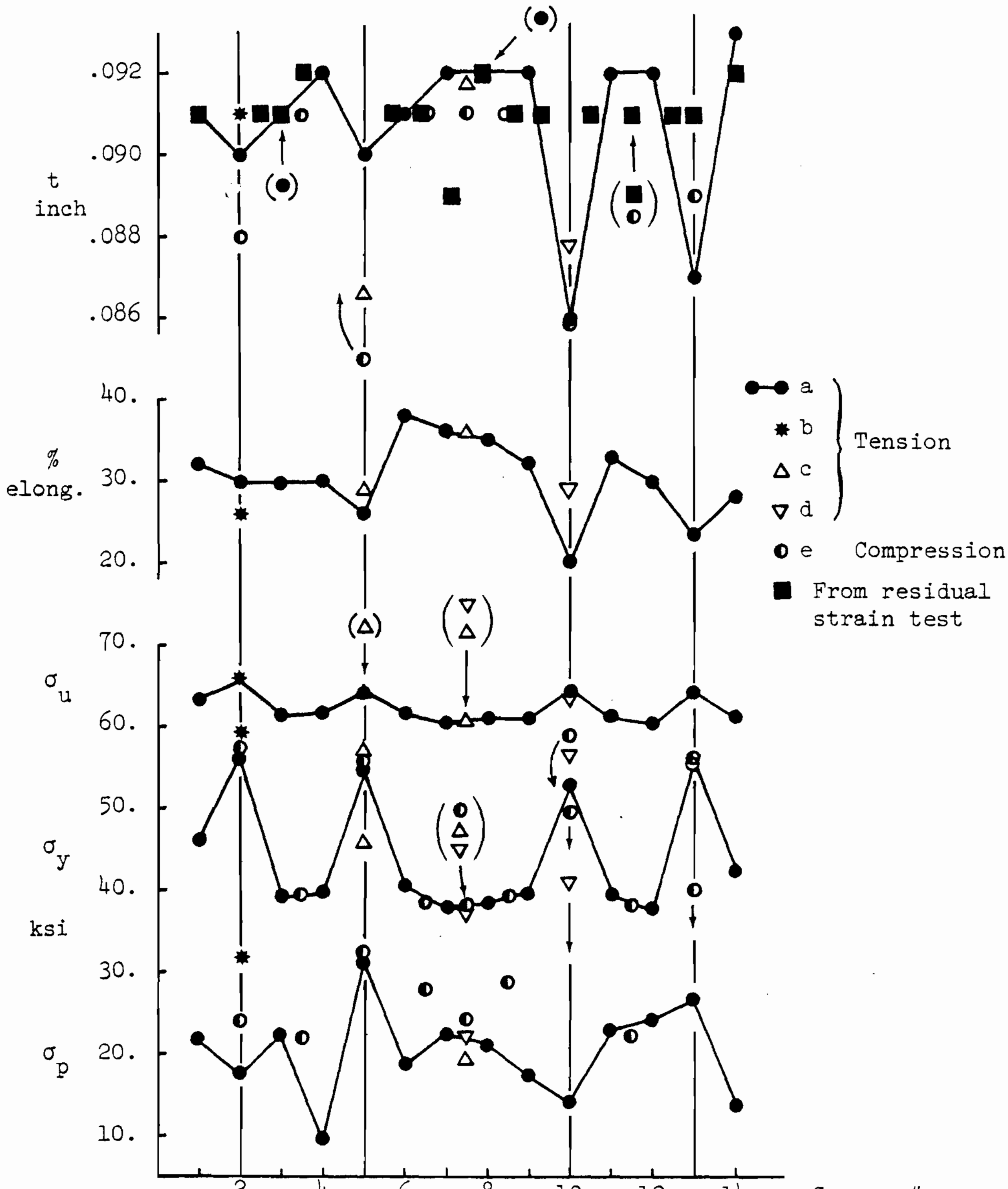

For coupon locations, see Fig. 3.10.

Fig. 3.14 PBC 13 Tensile and Compressive Coupon Tests.

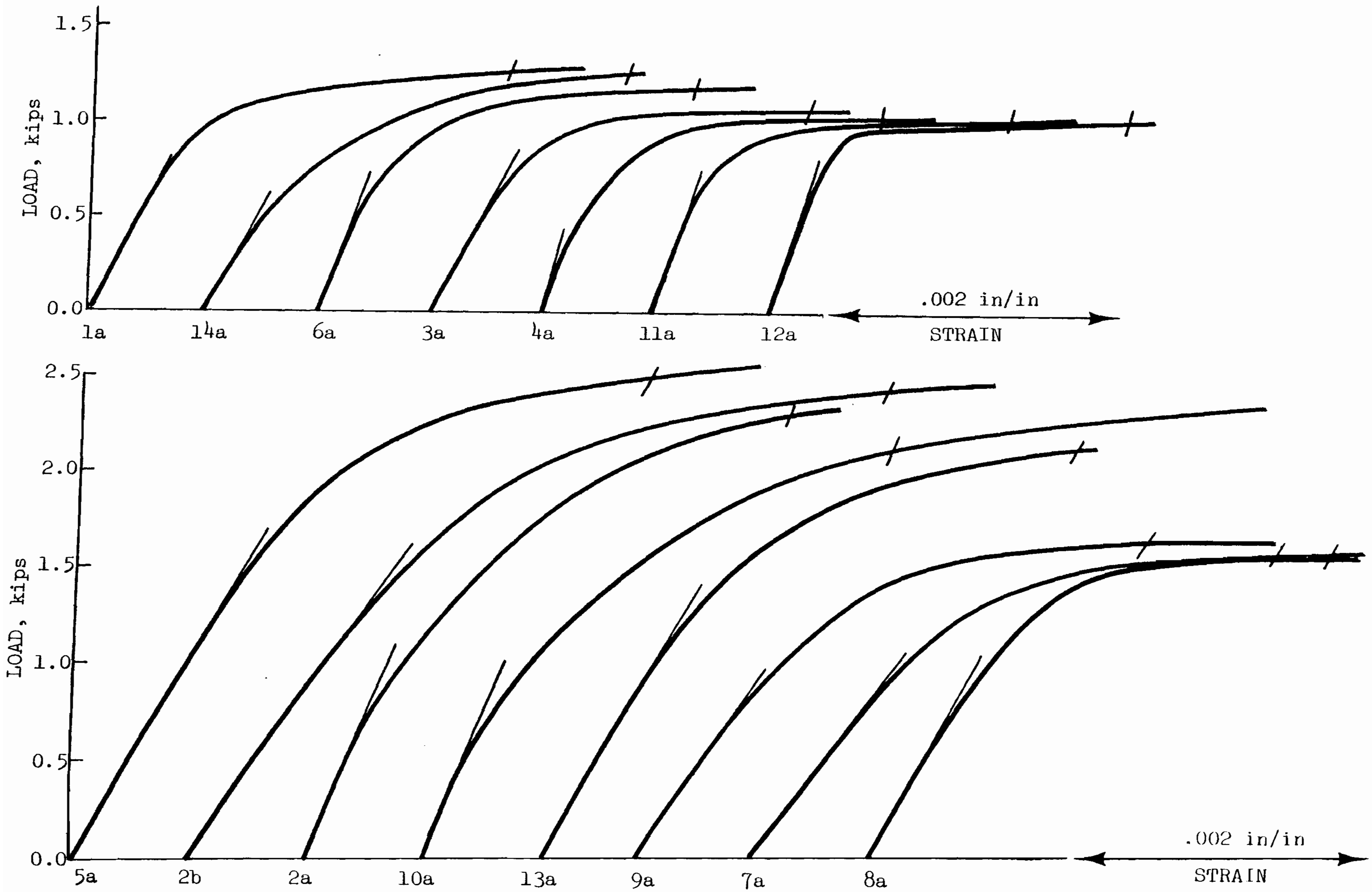

Fig. 3.15a PBC 13 Tensile Coupon Tests.

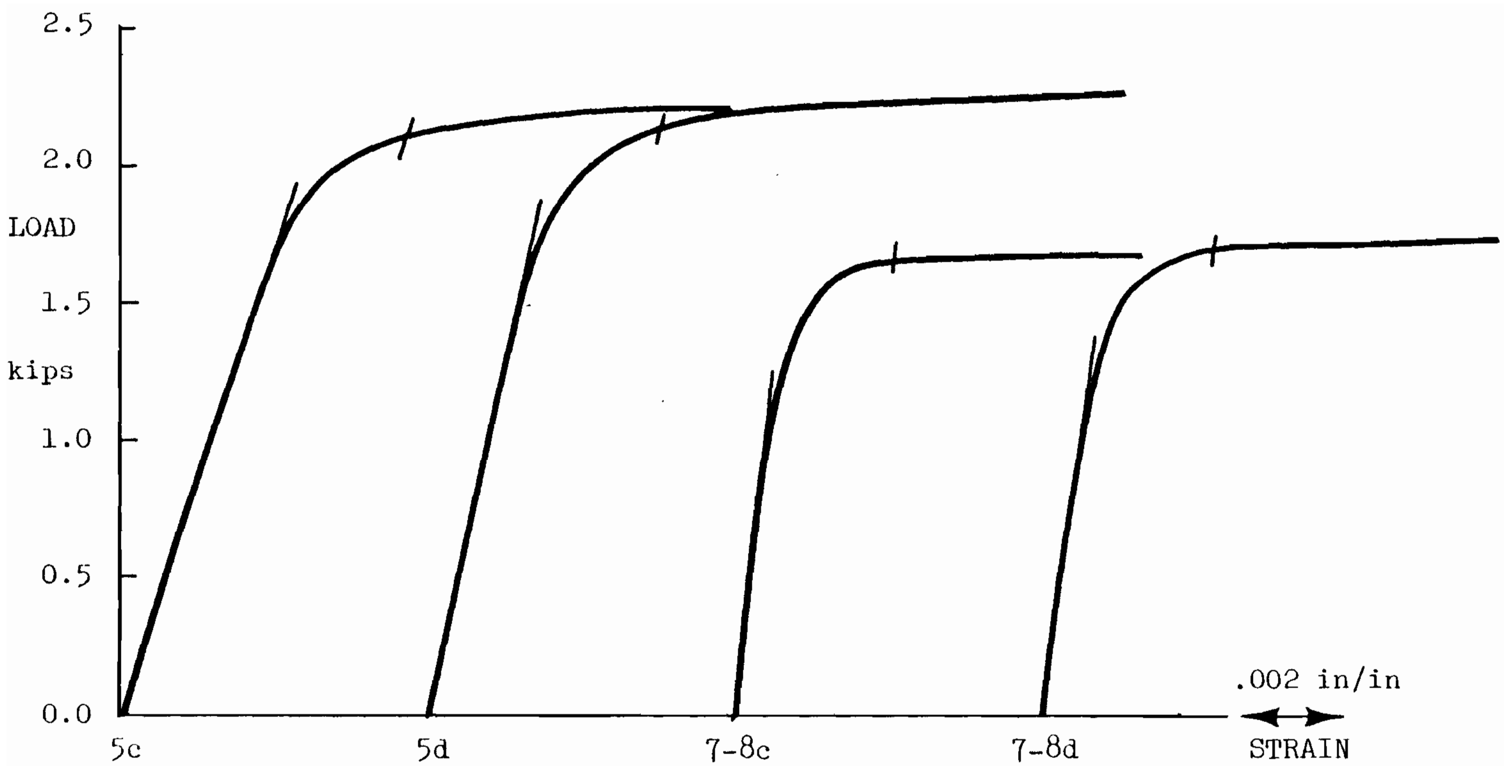

Fig. 3.15b PBC 13 Tensile Coupon Tests.

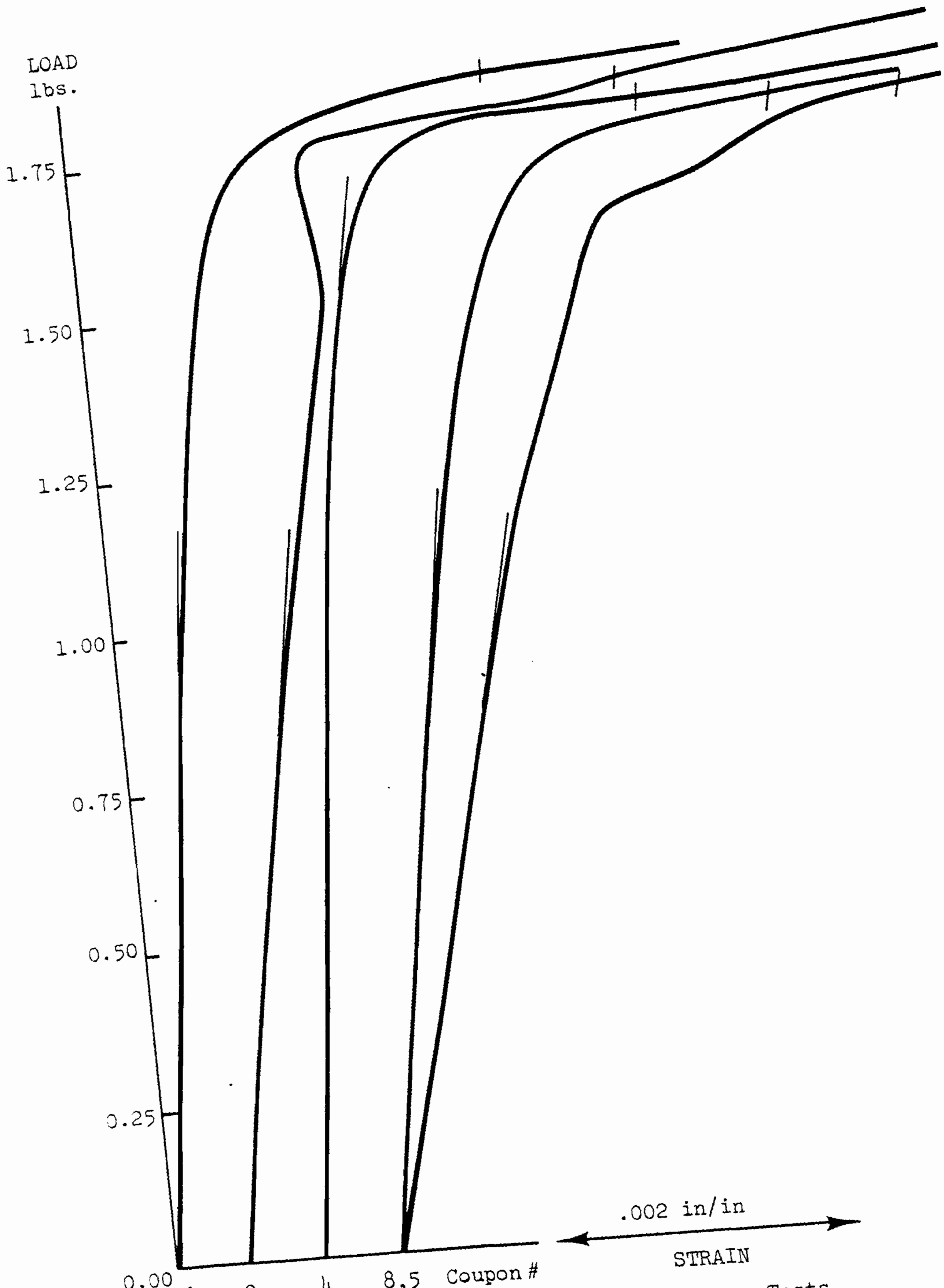

Fig. 3.16a PBC 13 Compressive Coupon Tests.

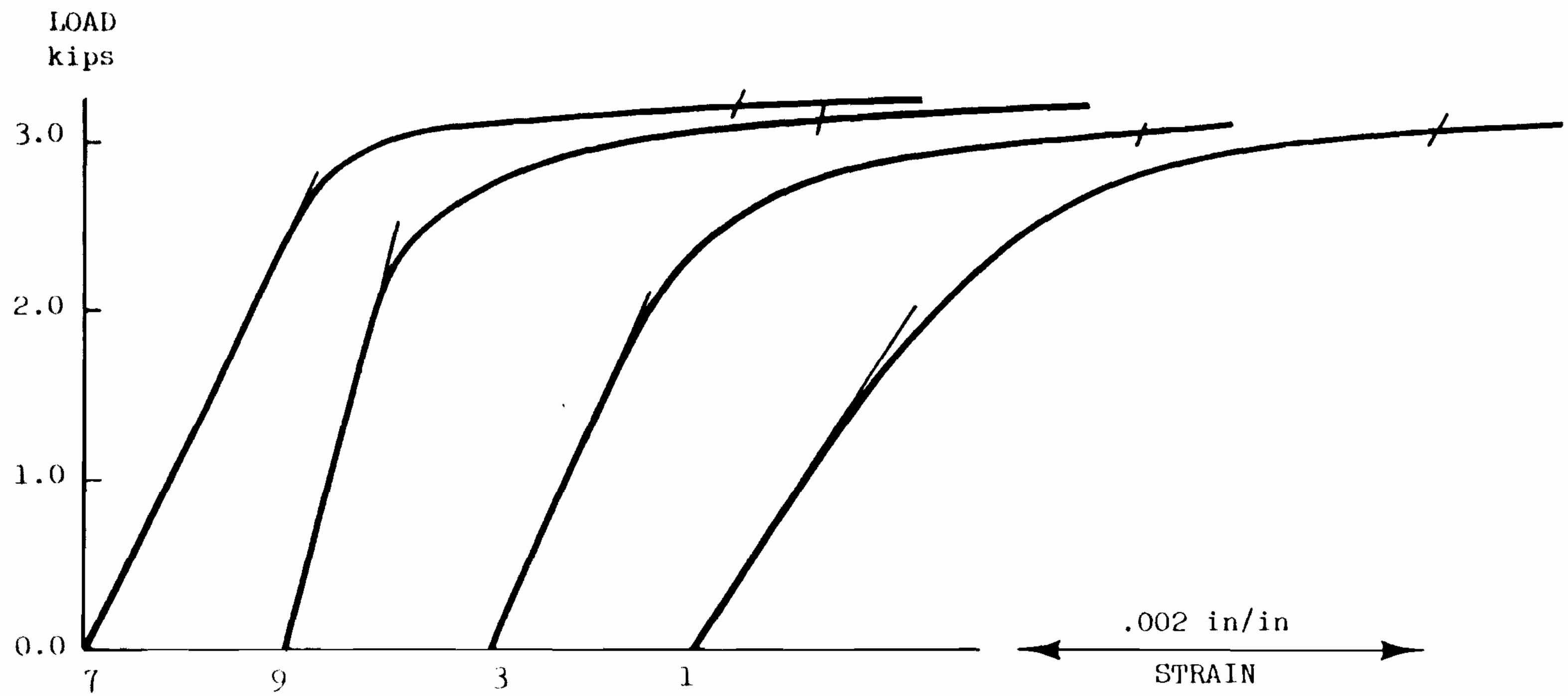

Fig. 3.16b PBC 13 Compressive Coupon Tests.

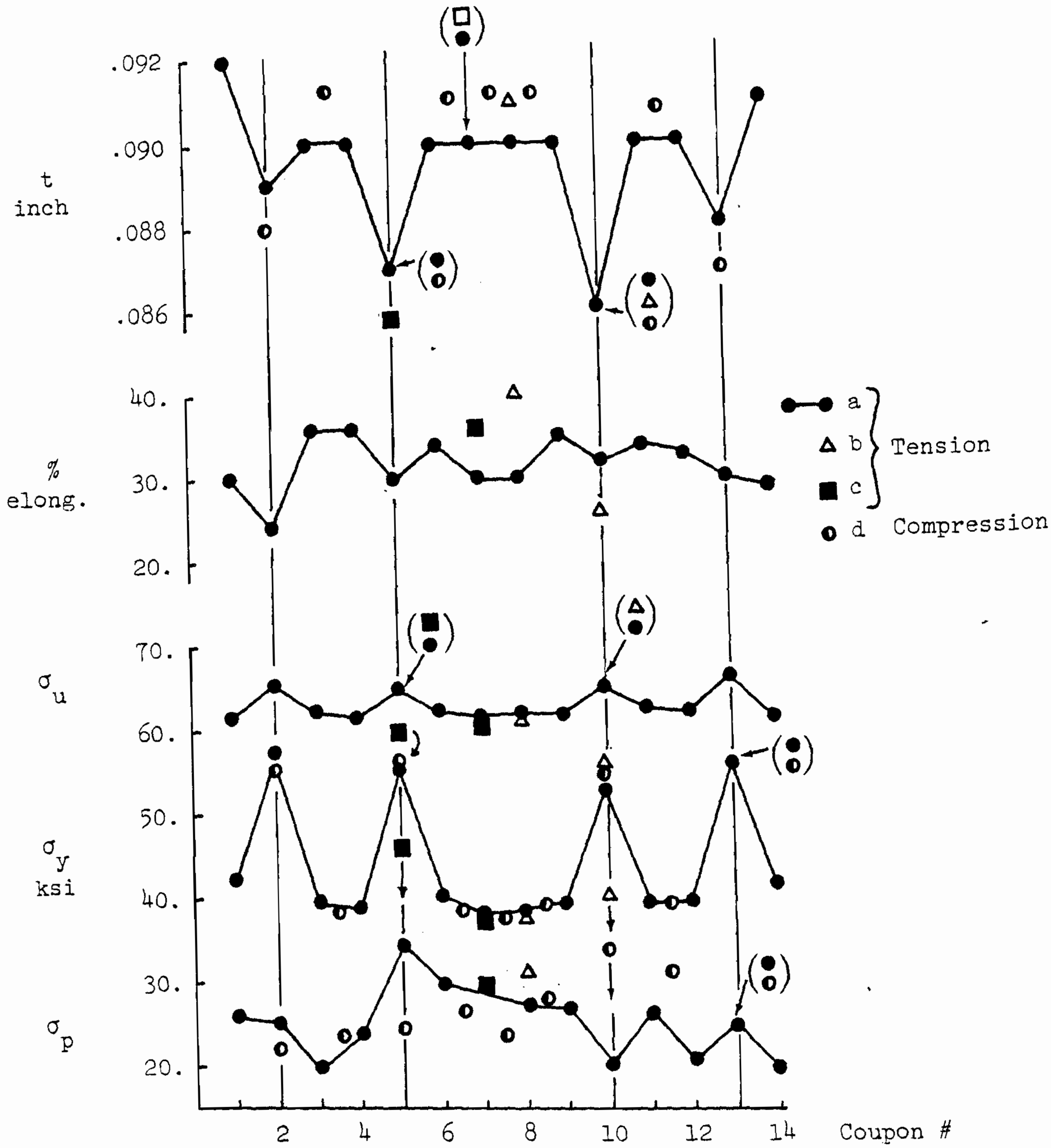

For coupon locations, see Fig. 3.10.

Fig. 3.17 RFC 13 Tensile and Compressive Tests.

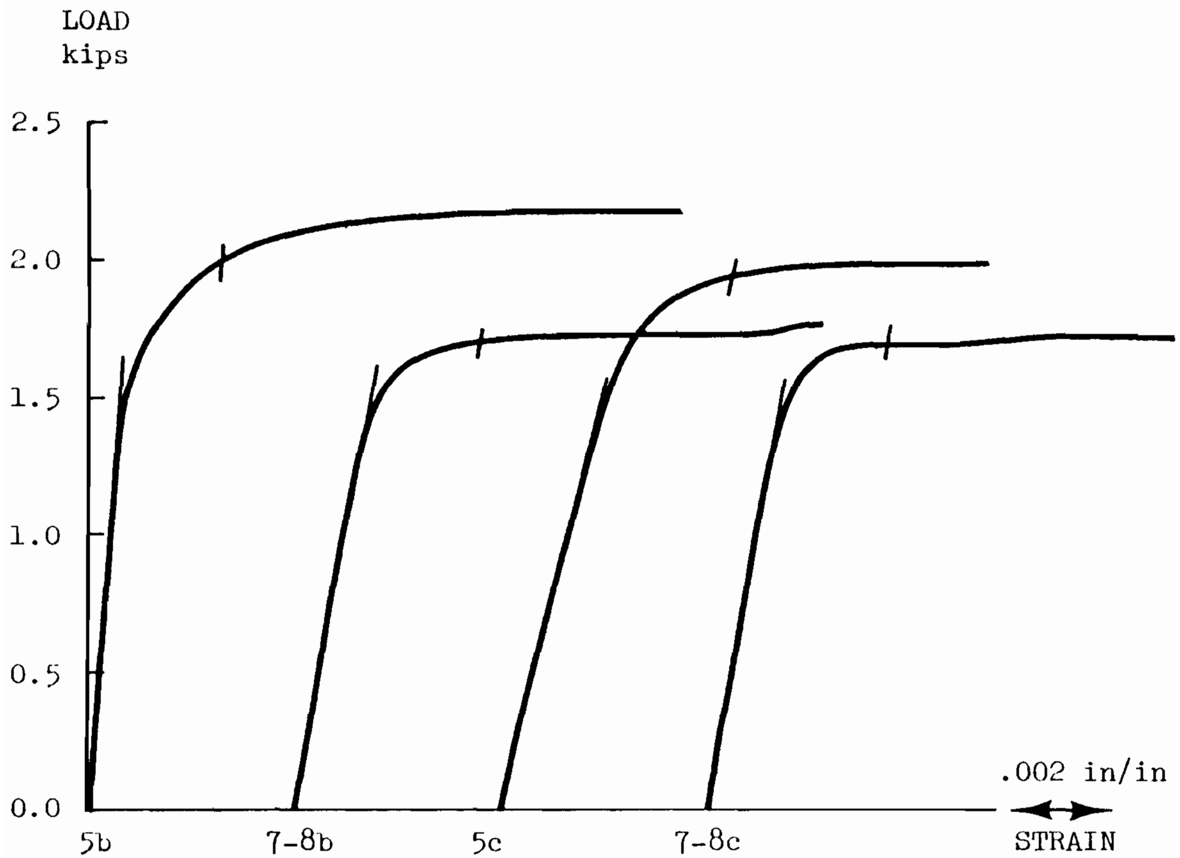

Fig. 3.18a RFC 13 Tensile Coupon Tests.

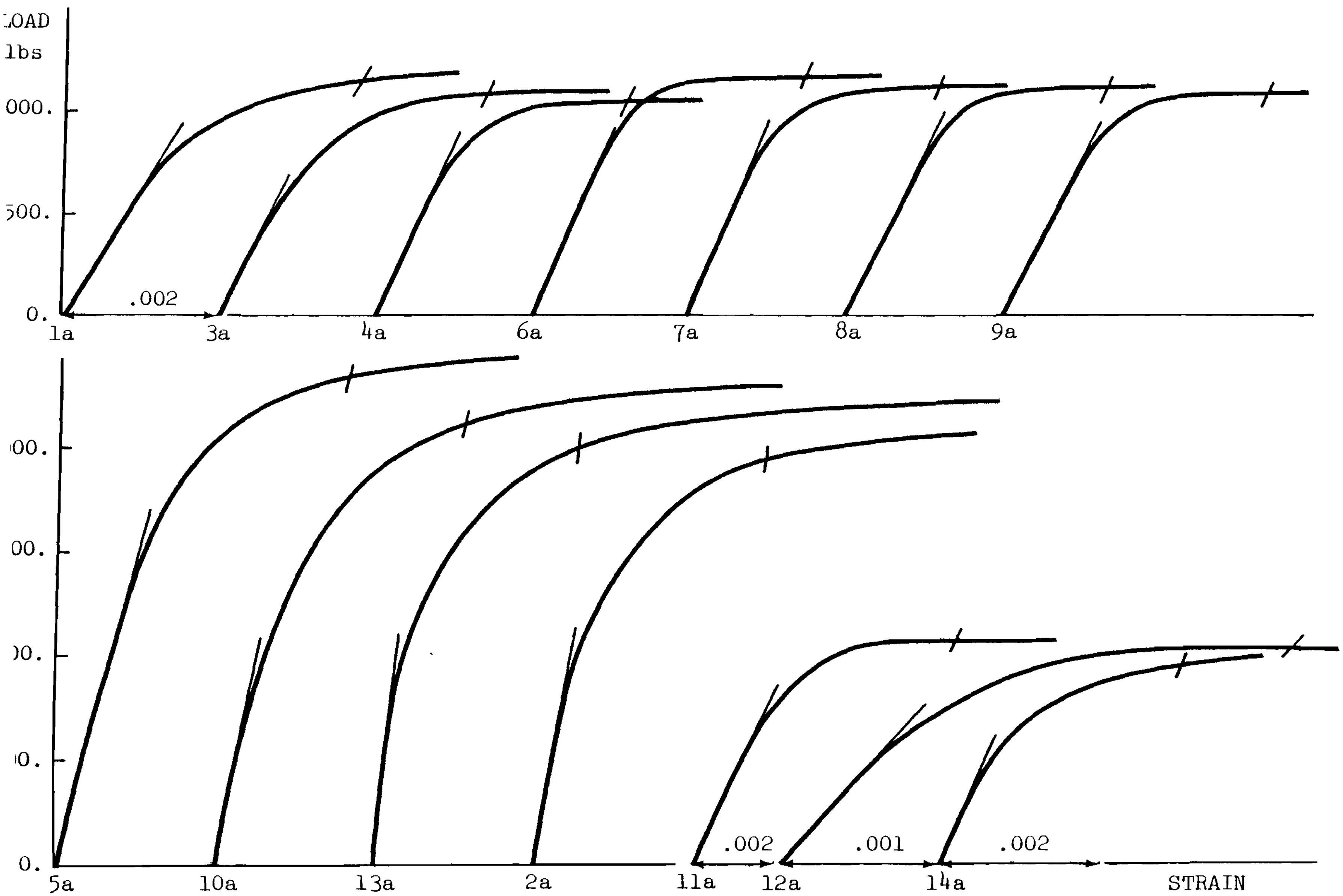

Fig. 3.18b RFC 13 Tensile Coupon Tests (specimen a)

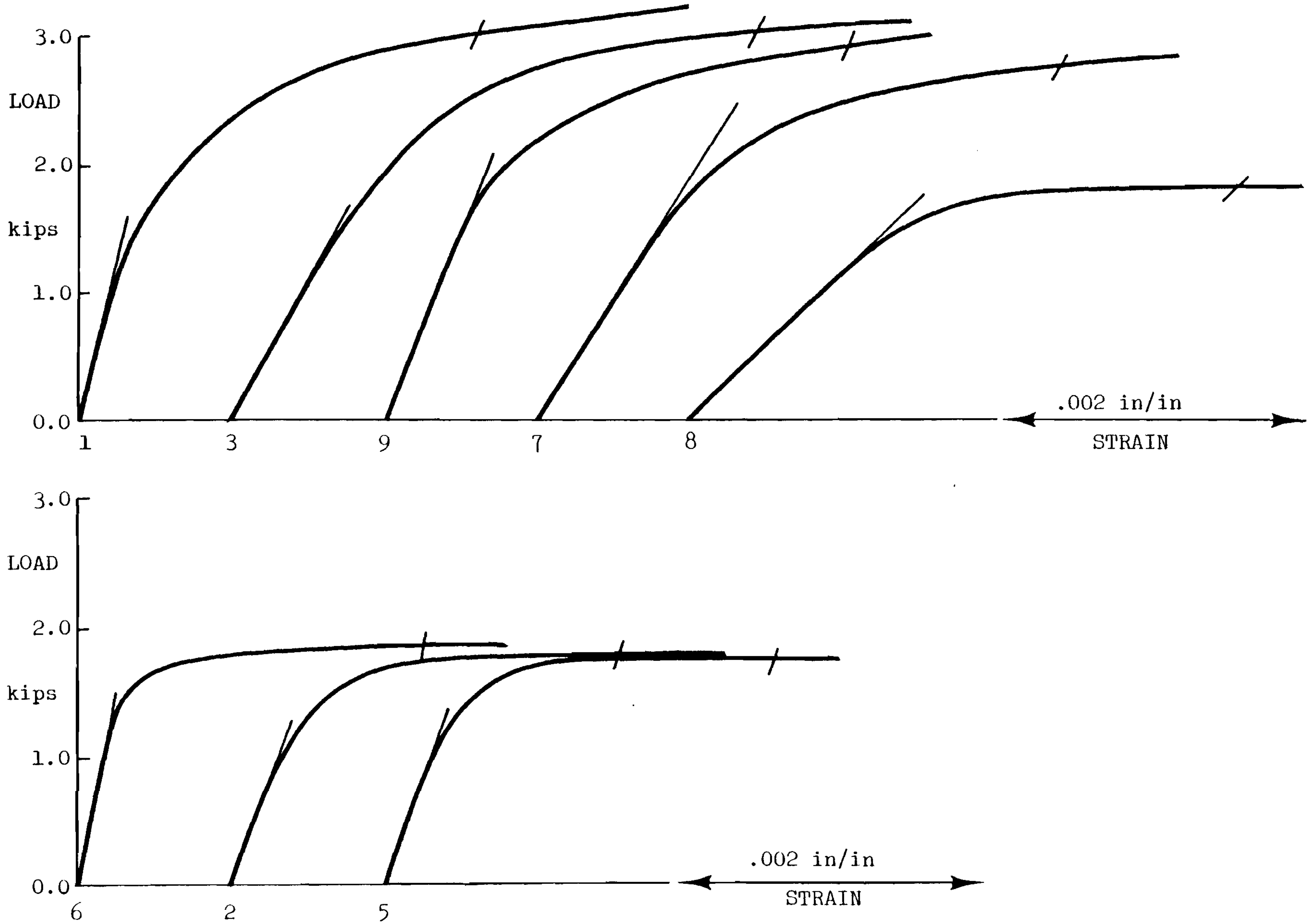

Fig. 3.19a PBC 13 Compressive Coupon Tests.

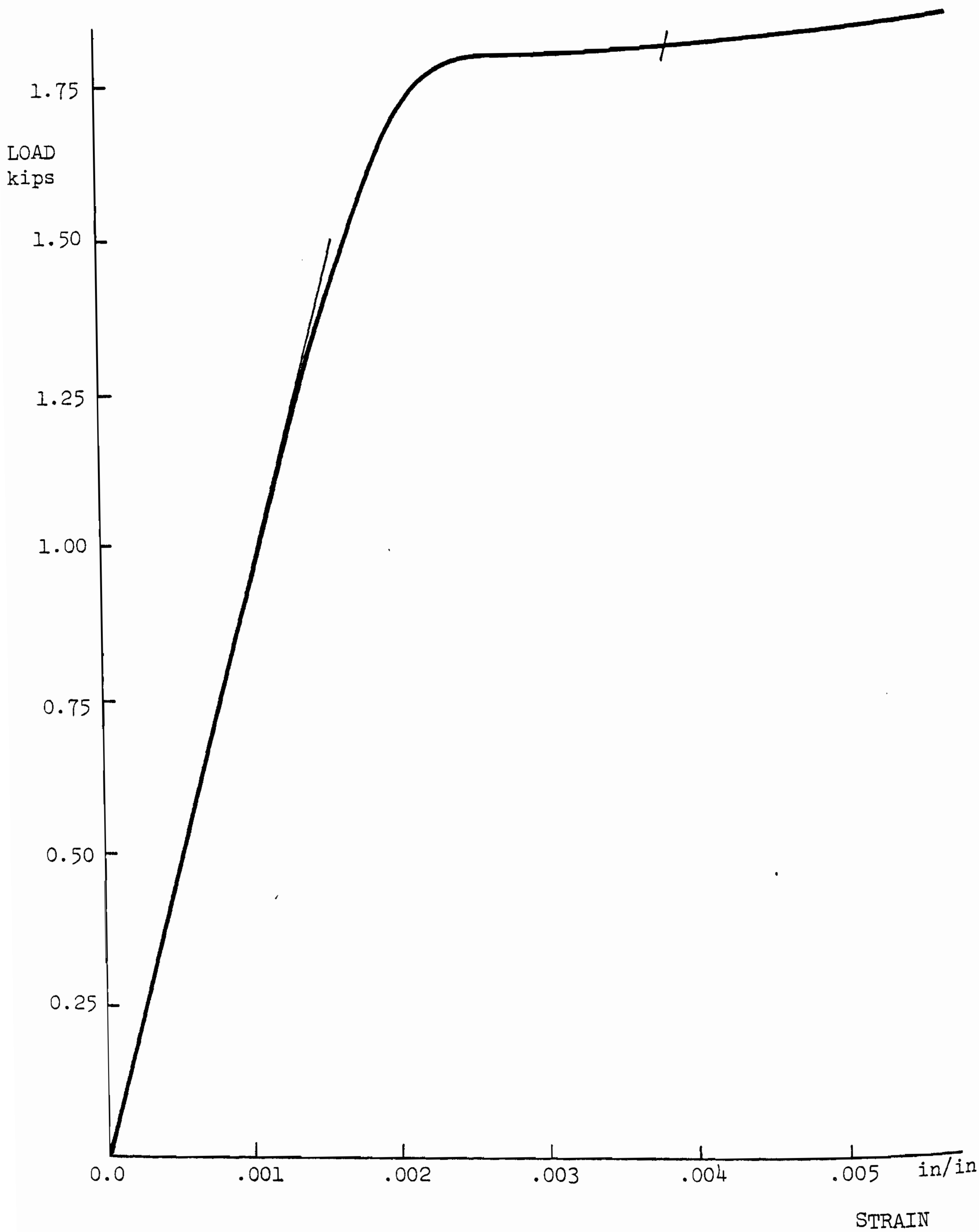

Fig. 3.19b RFC 13 Compressive Coupon 4.

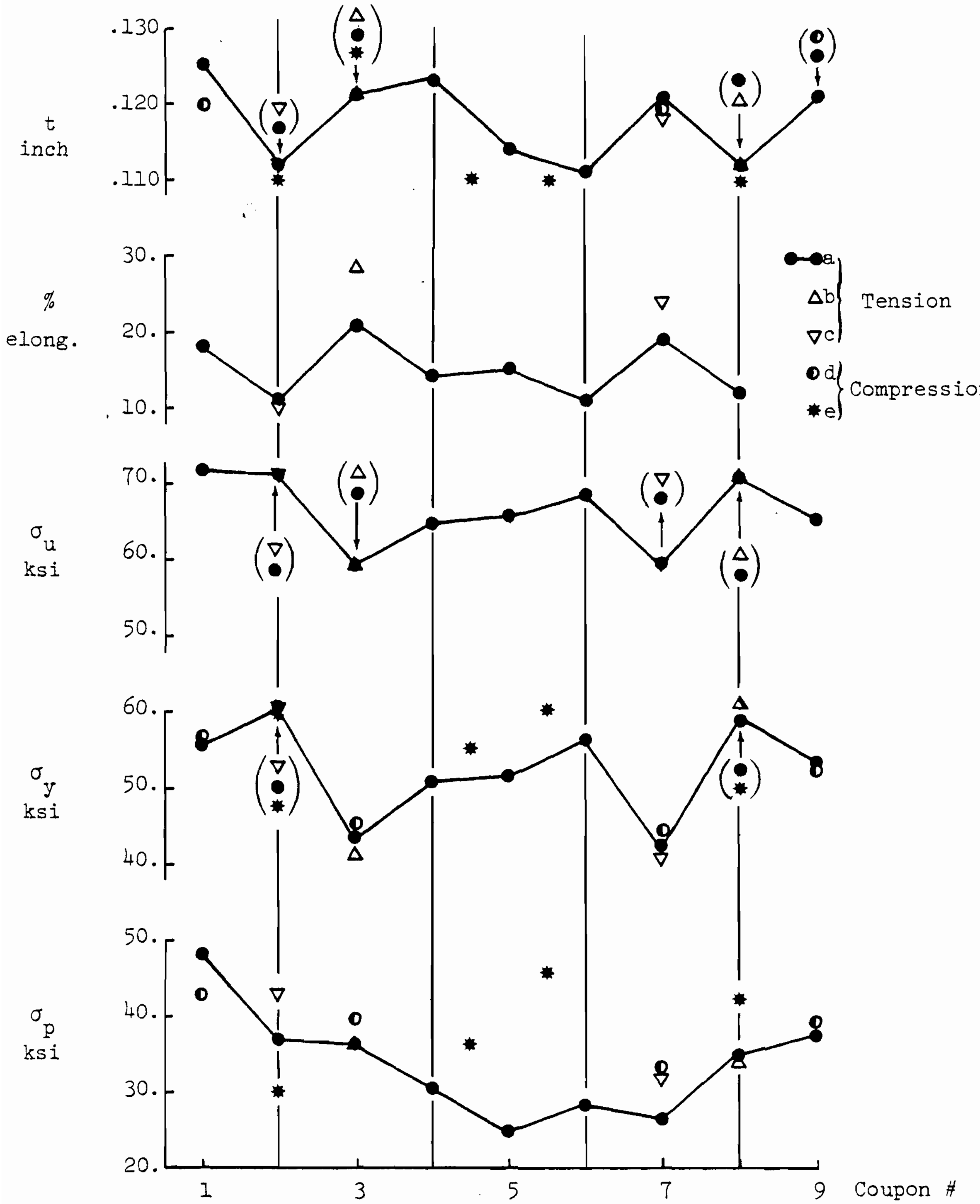

For coupon locations, see Fig. 3.21a.

Fig. 3.20 H 11 Tensile and Compressive Coupon Tests.

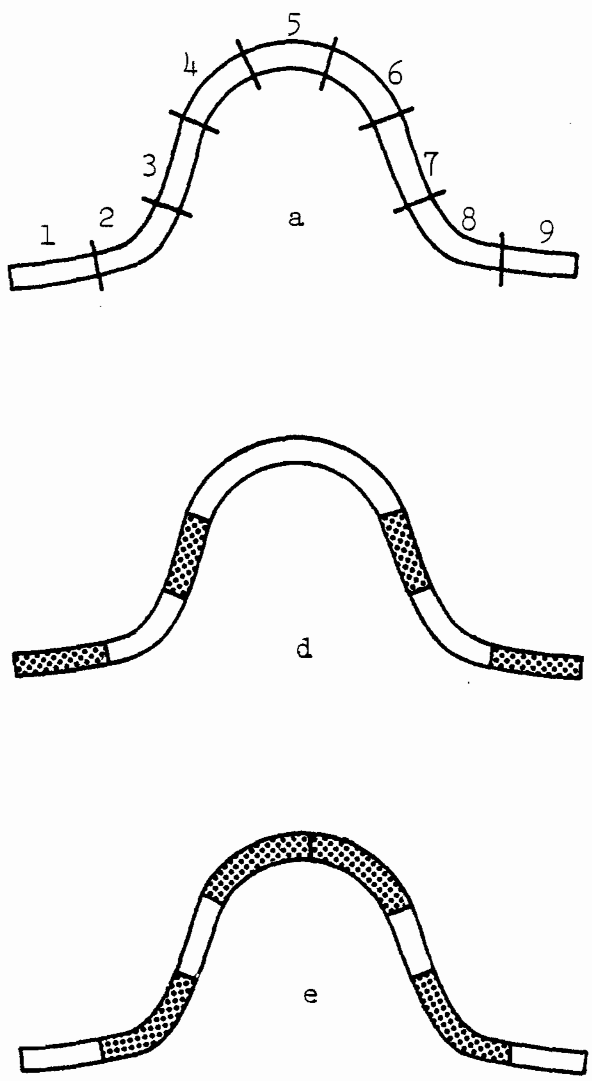

Fig. 3.21 H 11 Tensile (a) and Compressive (d,e) Coupons (a also corresponds to residual strain coupons).

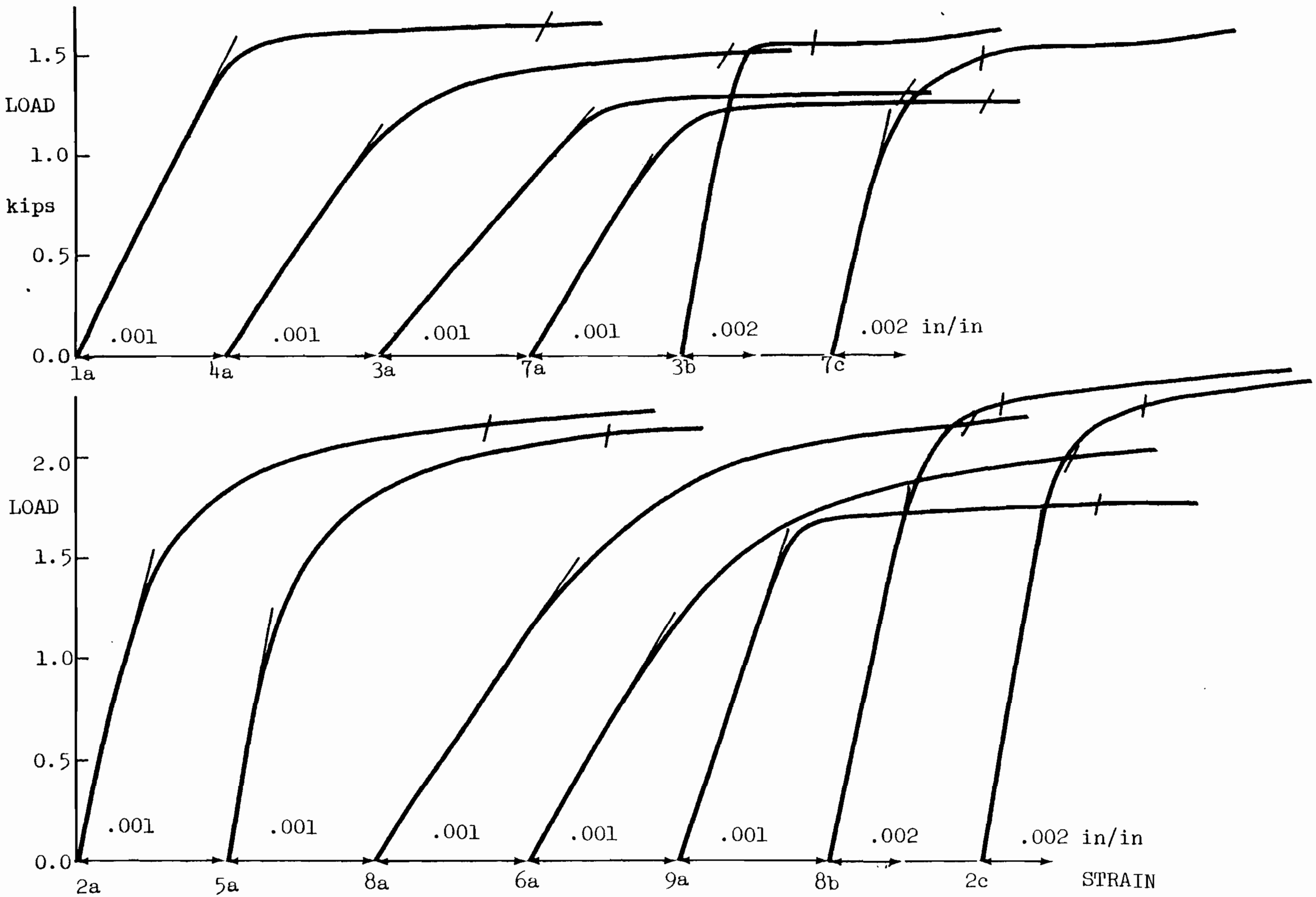

Fig. 3.22 H 11 Tensile Coupon Tests.

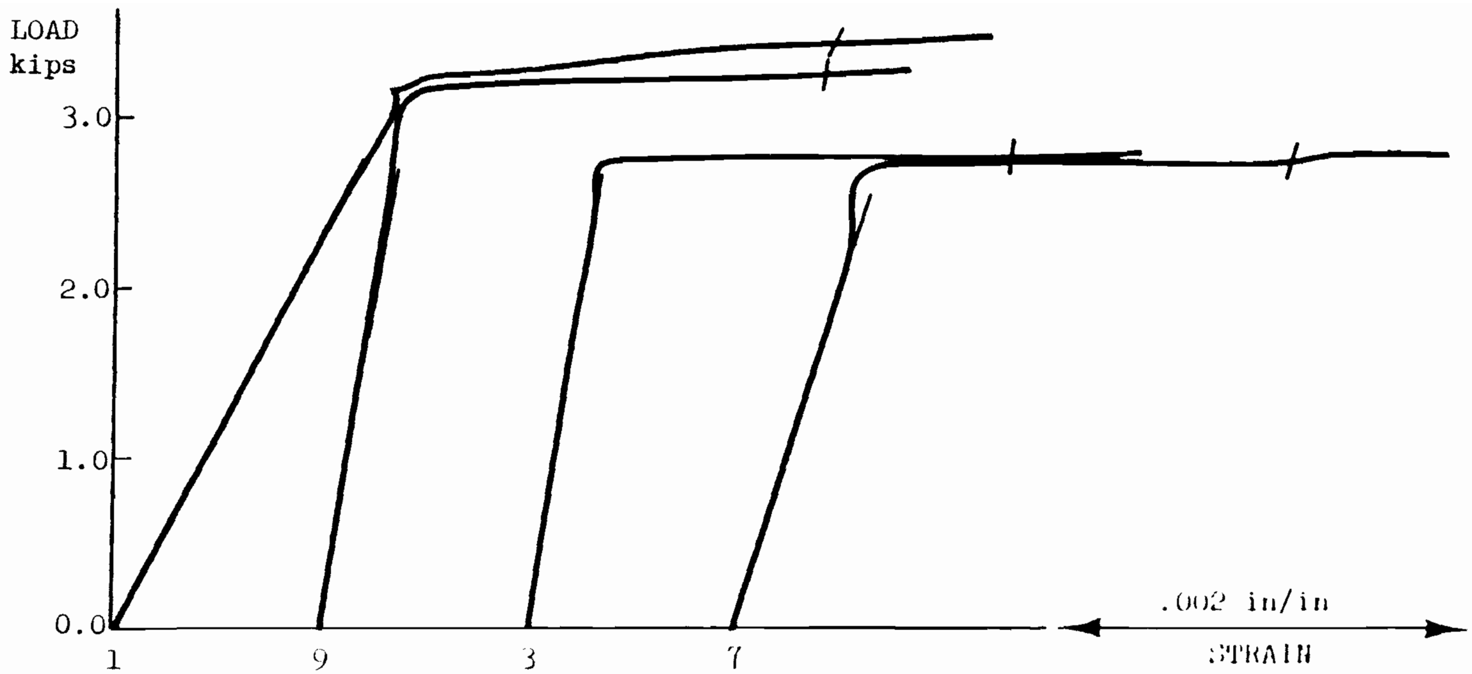

Fig. 3.23a: H 11 Compressive Coupon Tests.

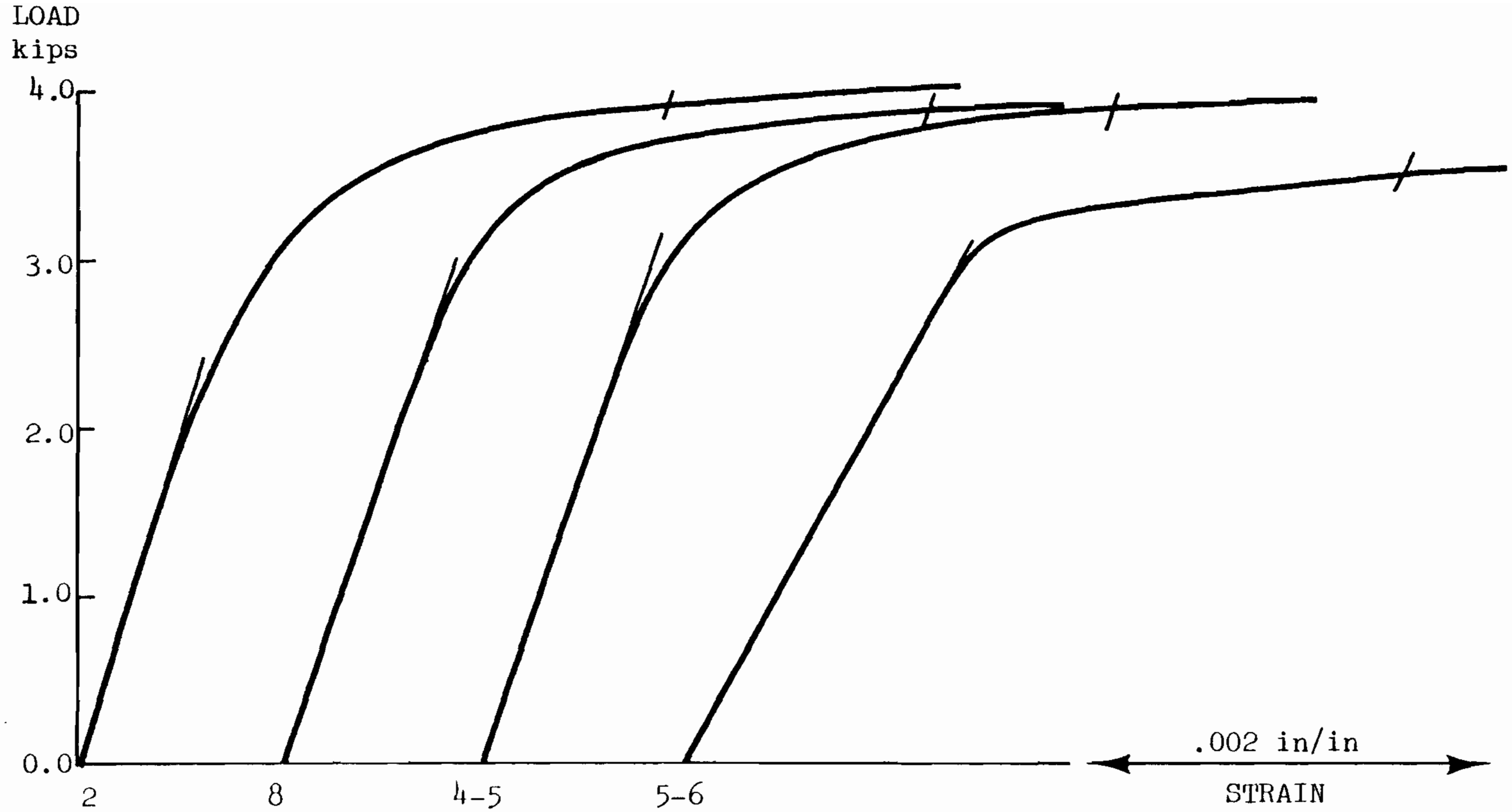

Fig. 3.23b: H 11 Compressive Coupon Tests.

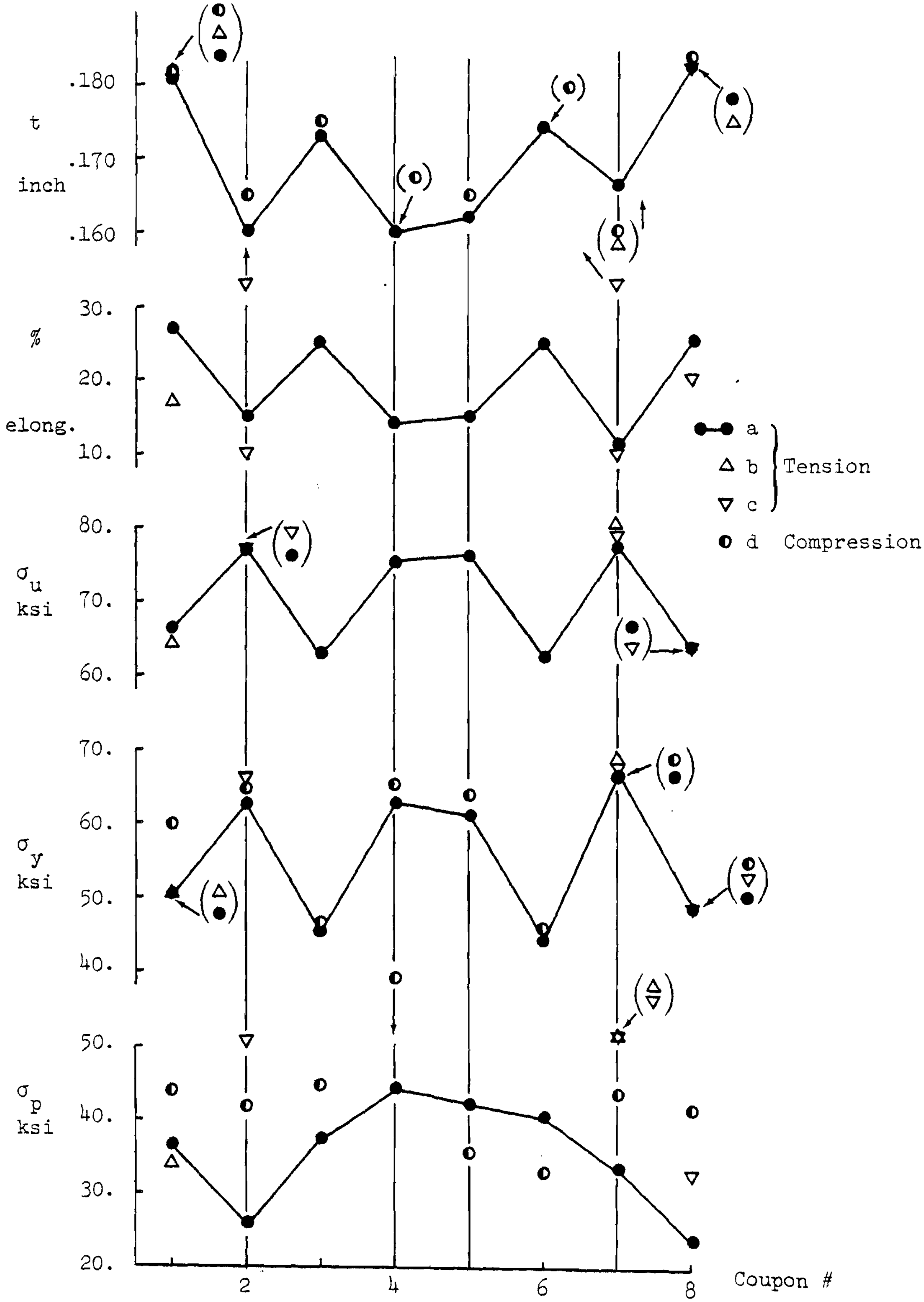

Fig. 3.24 H 7 Tensile and Compressive Coupon Tests.
For locations of coupons, see Fig. 3.25.

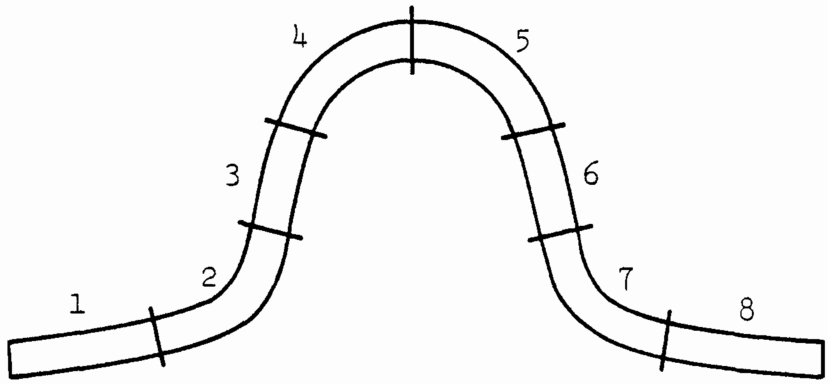

Fig. 3.25 H 7 Tensile and Compressive Coupons.

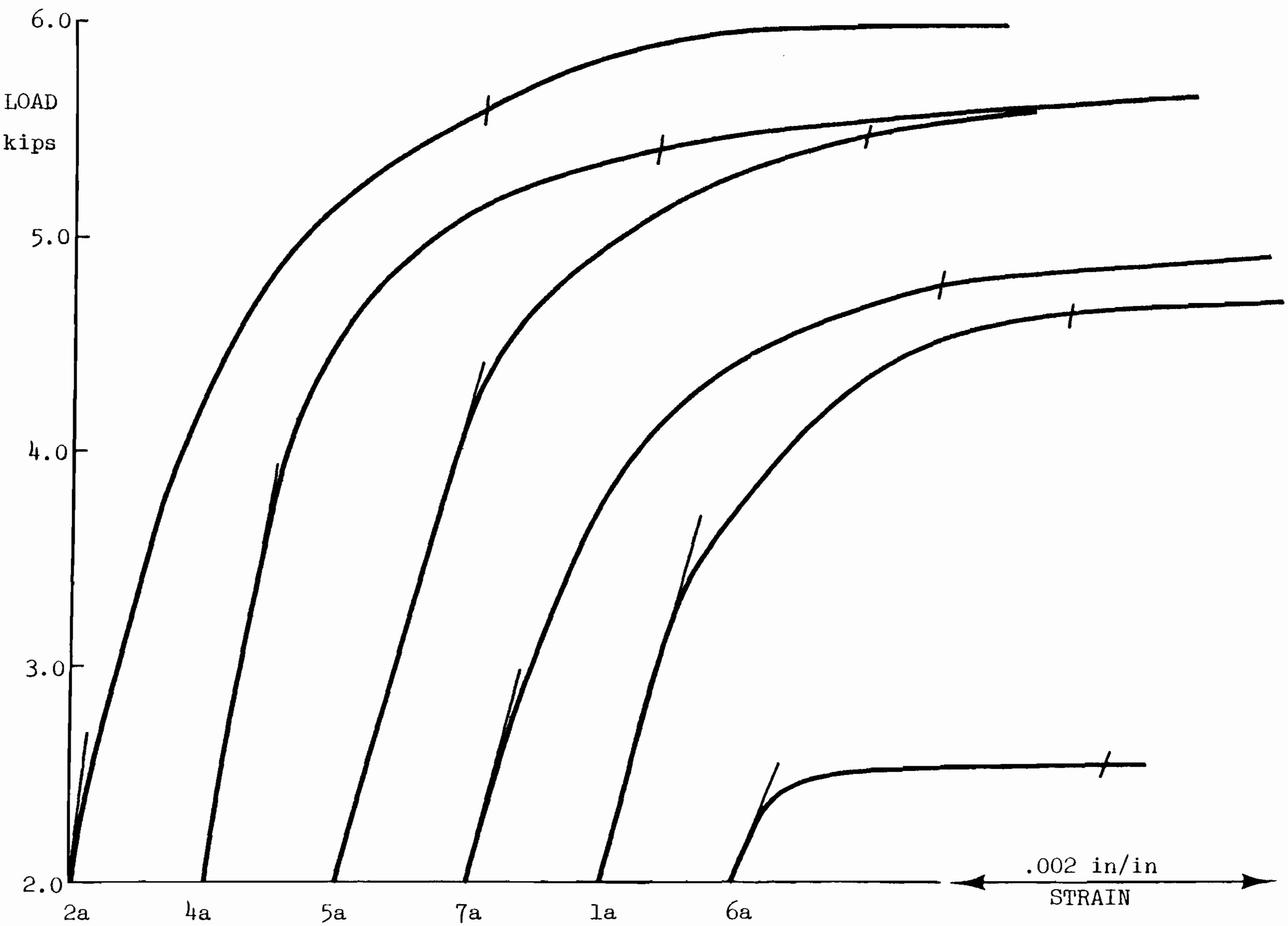

Fig. 3.26a H 7 Tensile Coupon Tests (specimen a).

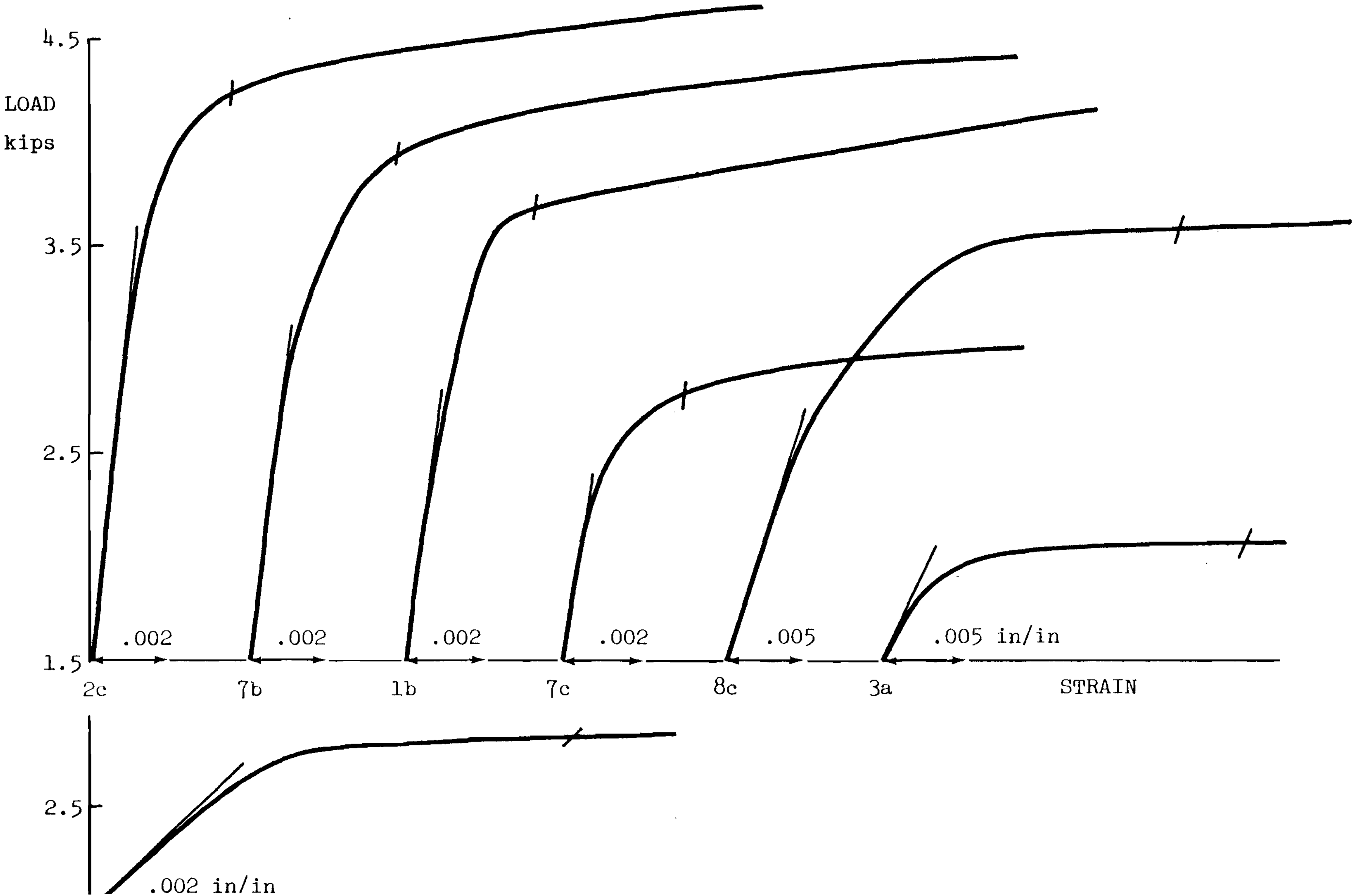

4.5
LOAD
kips
3.5
2.5
1.5
.002
.002
.002
.002
.005
.005 in/in
2c
7b
1b
7c
8c
3a
STRAIN
2.5
.002 in/in

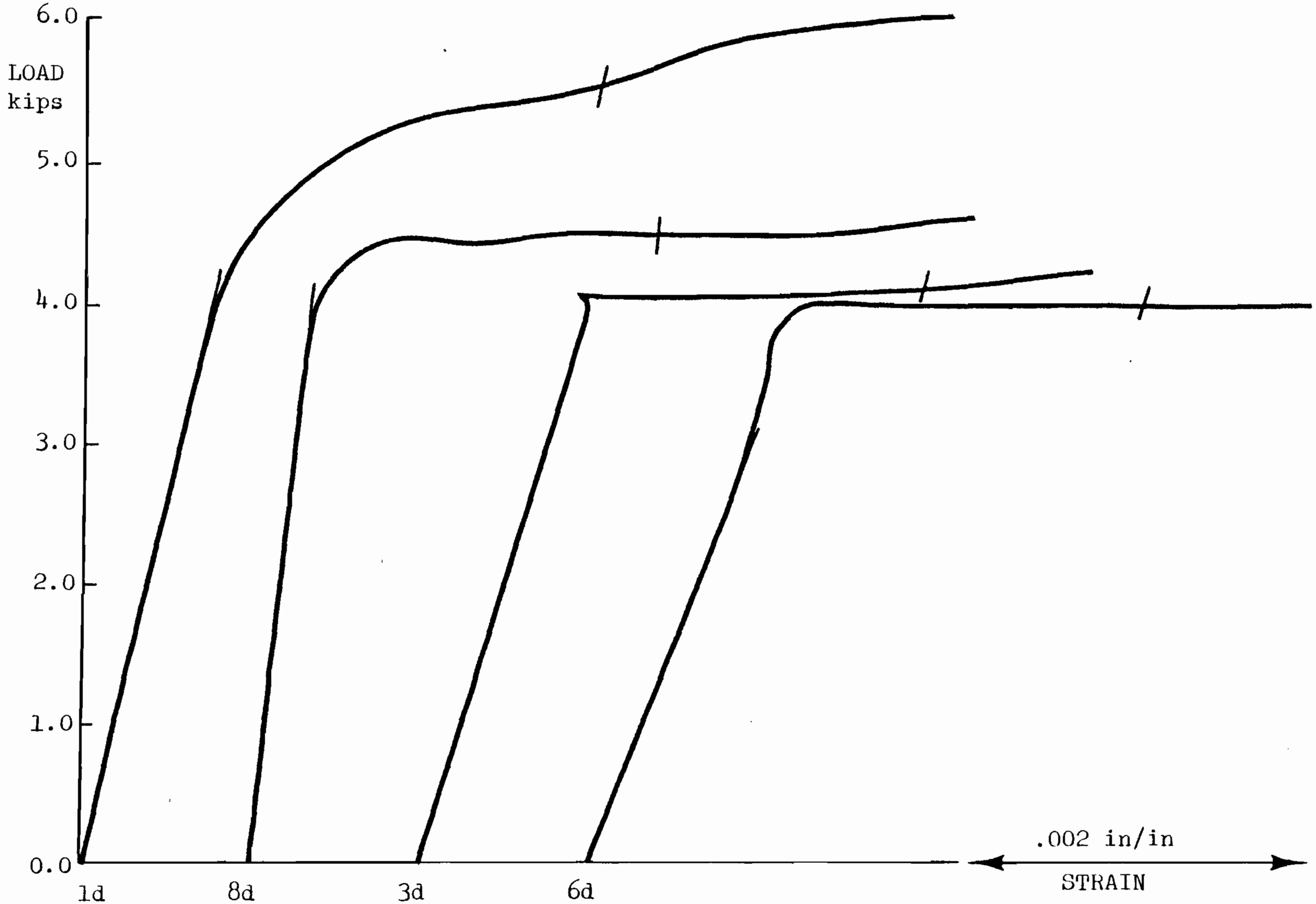

Fig. 3.27a H 7 Compressive Coupon Tests.

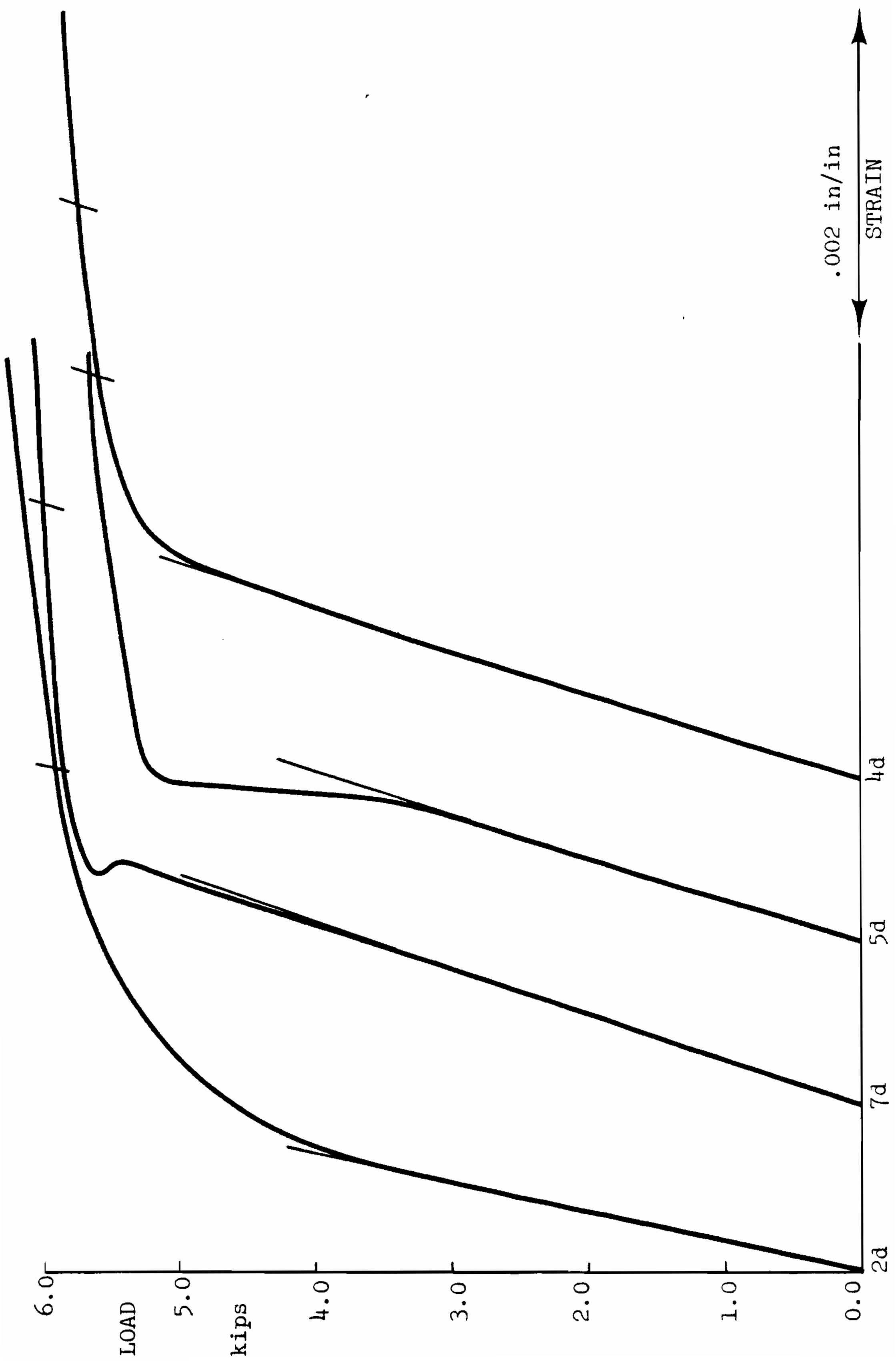
LOAD
kips
6.0
5.0
4.0
3.0
2.0
1.0
0.0
2d
7d
5d
4d
.002 in/in
STRAIN

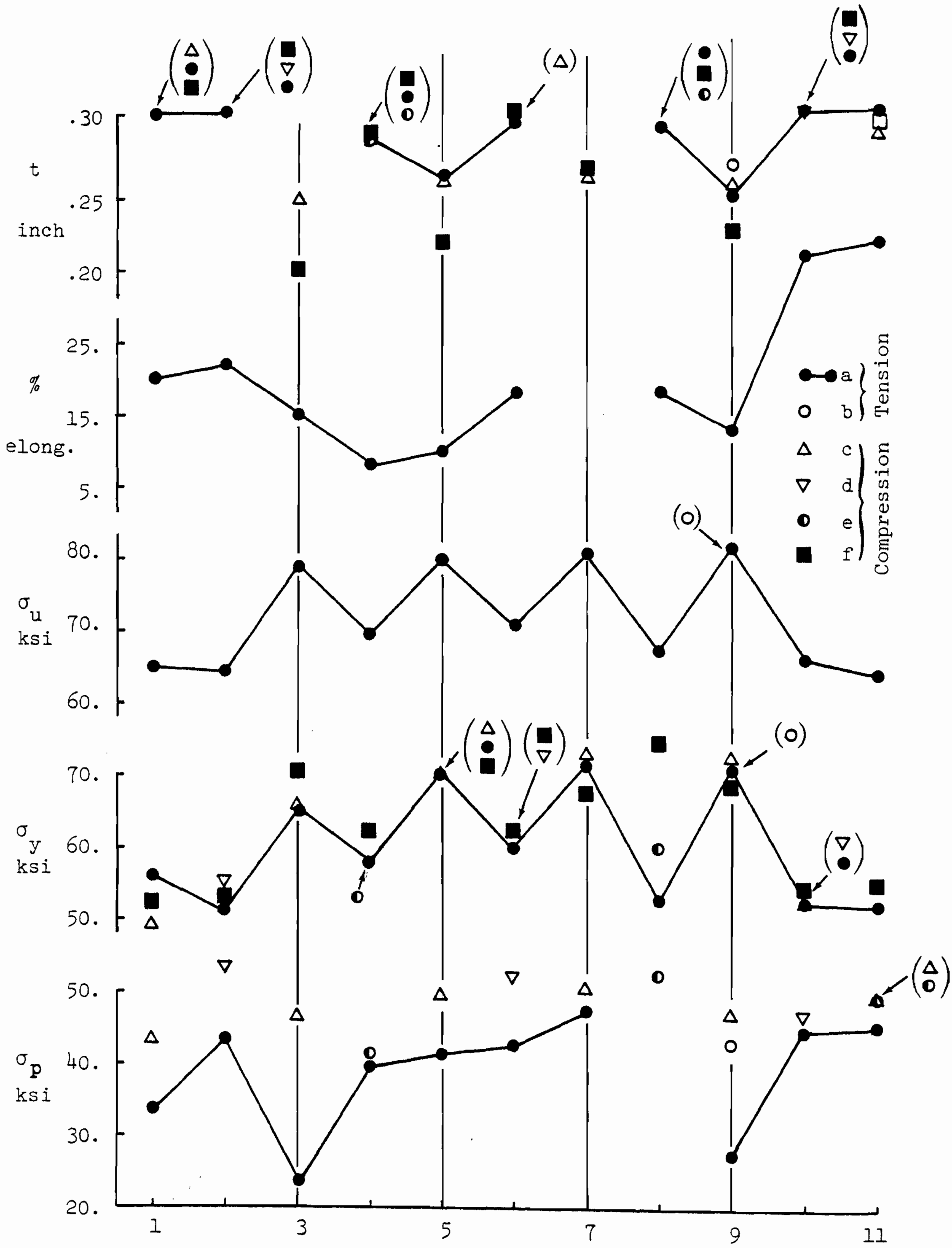

Fig. 3.28 HT Tensile and Compressive Tests.
For locations of coupons, see Fig. 3.29.

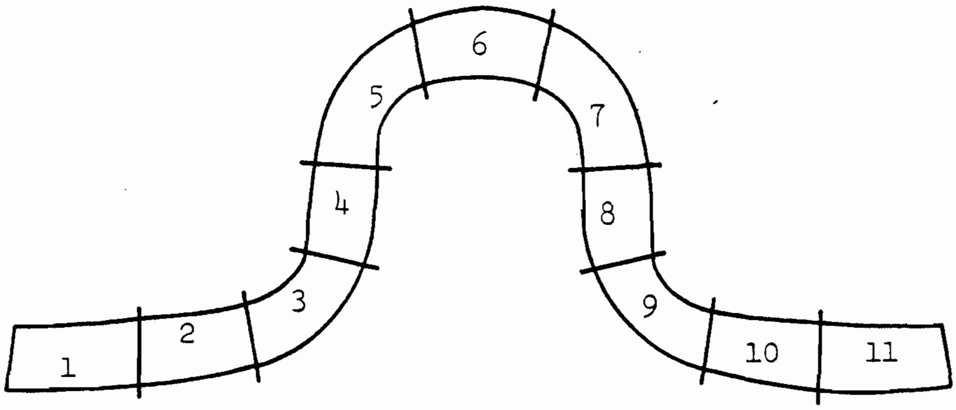

Fig. 3.29 HT Tensile and Compressive Coupons.
(also corresponds to residual strain
coupons).

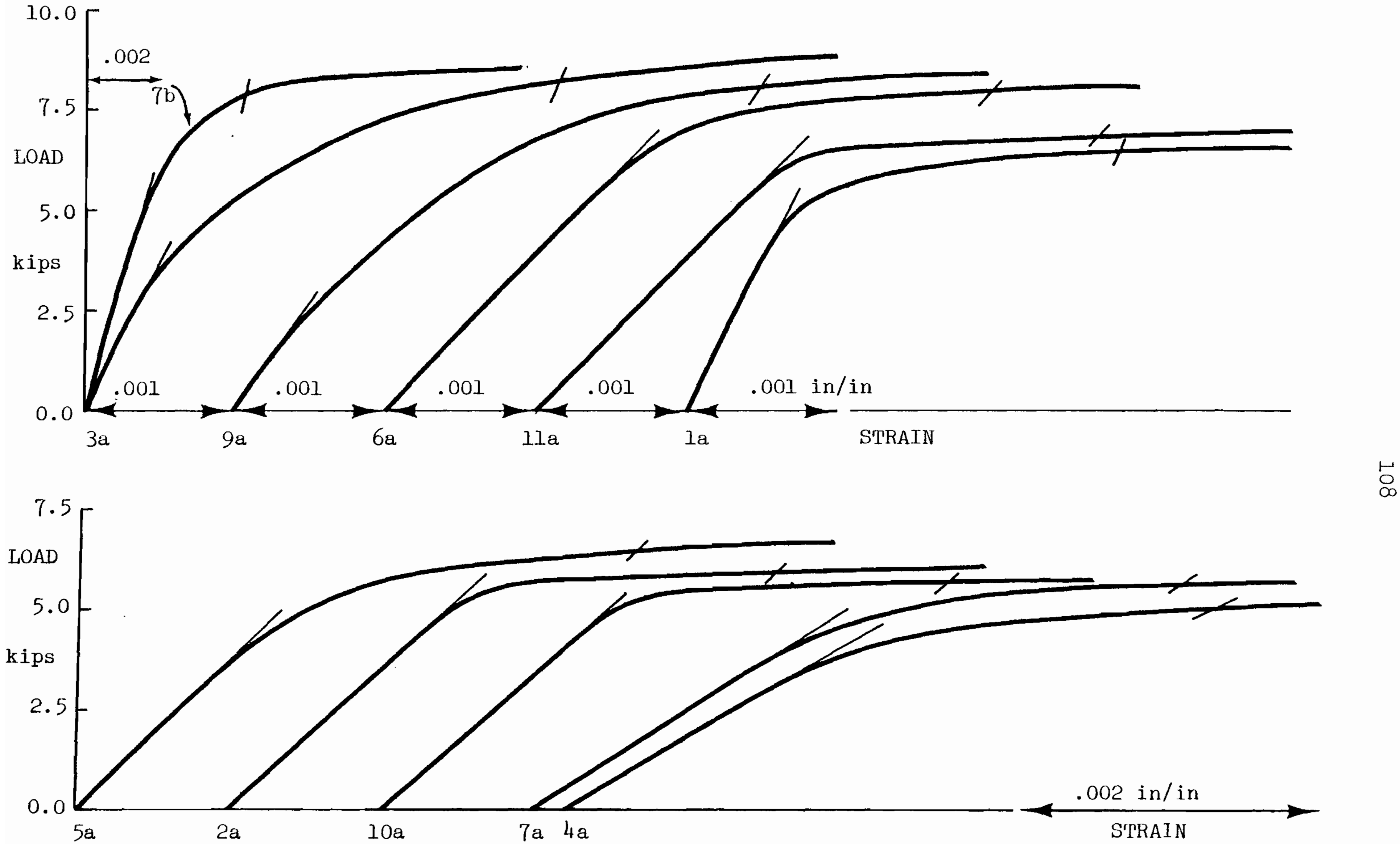

Fig. 3.30 H T Tensile Coupon Tests.

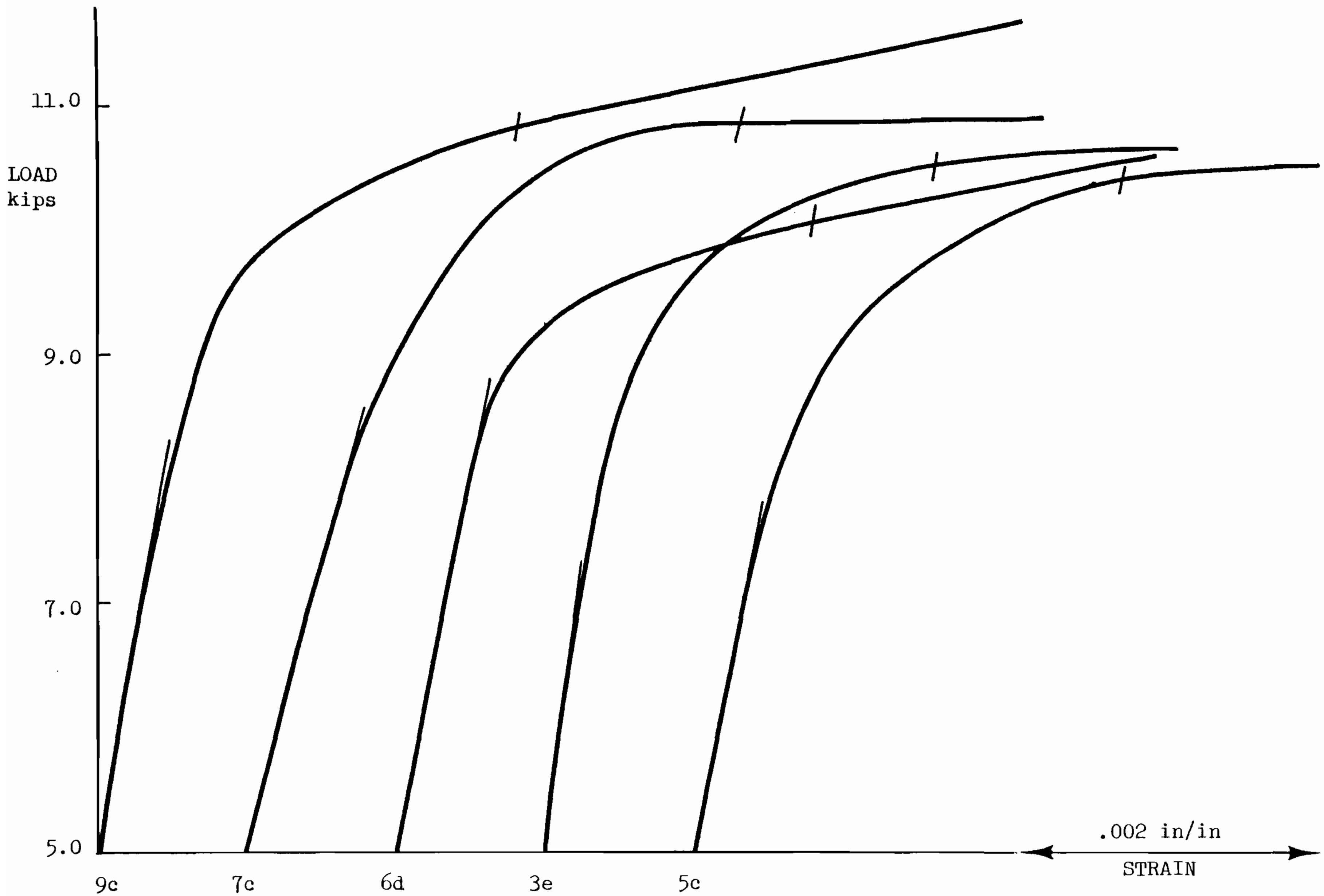

Fig. 3.31a H T Compressive Coupon Test.

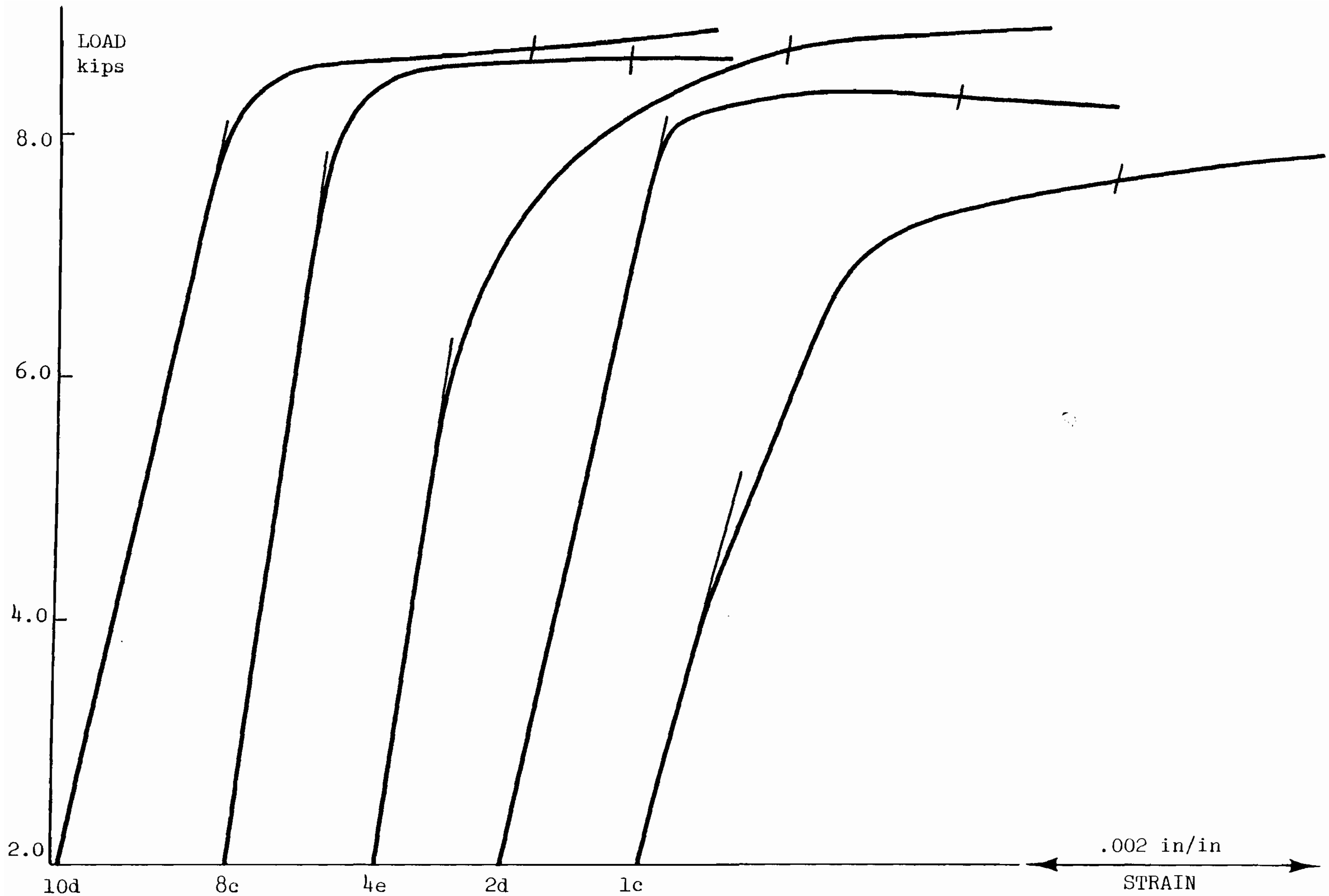

Fig. 3.31b H T Compressive Coupon Tests.

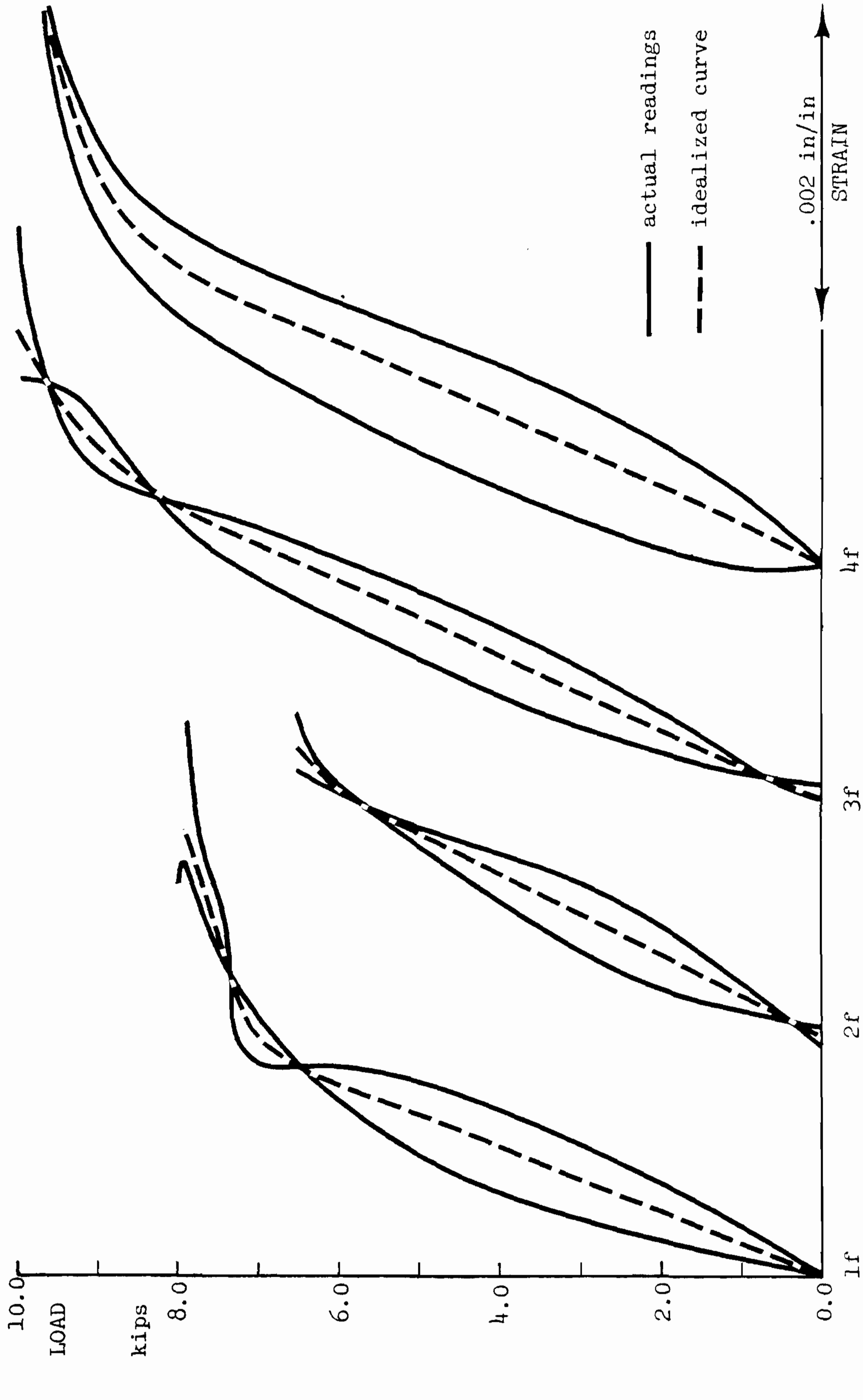

10.0
LOAD
kips
8.0
6.0
4.0
2.0
0.0
1f
2f
3f
4f
actual readings
idealized curve
.002 in/in
STRAIN

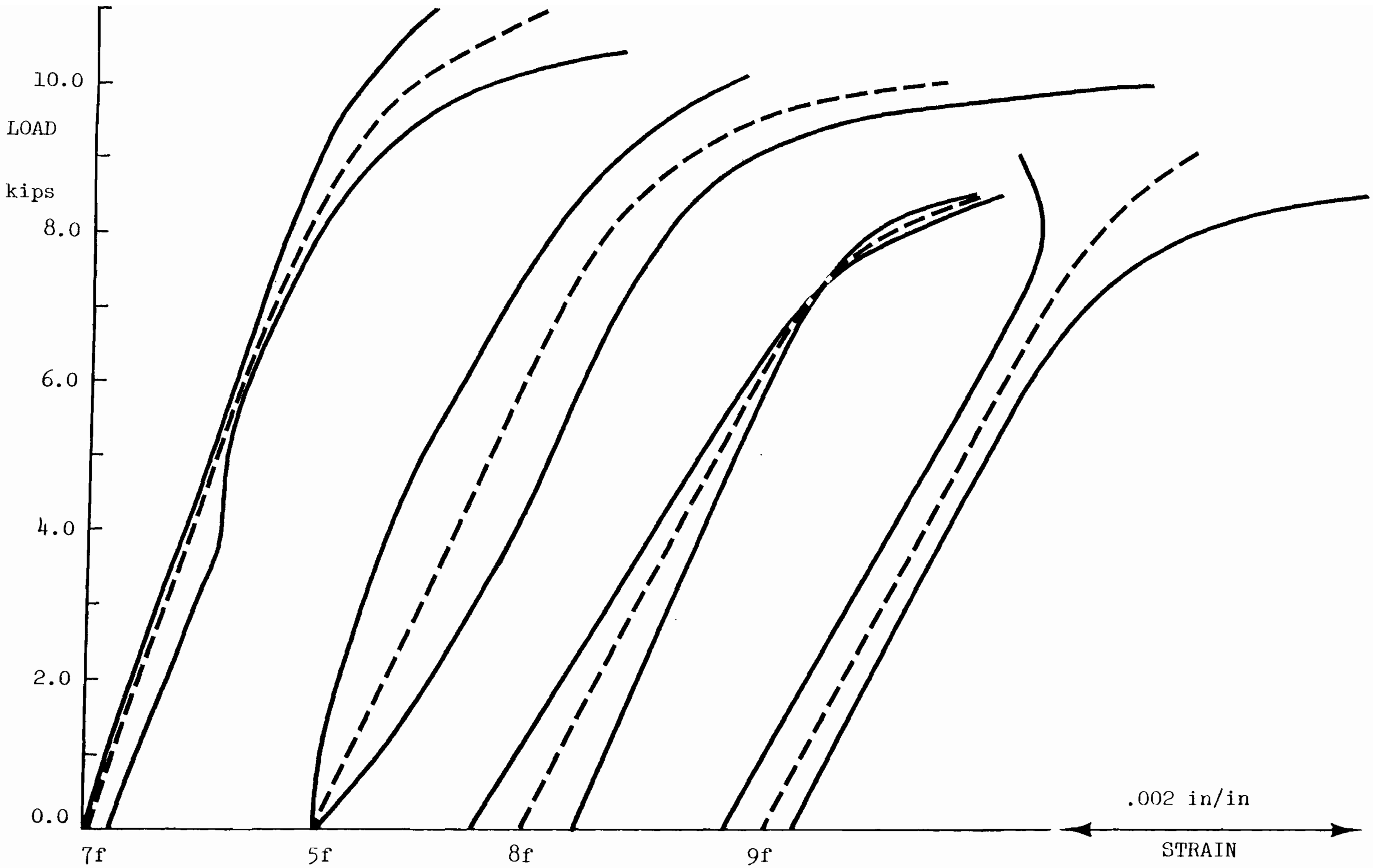

Fig. 3.32b H T Compressive Coupon Tests with Strain Gages (Specimen f).

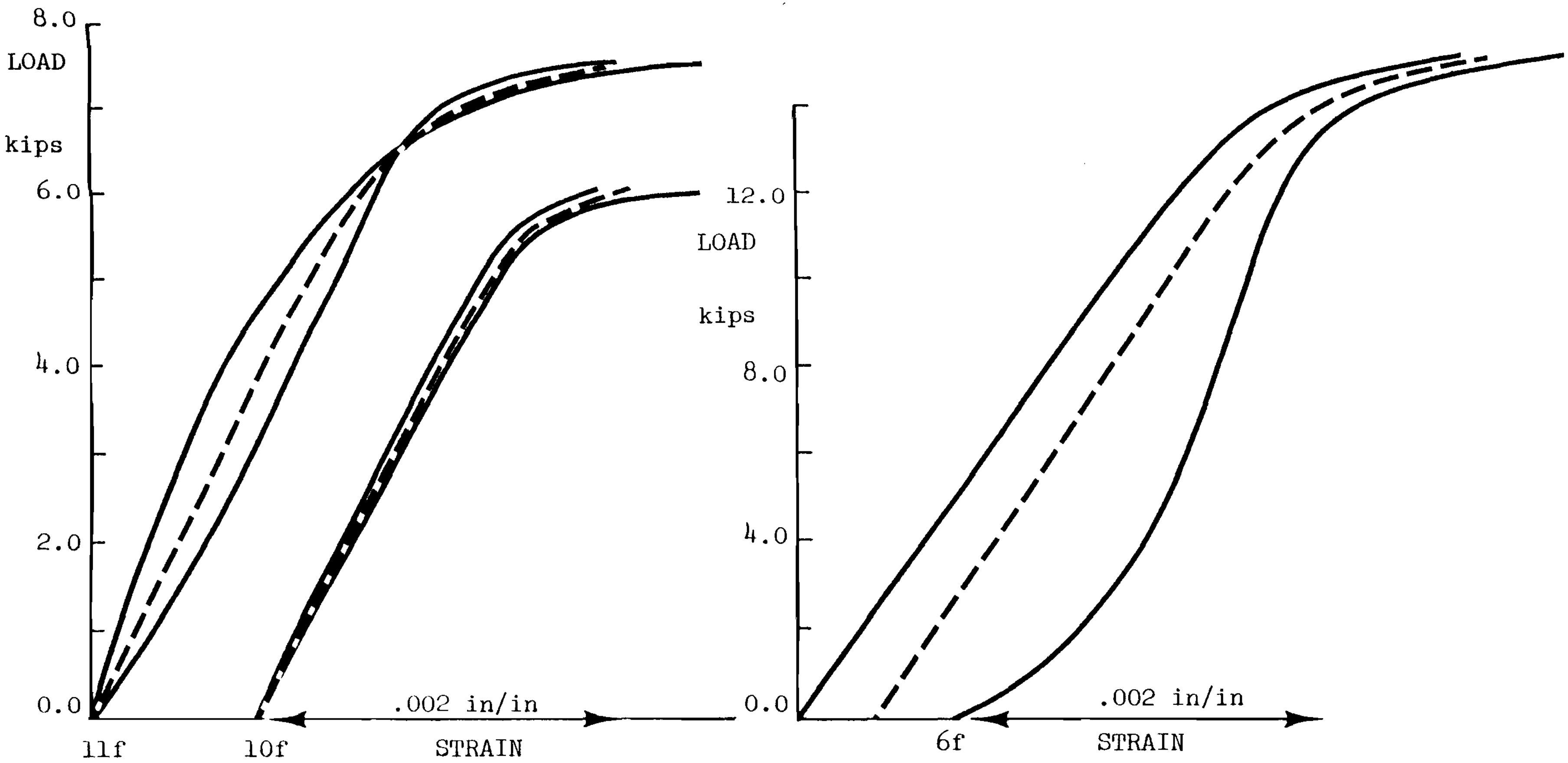

Fig. 3.32c H T Compressive Coupon Tests with Strain Gages (Specimen f).

CHAPTER 4

RESIDUAL STRESSES DUE TO COLD-FORMING: THEORY

4.1 Introduction

The cold forming of a structural section involves loading the metal into the plastic range followed by unloading. This sequence leaves residual stresses locked in the metal since loading and unloading follow different stress-strain paths. The loads are of mechanical origin here but they can also be of thermal origin (e.g. in the uneven cooling of hot-rolled sections) or a combination of both (e.g. in metal cutting).

Only the simplest problems have so far lent themselves to theoretical analysis, and accurate prediction of residual stresses is still the exception rather than the rule. Solutions do exist, however, for the bending of beams and sheets, a problem relevant to the present investigation, and the next easiest problem, the autofrettage of cylinders (prestraining by uniform internal pressure)* which produces an axisymmetric state of stress. Denton [1966a] cites several solutions to the problem, including one that produces results within 5% of experimental measurements obtained by the Sachs boring method (Chapter 5).

---

*"Guns, tanks to contain gases at high pressure, etc. may be tightly wound with wire so as to exert compression on the inside, or the guns are expanded by internal hydraulic pressure, so that, when this pressure is relieved, there will be residual compressive stress, so located that, when the gun is fired, the effective tensile stress is decreased. Thus the gun is strengthened, much as when an outer gun tube is shrunk upon an inner tube or when the gun is tightly wound with wire." Bullens [1948]

More recently, with the advent of electronic computation, a greater number of analytical solutions to residual stress problems have been developed. Incremental computer techniques have proved invaluable in solving the basic difficulty, which lies in the elasto-plastic loading stage rather than the elastic unloading stage (Pawelski [1970]). There is a possibility of further plastic flow in the unloading stage, but most investigators have neglected this possibility because of the great complications involved. It will be shown below this neglect is justified in the case of bending of sheets, except for a narrow range of internal pressure.

4.2 Literature Review

Hill [1950] solved the plane strain problem of bending of wide sheets by pure bending and by a combination of end moments and internal pressure (his solution is also reported in Hoffman and Sachs [1953]). Independently, Lubahn and Sachs [1950] solved both the plane stress and plane strain problems of pure bending of sheets. Stresses in the plane strain condition could be obtained directly, whereas the plane stress case required successive approximations. All the above solutions neglected strain-hardening, the presence of an elastic zone near the neutral axis at the end of the loading stage and assumed purely elastic unloading.

Alexander [1959] solved basically the same problem of pure bending of sheets but with slightly different assumptions. The plane strain condition and elasto-plastic loading were considered (not a fully plastified section like above), but the normal stresses in the thickness direction were neglected and a close-form solution was obtained. Using a simple three-sheet model, Alexander also found that a small amount of stretching reduces considerably the magnitude of transverse residual stresses. He concluded that stretching in a direction transverse to the major residual stresses is almost as effective in reducing them as stretching in a parallel direction.

Denton [1966b] extended Alexander's work to the plane strain pure bending of a work-hardening material but abandoned Alexander's geometrical method for a numerical one.

Shaffer and Ungar [1960] also considered the plane strain pure bending of sheets and assumed the formation of a full plastic hinge at the loading stage. They proved, however, that unloading cannot be fully elastic, and a thin plastic region remains around the neutral axis of the section after unloading. For severe bending (ratio of internal radius to thickness $a/t < 0.84$), an additional plastic region is left on the concave (internal) edge. This is one of the few solutions that consider the possibility of plastic flow in the unloading stage. The thickness of the residual plastic zones is small, however, especially when internal pressure is also applied, as will be shown below. The interior plastic residual region may be a consequence of the assumption of full plasticity after loading, and the assumption of elastic unloading appears to be justified. This problem, generalized to include the action of internal pressure, is reexamined in detail below.

More recently, Ingvarsson [1975, 1977b] studied the problem of plane stress and plane strain bending of bars and sheets under internal pressure, end moments and forces, taking into account elasto-plastic loading and strain hardening. A computer program takes the section through increments of loads followed by purely elastic unloading (the unloading stresses are not exact but assumed to vary linearly in the thickness direction). There is no mention of violation of the yield criterion in the unloading stage. This work appears to be the most complete and general to date and will be used subsequently.

Most of the studies about sheet bending mentioned so far only consider pure bending by end moments, a condition that creates strains varying linearly in the thickness direction. This is obviously the simplest case, but clearly it does not reflect the complexity of the forces between the dies or the rolls and the metal sheet. It is reassuring to note that, in modelling the bending of sheets by a three-roll pyramid type machine, Basset and Johnson [1966] obtained good agreement with experimental results in considering bending moments only.

The bending of sheets by pressure and moment and the resulting residual stresses are reexamined in detail. A first solution assumes purely elastic unloading, whereas a second solution allows for the possibility of inelastic unloading. Both solutions assume full plastification upon loading. The approach is therefore slightly different from Ingvarsson's [1975, 1977b] who does not assume full plastification upon loading but only considers elastic unloading. The present solution is also a generalization of the work of Shaffer and Ungar [1960] who did not consider pressure loading. The first solution is less exact than Ingvarsson's but offers the advantage of simplicity: without the need of a computer program an approximate, close-form solution can be obtained from the classical results of the theories of plasticity and elasticity.

4.3 Theory of Sheet Bending

The forming of a corner under internal pressure $\bar{p}$, end moments $\bar{M}$ and end forces $\bar{T}$ is now examined (Fig. 3.3). It is assumed that:

— forming occurs under plane strain conditions. This is obviously a good assumption since the structural member being formed is usually several dozen feet long and only a fraction of an inch thick.

— the material is elastic, perfectly plastic and does not strain-harden.

— plane sections remain plane.

— the section is entirely plastified after loading. The small elastic region near the neutral axis is neglected and the angle of curvature does not need to be considered.

It is clear that r, θ and z are the principal directions.

4.3.1 Yield Criterion

The yield criterion for plane strain is:

$$\bar{\sigma}_\theta - \bar{\sigma}_r = \pm 2\bar{k} \qquad (4.1)$$

where $\bar{\sigma}_\theta$ = tangential normal stress

$\bar{\sigma}_r$ = radial normal stress

$$2\bar{k} \begin{cases} = \sigma_y & \text{for the Tresca criterion} \\ = 2\sigma_y/\sqrt{3} & \text{for the Von Mises criterion} \end{cases}$$

σ_y = yield strength of the material in one dimension

Forces, moments and stresses are normalized with respect to $2\bar{k}$.

$$\sigma_\theta = \bar{\sigma}_\theta/2\bar{k}$$

$$\sigma_r = \bar{\sigma}_r/2\bar{k}$$

$$M = \bar{M}/2\bar{k}$$

$$T = \overline{T}/2\overline{k}$$

$$p = \overline{p}/2\overline{k}$$

The yield criterion is then:

$$\sigma_\theta - \sigma_r = \pm 1 \qquad (4.2)$$

This equation will be referred to as the '+' or '-' criterion depending on the sign on the right-hand side.

4.3.2 Equilibrium

Equilibrium requires:

$$T = ap \qquad (4.3)$$

where a is the internal radius.

The stresses must also satisfy the differential equation:

$$\frac{d\sigma_r}{dr} = \frac{\sigma_\theta - \sigma_r}{r} \qquad (4.4)$$

4.3.3 Plastic Loading

Hill's results [1950] on plastic loading are presented here. The state of stress is:

— for $a \leq r \leq c$

$$\begin{aligned} \sigma_{rp} &= -p - \ln r/a \\ \sigma_{\theta p} &= -p - 1 - \ln r/a \end{aligned} \qquad (4.5)$$

where σ_{rp} , $\sigma_{\theta p}$ are the plastic loading stresses in the radial and tangential directions.

$$c = (abe^{-p})^{1/2} \qquad (4.6)$$

is the radius of the neutral axis and b is the external radius. The location of the neutral axis depends on p and therefore, as will be seen below, on the thinning of a corner relative to the virgin flat.

— for $c \leq r \leq b$

$$\sigma_{rp} = \ln r/b$$
$$\sigma_{\theta p} = 1 + \ln r/b \tag{4.7}$$

The combination of pressure p and moment M necessary to obtain full plastification of the corner is given by:

$$M = (a^2 + b^2 - 2abe^{-p})/4 - abp/2 \tag{4.8}$$

The relative thinning of the sheet, $-\Delta t/t$, is proportional to the pressure:

$$-\Delta t/t = p/2 \tag{4.9}$$

This is of practical importance. $-\Delta t/t$ can be measured experimentally and thus, p, M and c evaluated. The combination of p and M determines the residual and the relaxation stresses.

p must, of course, be positive and it is natural to also require M to be positive, so the cold-forming actions do not work against one another. By (4.8), $M \geq 0$ implies

$$p + e^{-p} \leq \frac{a^2 + b^2}{2ab} \tag{4.10}$$

Thus a maximum value p_m can be defined, for which M = 0:

$$p_m + e^{-p_m} = \frac{a^2 + b^2}{2ab} \tag{4.10b}$$

Similarly, a maximum moment can be defined, for which p = 0:

$$M_m = t^2/4 \tag{4.10c}$$

where t = b - a is the corner thickness.

Another limiting value of p is one for which c = a. From (4.6) there results:

$$p_\ell = \ln(b/a) \tag{4.11}$$

where ln denotes the natural logarithm.

It is seen numerically that $p_\ell < p_m$, so $0 \le p \le p_\ell$. The greatest thickness reduction occurs at $p = p_\ell$:

$$(-\Delta t/t)_\ell = 1/2 \ln(b/a) \tag{4.12}$$

Equations (4.6) and (4.9) indicate that the highest value of the neutral axis,

$$c_0 = \sqrt{ab} \tag{4.13}$$

occurs at $p = 0$, where no thickness reduction takes place.

4.3.4 Elastic Unloading (to be added):

The problem is axisymmetric and its solution can be readily found in Timoshenko and Goodier [1970]:

$$\begin{aligned} \sigma_{re} &= A/r^2 + B(1 + \ln r^2) + C \\ \sigma_{\theta e} &= -A/r^2 + B(3 + \ln r^2) + C \end{aligned} \tag{4.14}$$

σ_{re} , $\sigma_{\theta e}$ are the elastic unloading stresses and A, B, C are constants to be determined.

The solution is the superposition of an internal pressure solution and a pure bending solution. Let the superscripts pu and bu denote pressure unloading and bending unloading respectively.

The pressure unloading stresses are:

$$\begin{aligned} \sigma_r^{pu} &= -\frac{a^2 p}{b^2 - a^2}\left(1 - \frac{b^2}{r^2}\right) \\ \sigma_\theta^{pu} &= -\frac{a^2 p}{b^2 - a^2}\left(1 + \frac{b^2}{r^2}\right) \end{aligned} \tag{4.15}$$

Subtracting:

$$\sigma_\theta^{pu} - \sigma_r^{pu} = -\frac{2a^2 p}{b^2 - a^2}\frac{b^2}{r^2}$$

With N defined by:

$$N = (\gamma^2 - 1)^2 - 4\gamma^2(\ln\gamma)^2 \tag{4.16}$$

where,

$$\gamma = b/a \tag{4.17}$$

the bending unloading stresses are:

$$\begin{aligned}\sigma_r^{bu} &= -\frac{4M}{a^2N}\left(\frac{b^2}{r^2}\ln\frac{b}{a} + \frac{b^2}{a^2}\ln\frac{r}{b} + \ln\frac{a}{r}\right)\\ \sigma_\theta^{bu} &= -\frac{4M}{a^2N}\left(-\frac{b^2}{r^2}\ln\frac{b}{a} + \frac{b^2}{a^2}\ln\frac{r}{b} + \ln\frac{a}{r} + \frac{b^2}{a^2} - 1\right)\end{aligned} \tag{4.18}$$

Subtracting:

$$\sigma_\theta^{bu} - \sigma_r^{bu} = \frac{4M}{a^2N}\left(2\frac{b^2}{r^2}\ln\frac{b}{a} - \frac{b^2}{a^2} + 1\right)$$

N is always positive (Shaffer and Ungar [1960]).

4.3.5 Residual Stresses

The residual stresses, denoted by superscript res, are the sum of the loading and the unloading stresses:

$$\begin{aligned}\sigma_r^{res} &= \sigma_{rp} + \sigma_r^{pu} + \sigma_r^{bu}\\ \sigma_\theta^{res} &= \sigma_{\theta p} + \sigma_\theta^{pu} + \sigma_\theta^{bu}\\ \sigma_z^{res} &= 0.5(\sigma_{rp} + \sigma_{\theta p}) + 0.3(\sigma_r^{pu} + \sigma_\theta^{pu} + \sigma_r^{bu} + \sigma_\theta^{bu})\end{aligned} \tag{4.19}$$

Poisson's ratio is 0.5 in the plastic range, 0.3 in the elastic range.

The resultant forces and moments on the corner vanish after unloading:

No tangential force:

$$\int_{o}^{z=1}\int_{a}^{b} \sigma_{\theta}^{res}\, drdz = 0 \quad \text{or} \quad \int_{a}^{b} \sigma_{\theta}^{res}\, dr = 0 \qquad (4.20a)$$

No moment:

$$\int_{o}^{z=1}\int_{a}^{b} \sigma_{\theta}^{res}\, rdrdz = 0 \quad \text{or} \quad \int_{a}^{b} \sigma_{\theta}^{res}\, rdr = 0 \qquad (4.20b)$$

4.4 Approximate Stresses

The expressions for the stresses are straightforward, but lengthy. In evaluating them, it was observed that linearization is justified for certain quantities and for large a/t ratios (mildly bent corners). In practice, the approximation is good for $a/t > 3$.

4.4.1 Plastic Loading (from 4.5 and 4.7):

— for $a \leq r \leq c$

$$\begin{aligned} \sigma_{rp} &\simeq 1 - p - r/a \\ \sigma_{\theta p} &\simeq -p - r/a \\ \sigma_{zp} &\simeq 1/2 - p - r/a \end{aligned} \qquad (4.21)$$

— for $c \leq r \leq b$

$$\begin{aligned} \sigma_{rp} &\simeq (r-b)/a \\ \sigma_{\theta p} &\simeq (r-t)/a \\ \sigma_{zp} &\simeq -1/2 + (r-t)/a \end{aligned} \qquad (4.22)$$

4.4.2 Elastic Pressure Unloading (from 4.15):

$$\sigma_{r}^{pu} \simeq \frac{2ap}{t} \cdot \frac{r-b}{a+b}$$

$$\sigma_\theta^{pu} \simeq \frac{2ap}{t}\left(1 - \frac{r}{a+b}\right) \tag{4.23}$$

$$\sigma_z^{pu} = \frac{2\nu a^2 p}{t(a+b)} \qquad \text{(exact)}$$

4.4.3 <u>Elastic Bending Unloading</u> (from 4.18):

$$\sigma_r^{bu} \simeq \frac{6M(r-a)(r-b)}{at^3}$$

$$\sigma_\theta^{bu} \simeq \frac{12M}{t^3}\left(r - \frac{a+b}{2}\right) \tag{4.24}$$

$$\sigma_z^{bu} \simeq \frac{6\nu Ma}{t^3}\left[\left(\frac{r}{a}\right)^2 - \left(\frac{t}{a}+4\right)\frac{r}{a} + 2\frac{t}{a} + \frac{t^2}{3a^2} + 3\right]$$

Unfortunately these expressions are obtained through neglect of (a/t) terms of different orders and care should be exerted in summing them. There is no simple expression for the residual stresses and expressions (4.19) should be used.

4.5 <u>Theory of Sheet Bending with Inelastic Unloading</u>

Following Shaffer and Ungar's work [1960], the unloading process is reexamined to see if it violates the yield criterion. From (4.19) and (4.2):

$$\sigma_\theta^{res} - \sigma_r^{res} = (\sigma_{\theta p} - \sigma_{rp}) + (\sigma_\theta^{pu} - \sigma_r^{pu}) + (\sigma_\theta^{bu} - \sigma_r^{bu}) = \begin{cases} -1 + \delta \\ \text{for } a \le r \le c \\ +1 + \delta \\ \text{for } c \le r \le b \end{cases} \tag{4.25}$$

where,

$$\delta \equiv (\sigma_\theta^{pu} - \sigma_r^{pu}) + (\sigma_\theta^{bu} - \sigma_r^{bu}) \tag{4.26}$$

From (4.15) and (4.18) and with

$$\eta \equiv a^2 p/M \tag{4.27}$$

$$\delta = \frac{2b^2M}{r^2}\left(\frac{4}{a^2N}\ln\frac{b}{a} - \frac{n}{b^2 - a^2}\right) - \frac{4M}{a^4N}(b^2 - a^2) \qquad (4.28)$$

Elastic unloading occurs in $a \leq r \leq c$ only if $\delta > 0$ and in $c \leq r \leq b$ only if $\delta < 0$.

If $M = 0$, $\delta = -\dfrac{2a^2b^2p}{(b^2 - a^2)r^2}$ and is always negative. The concave region $a \leq r \leq c$ then unloads inelastically regardless of a and b.

If $\eta \geq \dfrac{4(b^2 - a^2)}{a^2N}\ln\dfrac{b}{a}$, then δ is always negative. The concave region $a \leq r \leq c$ unloads inelastically. Therefore, inelastic unloading develops for high pressures.

For $\eta < \dfrac{4(b^2 - a^2)}{a^2N}\ln\dfrac{b}{a}$, r_y is defined as the radius at which $\delta = 0$; also $\delta < 0$ for $r > r_y$ and $\delta > 0$ for $r < r_y$. From (4.28):

$$r_y^2 = \left(\frac{ab}{b^2 - a^2}\right)^2\left[2(b^2 - a^2)\ln\frac{b}{a} - \frac{1}{2}\eta\, a^2N\right] \qquad (4.29)$$

The relative positions of r_y and c (i.e., $r_y < c$ or $r_y > c$) suggests two kinds of interior yield band. For severe bending (high b/a) at low pressures a third case arises whereby an additional yield band develops at the concave edge. As the pressure increases, the interior yield zone migrates towards the concave edge. A fourth case obtains as soon as one of the following holds:

$$t_o \leq a\ , \quad \eta \geq \frac{4(b^2 - a^2)}{a^2N}\ln\frac{b}{a} \quad \text{or} \quad M = 0.$$

t_o is defined as the lower boundary of the interior residual plastic zone.

4.5.1 Case 1: $t_o < c$. Interior yielding only.

An interior region bordered by t_o (by definition) and c unloads inelastically (Fig. 4.1).

The residual stresses are:

– for $a \leq r \leq t_o$ (from (4.5) and (4.14)):

$$\begin{aligned} \sigma_r^{res} &= \sigma_{rp} + \sigma_{re} = -p - \ln r/a + A/r^2 + B(1 + \ln r^2) + C \\ \sigma_\theta^{res} &= \sigma_{\theta p} + \sigma_{\theta e} = -1 - p - \ln r/a - A/r^2 + B(3 + \ln r^2) + C \\ \sigma_z^{res} &= 0.5(\sigma_{rp} + \sigma_{\theta p}) + 0.3(\sigma_{re} + \sigma_{\theta e}) = -0.5 - p - \ln r/a \\ &\quad + 0.3[B(4 + 2\ln r^2) + 2C] \end{aligned} \tag{4.30}$$

– for $t_o \leq r \leq c$ (from (4.2) and (4.4)):

$$\begin{aligned} \sigma_r^{res} &= \sigma_{rp-} = -\ln r/b - D \\ \sigma_\theta^{res} &= \sigma_{\theta p-} = -\ln r/b - D - 1 \\ \sigma_z^{res} &= 0.5(\sigma_{rp-} + \sigma_{\theta p-}) = -0.5 - \ln r/b - D \end{aligned} \tag{4.31}$$

The - in the subscript indicates satisfaction of the '-' yield criterion (4.2).

– for $c \leq r \leq b$ (from (4.7) and (4.14)):

$$\begin{aligned} \sigma_r^{res} &= \sigma_{rp} + \sigma_{re} = \ln r/b + A/r^2 + B(1 + \ln r^2) + C + H \\ \sigma_\theta^{res} &= \sigma_{\theta p} + \sigma_{\theta e} = 1 + \ln r/b - A/r^2 + B(3 + \ln r^2) + C + H \\ \sigma_z^{res} &= 0.5(\sigma_{rp} + \sigma_{\theta p}) + 0.3(\sigma_{re} + \sigma_{\theta e}) = 0.5 + \ln r/b \\ &\quad + 0.3[4B(1 + \ln r) + 2(C + H)] \end{aligned} \tag{4.32}$$

A constant H has been added here because there is no continuity requirement of the stresses from one side of the yield band to the other.

Boundary Conditions and Equilibrium:

Radial stresses vanish at both edges: $\sigma_r^{res} = 0$ at $r = a$, b and are continuous at t_o and c. Tangential stresses are also continuous at t_o. These conditions, added to the requirements of zero resultant force and moment (4.20a,b) provide seven equations to solve for the six unknowns A, B, C, D, H and t_o.

At $r = a$,

$$\sigma_r^{res} = -p + A/a^2 + B(1 + \ln a^2) + C = 0 \tag{4.33}$$

at $r = b$,

$$\sigma_r^{res} = A/b^2 + B(1 + \ln b^2) + C + H = 0 \tag{4.34}$$

at $r = t_o$, σ_r^{res} is continuous:

$$-p - \ln t_o/a + A/t_o^2 + B(1 + \ln t_o^2) + C = -\ln t_o/b - D \tag{4.35}$$

at $r = c$, σ_r^{res} is continuous:

$$-\ln b/c + A/c^2 + B(1 + \ln c^2) + C + H = -\ln c/b - D \tag{4.36}$$

and at $r = t_o$, σ_θ^{res} is continuous:

$$-1 - p - \ln t_o/a - A/t_o^2 + B(3 + \ln t_o^2) + C = -\ln t_o/b - D - 1 \tag{4.37}$$

Subtracting (4.37) from (4.35):

$$1 + 2A/t_o^2 - 2B = 1 \quad \text{or} \quad A = Bt_o^2 \tag{4.38}$$

From (4.33),

$$C = p - A/a^2 - B(1 + \ln a^2) \tag{4.39}$$

from (4.34),

$$H = -A/b^2 - B(1 + \ln b^2) - C \tag{4.40}$$

from (4.36),

$$D = 2(1 + B)\ln\frac{b}{c} + A\left(\frac{1}{b^2} - \frac{1}{c^2}\right) \tag{4.41}$$

from (4.35),

$$\ln\left(\frac{t_o}{a}\right)^2 + \frac{p}{B} - t_o^2\left(\frac{1}{a^2} - \frac{1}{b^2} + \frac{1}{c^2}\right) = -1 + \ln\left(\frac{c}{b}\right)^2 \tag{4.42}$$

and from (4.20b),

$$0 = \frac{1}{4}(a^2 + b^2 - 2c^2) + \frac{t_o^2 p}{2} - \frac{B}{2a^2}\left(t_o^2 - a^2\right)^2 + \frac{B(b^2 - c^2)}{2b^2}\left(b^2 - \frac{t_o^4}{c^2}\right) \tag{4.43}$$

Finally, the force equation (4.20a) is identical to (4.42). Integrals (4.20a) and (4.20b) are evaluated in Appendix A. All equations reduce to published results when $p = 0$. The system of six equations (4.38)-(4.43) is solved numerically for A, B, C, D, H and t_o and the residual stresses are obtained from (4.30)-(4.32).

4.5.2 Case 2: $t_o > c$. Interior yielding only.

Case 2 is similar to case 1 except that the interior plastic region now satisfies the '+' yield criterion (4.2).

For $a \leq r \leq c$ and $t_o \leq r \leq b$ the residual stresses are given by (4.30) and (4.32) respectively. For $c \leq r \leq t_o$, they are:

$$\sigma_r^{res} = \sigma_{rp+} = \ln r/b + D$$

$$\sigma_\theta^{res} = \sigma_{\theta p+} = \ln r/b + D + 1 \tag{4.44}$$

$$\sigma_z^{res} = 0.5(\sigma_{rp+} + \sigma_{\theta p+}) = 0.5 + \ln r/b + D$$

Boundary Conditions:

As in case 1 above:

at $r = a$,

$$\sigma_r^{res} = -p + A/a^2 + B(1 + 2\ln a) + C = 0 \tag{4.45}$$

at $r = b$,

$$\sigma_r^{res} = A/b^2 + B(1 + 2\ln b) + C + H = 0 \tag{4.46}$$

at $r = t_o$, σ_r^{res} is continuous:

$$-\ln b/t_o + A/t_o^2 + B(1 + 2\ln t_o) + C + H = \ln t_o/b + D \tag{4.47}$$

at $r = c$, σ_r^{res} is continuous:

$$-p - \ln c/a + A/c^2 + B(1 + 2\ln c) + C = \ln c/b + D \tag{4.48}$$

and at $r = t_o$, σ_θ^{res} is continuous:

$$1 - \ln b/t_o - A/t_o^2 + B(3 + 2\ln t_o) + C + H = \ln t_o/b + D + 1 \tag{4.49}$$

Subtracting (4.49) from (4.47):

$$2A/t_o^2 - 2B = 0 \qquad \text{or} \qquad A = Bt_o^2 \tag{4.50}$$

From (4.45),

$$C = p - A/a^2 - B(1 + 2\ln a) \tag{4.51}$$

from (4.46),

$$-H = A/b^2 + B(1 + 2\ln b) + C \tag{4.52}$$

from (4.48),

$$D = -p - \ln c^2/ab + A/c^2 + B(1 + 2\ln c) + C$$

from (4.6),

$$D = A/c^2 + B(1 + 2\ln c) + C$$

from (4.50) and (4.51),

$$D = Bt_o^2/c^2 + B(1 + 2\ln c) + p - Bt_o^2/a^2 - B(1 + 2\ln a)$$

or

$$D = B\left[\frac{p}{B} + t_o^2\left(\frac{1}{c^2} - \frac{1}{a^2}\right) + 2\ln\frac{c}{a}\right] \tag{4.53}$$

from (4.47),

$$D = 2B(1 + \ln t_o) - B(t_o^2/b^2) - B(1 + 2\ln b)$$

or

$$D = B(1 + 2\ln t_o/b - t_o^2/b^2) \tag{4.54}$$

and from (4.53) = (4.54),

$$\frac{p}{B} = 1 + 2\ln\left(\frac{t_o}{b}\right)\left(\frac{a}{c}\right) - t_o^2\left(-\frac{1}{a^2} + \frac{1}{b^2} + \frac{1}{c^2}\right) \tag{4.55}$$

<u>Equilibrium</u>:

The condition of moment equilibrium (3.20b) is equivalent to:

$$0 = \frac{1}{4}\left(a^2 + b^2 - 2c^2\right) + \frac{c^2}{2}p + \frac{Bc^2t_o^2}{2}\left(\frac{1}{b^2} - \frac{1}{a^2}\right)$$

$$+ \frac{B}{2}\left(b^2 - a^2\right) + B\left(c^2 - t_o^2\right)\ln\frac{bc}{at_o} \tag{4.56}$$

and the force equilibrium equation (4.20a) is equivalent to (4.47). The system of six equations (4.50)-(4.54) and (4.56) is evaluated numerically for A, B, C, D, H and t_o.

4.5.3 Case 3

In this case, there exists a yield band in the interior limited by t_o and c (as in case 1) and another yield band on the concave edge limited by a and t_i (by definition. See Fig. 4.2). The edge band satisfies the '+' criterion; the interior band, the '-' criterion.

Residual Stresses:

For $a \leq r \leq t_i$, they are expressed by:

$$\begin{aligned} \sigma_r^{res} &= \sigma_{rp+} = \ln r/a \\ \sigma_\theta^{res} &= \sigma_{\theta p+} = \ln r/a + 1 \\ \sigma_z^{res} &= 0.5(\sigma_{rp+} + \sigma_{\theta p+}) = 0.5 + \ln r/a \\ \sigma_{\theta p+} &- \sigma_{rp+} = +1 \end{aligned} \tag{4.57}$$

For $t_i \leq r \leq t_o$, $t_o \leq r \leq c$ and $c \leq r \leq b$, the residual stresses are given by (4.30), (4.31) and (4.32) respectively.

Boundary Conditions:

At r = a,

$$\sigma_r^{res} = 0 \quad \text{is satisfied.}$$

at r = b,

$$\sigma_r^{res} = A/b^2 + B(1 + 2\ln b) + C + H = 0 \tag{4.58}$$

at $r = t_i$, σ_r^{res} is continuous:

$$\ln t_i/a = -p - \ln t_i/a + A/t_i^2 + B(1 + 2\ln t_i) + C \tag{4.59}$$

at $r = t_o$, σ_r^{res} is continuous:

$$-\ln t_o/b - D = -p - \ln t_o/a + A/t_o^2 + B(1 + 2\ln t_o) + C \tag{4.60}$$

at $r = c$, σ_r^{res} is continuous:

$$-\ln c/b - D = -\ln b/c + A/c^2 + B(1 + 2\ln c) + C + H \tag{4.61}$$

at $r = t_i$, σ_θ^{res} is continuous:

$$\ln t_i/a + 1 = -1 - p - \ln t_i/a - A/t_i^2 + B(3 + 2\ln t_i) + C \tag{4.62}$$

at $r = t_o$, σ_θ^{res} is continuous:

$$-\ln t_o/b - D - 1 = -1 - p - \ln t_o/a - A/t_o^2 + B(3 + 2\ln t_o) + C \tag{4.63}$$

From (4.60) and (4.63)

$$0 = 2A/t_o^2 - 2B$$

which implies

$$A = Bt_o^2 \quad \text{or} \quad B = A/t_o^2 \tag{4.64}$$

from (4.59) and (4.62)

$$-1 = 1 + 2A/t_i^2 - 2B \quad \text{or} \quad B = 1 + A/t_i^2$$

so

$$A = \frac{t_i^2 t_o^2}{t_i^2 - t_o^2} \tag{4.65}$$

and

$$B = \frac{t_i^2}{t_i^2 - t_o^2} \tag{4.66}$$

From (4.58) and (4.61)

$$D = 2\ln b/c - A/c^2 - B(1 + 2\ln c) + A/b^2 + B(1 + 2\ln b)$$

from (4.64)

$$D = (B + 1)\ln\left(\frac{b}{c}\right)^2 - Bt_o^2\left(-\frac{1}{b^2} + \frac{1}{c^2}\right) \tag{4.67}$$

from (4.60)

$$C = -\ln t_o/b - 2(B + 1)\ln b/c - A\frac{c^2 - b^2}{b^2c^2} + p + \ln t_o/a$$
$$- A/t_o^2 - B(1 + 2\ln t_o)$$

from (4.6)

$$C = -B\left[\ln\left(\frac{bt_o}{c}\right)^2 + 2\right] + Bt_o^2\left(-\frac{1}{b^2} + \frac{1}{c^2}\right) \tag{4.68}$$

from (4.59)

$$C = \ln\left(\frac{t_i}{a}\right)^2 - B\left(\frac{t_o}{t}\right)^2 - B\left(1 + \ln t_i^2\right) + p \tag{4.69}$$

from (4.61)

$$-H = -2\ln b/c + Bt_o^2/c^2 + B(1 + 2\ln c) + 2\ln t_i/a + p - Bt_o^2/t_i^2$$
$$- B(1 + 2\ln t_i) + 2(B + 1)\ln\frac{b}{c} + Bt_o^2\frac{c^2 - b^2}{b^2c^2}$$

or

$$-H = -B\ln\left(\frac{t_i}{b}\right)^2 + \ln\left(\frac{t_i}{a}\right)^2 - Bt_o^2\left(-\frac{1}{b^2} + \frac{1}{t_i^2}\right) + p \tag{4.70}$$

From (4.68) = (4.69)

$$2 \ln \frac{t_i}{a} - B \frac{t_o^2}{t_i^2} - B(1 + 2 \ln t_i) + p = -2B \left(\ln \frac{bt_o}{c} + 1 \right) + Bt_o^2 \frac{b^2 - c^2}{b^2 c^2}$$

or

$$\ln \left(\frac{t_i}{a} \right)^2 + p = -B \ln \left[\left(\frac{b}{c} \right)^2 \left(\frac{t_o}{t_i} \right)^2 \right] + Bt_o^2 \left(-\frac{1}{b^2} + \frac{1}{c^2} - \frac{1}{t_o^2} + \frac{1}{t_i^2} \right) \tag{4.71}$$

and from (4.66)

$$\left(\frac{t_o}{t_i} \right)^2 \ln \left(\frac{a}{t_i} \right)^2 + \ln \left(\frac{b}{a} \right) \left(\frac{t_o}{a} \right)^2 = t_o^2 \left(-\frac{1}{b^2} + \frac{1}{c^2} \right) - 1 + \left(\frac{t_o}{t_i} \right)^2 + \left[\left(\frac{t_o}{t_i} \right)^2 - 2 \right] p$$

or

$$\left(\frac{t_o}{t_i} \right)^2 \ln \left(\frac{a}{t_i} \right)^2 + \ln \left(\frac{b}{a} \right) \left(\frac{t_o}{a} \right)^2 + t_o^2 \left(\frac{1}{b^2} - \frac{1}{c^2} - \frac{1}{t_i^2} \right) - \left[\left(\frac{t_o}{t_i} \right)^2 - 2 \right] p + 1 = 0 \tag{4.72}$$

Equilibrium:

Moment equilibrium (4.20b) requires:

$$\left(\frac{1}{t_o^2} - \frac{1}{t_i^2} \right) \left[1 + p + \frac{(-a^2 + b^2 - 2c^2)}{2t_o^2} + 2 \ln \frac{t_i}{a} \right] + \frac{1}{t_o^4} \left(b^2 - c^2 \right) + \left(\frac{1}{b^2} - \frac{1}{c^2} \right) = 0 \tag{4.73a}$$

or

$$\left\{\frac{1}{b^2} - \frac{1}{c^2} - \frac{1}{t_i^2}\left[1 + p + \ln\left(\frac{t_i}{a}\right)^2\right]\right\} t_o^4 + \left[1 + p + \ln\left(\frac{t_i}{a}\right)^2 + \frac{a^2 - b^2 + 2c^2}{2t_i^2}\right] t_o^2 + \frac{-a^2 + 3b^2 - 4c^2}{2} = 0 \qquad (4.73)$$

It is shown in Appendix A that the force equilibrium (4.20a) is equivalent to (4.71). It can also be seen from inspection that the equations in case 3 reduce to published results (Shaffer and Ungar [1960]) for $p = 0$, $c^2 = ab$. t_o and t_i can be solved for from (4.72) and (4.73). Substitution into (4.71), (4.72), (4.74) and (4.75) gives A, B, D, C and H.

4.5.4 Case 4

The region below the neutral axis ($a \le r \le c$) unloads inelastically. As discussed earlier this case arises at high pressure, namely

— when $p = p_{max}$, i.e., $M = 0$

— when $\eta = \frac{a^2 p}{M} \ge \frac{4(b^2 - a^2)}{a^2 N} \ln \frac{b}{a}$

— when $t_o \le a$.

As will be shown below, r_y is a useful estimate of t_o. From (4.17), (4.27) and (4.20):

$$r_y^2 = a^2 \Leftrightarrow \left(\frac{\gamma^2 - 1}{\gamma}\right)^2 = 2(\gamma^2 - 1)\ln\gamma - \frac{1}{2}\eta N$$

or

$$\frac{a^2 p}{M} N = 4Q$$

where

$$Q \equiv (\gamma^2 - 1)\ln\gamma - \frac{1}{2}\left(\frac{\gamma^2 - 1}{\gamma}\right)^2 \tag{4.74}$$

From (4.8)

$$M = a^2(1 + \gamma^2 - 2\gamma e^{-p} - 2\gamma p)/4$$

so

$$(N + 2\gamma Q)p + 2\gamma Q e^{-p} - (1 + \gamma^2)Q = 0 \tag{4.75}$$

The solution of (4.75) gives p_a , the internal pressure at which $r_y = a$. Case 4 does not arise before p reaches p_a.

Residual Stresses:

The residual stresses in this case are:

— for $a \leq r \leq c$

$$\begin{aligned}
\sigma_r^{res} &= \sigma_{rp-} = -\ln r/a \\
\sigma_\theta^{res} &= \sigma_{\theta p-} = -\ln r/a - 1 \\
\sigma_z^{res} &= 0.5(\sigma_{rp-} + \sigma_{\theta p-}) = -0.5 - \ln r/a \\
\sigma_{\theta p-} - \sigma_{rp-} &= -1
\end{aligned} \tag{4.76}$$

— for $c \leq r \leq b$, equations (4.32) apply with H = 0.

Boundary Conditions:

At r = a,

$\sigma_r^{res} = 0$ is satisfied.

At r = c , σ_r^{res} is continuous:

$$\ln c/b + A/c^2 + B(1 + \ln c^2) + C = \ln a/c$$

From (4.6)

$$A/c^2 + B(1 + \ln c^2) + C = p \tag{4.77}$$

At $r = b$,

$$\sigma_r^{res} = 0 = A/b^2 + B(1 + \ln b^2) + C \tag{4.78}$$

Equilibrium requires resultant residual force and moment to be zero (4.20a, b):

$$\text{Force} = -\int_a^c (\ln r/a + 1)dr + \int_c^b (1 + \ln r/b - A/r^2 + B(3 + 2\ln r) + C)dr$$

$$= -\int_a^c (\ln r - \ln a + 1)dr + \int_c^b [(1 + 3B + C - \ln b) + (1 + 2B)\ln r - A/r^2]dr$$

$$= -[r \ln r - r - r \ln a + r]_a^c + (1 + 3B + C - \ln b)(b - c) + (1 + 2B)[r \ln r - r]_c^b + [A/r]_c^b$$

$$= A(\frac{1}{b} - \frac{1}{c}) + B[b(1 + \ln b^2) - c(1 + \ln c^2)] + C(b - c) + cp = 0 \tag{4.79}$$

It is clear that (4.79) can be derived from (4.77) and (4.78).

$$\text{Moment} = -\int_a^c (\ln r - \ln a + 1)rdr + \int_c^b [(1 + 3B + C - \ln b) + (1 + 2B)\ln r - A/r^2]rdr$$

$$= [-\frac{r^2}{4}(2\ln r - 1) + (\ln a - 1)\frac{r^2}{2}]_a^c + [(1 + 3B + C - \ln b)\frac{r^2}{2}$$

$$+ (1 + 2B)\frac{r^2}{4}(2\ln r - 1) - A\ln r]_c^b - A\ln b^2/c^2$$

$$+ B[b^2(2 + \ln b^2) - c^2(2 + \ln c^2)] + C(b^2 - c^2) + \frac{a^2}{2} + \frac{b^2}{2} + (p - 1)c^2 = 0 \tag{4.80}$$

Equations (4.77), (4.78) and (4.80) are solved for A, B and C.

From (4.78)

$$C = -A/b^2 - B(1 + \ln b^2)$$

from (4.77)

$$A\left(\frac{1}{c^2} - \frac{1}{b^2}\right) + B(\ln c^2 - \ln b^2) = p$$

or (4.81)

$$A = \frac{b^2c^2}{b^2 - c^2}\left(p + B\ln\frac{b^2}{c^2}\right)$$

so

$$-C(b^2 - c^2) = c^2(p + B\ln b^2 - B\ln c^2) + B(1 + \ln b^2)(b^2 - c^2)$$

$$= c^2 p + B[b^2(\ln b^2 + 1) - c^2(\ln c^2 + 1)] \ . \tag{4.82}$$

Introducing (4.81) and (4.82) into (4.80):

$$A(b^2 - c^2)\ln\frac{b^2}{c^2} - B(b^2 - c^2)[b^2(2 + \ln b^2) - c^2(2 + \ln c^2)] - C(b^2 - c^2)^2 =$$

$$\frac{(a^2 + b^2 - 2c^2)}{2}\,(b^2 - c^2) + pc^2(b^2 - c^2)$$

or

$$b^2c^2\left(p + B\ln\frac{b^2}{c^2}\right)\ln\frac{b^2}{c^2} - B(b^2 - c^2)^2 = (a^2 + b^2 - 2c^2)(b^2 - c^2)/2 \ .$$

From which

$$B = \frac{(a^2 + b^2 - 2c^2)(b^2 - c^2)/2 - b^2c^2 p\ln(b^2/c^2)}{[bc\ln(b^2/c^2)]^2 - (b^2 - c^2)^2} \tag{4.83}$$

The constants of integration are thus obtained in close form.

In particular, $p = \ln(b/a)$ gives $c = a$, $B = -1/2$, $A = 0$, $C = 1/2 + \ln b$ and $\sigma_r^{res} = \sigma_\theta^{res} = 0$ for any r.

4.6 Springback

Springback occurs upon unloading. The constants A and B are related to the rotation of radial sections and the change in radius of curvature (Shaffer and Ungar [1960]).

$$2B = \frac{G}{\bar{k}} \frac{\Delta\theta}{\theta} \tag{4.84}$$

and

$$\frac{G}{\bar{k}}\left(\frac{\Delta a}{a}\right) = -\frac{A}{a^2} - B \tag{4.85}$$

where G is the shear modulus, $2\bar{k}$ is the yield stress in two-dimensional space, a is the internal radius and θ is the angle of curvature.

Continuity of displacements requires A and B to remain the same throughout the thickness. No such requirement exists for C; H is therefore introduced in (4.32).

4.7 Elastic Relaxation of the Longitudinal Residual Stresses

The longitudinal residual stresses are released by sectioning (see Chapter 5). The force resultant per unit angle is:

$$\bar{F} = \int_o^{\theta=1} \int_a^b \bar{\sigma}_z^{res}\ r dr d\theta = \int_a^b \bar{\sigma}_z^{res}\ r dr \tag{4.86}$$

The axial elastic relaxation stress is:

$$\bar{\sigma}_a^{rel} = -\frac{\bar{F}}{(b^2 - a^2)/2} \tag{4.87}$$

The moment resultant per unit angle about the center of curvature is:

$$\bar{M}_z = \int_o^{\theta=1} \int_a^b \bar{\sigma}_z^{res}\ r^2 dr d\theta = \int_a^b \bar{\sigma}_z^{res}\ r^2 dr \tag{4.88}$$

The elastic response $\bar{\sigma}$ to this moment, which is uniformly distributed over the corner width is linear in the radial direction:

$$\bar{\sigma} = -\frac{2\bar{\sigma}_b^{rel}}{b - a}\left(r - \frac{a + b}{2}\right) \tag{4.89}$$

such that, at $r = a$, $\bar{\sigma} = +\bar{\sigma}_b^{rel}$ and at $r = b$, $\bar{\sigma} = -\bar{\sigma}_b^{rel}$.

The relaxation moment is:

$$\bar{M}_z^{rel} = -\frac{2\bar{\sigma}_b^{rel}}{b - a}\int_a^b (r - \frac{a + b}{2})r^2 dr = -\frac{\bar{\sigma}_b^{rel}}{b - a}\left[\frac{b^4 - a^4}{2} - \frac{(a + b)}{3}(b^3 - a^3)\right] \tag{4.90}$$

Since $\bar{M}_z^{rel} = -\bar{M}_z$, one obtains the bending elastic relaxation stress:

$$\bar{\sigma}_b^{rel} = \frac{\bar{M}_z(b - a)}{\frac{b^4 - a^4}{2} - \frac{(a + b)(b^3 - a^3)}{3}} \tag{4.91}$$

Table 4.1 shows $\bar{\sigma}_a^{rel}$ and $\bar{\sigma}_b^{rel}$ for purely elastic unloading (*) and elasto-plastic unloading (o) for some actual corners. Comparison with experimental results will be discussed in the following chapter.

4.8 Results and Discussion

Various combinations of pressure and moment (characterized by the ratio of the pressure p to the maximum pressure p_m for which the applied moment is zero) applied to different geometries (characterized by the ratio of the external radius b to the internal radius a) were examined. Von Mises yield criterion was used. The location and extent of the yield zones are tabulated in Tables 4.2-4.6 and plotted in Fig. 4.3 for some selected b/a values. Any consistent system of units may be used with the figures and tables of this chapter, e.g. ksi for stress and inch for distance. For pure bending situations ($p = 0$), there exists an interior yield zone limited on the upper side by the neutral axis for all values of b/a. For severe bending ($a/t < 0.84$ or, equivalently, $b/a > 2.2$) with little or no pressure, an additional yield zone develops at the concave edge (in Fig. 4.3, this is shown for $b/a = 3.0$). The preceding observations were first made by Shaffer and Ungar [1960], but the following remarks have to do with the existence of pressure and are new, as far as the author knows.

The edge yield zone is small, however, and disappears rapidly as the forming pressure increases. For mild bending ($b/a < 1.80$), the interior yield zone is located above the neutral axis for moderate pressures, but below it for very small or very large pressures (e.g. $b/a = 1.2$ in Fig. 4.3). For such cases, there are two values of p for which the whole section remains elastic (these are the abscissas of the intersections of c and t_o in Fig. 4.3). For $b/a > 1.80$ the interior yield zone remains below the neutral axis for all pressures and yielding is minimal for moderate pressures ($p \approx 0.4p_m$).

In Fig. 4.3, the extent of yielding is given by the vertical height, parallel to the r-axis, of the darkened areas. Except for the cases where there are two separate yield bands (high b/a), the extent of yielding is greatest (about 13% of the thickness) when $t_o = a$, at $p \equiv p_t$, i.e., the lowest pressure at which the whole area below the neutral axis is plastic. When there are two separate yield zones, the extent of yielding may be maximum at $p = 0$. Thus, errors in residual stresses due to the assumption of purely elastic unloading are significant only for $p \simeq p_t$ and, in addition, for $p \approx 0$ when b/a is large (> 3.0).

It is recalled that r_y (Eq. 4.29) denotes a limiting radius between elastic and inelastic unloading zones. t_o is also defined as one of the limits (the other being the neutral axis c) of the interior yield zone. t_o is obtained by solving a system of equations, such as Eqs. (4.38)-(4.43), whereas r_y can be obtained directly in one step. If t_o were not assumed unknown (a logical assumption is $t_o = r_y$), the system of equations would have been overdeterminate. r_y and t_o are identical for small pressures, but strangely enough, their difference increases with p (Fig. 4.4). If r_y , and not t_o were considered, one would have reached the erroneous conclusion that the interior yield zone remains below the neutral axis for all pressures when $b/a > 1.60$ (correct value is 1.80).

Using Von Mises's yield criterion, the loading stresses and the residual stresses after both purely elastic unloading and elasto-plastic unloading (dotted lines) are studied for $b/a = 4/3$, which corresponds to $p_m = .3502\sigma_y$, and various positions of the neutral axis (Figs. 4.5a - 4.10a and Tables 4.7 - 4.18). Except for the case $c = 3.10$, for which p is close to p_t , the two solutions agree well. The assumption of elastic unloading is therefore justified, except for p close to p_t (which is expected from the discussion above, since there is only one yield zone). The two solutions compare well also with Ingvarsson's solution [1977b], shown in Figs. 4.5b - 4.10b. One reservation, however: at difference with Ingvarsson, this theory predicts that c cannot reach the value 3.50 (i.e., the neutral axis is always below midthickness) unless p becomes negative and the corner thickens upon forming (Fig. 4.10a, b).

Results also confirm that radial residual stresses are small and can reasonably be neglected (Alexander [1959]).

4.9 Summary

The first part of this study presents a simple, approximate, close-form expression for the residual stresses caused by sheet bending. This is a recast of Ingvarsson's solution [1975, 1977b], but has the advantage of simplicity without much sacrifice in accuracy.

The second part extends Shaffer and Ungar's work [1960] to include internal pressure. The validity of the assumption of purely elastic unloading is evaluated.

TABLE 4.1

RELAXATION OF z RESIDUAL STRESSES:

AXIAL AND BENDING COMPONENTS

	$\frac{p}{p_m}$	$-\frac{\Delta t}{.01t}$	° $-\frac{\bar{\sigma}_a^{rel}}{.01\sigma_y}$	° $\frac{\bar{\sigma}_b^{rel}}{.01\sigma_y}$	* $-\frac{\bar{\sigma}_a^{rel}}{.01\sigma_y}$	* $\frac{\bar{\sigma}_b^{rel}}{.01\sigma_y}$
PBC 14	0.00	0.0	.376	19.4	0.0	17.3
RFC 14	0.25	6.5	3.54	37.3	3.28	37.0
a = .109"	0.50	13.0	6.72	53.9	6.56	55.2
b = .184"	0.75	19.5	11.2	75.5	9.84	72.4
$p_m = .602\sigma_y$	1.00	26.0	13.1	84.7	13.1	88.9
PBC 13	0.00	0.0	.532	19.8	.001	17.3
	0.25	7.8	3.63	34.2	2.89	32.2
a = .102	0.50	15.7	6.22	45.1	5.78	45.8
b = .190	0.75	23.5	10.1	60.1	8.67	58.5
$p_m = .724\sigma_y$	1.00	31.3	11.6	65.7	11.6	70.7
RFC 13	0.00	0.0	.618	19.9	.001	17.3
	0.25	8.5	3.68	32.9	2.71	30.4
a = .0937	0.50	17.0	5.99	41.7	5.42	42.3
b = .185	0.75	25.5	9.63	54.3	8.12	53.3
$p_m = .786\sigma_y$	1.00	34.0	10.8	58.7	10.8	64.0
H 11	0.00	0.0	.331	19.3	0.0	17.3
Corner 1	0.25	6.1	3.51	38.6	3.41	39.1
a = .195	0.50	12.2	6.89	57.7	6.82	59.3
b = .318	0.75	18.3	11.6	82.1	10.2	78.4
$p_m = .562\sigma_y$	1.00	24.3	13.6	92.8	13.6	96.8
H 11	0.00	0.0	.263	19.1	0.0	17.3
Corner 2	0.25	5.4	3.55	41.7	3.63	43.1
a = .227	0.50	10.8	7.22	65.2	7.27	67.3
b = .349	0.75	16.2	12.1	94.8	10.9	90.3
$p_m = .499\sigma_y$	1.00	21.6	14.5	109.	14.5	112.

°elasto-plastic unloading

*elastic unloading

Table 4.1 (continued)

RELAXATION OF z RESIDUAL STRESSES:

AXIAL AND BENDING COMPONENTS

	$\frac{p}{p_m}$	$-\frac{\Delta t}{.01t}$	° $-\frac{\bar{\sigma}_a^{rel}}{.01\sigma_y}$	* $\frac{\bar{\sigma}_b^{rel}}{.01\sigma_y}$	* $-\frac{\bar{\sigma}_a^{rel}}{.01\sigma_y}$	* $\frac{\bar{\sigma}_b^{rel}}{.01\sigma_y}$
H7	0.00	0.0	.769	20.1	0.0	17.3
corner 1	0.25	9.6	3.77	31.2	2.43	28.1
a = .156	0.50	19.2	5.62	37.2	4.85	37.7
b = .338	0.75	28.9	8.82	46.6	7.28	46.7
$p_m = .889\sigma_y$	1.00	38.5	9.70	49.6	9.70	55.4
H7	0.00	0.0	.472	19.6	0.0	17.3
corner 2	0.25	7.3	3.59	35.2	3.03	33.7
a = .227	0.50	14.7	6.40	48.0	6.06	48.8
b = .408	0.75	22.0	10.5	65.1	9.09	63.0
$p_m = .679\sigma_y$	1.00	29.4	12.1	71.8	12.1	76.5
HT	0.00	0.0	.961	20.3	.002	17.3
corner 1	0.25	11.4	2.46	25.0	2.02	25.4
a = .203	0.50	22.8	5.06	31.9	4.05	32.7
b = .506	0.75	34.2	7.63	37.9	6.07	39.4
$p_m = 1.054\sigma_y$	1.00	45.6	8.10	39.5	8.09	46.1
HT	0.00	0.0	.727	20.1	.001	17.3
corner 2	0.25	9.3	3.74	31.6	2.50	28.6
a = .273	0.50	18.6	5.72	38.3	5.00	38.8
b = .576	0.75	28.0	9.04	48.5	7.50	48.3
$p_m = .861\sigma_y$	1.00	37.3	10.0	51.8	10.0	57.5

TABLE 4.2

LOCATION AND EXTENT OF YIELD ZONE

$a = 10.0$, $b = 12.0$, $t = 2.0$, $p_m = .217\sigma_y$, $M_m = 1.155\sigma_y$,

$p_a/p_m = .682$ (M_m is maximum moment, when $p = 0$.)

$\frac{p}{p_m}$	$\frac{c-a}{t}$	$\frac{r_y-a}{t}$	$\frac{t_o-a}{t}$	$\frac{t_o-r_y}{.01t}$	$\frac{\lvert t_o-c\rvert}{.01t}$	$\frac{c-a}{.01t}$	case
0.0	.477	.462	.462	0.00	1.52		1
0.1	.426	.428	.428	0.00	0.00		2
0.2	.375	.390	.391	0.02	1.63		2
0.3	.325	.348	.351	0.05	2.59		2
0.4	.275	.296	.301	0.10	2.64		2
0.5	.225	.227	.237	0.19	1.14		2
0.6	.176	.127	.145	0.35	3.11		1
0.7	.128	(-.038)	(-.081)			12.8	4
0.8	.080					7.98	4
0.9	.032					3.22	4
1.0	(-.015)					0.0	4

TABLE 4.3

LOCATION AND EXTENT OF YIELD ZONE

$a = 3.0,\ b = 4.0,\ p_m = .350\sigma_y,\ p_a/p_m = .659,\ M_m = .289\sigma_y$

$\frac{p}{p_m}$	$\frac{c-a}{t}$	$\frac{r_y-a}{t}$	$\frac{t_o-a}{t}$	$\frac{t_o-r_y}{.01t_o}$	$\frac{c-t_o}{.01t}$	$\frac{c-a}{.01t}$	case
0.0	.464	.440	.440	-.008	2.40		1
0.1	.412	.405	.406	.009	.63		1
0.2	.361	.368	.369	.046	.85		2
0.25	.335	.347	.349	.077	1.41		2
0.3	.310	.324	.328	.12	1.80		2
0.4	.260	.270	.278	.25	1.82		2
0.5	.211	.198	.214	.49	.30		2
0.6	.163	.092	.122	.95	4.08		1
0.7	.115					11.5	4
0.75	.092					9.17	4
0.8	.068					6.84	4
0.9	.022					2.22	4
1.0	(-.023)					0.	4

TABLE 4.4

LOCATION AND EXTENT OF YIELD ZONE

$a = 10.0,\ b = 18.0,\ p_m = .764\sigma_y,\ p_a/p_m = .596,\ M_m = 16.0\sigma_y$

$\frac{p}{p_m}$	$\frac{c-a}{t}$	$\frac{r_y-a}{t}$	$\frac{t_o-a}{t}$	$\frac{t_o-r_y}{.01t_o}$	$\frac{c-t_o}{.01t}$	$\frac{c-a}{.01t}$	case
0.0	.427	.380	.379	-.071	4.82		1
0.1	.372	.345	.345	.020	2.75		1
0.2	.320	.306	.309	.20	1.08		1
0.3	.268	.260	.268	.53	.068		1
0.4	.219	.201	.219	1.17	.049		1
0.5	.171	.120	.155	2.47	1.63		1
0.6	.125	(-.006)	.060	5.00	6.54		1
0.7	.080				8.02		4
0.8	.037				3.69		4
0.9	(-.005)				0		
1.0	(-.045)				0		

TABLE 4.5

LOCATION AND EXTENT OF YIELD ZONES

$a = 10.0,\ b = 22.0,\ p_m = 1.079\sigma_y,\ p_a/p_m = .556,\ M_m = 3.60\sigma_y$

$\frac{p}{p_m}$	$\frac{c-a}{t}$	$\frac{r_y-a}{t}$	$\frac{t_o-a}{t}$	$\frac{t_o-r_y}{.01t_o}$	$\frac{c-t_o}{.01t}$	$\frac{c-a}{.01t}$	$\frac{t_i-a}{.01t}$	case
0.0	.403	.341	.339	-.17	6.32		.034	3
0.1	.346	.306	.306	.007	3.98			1
0.2	.292	.267	.271	.35	2.12			1
0.3	.241	.220	.231	1.01	1.00			1
0.4	.192	.159	.182	2.31	.95			1
0.5	.145	.071	.119	5.05	2.61			1
0.6	.100					10.05		4
0.7	.058					5.79		4
0.8	.017					1.72		4
0.9	-.022					0.0		
1.0	-.059					0.0		

TABLE 4.6

LOCATION AND EXTENT OF YIELD ZONES

$a = 10.0,\ b = 30.0,\ p_m = 1.648\sigma_y,\ p_a/p_m = .498,\ M_m = 100.0\sigma_y$

$\frac{p}{p_m}$	$\frac{c-a}{t}$	$\frac{r_y-a}{t}$	$\frac{t_o-a}{t}$	$\frac{t_o-r_y}{.01t_o}$	$\frac{c-t_o}{.01t}$	$\frac{c-a}{.01t}$	$\frac{t_i-a}{.01t}$	case
0.0	.366	.286	.284	-.26	8.20		1.97	3
0.1	.306	.252	.252	-.06	5.48		.05	3
0.2	.251	.213	.218	.67	3.27			1
0.3	.199	.165	.180	2.13	1.96			1
0.4	.151	.099	.132	5.21	1.88			1
0.5	.106	-.003	.068	12.5	3.78			1
0.6	.064					6.45		4
0.7	.026					2.56		4
0.8	-.010					0.0		
0.9	-.044					0.0		
1.0	-0.076					0.0		

TABLE 4.7

LOADING STRESSES

$c = 3.00,\ p = .332\sigma_y,\ M = .0276\sigma_y,$

$\Delta t/t = -14.4\%$

r	$\bar{\sigma}_{rp}/\sigma_y$	$\bar{\sigma}_{\theta p}/\sigma_y$	$\bar{\sigma}_{zp}/\sigma_y$
a = c = 3.0	-.332	-1.487	-.909
a = c = 3.0	-.332	.822	.245
3.1	-.294	.860	.283
3.2	-.258	.897	.320
3.3	-.222	.933	.355
3.4	-.188	.967	.390
3.5	-.154	1.001	.423
3.6	-.122	1.033	.456
3.7	-.0900	1.065	.487
3.8	-.0592	1.095	.518
3.9	-.0292	1.125	.548
b = 4.0	0.0	1.155	.577

TABLE 4.8

LOADING STRESSES

$c = 3.10,\ p = .256\sigma_y,\ M = .130\sigma_y,$

$\Delta t/t = -\ 11.1\%$

r	$\bar{\sigma}_{rp}/\sigma_y$	$\bar{\sigma}_{\theta p}/\sigma_y$	$\bar{\sigma}_{zp}/\sigma_y$
a = 3.0	-.256	-1.411	-.834
c = 3.1	-.294	-1.449	-.872
c = 3.1	-.294	.860	.283
3.2	-.258	.897	.320
3.3	-.222	.933	.355
3.4	-.188	.967	.390
3.5	-.154	1.001	.423
3.6	-.122	1.033	.456
3.7	-.0900	1.065	.487
3.8	-.0592	1.095	.518
3.9	-.0292	1.125	.548
b = 4.0	0.0	1.155	.577

TABLE 4.9

LOADING STRESSES

$c = 3.20$, $p = .183\sigma_y$, $M = .206\sigma_y$,

$\Delta t/t = -7.93\%$

r	$\bar{\sigma}_{rp}/\sigma_y$	$\bar{\sigma}_{\theta p}/\sigma_y$	$\bar{\sigma}_{zp}/\sigma_y$
a = 3.0	-.183	-1.338	-.760
3.1	-.221	-1.376	-.798
c = 3.2	-.258	-1.412	-.835
c = 3.2	-.258	.897	.320
3.3	-.222	.933	.355
3.4	-.188	.967	.390
3.5	-.154	1.001	.423
3.6	-.122	1.033	.456
3.7	-.0900	1.065	.487
3.8	-.0592	1.095	.518
3.9	-.0292	1.125	.548
4.0	0.0	1.155	.577

TABLE 4.10

LOADING STRESSES

$c = 3.30$, $p = .112\sigma_y$, $M = .257\sigma_y$,

$\Delta t/t = -4.85\%$

r	$\bar{\sigma}_{rp}/\sigma_y$	$\bar{\sigma}_{\theta p}/\sigma_y$	$\bar{\sigma}_{zp}/\sigma_y$
a = 3.0	-.112	-1.267	-.689
3.1	-.150	-1.305	-.727
3.2	-.187	-1.341	-.764
c = 3.3	-.222	-1.377	-.800
c = 3.3	-.222	.933	.355
3.4	-.188	.967	.390
3.5	-.154	1.001	.423
3.6	-.122	1.033	.456
3.7	-.0900	1.065	.487
3.8	-.0592	1.095	.518
3.9	-.0292	1.125	.548
4.0	0.0	1.155	.577

TABLE 4.11

LOADING STRESSES

$c = 3.40,\ p = .0431\sigma_y,\ M = .284\sigma_y,$

$\Delta t/t = -1.87\%$

r	$\bar{\sigma}_{rp}/\sigma_y$	$\bar{\sigma}_{\theta p}/\sigma_y$	$\bar{\sigma}_{zp}/\sigma_y$
a = 3.0	-.0431	-1.198	-.620
3.1	-.0810	-1.236	-.658
3.2	-.118	-1.272	-.695
3.3	-.153	-1.308	-.730
c = 3.4	-.188	-1.342	-.765
c = 3.4	-.188	.967	.390
3.5	-.154	1.001	.423
3.6	-.122	1.033	.456
3.7	-.0900	1.065	.487
3.8	-.0592	1.095	.518
3.9	-.0292	1.125	.548
b = 4.0	0.0	1.155	.577

TABLE 4.12

LOADING STRESSES

$c = 3.464,\ p = 0.0,\ M = .289\sigma_y,$

$\Delta t/t = 0.0$

r	$\bar{\sigma}_{rp}/\sigma_y$	$\bar{\sigma}_{\theta p}/\sigma_y$	$\bar{\sigma}_{zp}/\sigma_y$
a = 3.0	0.0	-1.155	-.577
3.1	-.0379	-1.193	-.615
3.2	-.0745	-1.229	-.652
3.3	-.110	-1.265	-.687
3.4	-.144	-1.299	-.722
c = 3.464	-.166	-1.321	-.743
c = 3.464	-.166	.989	.411
3.5	-.154	1.001	.423
3.6	-.122	1.033	.456
3.7	-.0900	1.065	.487
3.8	-.0592	1.095	.518
3.9	-.0292	1.125	.548
b = 4.0	0.0	1.155	.577

TABLE 4.13

RESIDUAL STRESSES

$c = 3.00,\ p = p_\ell = .332\sigma_y,\ M = .0276\sigma_y,\ \Delta t/t = -14.4\%$

r	° $\bar{\sigma}_r^{res}/\sigma_y$	* $\bar{\sigma}_r^{res}/\sigma_y$	° $\bar{\sigma}_\theta^{res}/\sigma_y$	* $\bar{\sigma}_\theta^{res}/\sigma_y$	° $\bar{\sigma}_r^{res}/\sigma_y$	* $\bar{\sigma}_r^{res}/\sigma_y$
a = c = 3.0	0.0	0.0	-1.155	-2.49	-.577	-1.111
a = c = 3.0	0.0	0.0	0.0	-.181	.0981	.0439
3.1	0.0	-.0051	0.0	-.138	.113	.0703
3.2	0.0	-.0086	0.0	-.0980	.128	.0959
3.3	0.0	-.0108	0.0	-.0606	.142	.121
3.4	0.0	-.0117	0.0	-.0254	.156	.145
3.5	0.0	-.0116	0.0	.0077	.169	.168
3.6	0.0	-.0107	0.0	.0391	.182	.191
3.7	0.0	-.0089	0.0	.0687	.195	.213
3.8	0.0	-.0065	0.0	.0969	.207	.234
3.9	0.0	-.0035	0.0	.124	.219	.255
b = 4.0	0.0	0.0	0.0	.149	.231	.276

*elastic unloading   °elasto-plastic unloading

TABLE 4.14

RESIDUAL STRESSES

$c = 3.10,\ p = .256\sigma_y,\ M = .130\sigma_y,\ \Delta t/t = -11.1\%$

r	° $\bar{\sigma}_r^{res}/\sigma_y$	* $\bar{\sigma}_r^{res}/\sigma_y$	° $\bar{\sigma}_\theta^{res}/\sigma_y$	* $\bar{\sigma}_\theta^{res}/\sigma_y$	° $\bar{\sigma}_z^{res}/\sigma_y$	* $\bar{\sigma}_z^{res}/\sigma_y$
a = 3.0	0.0	0.0	-1.155	-1.466	-.577	-.773
c = 3.1	-.0379	-.0506	-1.193	-1.670	-.615	-.865
c = 3.1	-.0379	-.0506	.606	.639	.284	.290
3.2	-.0197	-.0310	.484	.519	.267	.274
3.3	-.0062	-.0160	.369	.407	.251	.259
3.4	.0033	-.0051	.261	.302	.235	.245
3.5	.0092	.0022	.160	.203	.220	.231
3.6	.0120	.0065	.0647	.110	.205	.217
3.7	.0122	.0081	-.0256	.220	.191	.204
3.8	.0101	.0074	-.111	-.0614	.177	.191
3.9	.0059	.0046	-.192	-.141	.163	.178
b = 4.0	0.0	0.0	-.270	-.216	.150	.166

*elastic unloading   °elasto-plastic unloading

TABLE 4.15

RESIDUAL STRESSES

$c = 3.20$, $t_o = 3.196$, $p = .183\sigma_y$, $M = .206\sigma_y$, $\Delta t/t = -7.93\%$

r	° $\bar{\sigma}_r^{res}/\sigma_y$	* $\bar{\sigma}_r^{res}/\sigma_y$	° $\bar{\sigma}_\theta^{res}/\sigma_y$	* $\bar{\sigma}_\theta^{res}/\sigma_y$	° $\bar{\sigma}_z^{res}/\sigma_y$	* $\bar{\sigma}_z^{res}/\sigma_y$
a = 3.0	0.0	0.0	-.526	-.625	-.462	-.492
3.1	-.0228	-.0256	-.884	-.960	-.591	-.615
t_o = 3.196	-.0537		-1.208		-.712	
t_o = 3.196	-.0537		-1.208		-.631	
c = 3.2	-.0550	-.0598	-1.210	-1.274	-.632	-.734
c = 3.2	-.0550	-.0598	1.089	1.035	.438	.420
3.3	-.0241	-.0300	.843	.810	.388	.376
3.4	-.0020	-.0085	.612	.598	.339	.333
3.5	.0124	.0059	.395	.399	.291	.291
3.6	.0201	.0142	.190	.211	.245	.250
3.7	.0221	.0171	-.0038	.0341	.200	.210
3.8	.0190	.0154	-.187	-.134	.157	.172
3.9	.0114	.0095	-.361	-.293	.114	.134
4.0	0.0	0.0	-.527	-.445	.0728	.0974

*elastic unloading   °elasto-plastic unloading

TABLE 4.16

RESIDUAL STRESSES

$c = 3.30,\ p = .112\sigma_y,\ M = .257\sigma_y,\ \Delta t/t = -4.85\%$

r	° $\bar{\sigma}_r^{res}/\sigma_y$	* $\bar{\sigma}_r^{res}/\sigma_y$	° $\bar{\sigma}_\theta^{res}/\sigma_y$	* $\bar{\sigma}_\theta^{res}/\sigma_y$	° $\bar{\sigma}_z^{res}/\sigma_y$	* $\bar{\sigma}_z^{res}/\sigma_y$
a = 3.0	0.0	0.0	.101	.0388	-.245	-.264
3.1	-.0039	-.0057	-.338	-.386	-.394	-.408
3.2	-.0209	-.0239	-.751	-.785	-.537	-.548
c = 3.3	-.0489	-.0527	-1.139	-1.161	-.676	-.684
c = 3.3	-.0489	-.0527	1.106	1.149	.528	.471
t_o = 3.319	-.0423		1.112		.535	
t_o = 3.319	-.0423		1.112		.466	
3.4	-.0177	-.0216	.873	.863	.412	.408
3.5	.0037	.0002	.593	.595	.348	.348
3.6	.0164	.0128	.329	.342	.286	.289
3.7	.0215	.0185	.0804	.103	.225	.231
3.8	.0199	.0177	-.156	-.123	.166	.176
3.9	.0125	.0113	-.380	-.338	.109	.121
b = 4.0	0.0	0.0	-.593	-.542	.0532	.0682

* elastic unloading   ° elasto-plastic unloading

TABLE 4.17

RESIDUAL STRESSES

$c = 3.40$, $p = .0431\sigma_y$, $M = .284\sigma_y$, $\Delta t/t = -1.87\%$

r	° $\bar{\sigma}_r^{res}/\sigma_y$	* $\bar{\sigma}_r^{res}/\sigma_y$	° $\bar{\sigma}_\theta^{res}/\sigma_y$	* $\bar{\sigma}_\theta^{res}/\sigma_y$	° $\bar{\sigma}_z^{res}/\sigma_y$	* $\bar{\sigma}_z^{res}/\sigma_y$
$a = 3.0$	0.0	0.0	.556	.532	-.0815	-.0886
3.1	.0100	.0094	.0729	.0548	-.238	-.0244
3.2	.0049	.0037	-.380	-.392	-.390	-.0395
3.3	-.0133	-.0147	-.805	-.813	-.538	-.0540
$t_o = 3.397$	-.0417		-1.196		-.677	
$t_o = 3.397$	-.0417		-1.196		-.619	
$c = 3.4$	-.0425	-.0441	-1.197	-1.210	-.620	-.682
$c = 3.4$	-.0425	-.0441	1.103	1.100	.474	.473
3.5	-.0143	-.0158	.791	.792	.402	.402
3.6	.0039	.0025	.497	.502	.332	.334
3.7	.0135	.0123	.219	.228	.265	.267
3.8	.0154	.0145	-.0444	-.0317	.199	.202
3.9	.0106	.0101	-.294	-.278	.134	.139
$b = 4.0$	0.0	0.0	-.532	-.512	.0715	.0773

*elastic unloading   °elasto-plastic unloading

TABLE 4.18

RESIDUAL STRESSES

$c = 3.464,\ p = 0.0,\ M = .289\sigma_y,\ \Delta t/t = 0.0$

r	° $\bar{\sigma}_r^{res}/\sigma_y$	* $\bar{\sigma}_r^{res}/\sigma_y$	° $\bar{\sigma}_\theta^{res}/\sigma_y$	* $\bar{\sigma}_\theta^{res}/\sigma_y$	° $\bar{\sigma}_z^{res}/\sigma_y$	* $\bar{\sigma}_z^{res}/\sigma_y$
a = 3.0	0.0	0.0	.760	.761	-.0031	-.0027
3.1	.0165	.0165	.269	.270	-.161	-.160
3.2	.0171	.0172	-.191	-.190	-.313	-.313
3.3	.0042	.0043	-.623	-.622	-.461	-.460
3.4	-.0203	-.0202	-1.031	-1.030	-.604	-.604
t_o = 3.440	-.0330		-1.188		-.660	
t_o = 3.440	-.0330		-1.188		-.610	
c = 3.464	-.0410	-.0412	-1.196	-1.279	-.618	-.693
c = 3.464	-.0410	-.0412	1.030	1.030	.461	.461
3.5	-.0306	-.0308	.918	.918	.435	.436
3.6	-.0085	-.0086	.618	.619	.365	.365
3.7	.0046	.0045	.335	.336	.297	.297
3.8	.0097	.0097	.0673	.0682	.230	.231
3.9	.0079	.0079	-.187	-.186	.166	.166
b = 4.0	0.0	0.0	-.428	-.427	.102	.103

*elastic unloading   °elasto-plastic unloading

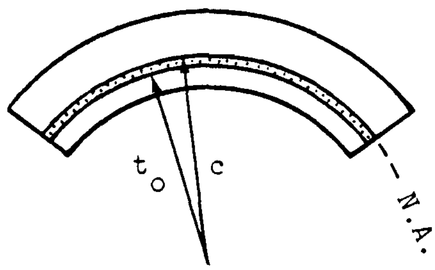

Fig. 4.1 Yielded Zone After Unloading (Case 1)

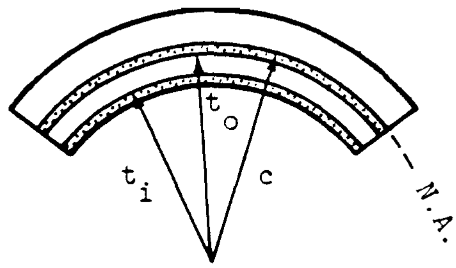

Fig. 4.2 Yielded Zones After Unloading (Case 3)

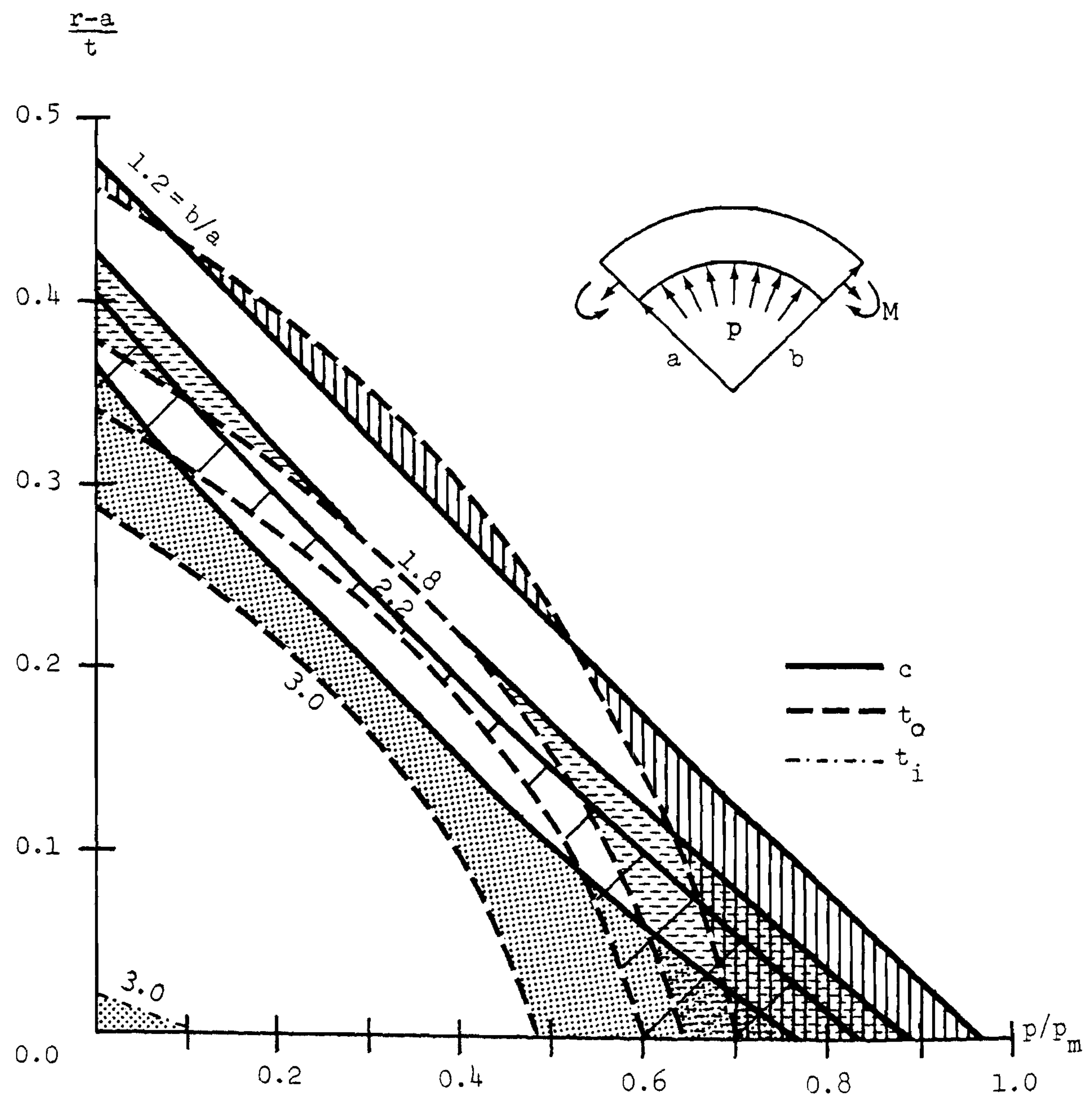

Fig. 4.3 Location and Extent of Yield Zones.

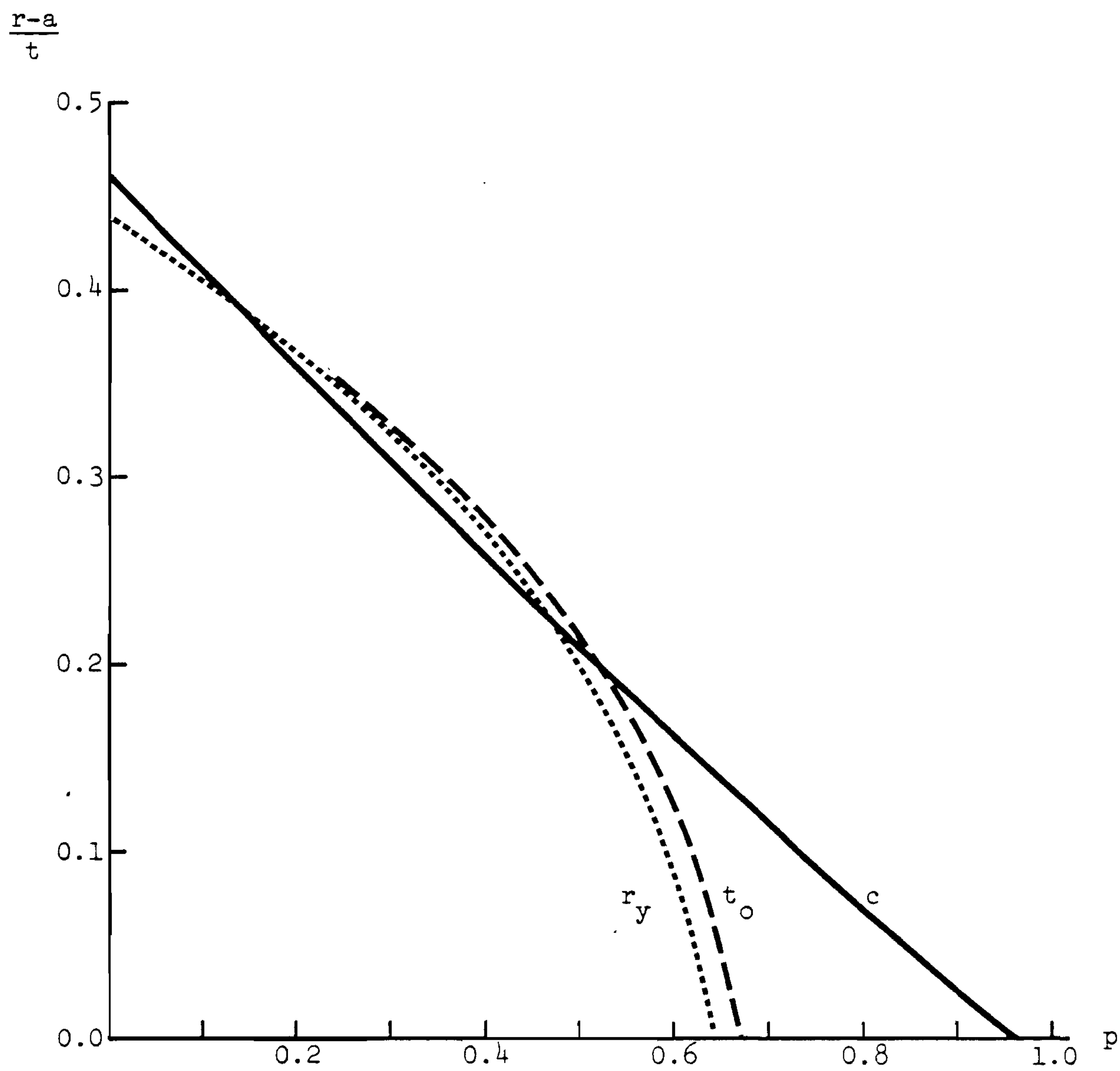

Fig. 4.4 Some Radii of Interest for the Case b/a = 1.33

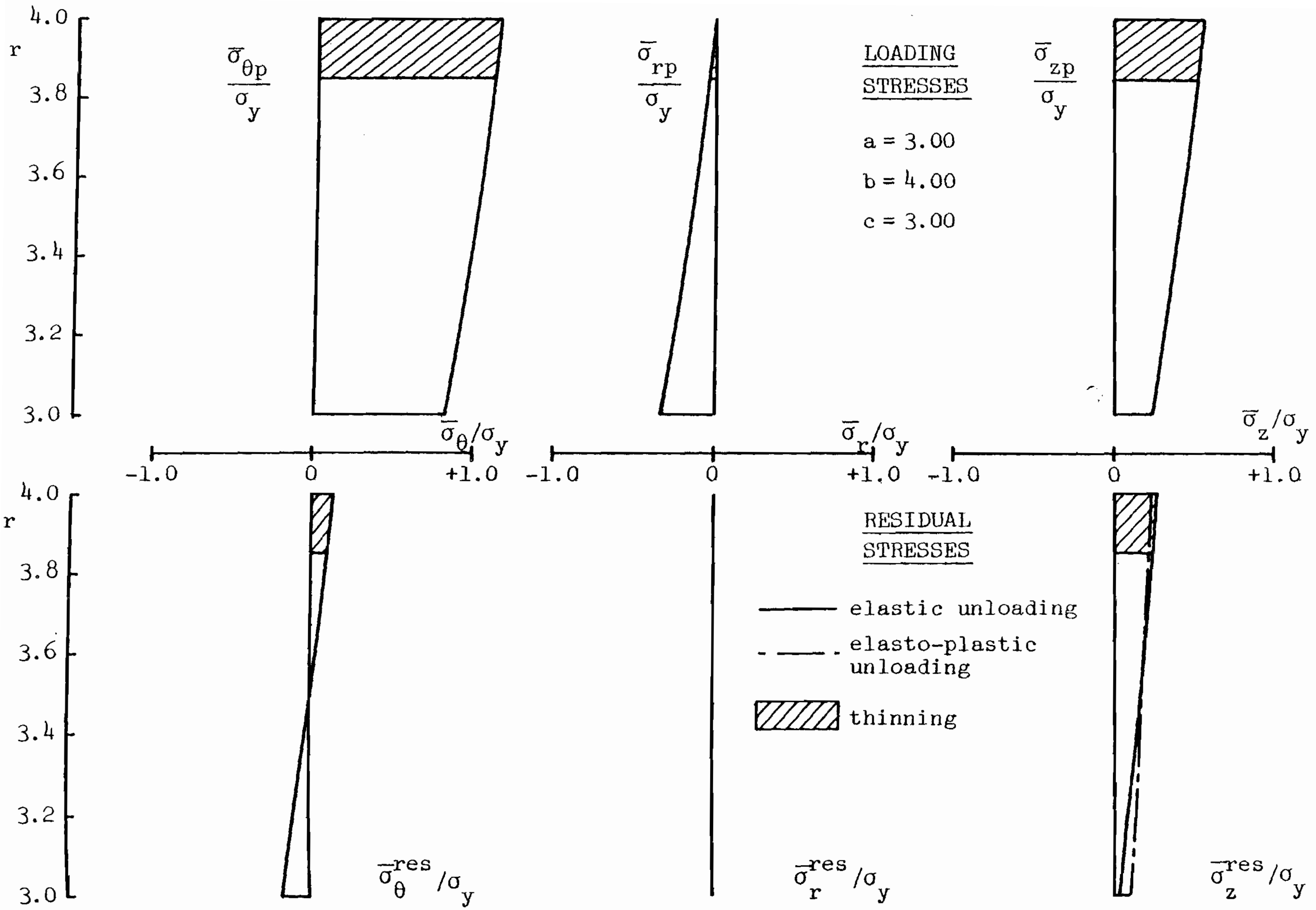

Fig. 4.5a Loading and Residual Stresses

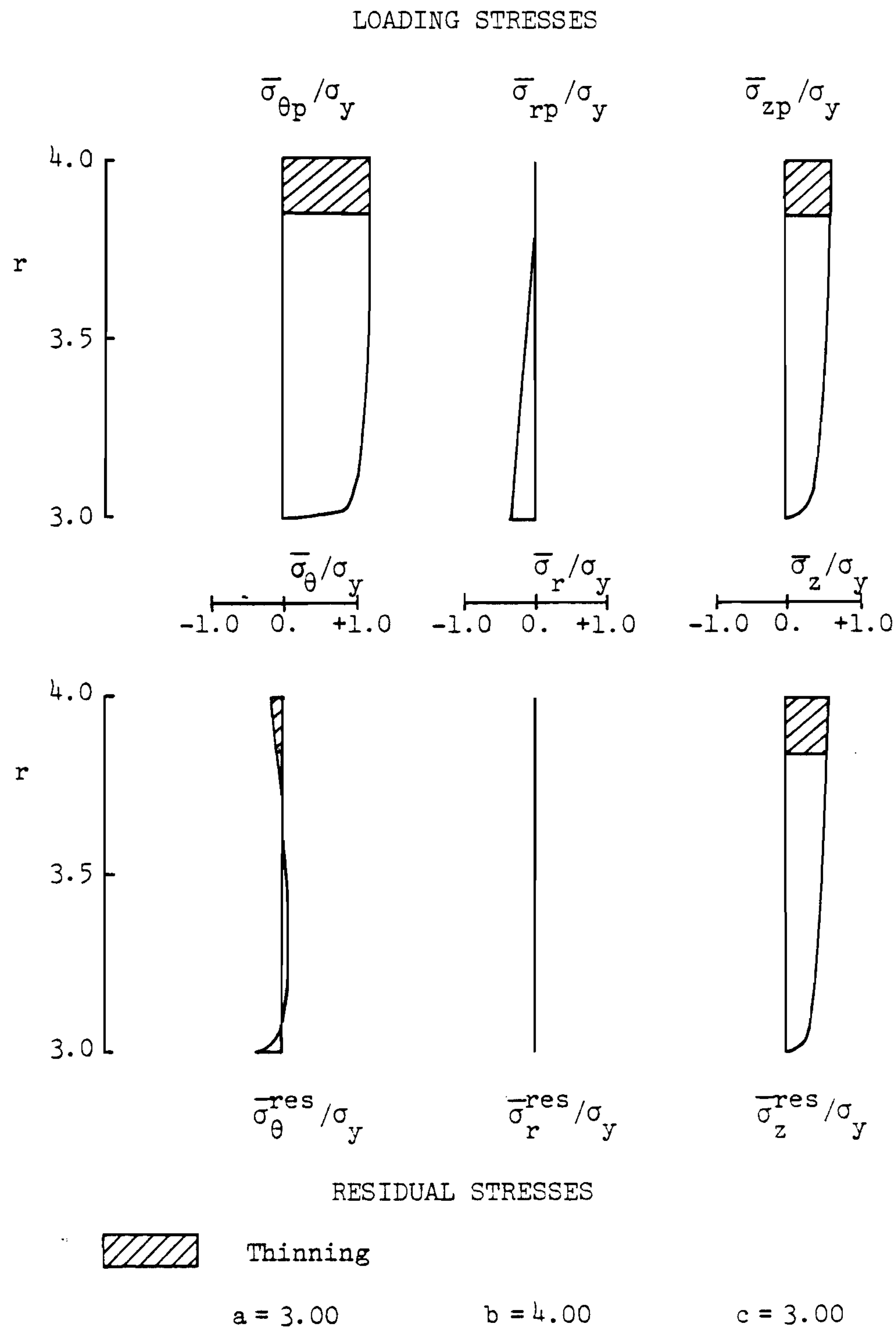

Fig. 4.5b Loading and Residual Stresses (Ingvarsson [1977b])

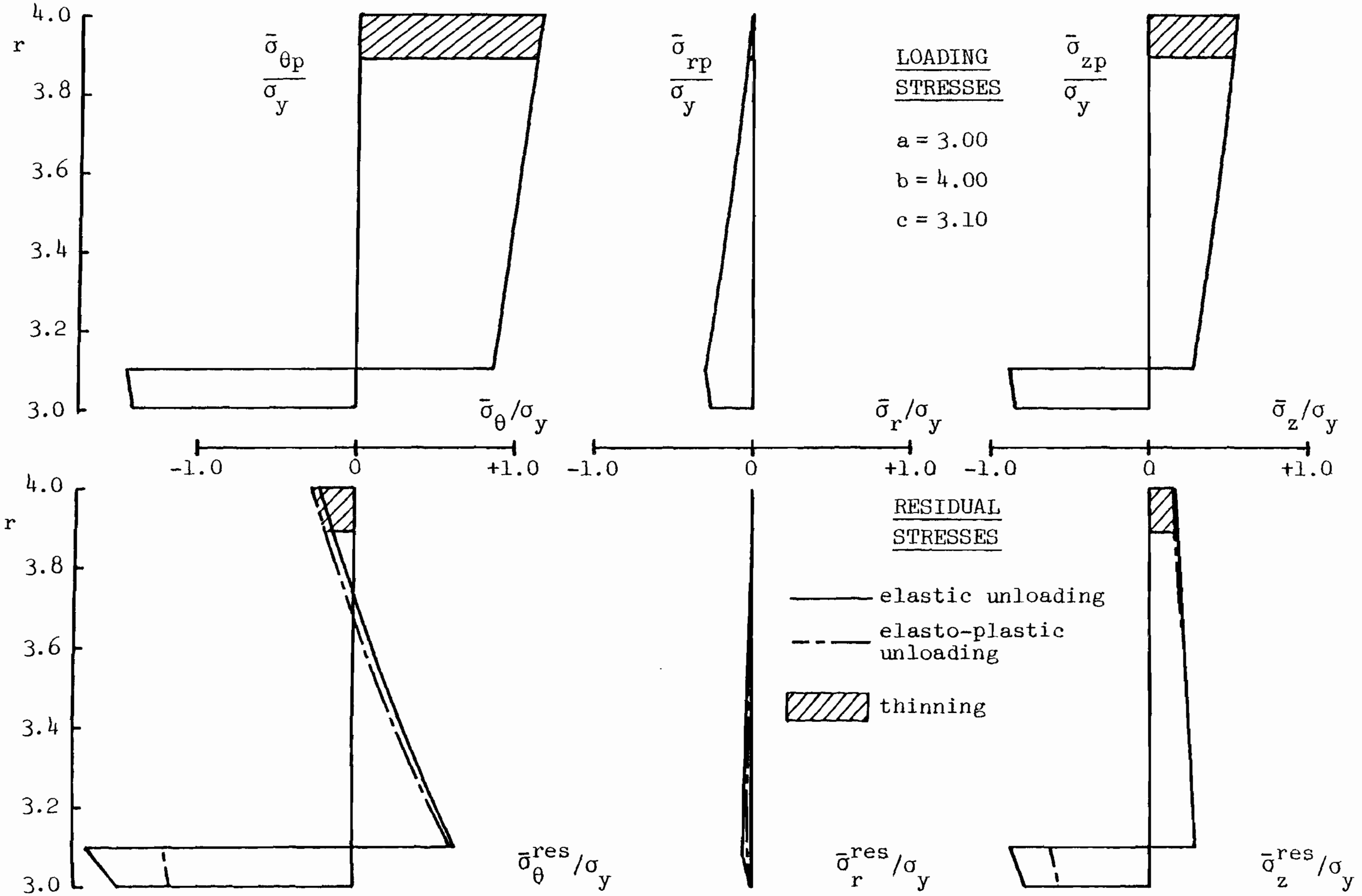

Fig. 4.6a Loading and Residual Stresses

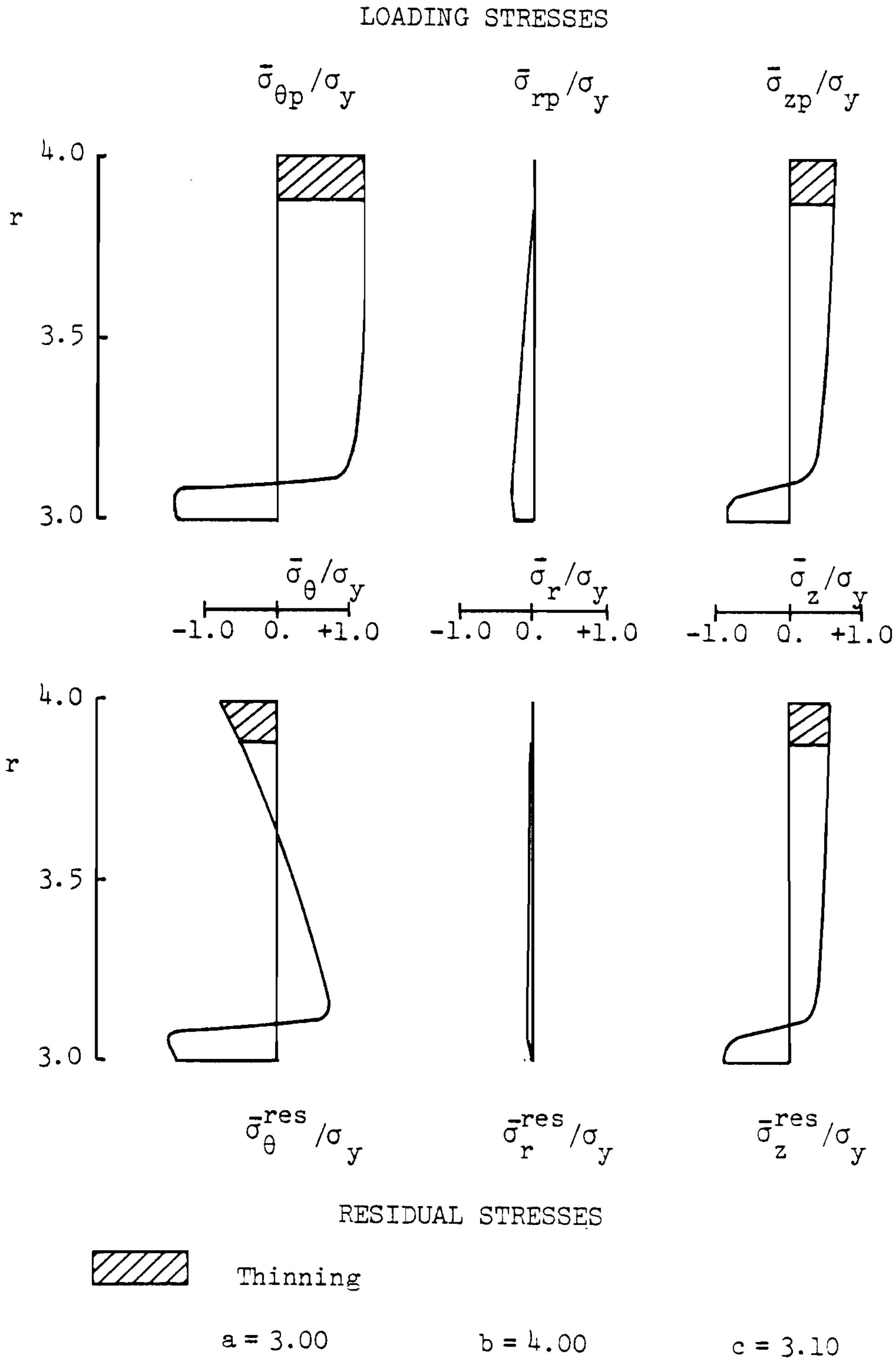

Fig. 4.6b Loading and Residual Stresses (Ingvarsson [1977b])

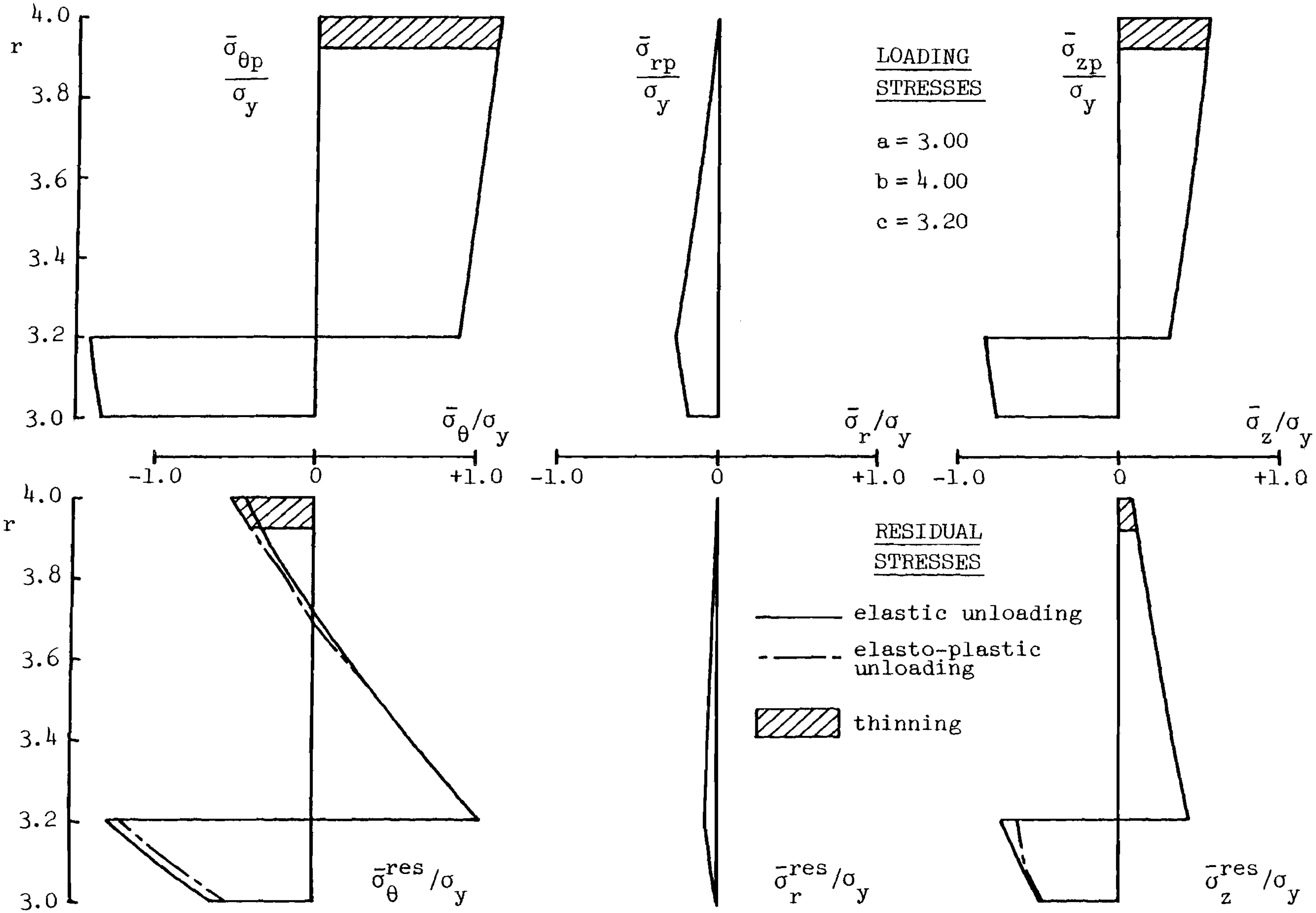

Fig. 4.7a Loading and Residual Stresses

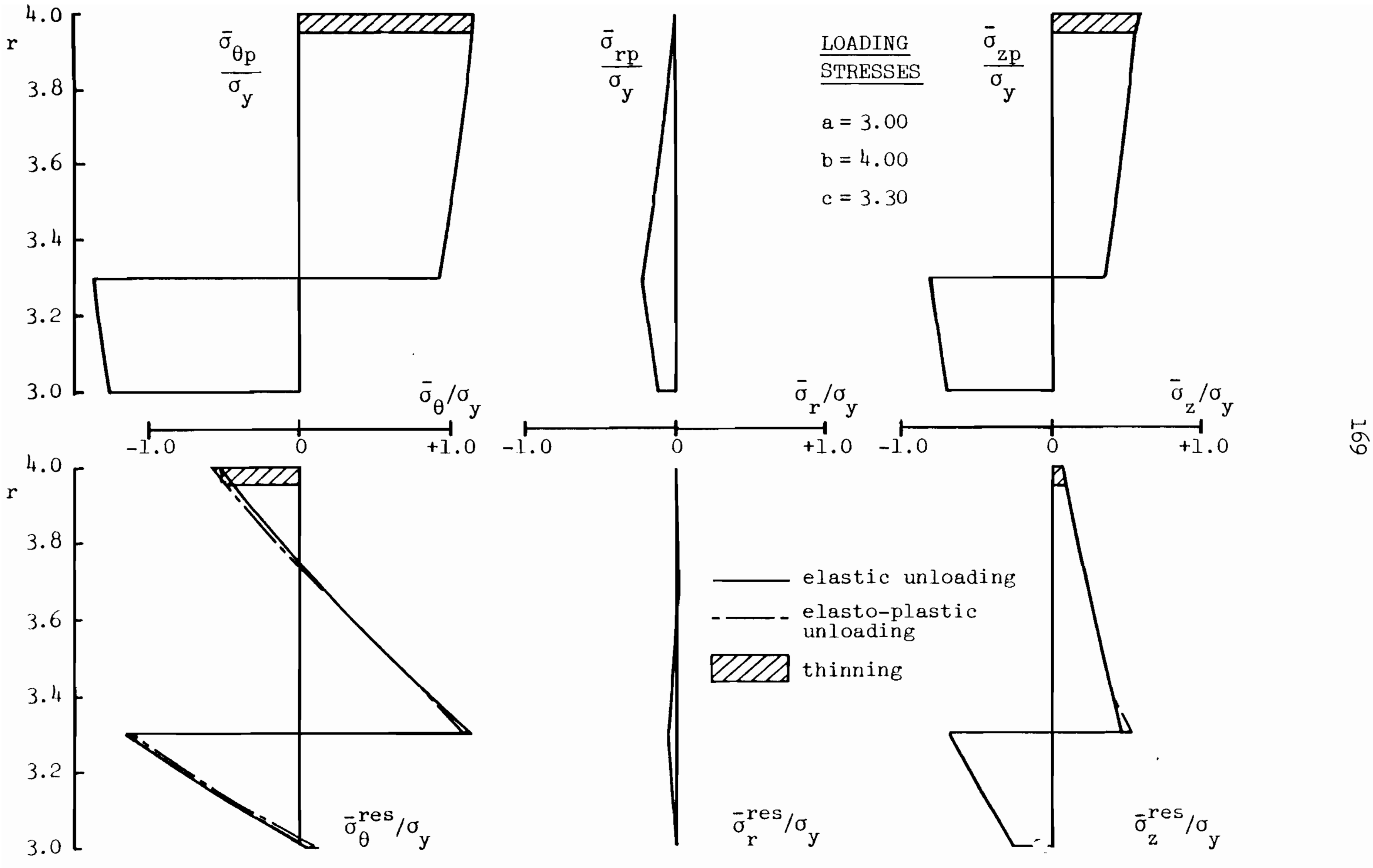

Fig. 4.8a Loading and Residual Stresses

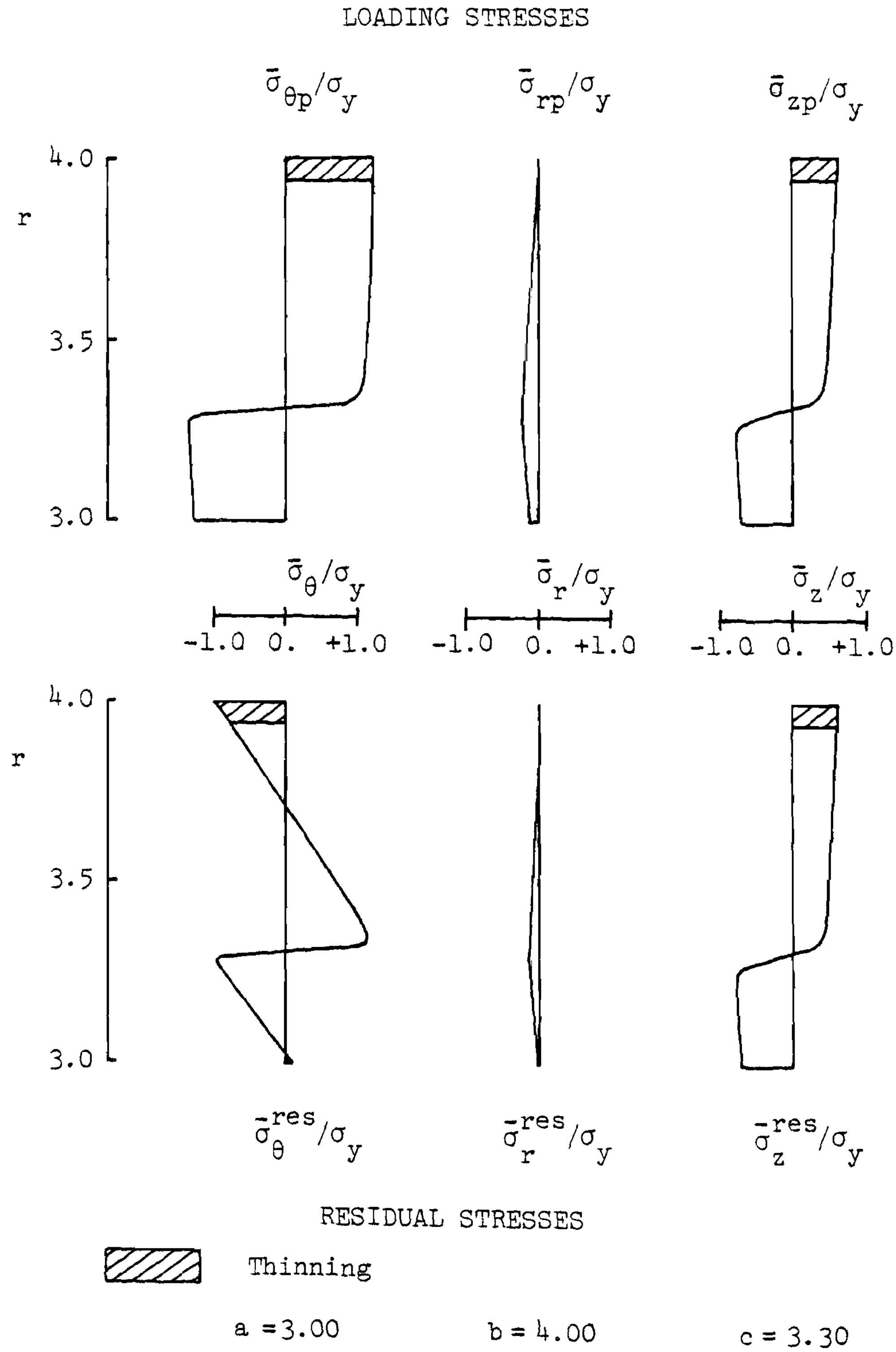

Fig. 4.8b Loading and Residual Stresses (Ingvarsson [1977])

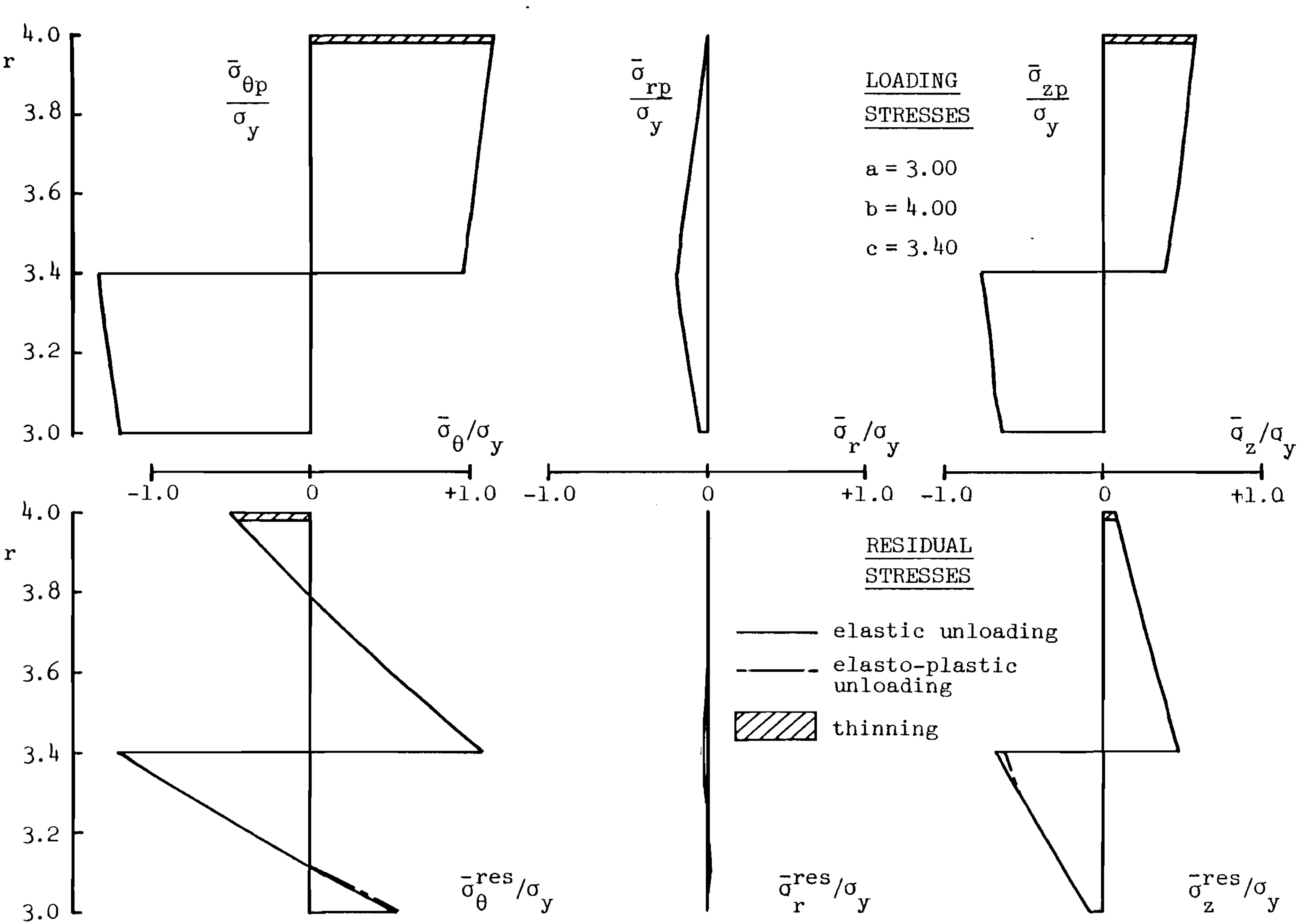

Fig. 4.9a Loading and Residual Stresses

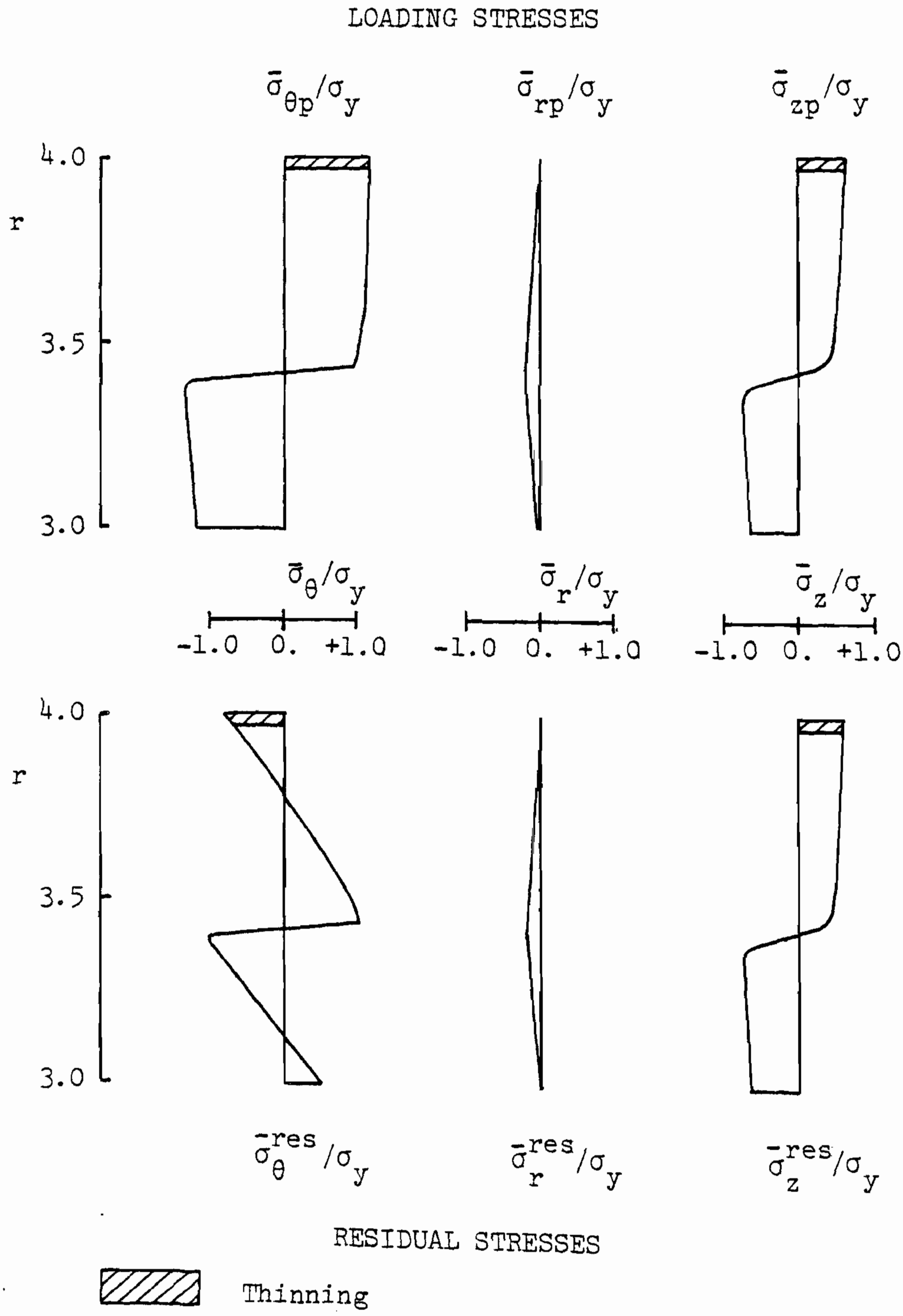

a = 3.00 b = 4.00 c = 3.40

Fig. 4.9b Loading and Residual Stresses (Ingvarsson [1977b])

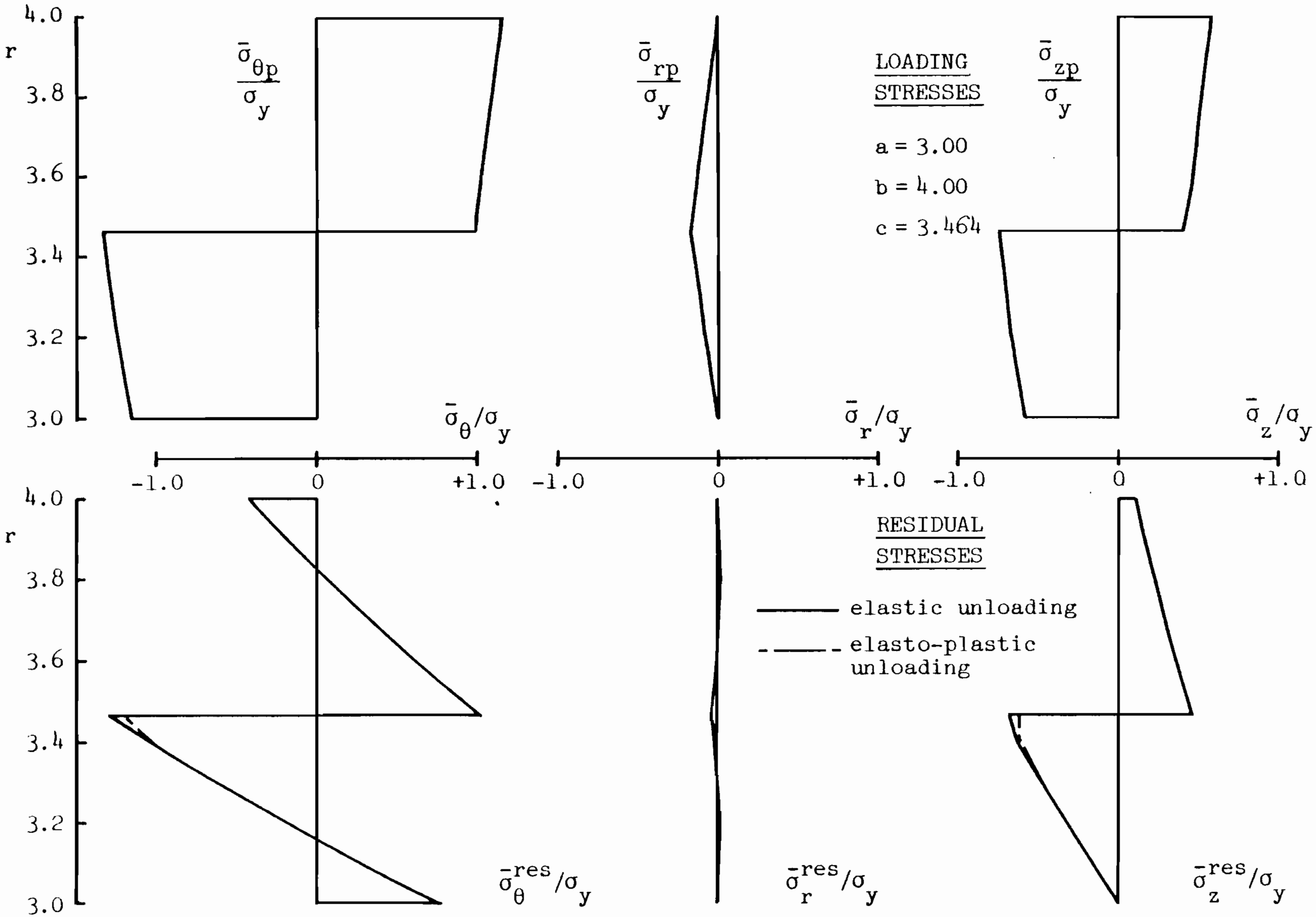

Fig. 4.10a Loading and Residual Stresses

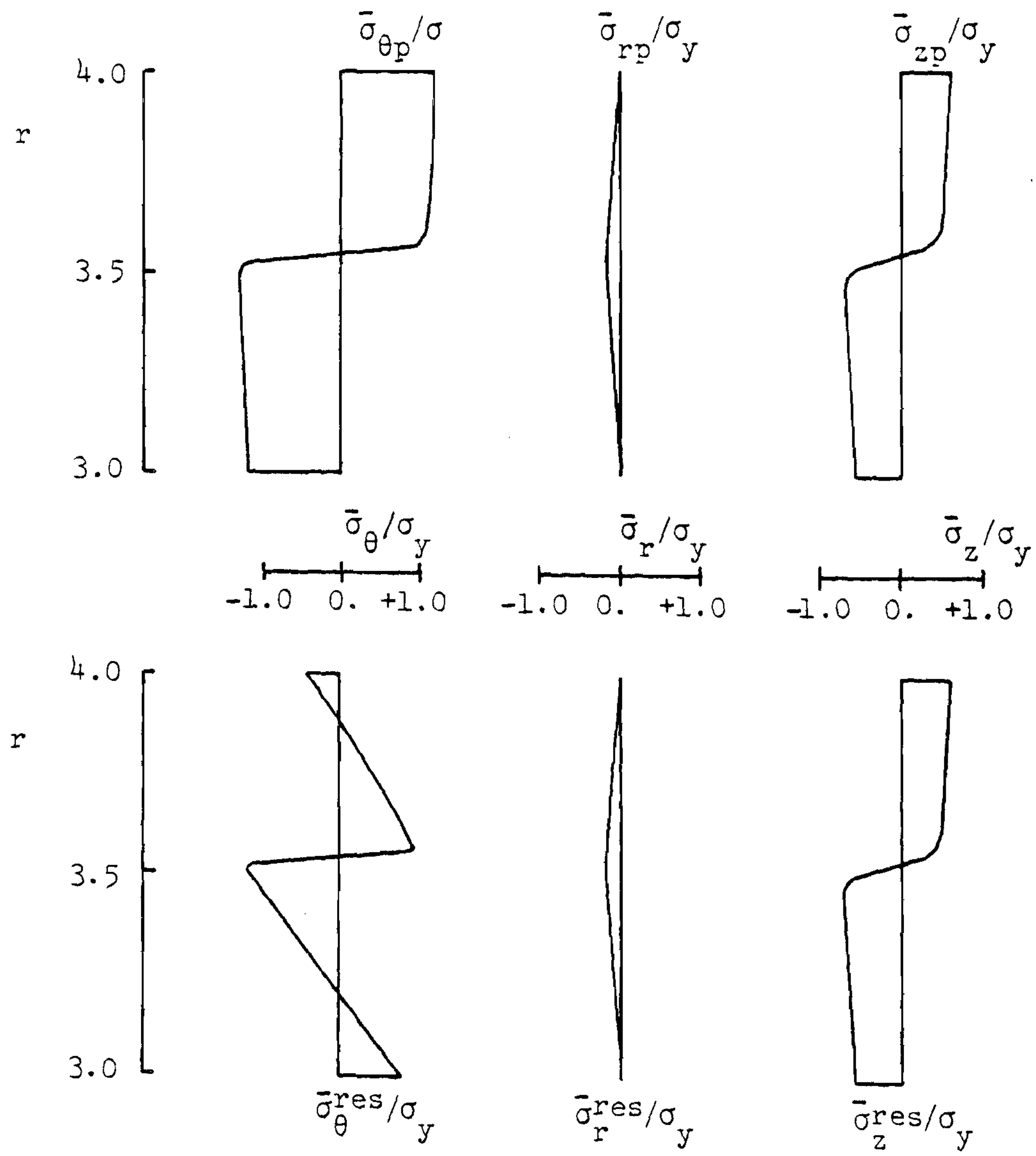

RESIDUAL STRESSES

a=3.00 b=4.00 c=3.50

Fig. 4.10b Loading and Residual Stresses.
(Ingvarsson [1977])

CHAPTER 5

RESIDUAL STRESSES DUE TO COLD-FORMING: EXPERIMENTS

5.1 Introduction

Residual stresses are in equilibrium and are most often measured by disturbing this equilibrium by more or less destructive methods and measuring the effect of this disturbance. Denton [1966a] and Meyer [1967] have provided very good surveys of the various methods of measuring residual stresses. The following brief summary is not meant to be exhaustive.

5.2 Literature Survey

5.2.1 Non-Destructive Techniques

Of the non-destructive techniques, measurement by X-ray is the most frequently used. The locked-in stresses change the crystal lattice spacing, which can be measured by X-Ray diffraction. However, only surface stresses resulting from a superposition of micro- and macrostresses can be detected in this way. (Macrostresses are produced by external factors influencing various parts of a body <u>differently</u>, even though the material may be isotropic and homogeneous. On the other hand, external factors acting <u>uniformly</u> upon the body may give rise to internal microstresses due to textural inhomogeneities of the material. Microstresses (caused, for example, by quenching a two-phase alloy) are usually on a granular scale and often randomly distributed).

Ultrasound techniques have also been used. The velocity of propagation of sound is a function of the density, which increases in the presence of compression and decreases in the presence of tension. Since the ease of penetration is inversely proportional to the wavelength, ultrasound is more effective than audible sound. Unfortunately, ultrasonic methods only provide information on the difference between the principal residual stresses and not on their absolute magnitude.

It has also been noticed that residual tension makes metal appear softer and, conversely, residual compression makes them appear harder than stress-free metals. This is the basis of the hardness test, used as a non-destructive means to measure residual stresses.

5.2.2 Semi Destructive Techniques

One relatively non-destructive technique is that of hole drilling. It can only determine local stresses at depths not exceeding half the hole diameter. Tebedge et al [1972] provided a detailed description of the method, together with a discussion of the relative merits of two different methods of strain measurement (electric strain gages gave good results whereas a mechanical gage did not, when used with the hole-drilling technique). Ross and Chen [1975], Chen and Ross [1977] used this technique to measure the variation of residual stresses in the thickness direction of a circular tube. Only few investigators have concerned themselves with the distribution of residual stresses over the thickness. Another such study, on a jumbo section, was performed at Lehigh (Brozetti et al [1970]).

5.2.3 Destructive Techniques

Of the destructive techniques, the most commonly used is the Sachs boring method. It is a bulk machining technique, which involves boring out a cylinder or tube in stages and measuring the longitudinal and circumferential strains at the outer surface at each stage, usually by means of electric resistance strain gages.

A common criticism of the Sachs boring technique, criticism shared by most other destructive techniques, is that it does not account for the stresses introduced by cutting or boring. One way of overcoming this difficulty is by using a stress-free way of layer removal, e.g. by acid etching; this method presents, however, problems of dimension control and protection of the measuring equipment. Electropolishing also removes material without introducing additional stresses.

Bending-deflection techniques offer the advantage over bulk machining techniques of amplifying the strains to be measured. The measurement of circumferential residual stresses in a thin-walled tube by slitting it falls under this category. Interferometric techniques have been used successfully and show promise in this technique.

5.2.4 The Method of Sectioning

When a specimen is cut into small "sections", the locked-in residual stresses are released. The cutting process and measurement of such released stresses constitute the method of sectioning. If only longitudinal stresses are measured, the specimen is cut into long and narrow strips; but, if transverse stresses are measured also, the strips are further cut into little square pieces. In the latter case, two-gage rosettes are generally used.

The method of sectioning is described in detail by Sherman [1969], Tebedge, Alpsten and Tall [1972, 1973] and in Technical Memorandum No.

6 of the Structural Stability Research Council (SSRC [1978]). It has been used extensively (Huber and Beedle [1954], Beedle and Tall [1960], Tall [1964], Ingvarsson [1975, 1977a, 1977b], Ross and Chen [1975], Brazetti, Alpsten and Tall [1970], Kato and Aoki) for the determination of residual stresses in wide-flange shapes, tubes of rectangular or circular cross-section and other geometries.

Some of the investigators whose works are referred to above use a mechanical gage of the Whittemore type, placed on two reference holes, to measure strains. Clearly the procedure does work quite nicely, as proved by the reproducible results quoted above. But a great deal of care and experience are required.

Sherman [1969] studied the errors associated with the use of a mechanical gage on a curved strip (the gage measures the chord length and not the arc length, the gage points are not aligned with the hole axis) and derived correction factors. It should be emphasized, however, that the hole drilling operation is quite difficult, especially on a curved surface such as a corner. It is necessary to drill the gage holes in one single pass to insure uniformity of diameter. In addition, wander of the drill bits may cause poor alignment of the holes; this would make the Whittemore gage unstable and would give irreproducible results. For close tubes, whose inside is unaccessible before sectioning, the gage holes are usually drilled through the thickness. In such cases, misalignment of the holes may cause significant error if it is assumed that the initial reference distance between the holes on the inside is equal to the distance on the outside of the tube. Also, the constant need to check and recalibrate the mechanical gage, as recommended by the SSRC [1978] makes the whole procedure lengthy; the apparatus heats up slightly with prolonged use and causes significant errors. A slight difference in pressure with which the gage is applied over the holes also makes a difference in the readings.

For all these reasons, the use of electric resistance strain gages was thought preferable. Denton [1966a] discussed some associated techniques and errors: strain gages are often disconnected during the cutting process and silver plated brass plugs have been found to provide reliable means of disconnecting and reconnecting leads; a difference in temperature of 1°C between the active and dummy gages has been reported to cause an error of about 50 μ in/in.

5.2.5 Effect of Cutting on Residual Stresses

In spite of the extensive use of machining in various destructive methods, studies of the stresses introduced by cutting and boring are few. It is recommended to use sharp tools and a liberal amount of coolant to minimize thermal stresses. It is also generally agreed, the coarser the cut, the greater the disturbance of the stress pattern.

Several investigations of the tensile residual stresses introduced by grinding are cited by Denton [1966a]. Okushima and Kakino [1972] made an analytical (by the Finite Element Method) and experimental study of the residual stresses produced by metal cutting. The study deals with surface cuts, but not with through thickness sectioning as used in the sectioning method. The parameters of significance are the depth of the cut, the speed of cutting and the rake angle of the blade. For a depth of cut of 0.1 mm, tensile residual stresses in the cutting direction as high as the yield stress of the cut metal are found in a subsurface layer, but drop off rapidly to become slightly compressive at levels deeper than 30 μm. Stresses normal to the cut are of the same sign and magnitude as those parallel to it.

Tebedge, Alpsten and Tall [1973] reported that, for one set of parameters, the local stress at the saw-cut edge is of the order of 0.5 to 1.5 ksi in compression. Huber and Beedle [1954] showed that residual stresses of annealed steel sections, measured by the sectioning method, are very small and of the order of the measurement errors. This means that annealing effectively removes residual stresses and cutting introduces negligible residual stresses. This is confirmed by the author's own measurements.

5.2.6 Accuracy of Measurements

Denton [1966a] reports that agreement within 10% is obtained by X-Ray diffraction applied to a bent strip of high strength steel with known surface residual stresses. It is estimated that errors in estimating the shift of sharp lines after diffraction from steel are of the order of 1500 psi.

For bending-deflection methods, the validity of the stress-deflection relationships is the limiting factor and one can only hope for an accuracy of ±1000 psi. The requirement of the knowledge of stress-deflection relationships can be avoided by a null deflection technique, whereby the force necessary to restore, say, a slit cut to its original dimension is measured.

To be competitive with a bending-deflection method, the stress in the Sachs boring technique should be measured to ±1000 psi, but the thickness of the layer removed should not be increased to meet this demand, if in doing so, a high stress gradient is obscured. This accuracy has been achieved in autofrettaged gun barrels from a strain measurement sensitivity of 2 μ in/in (Denton [1966a]).

Accuracy of about 20% can be expected with the hole drilling method.

Ingvarsson [1977a] reports errors less than ±10 MPa (±1.450 ksi) in measurement of residual stresses in welded box sections with the sectioning method and electric resistance strain gages. The sections are made of ordinary steel (σ_y = 332 MPa or 48 ksi) or high-strength steel (σ_y = 817 MPa or 118 ksi).

5.3 Residual Strain Measurements

5.3.1 Description of Experiments

The method of sectioning is used to measure the longitudinal residual strains in all sections studied (PBC 14, RFC 14, PBC 13, RFC 13, H 11, H 7 and HT). Specimens are about 3.0" in length and cut at least 6.0" from the ends of a member prior to any test. The ends of the specimen are machined precisely flat and perpendicular to the specimen axis. This step is necessary because the specimen is to be held by its ends in a vice for further sectioning. After scale and grease have been removed with emery cloth and solvent, longitudinal lines are scribed on both faces of the specimen. These lines serve the dual purpose of guidelines for mounting the strain gages and for sectioning. The distance between two adjacent lines is a compromise between several factors. On the one hand it is desirable to study the distribution of residual stresses in as much detail as possible; on the other hand the cuts should not be too close to the gages to avoid damage and to minimize the influence of cutting upon the measured strains. The gages are narrower than 1/8", but the necessity to mount them exactly opposite one another on both faces of the specimen and to align them with the lines makes a wider spacing necessary. Other factors are the width of the saw blade (0.040"; thinner blades tend to break teeth) and clearance for the wires. From experience, a spacing of no less than 3/8" is found desirable; where little variation is expected in the residual strains, a spacing of 1/2" is sometimes used.

After the lines have been scribed, the metal surfaces undergo the usual preparations for mounting gages, the gages are cemented, given time to cure and wired. The process is tedious and the inside corner gages especially require some skill.

The sectioning itself is usually done in a single working day to minimize time-drift of the gages. The temperature of the machine shop is maintained constant to within 1°C and cutting is slow enough so that the specimen only feels warm to the touch during machining. No coolant is thus necessary. Readings of all gages are taken twice initially and at least once after each cut.

5.3.2 Results and Discussion

On Tables 5.12 to 5.19 a small horizontal line is drawn to indicate the cut which completely severs a section from the specimen. Readings of gages adjacent to a fresh cut are disregarded because of the heat generated by machining; but the readings rapidly stabilize and the large majority of gages left undisturbed after complete separation exhibit a drift smaller than 15 μ in/in, which corresponds to a stress of 440 psi. The reading of all gages after each cut thus provides a measure of experimental error. Indeed, if strain relaxation due to cutting is assumed purely elastic, the cutting sequence is immaterial and it should only be necessary to record the initial readings before any cutting and the final readings after all cutting. This simplified procedure would shorten the experiment significantly but would deprive the experimenter of a measure of any possible drift. Such a measure is necessary in interpreting the results. The cutting sequence is left to the discretion of the machinist.

Since residual stresses are theoretically in equilibrium, another measure of experimental error is the unbalance strain which is the weighted average of the measured strains. The weights are either the physical weights of the coupons or their widths. The unbalance strain is only meaningful if the strain released on all coupons are available (i.e. no damaged gages). The available unbalance strains are:

-for RFC 14: -20. μin/in
-for PBC 14: 0.4
-for RFC 13: -91.
-for PBC 13: -40.
-for H7: 15.
-for H11: 21.
-for HT: 1.9

The average of the absolute values of the unbalance strains is 27 μin/in, which corresponds to a stress of 800 psi.

Another source of error, probably the most important, is the cutting process itself and will be discussed in the next section.

The relaxation strain patterns, shown in Fig. 5.1 to 5.7, are roughly symmetrical and exhibit negative values on the convex side. These observations agree with theoretical predictions (Fig. 4.5 to 4.10). According to the theory, to each corner geometry (defined by b/a or a/t) and to each change in thickness $\Delta t/t$ of a corner compared to a flat, corresponds a combination of internal pressure and moment; this combination, in turn, determines the residual stresses and the relaxation stresses. The relaxation stresses are worked out in Table 4.1 using the geometrical data collected in Tables 3.2a,b. Comparison with the experimental data is difficult, as shown in Table 5.22, because of the large scatter of these data. Ideally, the bending relaxation strains on both faces of a corner should be equal and opposite; corners of the same geometry should also relax identically. This is, however, not the case. Table 5.22 shows that, in general, the ranges of predicted relaxation stresses corresponding to the ranges of measured changes in thickness overlap with the ranges of measured relaxation stresses.

The global average of the relaxation strains over a cross-section is zero, as required by equilibrium.

It is remarkable that the local average is also zero, within experimental accuracy, as seen in Figs. 5.1 to 5.7.* The values of

*The average is computed as half the sum of the inside and outside values. This is correct for a flat but only approximate for a corner. In all rigor, assuming a linear distribution of strain and the value ε_i at the concave face, $r = a$, and ε_o at the convex face, $r = b$:

$$\varepsilon = (\varepsilon_o - \varepsilon_i)\,\frac{(r-a)}{(b-a)} + \varepsilon_i$$

axial strain relaxation predicted by theory are virtually zero for no internal pressure, and small (compared to the bending strain relaxation) for other values of pressure (Table 4.1). The contribution of the axial relaxation strain can thus be neglected in the comparison between theory and experiment in Table 5.22.

There is, surprisingly, no difference between the residual stresses of press-braked channels and those of cold-formed channels.

97% (216 out of 223) of the data points of residual strains fall within a band of ± 60% of the yield strength of the flat portion of the relevant cross-section. Of the points that fall outside that band, all except one occur at the extremities of the sections (Figs. 5.1-5.7).

The residual resultant force in the longitudinal direction of a corner is not zero if cold-forming occurs under any amount of internal pressure at all (Table 4.1). This residual force must be balanced by an opposite residual force in the flats. But this force is small and cannot explain the experimental observation that all channel sections

---

the average strain over a unit angle of corner is:

$$\frac{\int_0^{\theta=1}\int_a^b \varepsilon r dr d\theta}{\int_0^{\theta=1}\int_a^b r dr d\theta} = \frac{\int_a^b \varepsilon r dr}{\int_a^b r dr} = \frac{2}{3}(\varepsilon_o - \varepsilon_i)\,\frac{(b^2+ab+a^2)}{b^2-a^2} + \frac{\varepsilon_i b - \varepsilon_o a}{b-a} \neq \frac{\varepsilon_o+\varepsilon_i}{2}\,.$$

The refined formula is considered unnecessary here since corners contribute only a small part to the total area, and corner residual strains are small.

exhibit higher residual stresses at the flats (especially the web) than at the corners. Pending further study, it is suggested that these high stresses may be caused by the coiling and uncoiling of the steel sheet out of which the sections were cold-formed. It is also possible that these stresses are caused by straightening of the member. In puzzling contrast, the hat sections exhibit high residual stresses at the corners and low stresses at the flats. H7 shows little residual stress, except at the tips of the section.

5.4 Sectioning of Annealed Specimens

Five specimens (PBC13, PBC14, H11, H7 and HT) were stress-relieved by annealing. The procedure used was keeping them at a temperature of 1200°F for one hour, then slowly cooling them to room temperature at the rate of 50°F/hr. Chapter 7 examines this process in more detail. These specimens were subsequently sectioned, as described previously, in an attempt to determine the residual stresses induced by cutting.

Fig. 5.8 shows that, out of 32 data points, 25 (78%) fall within ± 50 μ in/in and 27 (84%) within ± 75 μ in/in. It was seen previously that values of 500-600 μ in/in are common for residual strains due to cold-forming. Fig. 5.9 shows the results of the sectioning of an annealed PBC14. The strains obtained are higher than in the previous experiments, but the switching unit did not work properly and may have contributed to the high readings.

5.5 Closure

Residual strains were measured by the sectioning method with electric resistance strain gages. If the errors introduced by cutting, temperature change and gage drift are added, one obtains an estimated error of 50 + 15 = 65 μ in/in (about 2000 psi). This is comparable to measurement by other investigators (§ 5.2.6).

The cold-forming residual stresses measured here have a completely different origin from the cooling residual stresses, which have been measured extensively, but to the author's knowledge, only on hot-rolled wide flange sections (Johnston [1976]). In these sections, the parts that cool the most rapidly (namely the tips of the section, the middle of thin elements) are in compression and the rest (corners, intersections of webs with flanges) are in tension. Cooling residual stresses are often assumed to be uniform across the thickness. Comparison between these two types of residual stresses on similar shapes would have been interesting; because of the different origins and mechanisms, the residual stresses are expected to be quite different.

TABLE 5.1

PBC14 RESIDUAL STRAINS

Gage #	Outside Strain (10^{-6})	Gage #	Inside Strain (10^{-6})	Average Strain (10^{-6})
1	-397	2	489	46.
3a	-414			
3b	-84	4	56	-14
5	-97	6	185	44
7	-246	8	269	11.5
9	-201	10	287	43.
11	-422	12	254	-84.
13	-640	14	528	-56.
15	-464	16	594	65.
17	-427	18	547	60.
19	-486	20	581	47.5
21	-590	22	566	-12
23	-768	24	581	-93.5
25	-169	26	128	-20.5
27	-202	28	154	-24.
29	-280	30	294	7.
31	-85	32	103	9.
33a	55	34	27	41.
33b	-269			
35	-688	36	651	-18.5

$$\frac{\text{Corner width}}{\text{Flat width}} = 1.56$$

Out-of-balance strain = 0.4×10^{-6}

TABLE 5.2

RFC14 RESIDUAL STRAINS

Gage #	Weight (gram)	Outside Strain (10^{-6})	Inside Strain (10^{-6})	Average Strain (10^{-6})
1	12.865	-334	321	-6.5
2	19.218	-168	-3	-85.5
3	15.682	-169	156	-6.5
4	14.979	-397	344	-26.5
5	22.318	-26	28	1.0
6	15.109	-599	544	-27.5
7	18.479	-582	649	33.5
8	13.514	-594	699	52.5
9	21.174	-361	408	23.5
10	20.418	-207	-24	-115.5
11	14.670	-338	351	6.5
12	16.004	-153	174	10.5
13	15.983	-182	-24	-103.
14	15.374	-231	206	-12.5

Out-of-balance strain

$$= \frac{\Sigma \text{ average strain x weight}}{\Sigma \text{ Weight}} = -20.0 \times 10^{-6}$$

TABLE 5.3

PBC13 RESIDUAL STRAINS

(coupon a)

Gage #	Outside Strain (10^{-6})	Gage #	Inside Strain (10^{-6})	Average Strain (10^{-6})	Thickness (inch)
1	-417	2	529	56.	.091
3	-820	4	151	-334.5	
5	-202	6	131	-35.5	.091
7	-205	8	156	-24.5	.091
9	-327	10	478	75.5	.092
11	-415	12	322	-46.5	
13	-834	14	715	-59.5	.091
15	-709	16	749	20.	.091
17	-647	18	709	31.	.089
19	-634	20	679	22.5	.092
21	-711	22	691	-10.	.091
23	-697	24	620	-38.5	.091
25	-246	26	285	19.5	
27	-398	28	273	-62.5	.091
29	-220	30	249	14.5	.091
31	-255	32	140	-57.5	.091
33	-412	34	315	-48.5	.091
35	-1497	36	1305	-96.	.092

$$\frac{\text{Corner width}}{\text{Flat width}} = \frac{.585}{.375} = 1.56$$

Out-of-balance strain = -39.7×10^{-6}

TABLE 5.4

PBC13 RESIDUAL STRAINS

(partial pilot test. Coupon b)

Gage #	Outside Strain (10^{-6})	Gage #	Inside Strain (10^{-6})	Average Strain (10^{-6})
19	-714			
27	-431			
27-29	-361			
29-31	-244			
31	-355			
33	-654	34	213	-220.5
35	-1426	36	1517	45.5

TABLE 5.5

RFC13 RESIDUAL STRAINS

Gage #	Weight (gram)	Outside Strain (10^{-6})	Inside Strain (10^{-6})	Average Strain (10^{-6})
1	20.086	-704	374	-165
2	23.486	-933	-212	-572.5
3	19.230	-132	191	29.5
4	19.060	-289	268	-10.5
5	30.332	-116	-2	-59
6	22.992	-684	611	-36.5
7	21.235	-537	587	25.
8	21.463	-514	545	15.5
9	19.663	-634	608	-13.
10	30.419	-284	148	-68.
11	20.102	-180	277	48.5
12	21.218	-100	-48	-74
13	22.499	-566	-95	-330.5
14	18.242	-447	476	14.5

Out-of-balance strain = -91.1×10^{-6}

$$= \frac{\Sigma \text{ average strain} * \text{weight}}{\Sigma \text{ weight}}$$

TABLE 5.6

H11 RESIDUAL STRAINS

Gage #	Inside Strain (10^{-6})	Outside Strain (10^{-6})	Average Strain (10^{-6})	Coupon Area (in^2)
1	-46	11	-17.5	.04087
2	-176	362	93.	.04413
3	-199	150	-24.5	.04473
4	212	-298	-43.	.04405
5	187	64	125.5	.05428
6	571	-288	141.5	.03979
7	-461	7	-227.	.04731
8	-58	390	166.	.04724
9	-152	94	-29.	.04897

Out-of-balance strain = 20.7×10^{-6}

TABLE 5.7

H7 RESIDUAL STRAINS

Specimen a

Gage #	Outside Strain (10^{-6})	Gage #	Inside Strain (10^{-6})	Average Strain (10^{-6})
1	610	2	-724	-57
3	140	4	-694	-277
5	246	6	495	370.5
7	-103	8	223	60
9	513	10	67	294
11	529			
13	-126	14	78	-24
15	-179	16	-253	-216
17	-226	18	-18	-122
19		20	372	
21	54	22	400	227
23	797	24		
25	826	26	-893	-33.5

TABLE 5.8

H7 RESIDUAL STRAIN

Specimen b

Gage #	Outside Strain (10^{-6})	Gage #	Inside Strain (10^{-6})	Average Strain (10^{-6})
1	662	2	-725	-31.5
3	39	4	-507	-234
5	128	6	489	308.5
7	-200	8	164	-18
9	-55	10	149	47
11	212	12	-18	97
13	-143	14	61	-41
15	60	16	-258	-99
17	-203	18	-6	-104.5
19	-12	20	256	122
21	246	22	44	145
23	-134	24	-56	-95
25	1237	26	-1205	16

$$\frac{\text{Corner Width}}{\text{Flat Width}} \simeq 1.25$$

Out-of-balance strain = 15.1×10^{-6}

TABLE 5.9

HT RESIDUAL STRAINS

Gage #	Outside Strain (10^{-6})	Inside Strain (10^{-6})	Average Strain (10^{-6})
1	-196	498	151
2	-211	-205	-208
3	671	-429	121
4	136	-371	-117.5
5	-535	232	-151.5
6	-157	147	-5
7	-117	223	53
8	44	-240	-98
9	742	-751	-4.5
10	141	-138	1.5
11	230	329	279.5

$$\frac{\text{Corner Width}}{\text{Flat Width}} = 1.1$$

Out-of-balance strain = 1.9×10^{-6}

TABLE 5.10

RESIDUAL STRAINS (10^{-6} in/in)

DUE TO MILLING; ANNEALED SPECIMENS

Specimen → Gage ↓	PBC13	H11	H7	HT
1	-12	-6	304	-38
2	-5	132	-137	-120
3	-9	-4	4	70
4	-23	24	21	12
5	-8	20	-44	-7
6	-11	140	33	60
7	23	18	-16	-44
8	27	0	-3	20

TABLE 5.11

RESIDUAL STRAINS DUE TO

MILLING; ANNEALED SPECIMEN
(switch unit gave trouble)

PBC 14				
Gage #	Inside Strain (10^{-6})	Gage #	Outside Strain (10^{-6})	Width (inch)
1	-25	15	29	.44
2	77	16	16	.48
3	-114	17	46	.50
4	-145	18	-47	.50
5	65	19	133	.66
6	3	20	-16	.50
7	25	21	-59	.50
8	-20	22	-97	---
9	-66	23	-26	Symmetrical
10	-23	24	-190	
11	-103	25	10	
12	-52	26	59	
13	-60	27	-152	
14	-8	28	15	

TABLE 5.12

PBC 14 RESIDUAL STRAINS (10^{-6} in/in): detail

Gage #

Cut#	OUT	1	3a	3b	5	7	9	11	13	15	17	19	21	23	25	27	29	31	33a	33b	35
		0	0	0	0	0	0	0	0	0	0	0	0	0	0	0	0	0	0	0	0
	1	-23	-6	-5	4	-18	-26	-44	-19	21	84	60	8	-12	-29	-23	-13	-6	0	1	-9
	2	-8	7	12	12	-5	-17	-37	-13	28	94	-488	52	27	0	-24	-16	-9	-1	5	6
	3	-4	8	12	17	-6	-16	-35	-13	30	94	-486	-583	4	34	-10	-19	-19	-14	-1	11
	4	+1	12	13	10	-5	-13	-33	-10	32	97	-484	-579	-773	66	12	-13	-25	-27	-9	21
	4b	-9	6	7	2	-10	-21	-44	-20	20	87	-497	-584	-778	61	11	-17	-30	-33	-18	17
	5	2	9	11	15	-7	-17	-42	-18	24	91	-492	-582	-776	-181	-37	-42	-55	-38	-15	31
	6	-2	10	11	16	-7	-19	-40	-14	27	93	-489	-580	-772	-166	-205	-5	-47	-51	-36	26
	7	-12	4	4	16	-15	-23	-45	-21	21	84	-494	-585	-778	-168	-208	-285	43	-77	-103	-8
	8	-24	-9	-6	6	-20	-30	-52	-28	12	78	-498	-592	-784	-174	-213	-293	-104	102	-401	-154
	9	-13	6	6	4	-7	-17	-39	-15	27	92	-487	-580	-771	-163	-199	-280	-82	49	-272	-687
	10	-8	9	0	-5	-33	-45	-39	30	118	-436	-482	-579	-769	-160	-198	-277	-78	56	-264	-680
	11	-11	-11	-27	-24	-52	-55	-20	16	-482	-451	-502	-600	-794	-188	-219	-300	-102	34	-290	-706
	12	26	4	-32	-53	-64	-53	62	-646	-470	-436	-488	-584	-776	-179	-206	-283	-91	48	-276	-693
	13	32	-31	-82	-68	-81	-30	-438	-646	-470	-435	-487	-584	-777	-178	-205	-283	-92	49	-271	-691
	14	40	-42	-82	-47	-36	-207	-428	-643	-466	-435	-486	-581	-775	-184	-204	-282	-89	53	-269	-691
	15	29	-113	-118	64	-265	-212	-433	-652	-479	-441	-488	-591	-778	-178	-203	-282	-91	51	-274	-691
	16	-92	-460	70	-93	-254	-205	-419	-673	-465	-433	-487	-580	-776	-174	-201	-281	-85	53	-268	-706
	17	-402	-419	-89	-102	-247	-199	-409	-635	-458	-427	-480	-575	-768	-164	-196	-273	-78	61	-264	-678

—— line indicates complete separation

TABLE 5.12 PBC 14 RESIDUAL STRAINS (10^{-6} in/in): detail (continued)

Gage #

	IN	2	4		6	8	10	12	14	16	18	20	22	24	26	28	30	32	34		36
		0	0		0	0	0	0	0	0	0	0	0	0	0	0	0	0	0		0
	1	-16	-7		-5	-25	-15	-45	-15	12	19	-65	-25	-16	-22	-16	-9	-12	-5		-8
	2	-5	6		3	-15	-4	-31	-5	24	28	576	-133	-34	-6	0	4	-4	-1		-1
Cut#	3	-1	18		6	-16	-3	-31	-6	22	27	579	557	-96	10	19	13	-7	-7		-1
	4	-1	16		4	-13	-2	-29	2	23	28	598	561	597	38	39	27	0	-13		9
	4b	-11	8		-5	-21	-7	-37	-11	16	22	591	553	592	34	34	18	-11	-17		3
	5	-5	0		-1	-20	-3	-34	-8	38	23	579	557	594	123	65	30	-8	-17		5
	6	-5	16		2	-18	-1	-29	-6	39	25	581	560	598	126	152	97	12	-27		14
	7	-11	1		-8	-22	-7	-37	-13	34	19	575	552	591	119	147	278	116	-58		26
	8	-25	13		-9	-29	-18	-47	-20	26	14	566	546	586	113	143	278	88	-4		167
	9	-10	1		0	-17	-15	-34	-7	42	22	580	561	597	127	158	294	109	23		645
	10	-13	-2		3	-18	-9	-41	-34	-64	539	584	561	599	129	158	298	107	30		649
	11	-22	-19		-11	-15	-3	-32	-154	541	525	562	543	574	112	136	273	89	11		629
	12	-5	-8		6	30	49	70	519	591	548	582	558	591	127	150	290	101	23		646
	13	-10	-45		5	64	125	259	520	589	546	575	560	592	128	151	291	96	23		647
	14	6	-44		38	148	278	269	524	593	548	577	558	593	124	153	288	94	26		649
	15	26	-72		171	259	275	259	521	582	546	575	553	593	130	150	289	97	23		643
	16	223	21		194	261	286	268	525	594	548	561	563	594	132	156	294	95	26		650
	17	484	51		201	270	294	278	534	601	547	585	569	596	135	160	301	92	32		654

—— line indicates complete separation

TABLE 5.13

RFC 14 RESIDUAL STRAIN (10^{-6} in/in): detail

Gage #

Cut #	OUT	1	2	3	4	5	6	7	8	9	10	11	12	13	14
		0	0	0	0	0	0	0	0	0	0	0	0	0	0
	1	-7	12	0	-22	-58	-28	20	115	-2	-82	-26	1	23	-2
	2	-7	8	-12	-45	-66	0	6	123	2	-77	-24	4	26	-1
	3	-7	-12	-22	-29	-14	-627	-578	120	4	-75	-24	2	29	1
	4	-6	-34	-69	-78	-72	-603	-578	118	3	-77	-27	1	27	3
	5	-5	-54	4	-405	-28	-596	-580	119	4	-81	-28	0	28	2
	6	5	-21	-184	-403	-29	-600	-581	117	2	-84	-29	-4	27	0
	7	-341	-175	-167	-398	-26	-599	-582	119	3	-88	-30	-5	24	0
	8	-337	-171	-170	-410	-27	-600	-582	-605	23	-113	-62	-28	14	2
	9	-337	-170	-173	-410	-27	-605	-583	-603	-372	-79	-18	-25	-5	2
	10	-333	-167	-168	-395	-26	-598	-582	-595	-360	-218	-66	-67	-20	57
	11	-333	-167	-163	-390	-26	-597	-583	-592	-359	-207	-345	-39	-50	30
	12	-335	-167	-169	-391	-26	-598	-584	-593	-363	-207	-352	-190	-97	-6
	13	-333	-167	-168	-389	-26	-596	-581	-589	-359	-204	-334	-153	-182	-231
grams	w	12.9	19.2	15.7	15.0	22.3	15.1	18.5	13.5	21.2	20.4	14.7	16.0	16.0	15.4

—— line indicates complete separation

TABLE 5.13 RFC 14 RESIDUAL STRAIN (10^{-6} in/in): detail (continued)

Cut # \ Gage # IN	1	2	3	4	5	6	7	8	9	10	11	12	13	14
	0	0	0	0	0	0	0	0	0	0	0	0	0	0
1	-4	-22	0	-20	-48	8	66	94	17	-46	-27	-6	18	1
2	-8	-18	-4	-21	-48	-22	641	97	19	-50	-24	-7	18	1
3	-2	-36	-12	-16	-32	531	652	98	20	-50	-24	-3	20	4
4	-2	-12	-13	31	3	541	652	98	17	-51	-26	-4	22	4
5	16	-28	25	341	27	547	650	98	17	-50	-24	-4	24	4
6	93	-29	44	339	27	544	650	99	15	-45	-25	-6	25	4
7	317	-26	152	342	29	544	650	97	15	-42	-24	-5	25	2
8	317	-1	156	351	26	538	650	693	41	-47	-22	-13	20	-10
9	320	-14	152	355	28	544	650	699	400	-44	-22	-15	14	-8
10	321	-8	156	342	28	545	647	700	408	-23	70	8	10	-3
11	321	-10	156	341	29	545	647	699	409	-19	344	53	-2	-16
12	326	2	158	342	27	546	646	699	405	-26	346	157	63	12
13	323	4	160	344	28	547	646	700	409	-23	354	174	-24	206

—— line indicates complete separation

TABLE 5.14

PBC 13 RESIDUAL STRAINS (coupon a. Detail) 10^{-6} in/in.

Cut # \ Gage #	1	3	5	7	9	11	13	15	17	19	21	23	25	27	29	31	33	35
Initial	0	0	0	0	0	0	0	0	0	0	0	0	0	0	0	0	0	0
1	3	-9	-1	1	1	11	7	-3	-19	-31	-16	-9	16	-16	-15	-47	-36	3
2	5	-27	-27	-27	-12	29	24	5	-667	-35	-20	-10	14	-16	-16	-46	-35	6
3	10	-50	-42	-31	1	72	1	-729	-656	-30	-16	-9	16	-12	-13	-50	-34	3
4	12	-69	-65	-45	2	132	-842	-717	-656	-29	-16	-9	17	-13	-15	-60	-33	7
5	42	-119	-132	-117	-52	-435	-841	-719	-655	-28	-16	-10	19	-12	-14	-58	-32	9
5b	25	-126	-141	-126	-74	-444	-854	-731	-665	-44	-24	-18	6	-23	-24	-71	-42	-5
6	18	-182	-159	-103	-379	-443	-860	-725	-662	-35	-20	-13	12	-17	-16	-42	-37	1
7	-21	-296	-53	-234	-362	-432	-844	-720	-659	-34	-18	-11	13	-15	-15	-45	-34	5
8	-250	-624	-221	-219	-364	-433	-843	-722	-659	-32	-19	-12	14	-16	-15	-45	-35	3
9	-439	-841	-212	-207	-348	-421	-832	-712	-648	-21	-9	-4	23	-18	-8	-27	-26	13
10	-439	-830	-213	-216	-369	-431	-838	-723	-659	-661	-18	-12	20	-30	-40	-78	-57	-2
11	-435	-825	-212	-213	-354	-427	-833	-718	-655	-652	-711	-11	51	-15	-31	-84	-72	11
12	-431	-820	-203	-208	-342	-418	-830	-713	-650	-649	-702	-717	76	-42	-54	-94	-76	29
13	-429	-822	-206	-211	-345	-421	-832	-715	-650	-646	-704	-711	-271	-86	-114	-134	-121	61
14	-436	-829	-213	-215	-352	-428	-834	-728	-656	-653	-708	-716	-261	-401	-53	-149	-174	52
15	-439	-832	-212	-231	-341	-429	-834	-719	-655	-649	-756	-753	-273	-408	-227	-80	-264	26
16	-432	-827	-208	-218	-331	-429	-857	-718	-656	-648	-722	-717	-255	-423	-237	-276	-331	18
17	-430	-828	-219	-215	-336	-426	-863	-749	-686	-666	-743	-713	-257	-395	-224	-268	-422	-1511

—— line indicates complete separation

TABLE 5.14: PBC 13 RESIDUAL STRAINS (coupon a. Detail) 10^{-6} in/in. (continued)

Cut # \ Gage #	2	4	6	8	10	12	14	16	18	20	22	24	26	28	30	32	34	36
Initial	0	0	0	0	0	0	0	0	0	0	0	0	0	0	0	0	0	0
1	-1	-12	9	-2	29	10	8	2	-3	12	14	12	12	-1	-5	-23	-23	3
2	-7	-22	-1	-8	34	-8	-27	-84	684	10	14	8	5	6	-2	-23	-22	4
3	15	-25	-6	3	54	23	-109	730	693	16	12	11	2	14	2	-19	-20	1
4	27	-46	-19	12	72	76	703	732	693	15	14	9	-1	11	-1	-23	-23	4
5	36	-73	-34	65	204	296	709	736	695	15	14	12	-1	18	2	-18	-20	7
5b	41	-100	-54	47	184	300	698	719	679	7	6	-4	-17	20	-18	-37	-42	-13
6	58	-120	-56	92	434	293	695	725	687	13	9	6	-12	30	-8	-27	-31	-4
7	92	-147	78	125	449	309	707	729	688	13	11	6	-10	32	-3	-25	-27	0
8	336	14	92	132	471	308	708	729	692	13	10	9	-10	33	-3	-23	-27	1
9	485	146	108	142	480	319	716	739	700	22	19	21	-12	42	9	-11	-14	11
10	533	127	110	133	454	310	705	731	690	661	-63	-7	-12	21	-1	-15	-36	8
11	538	123	116	137	459	315	711	734	695	676	684	-39	12	40	13	-9	-44	23
12	541	127	119	146	463	319	715	741	701	680	691	610	79	45	-6	-32	-46	31
13	542	126	115	143	461	314	712	741	701	678	691	609	261	126	52	-20	-78	42
14	531	121	110	136	452	307	675	736	696	672	685	606	275	295	159	8	-109	49
15	519	119	110	128	447	308	709	737	698	624	646	596	257	275	229	117	-152	47
16	529	129	110	139	457	310	614	737	696	673	681	609	271	240	226	119	118	266
17	531	110	104	140	460	280	710	709	674	655	677	598	267	280	232	121	293	1285

—— line indicates complete separation

TABLE 5.15

RFC 13 RESIDUAL STRAINS (detail)

	Gage # →	1	2	3	4	5	6	7	8	9	10	11	12	13	14
		0	0	0	0	0	0	0	0	0	0	0	0	0	0
Outside	1	-42	-30	-23	-17	-20	-29	-57	-50	-57	-38	3	-45	-157	-121
	2	-42	-47	-43	-36	-15	-33	-613	-44	-50	-30	14	-40	-150	-114
	3	-24	-60	-58	-34	17	-707	-555	-46	-50	-30	11	-42	-153	-115
	4	-6	-98	-99	-40	-157	-677	-534	-26	-33	-14	29	-22	-132	-94
	5	-85	-206	12	-329	-115	-679	-536	-30	-35	-18	28	-25	-132	-92
Cut #	6	-158	-368	-161	-286	-114	-679	-531	-29	-34	-16	29	-24	-136	-98
	7	-724	-948	-129	-286	-115	-680	-533	-32	-38	-19	25	-27	-136	-97
	8	-698	-930	-126	-288	-114	-687	-531	-586	-48	-35	-12	-64	-160	-120
	9	-703	-932	-133	-290	-112	-689	-539	-514	-653	-22	-4	-66	-178	-104
	10	-703	-932	-133	-290	-112	-685	-541	-514	-632	-314	-108	-156	-220	-58
	11	-703	-935	-134	-292	-112	-687	-543	-512	-634	-285	-183	-133	-248	-60
	12	-703	-935	-138	-296	-112	-693	-542	-514	-626	-283	-180	-120	-487	-201
	13	-713	-947	-147	-302	-128	-700	-554	-521	-636	-291	-191	-109	-576	-457
	ε^{res}	-704	-933	-132	-289	-116	-684	-537	-514	-634	-284	-180	-100	-566	-447

—— line indicates complete separation

w is the coupon weight in grams, ε^{res} in μin/in.

TABLE 5.15: RFC 13 RESIDUAL STRAINS (detail) continued

		Gage # 1	2	3	4	5	6	7	8	9	10	11	12	13	14
		0	0	0	0	0	0	0	0	0	0	0	0	0	0
	1	-26	-26	-23	-19	-17	7	39	68	18	-40	20	-60	-112	-4
Inside	2	-35	-46	-35	-23	-21	-41	548	70	22	-36	19	-57	-108	-1
	3	-27	-54	-41	-20	33	595	575	70	21	-36	19	-58	-107	-3
	4	-37	-79	-9	113	-40	620	593	90	38	-22	37	-38	-90	16
	5	-71	-116	115	247	-1	613	592	86	35	-24	35	-43	-90	14
	6	21	-29	180	267	0	614	592	86	38	-22	34	-43	-86	14
Cut #	7	366	-215	198	268	-1	613	587	83	35	-23	34	-45	-91	13
	8	373	-210	190	272	-1	609	591	505	-4	-38	20	-65	-114	-6
	9	375	-212	189	269	-3	607	585	544	598	-18	22	-71	-120	4
	10	375	-211	196	270	-3	608	584	546	607	132	222	-35	-136	8
	11	373	-213	189	267	-4	606	583	544	611	152	277	28	-136	12
	12	373	-212	191	265	-6	613	581	542	608	144	277	-67	-76	119
	13	363	-224	181	241	-19	595	571	535	598	131	268	-60	-106	466
	ε^{res}	374	-212	191	268	-2	611	587	545	608	148	277	-48	-95	476
	w	20.1	23.5	19.2	19.1	30.3	23.0	21.2	21.5	19.7	30.4	20.1	21.2	22.5	18.2

—— line indicates complete separation

w is the coupon weight in grams, ε^{res} in μin/in.

TABLE 5.16

H11 RESIDUAL STRAIN (10^{-6} in/in): detail

INSIDE OR LOWER

Cut # \ Gage #	1	2	3	4	5	6	7	8	9
Initial	0	0	0	0	0	0	0	0	0
1	26	5	-45	-159	-18	-166	-101	24	-16
2	28	34	-30	-136	-3	465	-366	64	-70
3	26	35	-40	-125	5	559	-533	107	31
4	10	32	-42	-127	3	560	-481	-71	-181
5	18	47	-71	-230	169	570	-464	-62	-154
6	128	67	-50	186	187	576	-467	-52	-141
7	-59	137	-206	204	187	571	-471	-58	-150
8	-46	-176	-199	212	187	571	-461	-58	-152

OUTSIDE OR UPPER

Cut # \ Gage #	1	2	3	4	5	6	7	8	9
Initial	0	0	0	0	0	0	0	0	0
1	15	46	3	38	159	31	25	34	-45
2	15	67	13	-27	176	-355	-138	232	-4
3	20	76	12	-14	183	-293	-37	117	-83
4	18	75	15	-7	190	-292	-3	329	65
5	-3	107	43	-12	50	-307	5	388	90
6	9	148	80	-332	66	-315	7	391	94
7	-152	-88	142	-288	63	-291	7	389	94
8	11	362	150	-298	64	-288	7	390	94

——— line indicates complete separation

TABLE 5.17

H7 RESIDUAL STRAINS (Specimen a. Detail) 10^{-6} in/in.

gage → / cut ↓	25	23	21	19	17	15	13	11	9	7	5	3	1
0	0	0	0	0	0	0	0	0	0	0	0	0	0
1	822	98	56	26	36	27	16	12	10	16	26	27	14
2	822	793	107	53	34	20	-13	-6	-14	15	18	24	7
3	822	787	45	*	10	41	18	17	2	26	24	33	8
4	877	844	101		26	38	58	92	91	115	140	267	620
5	886	849	110		-73	-123	36	192	253	308	440	298	658
6	842	805	68		-119	-168	-2	144	210	245	254	146	624
7	841	797	58		-149	-301	111	284	265	179	250	137	613
8	834	796	56		-148	-298	-126	316	270	183	250	140	610
9	837	796	58		-268	-173	-124	305	266	179	240	134	612
10	834	795	58		-231	-179	-118	310	273	191	246	146	612
11	826	797	54		-226	-179	-126	529	513	-103	240	139	606
ε_r	826	797	54		-226	-179	-126	529	513	-103	246	140	610

* Gage damaged

—— line indicates complete separation

TABLE 5.17: H7 RESIDUAL STRAINS (Specimen a. Detail) 10^{-6} in/in. (continued)

gage → / cut ↓	26	24	22	20	18	16	14	12	10	8	6	4	2
0	0	0	0	0	0	0	0		0	0	0	0	0
1	-894	17	20	11	18	10	8		-6	18	21	24	-5
2	-890	*	53	43	26	19	-6		-8	10	29	25	24
3	-886		415	-66	-22	25	18		14	26	37	26	28
4	-801		503	48	66	91	58		68	78	95	212	-663
5	-782		516	189	86	4	22		121	138	217	-684	-654
6	-880		414	93	-9	-93	19		90	100	507	-680	-717
7	-886		409	182	-13	-165	-73		134	-7	494	-690	-724
8	-888		407	182	-6	-165	84		204	-42	493	-692	-724
9	-893		400	294	50	-243	78		214	-38	495	-689	-724
10	-893		403	372	-13	-237	74		214	-42	502	-694	-722
11	-893		400	372	-18	-253	92		67	223	495	-697	-726
ε_r	-893		400	372	-18	-253	78		67	223	495	-694	-724

* Gage damaged

—— line indicates complete separation

TABLE 5.18

H7 RESIDUAL STRAINS (Specimen b. Detail) 10^{-6} in/in.

Gage→ / Cut ↓	1	3	5	7	9	11	13	15	17	19	21	23	25
Initial	0	0	0	0	0	0	0	0	0	0	0	0	0
1	-21	-33	-40	-59	-127	-61	-123	-91	-55	-40	-37	-46	-58
2	12	0	-1	-31	-97	-24	-172	-65	-11	-16	-37	-41	-49
3	12	0	-3	-37	-97	-23	-148	49	-40	-23	-3	-12	-25
4	14	5	-3	-34	-96	-24	-145	57	-234	192	3	-4	41
5	12	-1	-1	-35	-97	-27	-147	57	-219	-21	255	130	230
5b	22	12	4	-29	-87	-15	-138	65	-206	-5	280	147	248
6	12	6	-2	-39	-94	-20	-146	59	-202	-11	227	-406	656
7	18	6	2	-33	-90	-17	-137	63	-201	-6	246	-131	1253
8	-19	-6	-2	-91	-191	194	-139	65	-200	-8	246	-130	1237
9	24	20	25	67	-74	215	-135	66	-197	-3	252	-129	1249
10	283	226	363	-211	-54	211	-139	64	-197	-10	248	-132	1241
11	554	372	107	-195	-48	220	-131	70	-189	-3	253	-125	1315
12	650	31	134	-193	-45	223	-131	73	-190	-1	258	-125	1245
ε_r	662	39	128	-200	-55	212	-143	60	-203	-12	246	-134	1237

—— line indicates complete separation

TABLE 5.18: H7 RESIDUAL STRAINS (Specimen b. Detail) 10^{-6} in/in. (continued)

Gage → / Cut ↓	2	4	6	8	10	12	14	16	18	20	22	24	26
Initial	0	0	0	0	0	0	0	0	0	0	0	0	0
1	-97	-82	-56	-2	44	-71	-73	-100	-66	-42	-38	-27	-27
2	-60	-46	-9	30	79	-28	42	-111	-60	-44	-30	-13	8
3	-60	-48	-13	30	96	-30	62	-263	14	8	-5	-20	-26
4	-58	-45	-7	28	167	-30	64	-260	-17	145	-96	-117	-28
5	-61	-56	-8	28	114	-27	59	-262	-12	246	-138	-339	-175
5b	-54	-40	7	37	147	-18	64	-252	0	262	-114	-319	-162
6	-57	-43	10	32	214	-26	60	-257	-5	256	33	-756	-623
7	-54	-37	13	40	321	-21	64	-255	-2	262	48	-55	-1197
8	-93	-43	71	34	234	-45	65	-254	-1	314	50	-58	-1195
9	-119	-93	20	24	160	-22	69	-257	2	321	50	-51	-1200
10	-358	-400	-76	150	154	-18	67	-257	-6	306	45	-54	-1204
11	-599	-789	480	168	-492	-8	73	-247	4	266	54	-46	-1194
12	-727	-511	495	174	-475	-5	73	-245	7	269	56	-46	-1203
ε_r	-725	-507	489	164	149	-18	61	-258	-6	256	44	-56	-1205

*This is only 1/2 of the data. Each reading repeated twice 1-26, 1-26. This is the 2nd reading, deemed more reliable after more cooling time.
*Cut 1-5 on 4/26. Cut 6-12 on 4/27. Shift 5-5b is accounted for.
*Wire leading to gage 10 was a bit loose. Bad readings.

—— line indicates complete separation.

TABLE 5.19

HT RESIDUAL STRAINS (10^{-6} in/in): detail

outside - upper

Gage → / Cut ↓	1	2	3	4	5	6	7	8	9	10	11
Initial	0	0	0	0	0	0	0	0	0	0	0
1	-74	-21	-13	-79	-81	-147	157	29	61	92	82
2	-61	-21	6	1	11		171	61	24	55	46
3	-105	-29	100	-24	-824	-195	175	67	16	45	36
4	-92	-1	182	-138	-587	-175	174	68	13	43	34
5	-185	-289	612	88	-553	-170	175	68	14	41	32
6	-346	-316	666	116	-541	-164	177	71	9	38	32
7	-211	-217	672	128	-539	-161	344	89	93	266	66
8	-194	-209	673	136	-531	-158	-119	7	174	27	74
9	-196	-208	672	131	-531	-150	-119	43	736	262	246
10	-196	-211	671	142	-532	-147	-114	44	736	452	338
11	-196	-214	666	144	-535	-147	-102	45	742	141	230

inside - lower

Gage → / Cut ↓	1	2	3	4	5	6	7	8	9	10	11	
Initial	0	0	0	0	0	0	0	0	0	0	0	
1	-73	-81	-79	-68	-58	-84	-117	-77	-42	-23	-25	
2	-64	-35	7	-49	-126		-77	-32	2	17	11	
3	-109	-113	-99	-201	-131	124	-68	-24	11	22	20	
4	-137	-118	-51	-690	195	145	-64	-24	14	25	21	
5	66	-12	-759	-405	223	145	-66	-24	13	25	23	
6	343	-665	-475	-379	229	145	-64	-18	17	29	27→20	resolder
7	490	-219	-434	-371	232	146	-370	-501	-437	-291	-322	
8	495	-203	-430	-370	233	145	215	-301	-217	-109	-168	
9	497	-204	-426	-371	233	150	223	-240	-772	7	-24	
10	494	-208	-428	-370	235	156	221	-243	-772	-473	195	
11	505	-204	-426	-366	238	148	225	-237	-751	-138	329	

—— line indicates complete separation

TABLE 5.20

RESIDUAL STRAINS OF ANNEALED SPECIMENS (10^{-6} in/in)

Specimen	Gage → / Cut ↓	1	2	3	4	5	6	7	8
PBC 13	Initial	0	0	0	0	0	0	0	0
	1	-42	-10	-10	-24	-30	-24	-8	-2
	2	-14	-21	-18	-26	-10	-25	-10	-9
	3	-13	-9	-22	-30	-9	-12	8	-2
	4	-10	-2	-72	-36	-9	-12	-18	-8
	5	-8	-2	-12	-30	-4	-10	22	3
	6	-13	-8	-11	-34	-8	-8	23	27
	6	-12	-5	-9	-23	-8	-11	23	27
H11	Initial	0	0	0	0	0	0	0	0
	1	-48	68	-32	-12	4	114	2	-15
	2	-18	102	-12	6	7	120	12	0
	3	-8	132	-1	22	18	140	20	10
	4	-6	132	-4	24	20	140	18	0
HT	Initial	0	0	0	0	0	0	0	0
	1	-96	-30	-10	-10	-58	-29	-23	-14
	2	-40	-180	14	2	-7	-29	-14	-4
	3	-40	-180	-56	-32	-8	1	-64	-28
	4	-38	-120	70	12	-7	60	-44	20

TABLE 5.21

RELAXATION OF z RESIDUAL STRESSES: THEORY AND EXPERIMENT

SECTION	THEORY		EXPERIMENT	
	p/p_m %	$\bar{\sigma}_b^{rel}/\sigma_y$ %	$\Delta t/t$ %	$\bar{\sigma}^{rel}/\sigma_y$ %
PBC 14	0. to 25.	17. to 37.	1.9 to 4.7	$\frac{27}{1350} = 2.$ to $\frac{422}{1350} = 31.$
RFC 14	0. to 25.	17. to 37.	.13 to 5.7	$\frac{3}{1350} = .2$ to $\frac{207}{1350} = 15.$
PBC 13	0. to 25.	17. to 32.	3.4 to 4.4	$\frac{151}{1350} = 12.$ to $\frac{820}{1350} = 63.$
RFC 13	0. to 25.	17. to 30.	3.4 to 6.5	$\frac{2}{1300} = .15$ to $\frac{933}{1300} = 72.$
H11 (1)	~ 25.	~ 39.	4.3 to 8.6	$\frac{58}{1460} = 4.$ to $\frac{390}{1460} = 27.$
H11 (2)	0. to 50.	17. to 67.	2.2 to 10.8	$\frac{212}{1460} = 14.$ to $\frac{571}{1460} = 39.$
H7 (1)	25. to 50.	28. to 38.	11.3 to 15.7	$\frac{44}{1530} = 3.$ to $\frac{489}{1530} = 32.$
H7 (2)			33.9 to 39.7	$\frac{18}{1530} = 1.$ to $\frac{258}{1530} = 17.$
HT (1)	25. to 50.	25. to 33.	11.6 to 16.3	$\frac{429}{1830} = 23.$ to $\frac{751}{1830} = 41.$
HT (2)	25. to 50.	29. to 39.	10.8 to 14.6	$\frac{117}{1830} = 6.$ to $\frac{535}{1830} = 29.$

(1), (2) refer to corner numbers

TABLE 5.22

LIST OF TABLES AND FIGURES

FOR RESIDUAL STRAIN MEASUREMENTS

PBC 14	Fig. 5.1 Tables 5.1, 5.12
RFC 14	Fig. 5.2 Tables 5.2, 5.13
PBC 13	Fig. 5.3 Tables 5.3, 5.4, 5.14
RFC 13	Fig. 5.4 Tables 5.5, 5.15
H11	Fig. 5.5 Tables 5.6, 5.16
H7	Fig. 5.6 Tables 5.7, 5.8, 5.17, 5.18
HT	Fig. 5.7 Tables 5.9, 5.19
Annealed PBC 13, H11, H7, HT	Fig. 5.8 Tables 5.10, 5.20
Annealed PBC 14	Fig. 5.9 Tables 5.11
Comparison theory-experiment	Table 5.21

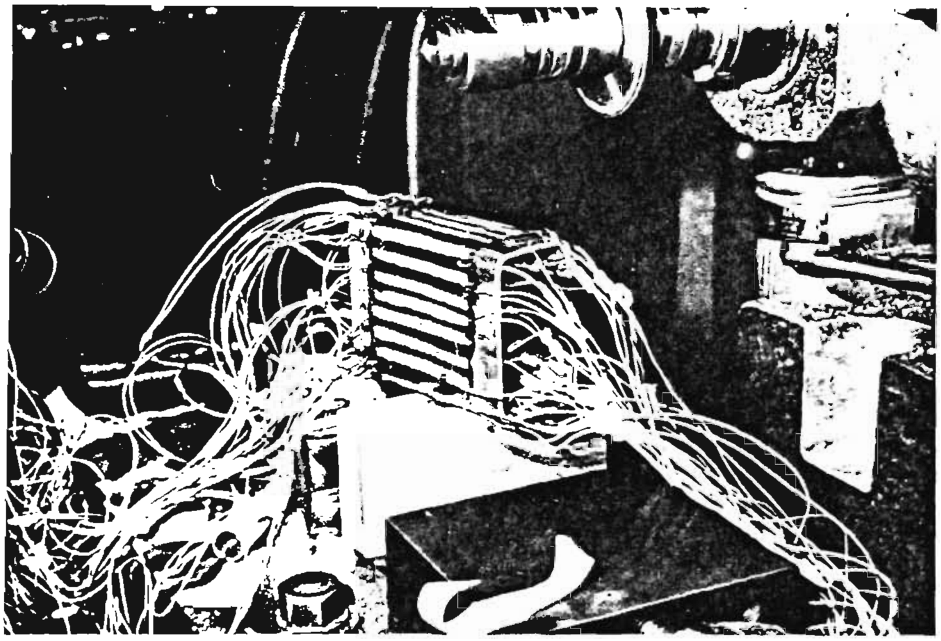

Photo 5.1 Residual Strain Measurement:
Channel Section Ready for Sectioning

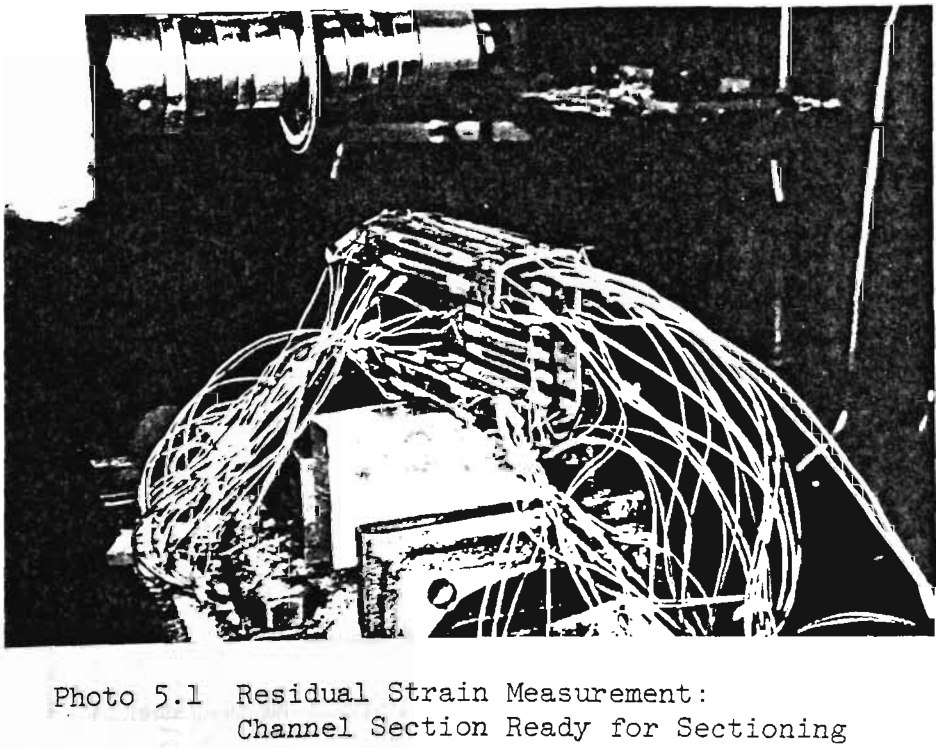

Photo 5.1 Residual Strain Measurement:
Channel Section Ready for Sectioning

Photo 5.3 Residual Strain Measurement:
Channel Section Ready for Sectioning

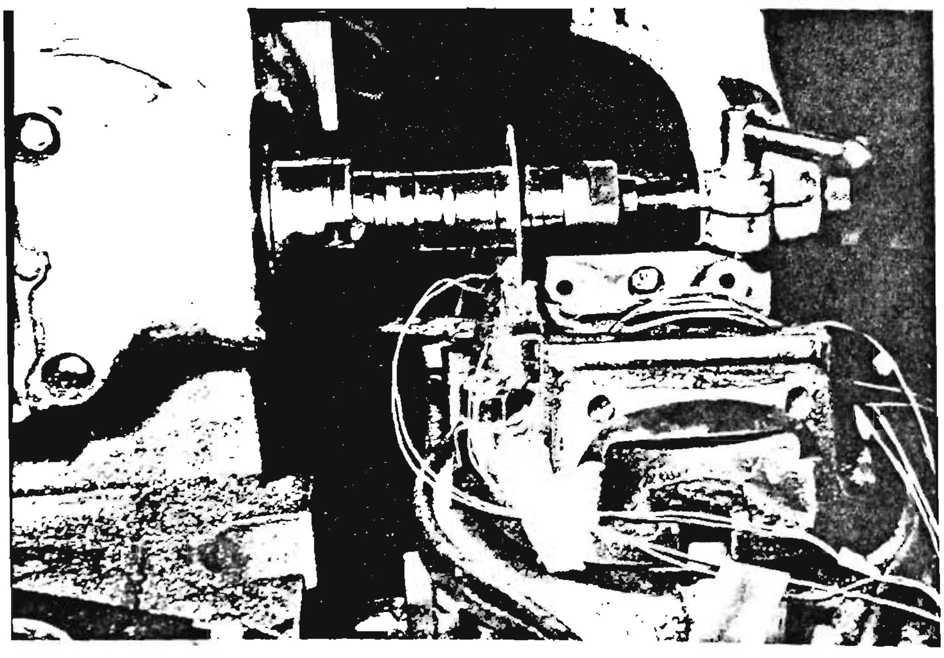

Photo 5.4 Residual Strain Measurement:
Sectioning

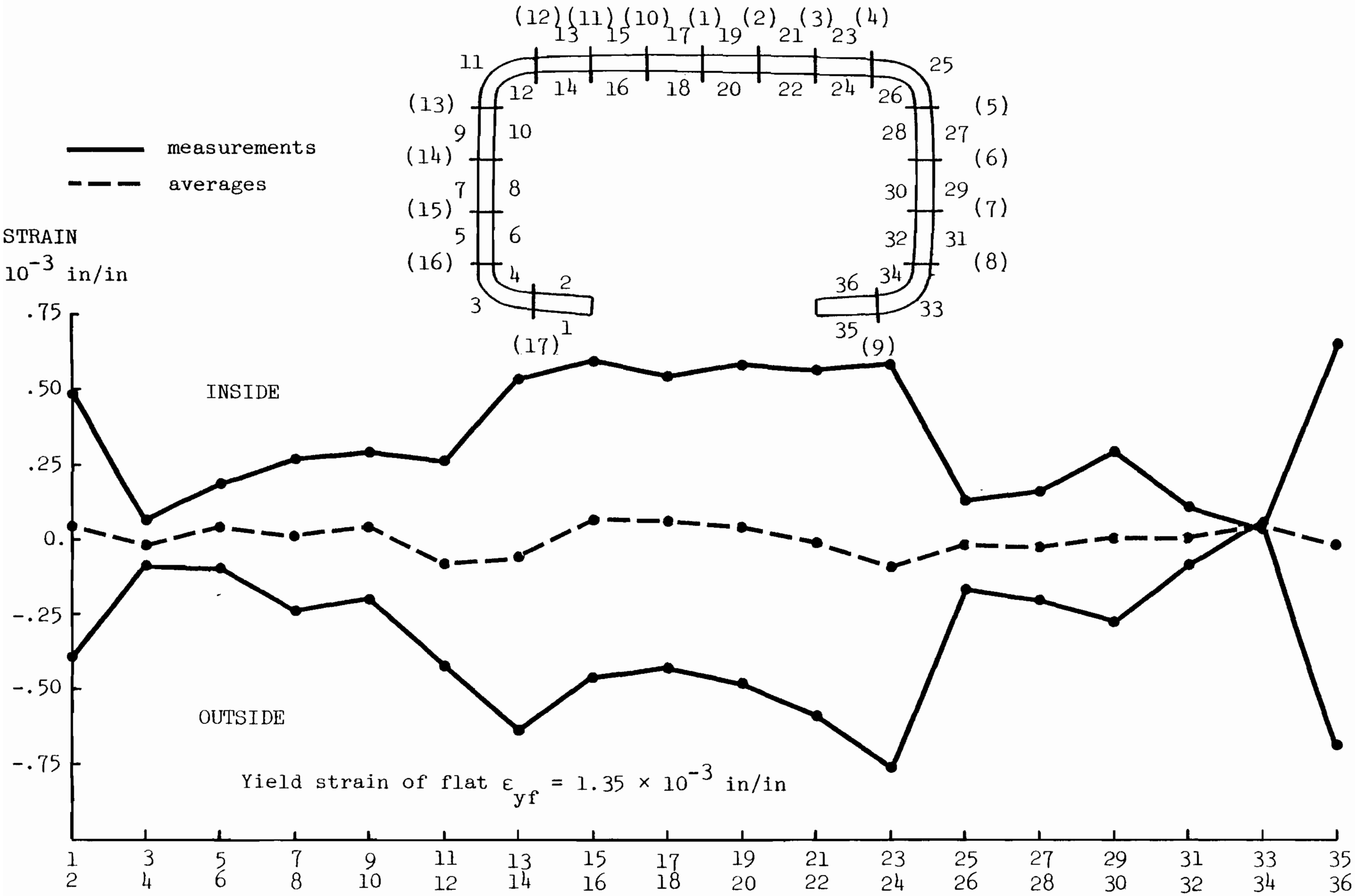

Fig. 5.1 PBC 14 Residual Strains

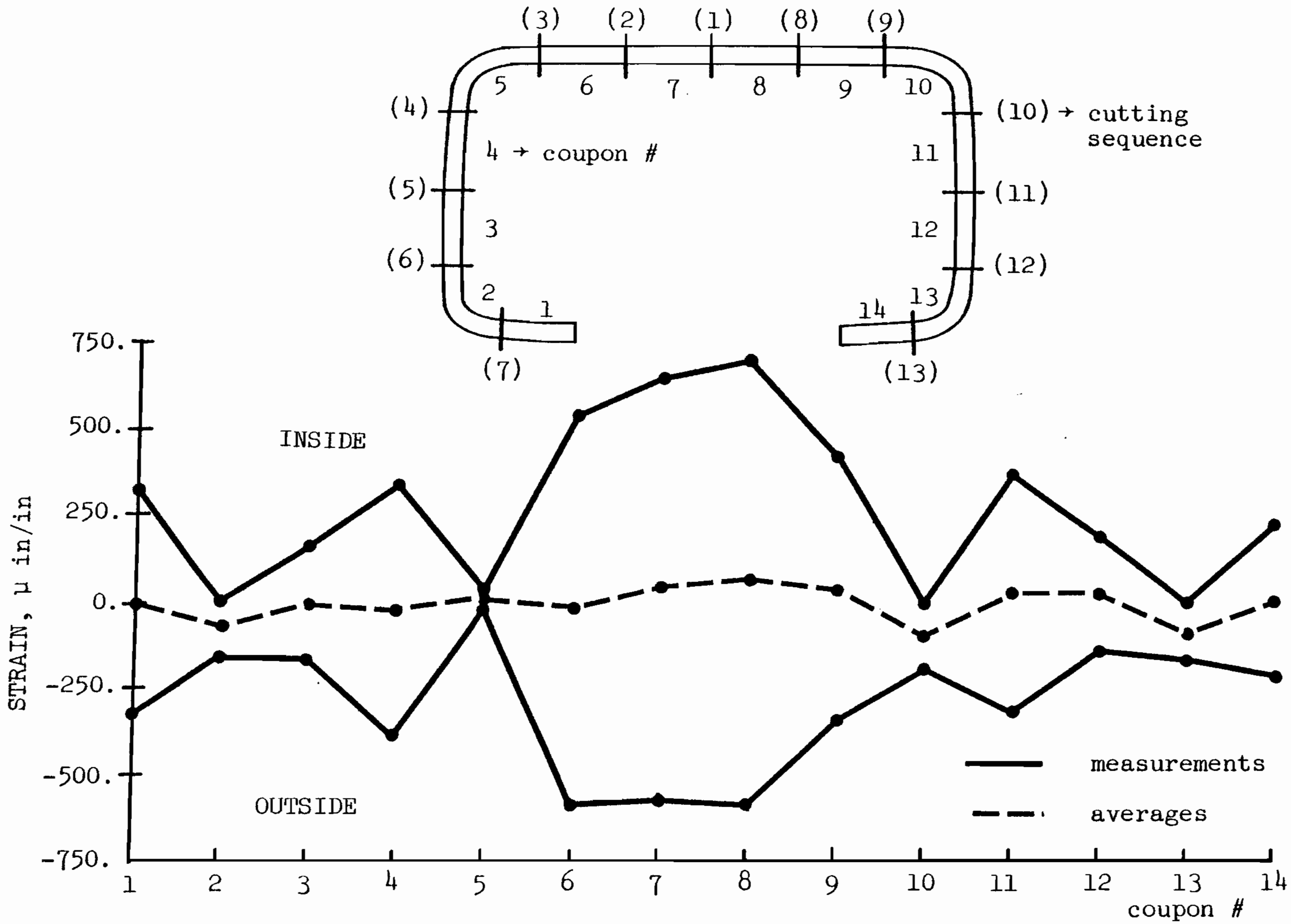

Fig. 5.2 RFC 14 Residual Strains
(Yield strain of flat ε_{yf} = 1350 μ in/in)

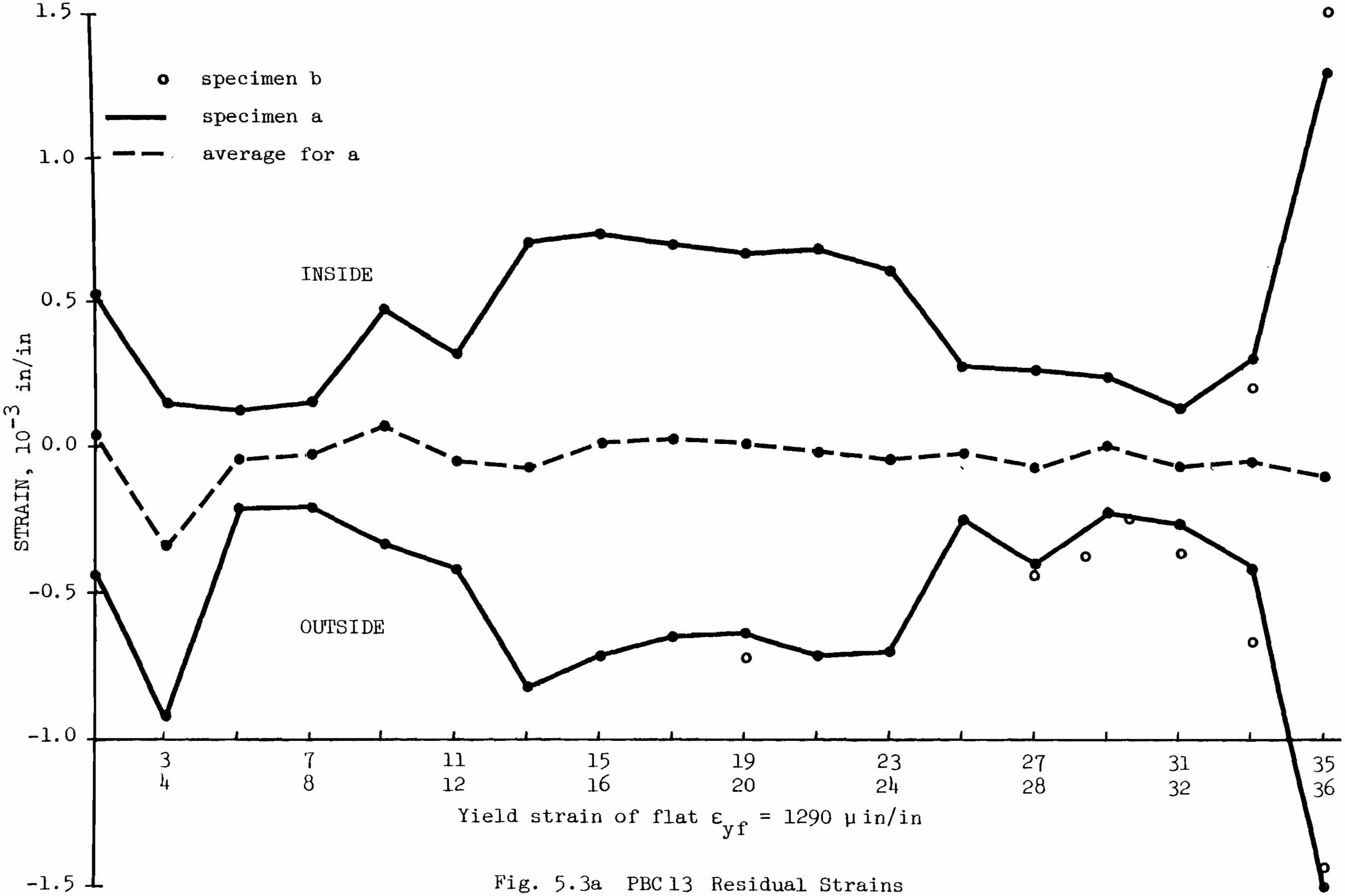

Fig. 5.3a PBC 13 Residual Strains

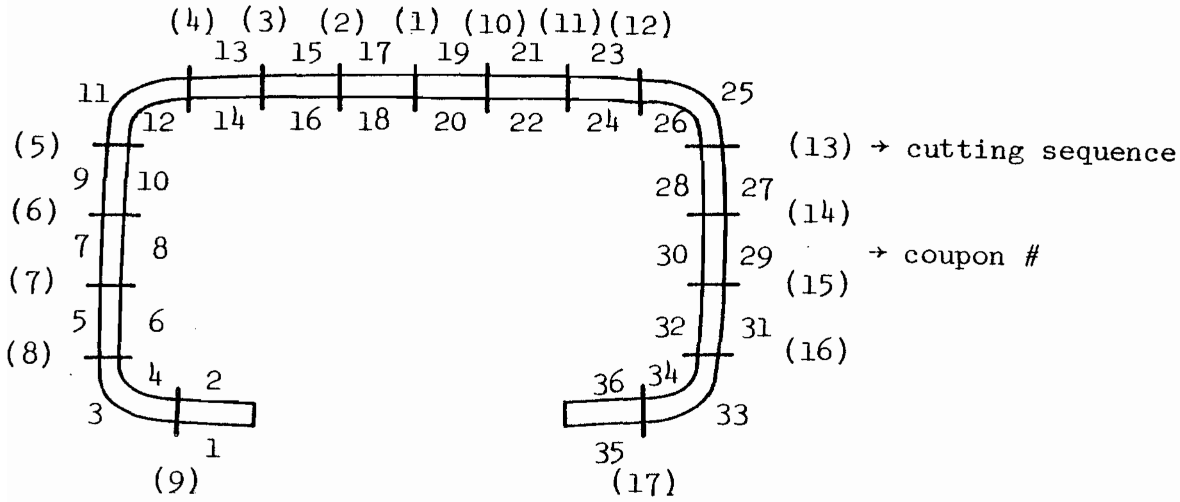

Fig. 5.3b PBC 13 Specimen for Residual Strains

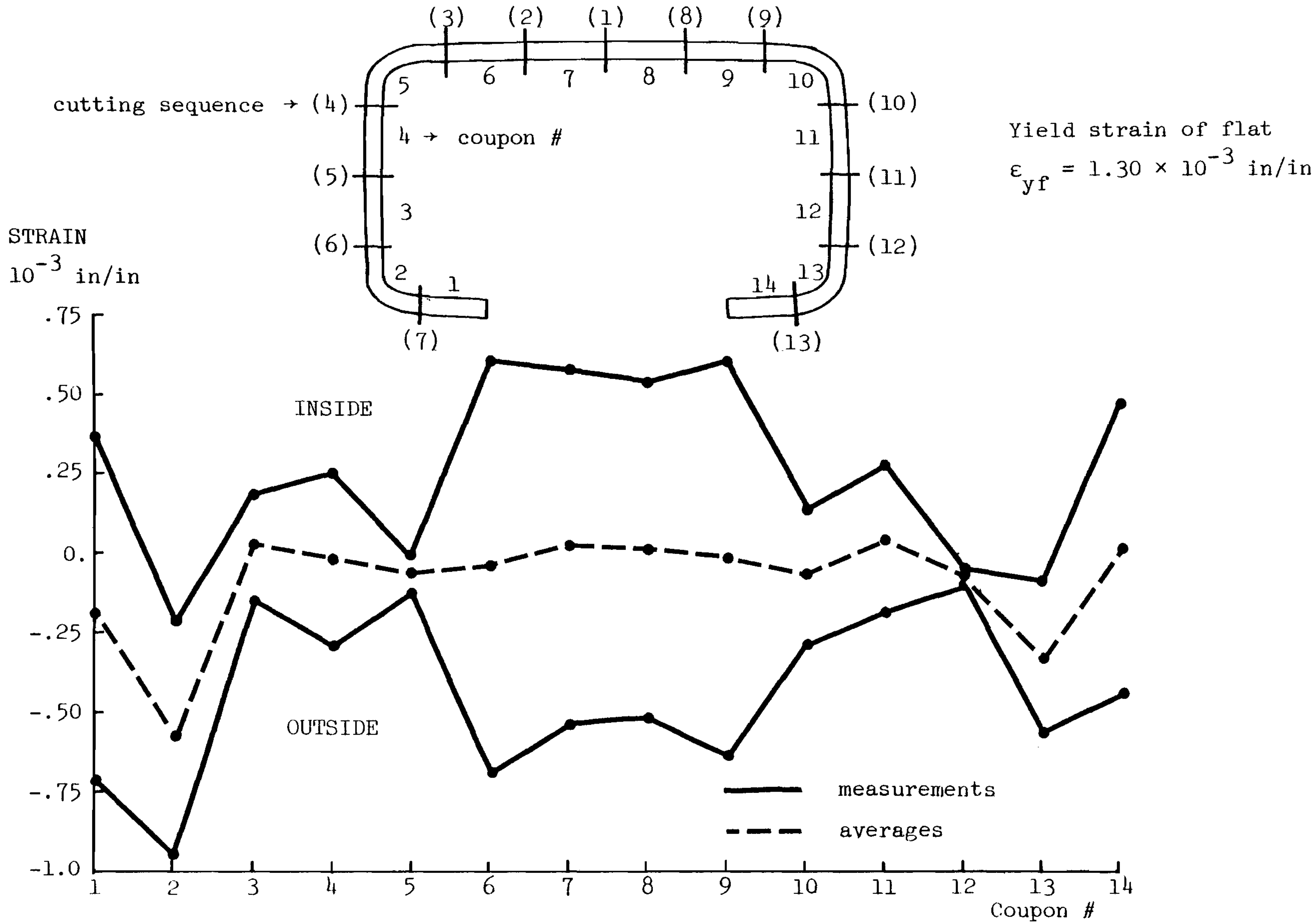

Fig. 5.4 RFC 13 Residual Strains

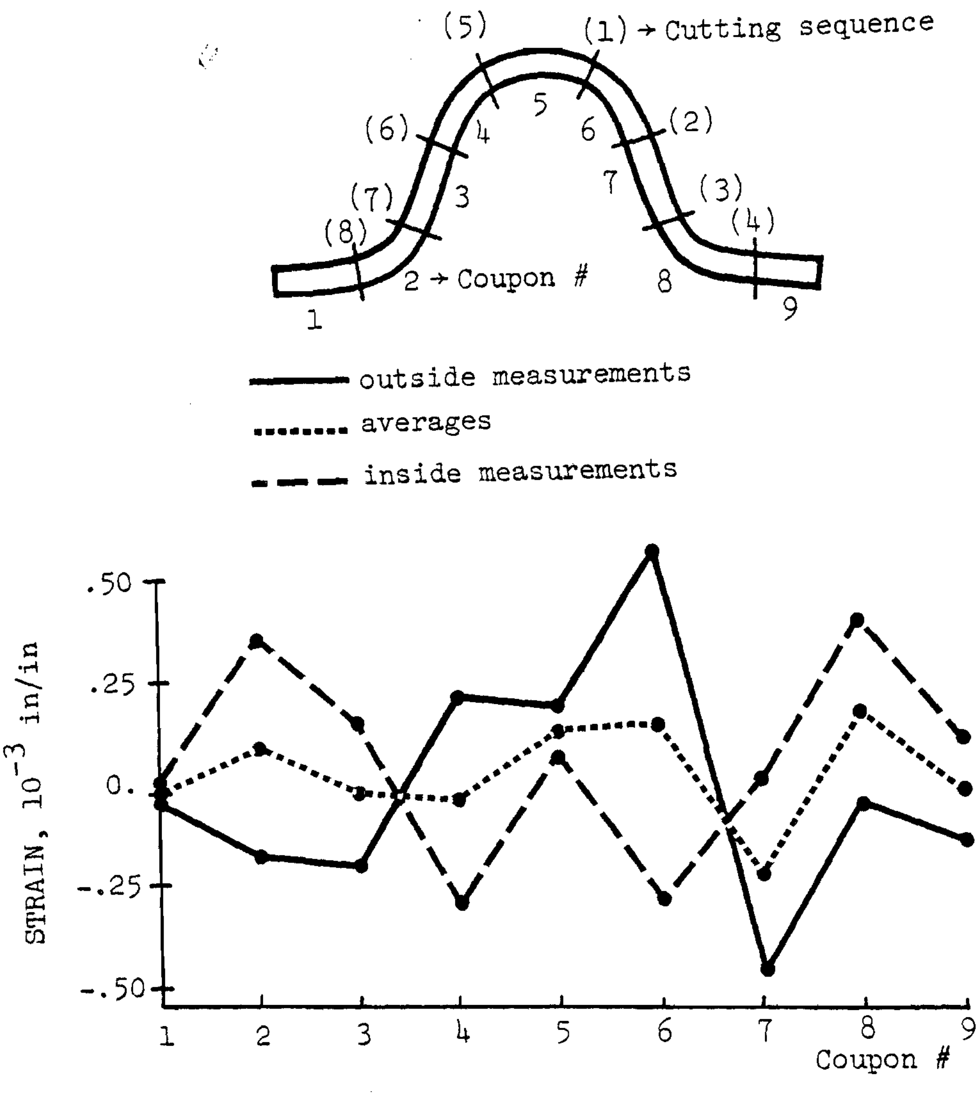

Yield strain of flat $\varepsilon_{yf} = 1.46 \times 10^{-3}$ in/in

Fig. 5.5 H11 Residual Strains.

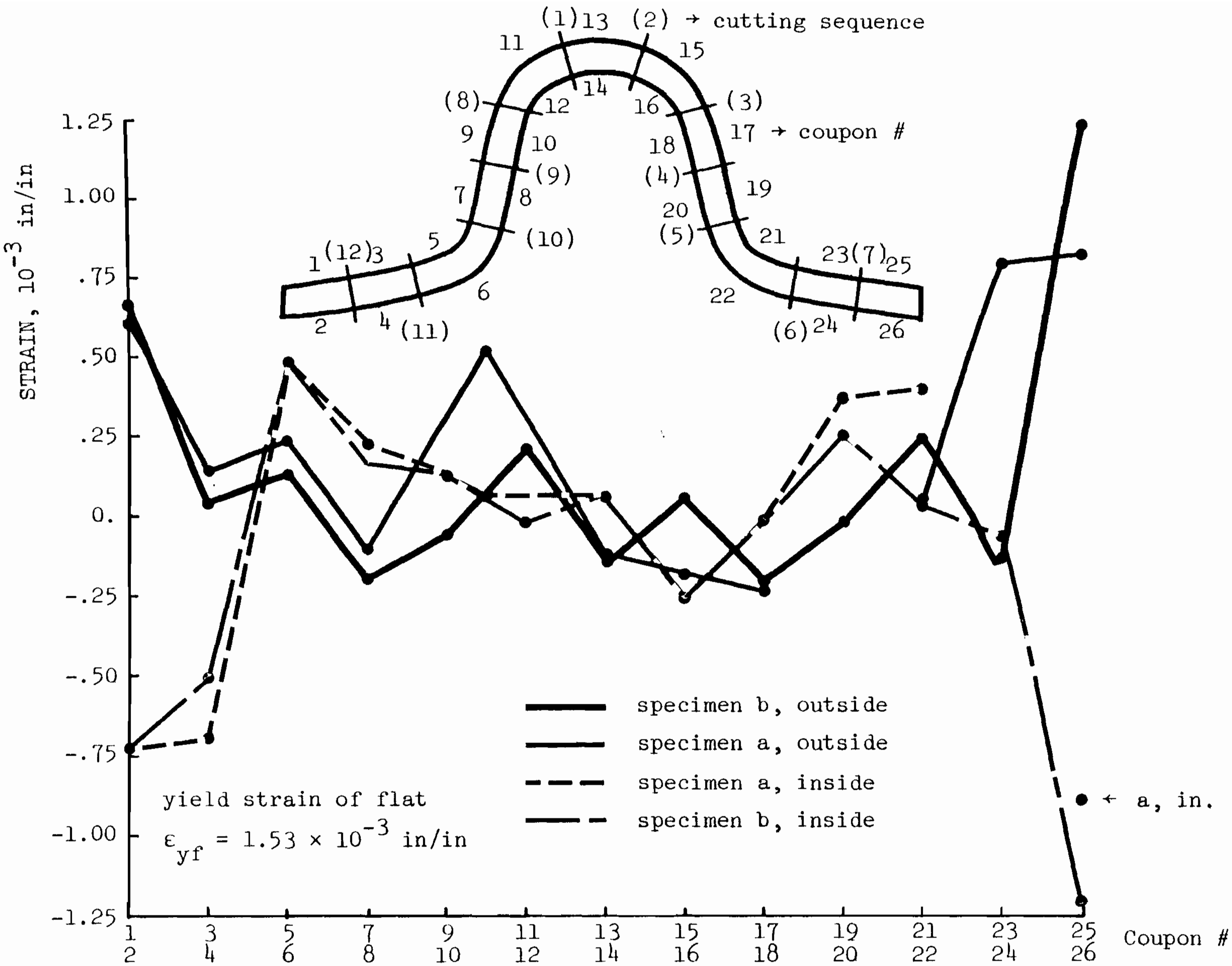

Fig. 5.6 H7 Residual Strains

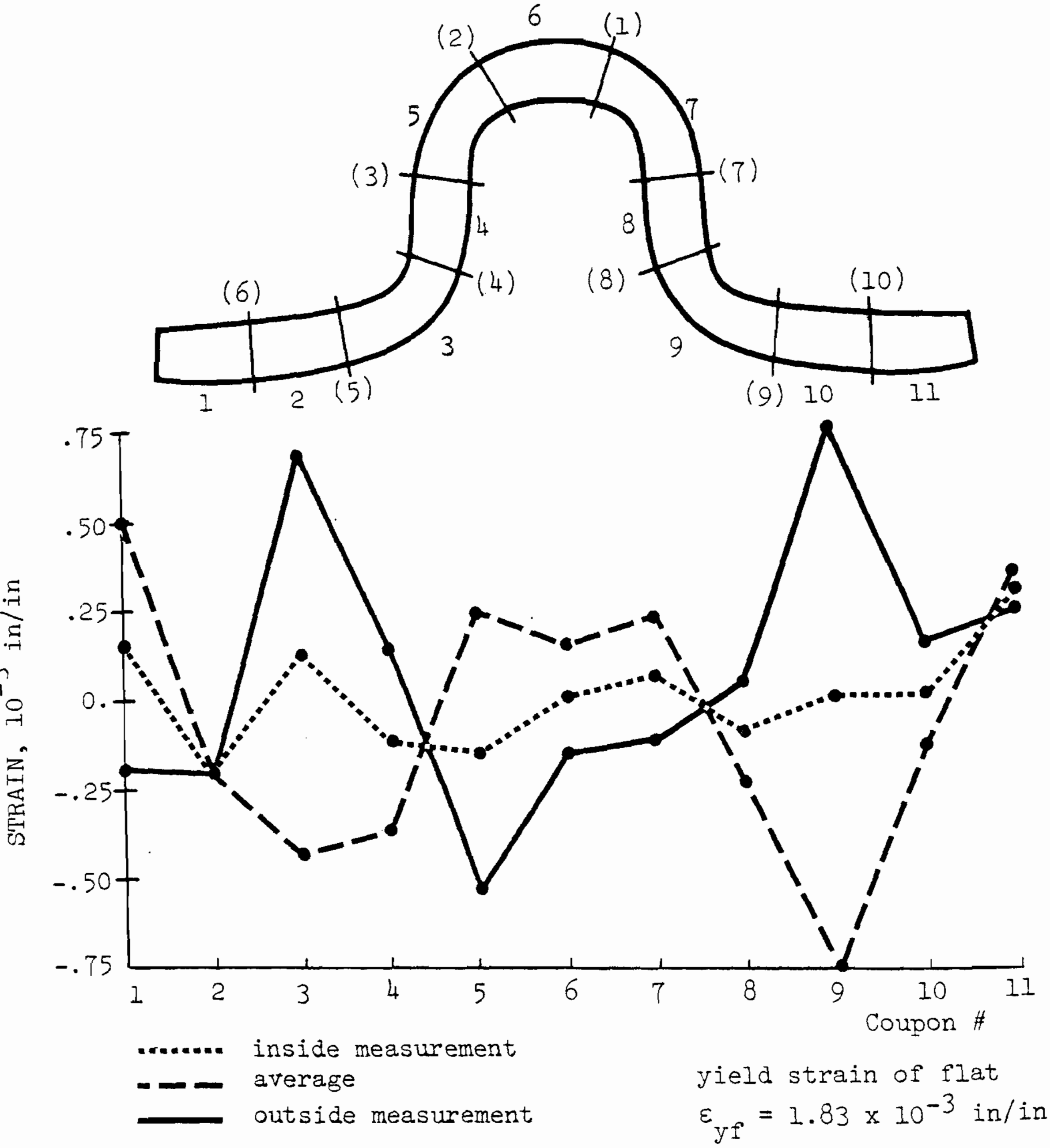

Fig. 5.7 HT Residual Strains

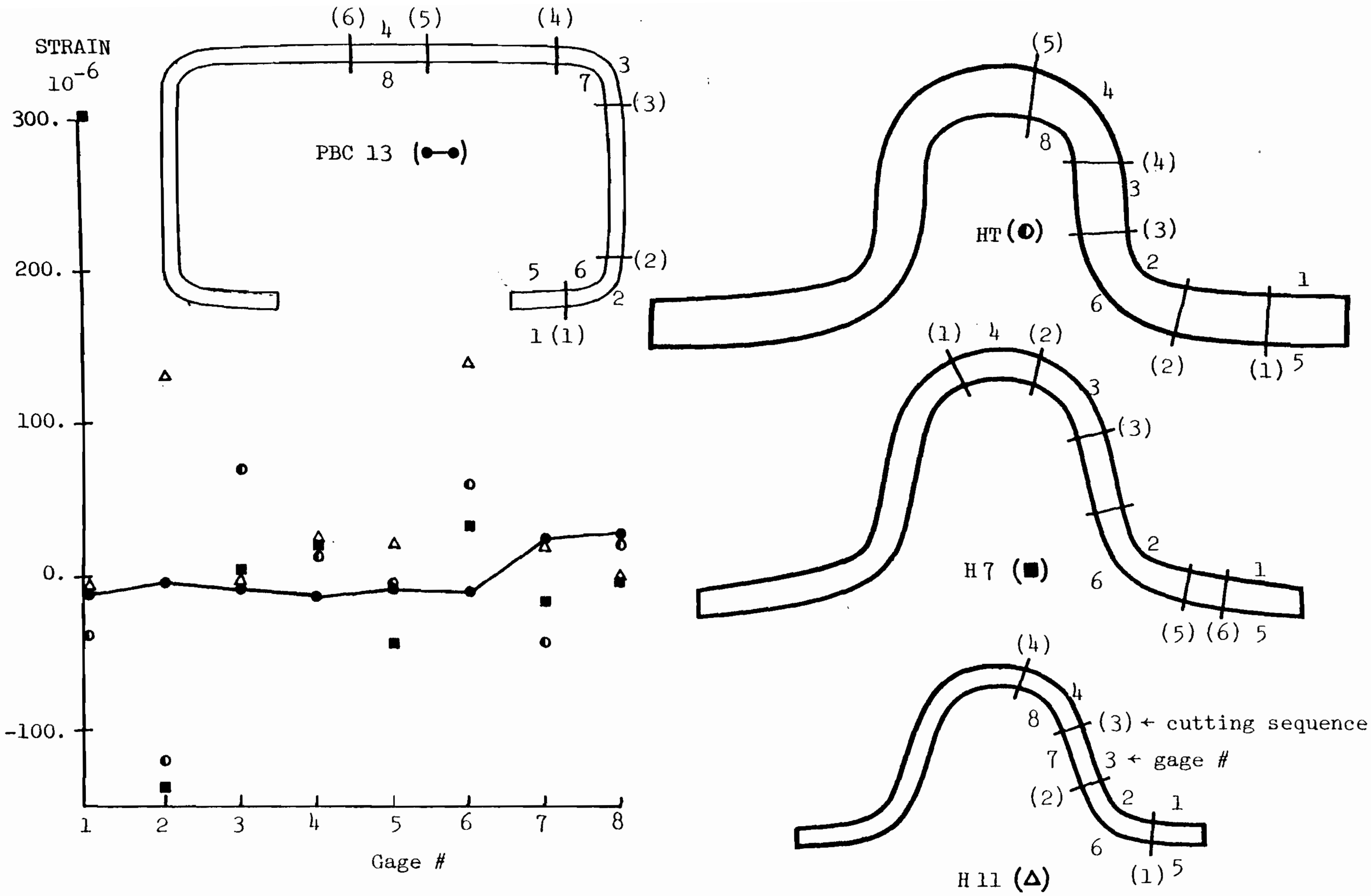

Fig. 5.8 Annealed Specimens: Residual strains due to milling.

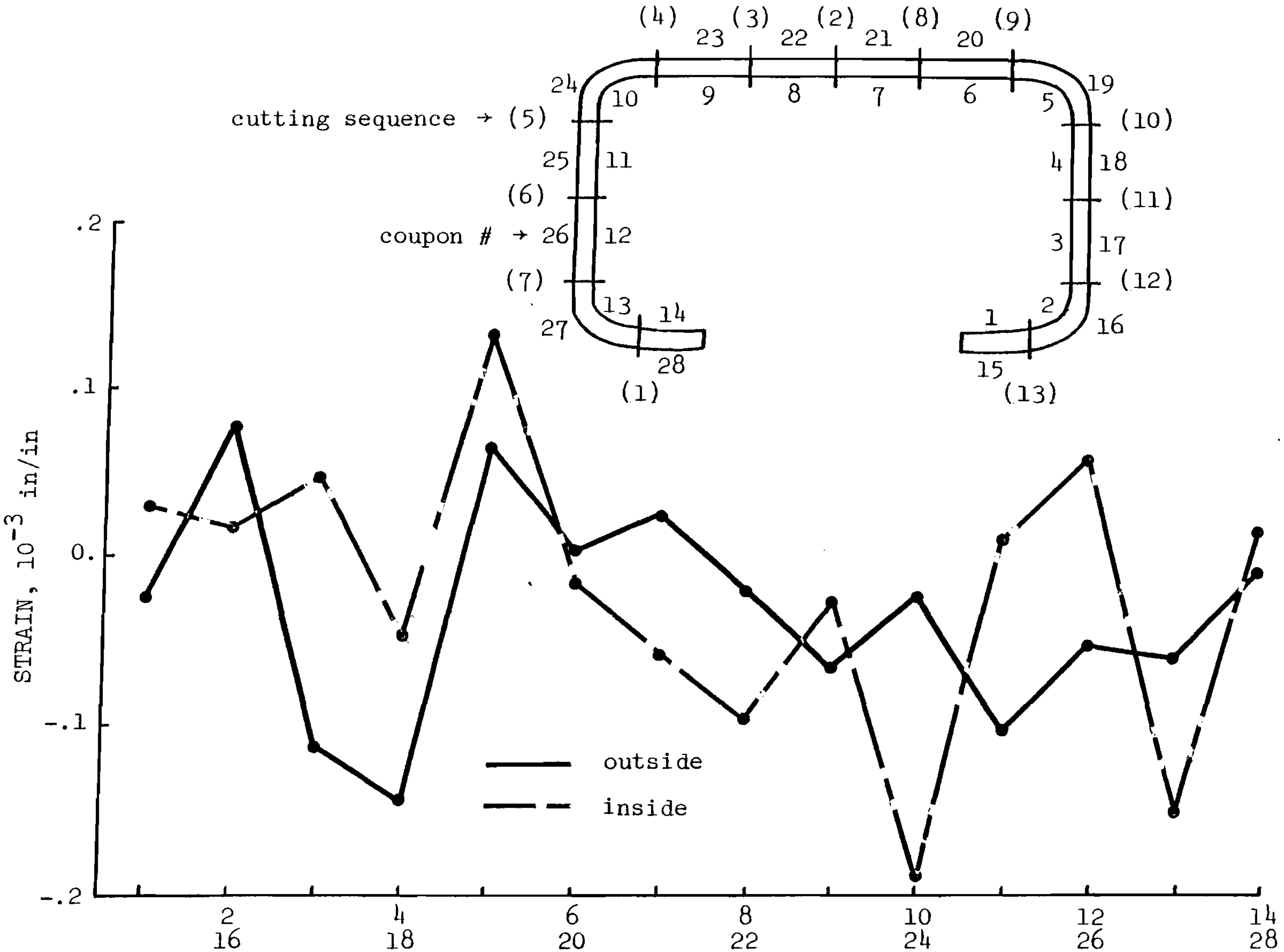

Fig. 5.9 Residual Strains Due to Milling; Annealed PBC 14
(switching unit was probably malfunctioning)

CHAPTER 6

COLUMN STRENGTH: THEORY

6.1 Literature Survey

In their two volumes on beam-columns, Chen and Atsuta [1976, 1977] made a complete and detailed survey of analytical methods for elastic and inelastic beam-columns, including contributions of their own. This was updated in a recent paper by Chen [1977]. The following literature survey follows Chen and Atsuta's classification.

The most important feature of the problem is the development of a relation between the slenderness ratio and the critical load. The problem involves a non-linear differential equation. The non-linearity, due to the dependence of the stiffness upon the loads and location of the section being considered along the column length, is the source of the difficulties. Depending on what the main dependent variable of the differential equation is, the various methods can be classified as deflection, curvature or moment methods. Some methods are general so they do not fall under this classification.

6.1.1 Deflection Methods

All of the early solutions and many of the more recent ones are of this type. It is required to solve the following differential equation under various boundary conditions:

$$\frac{d^2}{dz^2}\left(EI\,\frac{d^2v}{dz^2}\right) + P\,\frac{d^2v}{dz^2} = q(z) \tag{6.1}$$

where z = longitudinal coordinate

$v(z)$ = lateral deflection

$EI(z)$ = stiffness

P = applied axial load

$q(z)$ = lateral load

Initial deflection may be expressed as an equivalent lateral load. Once v is known, slope, curvature and moments can be obtained by differentiation. In the elastic range, analytically exact solutions can be obtained in most cases. Beyond the elastic limit, the solution is difficult because the moment-curvature-thrust relationship for commonly used structural sections is complicated.

6.1.1.1 Exact Approach: Jezek's Method

Jezek [1934] derived a close-form solution to an eccentrically loaded, elastic-perfectly plastic column of rectangular section loaded beyond the elastic limit. The method requires solving the differential equation (6.1) in three regions: elastic, primary plastic (yielding on the concave side only), secondary plastic (yielding on both the convex and concave sides) and matching the proper boundary conditions. Even for such a simple section and stress-strain diagram, the solution is quite involved and requires elliptic integrals.

Horne [1956] extended the solution to account for a finite drop at yield in the stress-strain curve of the material.

6.1.1.2 Numerical Approach: The Column Deflection Curve Method

For more complicated sections a close-form solution is out of the question. Numerical schemes require the knowledge of the moment-curvature relationship for a given axial load. This is usually obtained by an incremental iterative procedure in which the column is idealized into a number of small, constant strain elements. The axial thrust and bending moment are computed for each segment for an assumed state of strain and if these agree with the external loading, the curvature corresponding to that strain profile is taken as correct. Otherwise the strain profile is modified and the procedure repeated. The entire moment-curvature relation corresponding to the given axial thrust can be traced up to the maximum load.

One particularly efficient variant of the above scheme is the Column Deflection Curve Method. Von Karman recognized that different portions of an Equivalent Column under end axial loads only can be considered as various beam-columns under symmetric or asymmetric axial, lateral end loads and end moments. The deflected axis of the Equivalent Column is called a Column Deflection Curve. There is one such curve for a given equivalent axial end load and end slope. To obtain a CDC for a given P, one divides the column into a number of intervals, within each of which the curvature is assumed to vary linearly; one starts at one end with an assumed slope and marches towards the middle (the CDC is symmetrical) computing deflection, moment, curvature and slope at each interval. The CDC method can also be modified to take into account lateral loads.

The solutions of Schwalla [1928], Ellis [1958], Galambos and Ketter [1959], Beer and Schulz [1969, 1970] all followed this basic scheme. T.H. Lin [1950] presented a deflection method which expressed the initial and final shapes as Fourier series. Ojalvo [1960] developed a convenient graphical solution under the form of a series of nomographs.

6.1.1.3 Approximate Approach: Jezek's Method

Any solution that traces the column behavior over the entire loading range, as the ones described above, is bound to be quite elaborate. Westergaard and Osgood (Bleich [1952]) simplified von Karman and Schwalla's solution considerably by assuming the deflected shape to be part of a sine wave. A further simplification was made by Jezek who assumed, besides sinusoidal deflections, an elastic-perfectly plastic stress-strain curve (Bleich [1952]). Both of these works dealt with rectangular cross-sections. Chen and Atsuta [1976] extended the same idea to eccentrically as well as laterally loaded columns of more complicated cross-sections.

Various investigators have confirmed that the assumption of sinusoidal deflections gives very good results (T.H. Lin [1950], Huber and Ketter [1958], Batterman and Johnston [1967], Duberg and Wilder [1952]).

Duberg and Wilder's solution [1952], developed for an idealized H-section column, is based on the method of collocation and assumes that the deflections can be expressed as a series of odd sine terms. A bilinear or a Ramberg-Osgood stress-strain curve is assumed. Results indicate that relatively few terms are required for an accurate solution of the load-deflection history of the column. The column strength is slightly lower when a second term is included but remains virtually unchanged when more terms are added to the first two.

Huber and Ketter [1958] showed that results from a sine curve approximation are very close to the "exact" (deflected shape) results for an eccentrically loaded wide-flange column with residual stresses. Whether the approximate results fall slightly below or slightly above the more exact ones depend on the slenderness ratio and the load eccentricity.

Batterman and Johnston [1967] found that the maximum strength of wide-flange columns computed with the sine shape assumption are only slightly less than those obtained from the exact deflected shape but warned that "no general conclusions can be drawn because this comparison was made for only nominal amounts of residual stresses and initial crookedness".

An example in Chen and Atsuta's book ([1976] p. 265) shows that Jezek's approximate solution gives a higher strength than the solution with real stress-strain curve and exact deflected shape. In that particular example, the assumption of sinusoidal deflection accounts for a maximum error of 4.5% in strength.

It is interesting to note that Yanev and Gjelsvik [1977] have demonstrated that the deflected shape of short columns, buckling in the plastic and strain-hardening ranges, is portions of three sine curves.

6.1.2 The Modified Deflection Method

A modified deflection method was developed by Keramati, Gaylord and Robinson [1972]. They set out to find the critical end eccentricities of a beam-column subject to a given applied axial load. A segment by segment numerical integration procedure is employed for both the deflection curve and the auxiliary curve, which involves the derivative of the deflection curve.

6.1.3 The Curvature Method

The curvature method was essentially developed by Chen (Chen and Atsuta [1976]).

The equilibrium equation for a beam-column can be written as:

$$- M'' + Pv'' = q(z) \tag{6.2}$$

where " denotes 2nd order differentiation and M is the moment.

The equation can be expressed in normalized form with the following variables:

$m = M/M_y$ where M_y = the yield moment = $\sigma_y s$, s = section modulus

$\phi = \Phi/\Phi_y$ Φ, Φ_y are curvature and curvature at yield ($\Phi_y = 2\varepsilon_y/D$, D = section depth).

$\tilde{p} = P/P_y$ $P_y = A\sigma_y$ = yield load

$\bar{q} = q/M_y$

$h^2 = P/EI$

So:

$$m'' + h^2\phi = -\bar{q} \tag{6.3}$$

The moment-curvature relations depend on the extent of plastification:

$$m = \begin{cases} a\phi & \phi \le \phi_1 & : \text{elastic} \\ b - c/\sqrt{\phi} & \phi_1 \le \phi \le \phi_2 & : \text{primary plastic} \\ m_{pc} - d/\phi^2 & \phi_2 \le \phi & : \text{secondary plastic} \end{cases} \tag{6.4}$$

In the primary plastic state, yielding has occurred in a zone adjoining the concave edge and in the secondary plastic state, in zones adjoining both the concave and convex edges. a, b, c, d, m_{pc}, ϕ_1 and ϕ_2 are functions of the load, the material and the shape of the cross-section. Substitution of (6.4) into (6.3) results in a second order differential equation for ϕ. Integration gives $\phi' = d\phi/dz$ explicitly and in close form, but ϕ is best evaluated for specific cases. The various integration constants are determined from the boundary conditions, the conditions of continuity of curvature and discontinuities of curvature slope (ϕ' jumps at boundaries between regimes and at concentrated loads).

Results include curves relating $\tilde{p}$ to the midspan curvature ϕ_m and curves of slenderness ratio λ versus ϕ_m. By combining the two sets of curves, curves of $\tilde{p}$ versus λ are obtained. As in the Deflection Method, an Equivalent Column and a Column Curvature Curve can be defined. These simplify the solution of asymmetric loading cases.

6.1.4 The Moment Method

The Moment Method was developed by Cheong Siat Moy [1974] and is closely related to the curvature method. Equilibrium is now expressed in terms of moments:

$$\frac{d^2M}{dz^2} = -Pg(M,P) - q \tag{6.5}$$

where $\Phi = g(M,P)$ is the moment-curvature-thrust relationship.

If $\tilde{q} = q/(M_y h^2)$

and $\phi = \Phi/\Phi_y = g(M,P)/\Phi_y = \bar{g}(m,\tilde{p})$.

(6.10) takes the form:

$$\frac{d^2m}{dz^2} = -h^2[\bar{g}(m,\tilde{p}) + \tilde{q}] \tag{6.6}$$

The inverse of (6.4) is:

$$\phi = \bar{g}(m,\tilde{p}) = \begin{cases} m/a & \text{for} \quad |m| \le m_1 \quad : \text{elastic} \\ \left(\dfrac{c}{b-m}\right)^2 & m_1 \le |m| \le m_2 \quad : \text{primary plastic} \\ \left(\dfrac{d}{m_{pc}-m}\right)^{1/2} & m_2 \le |m| \quad : \text{secondary plastic} \end{cases} \tag{6.7}$$

(6.6) and (6.7) can be integrated rather easily. The complete moment diagram can be obtained by a forward marching procedure starting, say, at the section of maximum bending moment.

6.1.5 The Finite Differences Method

The equilibrium equation can be rewritten in the following form:

$$\frac{d^2M}{dz^2} + P(\Phi + \Phi_{io}) = -q \tag{6.8}$$

where Φ_{io} is the initial curvature at point i and $M = f(\Phi,P)$. The derivative is replaced by a finite difference:

$$\left(\frac{d^2M}{dz^2}\right)_i \simeq \frac{1}{\Delta z^2}(M_{i-1} - 2M_i + M_{i+1}) \tag{6.9}$$

Since $M = f(\Phi,P)$ is non-linear for elasto-plastic beam-columns, Φ_i must be solved for by an iterative procedure.

Young [1972] used this method to calculate the ultimate load of an axially loaded column with initial sinusoidal deflection.

6.1.6 The Finite Element Method

In this particularly versatile numerical method, the beam-column is divided into an assembly of discrete elements and the element stiffness (or flexibility) is evaluated using an approximate displacement (or stress) field along the element length. The set of functions for displacements (or stresses) are so chosen that they ensure continuity (or equilibrium) throughout the entire system. The application of the method to a practical problem requires the solution of a large system of linear algebraic equations. Details can be found in Chen and Atsuta [1977], to mention just one reference, which also includes a chapter on a parent method called the Finite-Segment Method.

Epstein et al [1978] used the FEM to study the behavior of inelastic beam-columns under large displacements. Seide [1975] compared the accuracy and convergence rate of the finite-difference method and two finite-element methods based on the minimum potential energy and a mixed variational principle for elastic column buckling.

6.1.7 Newmark's Integration Method [1943]

Newmark's integration method is a useful means to compute the deflected shape from a given curvature distribution. By using this method, the maximum strength of a beam-column can be examined directly without tracing closely the load-deflection curve.

6.2 Approximate Determination of Column Strength Using Jezek's Method

An approximate deflection method is used here by assuming a sinusoidal deflected shape and an elastic-perfectly plastic, but inhomogeneous material (Jezek's approximate solution, § 6.1.1.3). The analysis is similar to the work of Bjorhovde and Tall [1971], who studied the strength of wide-flange hot-rolled columns, but the geometries and residual stresses in the present work are completely different.

An initially curved column of length L is subjected to an axial load P applied at the centroid of its cross-section. The column is assumed to bend about its weak axis only.

6.2.1 Equilibrium

Let $v_o(z)$ and $v(z)$ designate the initial and additional lateral deflections at elevation z (Fig. 6.1). Under the combined axial load and bending moment, part of the cross-section may yield. The moment of the applied load about the centroid of the cross-section is:

$$M = P[v_o(z) + v(z)] \tag{6.10}$$

Compressive stresses and P are positive. Positive moments cause positive lateral deflections (+v in the +x direction) and consequently compression to the left of the centroid (Fig. 6.2).

The internal force and moment are:

$$P_{in} = \int_A \sigma dA = E \int_{A_e} \varepsilon dA + E \int_{A_p} \varepsilon_y dA \tag{6.11}$$

$$M_{in} = \int_A \sigma(x_o - x)dA = E \int_{A_e} \varepsilon(x_o - x)dA + E \int_{A_p} \varepsilon_y(x_o - x)dA \tag{6.12}$$

where ε_y = yield strain of material

x_o = abcissa of centroid (Fig. 6.2)

A_e = area of elastic part of section

A_p = area of plastic part of section

$A = A_e + A_p$ = total area of section

The material is assumed to be elastic-perfectly plastic, but variations of the yield stress and the presence of residual stresses (both due to cold-forming) are accounted for.

6.2.2 Strain-Displacement Relationship

The lateral deflections are assumed to be sinusoidal

$$v_o(z) = V_o \sin \pi z/L \tag{6.13}$$

$$v(z) = V \sin \pi z/L \tag{6.14}$$

So the maximum moment is

$$M_m = P[V_o + V] \tag{6.15}$$

where v_o, v are the initial deflection and the additional deflection due to the load

and V_o, V are the maximum values of v_o, v at midheight.

In the elastic range v is exactly sinusoidal provided v_o is also sinusoidal. The load-deflection relationship needs only be established between the load P and the single parameter V. The curve P-V reaches a maximum P which is the column strength (buckling load of an imperfect column).

If plane sections are assumed to remain plane, the bending strain ε_b is related to the deflection $v(z)$ by the familiar relationship:

$$\Phi = \frac{\varepsilon_b}{x_o - x} \simeq -v''. \tag{6.16}$$

At midheight and from (6.14):

$$\frac{\varepsilon_b}{x_o - x} = \frac{\pi^2}{L^2} V \tag{6.17}$$

6.2.3 Computational Scheme:

For a given V, a value of P is assumed. A first assumption may correspond to the elastic solution:

$$P(V + V_o) = EI\left(\frac{\pi^2}{L^2} V\right) \tag{6.18}$$

where I is the moment of inertia of the cross-section.

Bending strains are calculated according to (6.17), but a value of the axial strain ε_a is assumed. Again a first assumption may correspond to the elastic situation:

$$\varepsilon_a = \frac{P}{EA} \quad . \tag{6.19}$$

The total strain is obtained by summing the axial strain, the bending strain and the adjusted residual strains, which are discussed below. The elastic and the plastified parts of the section are determined and (6.11), (6.12) used to calculate the internal force and moment. If equilibrium is satisfied, i.e.

$$P_{in} = P \tag{6.20a}$$

$$M_{in} = M \tag{6.20b}$$

then a point on the P - V curve of the column has been found. However, if $P_{in} \neq P$, ε_a is changed and P_{in} and M_{in} are recomputed. Once equilibrium of forces is satisfied, equilibrium of moments is checked. If moments do not balance, the assumed value of P is changed and the process repeated. After equilibrium is satisfied, V is incremented and a new iteration started. A flowchart is shown in Fig. 6.3.

6.2.4 Discretization

The problem is complicated by the presence of residual stresses and the non-uniformity of the yield stress and thickness over the cross-section. Since the mechanical properties of the material are measured at discrete locations by sectioning, it is natural to divide the cross-section, or half of it because of symmetry, into discrete elements.

The strain field in each element is assumed uniform in the width direction but linearly varying in the thickness direction. The reasons for the higher refinement in the thickness direction are 1) no partitioning is performed in that direction, i.e. the thickness of an element is that of the section and 2) it is desired to account for the variation of residual strains over the thickness. The locally measured values of the tensile yield stress and thickness are used for each element. As discussed in Chapter 3 tensile coupon yield stress is not appreciably different from compressive yield stress and is not much influenced by residual stresses.

6.2.5 Residual Strains

The elemental radial coordinate ρ originates from the midthickness of an element and is positive outward (Fig. 6.2 and 6.4). For a flat element, the outward, positive direction is the same as for the previous curved segment with segment numbering beginning at the axis of symmetry.

Let ε_{oj} and ε_{ij} be the values of the residual strains at the outside and inside faces of element j. Three distributions of residual strains, of increasing complexity, are studied:

Uniform Distribution:

Residual strains are constant over the thickness. This assumption is customarily made for thin sections (Sherman [1971], Beedle and Tall

[1960]).

$$\varepsilon_j^{res} = \varepsilon_{oj} = \varepsilon_{ij} = \text{constant} \tag{6.21}$$

Linear Distribution (Figs. B1 and B2)

The following is derived in Appendix B:

$$\varepsilon_j^{res} = \frac{1}{2}(\varepsilon_{oj} + \varepsilon_{ij}) + \frac{\rho}{t_j}(\varepsilon_{oj} - \varepsilon_{ij}) \tag{6.22}$$

Rectangular Distribution (Figs. B3 and B4)

This distribution consists of two rectangular blocks and incorporates the essential features of Ingvarsson's analysis [1975] and those of the approximate analysis of Chapter 4. A more exact distribution would complicate the algebra significantly.

Let ρ_{nj} be the coordinate of the neutral axis. Chapter 4 explains how ρ_{nj} can be derived from the thinning of a corner, $\Delta t_j/t_j$.

$$\varepsilon_j^{res} = \begin{cases} \varepsilon_{oj} = \text{constant for } \rho \geq \rho_{nj} \\ \\ \varepsilon_{ij} = \text{constant for } \rho \leq \rho_{nj} \end{cases} \tag{6.23}$$

6.2.6 Experimental Input

It is necessary to relate ε_{oj}, ε_{ij}, the values of the assumed residual stress distribution at the surfaces, to the measured values, $-\bar{\varepsilon}_{oj}$, $-\bar{\varepsilon}_{ij}$.

Uniform Distribution

The average of the measured values is clearly the best estimate.

$$\varepsilon_j^{res} = (\bar{\varepsilon}_{oj} + \bar{\varepsilon}_{ij})/2 \tag{6.24}$$

For the other two distributions, equilibrium must be considered.

The measured quantities are the surface values of the elastic release of the residual stresses. The force and moment released by sectioning are equal and opposite to the locked-in force and moment.

Linear Distribution

The released stresses are elastic and therefore linearly distributed.

So:

$$\varepsilon_{oj} = \bar{\varepsilon}_{oj}$$

$$\varepsilon_{ij} = \bar{\varepsilon}_{ij}$$

and

$$\varepsilon_j^{res} = \frac{1}{2}(\bar{\varepsilon}_{oj} + \bar{\varepsilon}_{ij}) + \frac{\rho}{t_j}(\bar{\varepsilon}_{oj} - \bar{\varepsilon}_{ij}) \tag{6.25}$$

Rectangular Distribution

The following variables are defined:

$$\begin{cases} u_j = \varepsilon_{oj} + \varepsilon_{ij} \\ w_j = \varepsilon_{oj} - \varepsilon_{ij} \end{cases} \iff \begin{cases} \varepsilon_{oj} = (u_j + w_j)/2 \\ \varepsilon_{ij} = (u_j - w_j)/2 \end{cases} \tag{6.26}$$

$$\begin{cases} \bar{u}_j = \bar{\varepsilon}_{oj} + \bar{\varepsilon}_{ij} \\ \bar{w}_j = \bar{\varepsilon}_{oj} - \bar{\varepsilon}_{ij} \end{cases} \iff \begin{cases} \bar{\varepsilon}_{oj} = (\bar{u}_j + \bar{w}_j)/2 \\ \bar{\varepsilon}_{ij} = (\bar{u}_j - \bar{w}_j)/2 \end{cases} \tag{6.27}$$

$$\zeta_j = 2\rho_{nj}/t_j \tag{6.28}$$

$$\psi_j = (1 + \zeta_j)(1 - \zeta_j) \tag{6.29}$$

B_j = width of segment at midthickness

$2\alpha_j$ = corner angle

$$\beta_j = t_j/B_j. \tag{6.30}$$

The following relationships are derived in Appendix B:

-for a straight element:

$$\varepsilon_{oj} = \frac{\bar{u}_j}{2} + \frac{\bar{w}_j}{3(1-\zeta_j)} \qquad (6.31a)$$

$$\varepsilon_{ij} = \frac{\bar{u}_j}{2} - \frac{\bar{w}_j}{3(1+\zeta_j)} \qquad (5.31b)$$

-for a curved element:

$$u_j = \frac{(\alpha_j^2\beta_j^2 - 3)(3\psi_j\bar{u}_j + 2\zeta_j\bar{w}_j)}{\Delta_j} \qquad (6.32a)$$

$$w_j = \frac{6\alpha_j\beta_j\psi_j\zeta_j\,\bar{u}_j + 2(\alpha_j^2\beta_j^2\psi_j\zeta_j + \alpha_j^2\beta_j^2 - 3)\bar{w}_j}{\Delta_j} \qquad (6.32b)$$

where $$\Delta_j = 3\psi_j[\alpha_j\beta_j\zeta_j(\alpha_j\beta_j\psi_j - 2\zeta_j) + \alpha_j^2\beta_j^2 - 3] \qquad (6.32c)$$

6.2.7 Equilibrium Corrections:

Due to experimental errors, the measured residual stresses do not exactly satisfy equilibrium of forces and moments. The following correction factors, derived in Appendix B, are required.

Axial Strain Correction:

The unbalance force is:

-for uniform distribution: $$F = \sum_{j=1}^{n} (E\,\varepsilon_j^{res}B_jt_j) \qquad (6.33)$$

with ε_j^{res} given by (6.24)

-for linear and rectangular distributions:

$$F = \sum_{j=1}^{n} f_j \qquad (6.34)$$

where f_j, the unbalance force for element j is derived in Appendix B:

$$f_j = EB_j t_j(\bar{\varepsilon}_{oj} + \bar{\varepsilon}_{ij})/2 + Et_j^2\alpha_j(\bar{\varepsilon}_{oj} - \bar{\varepsilon}_{ij})/6 \qquad (6.35)$$

This force is computed from the linear strains of relaxation, rather than the assumed locked-in distribution. $\alpha_j = 0$ for a straight element.

The axial strain correction is given by:

$$\varepsilon_1 = -\frac{F}{EA} \qquad (6.36)$$

Bending Strain Corrections:

-for uniform distribution:

Residual stresses are assumed uniform for each segment and the resultant force is applied at the centroid of the segment, whose abcissa is x_{cj}. The unbalance moment is:

$$M_u = \sum_{j=1}^{n} E\,\varepsilon_j^{res}\, B_j t_j\,(x_o - x_{cj}) \qquad (6.37)$$

x_o is the abcissa of the centroid of the entire cross-section and ε_j^{res} is given by (6.24).

-for linear and rectangular distributions:

$$M_u = \sum_{j=1}^{n} [m_j\cos\theta_j + f_j(x_o - x_{cj})] \qquad (6.38)$$

where θ_j is the angular coordinate of the centroid of the element (Fig. 6.4), f_j is given by (6.35) and m_j is the unbalance moment for element j.

$$m_j = -\frac{EB_j t_j^2}{12}(\varepsilon_{oj} - \varepsilon_{ij}) \text{ for a straight element} \qquad (6.39a)$$

and $$m_j = -\frac{EB_j t_j^2}{12}(\varepsilon_{oj} - \varepsilon_{ij})(1 - \frac{t_j^2 \alpha_j^2}{3B_j^2})\frac{\sin\alpha_j}{\alpha_j} \text{ for a curved element.} \quad (6.39b)$$

These expressions are derived in Appendix B.

The corrective bending strain is:

$$\varepsilon_2 = -\frac{M_u}{EI}(x_o - x) \quad (6.40)$$

where $$x = x_{dj} + \rho\cos\theta_j \quad (6.41)$$

and I is the moment of inertia of the entire cross-section.

6.2.8 Determination of the Extent of Yield

It is necessary to determine the extent of yield for each element. The total strain at any point of element j is given by:

$$\varepsilon_{tj} = \varepsilon_a + \varepsilon_b + \varepsilon_j^{res} + \varepsilon_1 + \varepsilon_2 \quad (6.42)$$

where ε_a = axial strain from Eq. (6.19)

ε_b = bending strain from Eq. (6.17)

ε_j^{res} = residual strain from Eq. (6.21), (6.22) or (6.23)

ε_1 = correction for force equilibrium from Eq. (6.36)

ε_2 = correction for moment equilibrium from Eq. (6.40).

Let ρ_{yj} be the radial coordinate at which the total strain equals the yield strain ε_{yj}:

-<u>for the uniform and rectangular distributions</u>:

$$\varepsilon_{yj} = \varepsilon_{tj} = \varepsilon_a + \varepsilon_1 + \varepsilon_j^{res} + (\frac{\pi^2}{L^2}V - \frac{M_u}{EI})(x_o - x_{dj} - \rho_{yj}\cos\theta_j) \quad (6.43)$$

$$\Longrightarrow \rho_{yj} = (\frac{\varepsilon_a + \varepsilon_1 + \varepsilon_j^{res} - \varepsilon_{yj}}{\frac{\pi^2}{L^2}V - \frac{M_u}{EI}} - x_o + x_{dj})\frac{1}{\cos\theta_j} \quad (6.44)$$

ε_j^{res} is given by (6.21) for the uniform distribution and by (6.23) for the rectangular distribution.

-<u>for the linear distribution</u>:

$$\varepsilon_{yj} = \varepsilon_a + \varepsilon_1 + \frac{1}{2}(\bar{\varepsilon}_{oj} + \bar{\varepsilon}_{ij}) + \frac{\rho_{yj}}{t_j}(\bar{\varepsilon}_{oj} - \bar{\varepsilon}_{ij}) + (\frac{\pi^2}{L^2} V - \frac{M_u}{EI})(x_o - x_{dj} - \rho_{yj}\cos\theta_j) \tag{6.45}$$

$$\Rightarrow \rho_{yj} = \frac{\varepsilon_a + \varepsilon_1 - \varepsilon_y + \frac{1}{2}(\bar{\varepsilon}_{oj} + \bar{\varepsilon}_{ij}) + (\frac{\pi^2}{L^2} V - \frac{M_u}{EI})(x_o - x_{dj})}{(\frac{\pi^2}{L^2} V - \frac{M_u}{EI}) \cos\theta_j - \frac{(\bar{\varepsilon}_{oj} - \bar{\varepsilon}_{ij})}{t_j}} \tag{6.46}$$

6.3 Implementation. Effect of Initial Deflection and Direction of Buckling

The mathematical developments of the preceding section are implemented in a computer program. Data fed into the program includes the geometrical properties of the section, the length of the column including the end plates and fixtures, the mechanical properties of the material and the initial deflection of the column. Values of yield strength and residual stresses come from the tensile coupon tests and residual stress tests described in Chapters 3 and 5.

Examples are shown here, but most of the results will be discussed in Chapter 9, together with experimental findings. Figures 6.5 and 6.6 show theoretical results for a PBC 13 Column, of length L = 51.0" and maximum initial deflection V_t = -.004 L (subscript t for theoretical). The yield strength at specific locations of the cross-section are obtained from Fig. 3.14, specimen a, but the residual stresses are only half of those corresponding to Fig. 5.3a (this particular result comes from a study reported below of the effect of the magnitude of the residual stresses on column strength). Because the computer program makes use of the geometrical symmetry of the section, the actual input consists of the average of these data over the two symmetrical halves of the section. In this particular example, significant plastification does not occur until the load reaches about 2/3 of ultimate (Fig. 6.5). Fig. 6.6 is a plot of the strain on the convex and concave sides. Since the initial deflection is negative and the load is centrally applied, the column deflects in the negative direction (i.e. to the left on Fig. 6.2) and the convex side is the web, the concave side the lips (strains are calculated at the locations of the strain gages, namely at the middle of the web and at the flanges, near the junctures with the lips). Both figures show clearly that the load reaches a maximum, then decreases as straining increases.

Figures 6.7 and 6.8 show studies of the same column, but with full residual stresses (from Fig. 5.3a); Figure 6.7 is a plot of load versus lateral deflection (additional deflection due to load) for buckling to the right and to the left about the weak axis, which is perpendicular to the axis of symmetry of the section. The load maxima are represented by the dotted lines on Fig. 6.7 and also shown on Fig. 6.8 and Table 6.1. As the initial deflection tends to zero and by extrapolating from these figures, it is seen that the phenomenon becomes one of unstable asymmetric bifurcation. Column strength is the limit point of the equilibrium path of a column with initial imperfection.

In order to compare theoretical with experimental results, a Southwell plot is drawn for this example (PBC 13, L = 51.0". Fig. 6.9,

Table 6.2). Except for the vicinity of the origin where the load is small and the measured deflections relatively inaccurate, the points fall on a straight line. The intercept with the V-axis gives an initial deflection of V_o = -.015 in = -.00029 L, equivalent to the combination of initial deflection and unavoidable load eccentricity. For V_t/L = -.00030, the computer program predicts a strength P_{th} = 21.32 k, which compares favorably with the experimental P_u = 21.60 k.

It was not convenient to transform all the experimental records into Southwell plots. An alternative approach was used, whereby the computer program was run for various values of V_o until a good match was found between the computed deflections and strains and the actual ones. In most cases, reasonable agreement was also obtained between the predicted and the actual value of P_u (Chapter 9). For the example mentioned above, a good match was found for an assumed V_t = .0004 L for which P_{th} = 20.96 k. Of course, V_t can be adjusted so the actual and computed column strengths agree exactly, but then the theoretical strains and deflections will usually not match the actual strains and deflections exactly.

6.4 Effect of Residual Stresses

The effect of the magnitude and distribution of the longitudinal residual stresses on column strength is shown in Table 6.3 for one example (PBC 73 , L = 51.0").

As expected, the strength is highest for no residual stresses.

The first distribution over the perimeter to be studied is close to the actual one but rendered symmetrical by averaging over the two halves of the cross-section. Three distributions across the thickness are assumed: constant, linear and rectangular (models 1, 2 and 3).

Because the average residual stress across the thickness is close to zero, model 1 gives strengths close to the case with no residual stress.

Model 2 accounts better for the presence of residual stresses and causes a reduction in strength of 5.4% for buckling to the left (negative deflection) and 6.4% for buckling to the right (positive deflection), compared to a column free of residual stress.

Model 3 is sensitive to the location of the neutral axis of residual stresses. It was seen in Chapter 4 that the location of the neutral axis depends on the amount of pressure used in cold-forming (Eq. 4.6), which in turn can be determined from the reduction in thickness (Eq. 4.9). It was also discussed in § 4.8 that the neutral axis is always below the midsurface of the sheet without ever reaching it. If ρ is a thickness coordinate, originating from midthickness and positive outward, then the coordinate ρ_n of the neutral surface is always negative: $\rho_n < 0$. For the case of no pressure, however, it was seen that the neutral surface is close to the midsurface: $\rho \simeq 0$. This value proves to be a convenient limiting case and gives reductions in strength of 15% for buckling to the left and 12% for buckling to the right. For smaller values of ρ (more negative), the reduction in strength is not as large. If the same distribution is kept but the magnitude of the residual stresses reduced to half of the actual values, the reduction in strength is only about 2.5%.

Another distribution consisting of residual stresses at corners only is also examined. Since the residual stresses affect only a small proportion of the cross-sectional area, there is no reduction in strength.

A brief study of the influence of the residual stress distribution across the thickness (Table 6.4) suggests the effect of residual stresses is less severe for larger initial deflections. If supported by a more systematic computer study, this conclusion would differ from Batterman and Johnston's conclusion [1967] concerning hot-rolled steel columns (§ 2.3.5).

6.5 Closure

An approximate method of determining column strength was developed, which accounts for cold-forming effects and initial deflections. The difference of residual stresses and initial deflections was discussed. Comparison with experimental data follows in Chapter 9.

Table 6.1

Effect of Initial Imperfection and Direction of Buckling on Column Strength

PBC 13 L = 51.0"

$\lvert V_t/L \rvert * 10^3$	P_{th} for $V_t = -\lvert V_t \rvert$	P_{th} for $V_t = \lvert V_t \rvert$
2.50	17.04	17.18
2.00	17.77	17.81
1.75	18.16	18.16
1.50	18.58	18.53
1.25	19.02	18.93
1.00	19.49	19.36
.75	20.04	19.83
.50	20.68	20.36
.40	20.96	20.59
.30	21.32	20.81
.25	21.58	20.94
.20	22.18	21.07

Table 6.2

Southwell Plot

PBC 13 L = 51.0"

P kips	V_1 10^{-3} inch	V_2 10^{-3} inch	V_1/P	V_2/P
1	0	0	0	0
2	0	0	0	0
3	1	0	.33	0
4	1	1	.25	.25
5	2	2	.40	.40
6	4	3	.66	.50
7	5	6	.71	.86
8	7	7	.87	.87
9	8	9	.89	1.0
10	10	12	1.0	1.2
11	13	14	1.18	1.27
12	15	16	1.25	1.33
13	18	19	1.38	1.46
14	22	23	1.57	1.64
15	26	27	1.73	1.80
16	32	33	2.00	2.06
17	40	42	2.35	2.47
18	49	52	2.72	2.89
19	62	66	3.26	3.47
20	84	89	4.20	4.45
21	141	146	6.71	6.95
21.60 Max				

V_1 and V_2 are lateral deflections measured at locations 1 and 2 (Fig. 6.9)

Table 6.3

Effect of Magnitude and Distribution of

Residual Stresses on Column Strength

PBC 13, L = 51.0"

$\lambda = 78.7 \qquad \overline{\lambda}_a = .970 \qquad \overline{\lambda}_f = .890$

Distribution Over Perimeter	Magnitude (μin/in)	Model Across Thickness (in)	P for $V_t/L = -.0004$ (kips)	(%)	P for $V_t/L = +.0004$ (kips)	(%)
No residual strains			22.80	100.	22.30	100.
Average over symmetrical halves	Actual	1(uniform)	22.74	99.74	22.00	98.65
		2(linear)	21.57	94.60	20.86	93.54
		3(rectangular)				
		ρ_n = 0.0*	19.26	84.47	19.69	88.30
		ρ_n = -.015**	21.99	96.45	20.90	93.72
	1/2 Actual	3,ρ_n = 0.0	22.28	97.72	21.72	97.40
ε^{res} = ±750 at corners, ±375 adjacent to corners, 0 elsewhere			22.80	100.	22.30	100.

*neutral surface at midthickness
**neutral surface at lower third of thickness

Table 6.4

Effect of Models of Residual Stresses and Direction of Buckling on Column Strength

Section	L (inch)	Model	P for $V_t/L = +.001$ (kips)	P for $V_t/L = -.001$ (kips)
PBC 14	33.0	1	20.70	22.60
		2	20.63	22.97
		3	20.57	22.85
RFC 14	63.0	1	13.70	12.69
		2	13.16	12.65
		3	12.99	12.63
PBC 13	51.0	1	20.27	20.63
		2	19.55	19.79
		3	19.37	19.49
RFC 13	69.0	1	14.03	12.80
		2	13.41	12.71
		3	13.26	12.68
H11	39.0	1	10.36	10.78
		2	10.17	10.73
		3	10.17	10.75
H7	45.0	1	37.19	34.99
		2	37.08	35.05
		3	36.99	34.95
HT	51.0	1	59.89	60.29
		2	60.06	59.53
		3	59.95	59.55

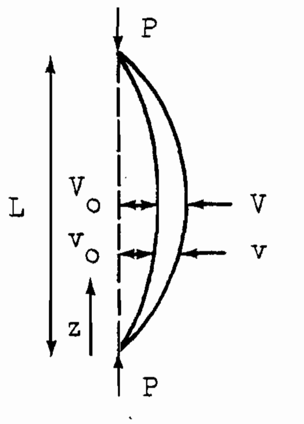

Fig. 6.1
Imperfect Column Under
Central Load

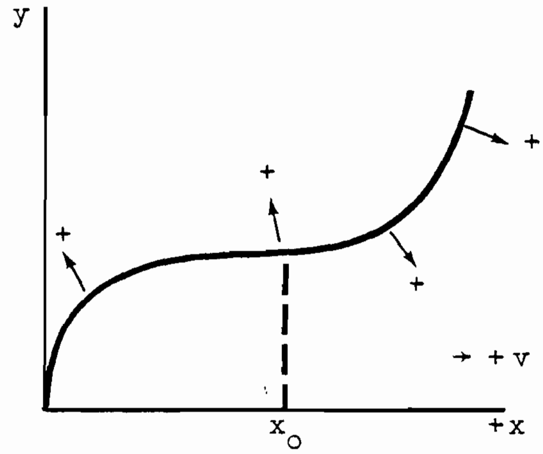

Fig. 6.2 Sign Convention

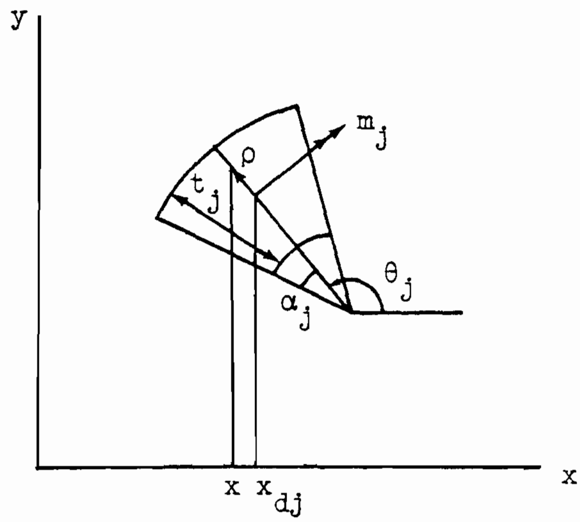

Fig. 6.4 Corner Element

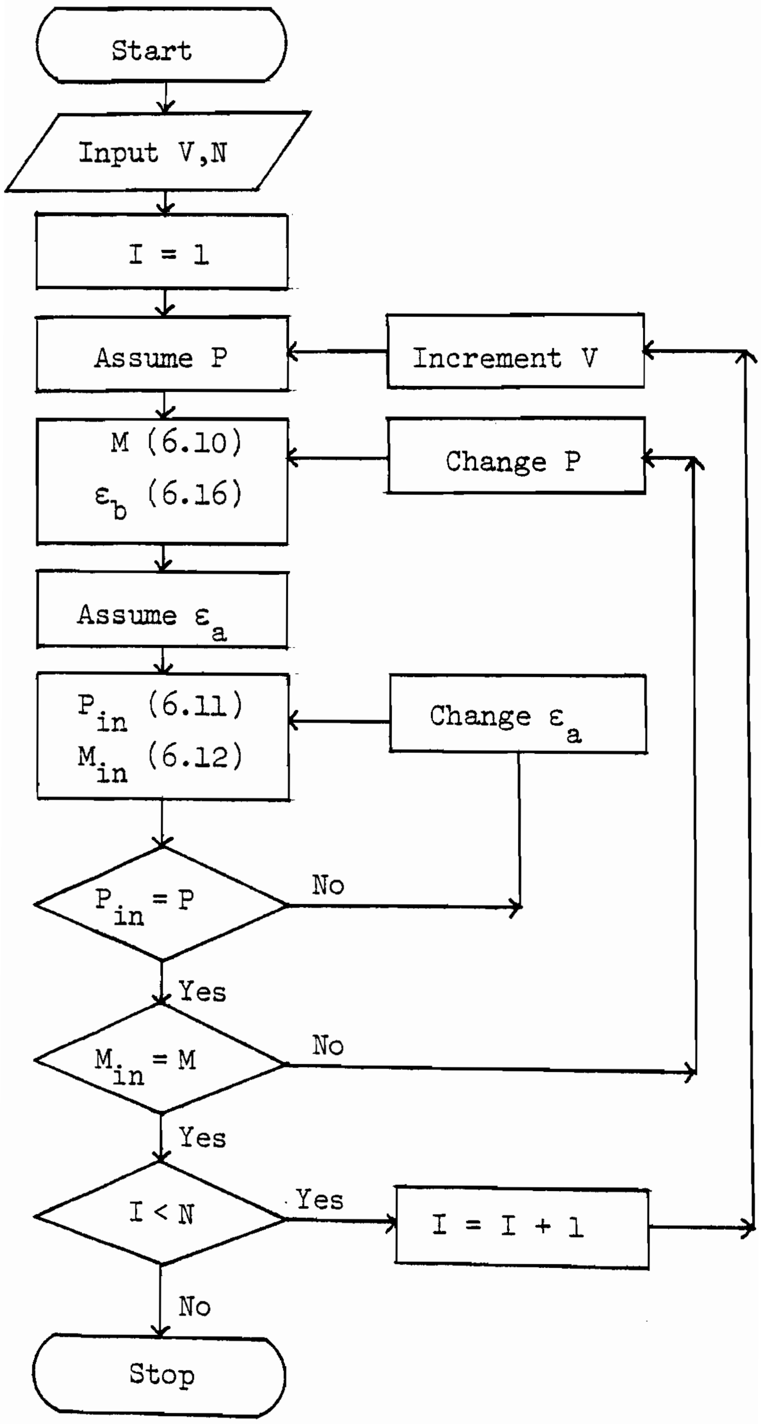

Fig. 6.3 Flowchart

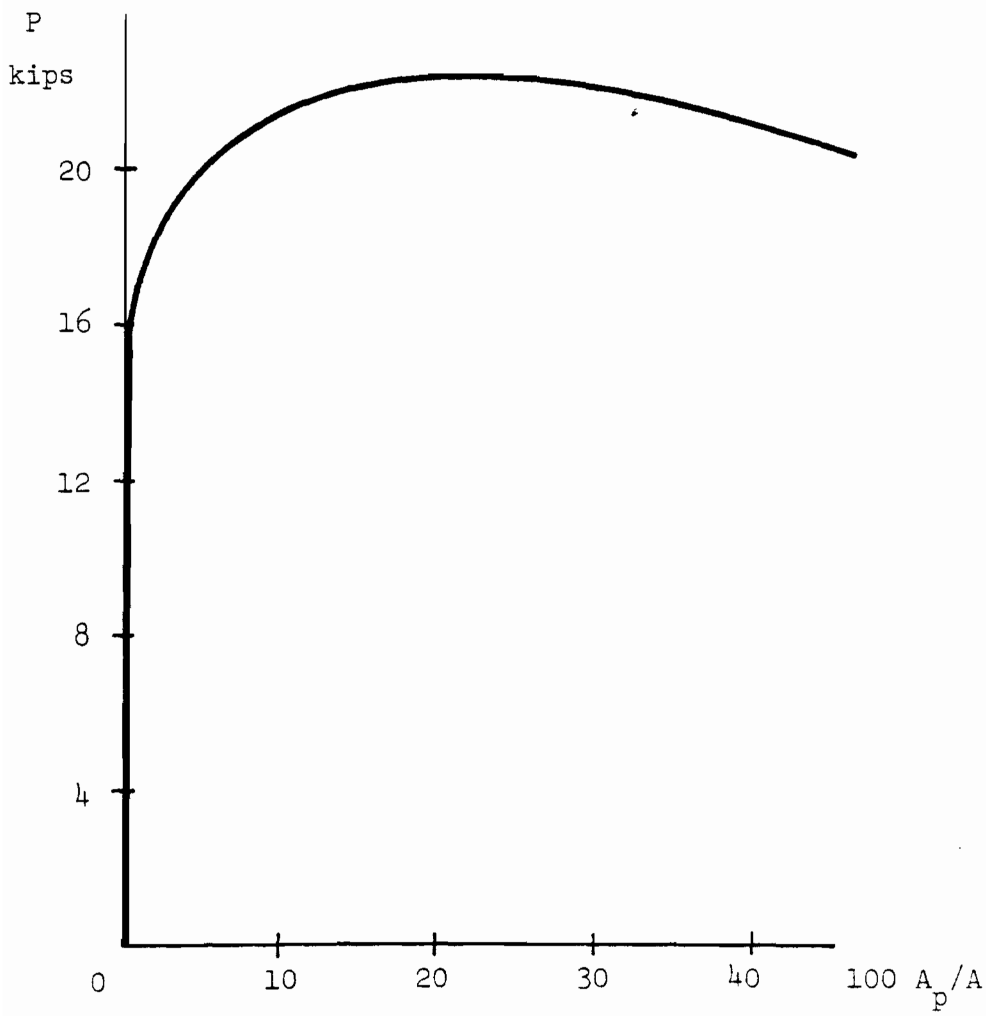

Fig. 6.5 Extent of Plastification
(PBC 13, L = 51.0", V_t/L = -.004, half
residual stress)

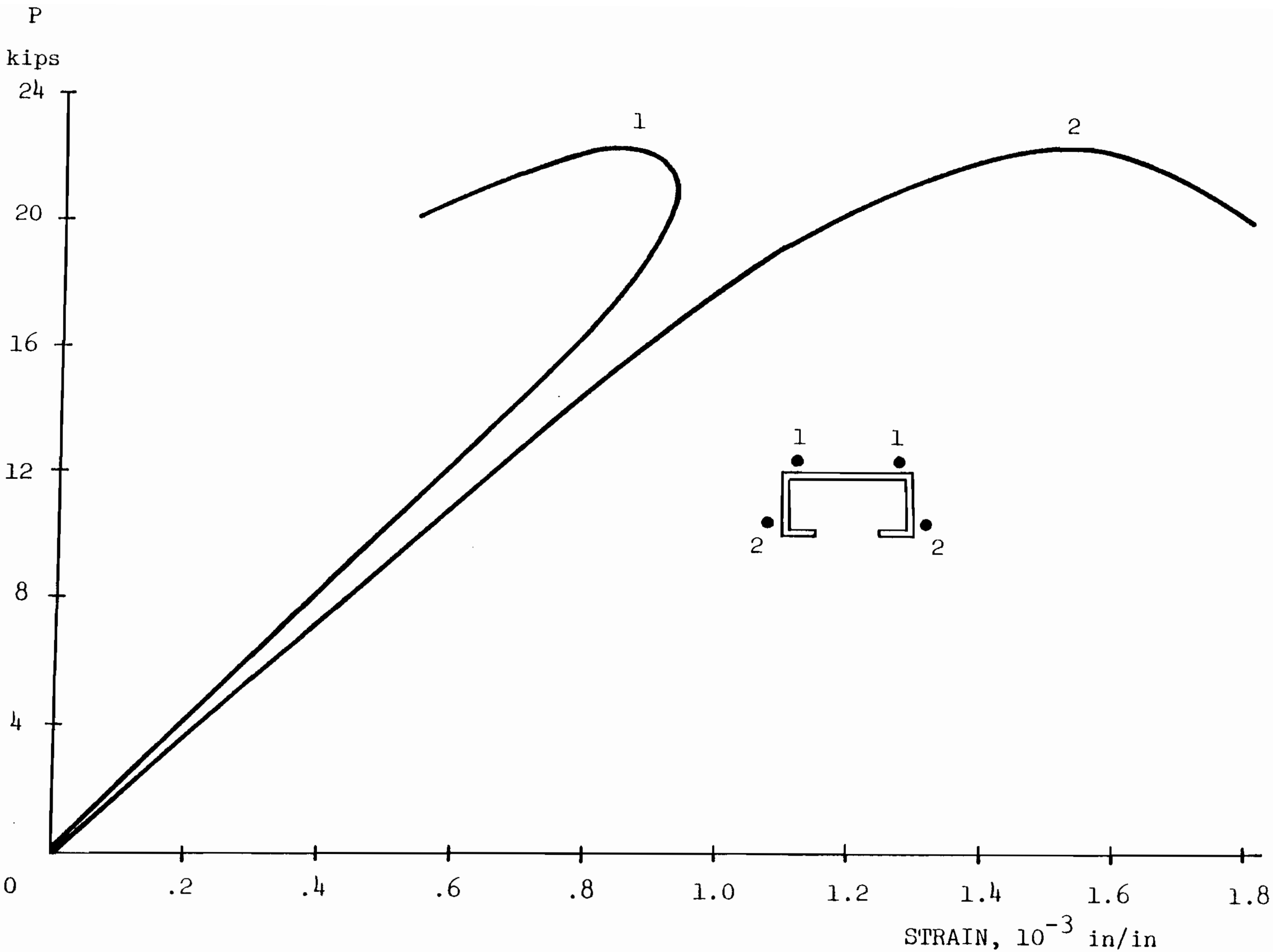

Fig. 6.6 Load-Strain Curves

(PBC 13 L = 51.0", V_t/L = -.004, half residual stress)

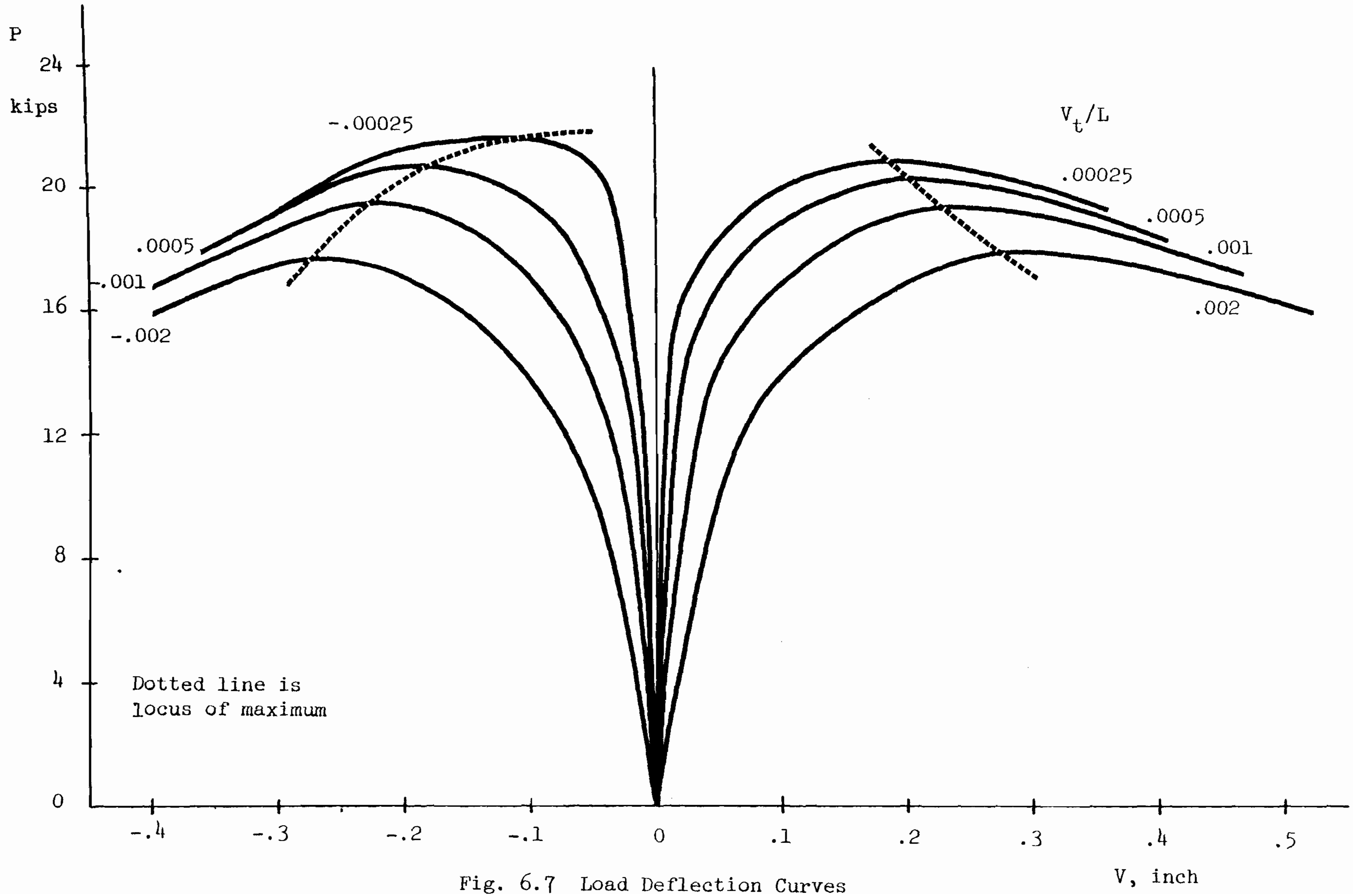

Fig. 6.7 Load Deflection Curves

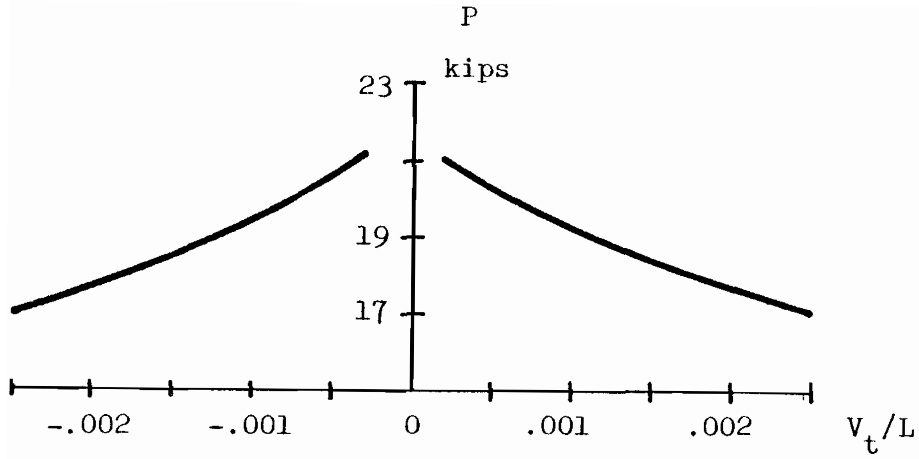

Fig. 6.8 Effect of Initial Deflection on Maximum Load
(PBC 13, L = 51.0", full residual stress)

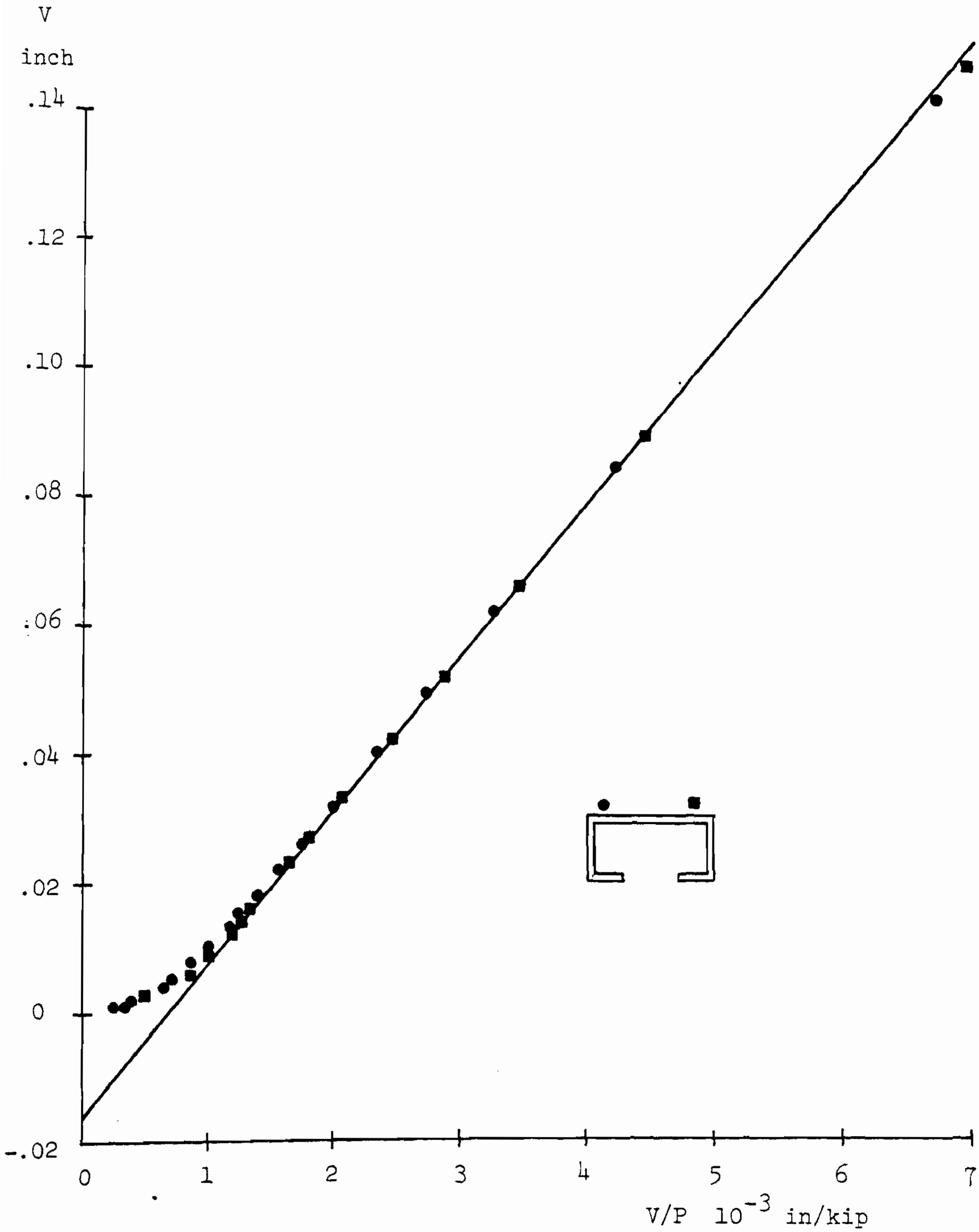

Fig. 6.9 Southwell Plot

PBC 13, L = 51.0"

CHAPTER 7

STUB COLUMN TESTS

7.1 Purpose

The behavior in compression of an entire section (as opposed to coupon tests) with its locked-in residual stresses and variations in yield strength can be studied through stub column tests. A stub column is short enough so global buckling does not occur, but long enough so end effects (due to cutting and, possibly, welding of end plates) are not significant and the residual stress and yield stress distributions are identical to those of a longer number.

7.2 Length

According to the SSRC Guide Technical Memorandum No. 3, "Stub Column Test Procedure" (Johnston [1976]), the length L of a stub column of a cold-formed section should be no less than three times the largest dimension of the section nor greater than twenty times the radius of gyration about the weak axis. It is thus required:

- for the C sections: $9.0'' = 3 \times 3.0 \leq L \leq 20 \times .648 = 12.96''$
- for H11 : $8.25'' = 3 \times 2.75 \leq L \leq 20 \times .379 = 7.58''$
- for H7 : $12.0'' = 3 \times 4.0 \leq L \leq 20 \times .575 = 11.50''$
- and for HT : $13.95'' = 3 \times 4.65 \leq L \leq 20 \times .586 = 11.72''$

Clearly, the requirements are contradictory and cannot be met for the hat sections. A length of 12.0" was chosen for the channel sections, 7.0" for the hat sections.

7.3 Testing Procedure

The procedure used follow SSRC recommendations (Technical Memorandum No. 3, Johnston [1976]). Stubs were cold-sawed no less than 6.0" from the end of a member. The stub ends were milled, then ground plane to within .0005" and perpendicular to the axis of the stub. When the cross-sectional area needed to be determined, the stub was cleaned with a wire brush and a solvent, and its height and weight measured. Strain gages were mounted at three, sometimes four mid-height locations. Since these strain gages were used for alignment, as well as to measure the response to loading, they were placed as far apart as possible, usually in the middle of the web and near the junction of the flanges and the lips for the channel sections, at the top and the lips for the hat sections (Figs. 7.2 - 7.8). The stub was then centered on the testing machine plates, between 3/4" thick (1/2" thick for some of the stubs), precisely ground end plates, plane to within .0005", of high strength steel, and two layers of hydrostone (Fig. 7.1). The end plates and the hydrostone help ensure uniformity of load. The bottom layer of hydrostone is spread first on the machine plate, then the bottom end plate and the stub are placed on top of it, well-centered with respect to the axis of the machine. Verticality of the stub is checked with a level and adjusted by pressing on the viscous hydrostone. The assembly is then topped by the other end plate on which is spread another layer of hydrostone about 1/2" thick. The head of the testing machine is lowered until it squeezes out part of the hydrostone and leaves a uniform layer about 1/4" thick. Although the wet hydrostone carries no appreciable load, some load may develop in the stub column as the hydrostone hardens, a process which takes about 40 minutes.

Alignment is considered satisfactory when strains are uniform to within ± 5% for loads up to 1/3 of the expected ultimate load. If this criterion is not attained, the hydrostone is broken and the setup repeated. Fortunately, this was not necessary in most cases.

A Tinius-Olsen compressometer was used on the lightest sections (C14 and H11) to record strains at one lip. Agreement with the electric resistance strain gages is good (Figs. 7.2, 7.3 and 7.6).

To investigate the effects of residual stresses, annealed stub columns were also tested.

Tests were conducted under static conditions; the load was incremented slowly and strain readings taken at various intervals.

Large deformations took place upon failure, which occurred by yielding. For the channel sections, the web would deform locally out-of-plane near one end, followed immediately by out-of-plane global bending of the flanges, accompanied by in-plane, global bending of the lips. One RFC14 and one PBC14 stub failed by local buckling of the web near one end. These tests were repeated. For the hat stubs, out-of-plane bending of the lips occurred. The deformations of the lips were either symmetrical or antisymmetrical. Because stubs fail by yielding, initial deformation is considered unimportant.

Before discussing the results of the stub column tests, a few words about the effects of annealing are called for.

7.4 Effects of Annealing

Crystals which have been plastically deformed, as for instance, by cold-work, have more energy than unstrained crystals because they are loaded with dislocations and other imperfections. Given a chance, atoms will move to form a more perfect, unstrained array. Such an opportunity arises when the crystals are subjected to high temperatures, through a process called annealing. The greater thermal vibrations of the lattice at high temperatures permit a reordering of the atoms into less distorted grains.

In full annealing the steel is heated to about 100°F above the upper critical temperature* and held for the desired length of time, followed by very slow cooling in a furnace.

The purpose of full annealing is three-fold: to soften the steel and improve ductility, to relieve internal stresses caused by previous treatment, and to refine the grain.

In process-annealing (so called because it intervenes between steps in the process), the steel is heated to a temperature below or close to the lower critical temperature followed by any desired rate of cooling. There is no change in the nature of the crystals, only in their

*The critical temperature is the temperature at which the eutectoid reaction occurs; the eutectoid reaction involves the decomposition of a solid solution into two other solid phases upon cooling and the reverse upon heating. The presence of impurities spreads the reaction temperature over a narrow range about 1333°F, which is the eutectoid temperature for a pure solid solution of iron and carbon. Thus, one can speak of an upper and a lower critical temperature. The solid solution is called Austenite or γ solid solution and its crystals are face-centered cubic. Austenite of eutectoid composition (0.8%C by weight) has the simplest decomposition behavior: the Austenite phase decomposes into the α solid solution or Ferrite, whose crystals are body-centered cubic, and the iron carbide phase or Cementite (Fe_3C). The two new phases form side by side in a given region of the Austenite to produce a nodule of Pearlite, the eutectoid microconstituent. The reverse reaction occurs upon heating: the Ferrite-Pearlite or Pearlite-Cementite structures are destroyed and transformed to the Austenite crystal form through heating past the critical temperature.

geometrical shape (they are less deformed) and size. Austenite and its transformation products are not involved. The principal purposes of this process are to soften the steel partially and to release internal stresses.

The recrystallization temperature, detectable by a marked softening, is not the same for all parts of a specimen but depends on the degree of cold-work. A highly strain-hardened metal is crystallographically more unstable than a metal with less cold-work and the metal with more cold-work softens at lower temperatures. Recrystallization temperature is also affected by the length of time of heating. Since a longer heating time gives atoms more opportunity to realign themselves, recrystallization occurs at lower temperatures.

Although for complete release of internal stresses, recrystallization must occur, a temperature of 1200°F for one hour is considered necessary to reduce residual stresses to a negligible figure. When recrystallization takes place, the crystals retain the orientation caused by cold-work.

Although softening is usually associated with annealing, the effects of reheating steel on its tensile and yield strength are complex. Stress-strain curves for a cold-drawn, 0.74%C steel reheated for one hour show marked increases in the yield strength, tensile strength and proportional limits for reheating temperatures below 400°F. The same is observed in cold-worked steels tempered for five hours and eight hours at 570°F (Bullens [1948] pp. 224, 225, 235). The same reference also shows that the response to annealing depends on the type of steel and the amount of cold-reduction (i.e. reduction of sheet thickness at a temperature below the recrystallization temperature). For instance, a rimmed steel core annealed at 1200°F for 16 hours exhibits increases of hardness, which implies increases in yield strength also, for various amounts of cold-reduction (Bullens [1948] p. 237).

Further information on this topic can be found in: Bullens [1948], Guy [1951], Clark and Varney [1952], Van Vlack [1964] and Hanson and Parr [1965].

7.5 Results and Discussion

The results of stub column tests, in the form of load versus strain curves, both for the annealed and not annealed sections, are presented in Figs. 7.2 to 7.8. Also presented, in dotted lines, are theoretical predictions using the model developed in the preceding chapter. In this particular application, strain is incremented but lateral deflection is kept at zero. Input includes the actual distribution of yield strength, measured by tensile coupon tests, and residual stresses. The computation is repeated for the case of no residual stresses.

Model 3 of residual stresses is used, with the neutral axis at midthickness, $\rho_{nj} = 0$.

Annealed stubs are gradually yielding because the yield strength is not uniform over the cross-section. The proportional limit of non-annealed stubs is lower than that of annealed stubs, a fact attributable to residual stresses.

From Table 7.1 and Figs. 7.2 to 7.8, the following observations can be made:

1) The C14 stubs all have lower strength than predicted. The same is observed for pin-ended columns of $\bar{\lambda} < 1.0$ (see Chapter 9). The possibility that this lower strength is due to a lower yield strength than used in the computer model is investigated in Figs. 7.2b and 7.3b. If the yield strength is everywhere lower by 3.0 ksi for PBC14 and by 3.5 ksi for RFC14 than measured in tensile specimens a (Chapter 3), then the agreement is more reasonable. This is justified in the case of RFC14 by the scatter in the measurements of yield strength (Fig. 3.9).

2) For the C13 and H11 stubs, the yield load is a good estimate of the ultimate load, i.e. the stub column fails as soon as the entire cross-section has yielded.

3) For the heavier sections (H7 and HT), strain-hardening is attained and the ultimate load is significantly higher than the yield load.

4) All except one annealed stubs have higher ultimate loads than the non-annealed ones. This increase in strength is small (less than 6% in all but one case).

Two flat tensile coupons cut from an annealed and a non-annealed specimen showed that yield strength decreases upon annealing (by 5.3 and 8.9%). The tensile specimens were cut from the same member, adjacent to one another. The author can offer no explanation for this apparent contradiction.

5) The theory developed in Chapter 6 underestimates the effects of residual stresses, both in lowering the proportional limit and in decreasing the column stiffness for loads above the proportional limit. It is recalled that the computer program uses as input the measured residual strains but assumes a rectangular (model 3) distribution across the thickness.

TABLE 7.1

STUB COLUMN TESTS

Section	EXPERIMENTS: Annealed $\frac{P_{pa}}{A}$	$\frac{P_{ua}}{A}$	Not Annealed $\frac{P_{pn}}{A}$	$\frac{P_{un}}{A}$	$\frac{P_{ua}-P_{un}}{.01\ P_{ua}}$	$\frac{P_{pa}-P_{un}}{A}$	THEORY: Annealed $\frac{P_{pa}}{A}$	Not Annealed $\frac{P_{pn}}{A}$	$\frac{P_y}{A}$	$\frac{P_{pa}-P_{pn}}{A}$
PBC 14	35.8 38.1	39.4 42.5	27.9	38.6	2.	7.9	32.1	21.4	40.2	10.7
RFC 14	40.5	45.7	31.4	42.9	6.	9.1	40.1	32.3	44.4	7.8
PBC 13	37.5 34.1	46.9 44.7	19.4 25.6	44.2 43.3	6. 3.	18.1 8.5	35.5	24.8	44.8	10.7
RFC 13	38.3	48.1	23.4	44.2	8.	14.9	35.8	25.5	44.2	10.3
H 11	50.3 48.1	56.3 49.2	37.9 38.5	53.5 51.5	5. -5.	12.4 9.6	43.0	43.0	51.6	0.
H 7	48.5	61.4	36.9	60.2	2.	11.6	41.1	26.5	54.8	14.6
H T	53.5	68.7	40. 43.4	68.3 66.9	6.	13.5	54.6	47.2	60.7	7.4

P_p = proportional limit load (kips)
P_y = yield load
P_u = ultimate load

A = cross-sectional area (in^2)
Subscripts a,n for annealed, not annealed

TABLE 7.2

STUB COLUMN TESTS:

NON-DIMENSIONALIZED RESULTS

Section	Column		L inch	P_u kips	$\bar{\lambda}_f$	P_u/P_{yf}	$\bar{\lambda}_a$	P_u/P_{ya}
PBC 14	A 15	a	12.0	21.18	.107	1.010	.115	0.880
	16	n		20.78		0.991		0.863
	17	a		22.85		1.090		0.949
RFC 14	B 12	a	12.0	23.7	.115	1.027	.119	0.955
	13	n		22.2		0.962		0.895
PBC 13	C 8	a	7.0	30.0	.0617	1.232	.0666	1.045
	9	n	7.0	28.3	.0617	1.162	.0666	0.986
	10	a	12.0	28.6	.106	1.174	.114	0.996
	11	n	12.0	27.7	.106	1.138	.114	0.965
RFC 13	D 14	a	12.0	30.8	.106	1.255	.114	1.087
	15	n		28.3		1.153		0.999
H 11	E 6	a	7.0	24.87	.112	1.314	.123	1.088
	7	n	7.0	23.67	.112	1.250	.123	1.036
	8	a	12.0	21.75	.192	1.149	.211	0.952
	9	n	12.0	22.75	.192	1.202	.211	0.996
H 7	F 6	a	7.0	60.8	.0753	1.379	.0835	1.119
	7	n		59.6		1.352		1.097
H T	G 6	a	7.0	128.4	.0843	1.184	.0862	1.131
	7	n	7.0	127.8	.0843	1.178	.0862	1.126
	8	n	12.0	125.2	.144	1.154	.148	1.103

a for annealed

A = cross-sectional area

σ_{yf} = yield strength of flat

$P_{yf} = A\sigma_{yf}$

$$\bar{\lambda}_f = \frac{1}{\pi}\sqrt{\frac{\sigma_{yf}}{E}}\,\frac{L}{R}$$

n for not annealed

R = radius of gyration

σ_{ya} = average yield strength

$P_{ya} = A\sigma_{ya}$

$$\bar{\lambda}_a = \frac{1}{\pi}\sqrt{\frac{\sigma_{ya}}{E}}\,\frac{L}{R}$$

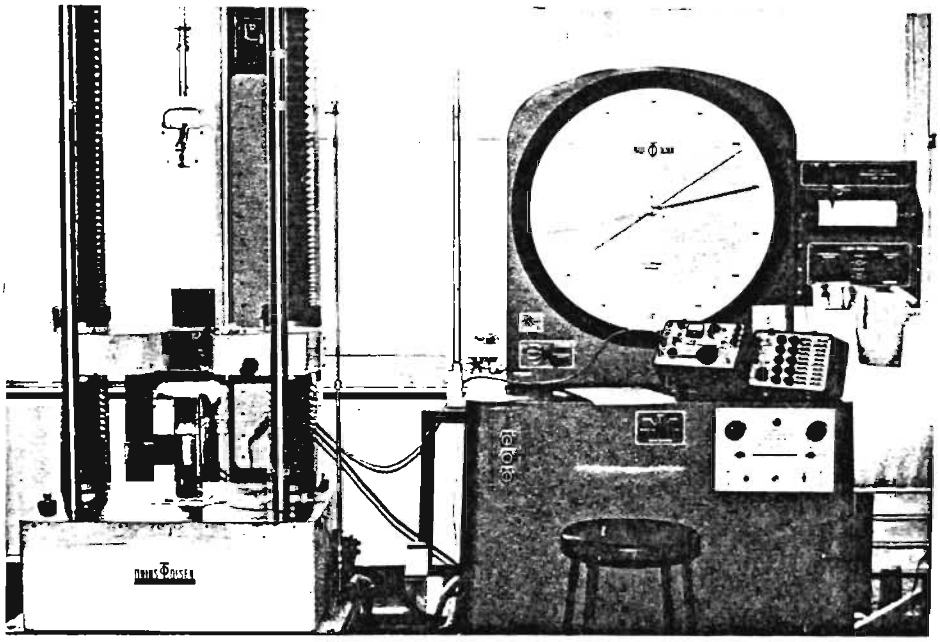

Photo 7.1 Stub Column Test: General Set-up

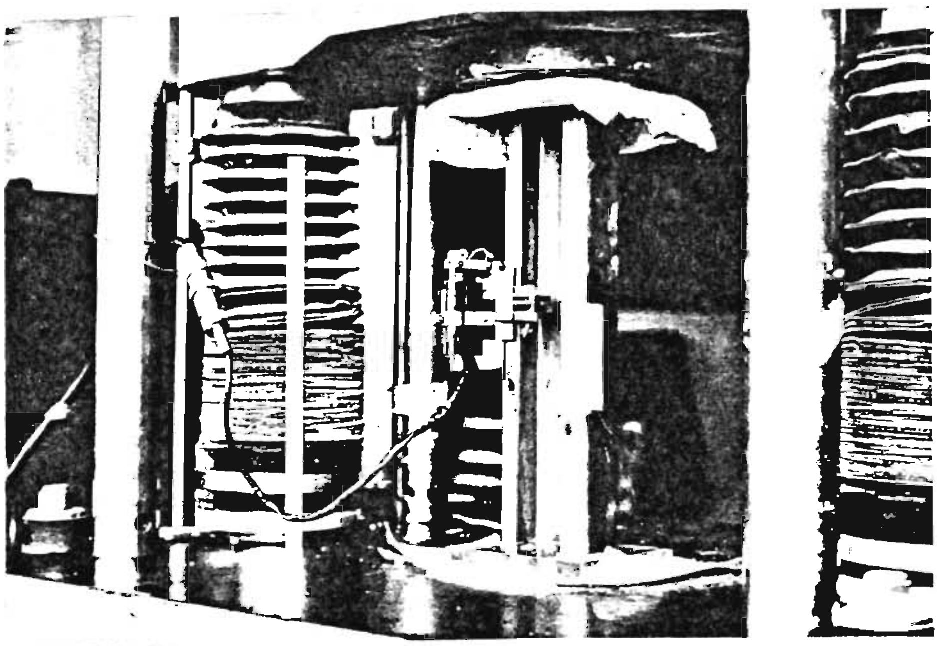

Photo 7.2 Stub Column Test: Use of Compressometer

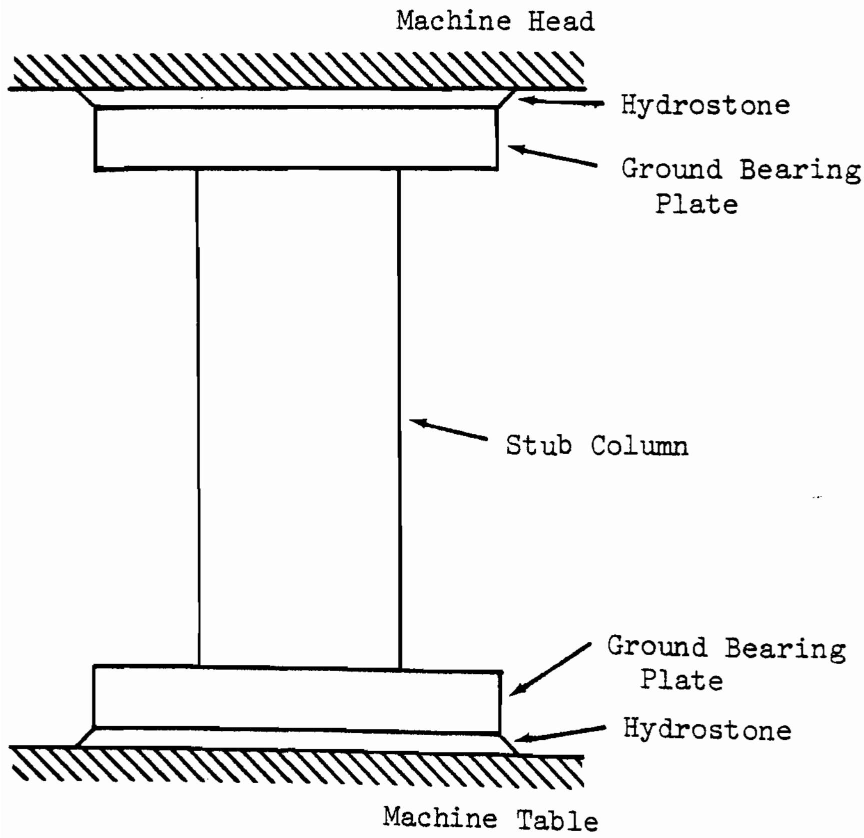

Fig. 7.1 Stub Column Test Set-up
(from Dewolf [1973])

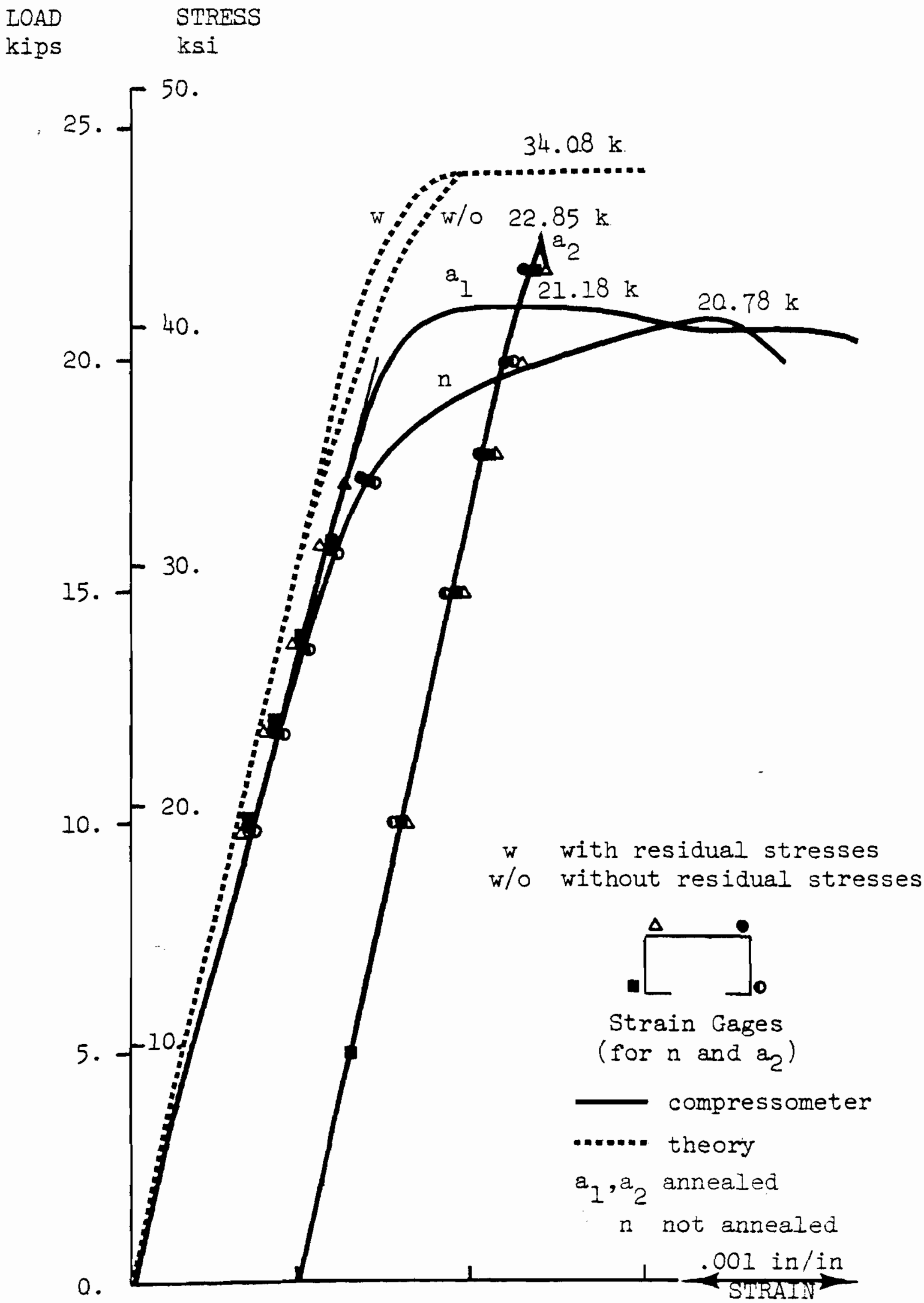

Fig. 7.2a PBC 14 Stub Column (12.0")

Theory uses coupon values of specimen a, Table 3.5.
Annealed stub a_2 failed by local buckling of web near one end, the others by yielding. Only compressometer record exists for a_1.

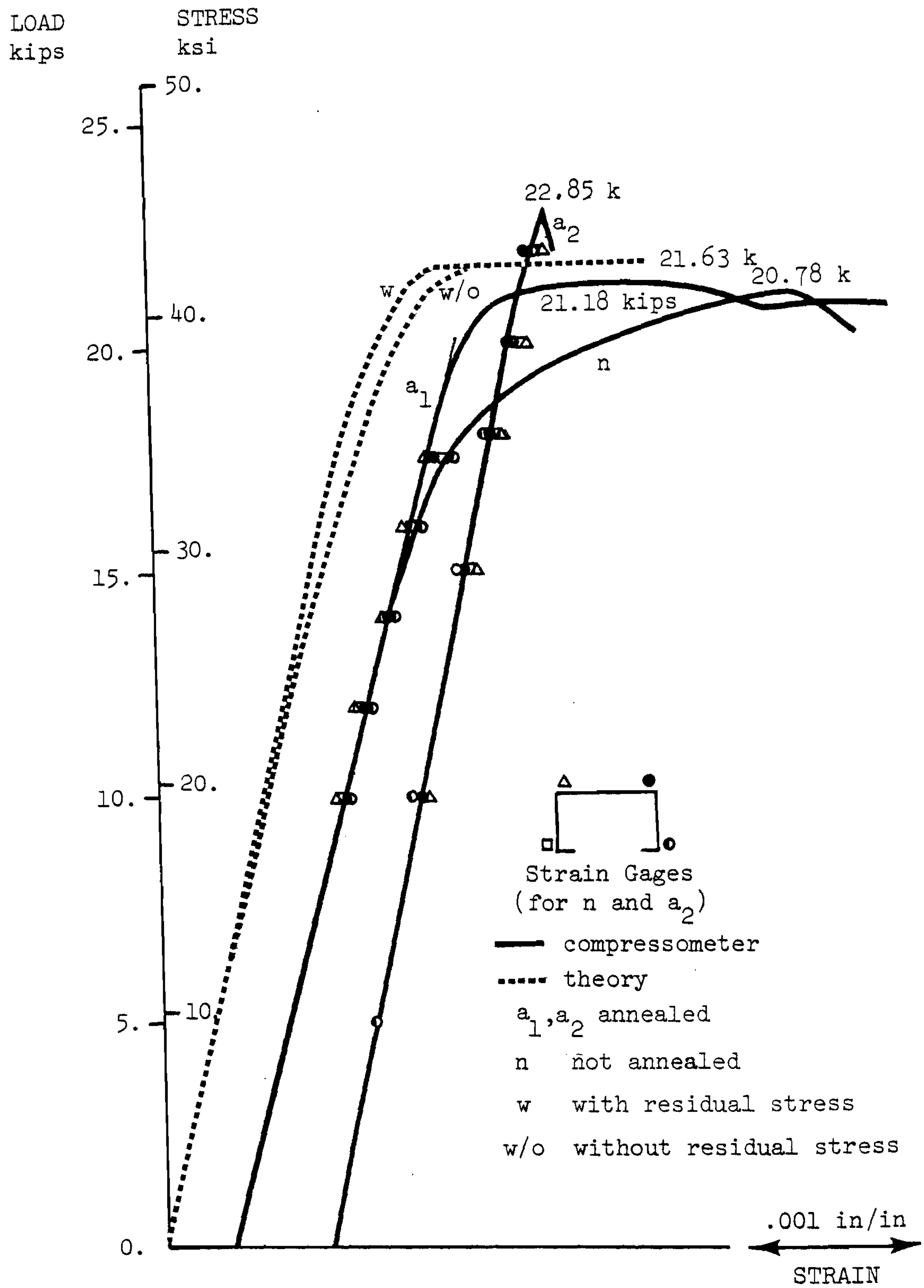

Fig. 7.2b PBC 14 Stub Column Tests

Theoretical curves use (σ_y - 3.0 ksi) and (.963t) where σ_y and t are coupon values of specimen a, Table 3.5.

Annealed stub a_2 failed by local buckling of web near one end, the others by yielding. Only compressometer record exists for a_1.

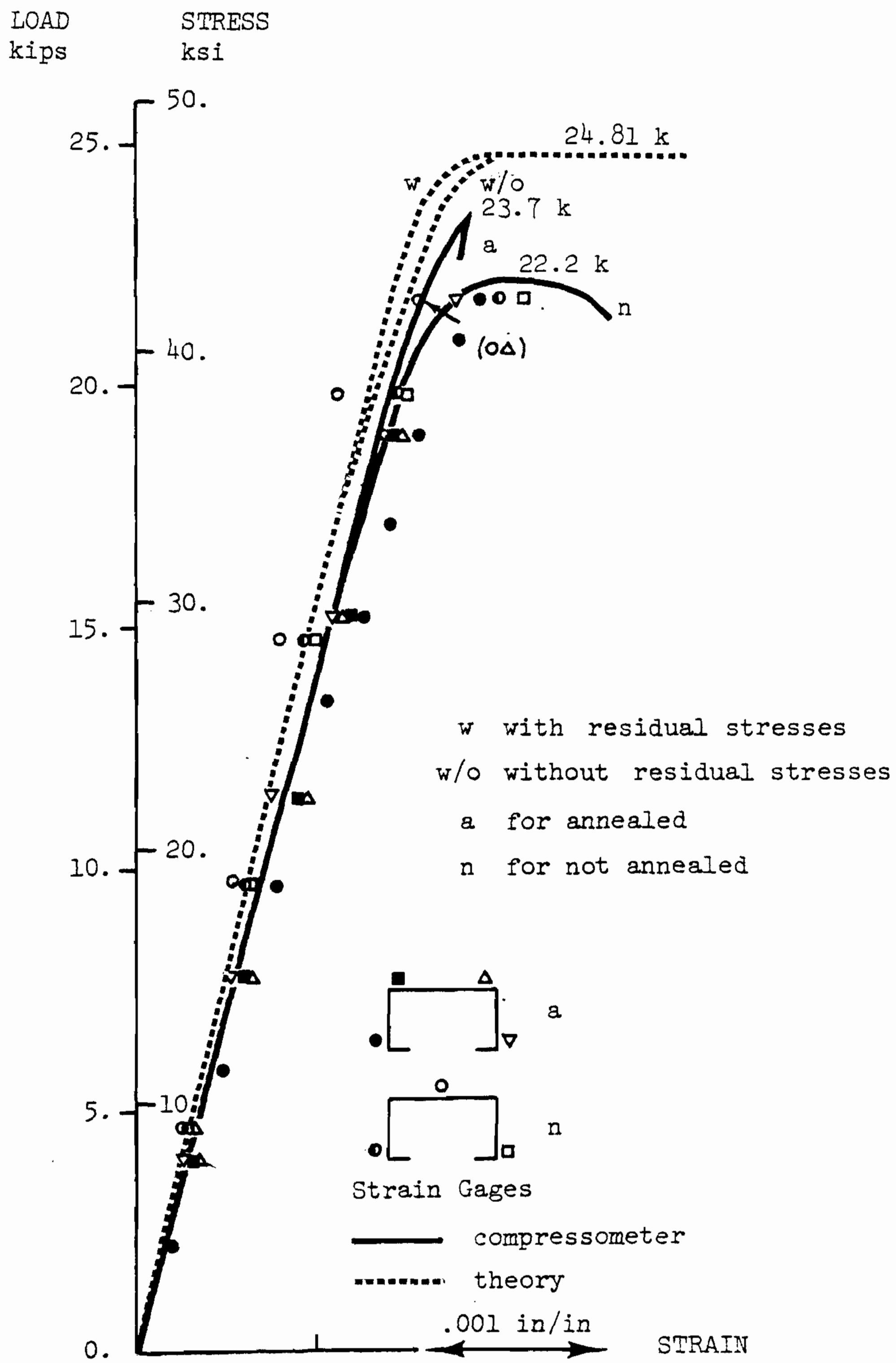

Fig. 7.3a RFC 14 Stub Column (12.0")

Theory uses coupon values of specimen a, Table 3.8.
Annealed stub failed by local buckling of web near one end.

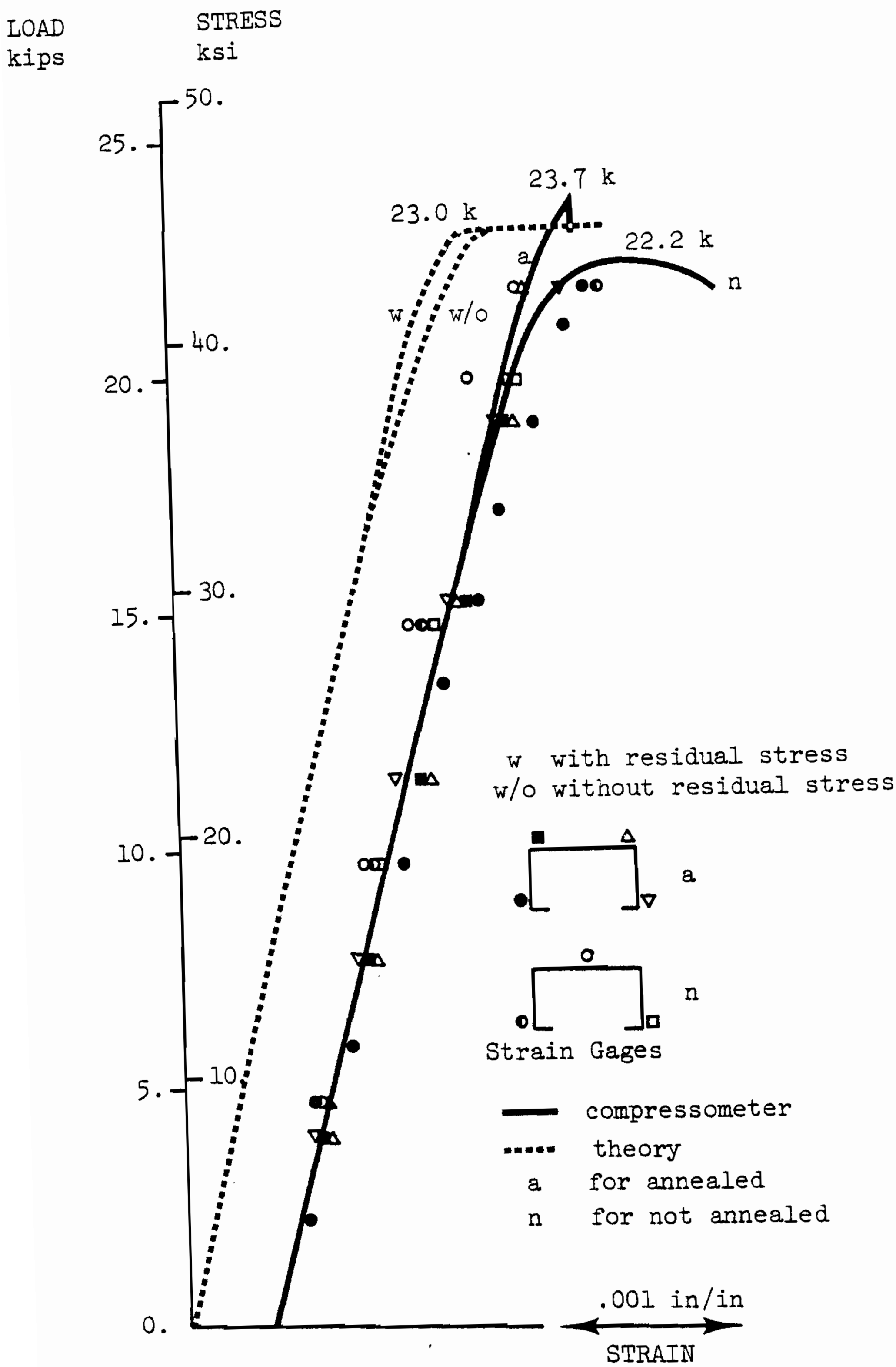

Fig. 7.3b RFC 14 Stub Column Tests

Theoretical curves use (σ_y - 3.5 ksi) where σ_y are coupon values of specimen a, Table 3.8.
Annealed stub failed by local buckling of web near one end.

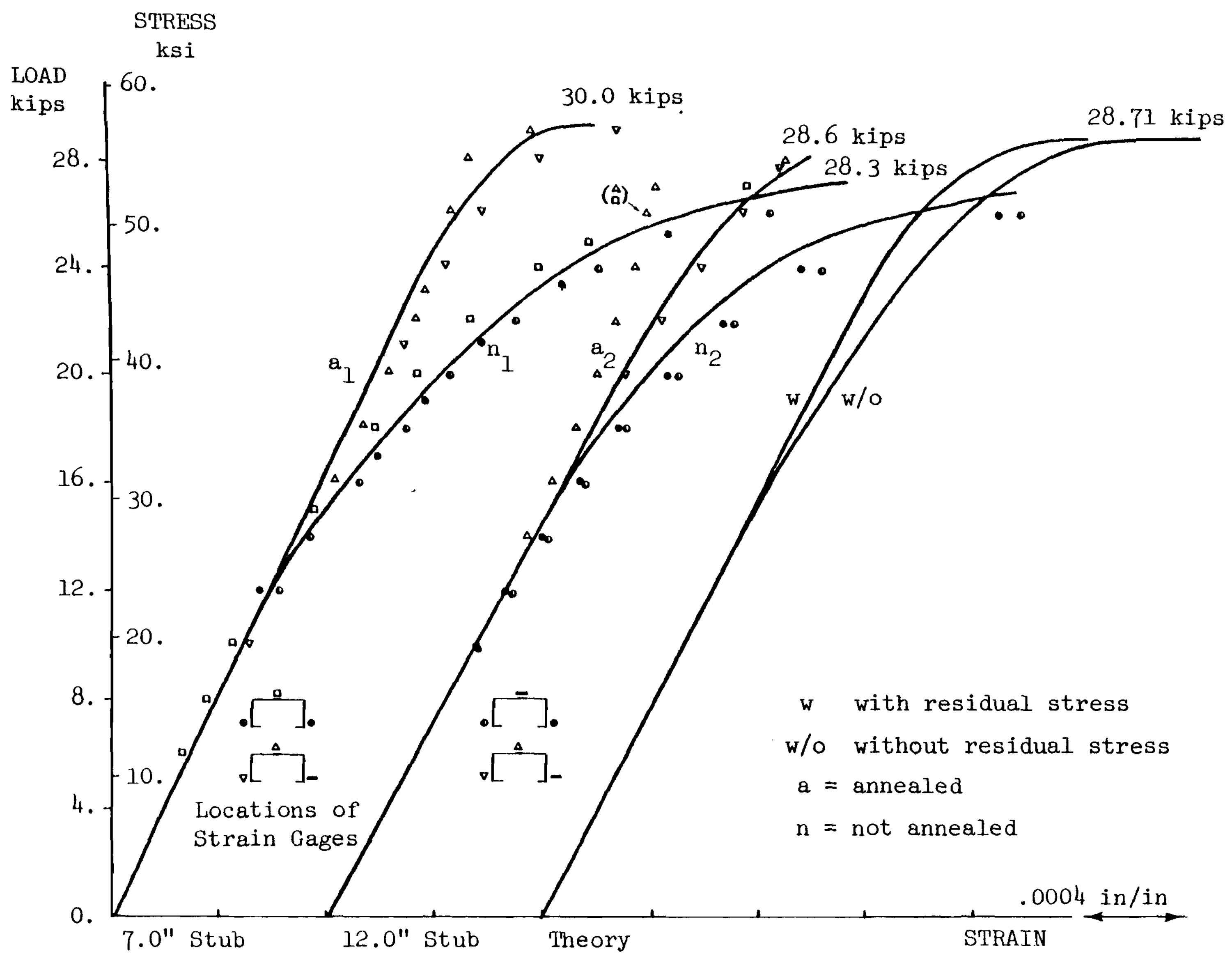

Fig. 7.4 PBC 13 Stub Column Tests

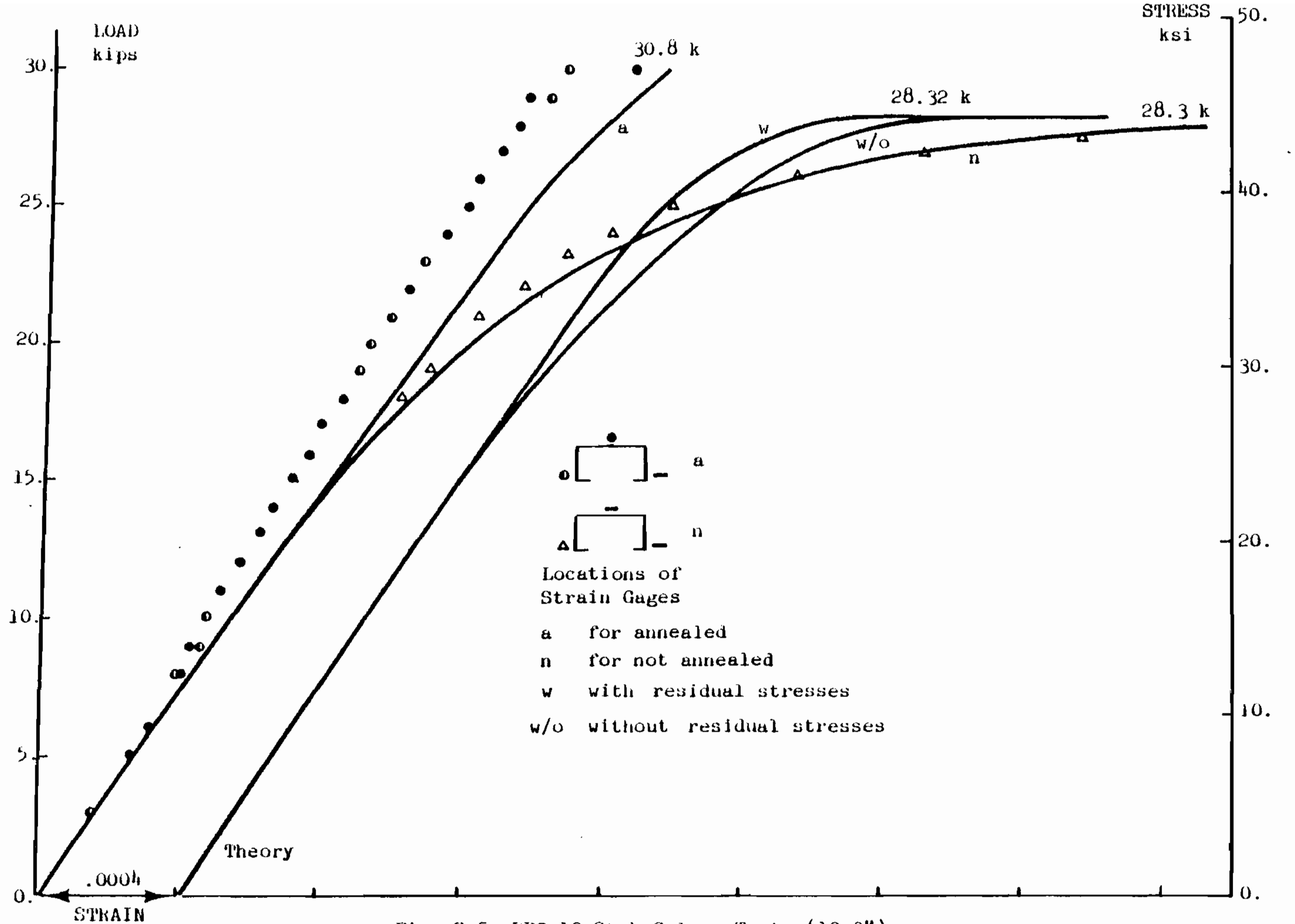

Fig. 7.5 RFC 13 Stub Column Tests (12.0")

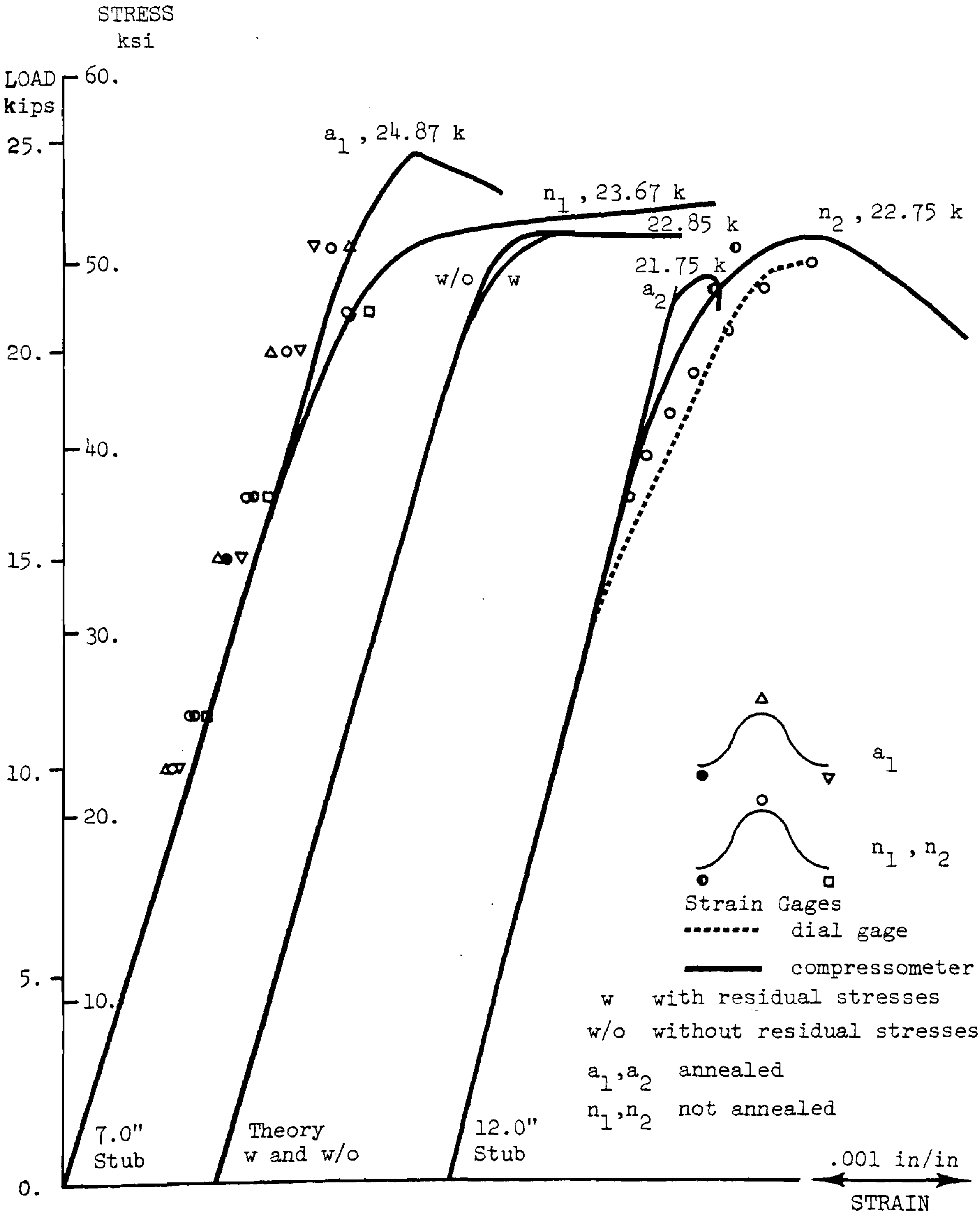

Fig. 7.6 H11 Stub Column Test

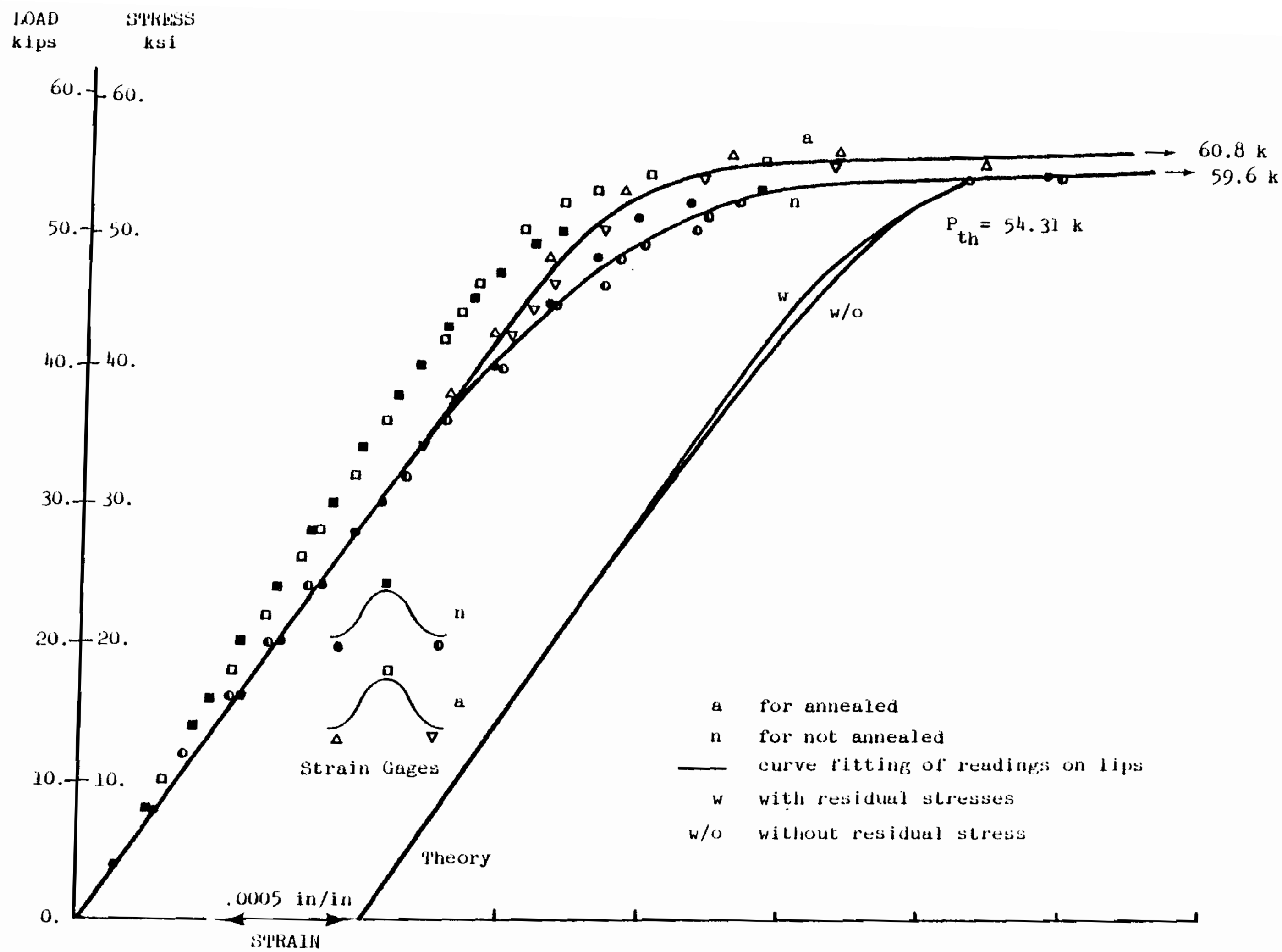

Fig. 7.7 H7 Stub Column Tests (7.0")

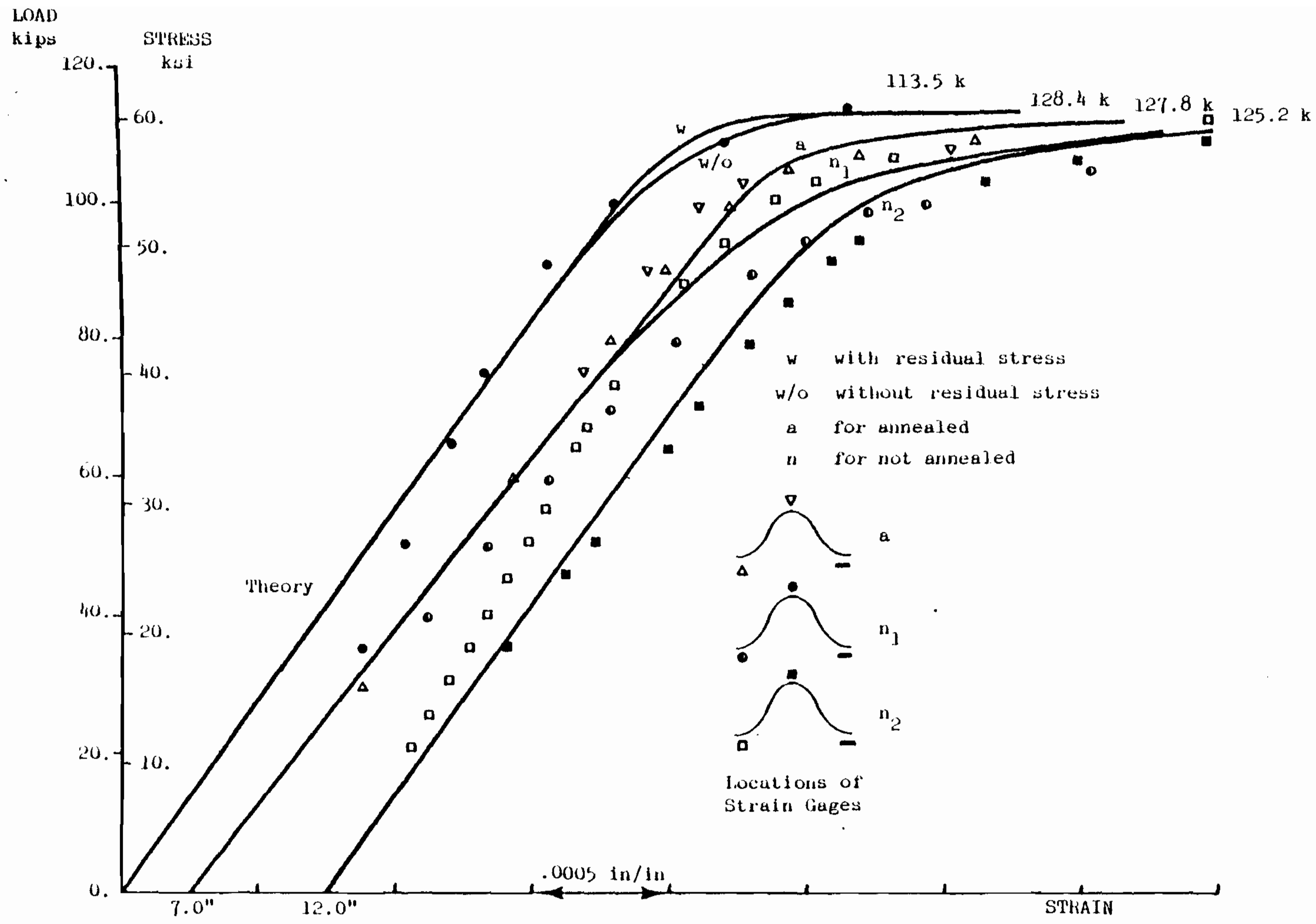

Fig. 7.8 HT Stub Column Tests

CHAPTER 8

INITIAL DEFLECTIONS AND COLUMN CENTERING

8.1 Literature Survey

The reduction of column strength caused by geometrical imperfections is an experimentally verified and well understood fact (Bleich [1952], Timoshenko and Gere [1951], Chen and Atsuta [1976], L'Hermite [1974, 1976]). The presence of initial deflections makes a qualitative difference: provided the load is centrally applied, a column with initial deflections bends continuously, whereas a perfectly straight column remains so until it reaches the bifurcation load, at which point it begins to deflect.

By using the method of characteristics and expressing the initial and additional deflections in terms of the buckling modes, it has been proved that the first term of the additional deflection proportional to the first buckling mode gets much more magnified than the other terms when the (first) buckling load is approached (Bleich [1952] p. 128, Timoshenko and Gere [1951] p. 32, Chen and Atsuta [1976] p. 97).

T.H. Lin [1950] derived formulas for the amplification of initial deflections and eccentricities both in the elastic and inelastic range. He expressed the initial deflection as a Fourier Series:

$$v_o = \sum_{n=1}^{\infty} V_{on} \sin n\pi z/L \qquad (8.1)$$

Similarly the additional deflection due to the load is:

$$v = \sum_{n=1}^{\infty} V_n \sin n\pi z/L \qquad (8.2)$$

In the elastic range the familiar amplification formula is obtained:

$$V_n = \frac{V_{on}}{n^2 P_{cr}/P - 1} \tag{8.3}$$

Clearly, the first term, $n = 1$, dominates the others when P approaches the critical load P_{cr}. In the inelastic range, partial yielding causes the neutral axis to shift away from the geometrical centroidal axis. There results an eccentricity of the load which may be assumed to be of the form:

$$e = \sum_{n=1}^{\infty} e_n \sin n\pi z/L \tag{8.4}$$

It can be proved that the rate of increase with respect to the load of each term of the total deflection is:

$$\frac{\Delta(V_n + V_{on})}{\Delta P} = \frac{V_n + V_{on} + e_n}{n^2 P_{cr} - P - \Delta P} \tag{8.5}$$

Upon summation: $$\sum_{n=1}^{\infty} \frac{V_n + V_{on} + e_n}{n^2 P_{cr} - P - \Delta P} \simeq \frac{V_1 + V_{01} + e_1}{P_{cr} - P - \Delta P} \tag{8.6}$$

So again the increase of the first harmonic is much more important than that of the other harmonics.

This fact has prompted Massonnet to state the following (L'Hermite [1976]): "No matter what the real (geometrical) imperfections of a strut are, it behaves, under a load close to the critical Euler load, as if it had an [initial] deformation affine to the buckled shape of a perfectly straight strut. (Quelles que soient les imperfections (géométriques) réelles de la barre, elle se comporte sous une charge voisine de la charge critique d'Euler comme si elle pessédait une déformation affine de la charge de flambage qu'elle aurait prise si elle avait été parfaitement rectilique.)"

In dealing with initial deflections, Chen (Chen and Atsuta [1976] p. 97) did not require the stiffness to be constant along the length of the column and his analysis could conceivably be extended to inelastic buckling. Chen [1970] also studied the effect of initial curvature on the strength of an inelastic column by the method of equivalent lateral loads, but the calculations were rather involved and no attempt was made to include initial deflected shapes other than those affine to the first buckling mode.

The effect of initial curvature on the strength of an inelastic column was also studied theoretically by Wilder, Brooks and Mathauser [1953] using an idealized H-section with a Ramberg-Osgood stress-strain curve. The initial and the additional deflections due to the load were assumed to be half-sine waves. The authors concluded that the maximum load for an initially curved column is always less than the maximum load for the corresponding straight column and may even be less than the tangent modulus load, depending upon the column proportions, the magnitude of the initial curvature and the shape of the stress-strain curve.

Calladine [1973] developed a geometrical construction to predict the maximum load of a Shanley column with or without initial curvature. The stress-strain curve is one of two types, elastic-perfectly plastic or gradually yielding. It turns out that, although the column curve based on the tangent modulus formula is sensitive to the precise shape of the stress-strain curve, the curves for the imperfect columns are insensitive to this shape, except for the stocky columns. A peak in imperfection sensitivity was found to exist at a slenderness ratio corresponding to a buckling stress equal to the proportional limit. This peak imperfection sensitivity had been observed experimentally by Chilver and Britvec [1963] and obtained by Batterman and Johnston in their computer study [1967]. Chilver and Britvec explained this phenomenon by examining the various postbuckling paths: the equilibrium path is stable, i.e. the load increases with lateral deflections, for a buckling load between the tangent modulus load and the reduced modulus load; it is neutral, i.e. the load remains constant as deflections increase, when the buckling load equals the reduced modulus load; and it is unstable, i.e. the load decreases with increasing deflections, for a buckling load between the reduced modulus load and the Euler load. This is similar to the concept of inelastic buckling gradient introduced by Johnston [1964].

Gilbert and Calladine [1964] extended Calladine's geometrical construction to account also for the effects of local imperfections. They concluded that the addition of local imperfections to a column already possessing an overall imperfection has little effect on the peak load.

Batterman and Johnston [1967] found through computer simulation that the effect of initial imperfections on the strength of columns diminishes with increasing slenderness ratio and with increasing yield strength of the material.

8.2 Measurement of Initial Deflections

As the testing of columns progresses, three different models of measuring initial deflections are used.

8.2.1 Method 1

The telescope of a transit is aimed at various locations alongside a column placed vertically about ten feet away (Fig. 8.1). Readings are taken of a ruler marked to 1/100" positioned perpendicular to the column surface. Deviations from the straight line joining the two end stations are computed. Thus it does not matter if the column axis deviates slightly from the vertical, or the axis of rotation of the telescope from the horizontal. For best accuracy and ease of computation these two conditions should, however, be fulfilled. The horizontality of the ruler is checked by aligning its graduations with the cross-hair of the telescope. The position perpendicular to the column surface is found by slightly rocking the ruler back and forth in a horizontal plane; this position corresponds to the smallest reading. Shimming is sometimes necessary to provide a stable support for the column. Accuracy is estimated to be of the order of 1/100".

8.2.2 Method 2

The column lies horizontally on a plane surface and a dial gage, whose support rests on the surface, is used to measure the elevation of various points of the column (Fig. 8.2 a,b). Self-weight deflection, usually negligible, is accounted for when the column is simply supported at its ends by the end plates. Of course, when the column rests on the table along its entire length, there is no dead weight deflection.

For short columns ($L \leq 4'$) a ground steel table, whose surface can be considered perfectly plane, is used. For longer columns, such a surface is not available and the imperfections of the table are accounted for by the scheme shown in Fig. 8.2 c: one set of x_1 measurements is taken, then the column is turned upside down and a set of x_2 measurements is recorded. Provided x_1 and x_2 are measured with respect to the same table location, the imperfections of the table can be eliminated from consideration and the initial out-of-straightness of the column is the average of x_1 and x_2.

When a good plane surface is used as reference, the measurements are as accurate as the dial gage (1/1000"). When the reference surface is not as good, the accuracy is estimated to be no better than 5/1000".

8.2.3 Method 3

This method is developed for long columns, as an alternative to the second method. The column rests horizontally on its two ends and a telescope placed about ten feet away is aimed along the column axis (Fig. 8.3 a). At the end of the telescope is mounted an optical micrometer (Fig. 8.3 b), which consists of a thick, parallel-faced glass plate, which can be rotated. A surveyor's scale is placed at various stations on the column surface and perpendicular to it (by the same techniques described in Method 1). A light ray emanating from the scale undergoes various vertical translations in a plane perpendicular to the axis of rotation of the glass plate, depending on the angle of incidence of the ray with the glass plate. It is thus possible, by rotating the glass plate, to always aim at the same graduation on the scale as the scale is positioned at various stations and as the graduation moves up or down by minute amounts. The micrometer is calibrated so that distances, rather than angles can be read directly. To check for possible movement of the telescope assembly, a sight is frequently taken of a fixed reference point; this is especially important since a small angular deviation causes a large linear displacement. The computed dead weight deflections are subtracted or added to the initial deflections depending on the direction of the latter.

The accuracy of the optical micrometer is 1/1000".

8.3 Computations

Let $\tilde{v}_{oj}$ be the elevations at locations z_j of the column. The deviations from straightness, $\bar{v}_{oj}$, are:

$$\bar{v}_{oj} = \bar{v}_o(z_j) = \tilde{v}_{oj} - [\tilde{v}_{oI} + (\tilde{v}_{oF} - \tilde{v}_{oI}) \frac{z_j - z_I}{z_F - z_I}]; j = 1,2,\ldots n \quad (8.7)$$

where the subscripts I and F refer to the measurements closest to the column ends. These readings are never at the ends themselves because of the presence of the end-welds.

Considering the horizontal column as simply supported, the self-weight deflection is:

$$v_d(\xi) = \frac{5\omega L^4}{384\ ER^2} [\frac{16}{5}(\xi^4 - 2\xi^3 + \xi)] \quad (8.8)$$

where L = column length

$\xi = z/L$ = abcissa

ω = density of steel = 490 lb/ft^3

E = modulus of elasticity = 29,500 ksi

R = radius of gyration

The computation of column strength described in Chapter 6 assumes initial sinusoidal deflections. These assumed values are now related to the measured initial deflections. It is convenient to approximate the dead load deflection by a half sine wave also, an approximation accurate to 2%:

$$s(\xi) = \frac{5\omega L^4}{384ER^2}\sin\pi\xi = S\sin\pi\xi \tag{8.9}$$

where $S \equiv 5\omega L^4/384ER^2$.

Since z_I and z_F are not the column ends, a least-square fit of a half-sine wave to v_{oj} is of the form:

$$v_{oj} = v_o(\xi_j) = A\sin\pi\xi_j - B \tag{8.10}$$

Minimization of

$$g = \sum_{j=1}^{n}(v_{oj} - \bar{v}_{oj})^2 = \sum_j (A\sin\pi\xi_j - B - \bar{v}_{oj})^2 \tag{8.11}$$

requires

$$\frac{\partial g}{\partial A} = 2\sum_j(\sin\pi\xi_j)(A\sin\pi\xi_j - B - \bar{v}_{oj}) = 0 \tag{8.12}$$

$$\frac{\partial g}{\partial B} = -2\sum_j(A\sin\pi\xi_j - B - \bar{v}_{oj}) = 0 \tag{8.13}$$

A and B are therefore determined by the system:

$$\begin{cases} (\sum_j \sin^2\pi\xi_j)A - (\sum_j\sin\pi\xi_j)B - \sum_j(\bar{v}_{oj}\sin\pi\xi_j) = 0 & (8.14) \\ (\sum_j\sin\pi\xi_j)A - nB - \sum_j\bar{v}_{oj} = 0 & (8.15) \end{cases}$$

from which:

$$\begin{cases} B = (A\sum\sin\pi\xi_j - \sum\bar{v}_{oj})/n & (8.16) \\ A = \dfrac{n(\sum\bar{v}_{oj}\sin\pi\xi_j) - (\sum\bar{v}_{oj})(\sum\sin\pi\xi_j)}{n(\sum\sin^2\pi\xi_j) - (\sum\sin\pi\xi_j)^2} & (8.17) \end{cases}$$

8.4 Results

Results are presented in Tables 8.1 - 8.11 (the ultimate load of the column is also recorded on these Tables as a means of identification). The sign convention follows that of Chapter 6: positive deflections go from the web toward the lips. The maximum measured deflections are about one-thousandth of the length, but the maximum amplitude of the sinusoidal fit is usually less.

8.5 Errors

Sources of error include:

- Limitations of measurement techniques. Although the best methods are theoretically accurate to 1/1000", it is unrealistic to expect an accuracy better than 2/1000" or 3/1000". Since initial deflection calculations involve the difference between nearly equal quantities, the relative error is sometimes high (up to 10%). This is explained in more detail below.
- Superposition of local and overall imperfections. To smooth out the local imperfections, which are of the order of 1/1000", would have required a greater number of readings than realistically feasible. Measurement stations are usually no closer than 6.0".
- The actual initial deflections are not sinusoidal.

8.5.1 Relative Error of Measurement of Initial Deflection

Let us assume the extreme readings to be at the column ends, drop the subscript j and rewrite Eq. (8.7) as:

$$\bar{v}_o = \tilde{v}_o - [\tilde{v}_{oI} + (\tilde{v}_{oF} - \tilde{v}_{oI})\,\frac{z}{L}] = \tilde{v}_o - (\frac{L - z}{L}\,\tilde{v}_{oI} + \frac{z}{L}\tilde{v}_{oF}) \qquad (8.18)$$

Differentiation gives the error in v_o:

$$\delta\bar{v}_o = \frac{\partial\bar{v}_o}{\partial\tilde{v}_o}\delta\tilde{v}_o + \frac{\partial\bar{v}}{\partial\tilde{v}_{oI}}\delta\tilde{v}_{oI} + \frac{\partial\bar{v}}{\partial\tilde{v}_{oF}}\delta\tilde{v}_{oF} = \delta\tilde{v}_o - \frac{L-z}{L}\delta\tilde{v}_{oI} - \frac{z}{L}\delta\tilde{v}_{oF} \tag{8.19}$$

The worst error is given by:

$$\delta\bar{v}_o = \delta\tilde{v}_o + \frac{L-z}{L}\delta\tilde{v}_{oI} + \frac{z}{L}\delta\tilde{v}_{oF} \tag{8.20}$$

Since the measurements are equally accurate, with a measurement error Δ:

$$\delta\tilde{v}_o = \delta\tilde{v}_{oI} = \delta\tilde{v}_{oF} = \Delta \quad \text{and} \quad \delta\bar{v}_o = 2\Delta \tag{8.21}$$

<u>Example</u>: For a 72" column, at a location where the initial deflection is .072" and with Δ = .003",

$$\frac{\delta\bar{v}_o}{\bar{v}_o} = \frac{.006}{.072} = \frac{1}{12} \approx 8\%.$$

8.6 Column Centering

In the testing of columns, the experimental procedure of column centering described in the next chapter, calls for the application of load at a small eccentricity to compensate for the initial deflection of the column. The criteria of load alignment are uniformity of strain and absence of appreciable lateral deflection at midheight for loads up to 1/3 or 1/2 or the expected ultimate. It is interesting to see how the introduction of load eccentricity, in effect, reduces the initial deflection.

A column with sinusoidal initial deflection,

$$v_o = V_o \sin \pi z/L, \tag{8.22}$$

is loaded eccentrically (Fig. 8.4). Its behavior, considered only in the elastic range, is compared with that of an elastic, centrally loaded column also with sinusoidal but smaller initial deflection

$$w_o = W_o \sin \pi z/L. \tag{8.23}$$

8.6.1 Curved Column Under Eccentric Load

Let v(z) be the additional deflection caused by the eccentric load. Moment equilibrium requires:

$$EIv'' = P[e - (V_o \sin \pi z/L + v)] \tag{8.24}$$

or

$$v'' + \frac{P}{EI} v = \frac{P}{EI} (e - V_o \sin \frac{\pi z}{L}). \tag{8.25}$$

e is the load eccentricity and " denotes double differentiation with respect to z.

Using the boundary conditions v(o) = v(L) = o and the notation

$$k^2 = \frac{P}{P_{cr}} = \frac{PL^2}{\pi^2 EI} \text{ and } \xi = z/L$$

the solution is:

$$v(\xi) = -e \cos\pi k\xi + e \frac{\cos\pi k - 1}{\sin\pi k} \sin\pi k\xi + \frac{k^2}{1 - k^2} V_o \sin\pi\xi + e \tag{8.26}$$

the midheight deflection V is:

$$V = v(1/2) = e(1 - \sec \frac{\pi k}{2}) + \frac{k^2}{1 - k^2} V_o \tag{8.27}$$

A similar analysis gives the midheight deflection W of a centrally loaded column:

$$W = \frac{k^2}{1 - k^2} W_o \tag{8.28}$$

Using the notations $\mu = V_o/e$ and $\bar{\mu} = W_o/e$, the last two equations can be rewritten as:

$$\frac{V}{e} = 1 - \sec\frac{\pi k}{2} + \frac{k^2}{1 - k^2}\mu \tag{8.29}$$

and

$$\frac{W}{e} = \frac{k^2}{1 - k^2}\bar{\mu} \tag{8.30}$$

It is possible to find $\bar{\mu}$ such that the midheight deflection of the eccentrically loaded column coincides with that of the centrally loaded column:

$$V = W \text{ implies} \qquad \mu - \bar{\mu} = \frac{1 - k^2}{k^2}\left(\sec\frac{\pi k}{2} - 1\right) \tag{8.31}$$

It is remarkable that $\mu - \bar{\mu}$ varies little and almost linearly with k^2:

k^2	.1	.2	.3	.4	.5	.6	.7	.8	.9
$\mu - \bar{\mu}$	1.237	1.241	1.244	1.248	1.252	1.256	1.260	1.264	1.269

The average value, $(\mu - \bar{\mu})_{av} = 1.25$, provides a good approximation over the whole range of elastic loading.

$$W_o \simeq V_o - 1.25e \tag{8.32}$$

So, if one was to align the column load by shifting the column ends while monitoring the midheight deflection, one ends up loading the column eccentrically and, in effect, reducing the initial sinusoidal out-of-straightness by 5/4 the eccentricity.

So far, only the midheight deflection has been considered. It is interesting to see how close the deflected shape of the eccentrically loaded column is to a half sine wave, which is the deflected shape of the centrally loaded column.

Fig. 8.5 shows that the curve $v/e = f(\xi)$, Equation (8.26), can be approximated fairly closely by a half sine-wave for values of $\mu < 1.10$ or $\mu > 1.40$. It is clear that the portions of the deflected shape close to the ends are to the left (when the eccentricity is to the right) of a half-sine-wave passing through the middle of the column.

If alignment is judged by absence of deflection or uniformity of strain at midheight, then the range $1.10 \leq \mu \leq 1.40$ corresponds to very good alignment. This is so because the column deflects in one direction close to the ends and in the opposite direction in the middle region (Fig. 8.6). For the greatest part of the loading, however, the maximum deflection is not at midheight.

Fig. 8.7 shows a reversal of the midheight deflection as the load increases for $1.23 < \mu < 1.27$. No such thing occurs for the quarter-point deflection. The value $\mu = V_o/e = 1.25$ can be considered the best alignment, judging from midheight deflection: up to $P = \frac{1}{2} P_{cr}$, $|V| \leq .0025\ e$.

<u>Example</u>: A 100" long column with initial deflection $W_o = L/1000 = .10"$ is loaded with an eccentricity $e = .040"$. (8.32) gives $V_o = .100 - 1.25 \times .040 = .050"$ and $V_o/e = 1.25$. So up to $P = P_{cr}/2$, $|V| \leq .0025 \times .04 = .0001"$. A very small deflection, not measurable even with a dial gage sensitive to 10^{-4}".

So, even with such average initial deflection as L/1000 and for rather long columns, the midheight deflection can remain virtually negligible up to 1/2 the buckling load by judicious load alignment. It should be emphasized, though, that the column cannot be considered straight since the midheight deflection in this case is not the maximum deflection.

8.6.2 Generalization

If the initial deflection is generalized to:

$$v_o = \sum_{n=1}^{\infty} V_{on} \sin n\pi z/L \qquad (8.33)$$

it is easily shown that:

$$\frac{v}{e} = -\cos\pi k\xi + \frac{\cos\pi k - 1}{\sin\pi k} \sin\pi k\xi + \sum_n \left(\frac{k^2\mu_n}{n^2 - k^2} \sin n\pi\xi\right) + 1 \qquad (8.34)$$

where $\mu_n = V_{on}/e$.

It is well known that, near the buckling load, the $n = 1$ term dominates and deflection reversals occur for the parts of the column which were initially deflected in the direction opposite to the first buckling mode (Timoshenko and Gere [1961]). Load eccentricity hastens these reversals.

The above was derived in the elastic range, which is the range of interest in the alignment process.

8.7 Summary

The effect of initial deflections on column strength was surveyed, initial out-of-straightness were measured by three different methods and the process of load alignment was examined. Since the maximum deflections are not always at midheight, monitoring deflections at the quarter points during the alignment process is justified.

TABLE 8.1

PBC 14, GROUP 1: INITIAL DEFLECTIONS

Column A3 $P_u = 20.20$ k

	#	z	$\bar{v}_o$
L = 24.0"			
Method 2	1	6.0	0.0
A = 3.1	2	12.0	0.9
B = 2.2	3	18.0	0.0
S = -.099			
V_o/L = .21			

Column A5 $P_u = 19.30$ k

	#	z	$\bar{v}_o$
L = 36.0"			
Method 3	1	6.0	0.0
A = -11.	2	12.0	-1.75
B = -5.7	3	18.0	-6.50
S = -.5	4	24.0	-4.25
V_o/L = -.48	5	30.0	0.0

Column A9 $P_u = 13.95$ k

	#	z	$\bar{v}_o$
L = 54.0"			
Method 2	1	6.0	0.0
A = -49.	2	12.0	-18.0
B = -18.	3	18.0	-25.0
S = -2.5	4	24.0	-43.0
V_o/L = -1.3	5	30.0	-27.0
	6	36.0	-14.0
	7	42.0	-9.0
	8	48.0	0.0

Column A11 $P_u = 11.20$ k

	#	z	$\bar{v}_o$
L = 66.0"			
Method 2	1	6.0	0.0
A = -33.	2	12.0	-14.0
B = -12.	3	18.0	-18.0
S = -5.6	4	24.0	-28.0
V_o/L = -.78	5	30.0	-28.0
	6	36.0	-20.0
	7	42.0	-11.0
	8	48.0	5.0
	9	54.0	6.0
	10	60.0	0.0

Column A13 $P_u = 10.50$ k

	#	z	$\bar{v}_o$
L = 75.0"			
Method 3	1	2.0	0.0
A = 25.	2	8.0	32.1
B = -10.	3	14.0	30.2
S = 9.4	4	20.0	26.2
V_o/L = .33	5	26.0	33.3
	6	32.0	31.4
	7	38.0	29.5
	8	44.0	29.6
	9	50.0	32.7
	10	56.0	32.7
	11	62.0	30.8
	12	68.0	26.9
	13	74.0	0.0

Column A14 $P_u = 8.20$ k

	#	z	$\bar{v}_o$
L = 86.0"			
Method 3	1	2.0	0.0
A = -.92	2	14.0	-2.4
B = 5.1	3	26.0	7.2
S = 16.3	4	38.0	1.8
V_o/L = -.24	5	50.0	-11.7
	6	62.0	-14.1
	7	74.0	-25.5
	8	84.0	0.0

A,B,S,$\bar{v}_o$ in 10^{-3} inch, V_o/L in 10^{-3}.

Column length without end plates.

z in inch.

TABLE 8.2

PBC 14, GROUP 2: INITIAL DEFLECTIONS

Column A1 $P_u = 19.0$ k

	#	z	$\bar{v}_o$
L = 18.0"			
Method 2	1	3.0	0.0
A = 1.7	2	6.0	3.5
B = .90	3	9.0	1.0
S = .031	4	12.0	-2.5
V_o/L = .15	5	15.0	0.0

Column A2 $P_u = 16.9$ k

	#	z	$\bar{v}_o$
L = 24.0"			
Method 2	1	2.0	0.0
A = 31.	2	11.0	23.3
B = 8.1	3	13.0	22.7
S = -.099	4	22.0	0.0
V_o/L = 1.6			

Column A4 $P_u = 16.3$ k

	#	z	$\bar{v}_o$
L = 30.0"			
Method 2	1	6.0	0.0
A = 36.0	2	12.0	14.0
B = 21.0	3	15.0	14.0
S = -.24	4	18.0	13.0
V_o/L = 1.9	5	24.0	0.0

Column A6 $P_u = 14.4$ k

	#	z	$\bar{v}_o$
L = 39.0"			
Method 1	1	0.0	0.0
A = 35.	2	18.0	35.0
B = 0.0	3	0.0	0.0
S = 0.0			
V_o/L = .97			

Column A7 $P_u = 13.5$ k

	#	z	$\bar{v}_o$
L = 42.0"			
Method 3	1	6.0	0.0
A = -3.7	2	12.0	-14.0
B = 1.2	3	18.0	-2.0
S = -.93	4	21.0	0.0
V_o/L = -.082	5	24.0	-3.0
	6	30.0	-9.0
	7	36.0	0.0

Column A8 $P_u = 13.66$ k

	#	z	$\bar{v}_o$
L = 48.0"			
Method 2	1	5.0	0.0
A = -26.	2	11.0	0.16
B = -3.5	3	17.0	-7.7
S = -1.6	4	23.0	-14.5
V_o/L = -.65	5	25.0	-19.5
	6	31.0	-33.3
	7	37.0	-46.2
	8	43.0	0.0

Column A10 $P_u = 10.45$ k

	#	z	$\bar{v}_o$
L = 60."			
Method 1	1	0	0.
A = 7.5	2	30.	-6.
B = 0.	3	60.	0.
S = 0.			
V_o/L = -.10			

Column A12 $P_u = 9.50$ k

	#	z	$\bar{v}_o$
L = 72."			
Method 2	1	6.0	0.
A = -94.	2	12.0	-17.
B = -24.	3	18.0	-34.
S = 8.0	4	24.0	-38.
V_o/L = -1.5	5	30.0	-73.
	6	36.0	-73.
	7	42.0	-69.
	8	48.0	-62.
	9	54.0	-54.
	10	60.0	-34.
	11	66.0	0.

Column length without end plates.

A,B,S in 10^{-3} inch, V_o/L in 10^{-3}, z in inch.

TABLE 8.3

RFC 14, GROUP 1: INITIAL DEFLECTIONS

Column B2 P_u = 19.5 k

	#	z	$\bar{v}_o$
L = 24.0"	1	3.0	0.0
Method 2	2	9.0	10.7
A = 17.	3	15.0	7.3
B = 6.4	4	21.0	0.0
S = -.099			
V_o/L = .95			

Column B4 P_u = 18.0 k

	#	z	$\bar{v}_o$
L = 36.0	1	3.0	0.0
Method 2	2	9.0	11.8
A = 20.	3	15.0	13.6
B = 4.3	4	21.0	13.4
S = .5	5	27.0	12.2
V_o/L = .66	6	33.0	0.0

Column B5 P_u = 16.00 k

	#	z	$\bar{v}_o$
L = 48.0"	1	6.0	0.0
Method 3	2	12.0	-4.3
A = -12.	3	18.0	-4.7
B = -4.4	4	24.0	-8.0
S = -1.6	5	30.0	-8.3
V_o/L = -.38	6	36.0	-5.7
	7	42.0	0.0

Column B6 P_u = 15.5 k

	#	z	$\bar{v}_o$
L = 48.0"	1	6.0	0.0
Method 3	2	12.0	10.8
A = 23.	3	18.0	10.7
B = 7.3	4	24.0	14.5
S = 1.6	5	30.0	14.3
V_o/L = -.66	6	36.0	14.2
	7	42.0	0.0

Column B9 P_u = 8.80 k

	#	z	$\bar{v}_o$
L = 77.5"	1	2.0	0.0
Method 3	2	14.0	-39.5
A = -69.	3	26.0	-66.0
B = -6.3	4	38.0	-55.5
S = 10.7	5	50.0	-51.0
V_o/L = -.83	6	62.0	-26.5
	7	74.0	0.0

Column B10 P_u = 8.00 k

	#	z	$\bar{v}_o$
L = 77.5"	1	2.0	0.0
Method 3	2	8.0	37.1
A = 46.	3	14.0	47.2
B = -8.5	4	20.0	45.3
S = -10.7	5	26.0	44.4
V_o/L = .35	6	32.0	49.5
	7	38.0	48.6
	8	44.0	47.8
	9	50.0	46.9
	10	56.0	46.0
	11	62.0	42.1
	12	68.0	40.2
	13	74.0	8.3
	14	76.0	0.0

Column B11 P_u = 9.05 k

	#	z	$\bar{v}_o$
L = 81.9"	1	4.5	0.0
Method 3	2	10.5	17.0
A = 26.	3	16.5	17.2
B = -1.5	4	22.5	18.6
S = 13.	5	28.5	22.1
V_o/L = .46	6	34.5	21.7
	7	40.5	26.3
	8	46.5	26.0
	9	52.5	27.1
	10	58.5	26.7
	11	64.5	23.8
	12	70.5	21.4
	13	76.5	0.0

Column length without end plates.
A,B,S in 10^{-3} inch. V_o/L in 10^{-3}.
z in inch.

TABLE 8.4

RFC 14, GROUP 2: INITIAL DEFLECTIONS

Column B1 $P_u = 18.5$ k

	#	z	$\bar{v}_o$
L = 24.0"			
Method 2	1	2.0	0.0
A = 20.	2	11.0	11.5
B = 5.1	3	13.0	17.5
S = -.099	4	22.0	0.0
$V_o/L = 1.0$			

Column B3 $P_u = 16.3$ k

	#	z	$\bar{v}_o$
L = 36.0"			
Method 2	1	6.0	0.0
A = 36.	2	12.0	12.5
B = 18.	3	17.0	18.1
S = -.50	4	19.0	17.9
$V_o/L = 1.5$	5	24.0	12.5
	6	30.0	0.0

Column B7 $P_u = 14.0$ k

	#	z	$\bar{v}_o$
L = 48.0"			
Method 2	1	3.0	0.0
A = 74.	2	10.0	34.2
B = 14.	3	17.0	51.3
S = -1.6	4	23.0	56.8
$V_o/L = 1.8$	5	25.0	60.2
	6	31.0	57.7
	7	38.0	28.8
	8	45.0	0.0

Column B8 $P_u = 11.5$ k

	#	z	$\bar{v}_o$
L = 60.0"			
Method 1	1	0.0	0.0
A = 7.0	2	30.0	7.0
B = 0.	3	60.0	0.0
S = 0.			
$V_o/L = .12$			

Column length without end plates.

A,B,S in 10^{-3} inch; V_o/L in 10^{-3}

z in inch.

Table 8.5

PBC 13, GROUP 1: INITIAL DEFLECTIONS

Column C3 $P_u = 26.40$ k

	#	z	$\bar{v}_o$
L = 36.0"	1	6.0	0.0
Method 2	2	12.0	4.5
A = 17.	3	18.0	10.
B = 9.	4	24.0	5.5
S = -.5	5	30.0	0.0
$V_o/L = .72$			

Column C4 $P_u = 21.60$ k

	#	z	$\bar{v}_o$
L = 48.0"	1	6.0	0.0
Method 2	2	12.0	8.8
A = 10.	3	18.0	5.7
B = 3.	4	24.0	5.5
S = -1.6	5	30.0	7.3
$V_o/L = .25$	6	36.0	4.2
	7	42.0	0.0

Column C5 $P_u = 15.85$ k

	#	z	$\bar{v}_o$
L = 60.0"	1	6.0	0.0
Method 2	2	12.0	-7.0
A = -30.	3	18.0	-22.0
B = -11.	4	24.0	-34.0
S = -3.9	5	30.0	-16.0
$V_o/L = -.74$	6	36.0	-11.0
	7	42.0	-1.0
	8	48.0	-4.0
	9	54.0	0.0

Column C6 $P_u = 9.95$ k

	#	z	$\bar{v}_o$
L = 79.0"	1	6.0	0.0
Method 3	2	12.0	0.36
A = -7.8	3	18.0	-3.3
B = -.05	4	24.0	-2.4
S = -12.	5	30.0	-6.0
$V_o/L = -.25$	6	36.0	-7.7
	7	42.0	-5.8
	8	48.0	-7.4
	9	54.0	-9.1
	10	60.0	-10.7
	11	66.0	-12.4
	12	72.0	0.0

Column C7 $P_u = 7.70$ k

	#	z	$\bar{v}_o$
L = 97.0"	1	2.0	0.0
Method 3	2	14.0	-18.0
A = -19.	3	26.0	-16.0
B = .73	4	38.0	-21.0
S = -26.	5	50.0	-18.0
$V_o/L = -.46$	6	62.0	-15.0
	7	74.0	-13.0
	8	86.0	-6.0
	9	95.0	0.0

Column length without end plates.
A,B,S in 10^{-3} inch; V_o/L in 10^{-3}.
z in inch.

TABLE 8.6

PBC 13, GROUP 2: INITIAL DEFLECTIONS

Column C1 P_u = 35.00 k

	#	z	$\bar{v}_o$
L = 24.0"			
Method 2	1	6.0	0.0
A = 0.0	2	12.0	0.0
B = 0.0	3	18.0	0.0
S = -.099			
V_o/L = -.10			

Column C2 P_u = 23.38 k

	#	z	$\bar{v}_o$
L = 24.0"			
Method 2	1	6.0	0.0
A = 10.	2	12.0	3.0
B = 7.2	3	18.0	0.0
S = -.099			
V_o/L = .72			

Column length without end plates.

A,B,S in 10^{-3} inch. V_o/L in 10^{-3}.

TABLE 8.7

RFC 13, GROUP 2: INITIAL DEFLECTIONS

Column D3 P_u = 35.0 k

	#	z	$\bar{v}_o$
L = 24.0"			
Method 2	1	6.0	0.0
A = 0.0	2	12.0	0.0
B = 0.0	3	18.0	0.0
S = -.099			
V_o/L = -4.1			

Column D4 P_u = 22.3 k

	#	z	$\bar{v}_o$
L = 24.0"			
Method 2	1	6.0	0.0
A = 3.1	2	12.0	0.9
B = 2.2	3	18.0	0.0
S = -.099			
V_o/L = .21			

A,B,S in 10^{-3} inch; V_o/L in 10^{-3}.

Column length without end plates, z in inch

The initial deflections of the columns of Group 1, RFC 13 were measured by method 1 and are not tabulated.

TABLE 8.8

H 11, GROUP 1: INITIAL DEFLECTIONS

Column E1 P_u = 18.50 k

	#	z	$\bar{v}_o$
L = 16.4"			
Method 2	1	2.25	0.0
A = 40.	2	8.25	23.5
B = 16.	3	14.25	0.0
S = .063			
V_o/L = 3.4			

Column E3 P_u = 18.20 k

	#	z	$\bar{v}_o$
L = 25.0"			
Method 2	1	2.0	0.0
A = 39.	2	6.5	17.6
B = 9.6	3	12.5	29.0
S = .34	4	18.5	19.4
V_o/L = 1.9	5	23.0	0.0

Column E4 P_u = 11.8 k

	#	z	$\bar{v}_o$
L = 36.0"			
Method 2	1	2.0	0.0
A = -24.	2	10.0	-7.8
B = -4.1	3	17.0	-19.9
S = -1.5	4	19.0	-19.9
V_o/L = -.83	5	26.0	-22.9
	6	34.0	0.0

Column E5 P_u = 7.00 k

	#	z	$\bar{v}_o$
L = 48.0"			
Method 2	1	0.0	0.0
A = -19.	2	6.0	-9.0
B = .93	3	12.0	-16.0
S = -4.6	4	18.0	-23.0
V_o/L = -.48	5	24.0	-13.0
	6	30.0	-19.0
	7	36.0	-18.0
	8	42.0	-8.0
	9	48.0	0.0

Column length without end plates.
A,B,S in 10^{-3} inch, V_o/L in 10^{-3}, z in inch

TABLE 8.9

H 11, GROUP 2: INITIAL DEFLECTIONS

Column E2 P_u = 15.7 k

	#	z	$\bar{v}_o$
L = 20.0"			
A = 9.2	1	3.	0.0
B = 4.2	2	10.	5.0
S = -.14	3	17.	0.0
V_o/L = .66			

Column length without end plates.

A,B,S in 10^{-3} inch; V_o/L in 10^{-3}, z in inch.

TABLE 8.10

H 7: INITIAL DEFLECTIONS

Column F1 $P_u = 45.00$ k

	#	z	$\bar{v}_o$
L = 28.0"	1	2.0	0.0
Method 2	2	8.0	-9.5
A = -17.	3	14.0	-13.4
B = -3.8	4	20.0	-10.5
S = +.23	5	26.0	0.0
V_o/L = -.75			

Column F2 $P_u = 41.80$ k

	#	z	$\bar{v}_o$
L = 36.0"	1	0.	0.
Method 2	2	18.	-4.
A = -5.4	3	36.	0.
B = -1.4			
S = -.63			
V_o/L = -.21			

Column F3 $P_u = 39.60$ k

	#	z	$\bar{v}_o$
L = 39.4"	1	1.69	0.0
Method 2	2	7.69	-10.3
A = -23.7	3	13.69	-18.7
B = -3.2	4	19.69	-21.0
S = .91	5	25.69	-16.3
V_o/L = -.66	6	31.69	-10.7
	7	37.69	0.0

Column F4 $P_u = 39.40$ k

	#	z	$\bar{v}_o$
L = 42.0"	1	6.0	0.0
Method 2	2	12.0	-3.2
A = -25.3	3	18.0	-13.0
B = -12.	4	24.0	-16.0
S = 1.2	5	30.0	-6.8
V_o/L = -.92	6	36.0	0.0

Column F5 $P_u = 30.90$ k

	#	z	$\bar{v}_o$
L = 48.0"	1	6.0	0.0
Method 2	2	12.0	0.0
A = 15.6	3	18.0	-22.0
B = .21	4	23.0	8.0
S = -2.0	5	25.0	19.0
V_o/L = .29	6	30.0	38.0
	7	36.0	49.0
	8	42.0	0.0

A,B,S in 10^{-3} inch. V_o/L in 10^{-3}.

Column length without end plates, z in inch.

TABLE 8.11

H T INITIAL DEFLECTIONS

Column G1 $P_u = 97.40$ k

L = 24.9"
Method 2
A = -3.6
B = -.82
S = .14
$V_o/L = -.17$

#	z	$\bar{v}_o$
1	2.0	0.0
2	6.5	-4.9
3	12.5	-2.5
4	18.5	.9
5	23.0	0.0

Column G2 $P_u = 78.00$ k

L = 36.0"
Method 2
A = -16.
B = -3.6
S = -.61
$V_o/L = -.57$

#	z	$\bar{v}_o$
1	2.0	0.0
2	9.0	-3.1
3	16.0	-12.
4	20.0	-16.
5	27.0	-7.9
6	34.0	0.0

Column G3 $P_u = 65.80$ k

L = 48.0"
Method 2
A = 7.6
B = 3.0
S = 1.9
$V_o/L = .26$

#	z	$\bar{v}_o$
1	6.0	0.0
2	12.0	4.5
3	18.0	10.0
4	23.0	5.1
5	25.0	2.9
6	30.0	0.0
7	36.0	-0.5
8	42.0	0.0

Column G4 $P_u = 42.75$ k

L = 62.4"
Method 3
A = -3.3
B = -.21
S = -5.7
$V_o/L = -.15$

#	z	$\bar{v}_o$
1	6.0	0.0
2	12.0	-0.9
3	18.0	-1.8
4	24.0	-2.7
5	30.0	0.4
6	36.0	-4.4
7	42.0	-5.3
8	48.0	-3.2
9	54.0	-2.1
10	60.0	0.0

Column G5 $P_u = 35.40$ k

L = 68.0"
Method 2
A = 20.
B = 7.6
S = -7.8
$V_o/L = .30$

#	z	$\bar{v}_o$
1	6.0	0.0
2	12.0	-3.3
3	18.0	11.0
4	24.0	16.0
5	30.0	15.0
6	36.0	9.0
7	42.0	10.0
8	48.0	4.0
9	54.0	7.0
10	60.0	0.0

A,B,S in 10^{-3} inch;
V_o/L in 10^{-3}, z in inch.
Column length without end plates.

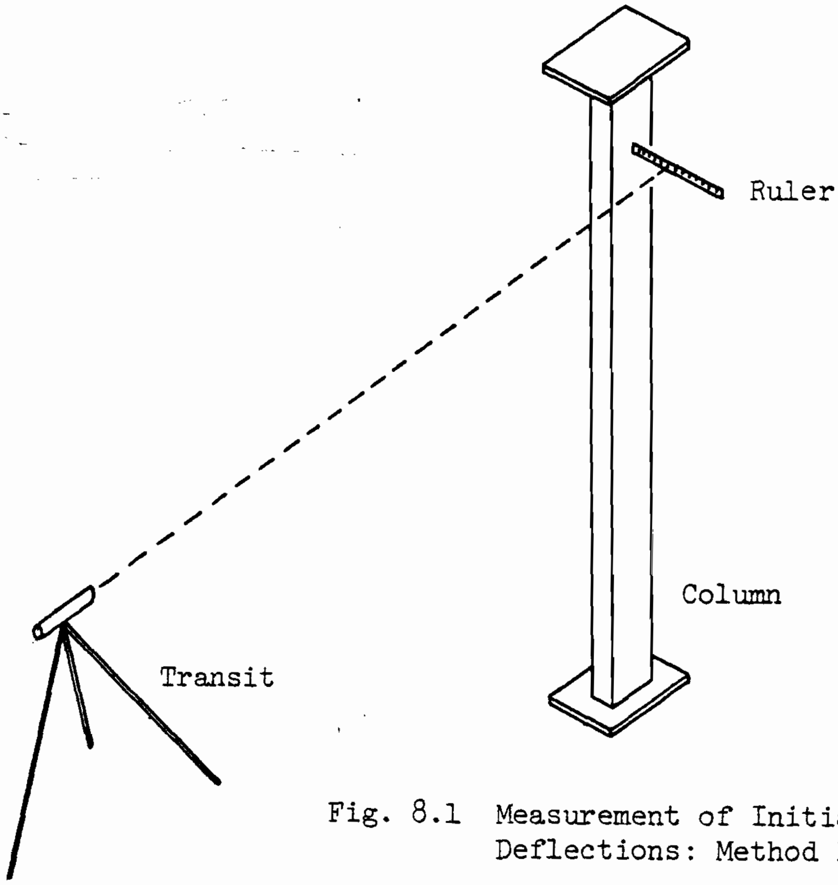

Fig. 8.1 Measurement of Initial Deflections: Method 1

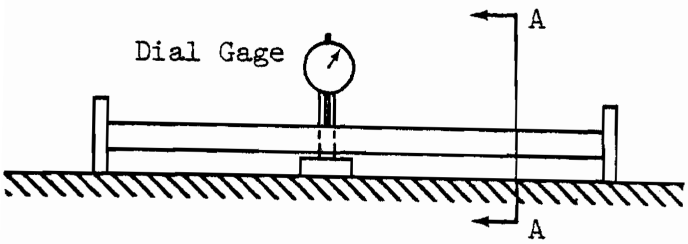

a)

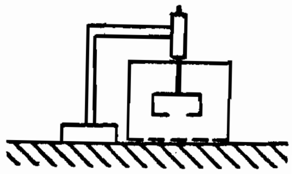

b) View A-A

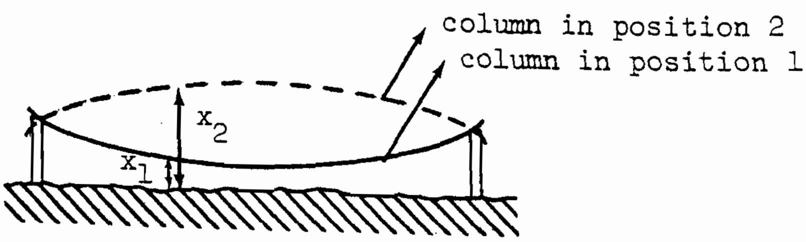

c) Imperfect table

Fig. 8.2 Measurement of Initial Deflections: Method 2

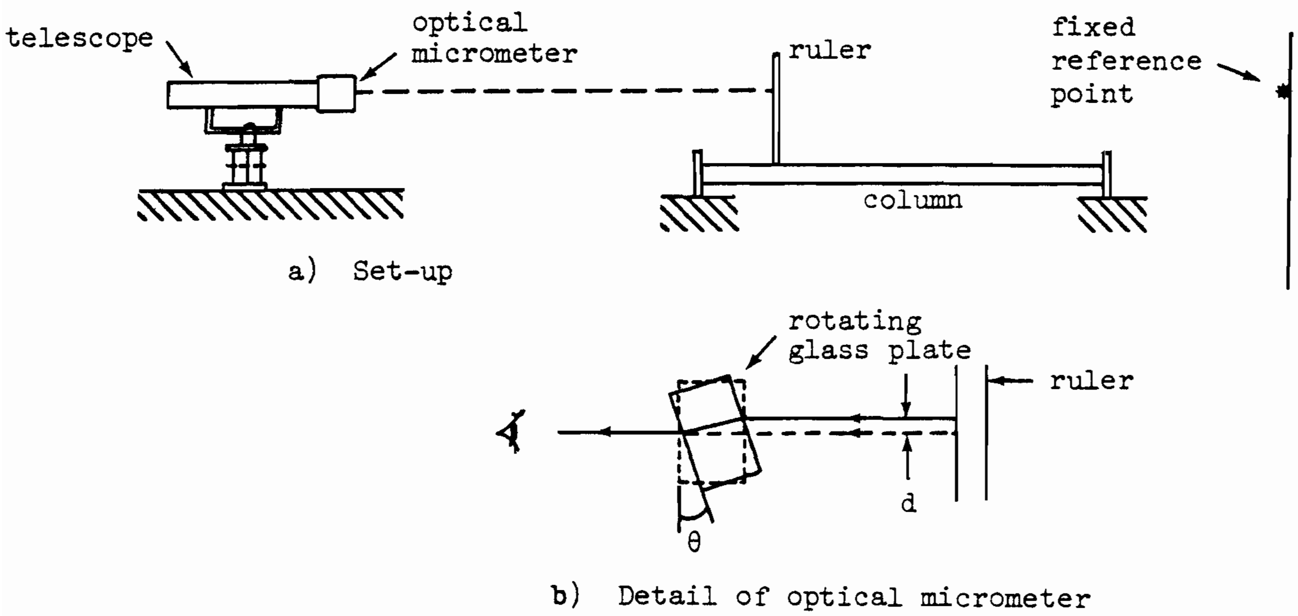

Fig. 8.3 Measurement of Initial Deflections: Method 3

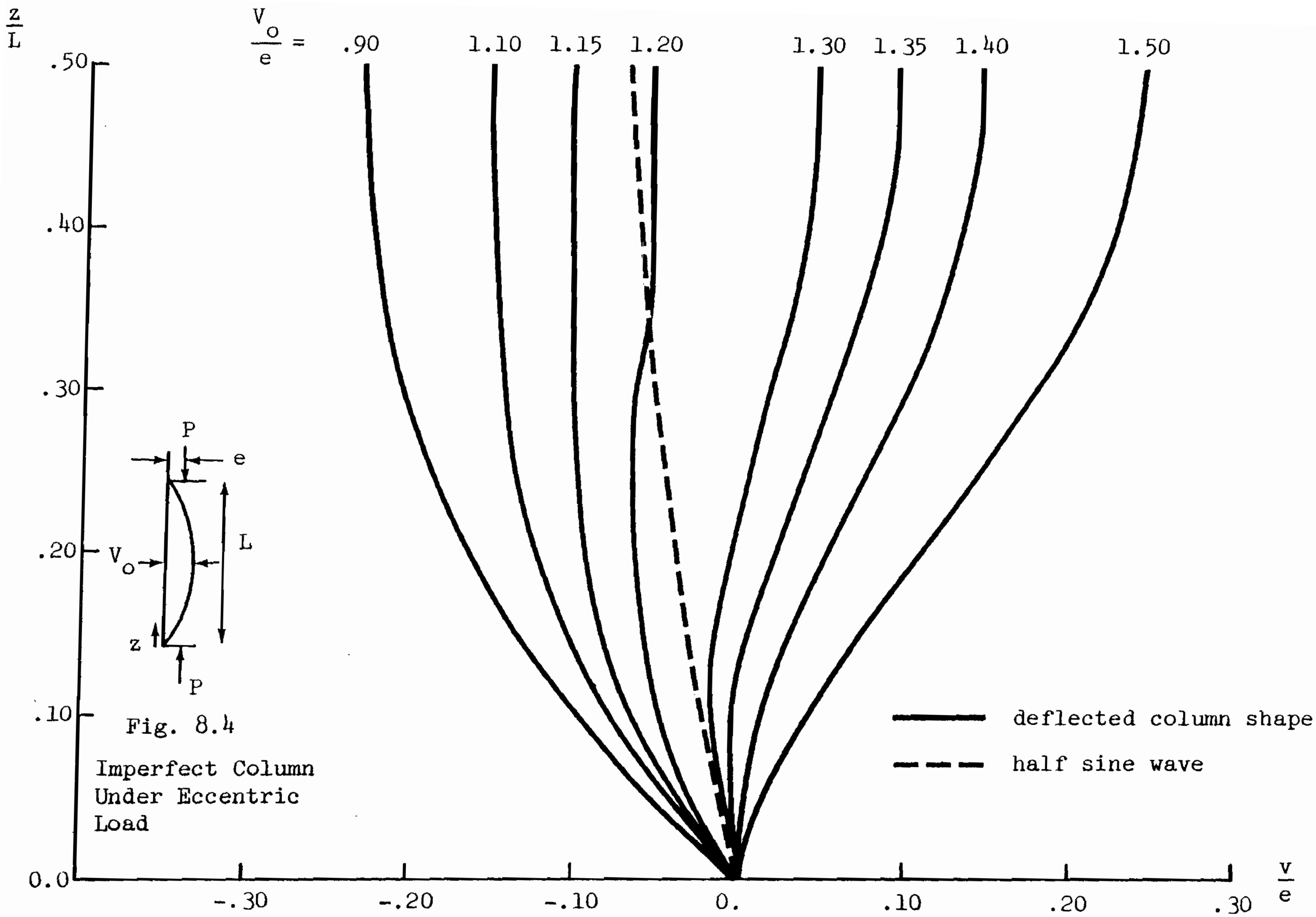

Fig. 8.4

Imperfect Column Under Eccentric Load

Fig. 8.5 Deflected Column Shapes

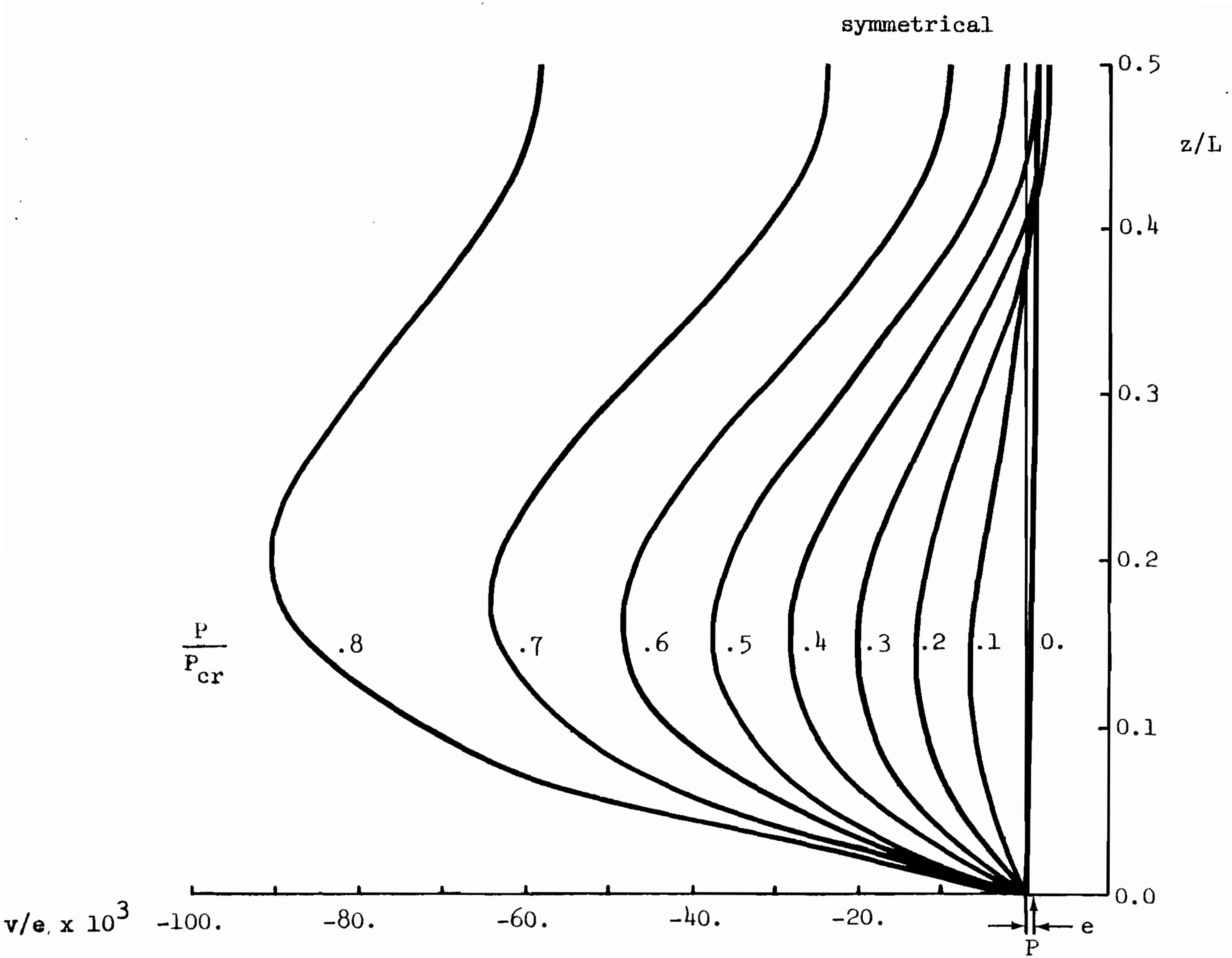

Fig. 8.6 Elastic Curve of Initially Deflected Column ($V_o/e = 1.25$) Loaded Eccentrically.

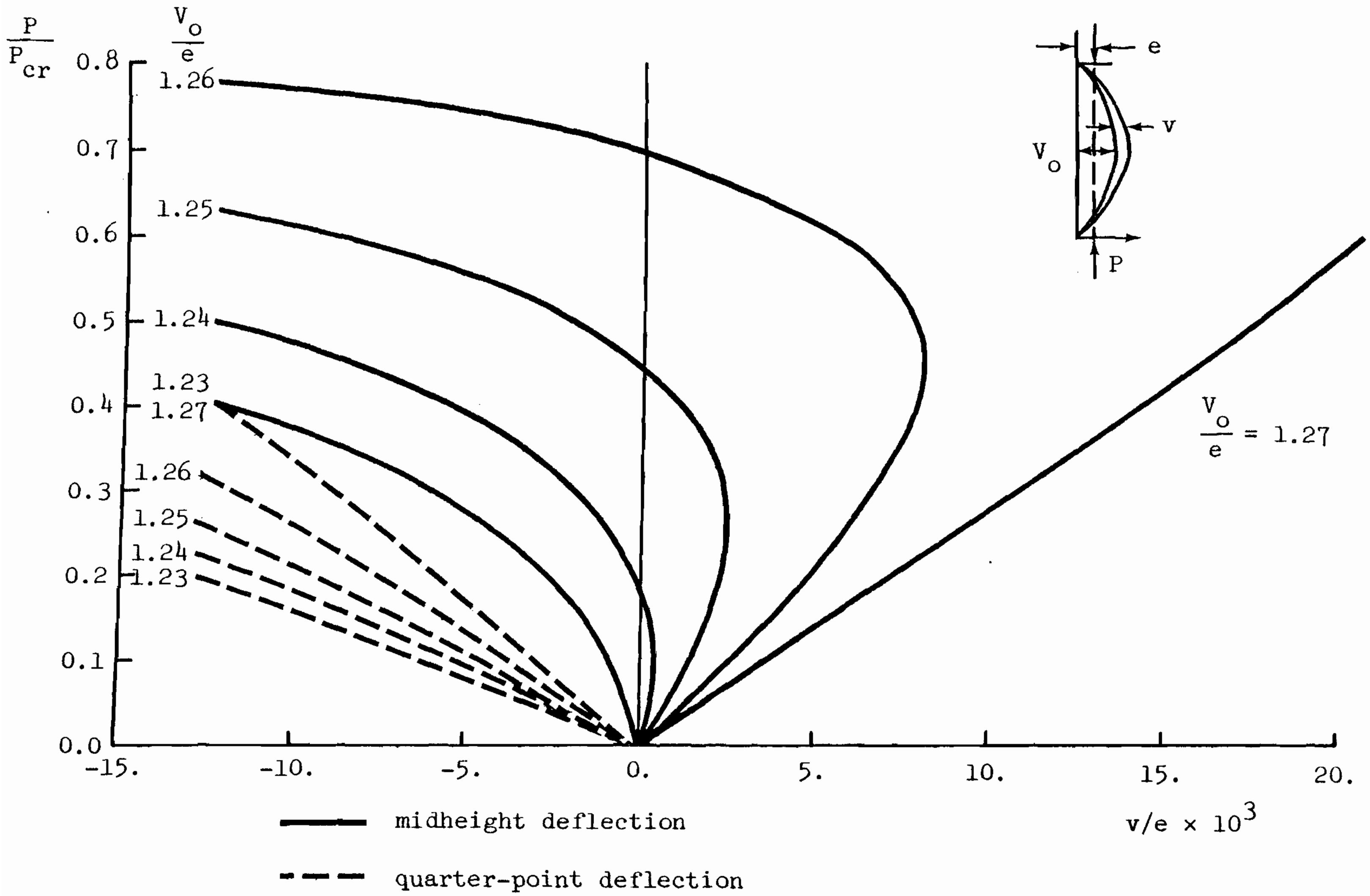

Fig. 8.7 Column Deflections

CHAPTER 9

COLUMN TESTS

Of central importance in this investigation is the experimental determination of column strength.

9.1 Review of Various Procedures

In the research proposal that initiated this work, Peköz [1975] listed the three principal methods of column testing procedures:

9.1.1 Dynamic Method

In the Dynamic Method (European Convention Testing Method), "the load is gradually and continuously increased and readings are taken at certain load increments without stabilizing the load. The initial imperfections are carefully measured and the column is centered in the test machine only geometrically with respect to the ends. The evaluation includes the effect of initial geometric imperfections. The geometric cross-sectional imperfections are not included in the evaluation. A static ultimate load is not obtained in this test." (Peköz [1975]).

9.1.2 Modified Dynamic Method

The Modified Dynamic Method (New Lehigh Procedure. SSRC Technical Memorandum No. 4, Johnston [1976]) is only different from the Dynamic Method in that it also obtains a static ultimate load. Upon reaching the maximum dynamic test load as above, the load is stabilized (usually a drop in load occurs) while the column shape is unchanged. For a screwtype machine this can be achieved by maintaining the cross-head in a stationary position. For a hydraulic machine, this can be done by slowly opening the bypass valve further until further lateral deflection of the column at midheight ceases. After recording the maximum static load, the test is resumed dynamically.

9.1.3 Static Method

In the Static Method, the load is slowly increased and stabilized at every load increment before readings are taken. The ultimate load obtained is the ultimate static load of the column. Column centering is elaborate and usually requires that stresses be uniform within certain tolerances at certain sections along the column.

The two dynamic methods are faster than the static method, at both stages of centering and testing. The dynamic methods also indicate the effect of initial imperfections directly. In the static method, it is possible to find the combined magnitude of initial imperfection and load eccentricity by a Southwell plot.

The static test is more appropriate than the dynamic tests for verifying the tangent modulus load. The static test has been used for all the cold-formed column tests conducted to date (Peköz [1975]). For consistency, it is also used here.

9.1.4 Boundary Conditions

Technical Memorandum No. 4 of the SSRC (Johnston [1976]) compares the fixed-end and the pinned-end conditions:

"In testing columns under the fixed-end condition, the full restraint may not be provided in the entire range of the test loads;

thus the effective length of the column is not a constant but a function of the applied load. This may be due partly to the fact that the rigidity of the testing machine varies with the applied load and partly to the indeterminate nature of the stress distribution at the column ends, particularly in the load range in which the material yields. These problems are eliminated by using pinned-end conditions because the critical condition exists at about the midheight cross-section."

A further advantage of the pinned-end condition is that, "for the same effective slenderness ratio, it requires the use of only half the column length used for the fixed-end condition."

The pinned-end condition is used here.

9.2 Description of Procedure

Columns are cut from relatively straight portions of stock, no closer than 6.0" inches to any flame cut ends. The column ends are cold-sawed perpendicular to the column axis at its ends. Due to initial deflections, the end surfaces are generally not exactly parallel, although deviations from parallelism are minimal and can be accommodated for by the use of hydrostone during alignment. 3/4" thick, rectangular end plates, ground flat to .0005 inches are welded to the column ends, so the centroidal axes of the plates and those of the column at its ends coincide. To minimize welding residual stresses, short fillet welds are placed sequentially and symmetrically so any given weld is allowed to cool before an adjacent weld is placed. The result is a continuous weld on both the inside and outside faces of the column.

Initial deflections are measured by the methods described in Chapter 8. Strain gages are mounted at various midheight locations after the necessary surface preparations. These gages monitor the test and are especially useful for alignment. Since uniformity of strain at midheight is the criterion used for load alignment, it is judicious to place the gages on opposite sides of the axes of bending and as far from them as possible. In the early column tests, up to eight gages are used, two at each corner; but in the later ones, only three are used. For the channel sections, one gage is placed at the middle of the web, the other two on the flanges, near their juncture with the lips. All gages are on the outside face (since there is no local buckling, it is not necessary to have gages in pairs on both faces). For the hat sections, one gage is at the top, the other two at the middle of the lips, but on the other face. At the same time as strain gages are mounted, strings to attach to dial gages are glued to the surface of the column at the corners between web and flanges.

Next, the column is placed in a hydraulic press between two end fixtures which have been centered on the machine plates beforehand. These end fixtures are basically knife edges and allow rotation in one direction only with negligible friction. The fixtures were devised by Peköz [1967] and used successfully in several research projects. Each fixture, shown in Fig. 9.1, has two separate sets of wedges which allow compensation for any lack of parallelism between the column ends in the direction parallel to the axis of rotation (i.e. the axes of rotation of the ends, say yy, are coplanar but not parallel). To compensate for lack of parallelism in the other direction, (i.e. the xx axes of the two ends are coplanar but not parallel), two layers of hydrostone are laid between the column base plates and the end fixtures. Sets of bolts on all four sides of each fixture allow precise positioning of the column base plates. They are used to move the xx axes of the column ends into the same vertical plane. The same can be done about the yy axes. Displacement of the base plate is possible, even after the hydrostone has set, if wax paper is placed between the hydrostone and the end fixture.

In chronological order, the bottom and top fixtures are first placed and centered in the testing machine. The wedges are brought back to the neutral position (both sides level) and the fixtures checked for any rotational restraint. A sheet of wax paper is placed on the bottom fixture, on which a layer of hydrostone, about 1/4" thick is spread. The column is then placed on top of the hydrostone, well centered with respect to the fixture and the bottom machine plate. Hydrostone is laid on top of the column and covered with wax paper. The top fixture attached to the machine cross-head is then lowered until it touches the hydrostone. The verticality of the column is checked with a level tube. To prevent motion from the vertical position, a small load of about 100 pounds is maintained while the hydrostone sets. This load may vary as setting progresses.

Load alignment is of crucial importance and the criterion used is uniformity of strains at midheight (the absence of lateral deflection is usually not stringent enough a criterion).

Alignment is considered satisfactory when strains are uniform to within ± 5% for loads up to 1/3 of the estimated ultimate. This goal is achieved by adjusting the wedges and shifting the base plates. On occasions, the column had to be removed from the machine, the hydrostone chipped off and the whole process repeated anew. These occasions are fortunately rare, but in all cases load alignment is a time-consuming and tedious process which may take days.

In shifting the base plates, a minute load eccentricity is, in effect, introduced to compensate for the initial deflections of the column. Chapter 8 examined the effect of this procedure.

After the load has been aligned, dial gages are attached to the strings or placed directly against the column. Typically, two gages are used to measure deflections in the direction of the strong axis, two in the direction of the short axis. Since bending occurs about the weak axis, deflections parallel to it are negligible and in the later experiments are not measured.

The column is loaded statically. Readings of strains and deflections are taken at various loads after the load has stabilized. Load increments are chosen smaller near the ultimate load than at the beginning. The load reaches a peak, then decreases rapidly and finally stabilizes. The column has failed by then and shows large lateral deflections.

9.3 Results and Discussion

Results are reported in Tables 9.1a to 9.12b. Records of individual tests, in the form of plots of strains and lateral deflections versus load as well as collective results plotted on non-dimensionalized column curves are shown in Fig. 9.2 to 9.77. On these tables and figures, predicted values based on the theory of Chapter 6 and on the measurements of yield strength and residual stresses of Chapters 3 and 5 are also shown for comparison.

Column results are non-dimensionalized in a way that incorporates the yield strength of the material, thus allowing results for steels of various strength to be plotted on the same column curve. Loads are non-dimensionalized with respect to the yield load of the section $P_y = A\sigma_y$; slenderness ratios $\lambda = L/R$ are non-dimensionalized with respect to the slenderness ratio λ_o for which the Euler critical stress equals the yield stress:

$$\sigma_{cr} = \frac{\pi^2 E}{\lambda_o^2} = \sigma_y \Longrightarrow \lambda_o = \pi\sqrt{\frac{E}{\sigma_y}} \tag{9.1}$$

So

$$\bar{\lambda} = \frac{\lambda}{\lambda_o} = \frac{1}{\pi}\sqrt{\frac{\sigma_y}{E}}\,\frac{L}{R}$$

Cold-forming destroys the homogeneity of the material; as a result, the yield strength is not uniform and the question arises, what value of the yield strength to use for non-dimensionalization. The average value of yield strength, $\sigma_{ya} = \frac{\Sigma\, \sigma_{yi}\, A_i}{\Sigma\, A_i}$, where σ_{yi} and A_i are the yield strength and cross-sectional area of coupons, is the most logical choice. This average value may also be obtained by full section test. Full section tests or coupon tests that cover the entire cross-section are, however, difficult, time-consuming and rarely performed in practice, and the yield strength of the flat portions σ_{yf} is commonly referred to as the measure of the yield strength of the section. Both alternatives are used here. For the channel sections, the yield strength of the flats σ_{yf} is about the same for the web and flanges (Fig. 3.5, 3.9, 3.14 and 3.17); for the hats, the flange value is chosen as σ_{yf} (Fig. 3.20, 3.24 and 3.28).

Tensile yield strength is used here, rather than the more logical choice, compressive yield strength. The reason is, tensile tests are much easier to perform than compressive tests and give about the same results for steel; tensile test values are also used in practice.

Column results are separated in two groups. In group 1, computer predictions and experimental observations match more or less closely. In group 2, no such match is found.

The channel sections of (thickness) gage 14, be they press-braked or roll-formed, exhibit strength markedly below (up to 25%) the SSRC Curve and theoretical expectations, for slenderness ratios $\bar{\lambda} \leq 1.0$ (Fig. 9.16, 9.17, 9.29 and 9.30). For RFC14, tensile coupon tests (Fig. 3.9) show an atypically large spread in yield strengths. The upper limit is the yield strength values of coupon a, the lower limit is about 5.0 ksi less. This lower limit is used in the computer model (Table 9.3a) for the short, low-strength columns; even then, predictions are higher than actuality, except in one case, column B6, where agreement is good. Limited tensile coupon tests for PBC14 justify the assumption that all PBC14 columns have the same mechanical properties. The behavior of the C14 columns during the tests was identical to that of the C13 columns, which did not exhibit this puzzling low strength. Appendix D examines alternative buckling modes of the C14 columns.

Four of the C13 columns had much higher strength than expected (C1,D1,D3 and D5). It is possible some end restraint was inadvertently introduced, thus reducing the effective lengths (D1 was tested with knife-edges rather than the regular fixtures). On the other hand, one RFC13 column (D2) was much weaker than expected because it failed by local buckling of the web, near one end weld; this weld may have caused some larger than usual local distortion.

All the other columns behave fairly much in agreement with theoretical predictions. The error between theory and experiment hovers about 5%, which is what other investigators have obtained with the assumption of sinusoidal deflection.

9.4 Column Curves

Linear regressions by ordinary least squares (OLS) as well as by generalized least squares (GLS) and analyses of variance are performed on the column test results (Tables 9.13-9.23, Figs. 9.76-9.80). The model fitted to the data by OLS assumes constant variance (homoscedasticity) whereas that fitted by GLS does not(heteroscedasticity). For more details the reader is referred to standard texts of econometrics (Goldberger [1964], Johnston [1972], Theil [1971]). Statistical concepts relevant to the analysis of variance are reviewed in Appendix C, which is largely taken from Draper and Smith [1966]. In particular, if the data fell exactly on the regression line, then the correlation coefficient R would equal ± 1 (+ for positive slope, - for negative slope. For higher order regressions, the line is no longer straight and the quantity R^2 called the multiple correlation coefficient is used). Table 9.13 lists the regression lines and correlation coefficients corresponding to the following data sets:

a) all the test results of the present work (80 points)

b) nearly all of them, with the exclusion of five points, C1,D1,D2,D3 and D5, which fall far from the remaining points. Compared to the previous set, the correlation coefficient is much better (75 points).

c) another set excludes the five points mentioned above and the stub columns. The correlation coefficient goes back to approximately the same value as in a) (55 points).

d) Karren's results, 17 points listed in Table 9.24, are pooled to the present 75 points. Karren's tests [1967] involve hot-rolled semi-killed double-channel (gage 10) and double-hat (gage 9) sections bolted or riveted together (92 points).

e) so far, ordinary least-square regressions, which assumes a constant variance about the regression, are performed. Inspection of the data reveals, however, that the scatter of the data is worse for the intermediate columns than for short or long ones. This has some theoretical justification as well.* A parabolic standard error s(X) is assumed:

$s(X) = -.070X^2 + .12\,X + .040$ if the average yield strength is used and $s(X) = -.069\,X^2 + .097\,X + .066$ if the yield strength of the flat is used, where $X = \bar{\lambda} = \frac{1}{\pi}\sqrt{\frac{\sigma_y}{E}}\,\frac{L}{R}$. Also $Y = P_u/P_y$.

Note that if the coefficients of s(X) are multiplied by a common factor results will not change.

---

*Applied Mechanics Reviews summarize Perry's work as follows:
(Perry, S.H. "Statistical Variation of Buckling Strength" PhD Thesis, University College, London, 1966).

"(This is a) study of random imperfections in columns; over the total range of slenderness ratios of a column, three distinct forms of post-buckling are possible: for long columns, stable, elastic post-buckling occurs, showing little dependence on geometric imperfections; for very short columns, stable plastic post-buckling occurs, again showing little dependence on imperfections; in the intermediate range of slenderness ratios, post-buckling can be plastic and unstable. In the three ranges, the dependence of collapse load on initial imperfections takes different forms; this leads to scatter of load becoming more serious at the intermediate loads than at the two extreme ends of the range of slenderness ratios."

An ordinary least-square regression is fitted to the transformed variables:

$$X' = X/s(X) \quad \text{and} \quad Y' = Y/s(X).$$

This generalized least-square regression is performed on the same 92 data points mentioned in d). An improvement in the correlation coefficient results.

The above statistical analysis is done twice, using the average yield strength and the yield strength of the flat. It is seen that a straight line fits the data quite well (the correlation coefficient is between -.87 and -.97) and the five different schemes a-e produce results fairly close to one another.

A closer look is taken of scheme d), which contains the most data and assumes a straightforward uniform variance. Let U1 and U2 define the ratios of the actual column strength to that predicted by the linear model and by the SSRC parabola respectively (SSRCO(X) = $1-X^2/4$ for $X \leq \sqrt{2}$, $= 1/X^2$ for $X > \sqrt{2}$. Tables 9.17 and 9.22). The mean, variance, standard deviation and coefficient of variation of these ratios are determined. If the average yield strength is used, the SSRC parabola slightly overestimates column strength (mean of U2 less than 1.0) but the data exhibit a smaller variance about the parabola than the straight line. If the yield strength of the flats is used, there is little difference between the SSRC parabola and the linear model, as far as U1 and U2 are concerned.

Fig. 9.76 and 9.77 show the column data, non-dimensionalized by using the average yield strength and the yield strength of the flats respectively. The regression line using 75 of the 80 points (scheme b), its corresponding 95% confidence interval, the SSRC curve (dotted line) and a minimum curve are also shown. All points, except one, D2, fall above the minimum curve, which is governed by the PBC14 and RFC14 columns. If the average yield strength is used, the minimum curve is:

$$
\begin{aligned}
Y &= .787 - .292\,X && \text{for } .847 \le X \le 2.0 \\
Y &= 1.218 - 1.307\,X + .599\,X^2 && \text{for } .182 \le X \le .847 \\
Y &= 1.0 && \text{for } X \le .182
\end{aligned}
\tag{9.2}
$$

If the yield strength of the flats is used, the minimum curve is:

$$
\begin{aligned}
Y &= 1.122 - .726\,X + .144\,X^2 && \text{for } .174 \le X \le 2.0 \\
Y &= 1.0 && X \le .174
\end{aligned}
\tag{9.3}
$$

Fig. 9.78 and 9.79 show the column data obtained in the present work (80 points) and Karren's data (17 points). Also shown are the regression line using generalized least-squares (scheme e) and the corresponding 95% confidence interval. (The interval of confidence looks different from the theoretical work of Bjorhovde [1972] who assumes $P_u/P_y = 1.0$ at $\bar{\lambda} = 0.0$. The reason is, at the limit of zero length, all the variations in column strength are due to material properties and are included in P_y. In the present work, P_y is based on measurements on one set of coupon tests).

Finally Fig. 9.80 compares the SSRC parabola (called here curve 0), the SSRC curves 1,2 and 3 (Johnston [1976]), the Swedish Code design curve (European Recommendations [1979]) and the two straight lines obtained by scheme b) using 75 data points.

A brief summary of the findings described in this Section is given in Section 10.2. The following are the equations for the various approaches discussed above.

SSRC curve 0:

- for $0 \leq \bar{\lambda} \leq \sqrt{2}$ $\quad P_u/P_y = 1.0 - (\bar{\lambda})^2/4$

- for $\lambda > \sqrt{2}$ $\quad P_u/P_y = 1.0/(\bar{\lambda})^2$

SSRC curve 1:

- for $0 \leq \bar{\lambda} \leq .15$ $\quad P_u/P_y = 1.0$
- for $.15 \leq \bar{\lambda} \leq 1.2$ $\quad P_u/P_y = .990 + .122\bar{\lambda} - .367(\bar{\lambda})^2$
- for $1.2 \leq \bar{\lambda} \leq 1.8$ $\quad P_u/P_y = .051 + .801(\bar{\lambda})^{-2}$ (9.4)
- for $1.8 \leq \bar{\lambda} \leq 2.8$ $\quad P_u/P_y = .008 + .942(\bar{\lambda})^{-2}$

SSRC curve 2:

- for $0 \leq \bar{\lambda} \leq .15$ $\quad P_u/P_y = 1.0$
- for $.15 \leq \bar{\lambda} \leq 1.0$ $\quad P_u/P_y = 1.035 - .202\bar{\lambda} - .222(\bar{\lambda})^2$ (9.5)
- for $1.0 \leq \bar{\lambda} \leq 2.0$ $\quad P_u/P_y = -.111 + .636(\bar{\lambda})^{-1} + .087(\bar{\lambda})^{-2}$

SSRC curve 3:

- for $0 \leq \bar{\lambda} \leq .15$ $\quad P_u/P_y = 1.0$
- for $.15 \leq \bar{\lambda} \leq .8$ $\quad P_u/P_y = 1.093 - .622\bar{\lambda}$ (9.6)
- for $.8 \leq \lambda \leq 2.2$ $\quad P_u/P_y = -.128 + .707(\bar{\lambda})^{-1} - .102(\bar{\lambda})^{-2}$

Swedish design curve:

- for $0 \leq \bar{\lambda} \leq .30$ $\quad P_u/P_y = 1.0$
- for $.30 \leq \bar{\lambda} \leq 1.85$ $\quad P_u/P_y = 1.126 - .419\bar{\lambda}$ (9.7)

Linear regression using average yield strength (scheme b)

- for $0 \leq \bar{\lambda} \leq .154$ $\quad P_u/P_y = 1.0$
- for $.154 < \bar{\lambda} \leq 2.0$ $\quad P_u/P_y = 1.065 - .423\bar{\lambda}$ (9.8)

Linear regression using yield strength of flats (scheme b)

- for $0 \leq \bar{\lambda} \leq .428$ $\quad P_u/P_y = 1.0$
- for $.428 < \bar{\lambda} \leq 2.0$ $\quad P_u/P_y = 1.225 - .526\bar{\lambda}$ (9.9)

9.5 Effect of Transverse Residual Stresses

It was assumed in Chapter 6 that yielding occurs when the total strain including the longitudinal residual strain equals the uniaxial yield strain (Eq. 6.43 and 6.45). In light of the results of Chapter 4, which reveals that the transverse residual stresses σ_θ^{res} are larger than the longitudinal residual stresses σ_z^{res}, this assumption needs to be reexamined.

Preliminary studies showed that the inclusion of the transverse residual stresses in the computations may lead to 5 to 15 percent reduction in the computed column strengths. Further more definitive studies are needed.

9.6 Closure

Column tests were described and their results compared with theoretical predictions. Agreement is satisfactory, except for the thinner channels (C14). The column data fall fairly closely along a straight line. The effect of transverse residual stresses deserve further attention.

TABLE 9.1a

PBC 14, GROUP 1: COLUMN TEST RESULTS

			EXPERIMENT		THEORY			
Column	L	L/R	V_o/L	P_u	V_t/L	P_{th}	A_e/A	Error
	inch		10^{-3}	kips	10^{-3}	kips	%	%
A 3	27.0	41.7	.21	20.20	.50	21.50	49.0	6.4
A 5	39.0	60.2	-.48	19.30	-1.0	20.75	47.4	7.5
A 9	57.0	88.0	-1.3	13.95	.50	15.14	81.7	8.5
A 11	69.0	106.5	-.78	11.20	.50	11.53	84.5	2.1
A 13	78.0	120.4	.33	10.50	-.05	10.62	99.3	1.1
A 14	89.0	137.3	-.24	8.20	.10	8.16	96.5	.5

Cross-sectional area $A = .538\ \text{in}^2$ Radius of gyration $R = .648$ in

A_e = area of part of cross-section that remains elastic when maximum theoretical load is attained.

V_t = midheight initial deflection used in computer program.

Column length includes end plates and end fixtures.

TABLE 9.1b

PBC 14, GROUP 1: NON-DIMENSIONALIZED COLUMN TEST RESULTS

Column	$\bar{\lambda}_f$	P_u/P_{yf}	$\bar{\lambda}_a$	P_u/P_{ya}
A 3	.482	.963	.517	.839
A 5	.696	.920	.746	.802
A 9	1.018	.665	1.090	.579
A 11	1.232	.534	1.320	.465
A 13	1.393	.501	1.492	.436
A 14	1.589	.391	1.703	.341

Yield strength of flat $\sigma_{yf} = 38.98$ ksi

Average yield strength of cross-section $\sigma_{ya} = 44.75$ ksi

$P_{yf} = A\sigma_{yf} = 20.97$ kips $\quad P_{ya} = A\sigma_{ya} = 24.08$ kips

$$\bar{\lambda}_f = \frac{1}{\pi}\sqrt{\frac{\sigma_{yf}}{E}}\,\frac{L}{R} \qquad \bar{\lambda}_a = \frac{1}{\pi}\sqrt{\frac{\sigma_{ya}}{E}}\,\frac{L}{R}$$

TABLE 9.2

PBC 14, GROUP 2: COLUMN TEST RESULTS

Column	L inch	V_o/L 10^{-3}	P_u kips	L/R	P_u/P_{yf}	$\overline{\lambda}_f$	P_u/P_{ya}	$\overline{\lambda}_a$
A 1	21.	.15	19.00	32.41	.906	.375	.789	.402
A 2	27.	1.6	16.90	41.67	.806	.482	.702	.517
A 4	33.	1.9	16.30	50.93	.777	.589	.677	.631
A 6	39.	.97	14.40	60.18	.687	.696	.598	.746
A 7	45.	-.08	13.50	69.44	.644	.803	.561	.861
A 8	51.	-.65	13.66	78.70	.651	.911	.567	.976
A 10	63.	-.10	10.45	97.22	.501	1.125	.436	1.205
A 12	75.	-1.5	9.50	115.7	.453	1.339	.394	1.435

For explanations of notations see Table 9.1.

TABLE 9.3a

RFC 14, GROUP 1: COLUMN TEST RESULTS

Column	L	L/R	V_o/L	P_u	V_t/L	P_{th}	A_e/A	Error	Remark
			EXPERIMENT			THEORY			
	inch		10^{-3}	kips	10^{-3}	kips	%	%	
B 2	27.0	41.7	.95	19.50	1.0	21.10	32.5	5.5	σ_y-5.
B 4	39.0	60.3	.66	18.00	1.0	19.36	53.4	7.6	σ_y-5.
B 5	51.0	78.8	-.38	16.00	-.5	16.62	78.8	3.7	σ_y-5.
B 6	51.0	78.8	-.66	15.50	-1.0	15.44	77.7	.39	σ_y-5.
B 9	80.5	124.4	-.83	8.80	-.25	9.27	97.9	5.3	
B 10	80.5	124.4	.35	8.00	-1.0	8.45	94.6	5.6	
B 11	84.9	131.2	.46	9.05	.10	8.65	99.3	4.4	

Notations are explained in Table 9.1a
Unless otherwise noted, theoretical strengths are based on yield strengths determined by tensile coupon test, specimen a, as reported in Table 3.8 and Fig. 3.9. (σ_y-5) means theoretical strengths are based on a yield strength which is everywhere lower by 5.0 ksi than for coupon a.

$A = .518 \text{ in}^2$, $R = .647$ in.

TABLE 9.3b

RFC 14, GROUP 1: NON-DIMENSIONALIZED COLUMN TEST RESULTS

Column	$\bar{\lambda}_f$	P_u/P_{yf}	$\bar{\lambda}_a$	P_u/P_{ya}
B 2	.516	.845	.535	.786
B 4	.745	.780	.773	.725
B 5	.975	.693	1.011	.645
B 6	.975	.672	1.011	.625
B 9	1.539	.381	1.596	.355
B 10	1.539	.347	1.596	.322
B 11	1.623	.392	1.683	.365

Notations are explained in Table 9.1b.
The actual values of yield strength of specimen a, Table 3.8 and Fig. 3.9, are used here, not σ_y-5. ksi.

$\sigma_{yf} = 44.54$ ksi, $\sigma_{ya} = 47.91$ ksi.

$P_{yf} = 23.07$ kips, $P_{ya} = 24.81$ kips.

TABLE 9.4

RFC 14, GROUP 2 COLUMN TEST RESULTS

Column	L inch	V_o/L 10^{-3}	P_u kips	L/R	P_u/P_{yf}	$\bar{\lambda}_f$	P_u/P_{ya}	$\bar{\lambda}_a$
B 1	27.0	1.0	18.50	41.73	.802	.516	.746	.535
B 3	39.0	1.5	16.30	60.28	.706	.745	.657	.773
B 7	51.0	1.8	14.00	78.82	.607	.975	.564	1.011
B 8	63.0	.12	11.50	97.37	.498	1.204	.463	1.249

P_{yf}, P_{ya}, $\bar{\lambda}_f$, $\bar{\lambda}_a$ based on σ_y of coupon a, Table 3.8.

TABLE 9.5a

PBC 13, GROUP 1: COLUMN TEST RESULTS

			EXPERIMENT		THEORY			
Column	L inch	L/R	V_o/L 10^{-3}	P_u kips	V_t/L 10^{-3}	P_{th} kips	A_e/A %	Error %
C 3	39.0	60.2	.72	26.40	-1.0	24.42	47.5	-7.5
C 4	51.0	78.7	.25	21.60	-.40	20.96	76.0	-3.1
C 5	63.0	97.2	-.74	15.85	+.50	15.76	80.8	-.57
C 6	82.0	126.5	-.25	9.95	.50	10.37	89.0	4.2
C 7	100.0	154.3	-.46	7.70	.10	7.79	96.3	1.2

$A = .640\ in^2$ $R = .648$ in

Notations are explained in Table 9.1a

TABLE 9.5b

PBC 13, GROUP 1: NON-DIMENSIONALIZED COLUMN TEST RESULTS

Column	$\bar{\lambda}_f$	P_u/P_{yf}	$\bar{\lambda}_a$	P_u/P_{ya}
C 3	.688	1.084	.742	.919
C 4	.890	.887	.970	.752
C 5	1.111	.651	1.199	.552
C 6	1.447	.409	1.560	.351
C 7	1.764	.316	1.903	.268

σ_{yf} = 38.05 ksi σ_{ya} = 44.26 ksi

P_{yf} = 24.35 k P_{ya} = 28.71 k

Notations are explained in Table 9.1b

TABLE 9.6

PBC 13, GROUP 2: COLUMN TEST RESULTS

Column	L	V_o/L	P_u	L/R	P_u/P_{yf}	$\bar{\lambda}_f$	P_u/P_{ya}	$\bar{\lambda}_a$
	inch	10^{-3}	kips					
C 1	27.0	-.10	35.00	41.7	1.437	.476	1.219	.514
C 2	27.0	.72	23.38	41.7	.960	.476	.814	.514

Notations are explained in Tables 9.1.

TABLE 9.7a

RFC 13, GROUP 1: COLUMN TEST RESULTS

			EXPERIMENT			THEORY		
Column	L	L/R	V_o/L	P_u	V_t/L	P_{th}	A_e/A	Error
	inch		10^{-3}	kips	10^{-3}	kips	%	%
D 6	39.0	60.2	-.14	29.50	.50	29.45	50.7	-.17
D 7	45.0	69.4	17.7	24.50	.50	22.92	54.2	-6.4
D 8	51.0	78.7	.83	23.00	.13	21.82	65.4	-5.1
D 9	57.0	88.0	1.7	20.00	-.10	18.99	83.0	-5.0
D 10	63.0	97.2	-1.1	16.00	-.15	16.53	89.3	3.3
D 11	69.0	106.5	.30	13.35	.35	14.14	86.8	5.9
D 12	75.0	115.7	-.62	12.20	-.35	12.07	93.5	-1.1
D 13	87.0	134.3		9.03	1.0	8.97	86.7	-.67

$A = .640 \text{ in}^2$ $R = .648 \text{ in}$

Notations are explained in Table 9.1a

All above initial deflections were measured by method 1.

TABLE 9.7b

RFC 13, GROUP 1: NON-DIMENSIONALIZED COLUMN TEST RESULTS

Column	$\bar{\lambda}_f$	P_u/P_{yf}	$\bar{\lambda}_a$	P_u/P_{ya}
D 6	.691	1.202	.742	1.041
D 7	.797	.998	.856	.865
D 8	.903	.937	.970	.812
D 9	1.009	.815	1.085	.706
D 10	1.116	.652	1.199	.565
D 11	1.222	.544	1.313	.471
D 12	1.328	.497	1.427	.431
D 13	1.541	.368	1.655	.319

$\sigma_{yf} = 38.34$ ksi $\sigma_{ya} = 44.27$ ksi $P_{yf} = 24.54$ k $P_{ya} = 28.32$ k

Notations are explained in Table 9.1b

TABLE 9.8

RFC 13, GROUP 2: COLUMN TEST RESULTS

Column	L inch	V_o/L 10^{-3}	P_u kips	L/R	P_u/P_{yf}	$\bar{\lambda}_f$	P_u/P_{ya}	$\bar{\lambda}_a$
D 1	19.25*		34.20	29.71	1.394	.341	1.208	.366
D 2	21.0**		17.00	32.41	.693	.372	.600	.400
D 3	27.0	.21	35.00	41.67	1.426	.478	1.236	.514
D 4	27.0	-4.1	22.30	41.67	.909	.478	.787	.514
D 5	33.0		34.50	50.93	1.406	.584	1.218	.628

*D 1 tested with knife edge fixtures, not the regular ones.

**D 2 failed by local buckling of web, near weld.

Notations are explained in Tables 9.1.

TABLE 9.9a

H 11, GROUP 1: COLUMN TEST RESULTS

			EXPERIMENT		THEORY			
Column	L inch	L/R	V_o/L 10^{-3}	P_u kips	V_t/L 10^{-3}	P_{th} kips	A_e/A %	Error %
E 1	19.4	51.2	3.4	18.50	1.0	19.26	67.1	4.1
E 3	28.0	73.9	1.9	18.20	.3	17.89	91.2	1.7
E 4	39.0	102.9	-.83	11.80	-.15	11.88	98.4	.67
E 5	51.0	134.6	-.48	7.00	-.25	6.96	97.2	-.57

$A = .442\ in^2$ $R = .379$ in

TABLE 9.9b

H 11, GROUP 1: NON-DIMENSIONALIZED COLUMN TEST RESULTS

Column	$\bar{\lambda}_f$	P_u/P_{yf}	$\bar{\lambda}_a$	P_u/P_{ya}
E 1	.621	.977	.682	.811
E 3	.896	.961	.984	.797
E 4	1.248	.623	1.370	.517
E 5	1.632	.370	1.792	.307

σ_{yf} = 42.83 ksi σ_{ya} = 51.62 ksi P_{yf} = 18.93 k P_{ya} = 22.85 k

TABLE 9.10

H 11, GROUP 2: COLUMN TEST RESULTS

Column	L	V_o/L	P_u	L/R	P_u/P_{yf}	$\bar{\lambda}_f$	P_u/P_{ya}	$\bar{\lambda}_a$
	inch	10^{-3}	kips					
E 2	23.0	.66	15.70	60.7	.829	.736	.687	.808

Notations are explained in Tables 9.1.

TABLE 9.11a

H 7 COLUMN TEST RESULTS

			EXPERIMENT			THEORY		
Column	L	L/R	V_o/L	P_u	V_t/L	P_{th}	A_e/A	Error
	inch			kips	10^{-3}	kips	%	%
F 1	31.0	53.9	-.75	45.00	-1.0	46.90	47.6	5.8
F 2	39.0	67.8	-.21	41.80	-.10	45.39	66.5	8.6
F 3	42.4	73.7	-.66	39.60	-.30	40.80	81.2	3.0
F 4	45.0	78.3	-.92	39.40	.50	39.99	84.5	1.5
F 5	51.0	88.7	.29	30.90	-.17	32.34	90.4	4.8

$A = .990\ in^2$ $R = 575\ in$

Notations are explained in Tables 9.1

TABLE 9.11b

H 7 NON-DIMENSIONALIZED COLUMN TEST RESULTS

Column	$\bar{\lambda}_f$	P_u/P_{yf}	$\bar{\lambda}_a$	P_u/P_{ya}
F 1	.667	1.021	.740	.829
F 2	.839	.948	.931	.770
F 3	.912	.698	1.012	.729
F 4	.968	.893	1.074	.726
F 5	1.097	.701	1.217	.569

$\sigma_{yf} = 44.54$ ksi $\sigma_{ya} = 54.85$ ksi $P_{yf} = 44.09$ k $P_{ya} = 54.31$ k

Notations are explained in Tables 9.1.

TABLE 9.12a

H T COLUMN TEST RESULTS

Column	L	L/R	V_o/L	P_u	V_t/L	P_{th}	A_e/A	Error
	inch		10^{-3}	kips	10^{-3}	kips	%	%
G 1	27.9	47.6	-.17	97.40	-.50	96.72	54.2	.7
G 2	39.0	66.5	-.57	78.00	-.50	85.26	76.6	9.3
G 3	51.0	87.0	.26	65.80	.40	65.61	97.4	-.29
G 4	65.4	111.6	-.15	42.75	.10	43.16	98.8	1.0
G 5	71.0	121.2	.30	35.40	.17	36.40	100.	2.7

$A = 1.97\ in^2$ $R = .586\ in$

Notations are explained in Tables 9.1.

TABLE 9.12b

H T NON-DIMENSIONALIZED COLUMN TEST RESULTS

Column	$\bar{\lambda}_f$	P_u/P_{yf}	$\bar{\lambda}_a$	P_u/P_{ya}
G 1	.672	.898	.687	.858
G 2	.939	.719	.961	.687
G 3	1.228	.607	1.256	.580
G 4	1.575	.394	1.611	.377
G 5	1.710	.326	1.749	.312

$\sigma_{yf} = 58.00$ ksi $\sigma_{ya} = 60.69$ ksi $P_{yf} = 108.46$ k $P_{ya} = 113.5$ k

Notations are explained in Tables 9.1.

TABLE 9.13

LEAST SQUARE REGRESSION ON COLUMN DATA

Data Base	Yield Strength	Ordinary or General	Model $\hat{Y}$ =	Corr. Coeff.	Origin
a)80	Average	OLS	1.090 - .437X	-.886	Dat's column tests
b)75	"	"	1.065 - .423X	-.936	Exclude C1,D1,D2,D3,D5
c)55	"	"	1.069 - .427X	-.885	Exclude stubs also
d)92	"	"	1.096 - .427X	-.906	Dat's 75 + Karren's 17
e)70	"	"	1.150 - .472X	-.864	Dat + Karren - stubs
f)92	"	GLS	1.088 - .433X	-.967	Dat's 75 + Karren's 17
a)80	Flat	OLS	1.255 - .543X	-.877	Dat's column tests
b)75	"	"	1.225 - .526X	-.926	Exclude C1,D1,D2,D3,D5
c)55	"	"	1.225 - .525X	-.872	Exclude stubs also
d)92	"	"	1.241 - .520X	-.913	Dat's 75 + Karren's 17
e)70	"	"	1.275 - .551X	-.867	Dat + Karren - stubs
f)92	"	GLS	1.241 - .531X	-.929	Dat's 75 + Karren's 17

Note: $X = \bar{\lambda} = \frac{1}{\pi}\sqrt{\frac{\sigma_y}{E}}\frac{L}{R}$, $\hat{Y} = \frac{P_u}{A\sigma_y}$

σ_y may be the yield strength of the flat or the average yield strength.

Column data are gathered from Tables 7.2, 9.1b, 9.2, 9.3b, 9.4, 9.5b, 9.6 9.7b, 9.8, 9.9b, 9.10, 9.11b, 9.12b and 9.26

TABLE 9.14

ANOVA USING AVERAGE YIELD STRENGTH

DAT'S 80 DATA POINTS

Model $\hat{Y} = 1.090 - .437\ X$

Correlation coefficient $R = -.886$

ANOVA

Source	Sum of Squares	Degrees of Freedom	Mean Square
Regression (b_o)	44.10	1	
Regression ($b_1 \mid b_o$)	4.256	1	$MS_R = 2.063^2$
Residual	1.169	78	$s^2 = .0150$
Total, uncorrected for mean	49.52	80	

Estimated standard error of slope b_1 .0259

95% confidence interval for slope $-.488 < b_1 < -.385$

Estimated standard error of intercept b_o .0248

95% confidence interval for intercept $1.041 < b_o < 1.139$

Define U1 = actual $Y/\hat{Y}$

U2 = actual Y/SSRCO(X)

where $$\begin{aligned} \text{SSRCO}(X) &= 1 - X^2/4 \quad \text{for } X \leq \sqrt{2} \\ &= 1/X^2 \quad \text{for } X < \sqrt{2} \end{aligned}$$

represents the present design curve of the SSRC. Then

	Mean	Variance	Standard Deviation	Coefficient of Variation
U1	.997	.0232	.152	.153
U2	.943	.0209	.144	.153

TABLE 9.15

ANOVA USING AVERAGE YIELD STRENGTH

DAT'S 75 DATA POINTS (ALL EXCEPT C1,D1,D2,D3,D5)

Model $\hat{Y} = 1.065 - .423\,X'$

Correlation coefficient R = -.936

ANOVA

Source	Sum of Squares	Degrees of Freedom	Mean Square
Regression (b_o)	38.76	1	
Regression ($b_1 \| b_o$)	3.901	1	$MS_R = 1.975^2$
Residual	.549	73	$s^2 = .00752$
Total, uncorrected for mean	43.21	75	

Estimated standard error of slope (b_1)	.0186
95% confidence interval for slope	$-.460 < b_1 < -.386$
Estimated standard error of intercept (b_o)	.0182
95% confidence interval for intercept	$1.028 < b_o < 1.101$

Closest point to Euler curve: X = 1.70, $\hat{Y}$ = Euler = .346

	Mean	Variance	Standard Deviation	Coefficient of Variation
U1	.998	.0142	.119	.119
U2	.928	.0134	.116	.125

U1 and U2 are defined in Table 9.14

TABLE 9.16

ANOVA USING AVERAGE YIELD STRENGTH

55 DATA POINTS (DAT'S 75 - STUBS)

Model $\hat{Y} = 1.069 - .427\ X$

Correlation coefficient R = -.885

ANOVA

Source	Sum of Squares	Degrees of Freedom	Mean Square
Regression (b_o)	20.58	1	
Regression ($b_1 \mid b_o$)	1.525	1	$MS_R = 1.235^2$
Residual	.424	53	$s^2 = .00799$
Total, uncorrected for mean	22.53	55	

Estimated standard error of slope b_1	.0309
95% confidence interval for slope	$-.489 \leq b_1 \leq -.365$
Estimated standard error of intercept b_o	.0353
95% confidence interval for intercept	$.999 \leq b_o \leq 1.140$

Closest point to Euler curve: $X = 1.70$, $\hat{Y} = .343$, Euler = .346

	Mean	Variance	Standard Deviation	Coefficient of Variation
U1	.997	.0170	.131	.131
U2	.895	.0119	.109	.122

U1 and U2 are defined in Table 9.14

TABLE 9.17

ANOVA USING AVERAGE YIELD STRENGTH

92 DATA POINTS (DAT'S 75 + KARREN'S 17)

Model $\hat{Y} = 1.096 - .427\ X$

Correlation coefficient $R = -.906$

ANOVA

Source	Sum of Squares	Degrees of Freedom	Mean Square
Regression (b_o)	52.40	1	
Regression ($b_1 \mid b_o$)	4.286	1	$MS_R = 2.070^2$
Residual	.930	90	$s^2 = .0103$
Total, uncorrected for mean	57.62	92	

Estimated standard error of slope b_1	.0210
95% confidence interval for slope	$-.469 \leq b_1 \leq -.385$
Estimated standard error of intercept b_o	.0198
95% confidence interval for intercept	$1.057 \leq b_o \leq 1.136$

Closest point to Euler curve: $X = 1.444$, $\hat{Y}$ = Euler = .479

	Mean	Variance	Standard Deviation	Coefficient of Variation
U1	.995	.0192	.139	.139
U2	.956	.0153	.124	.130

U1 and U2 are defined in Table 9.14

TABLE 9.18

ANOVA USING AVERAGE YIELD STRENGTH

70 DATA POINTS (DAT'S 55 + KARREN'S 15. NO STUBS)

Model $\hat{Y} = 1.150 - .472\,X$

Correlation coefficient $R = -.864$

ANOVA

Source	Sum of Squares	Degrees of Freedom	Mean Square
Regression (b_o)	31.410	1	
Regression ($b_1 \mid b_o$)	2.200	1	$MS_R = 1.483^2$
Residual	.745	68	$s^2 = .0109$
Total, uncorrected for mean	34.355	70	

Estimated standard error of slope b_1	.0333
95% confidence interval for slope	$-.539 \leq b_1 \leq -.406$
Estimated standard error of intercept b_o	.0361
95% confidence interval for intercept	$1.078 \leq b_o \leq 1.222$

	Mean	Variance	Standard Deviation	Coefficient of Variation
U1	.997	.0208	.144	.144
U2	.933	.0157	.125	.134

U1 and U2 are defined in Table 9.14

TABLE 9.19

WEIGHTED LEAST SQUARES AND ANOVA

USING AVERAGE YIELD STRENGTH

Assumed standard error

$$s(X) = -.07\ X^2 + .12\ X + .04$$

Transformed Variables $X/s = X'$ $Y/s = Y'$

Model $Y' = 1.088 - .433\ X'$

Multiple Correlation Coefficient $R^2 = .935$ or $R = -.967$

Variance-Covariance Matrix of Parameters $= \begin{pmatrix} 2.040 \times 10^{-4} & -1.353 \times 10^{-4} \\ -1.353 \times 10^{-4} & 1.369 \times 10^{-4} \end{pmatrix}$

Source	Sum of Squares	Degrees of Freedom	Mean Square
SS (b_o)	1.134×10^4	1	1.134×10^4
SS $(b_1 \vert b_o)$	2.325×10^3	1	2.325×10^3
Residual SS	1.624×10^2	90	$s^2 = 1.805 = 1.343^2$
Total SS	1.383×10^4	92	

Standard error of slope s.e.(b_1) = .0117

Standard error of intercept s.e. (b_o) = .0143

	Mean	Variance	Standard Deviation	Coefficient of Variation
U1	1.016	.0194	.139	.137
U2	.956	.0153	.124	.130

U1 and U2 are defined in Table 9.14

TABLE 9.20

ANOVA USING YIELD STRENGTH OF FLAT

DAT'S 80 DATA POINTS

Model $\hat{Y} = 1.255 - .543\ X$

Correlation coefficient $R = -.877$

ANOVA

Source	Sum of Squares	Degrees of Freedom	Mean Square
Regression (b_o)	57.84	1	
Regression $(b_1\|b_o)$	5.848	1	$MS_R = 2.418^2$
Residual	1.750	78	$s^2 = .0224$
Total, uncorrected for mean	65.44	80	

Estimated standard error of slope b_1	.0336
95% confidence interval for slope	$-.610 < b_1 < -.476$
Estimated standard error of intercept b_o	.0302
95% confidence interval for intercept	$1.195 < b_o < 1.316$

	Mean	Variance	Standard Deviation	Coefficient of Variation
U1	.997	.0261	.161	.162
U2	1.038	.0360	.190	.183

U1 and U2 are defined in Table 9.14

TABLE 9.21

ANOVA USING YIELD STRENGTH OF FLAT

DAT'S 75 DATA POINTS (ALL EXCEPT C1,D1,D2,D3,D5)

Model $\hat{Y} = 1.225 - .526\ X$

Correlation coefficient $R = -.926$

ANOVA

Source	Sum of Squares	Degrees of Freedom	Mean Square
Regression (b_o)	50.71	1	
Regression ($b_1 \mid b_o$)	5.344	1	$MS_R = 2.312^2$
Residual	.890	73	$s^2 = .0122$
Total, uncorrected for mean	56.95	75	

Estimated standard error of slope b_1	.0251
95% confidence interval for slope	$-.576 < b_1 < -.476$
Estimated standard error of intercept b_o	.0231
95% confidence interval for intercept	$1.179 < b_o < 1.271$

Closest point to Euler curve: $X = 1.55$, $\hat{Y} = .410$, Euler = .416

	Mean	Variance	Standard Deviation	Coefficient of Variation
U1	.998	.0168	.130	.130
U2	1.018	.0249	.158	.155

U1 and U2 are defined in Table 9.14.

TABLE 9.22

ANOVA USING YIELD STRENGTH OF FLAT

55 DATA POINTS (DAT'S 75 - STUBS)

Model $\hat{Y} = 1.225 - .525 X$

Correlation coefficient R = -.872

ANOVA

Source	Sum of Squares	Degrees of Freedom	Mean Square
Regression (b_o)	26.69	1	
Regression ($b_1 \mid b_o$)	2.078	1	$MS_R = 1.441^2$
Residual	.655	53	$s^2 = .0124$
Total, uncorrected for mean	29.42	55	

Estimated standard error of slope b_1	.0405
95% confidence interval for slope	$-.606 \leq b_1 \leq -.445$
Estimated standard error of intercept b_o	.0434
95% confidence interval for intercept	$1.138 \leq b_o \leq 1.311$

	Mean	Variance	Standard Deviation	Coefficient of Variation
U1	.998	.0198	.141	.141
U2	.962	.0177	.133	.138

U1 and U2 are defined in Table 9.14

TABLE 9.23

ANOVA USING YIELD STRENGTH OF FLAT

92 DATA POINTS (DAT'S 75 + KARREN'S 17)

Model $\hat{Y} = 1.241 - .520\ X$

Correlation coefficient $R = -.913$

ANOVA

Source	Sum of Squares	Degrees of Freedom	Mean Square
Regression (b_o)	66.25	1	
Regression ($b_1 \mid b_o$)	5.655	1	$MS_R = 2.378^2$
Residual	1.124	90	$s^2 = .0125$
Total, uncorrected for mean	73.03		

Estimated standard error of slope b_1	.0244
95% confidence interval for slope	$-.569 \leq b_1 \leq -.471$
Estimated standard error of intercept b_o	.0218
95% confidence interval for intercept	$1.198 \leq b_o \leq 1.285$

Closest point to Euler curve $X = 1.777$ $\hat{Y}$ = Euler = .3167

	Mean	Variance	Standard Deviation	Coefficient of Variation
U1	.996	.0179	.134	.134
U2	1.038	.0230	.152	.146

U1 and U2 are defined in Table 9.14.

TABLE 9.24

ANOVA USING YIELD STRENGTH OF FLAT

70 DATA POINTS (DAT'S 55 + KARREN'S 15. NO STUBS)

Model $\hat{Y} = 1.275 - .551\ X$

Correlation coefficient R = -.867

ANOVA

Source	Sum of Squares	Degrees of Freedom	Mean Square
Regression (b_o)	39.086	1	
Regression ($b_1 \mid b_o$)	2.650	1	$MS_R = 1.628^2$
Residual	.873	68	$s^2 = .0128$
Total, uncorrected for mean	42.609	70	

Estimated standard error of slope b_1	.0384
95% confidence interval for slope	$-.628 \leq b_1 \leq -.475$
Estimated standard error of intercept	.0392
95% confidence interval for intercept	$1.197 \leq b_o \leq 1.354$

	Mean	Variance	Standard Deviation	Coefficient of Variation
U1	.997	.0199	.141	.141
U2	.996	.0190	.138	.138

U1 and U2 are defined in Table 9.14

TABLE 9.25

WEIGHTED LEAST SQUARES AND ANOVA

USING YIELD STRENGTH OF FLAT

92 DATA POINTS (DAT'S 75 + KARREN'S 17)

Assumed standard deviation

$$s(X) = -.069\ X^2 + .097\ X + .066$$

Transformed Variables $\quad X/s = X' \qquad Y/s = Y'$

Model $\quad Y' = 1.241 - .531\ X'$

Multiple Correlation Coefficient $\quad R^2 = .864$ or $R = -.929$

$$\text{Variance-Covariance Matrix of Parameters} = \begin{pmatrix} 3.335 \times 10^{-4} & -2.414 \times 10^{-4} \\ -2.414 \times 10^{-4} & 2.402 \times 10^{-4} \end{pmatrix}$$

Source	Sum of Squares	Degrees of Freedom	Mean Square
SS (b_o)	9.669×10^3	1	9.669×10^3
SS $(b_1 \mid b_o)$	9.007×10^2	1	9.007×10^2
Residual SS	1.423×10^2	90	$s^2 = 1.581 = 1.257^2$
Total SS	1.071×10^4	92	

Standard error of slope s.e. $(b_1) = 1.550 \times 10^{-2}$

Standard error of intercept s.e. $(b_o) = 1.826 \times 10^{-2}$

	Mean	Variance	Standard Deviation	Coefficient of Variation
U1	1.010	.0179	.134	.133
U2	1.038	.0230	.152	.146

U1 and U2 are defined in Table 9.14

TABLE 9.26

KARREN'S COLUMN TEST RESULTS
HOT-ROLLED SEMI-KILLED DOUBLE
HATS AND DOUBLE CHANNELS
(KARREN [1967])

Section	Specimen	P_u/P_{yf}	$\bar{\lambda}_f$	P_u/P_{ya}	$\bar{\lambda}_a$	Bolted or Riveted
Double Channel	Stub	1.224	.0700	1.167	.0717	
HRSK 10-37.0	CT 1	1.048	.460	1.000	.471	B
σ_{yf} = 45.6 ksi	2	1.017	.576	.971	.589	B
σ_{ya} = 47.8 ksi	3	1.001	.691	.960	.707	B
	4	.947	.806	.904	.825	B
	5	.960	.806	.916	.825	B
	6	.960	.922	.916	.944	B
	7	.945	.806	.902	.825	R
	8	.862	1.108	.822	1.134	R
Double Hat	Stub	1.184	.112	1.108	.115	
HRSK 9-30.7	CT 9	1.015	.532	.950	.550	B
σ_{yf} = 46.8 ksi	10	.914	.758	.856	.784	B
σ_{ya} = 50.0 ksi	11	.726	.967	.680	1.000	B
	12	.731	1.160	.684	1.199	R
	13	.880	.980	.824	1.013	R
	14	.968	.739	.906	.764	R
	15	1.017	.498	.952	.515	R

Effective length of stubs was taken as 0.6 * total length, assuming milled ends nearly fixed.

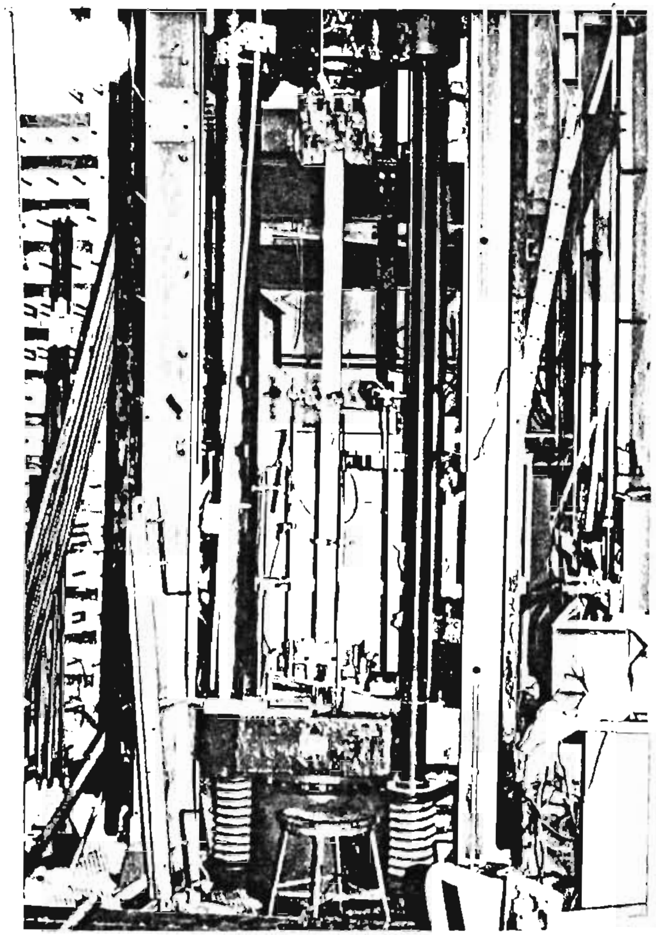

Photo 9.1 Long Column Test: General Set-up

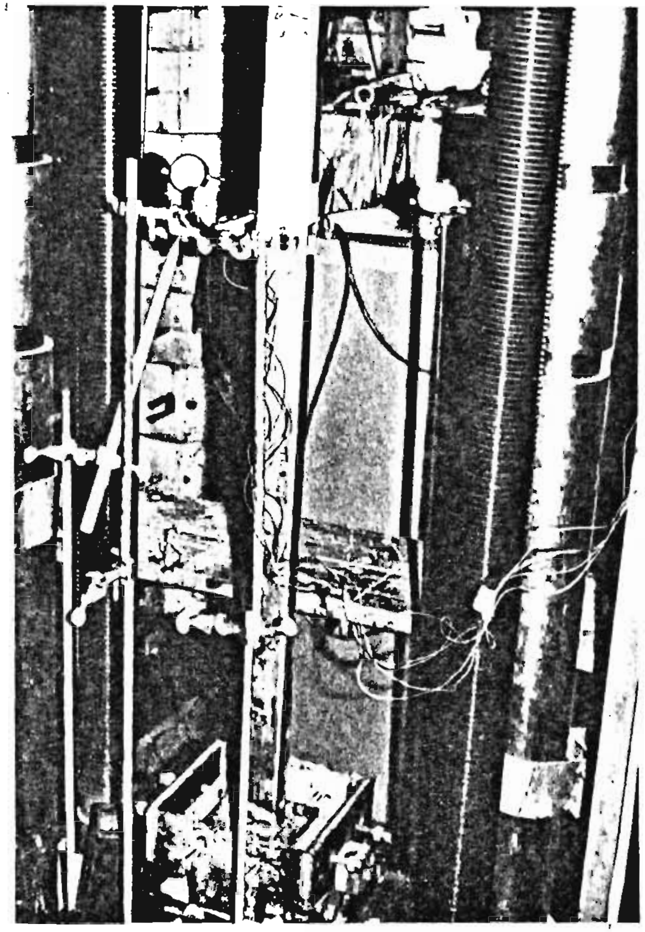

Photo 9.2 Long Column Test: Detail

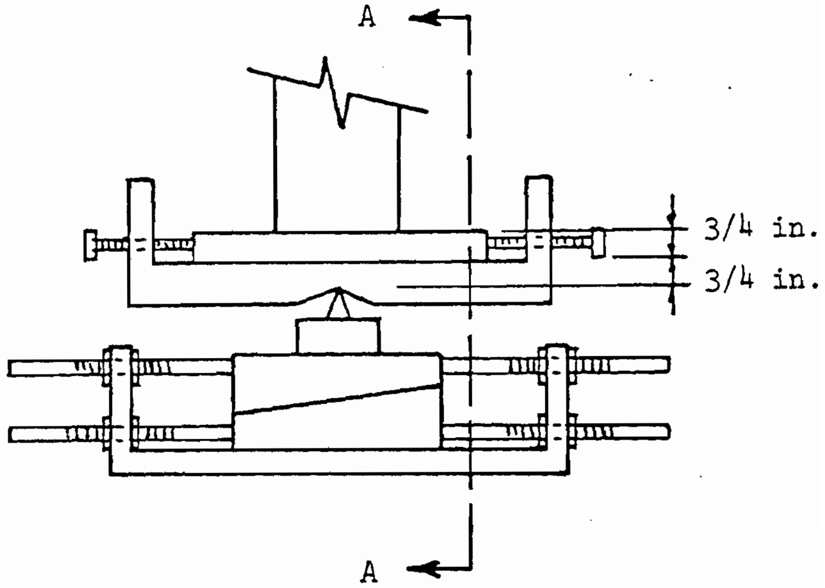

(a) Section Through Support in
Direction of Flexural Buckling

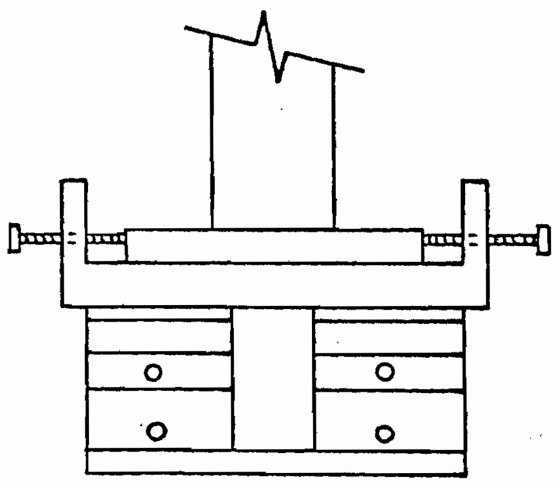

(b) Section A-A

Fig. 9.1 End Fixture for Column Tests
(from Peköz [1967])

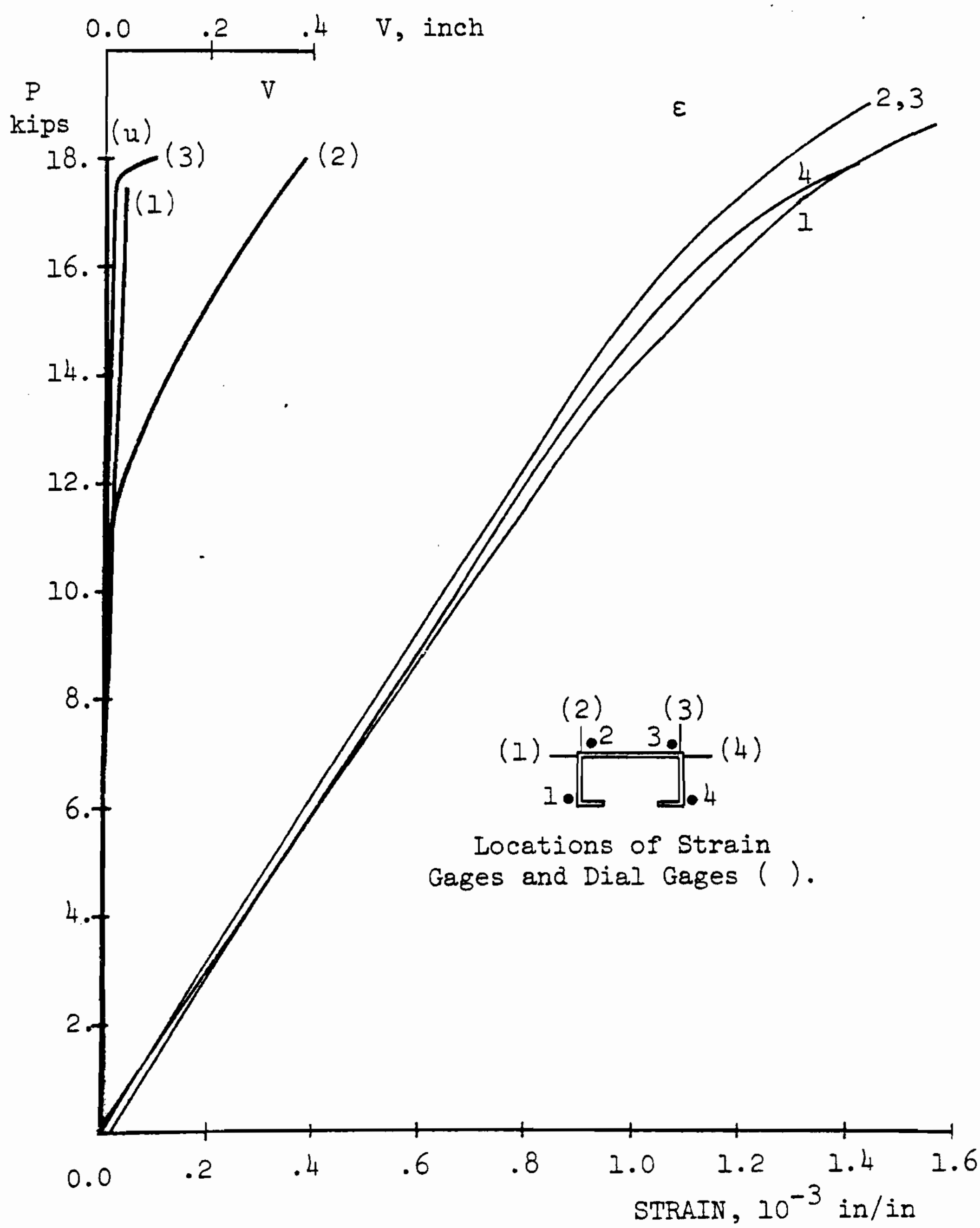

Fig. 9.2 PBC 14 Column A1, L = 18.0".

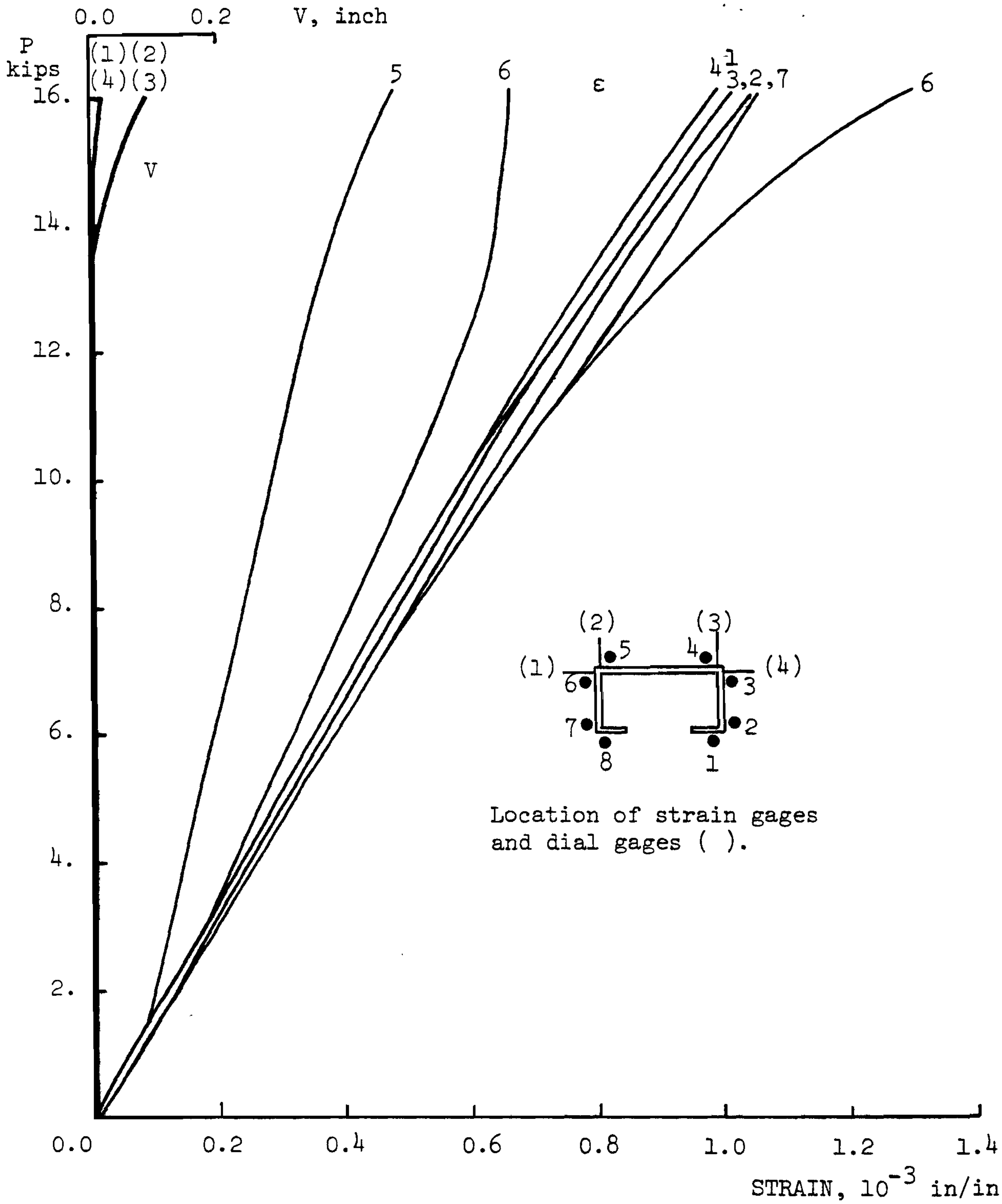

Fig. 9.3 PBC 14 Column A2, L = 27.0".

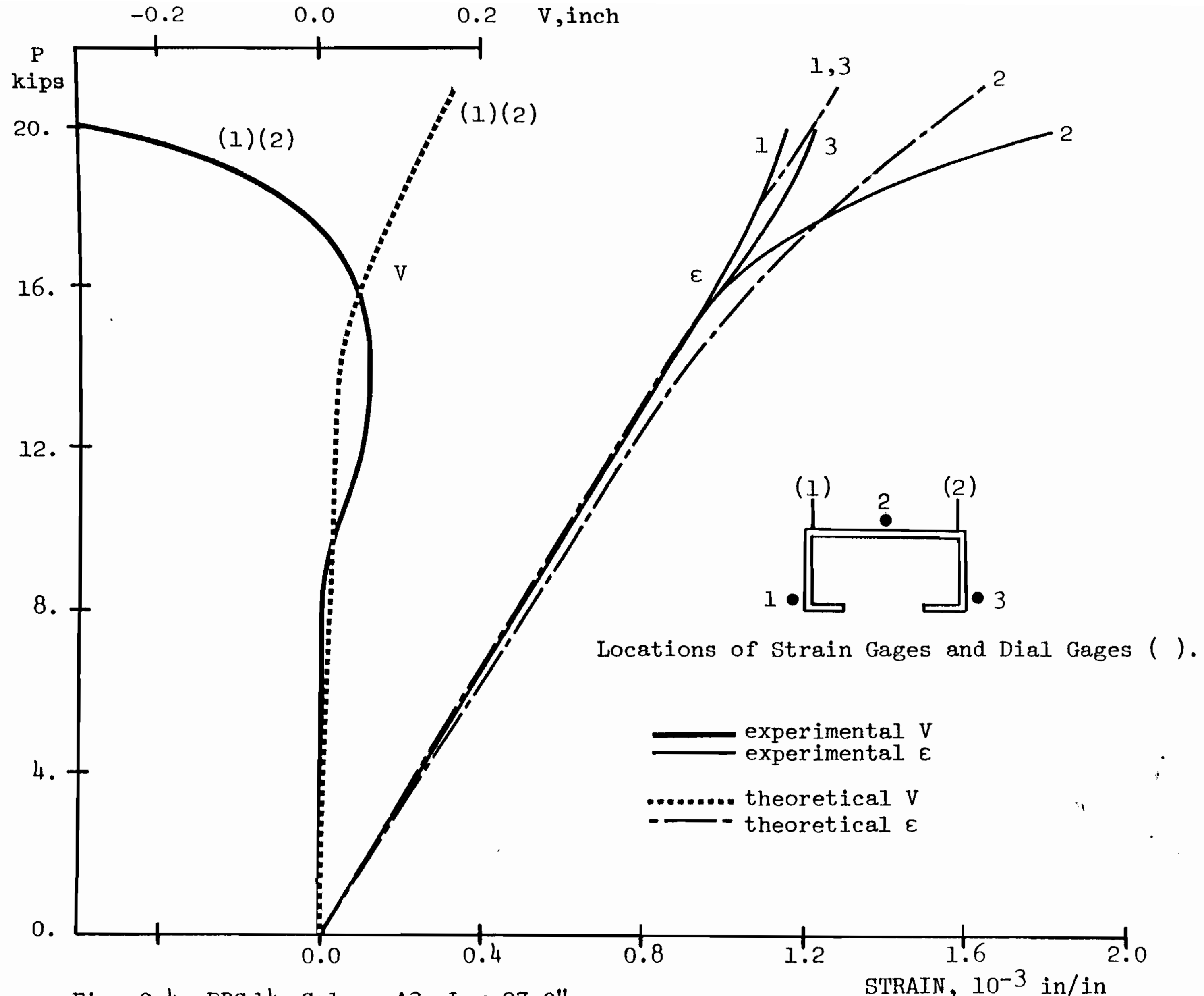

Fig. 9.4 PBC 14 Column A3, L = 27.0"

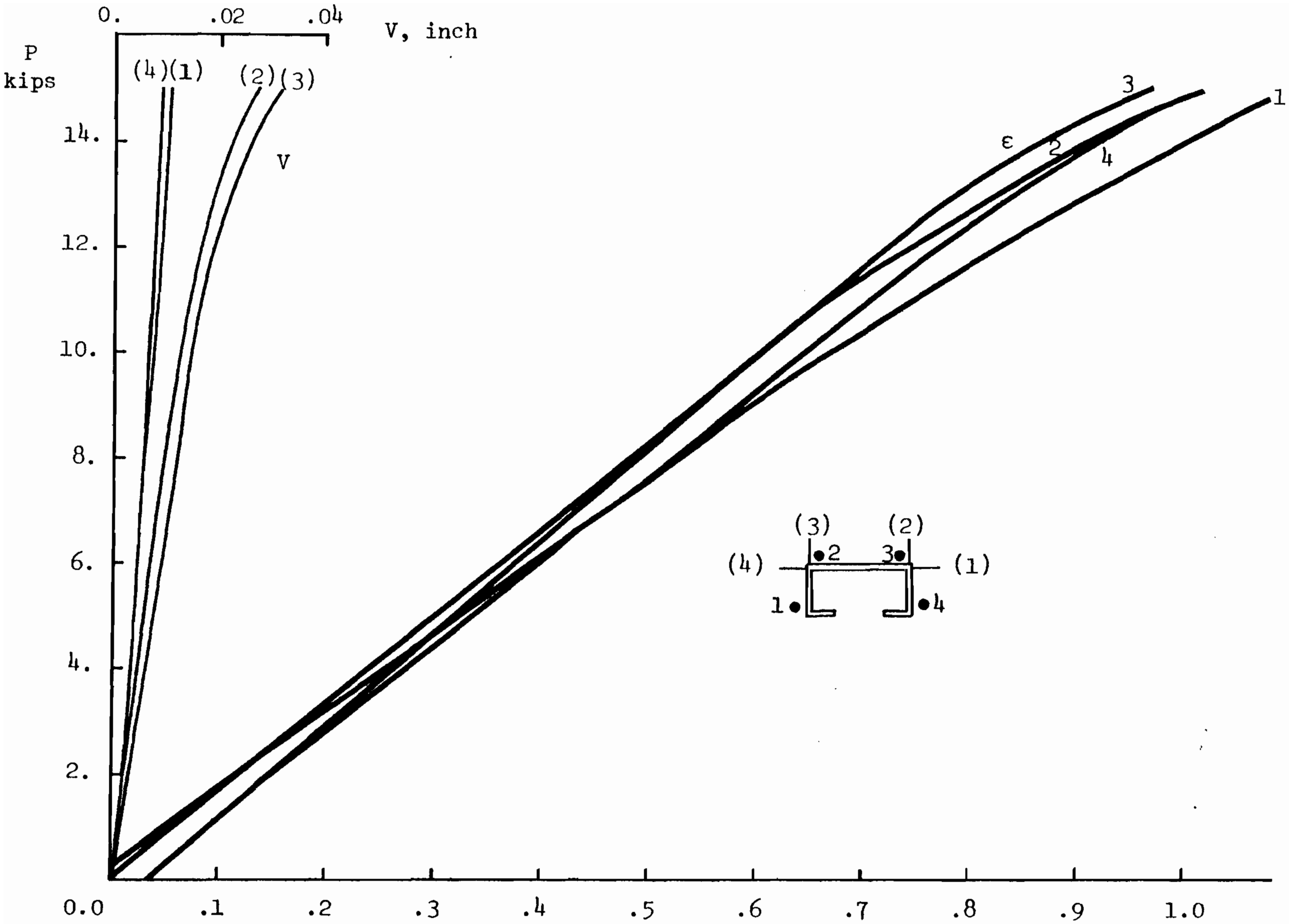

Fig. 9.5 PBC 14 Column A4, L = 33.0".

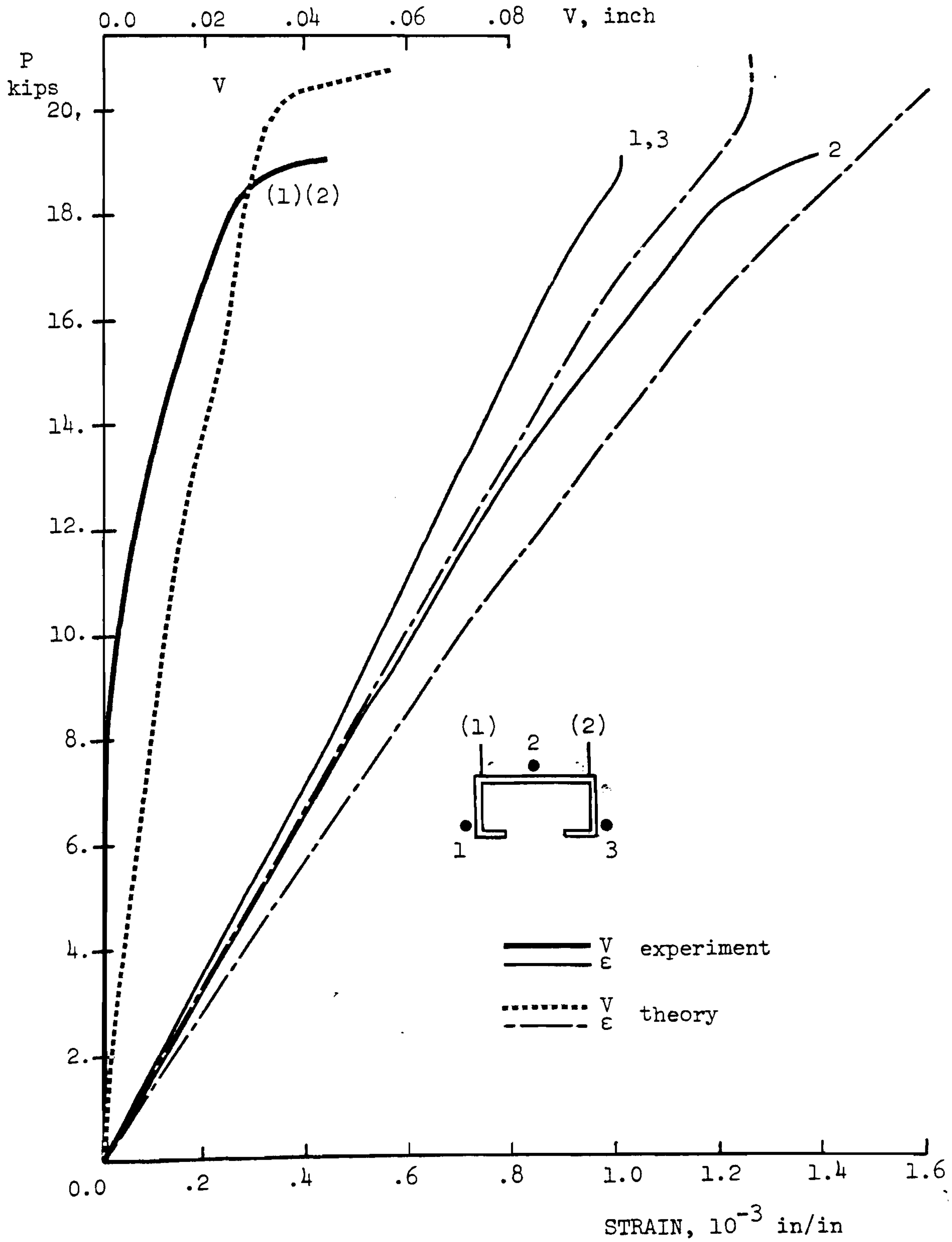

Fig. 9.6 Column A5, L = 39.0"

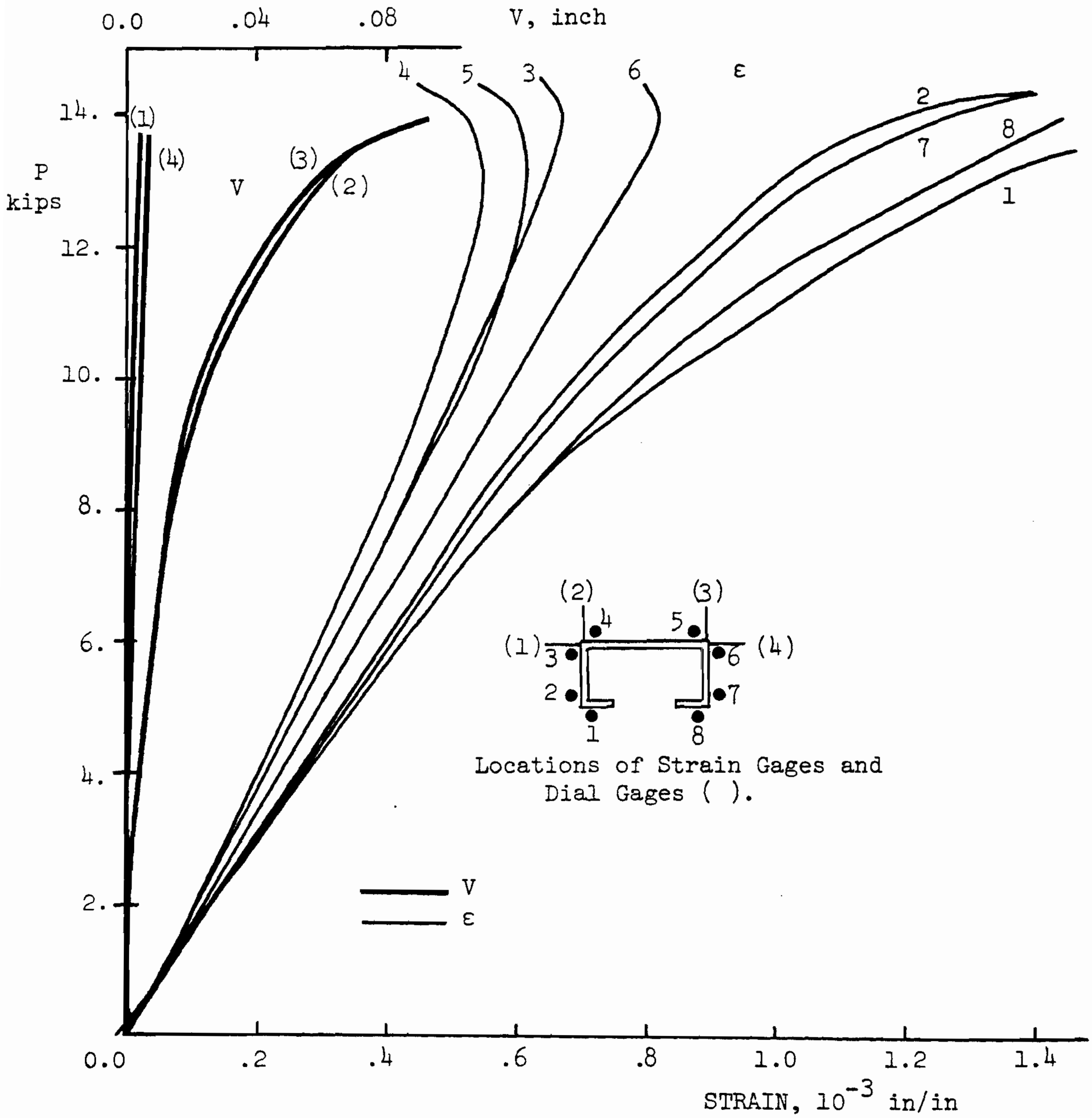

Fig. 9.7 PBC 14 Column A6, L = 39.0".

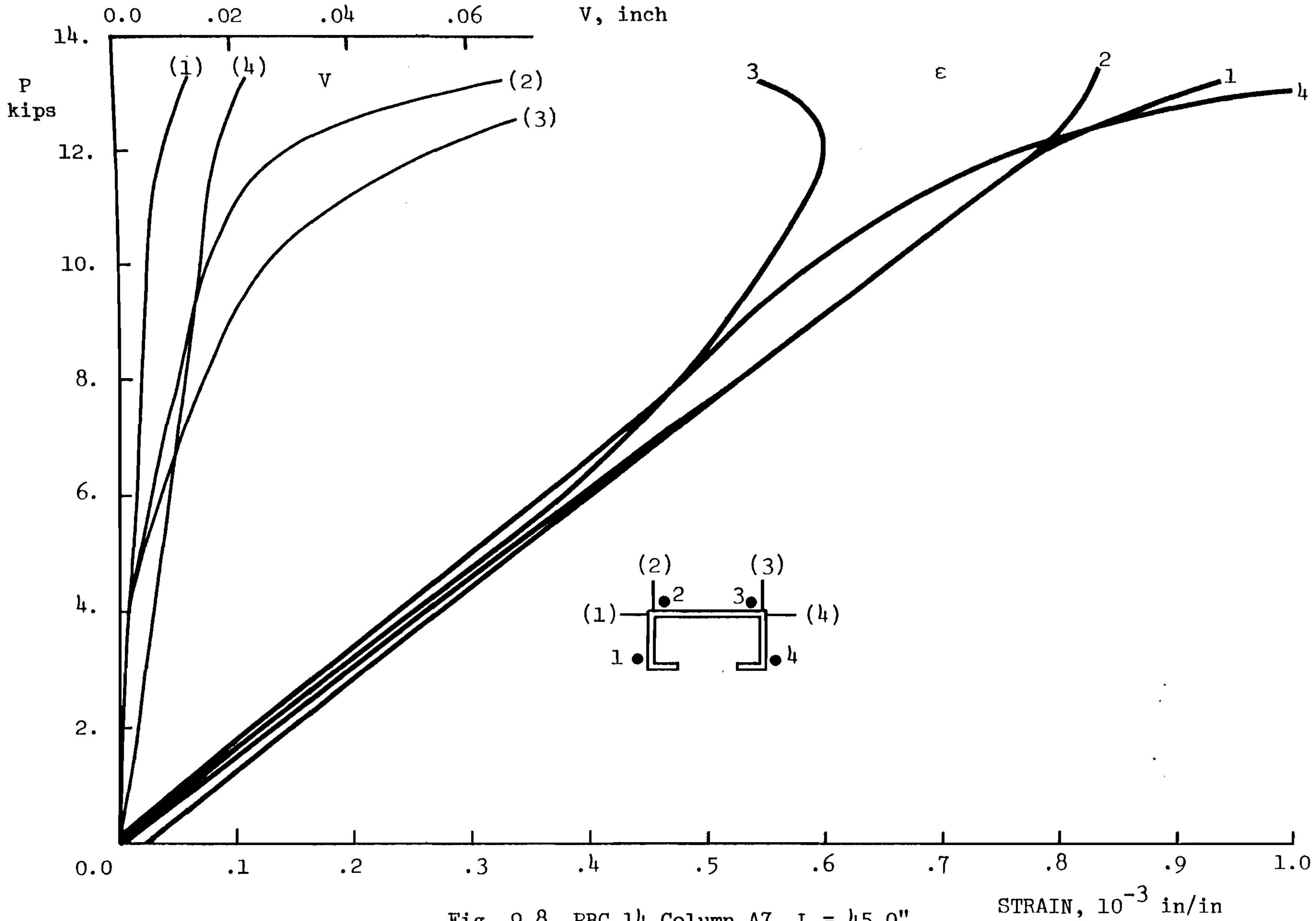

Fig. 9.8 PBC 14 Column A7, L = 45.0".

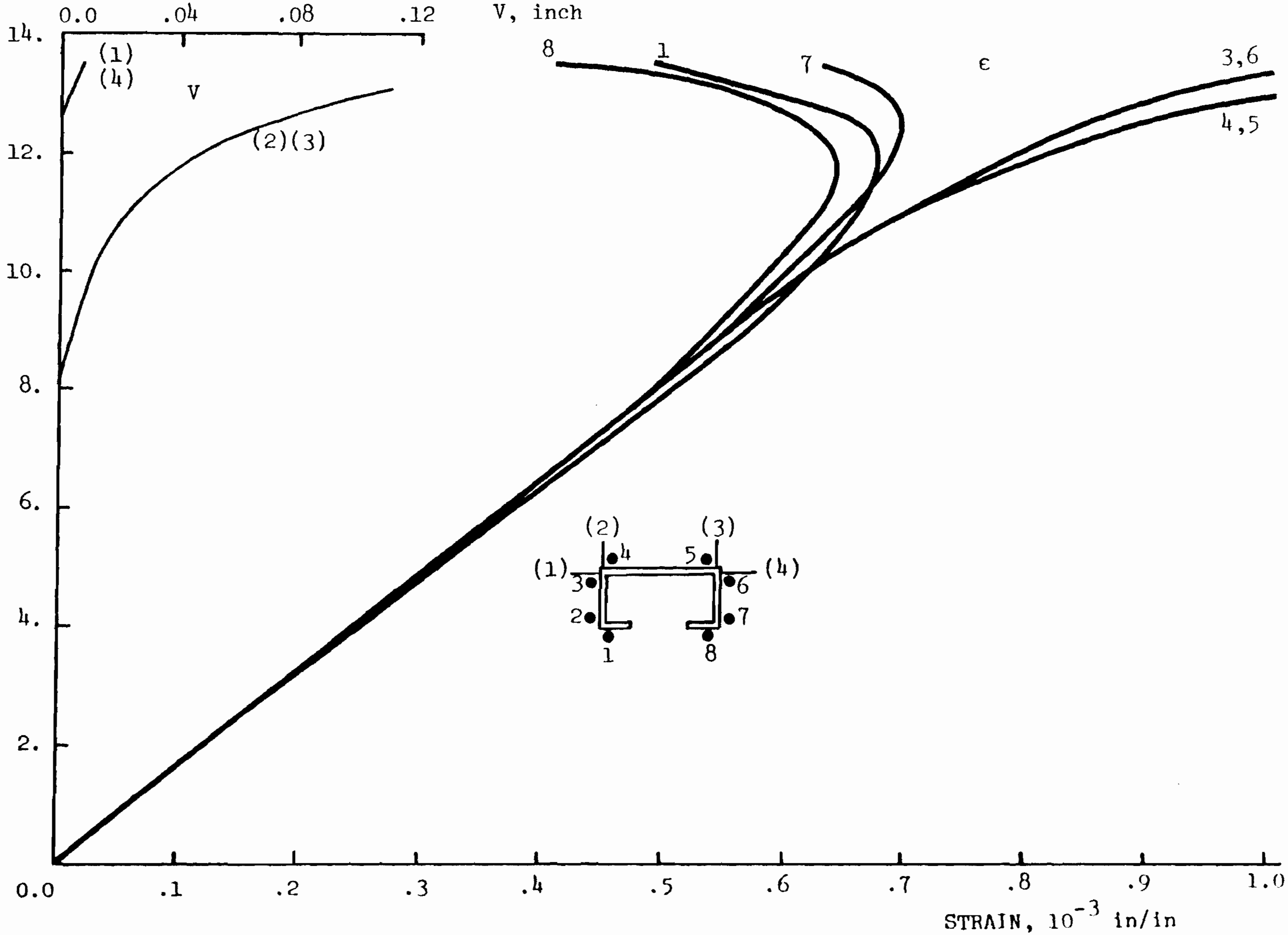

Fig. 9.9 PBC 14 Column A8, L = 51.0".

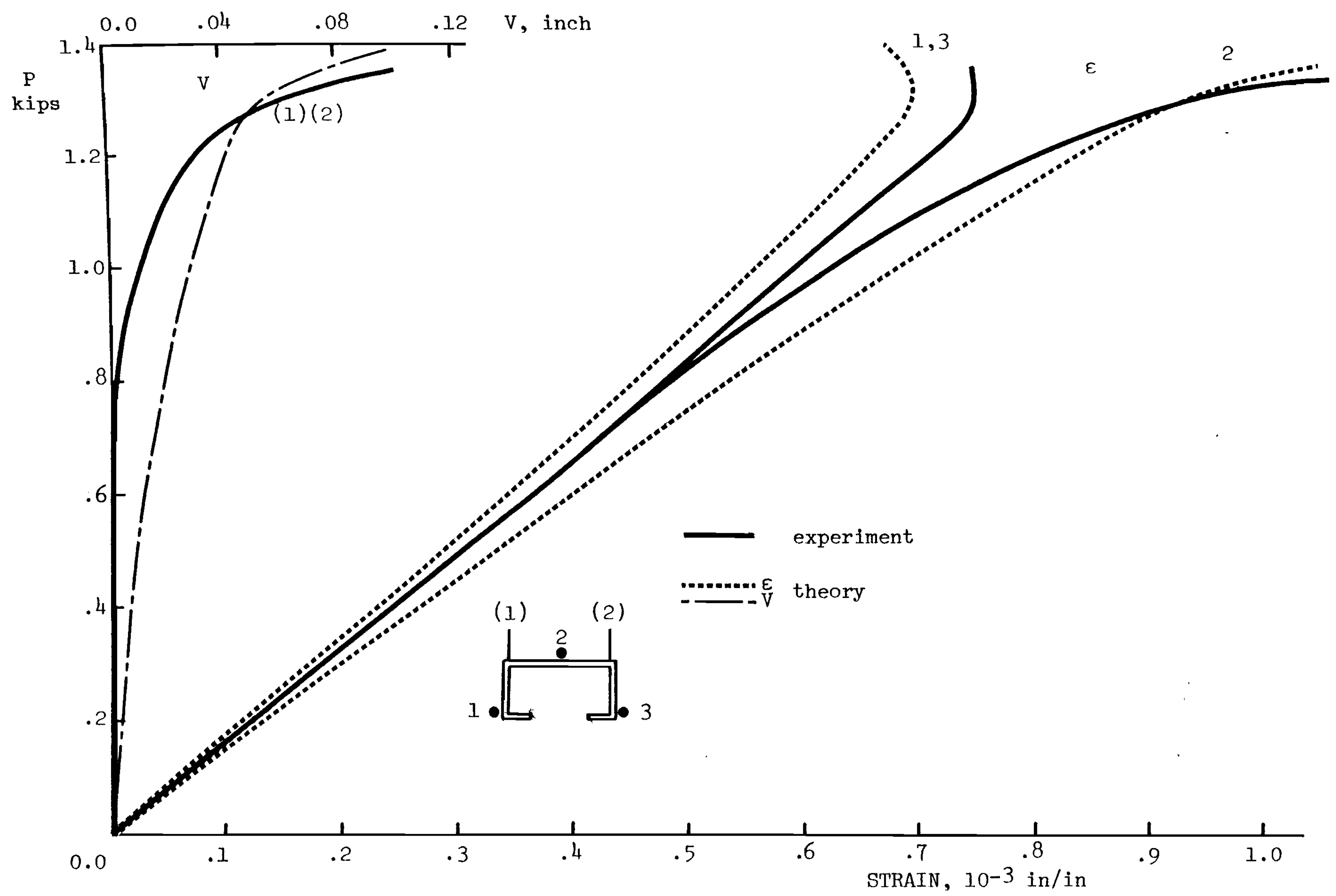

Fig. 9.10 PBC 14 Column A9, L = 57.0".

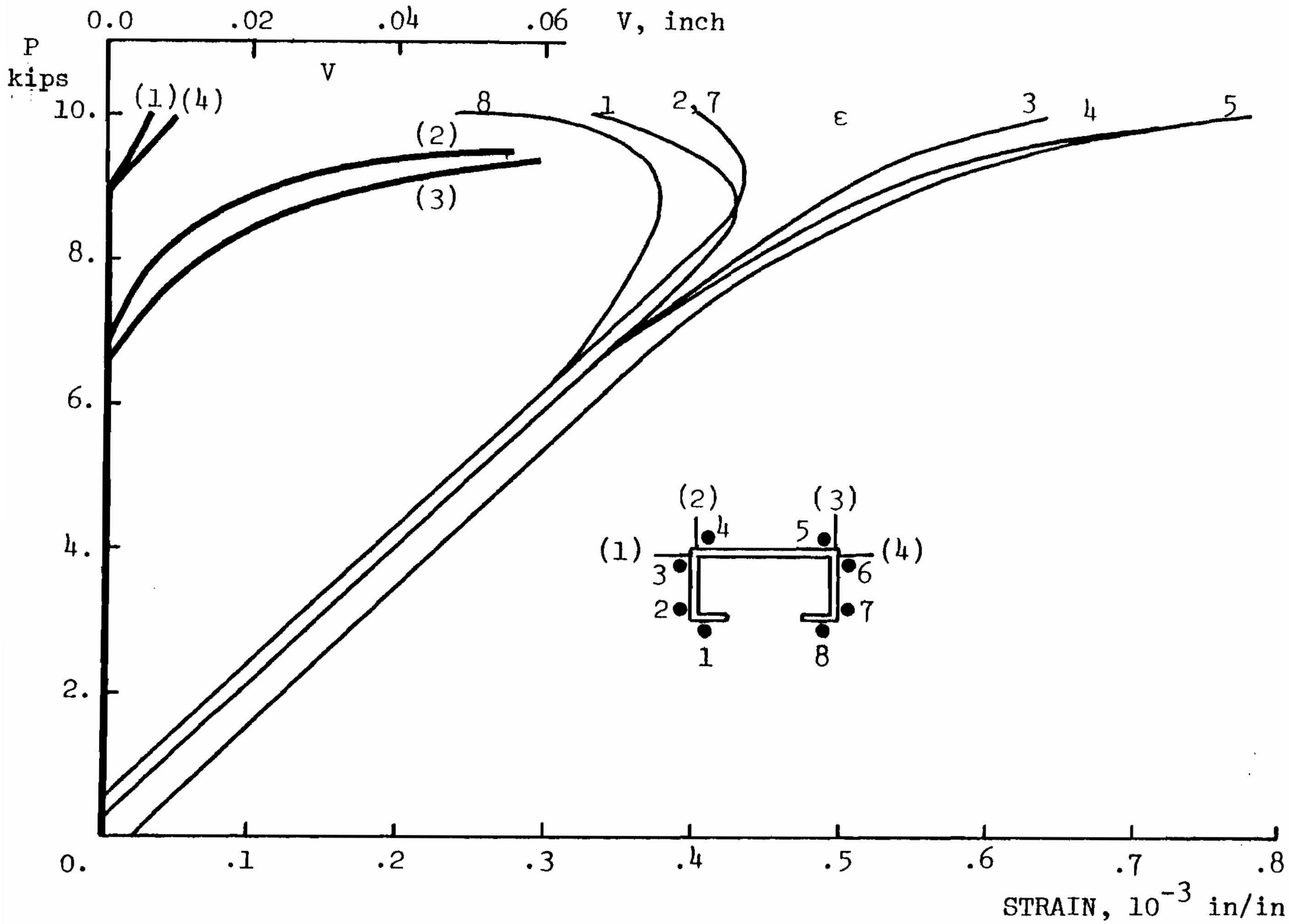

Fig. 9.11 PBC 14 Column A10, L = 63.0".

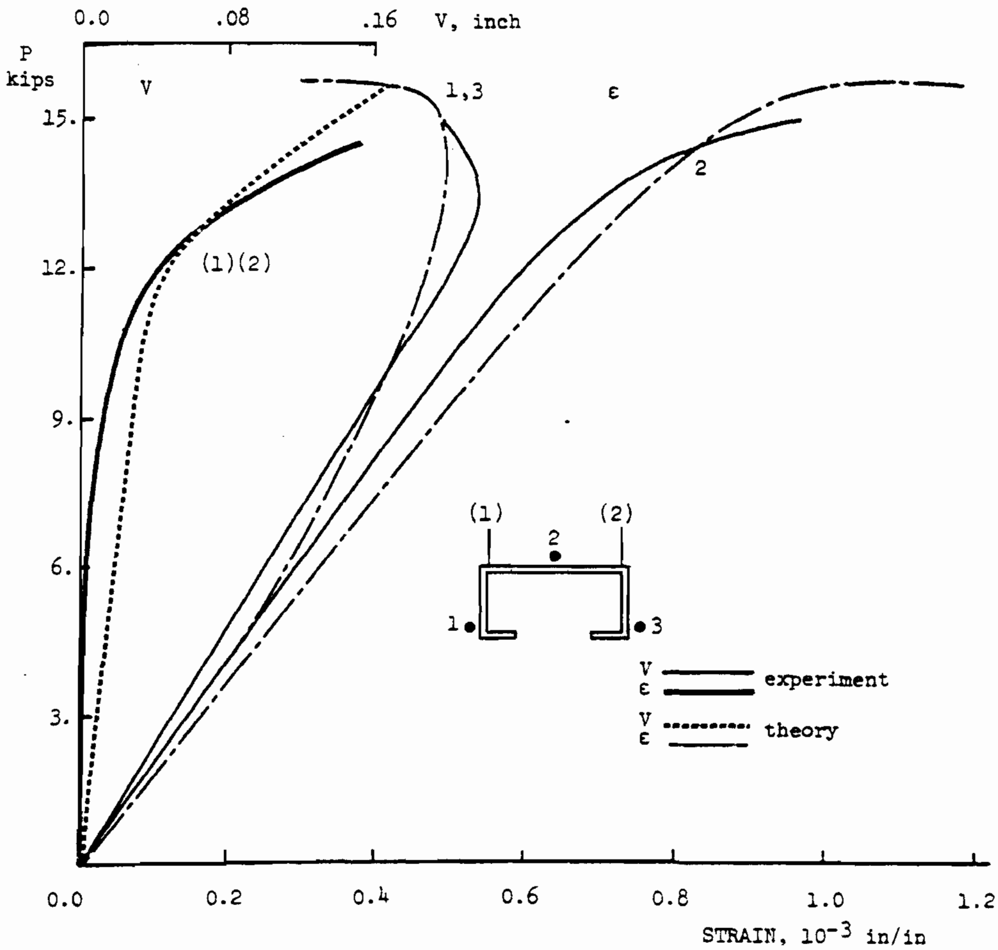

Fig. 9.12 PBC 14 Column A11, L = 69.0".

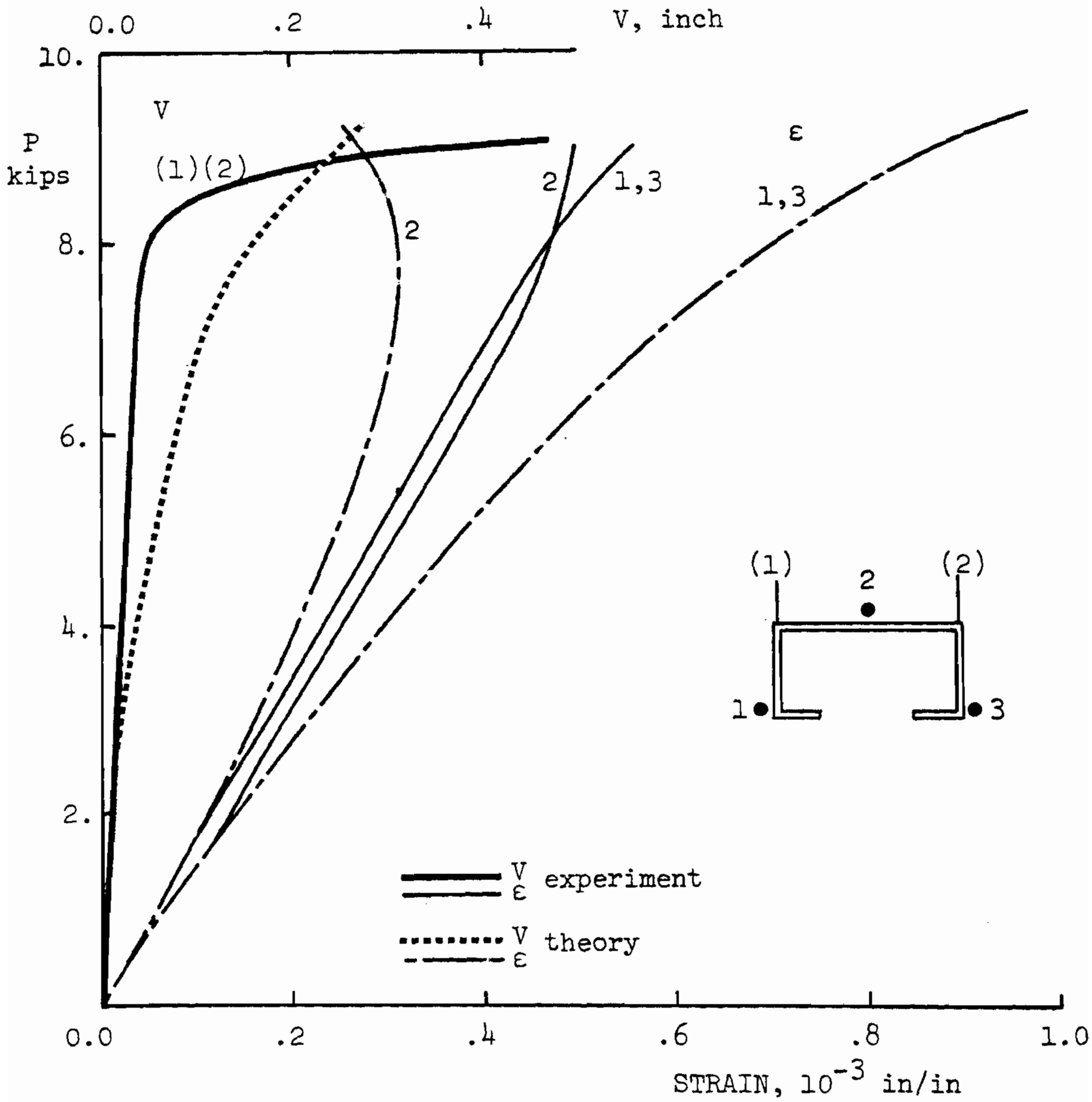

Theory: $V_t/L = -.001$, $P_{th} = 9.83$ k
$A_e/A = 92.9\%$, Error = 3.4%

Fig. 9.13 PBC 14 Column A12, L = 75.0".

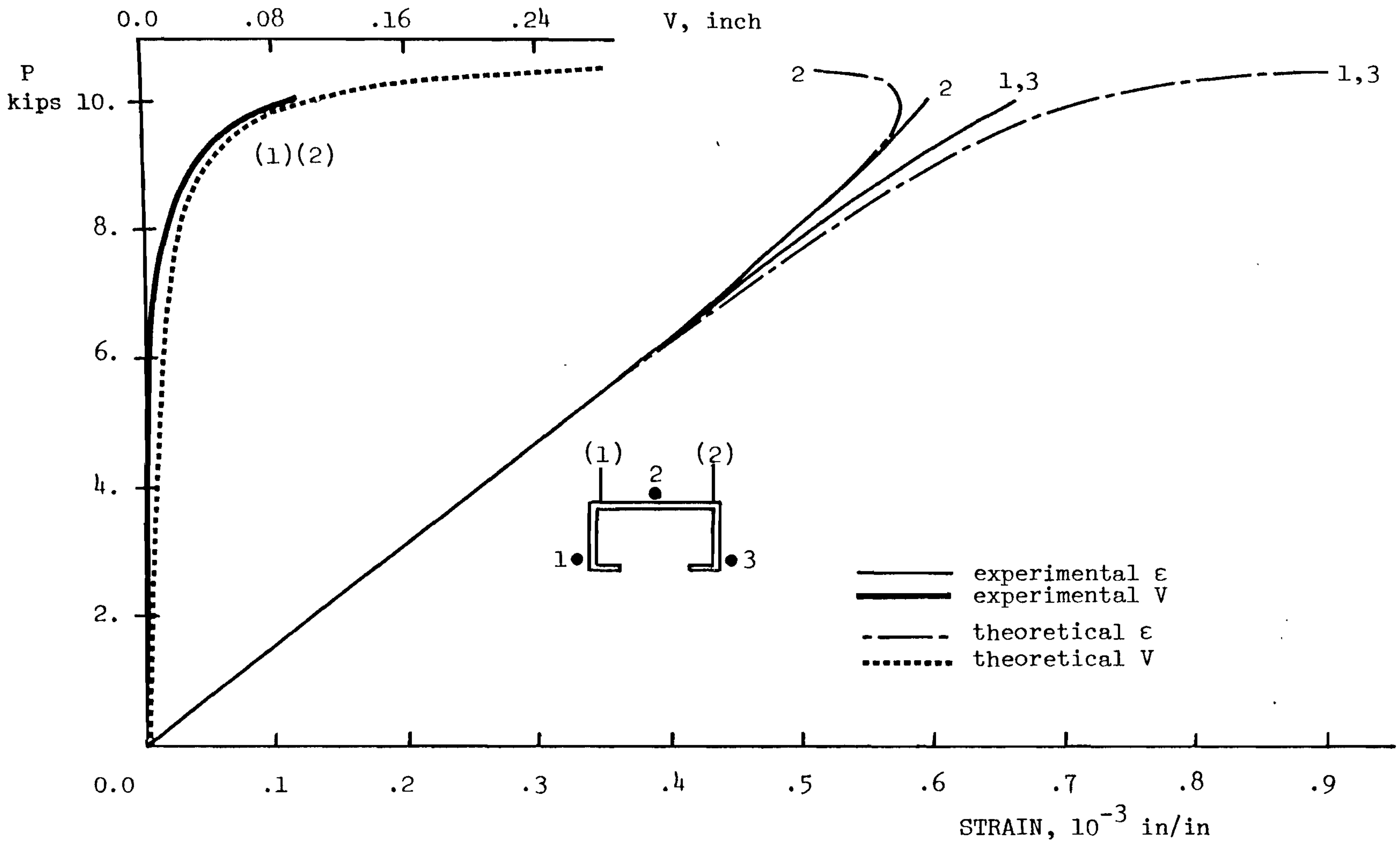

Fig. 9.14 PBC 14 Column A13, L = 78.0"

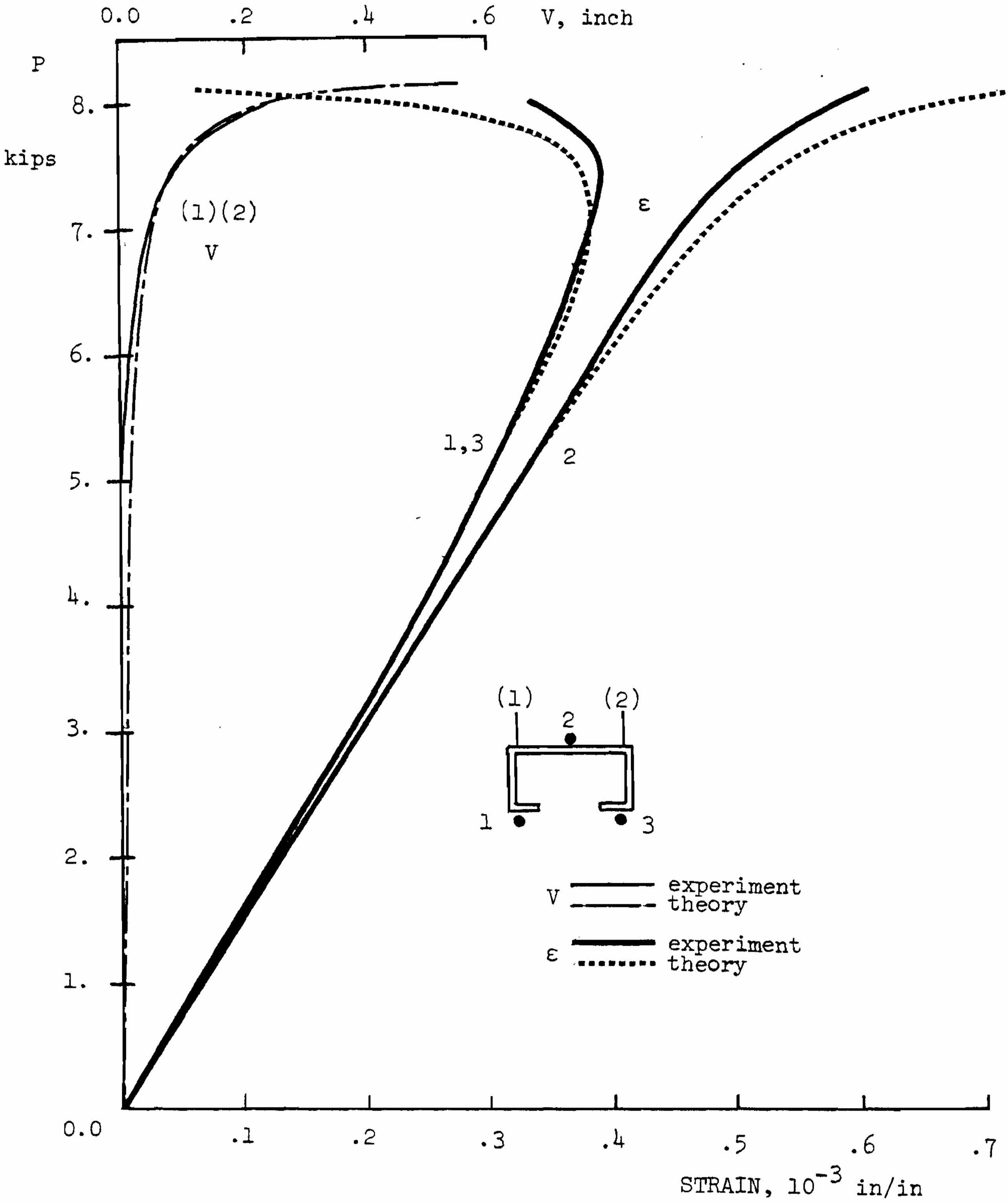

Fig. 9.15 PBC 14 Column A14, L = 89.0".

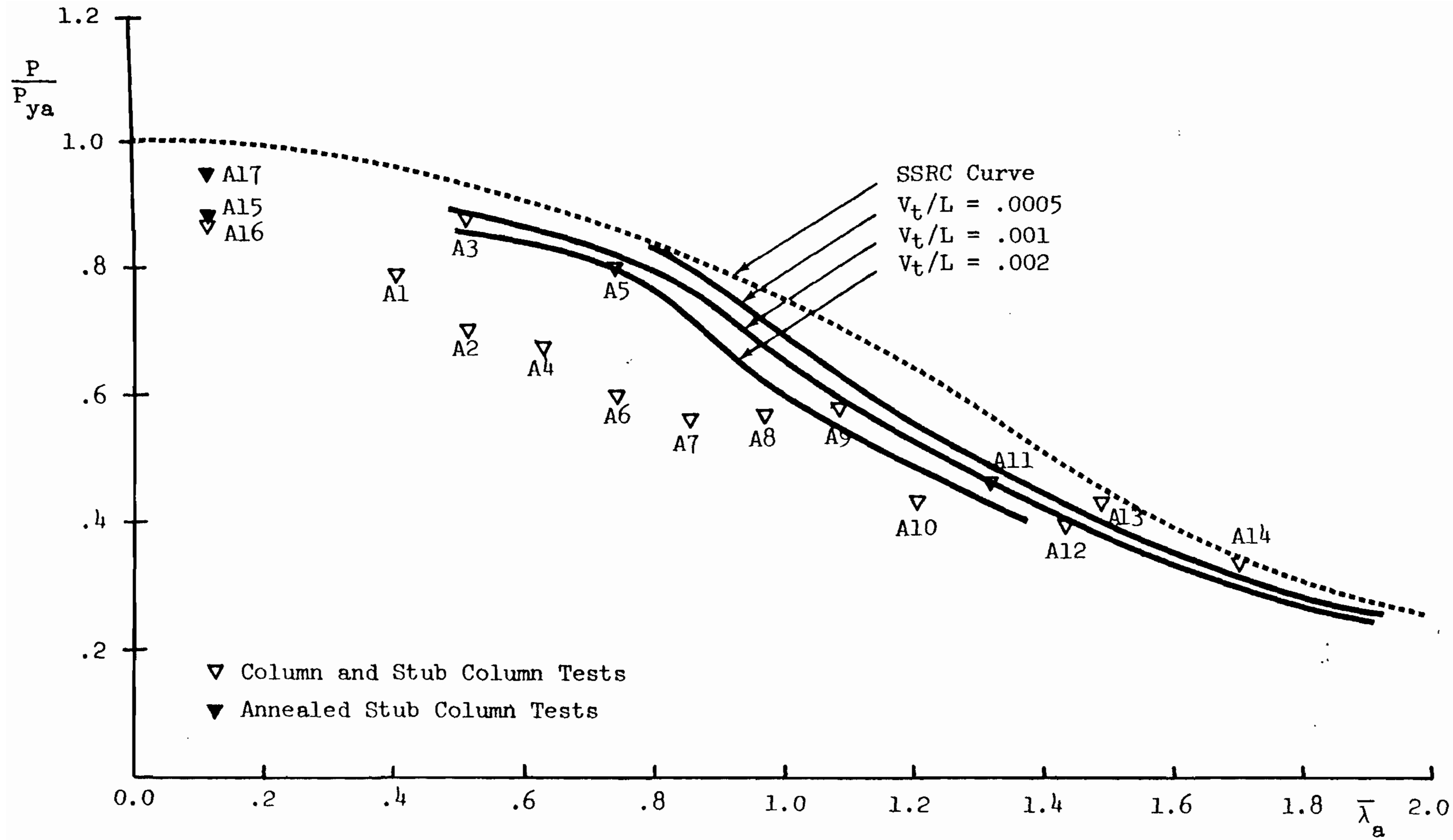

Fig. 9.16 PBC 14 Column Tests; average yield strength

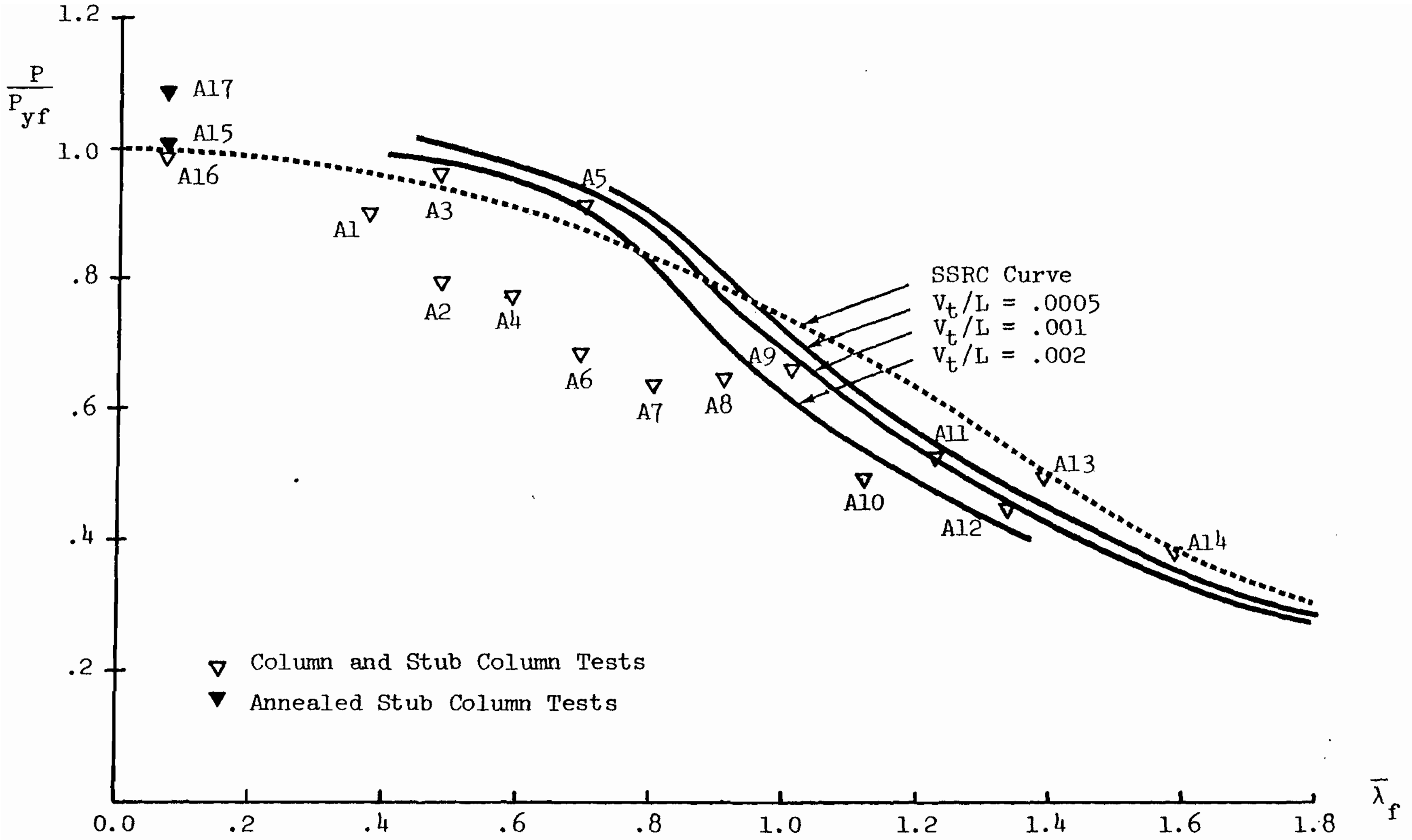

Fig. 9.17 PBC 14 Column Tests; yield strength of flat

364

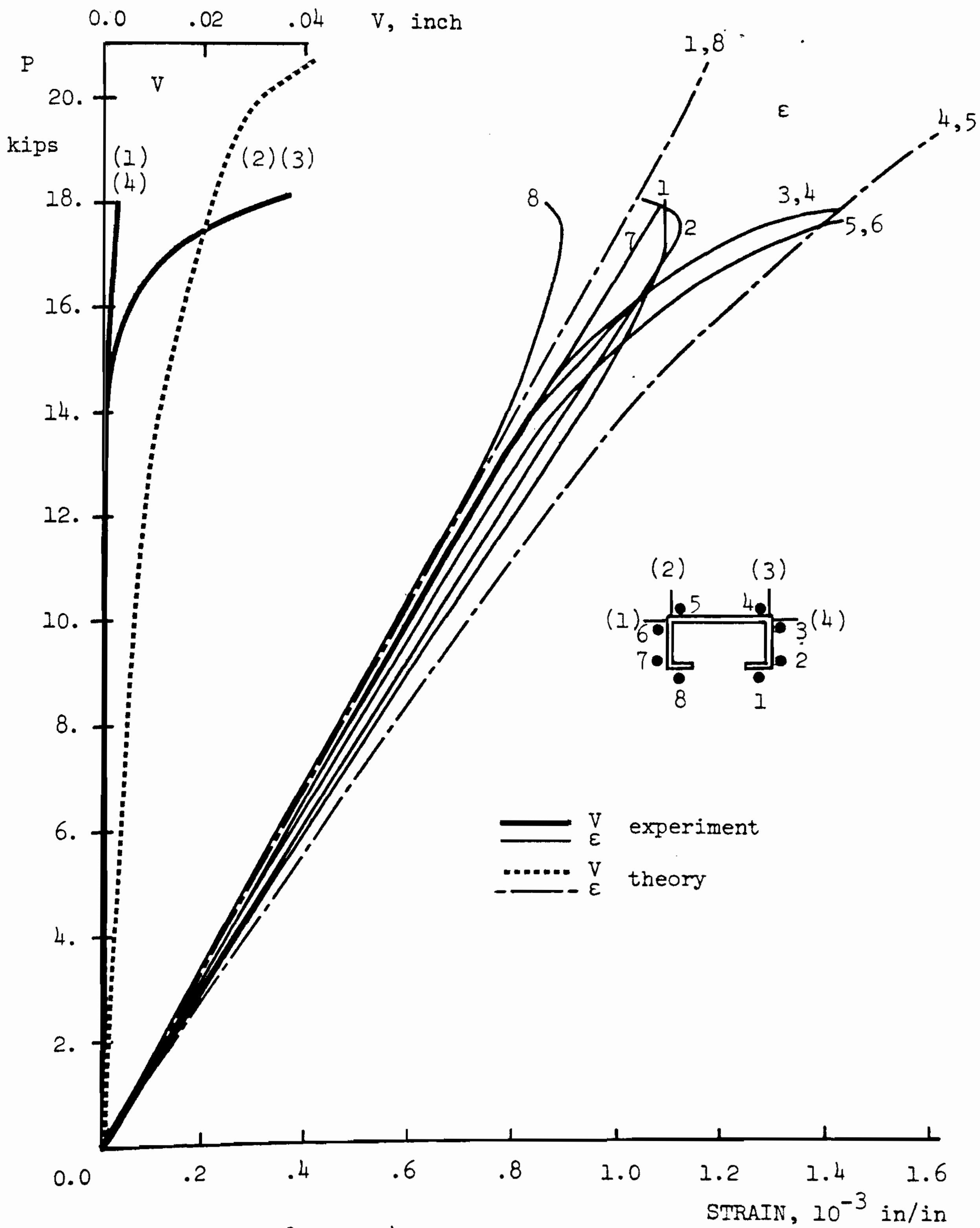

Fig. 9.18 RFC 14 Column B1, L = 27.0".

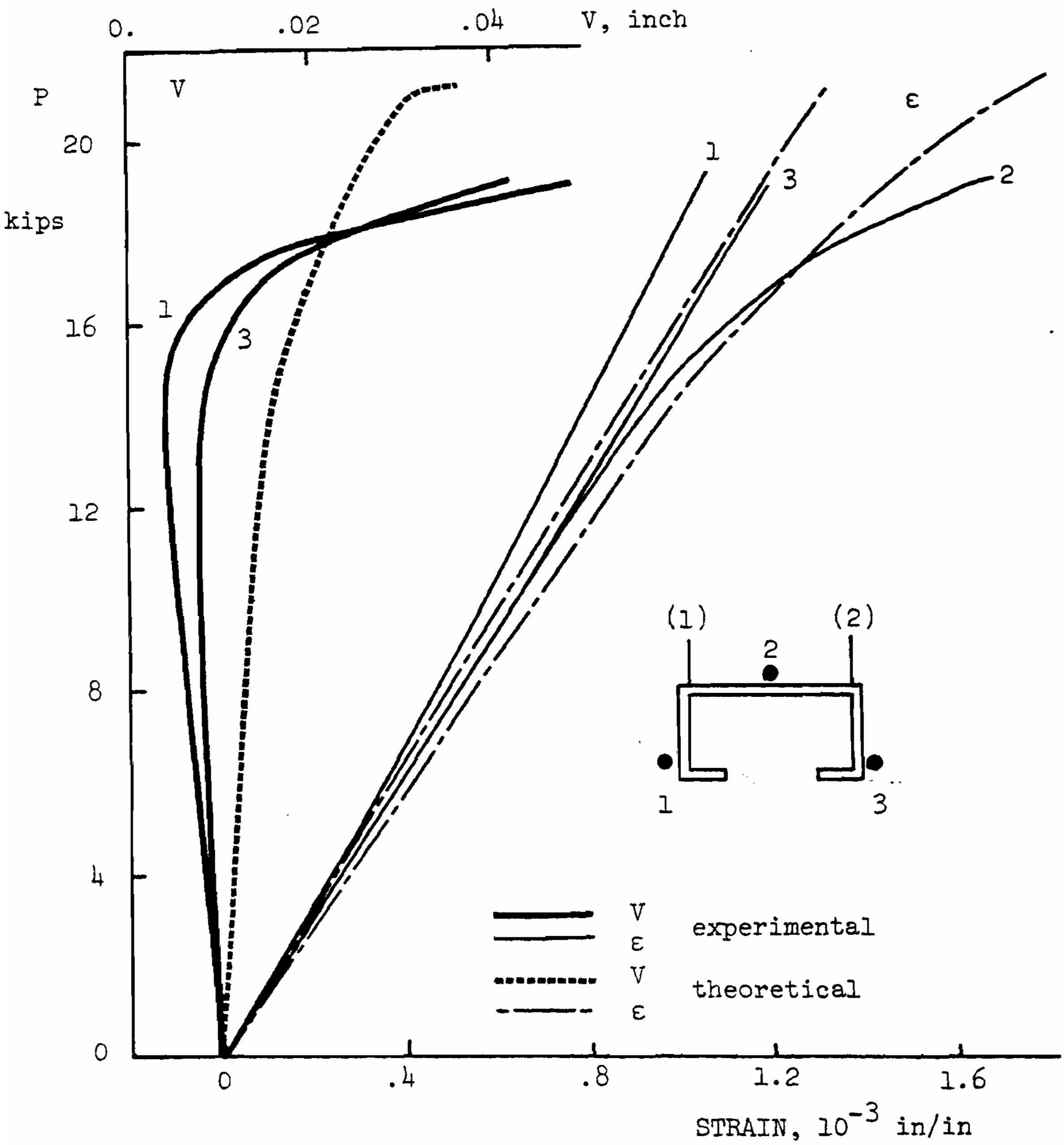

Fig. 9.19 RFC14, Column B2, L = 27.0".

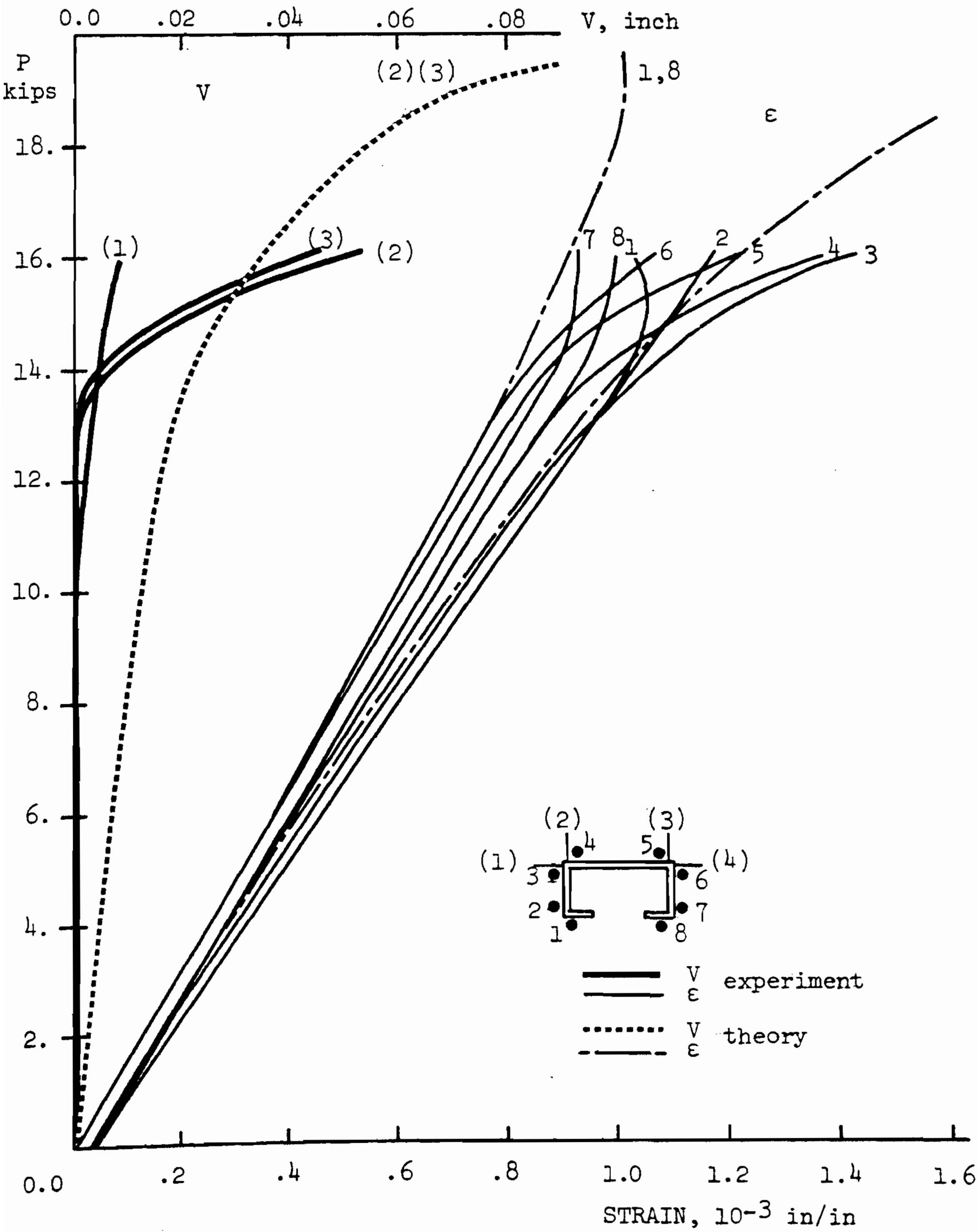

Fig. 9.20 RFC 14 Column B3, L = 39.0".

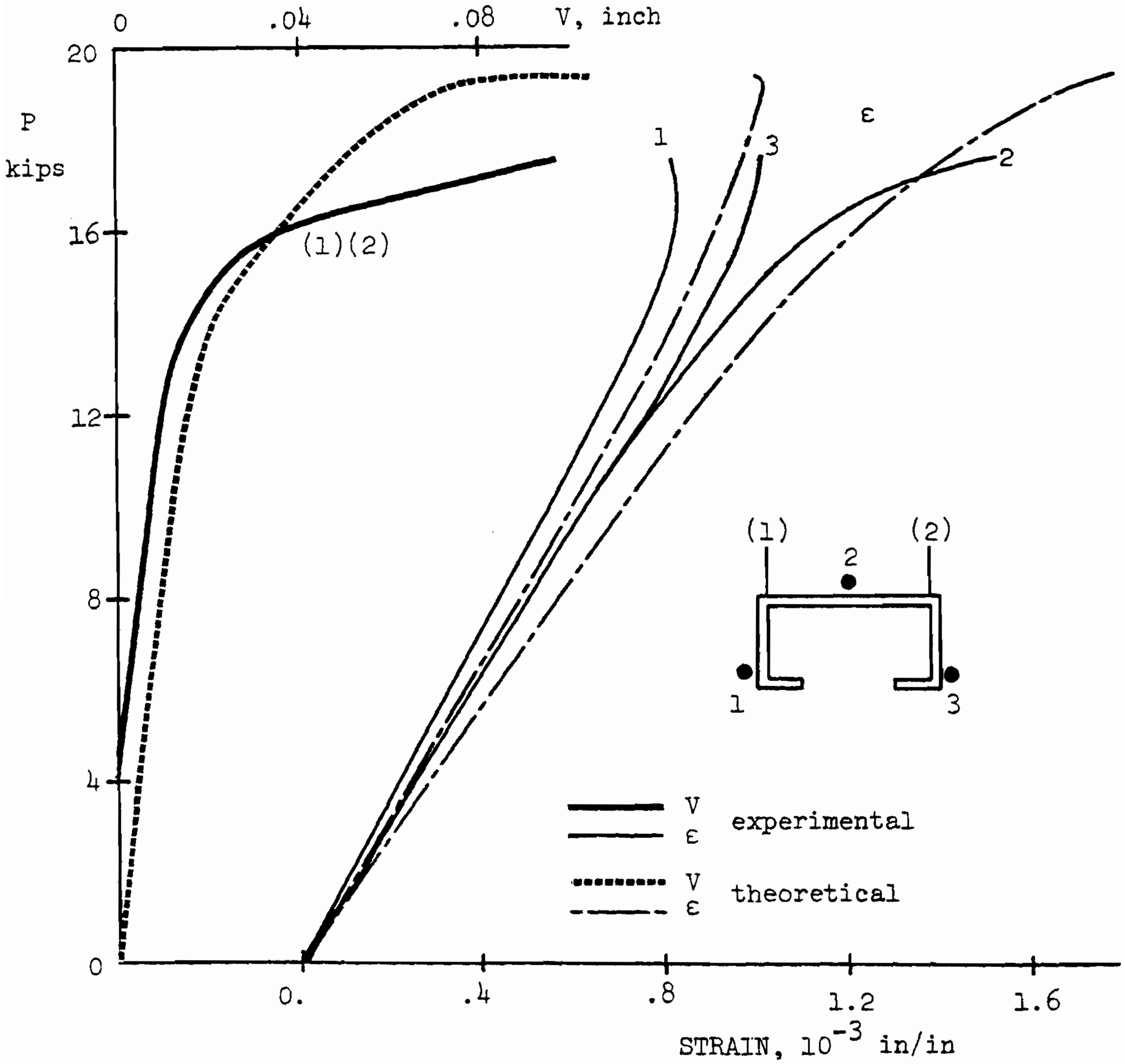

Fig. 9.21 RFC14, Column B4, L = 39.0"

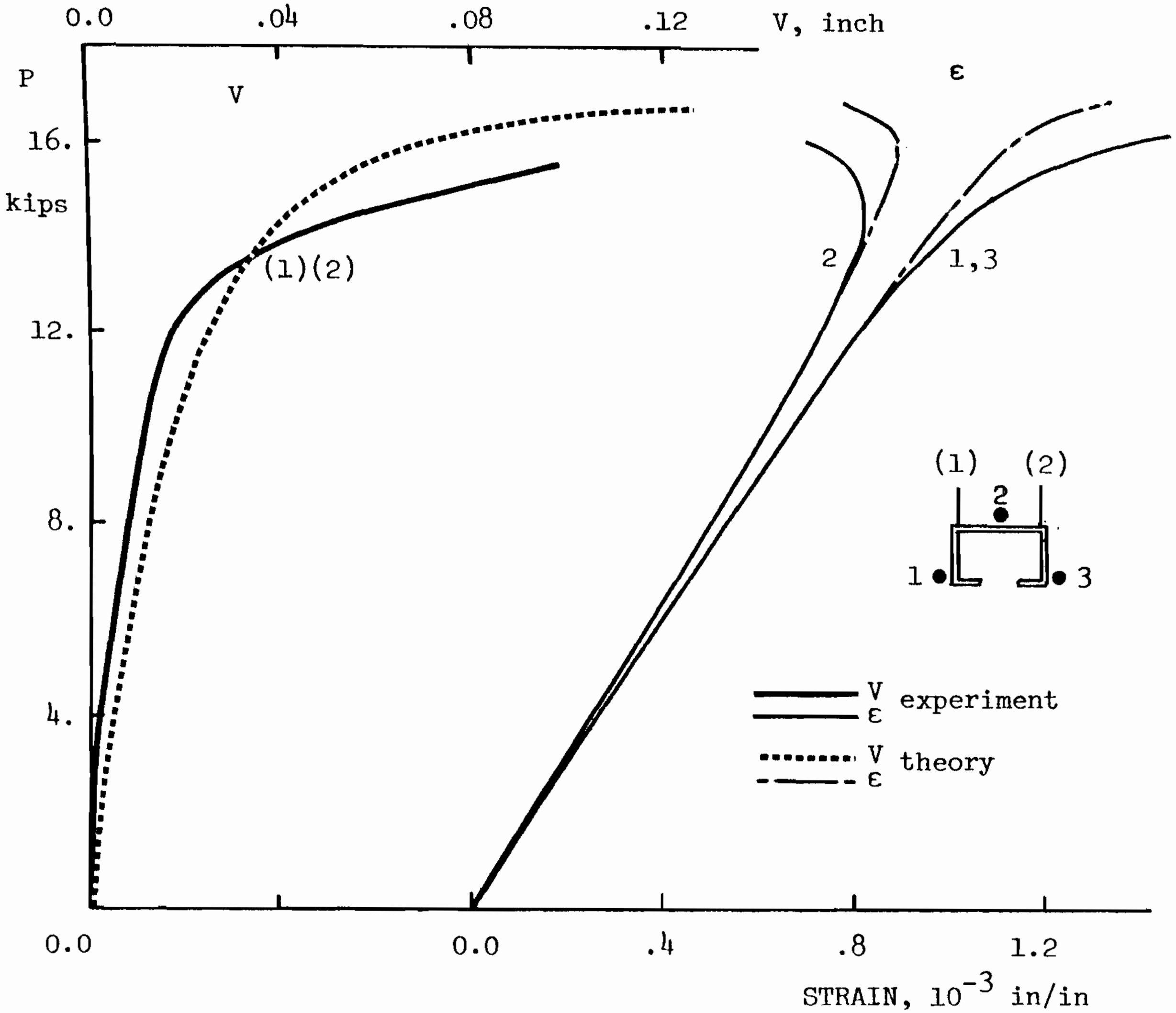

Fig. 9.22 RFC 14 Column B5, L = 51.0".

(Theory uses σ_y-5.0 ksi)

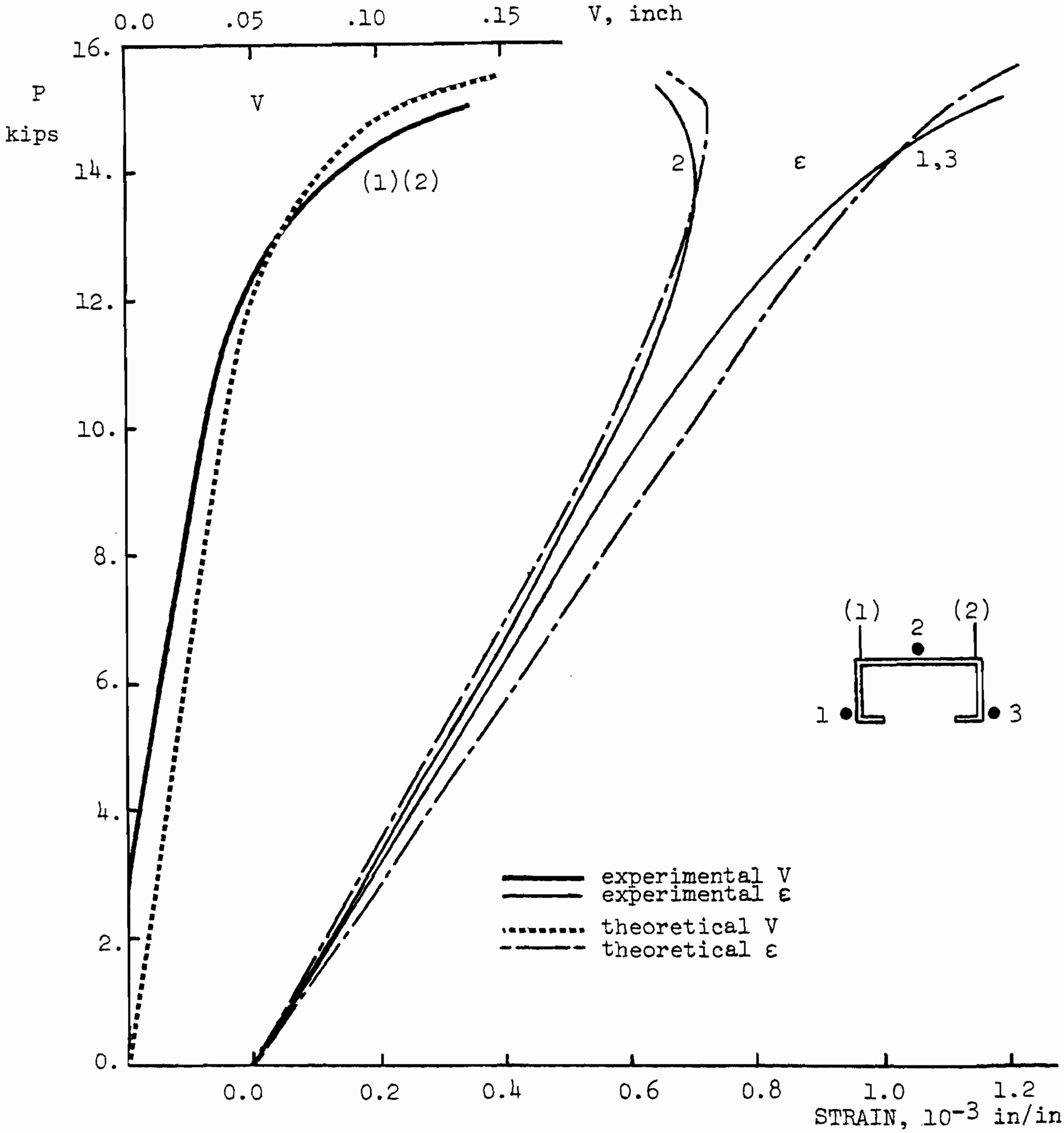

Fig. 9.23 RFC 14 Column B6, L = 51.0".

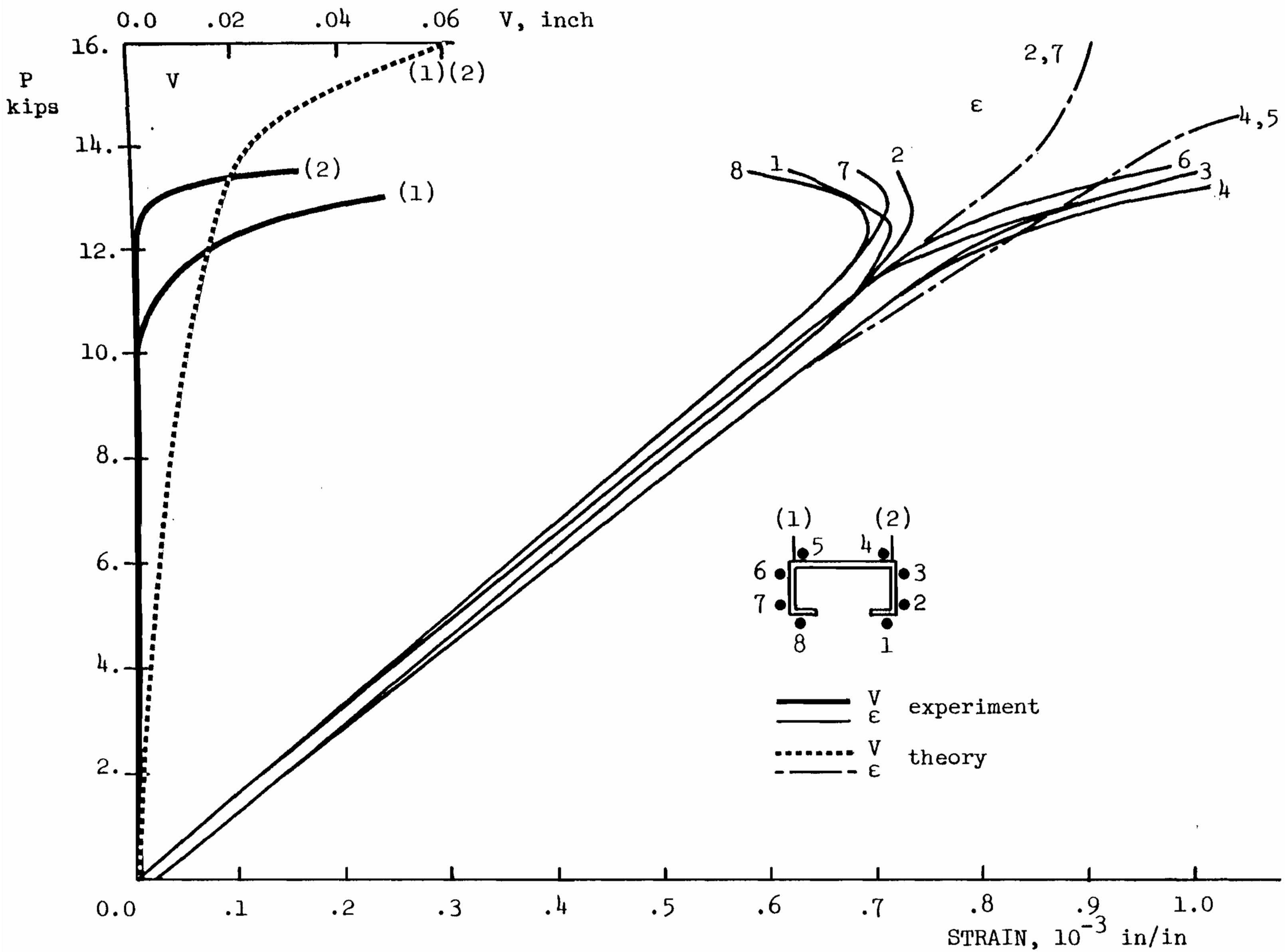

Fig. 9.24 RFC 14 Column B7, L = 51.0".

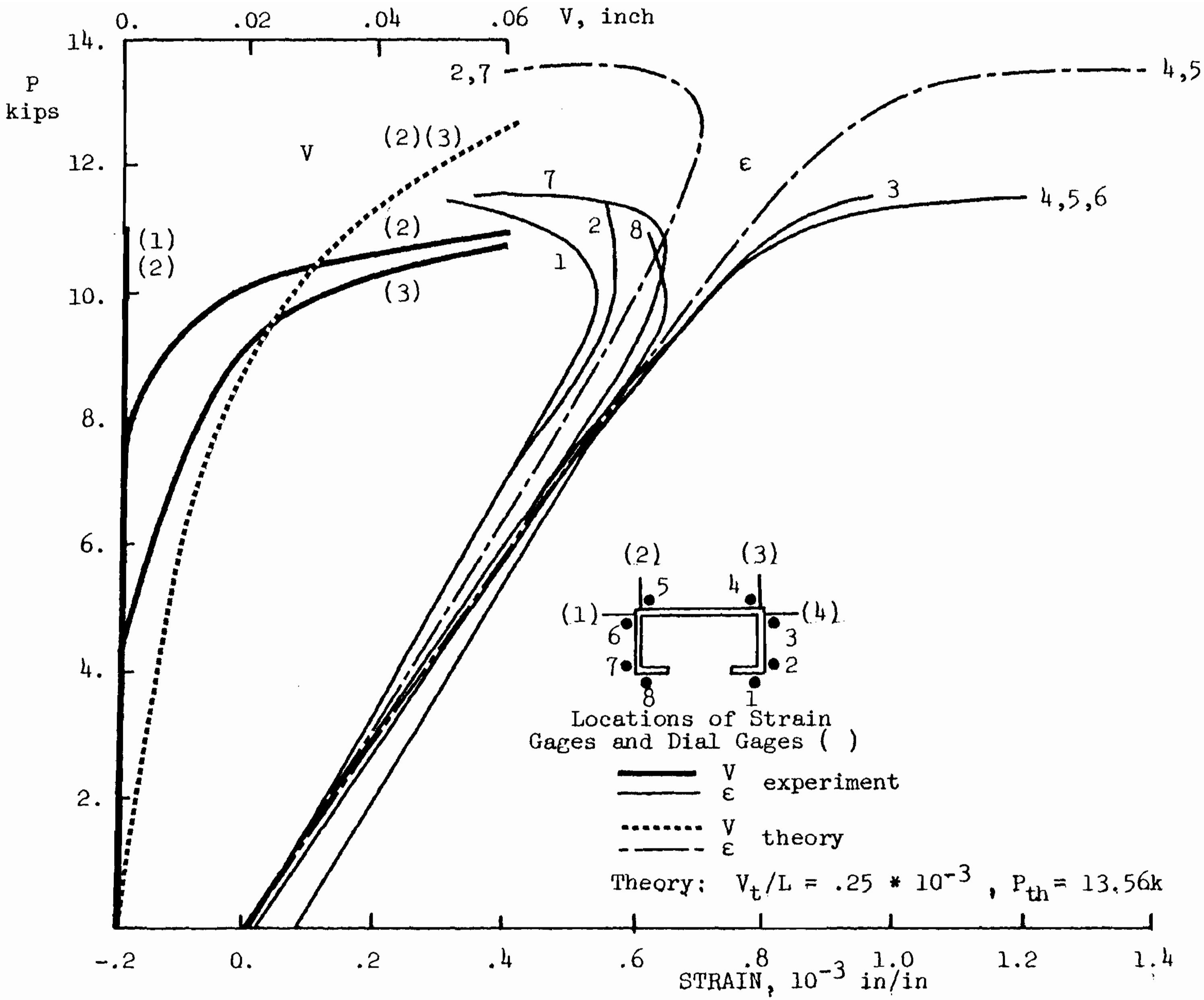

Fig. 9.25 RFC Column B8, L = 63.0"

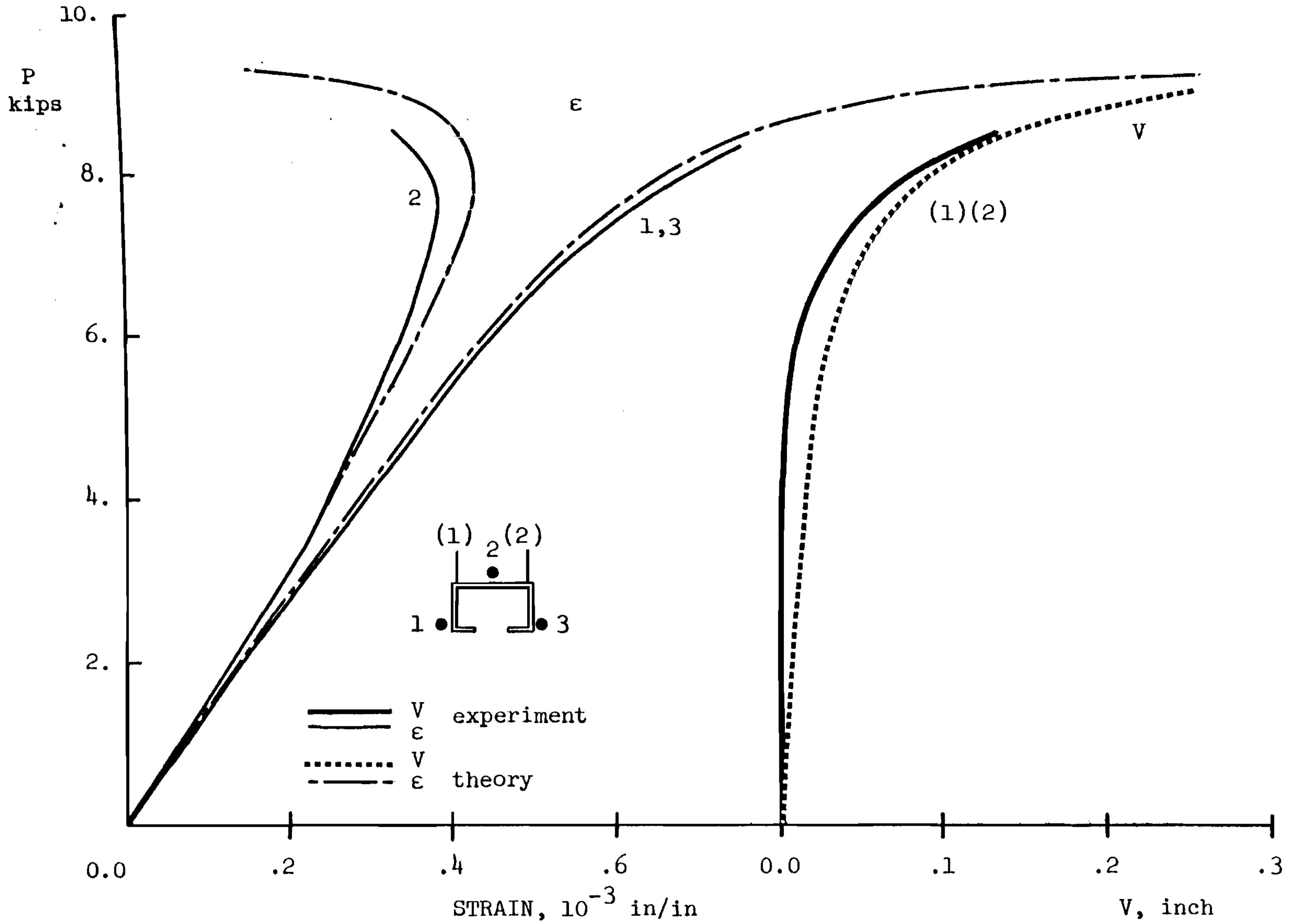

Fig. 9.26 RFC 14 Column B9, L = 80.5".

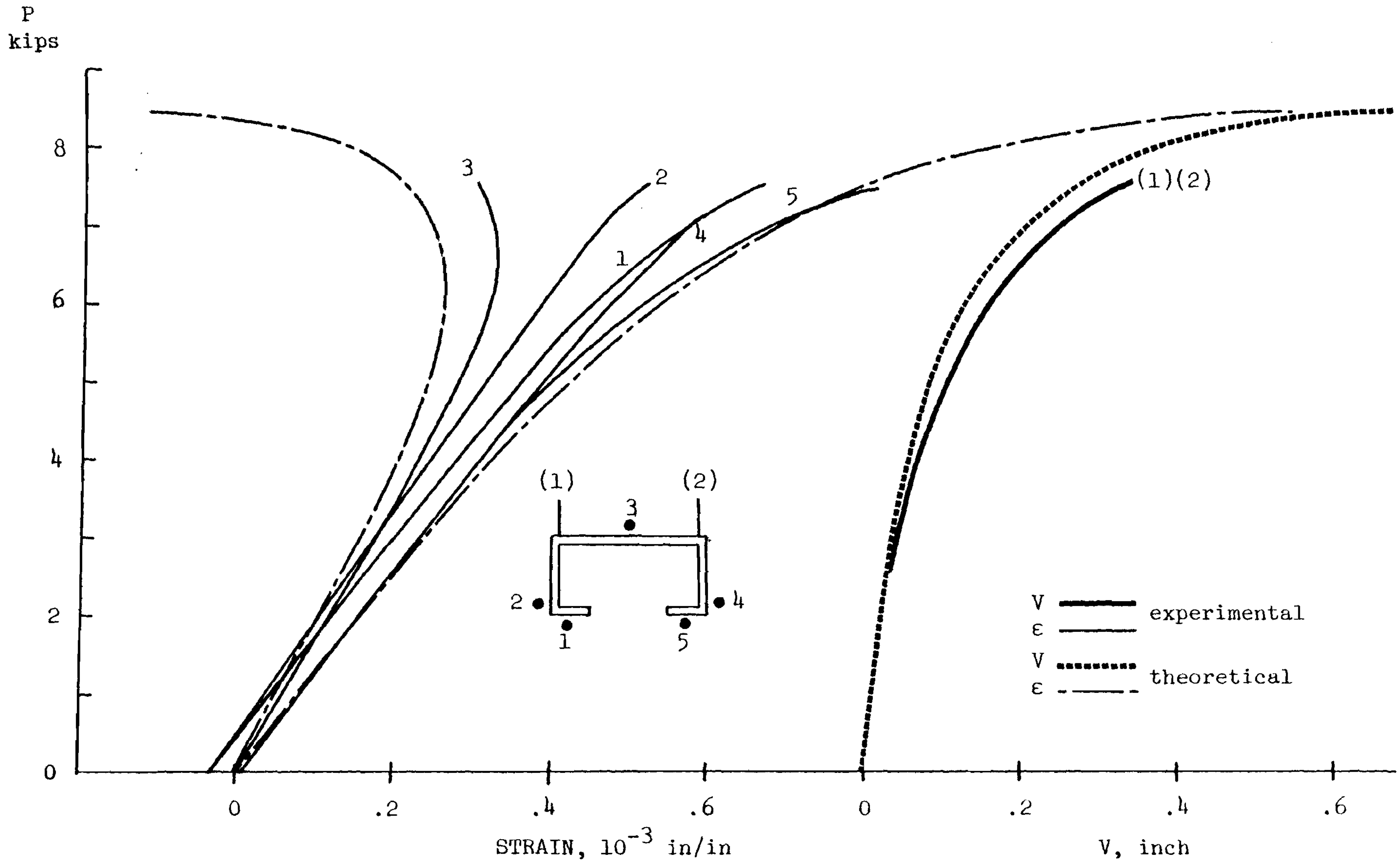

Fig. 9.27 RFC14, Column B10, L = 80.5"

374

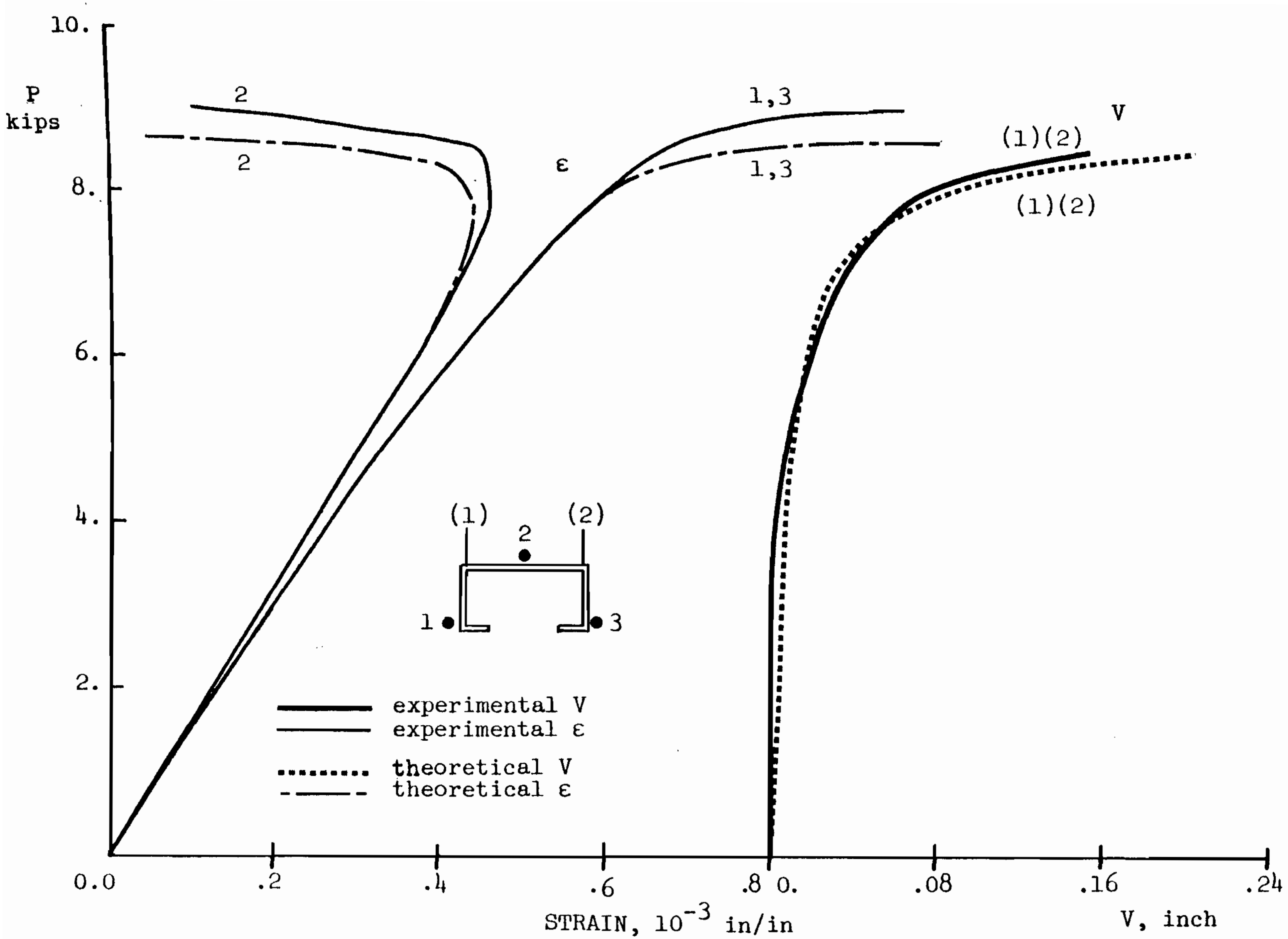

Fig. 9.28 RFC 14 Column B11, L = 84.9".

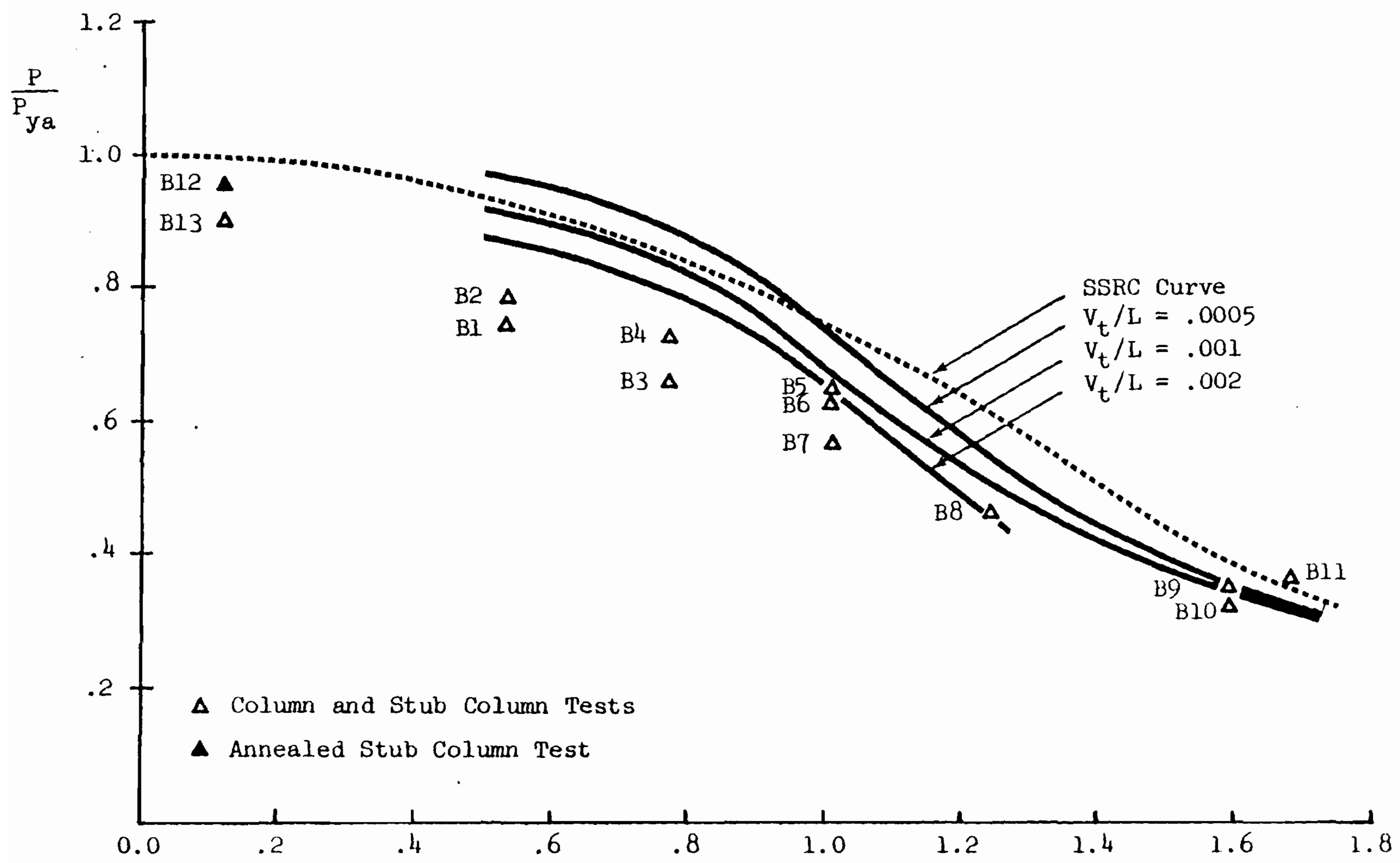

Fig. 9.29 RFC 14 Column Tests; average yield strength

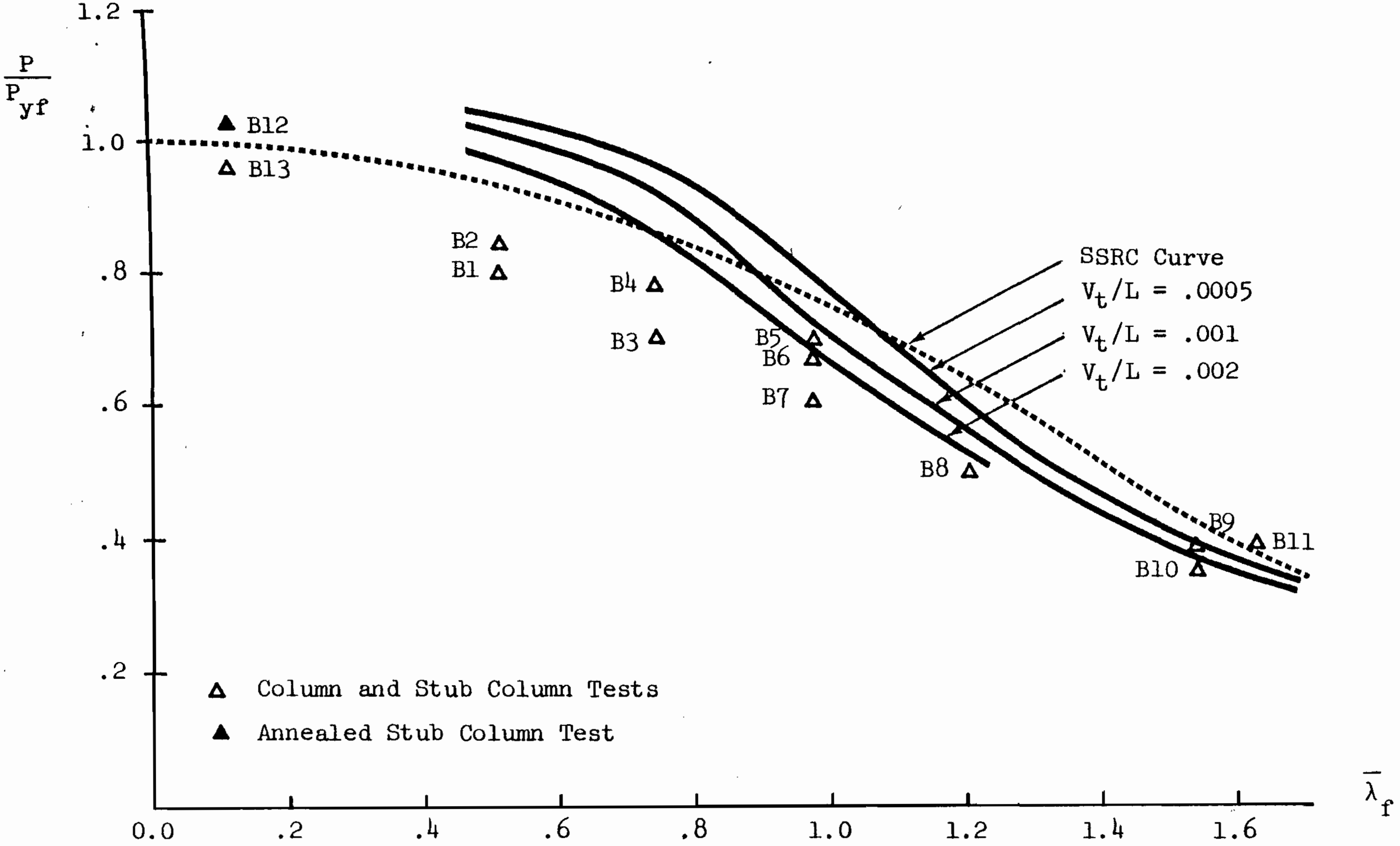

Fig. 9.30 RFC 14 Column Tests; yield strength of flat

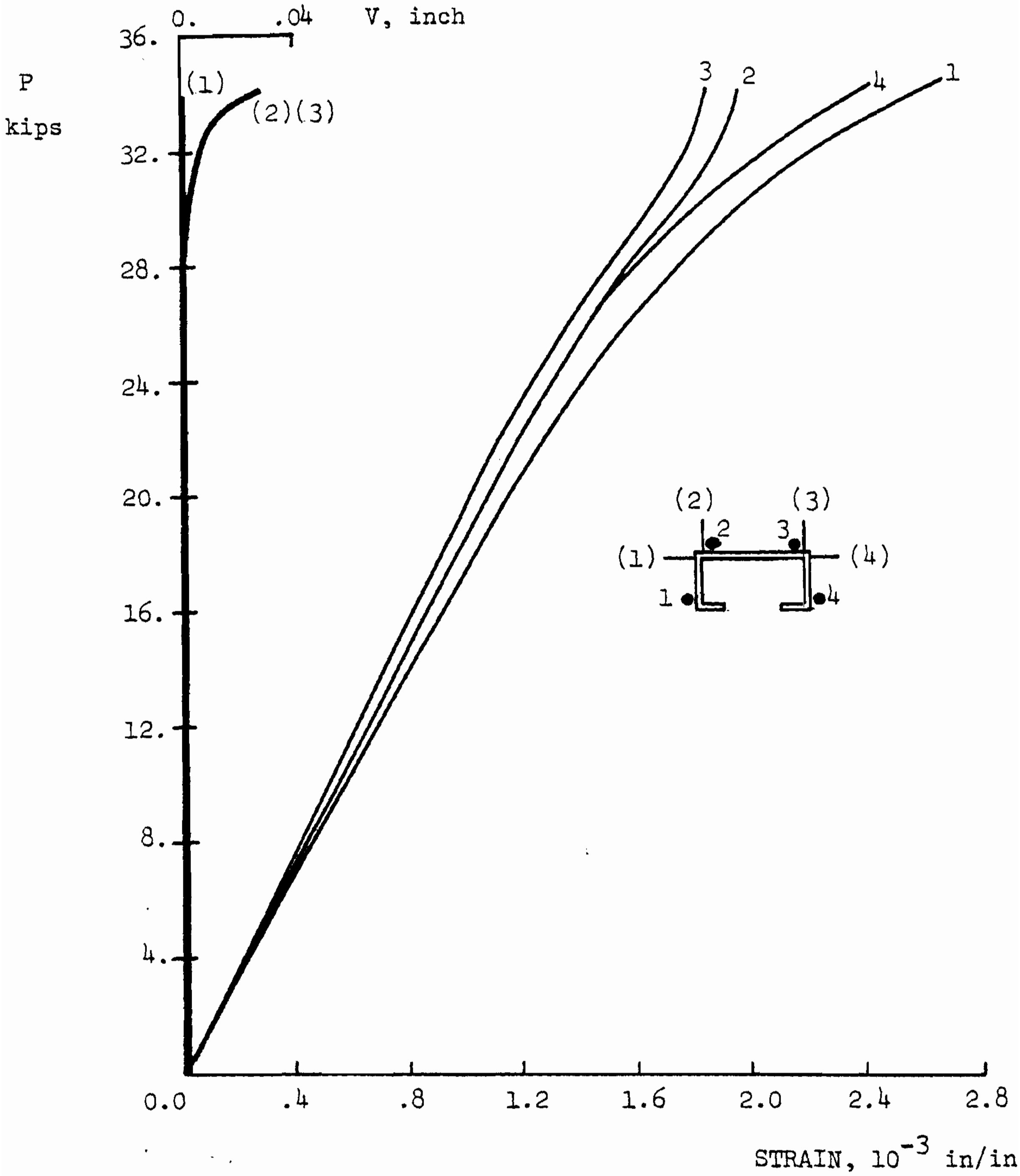

Fig. 9.31 PBC 13 Column C1, L = 27.0".

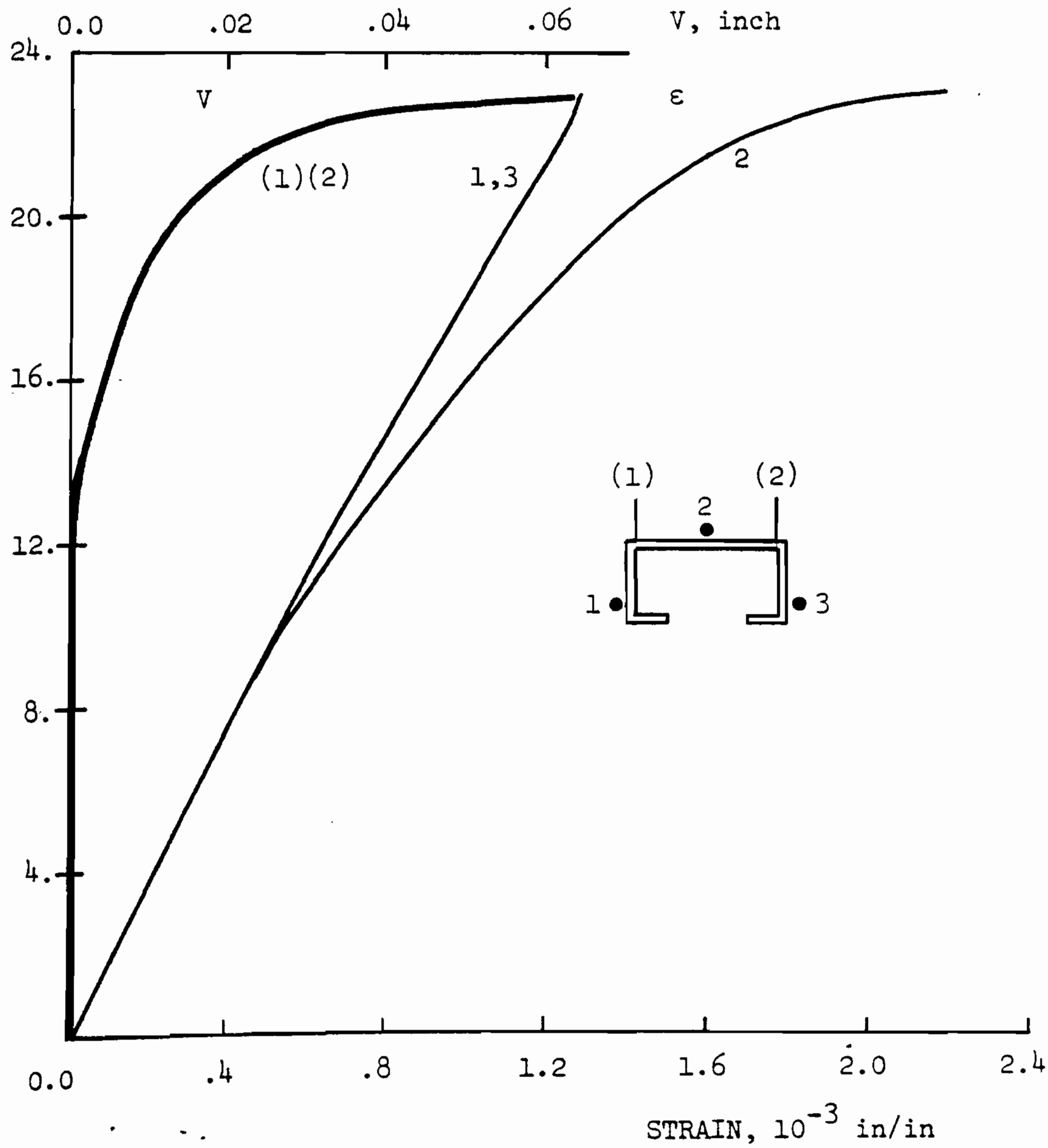

Fig. 9.32 PBC 13 Column C2, L = 27.0".

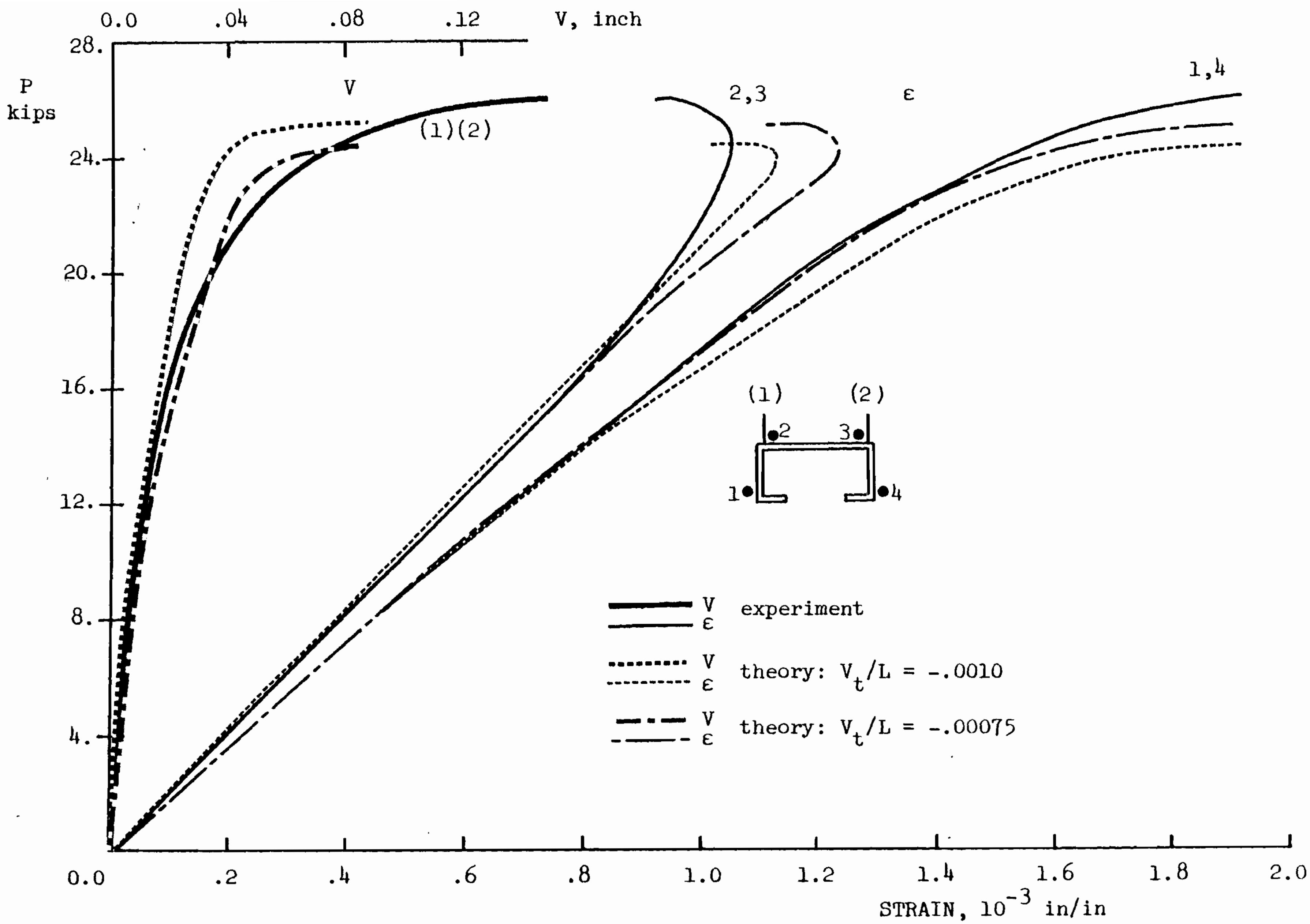

Fig. 9.33 PBC 13 Column C3, L = 39.0".

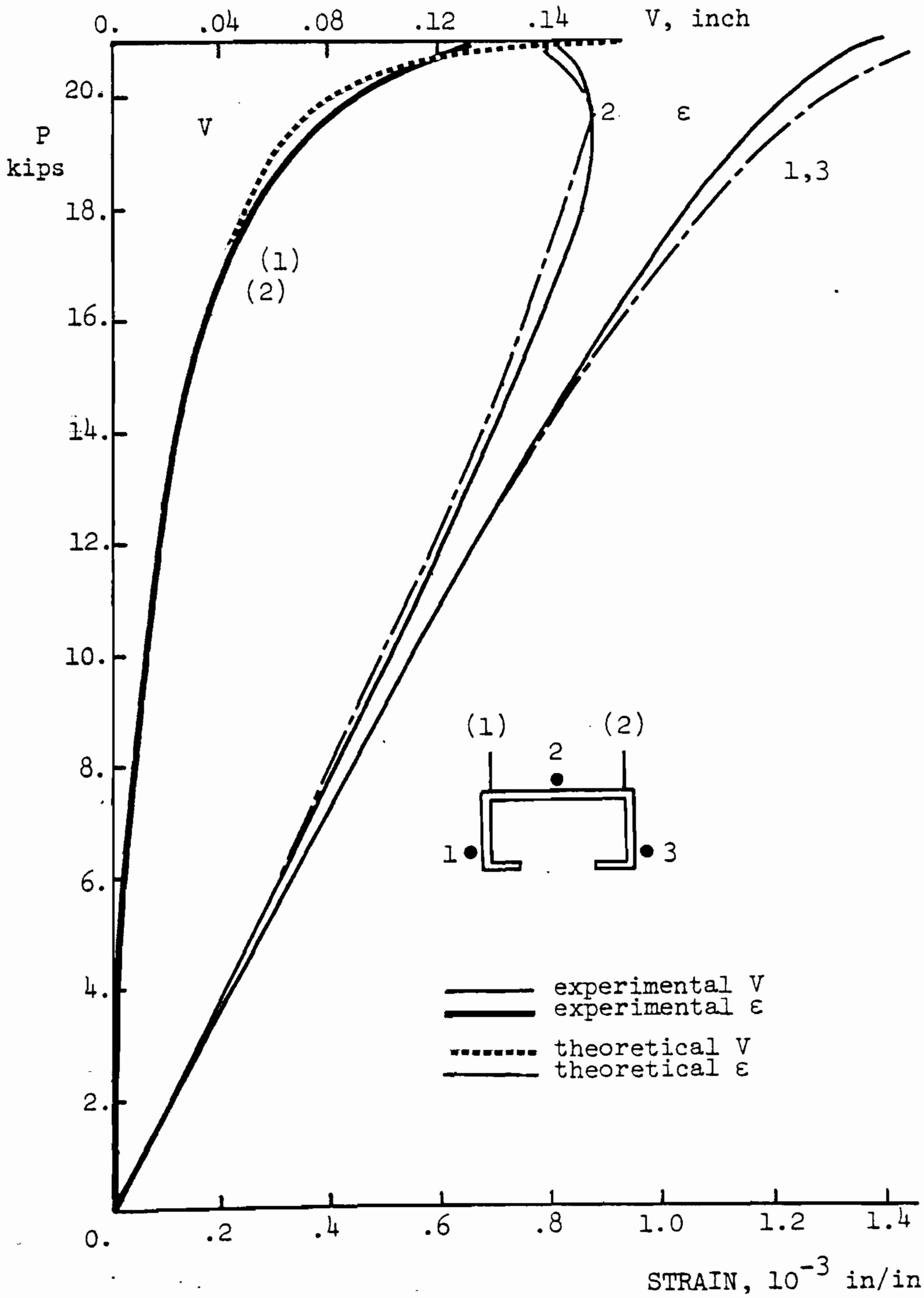

Fig. 9.34 PBC 13 Column C4, L = 51.0".

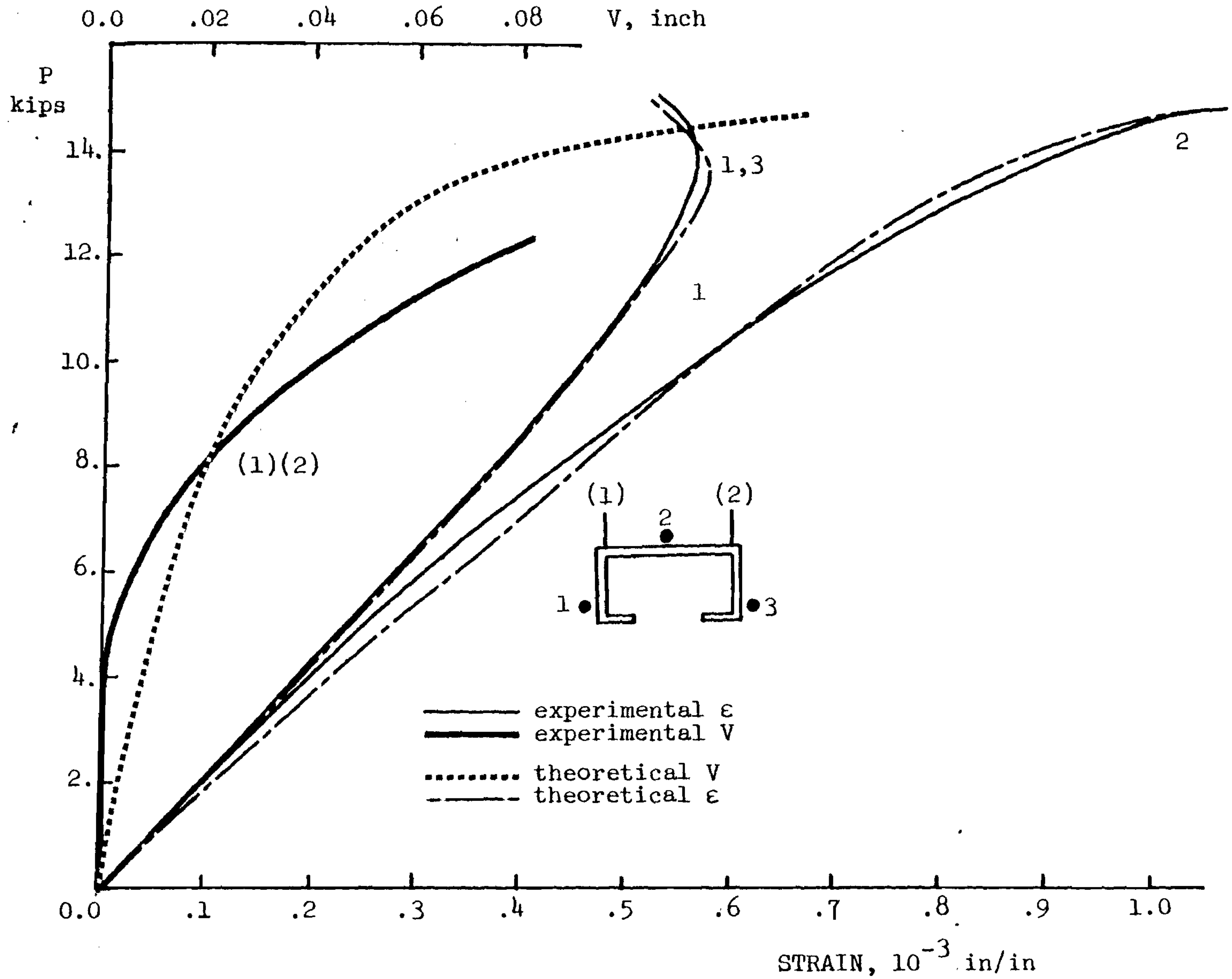

Fig. 9.35 PBC 13 Column C5, L = 63.0".

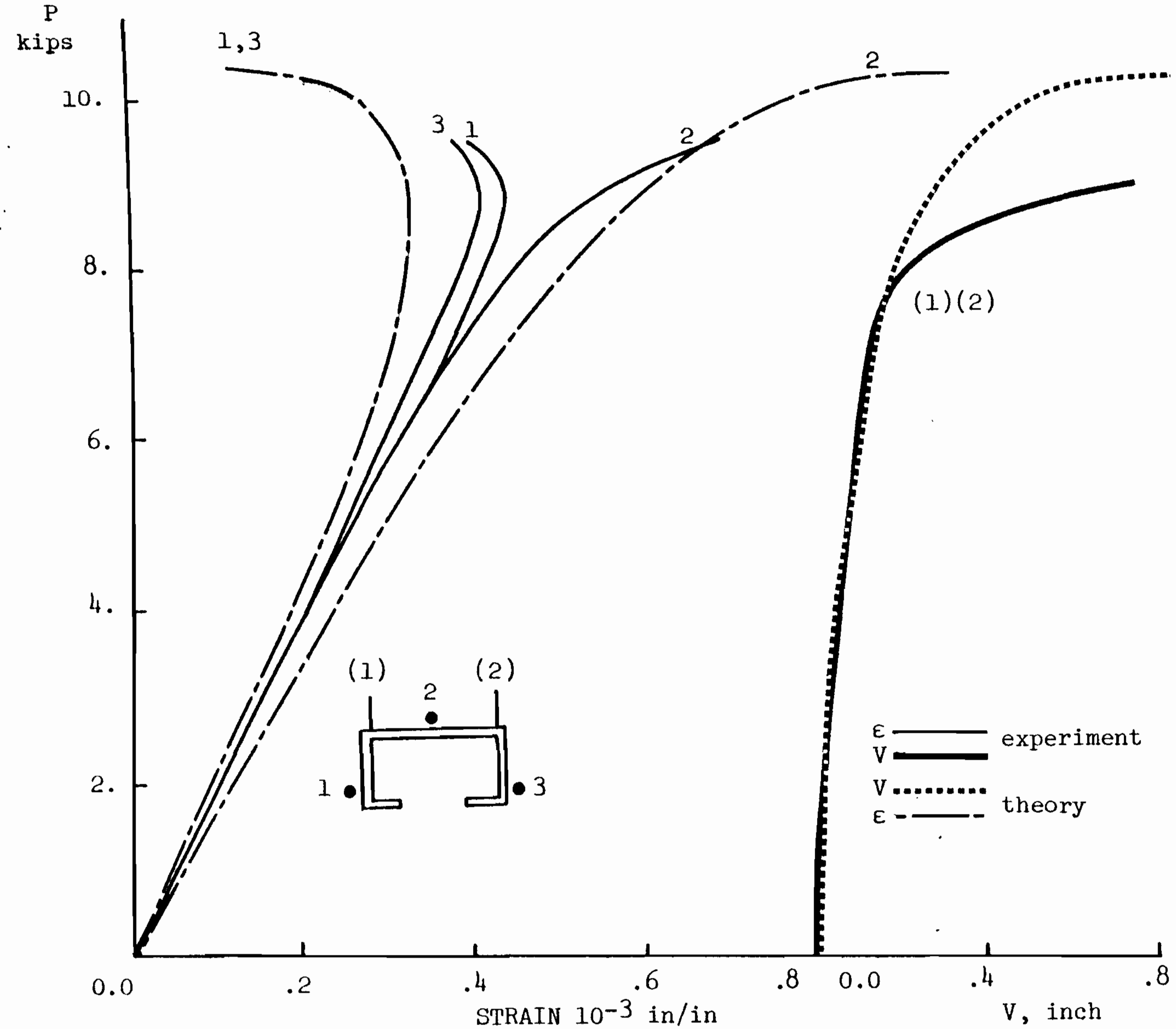

Fig. 9.36 PBC 13 Column C6, L = 82.0".

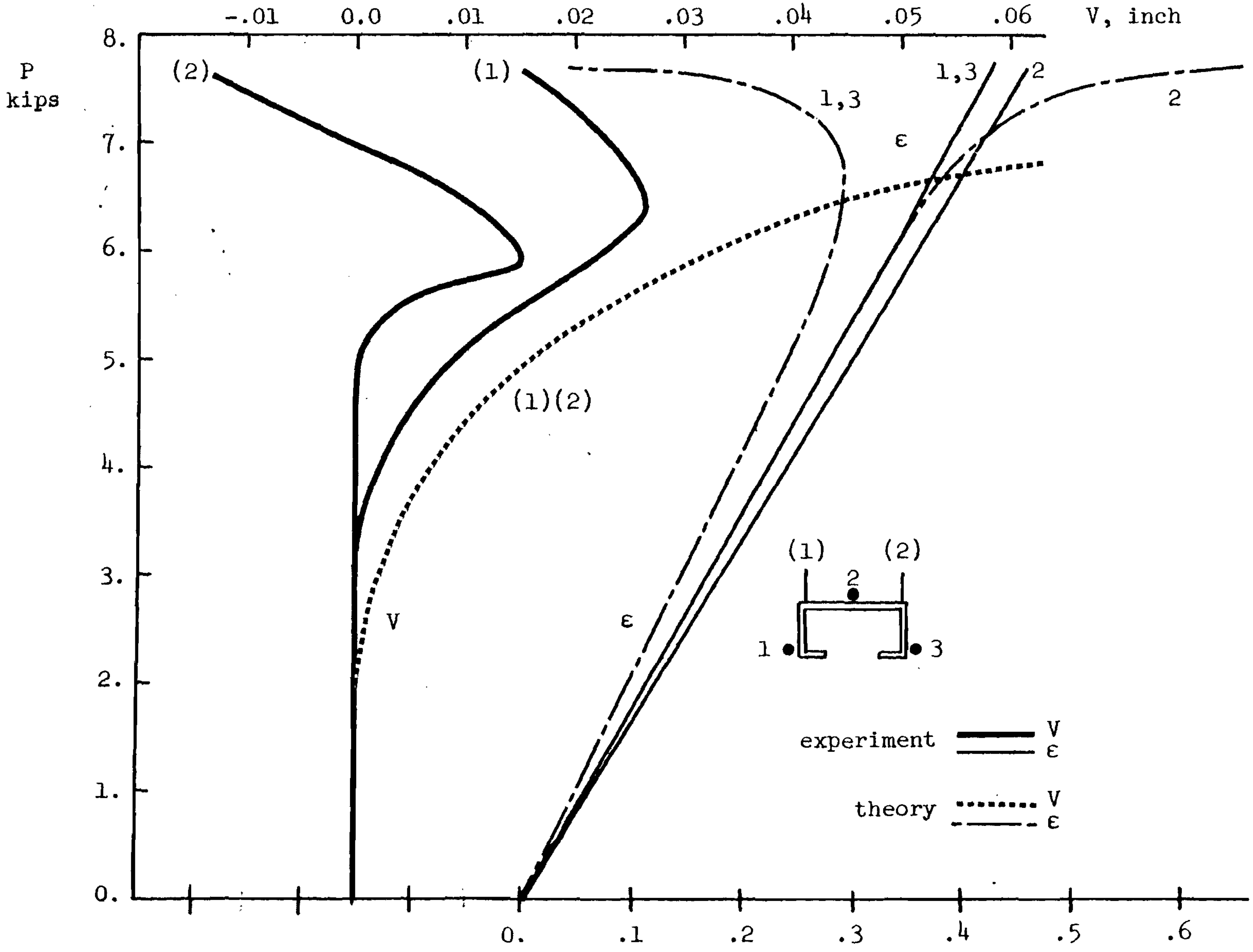

Fig. 9.37 PBC 13 Column C7, L = 100.0"

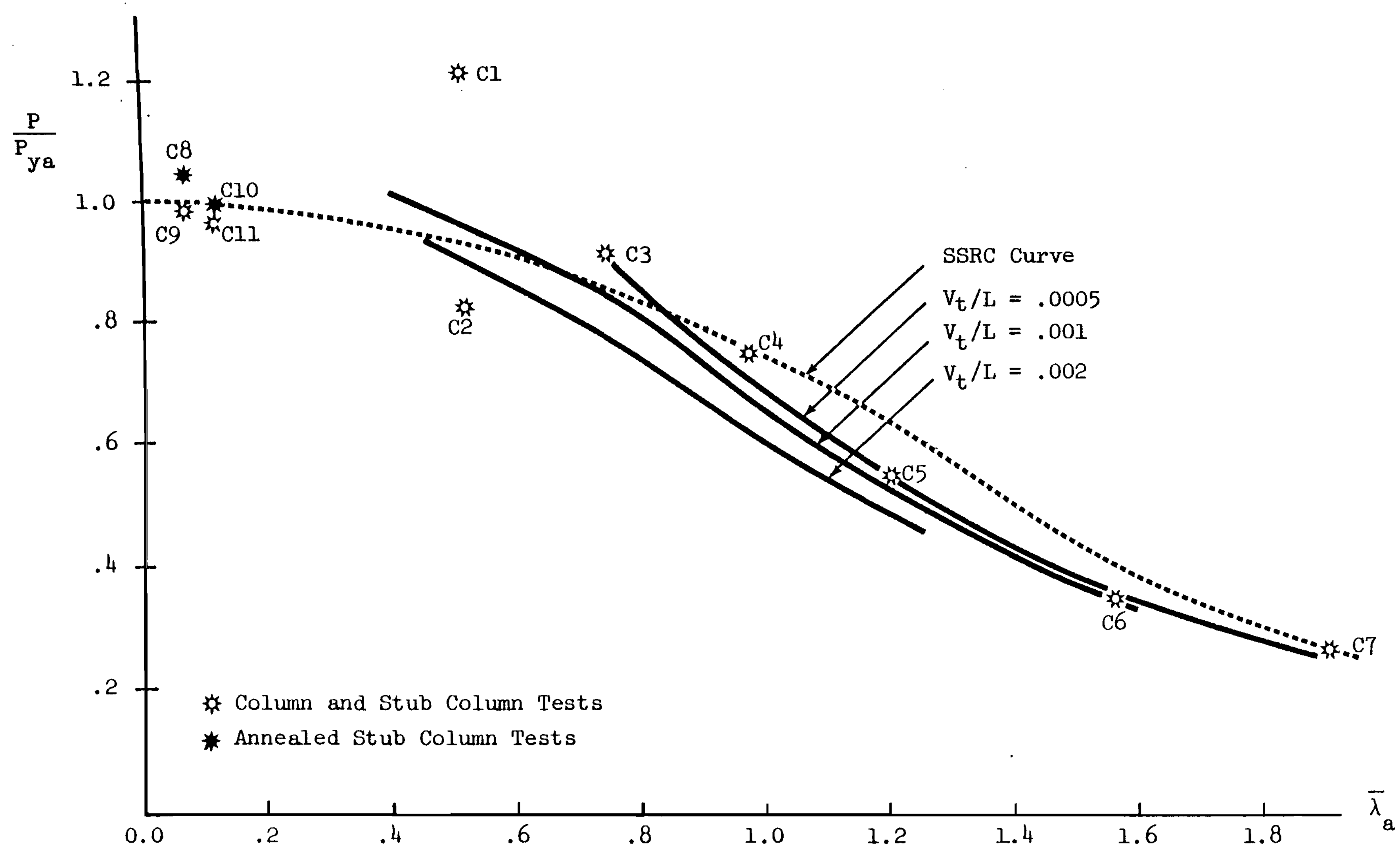

Fig. 9.38 PBC 13 Column Tests; average yield strength

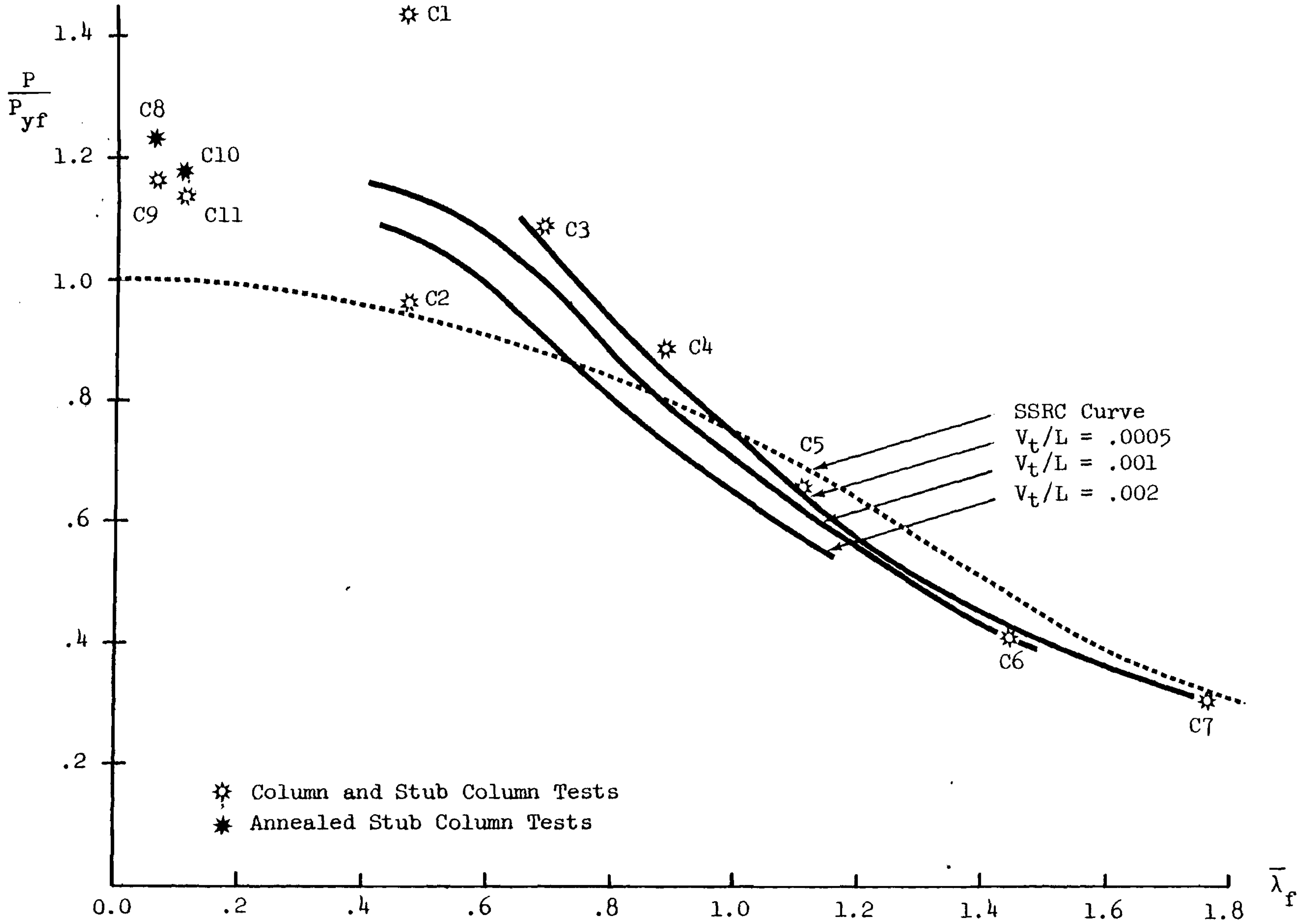

Fig. 9.39 PBC 13 Column Tests; yield strength of flat

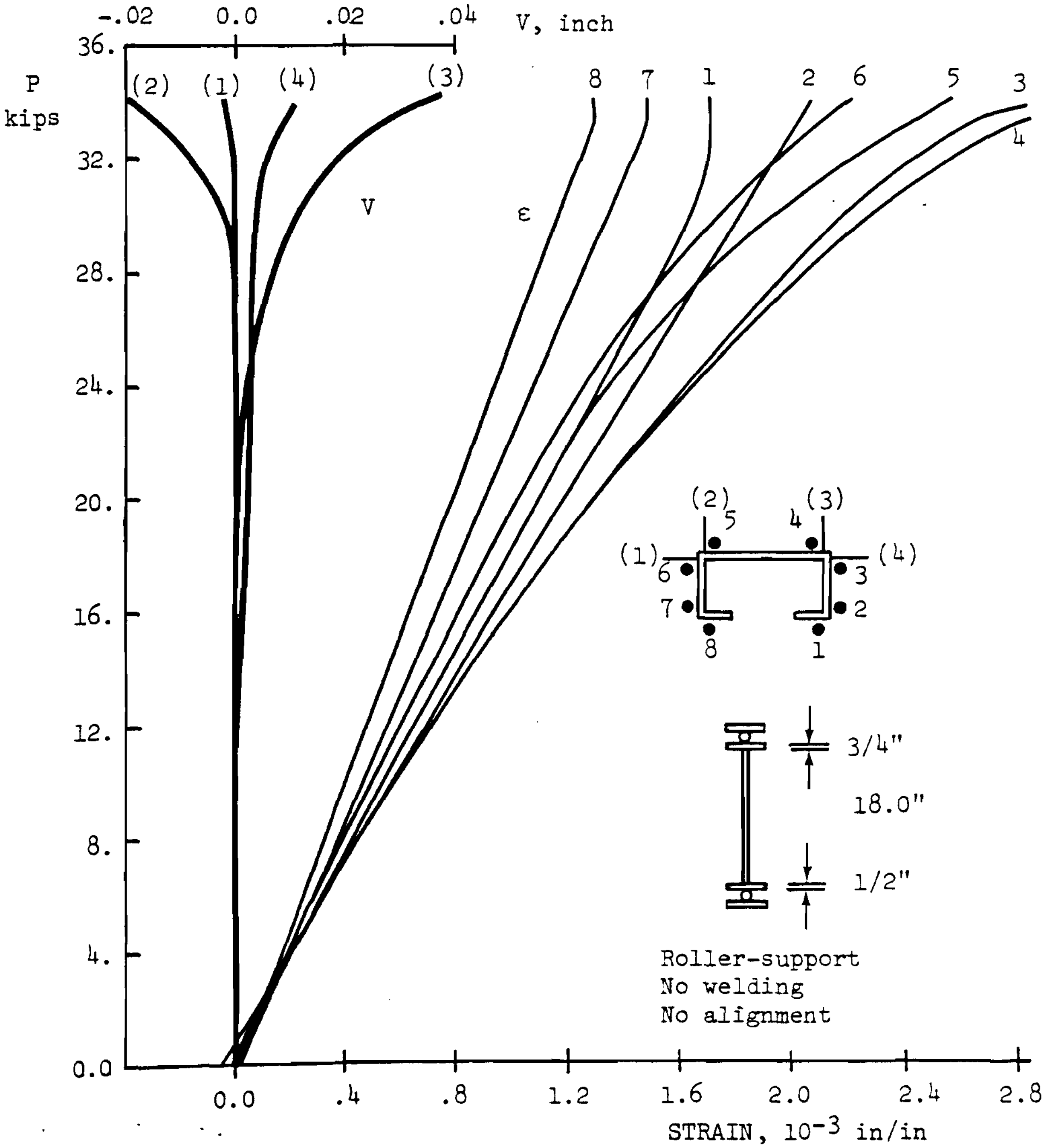

Fig. 9.40 RFC 13 Column D1, L = 19.25"

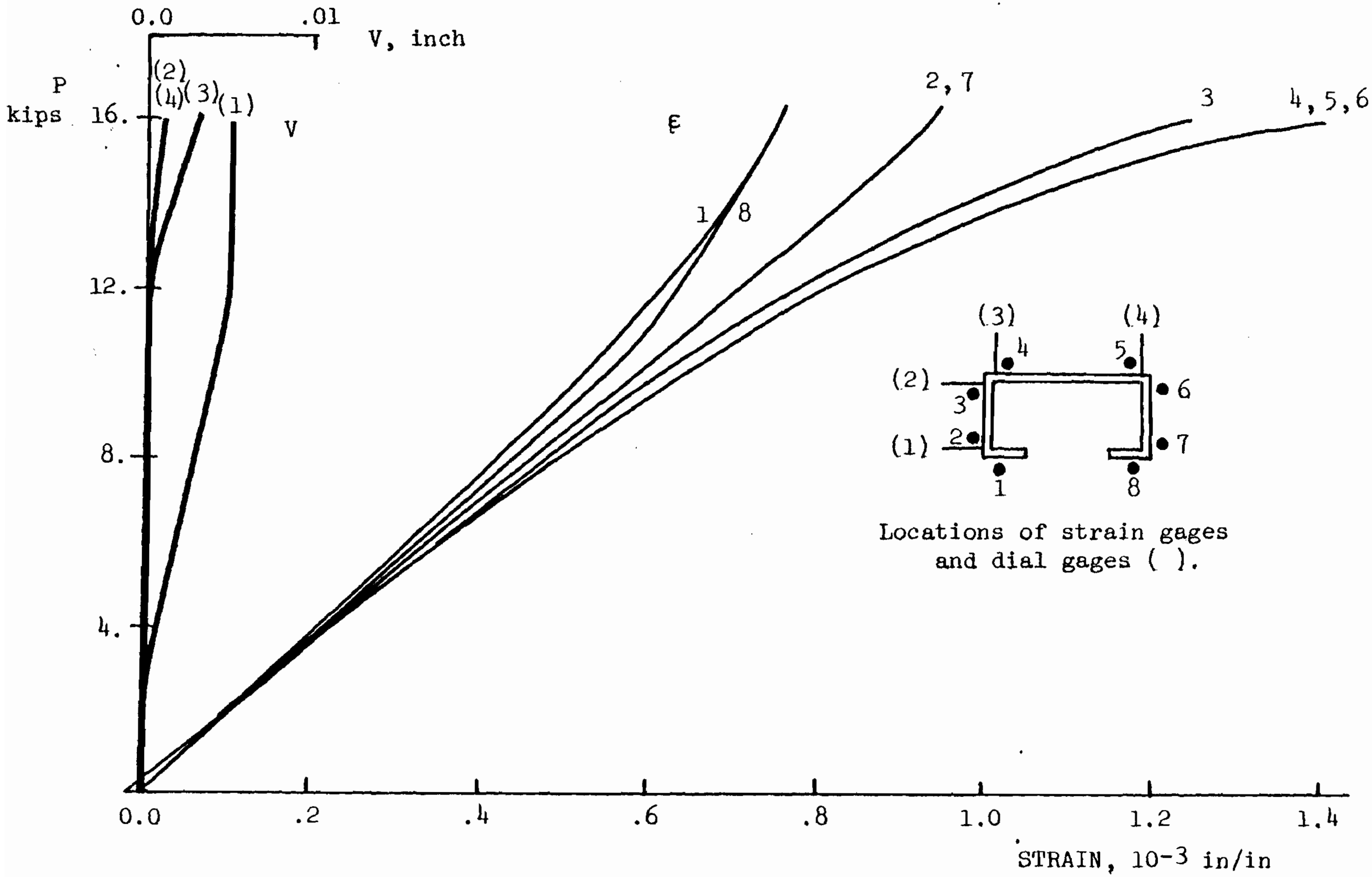

Fig. 9.41 RFC 13, Column D2, L = 21.0"
Failure by local buckling of web near top weld.

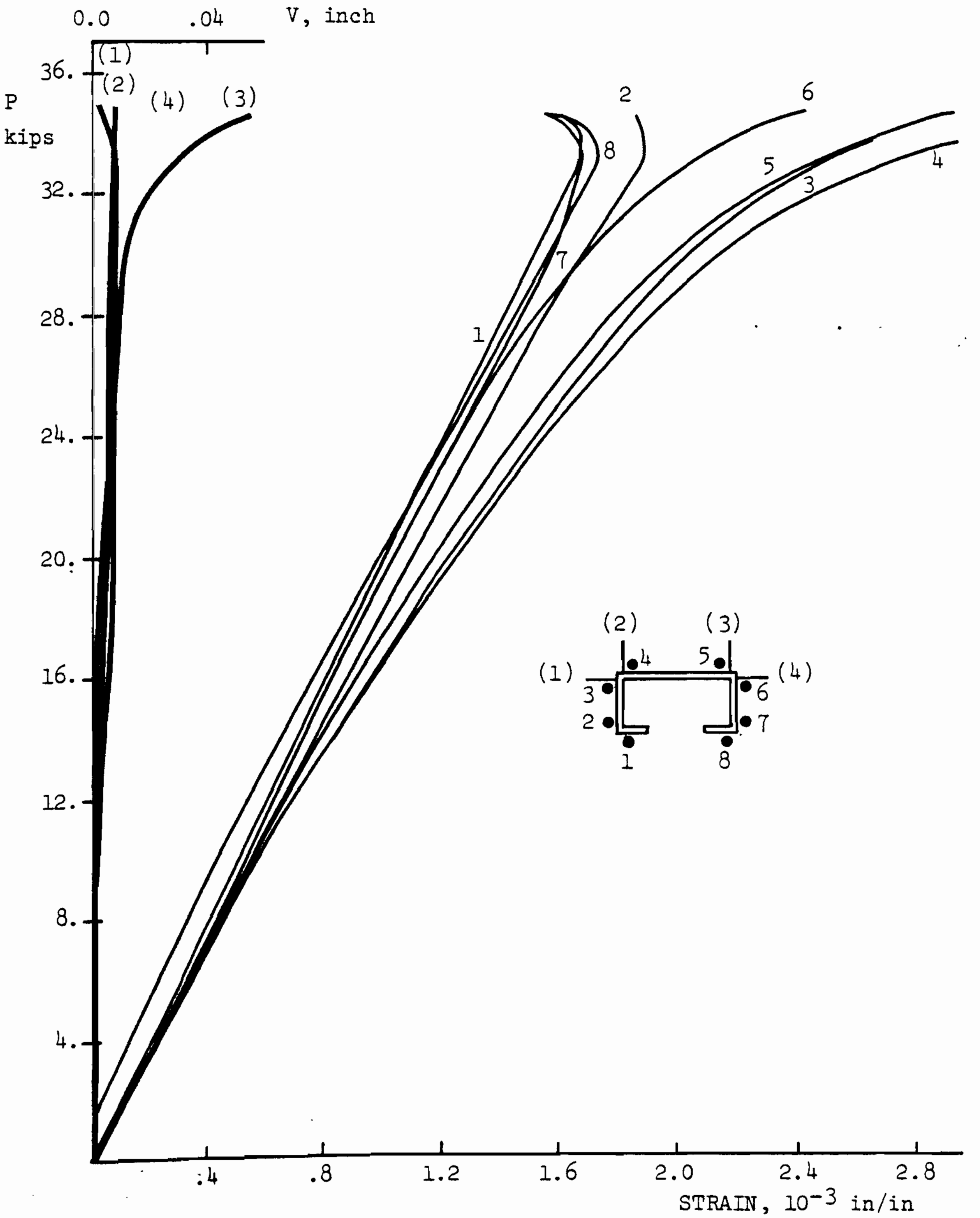

Fig. 9.42 RFC 13 Column D3, L = 27.0"

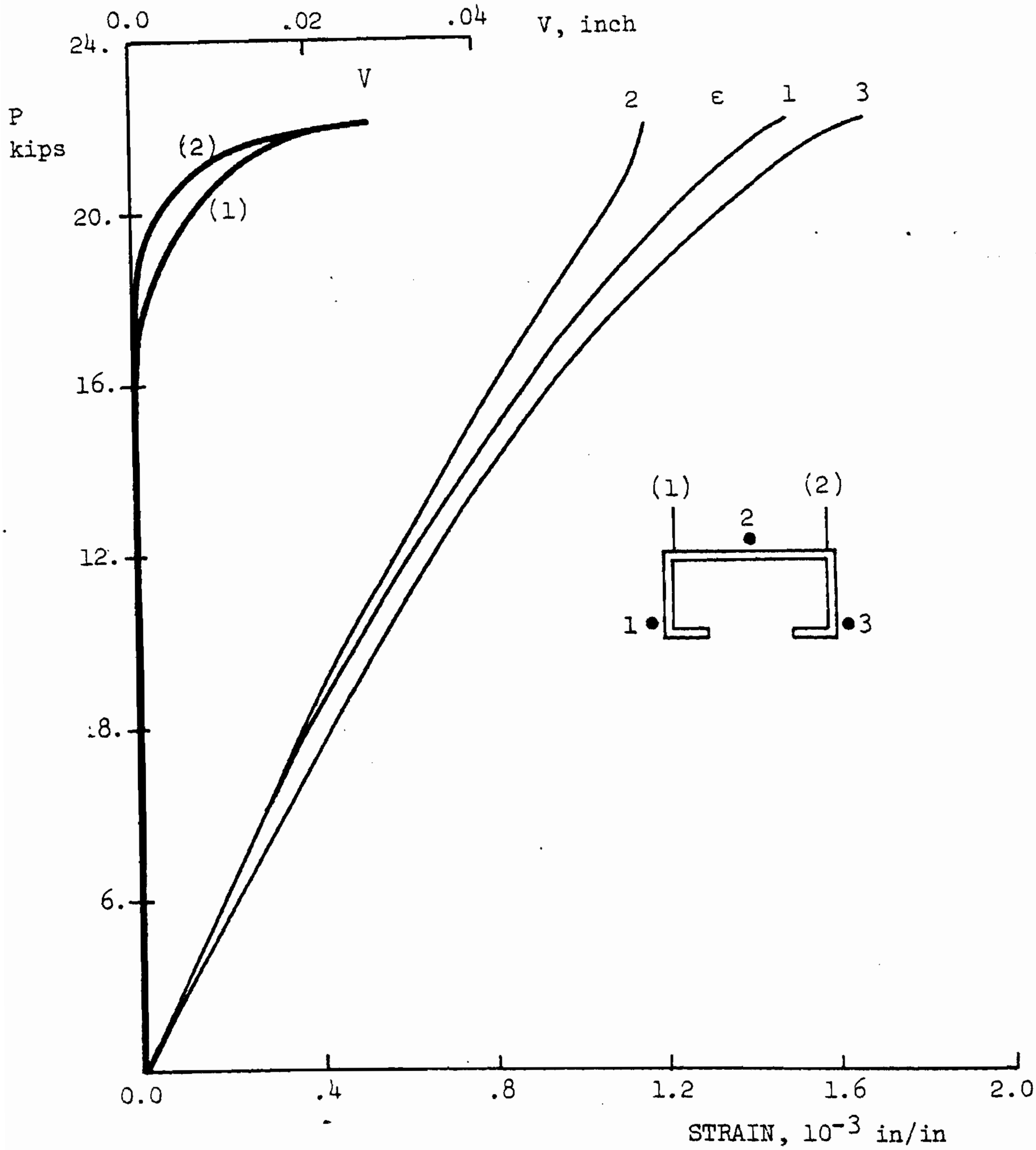

Fig. 9.43 RFC 13 Column D4, L = 27.0"

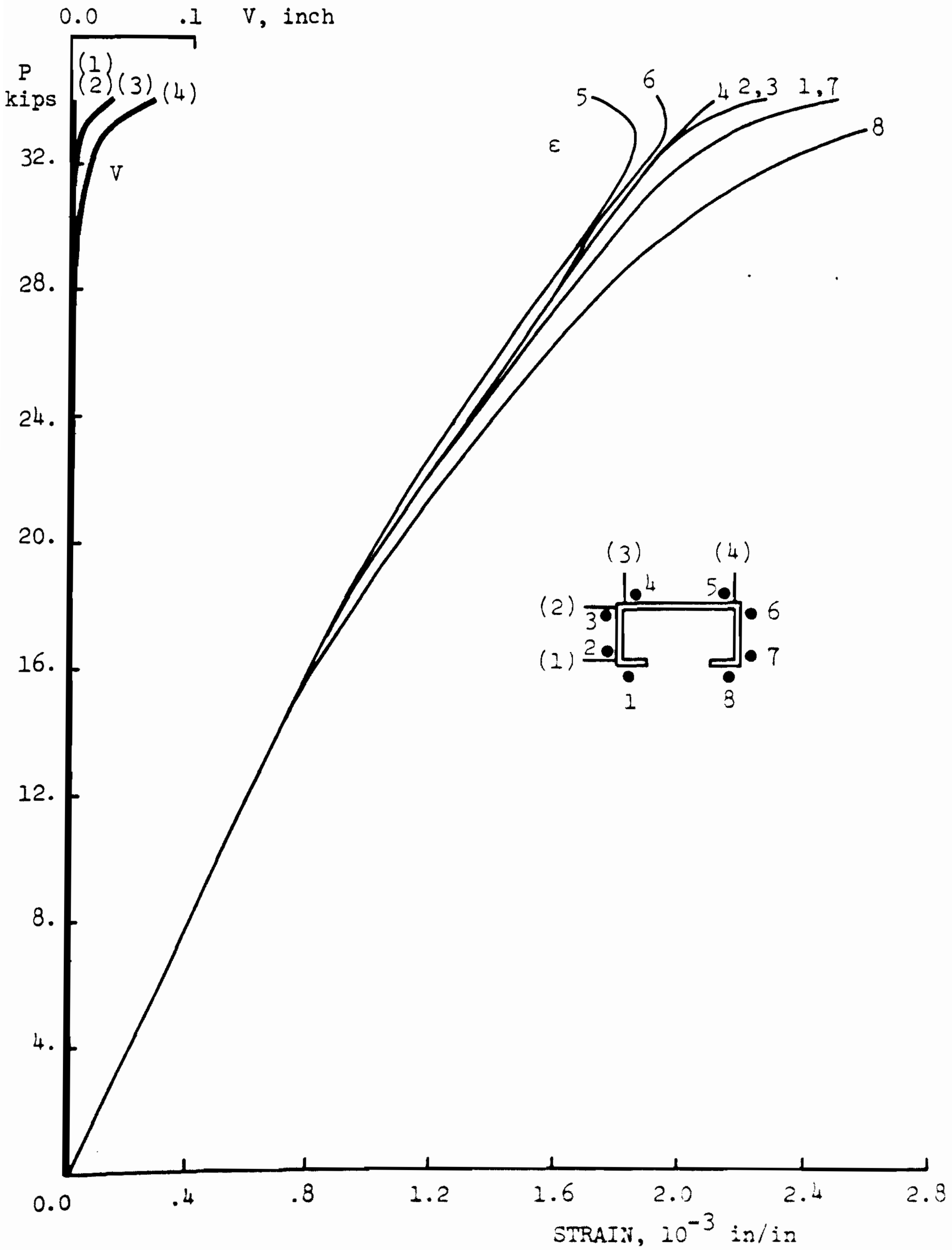

Fig. 9.44 RFC 13 Column D5, L = 33.0".

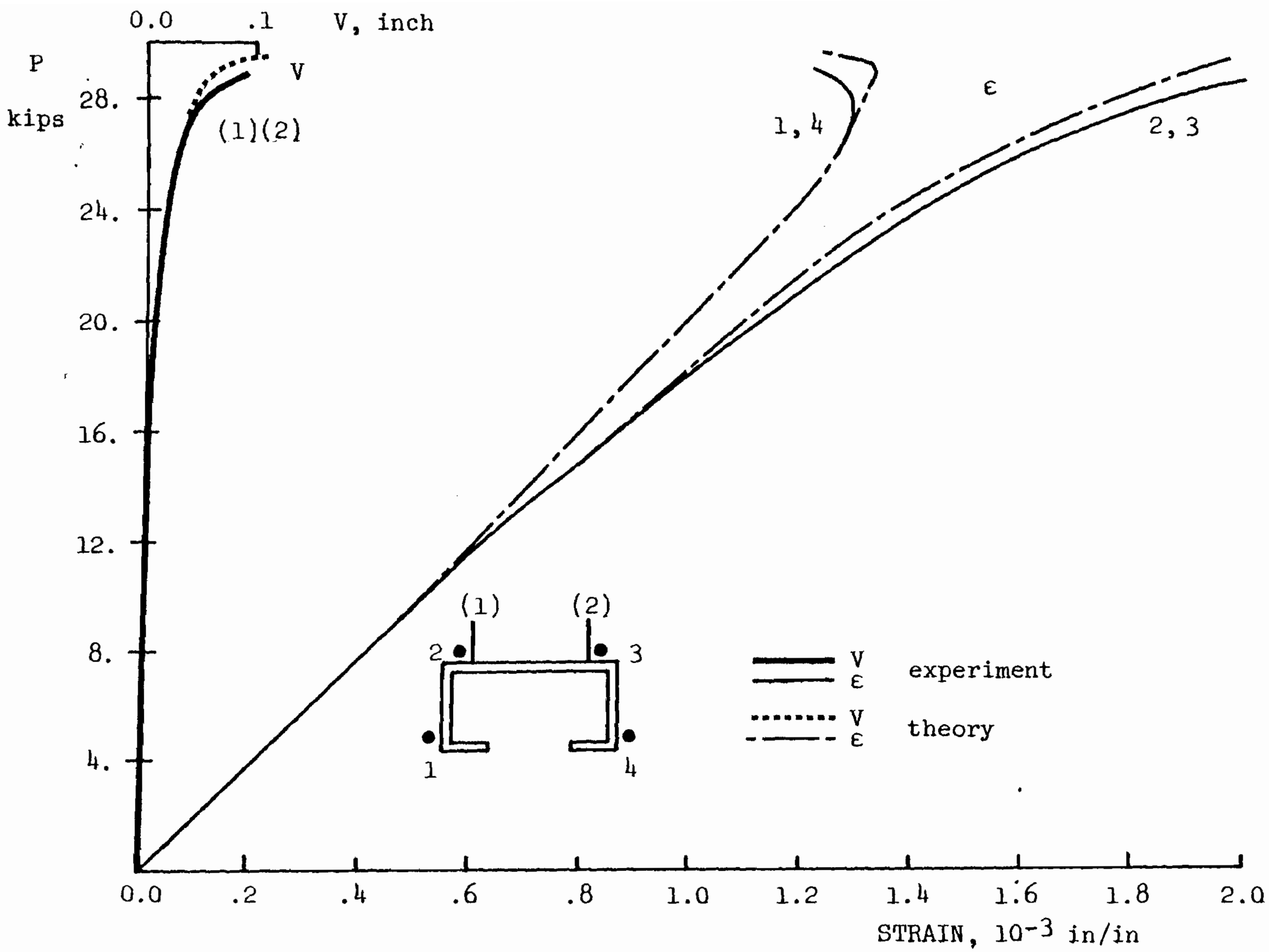

Fig. 9.45 RFC 13 Column D6, L = 39.0"

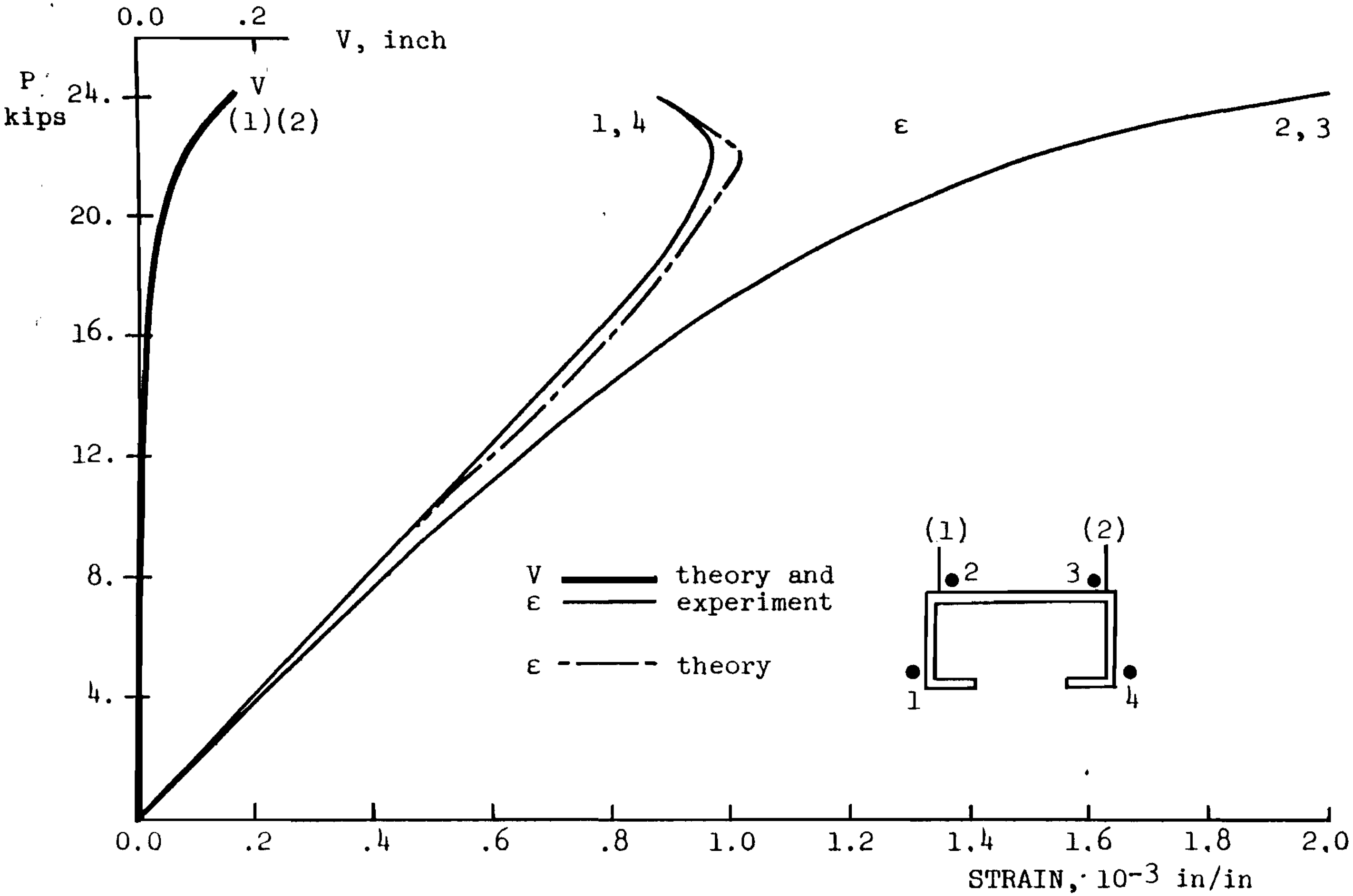

Fig. 9.46 RFC13 Column D7, L = 45.0"

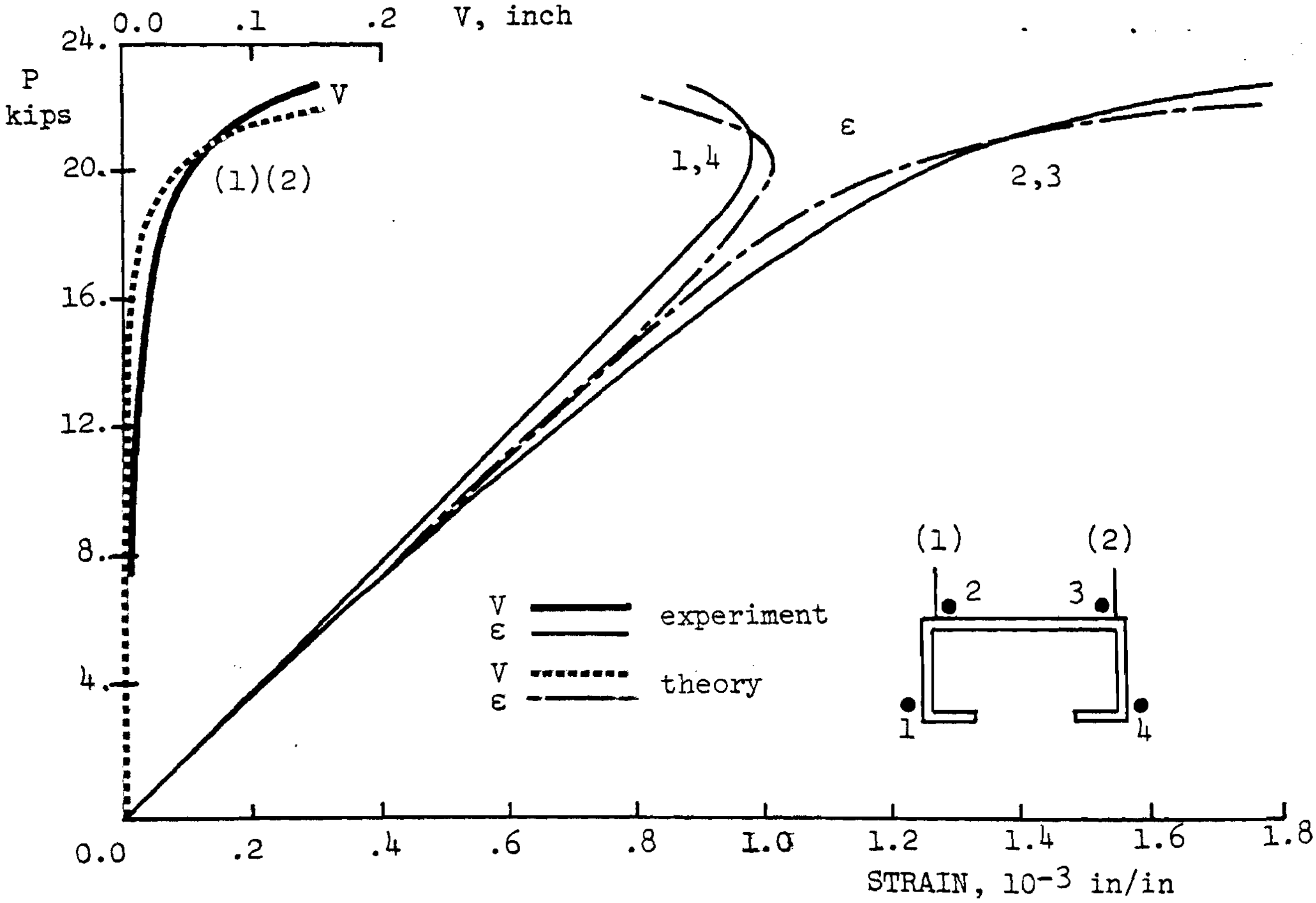

Fig. 9.47 RFC13 Column D8, L = 51.0"

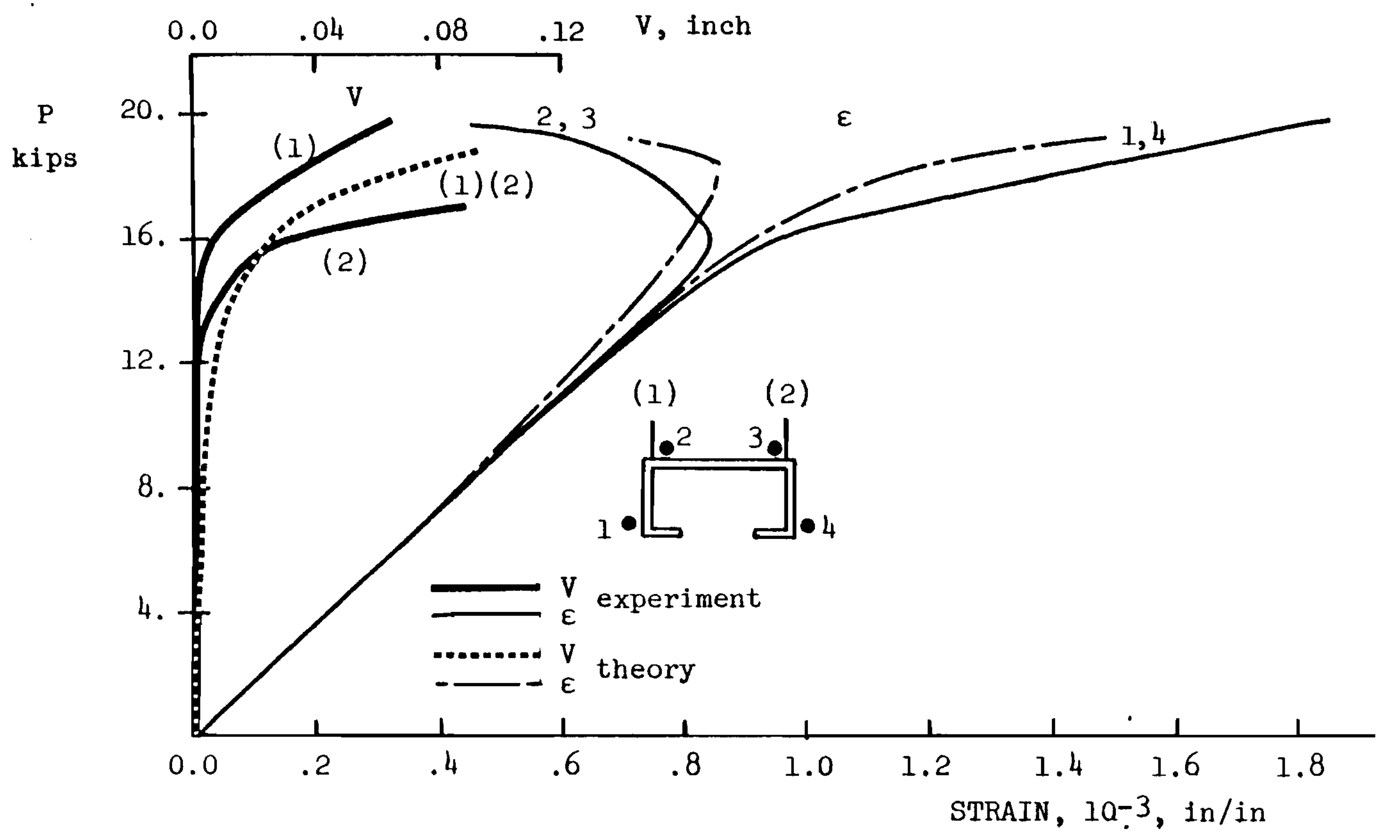

Fig. 9.48 Column D9, L = 57.0"

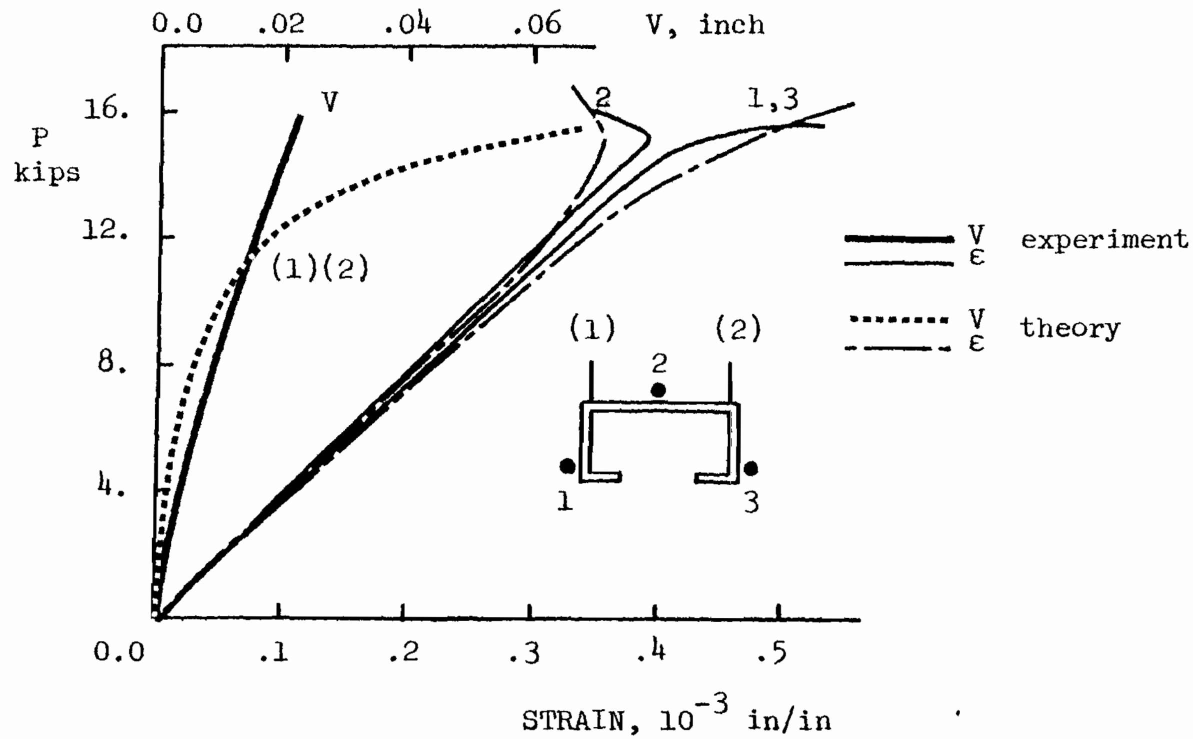

Fig. 9.49 RFC 13 Column D10, L = 63.0"

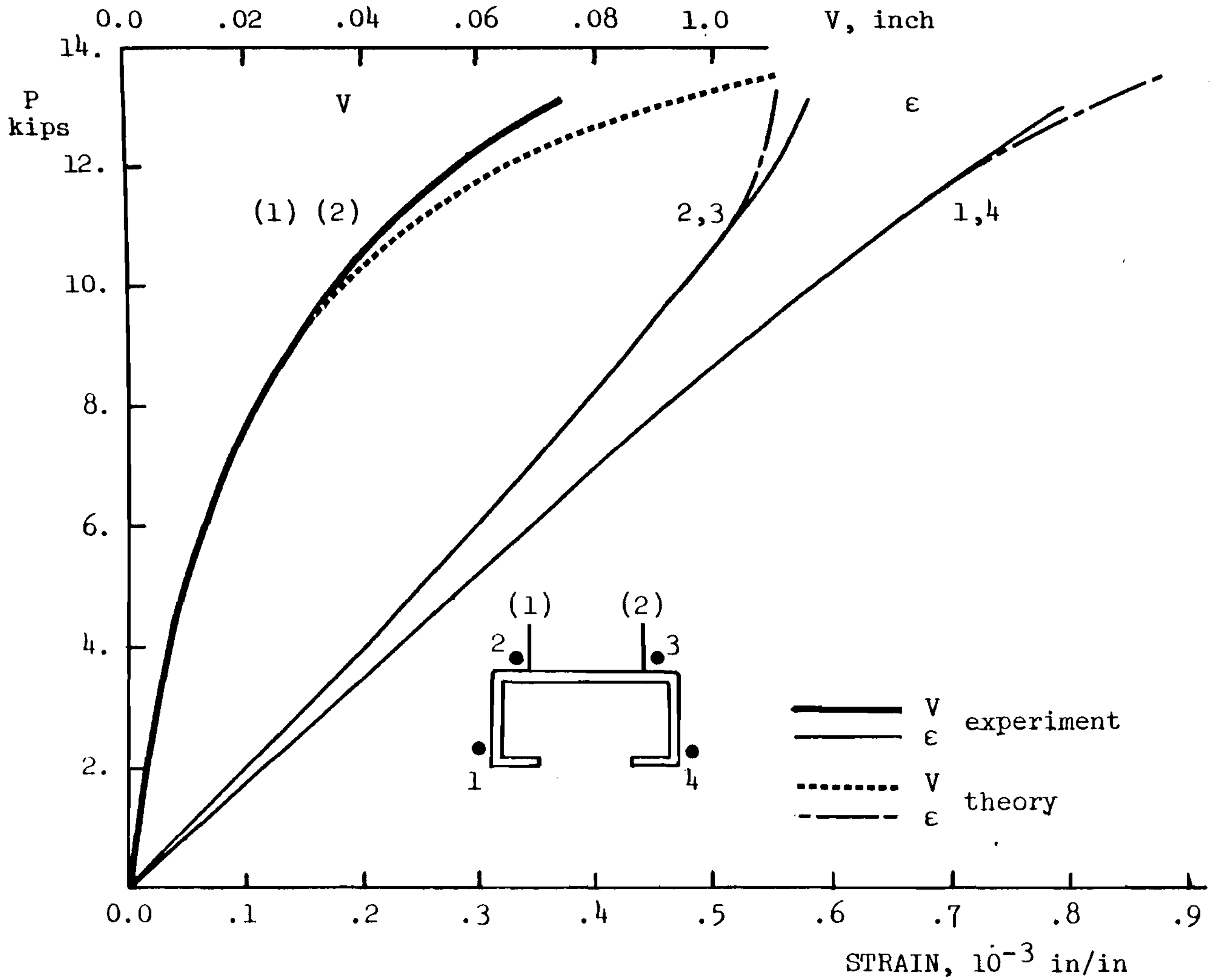

Fig. 9.50 RFC 13 Column D11, L = 69.0"

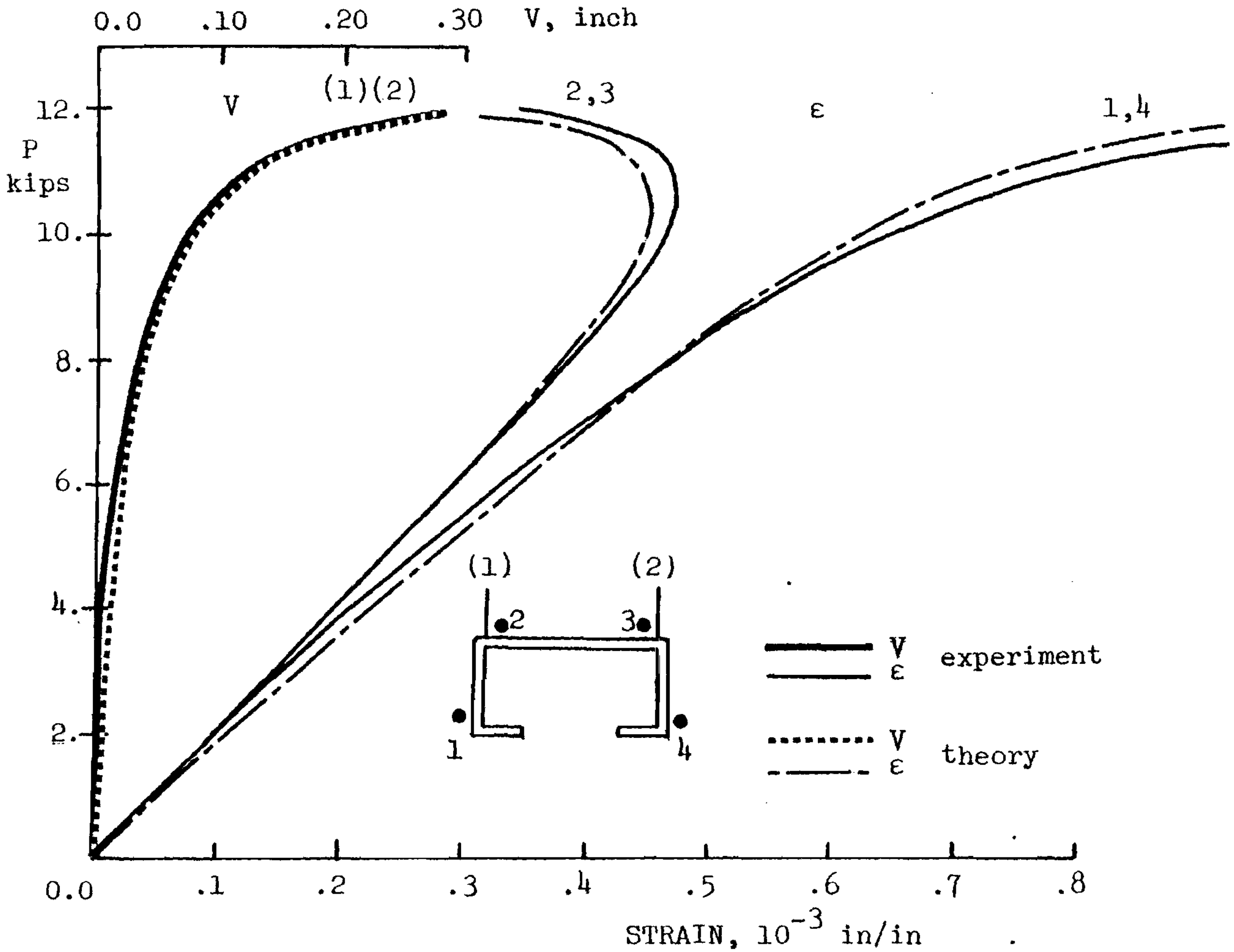

Fig. 9.51 RFC 13 Column D12, L = 75.0".

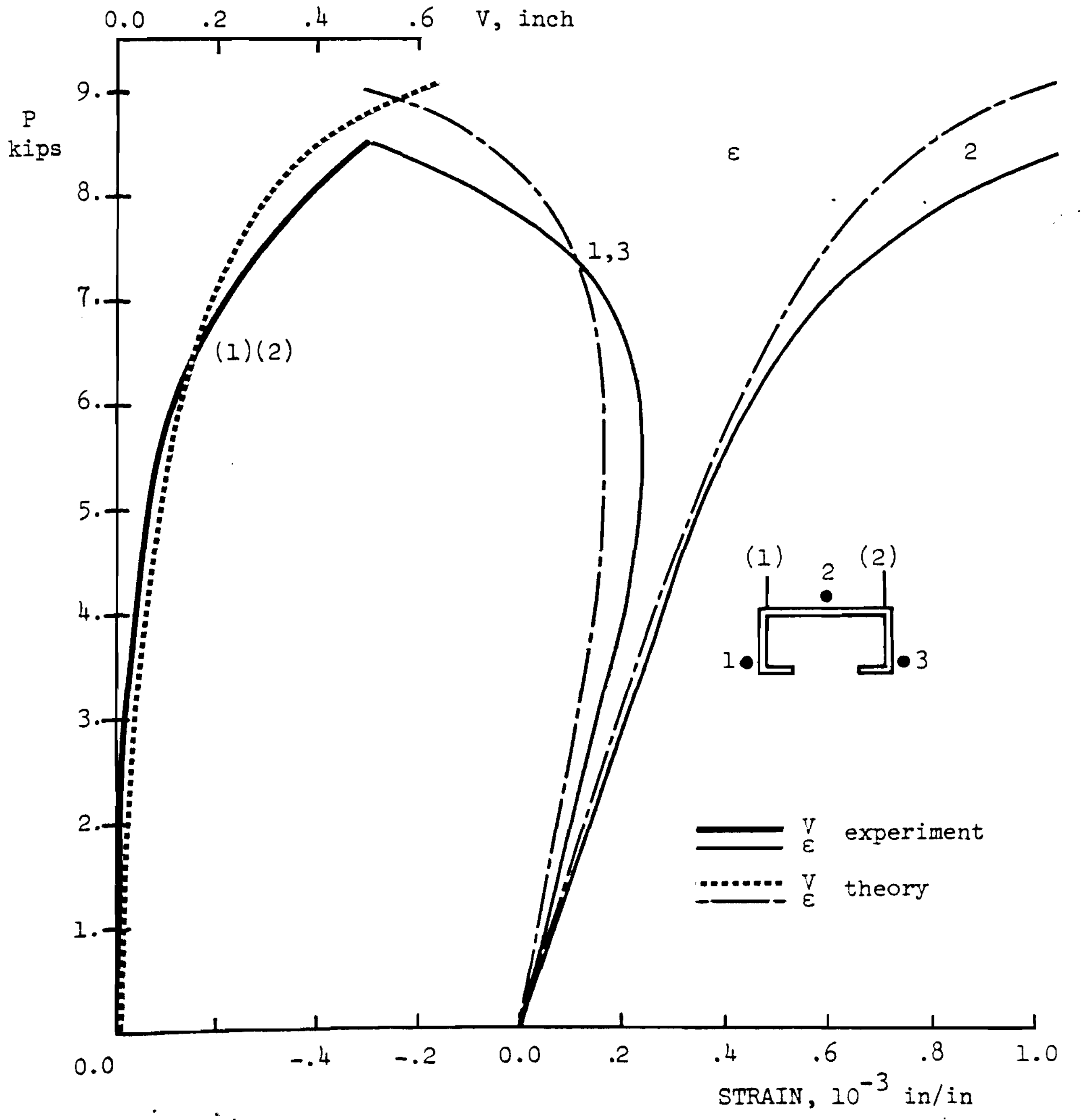

Fig. 9.52 RFC 13 Column D13, L = 87.0".

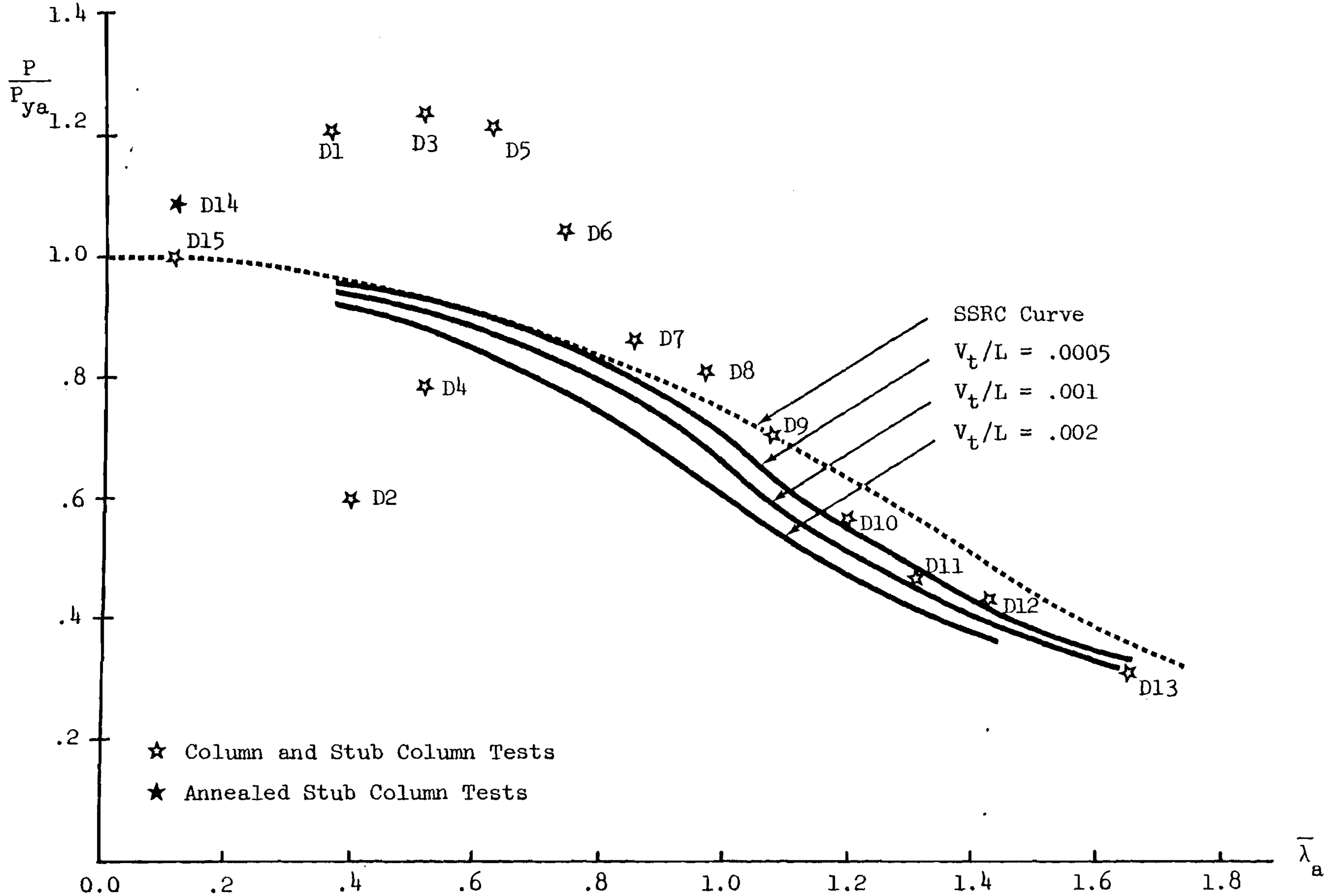

Fig. 9.53 RFC13 Column Tests; average yield strength

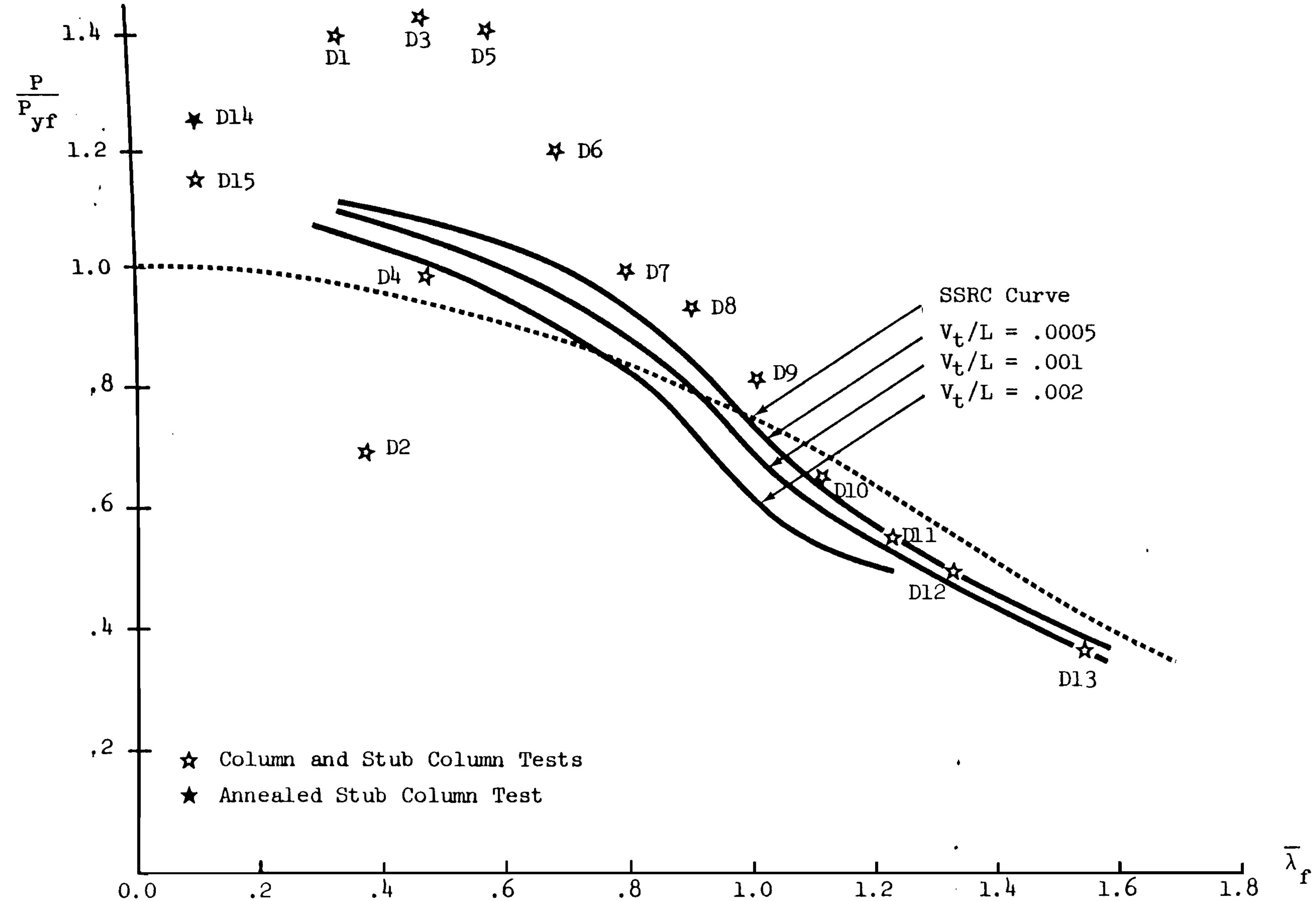

Fig. 9.54 RFC 13 Column Tests; yield strength of flat

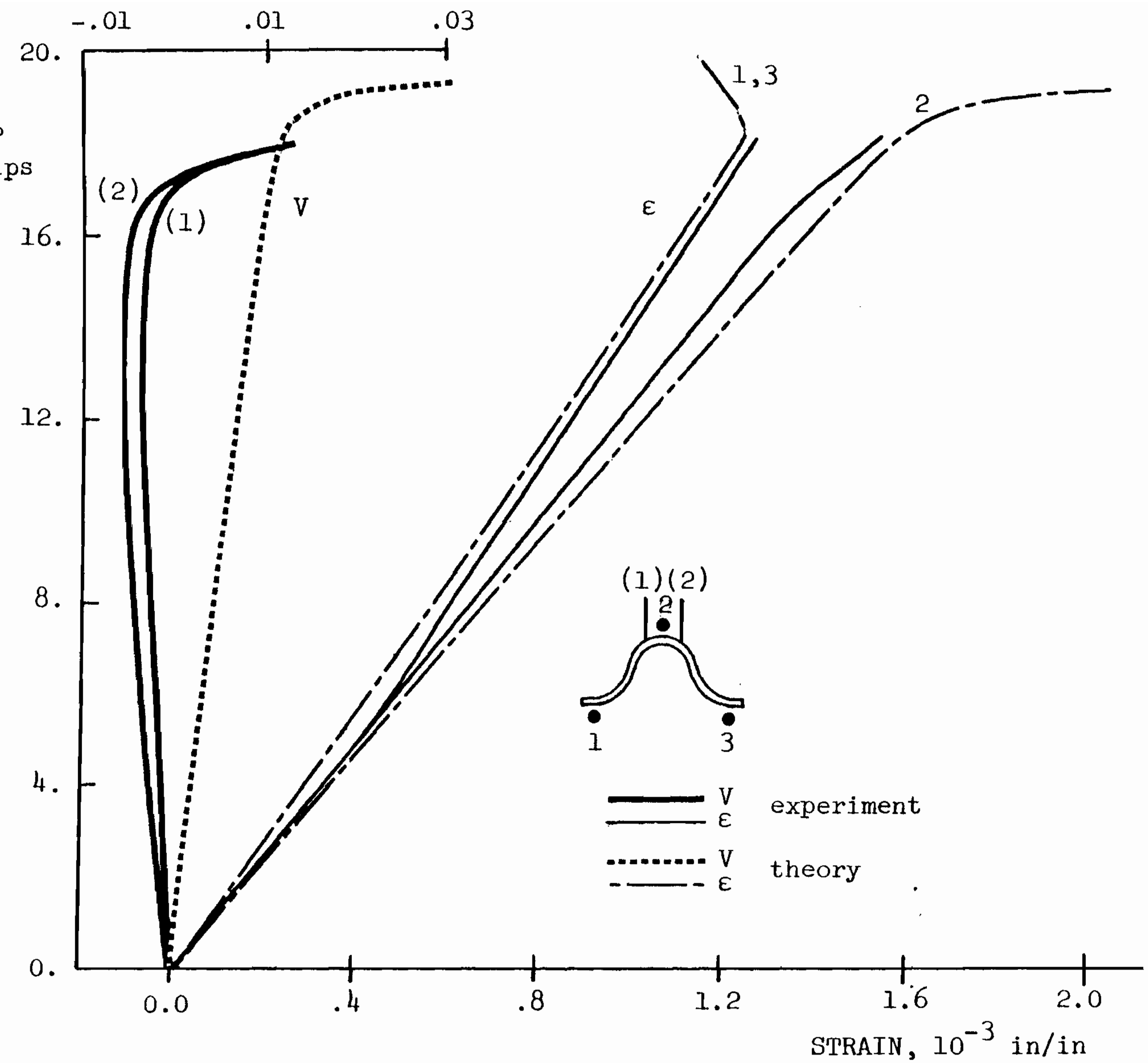

Fig. 9.55 H11 Column E1, L = 19.4".

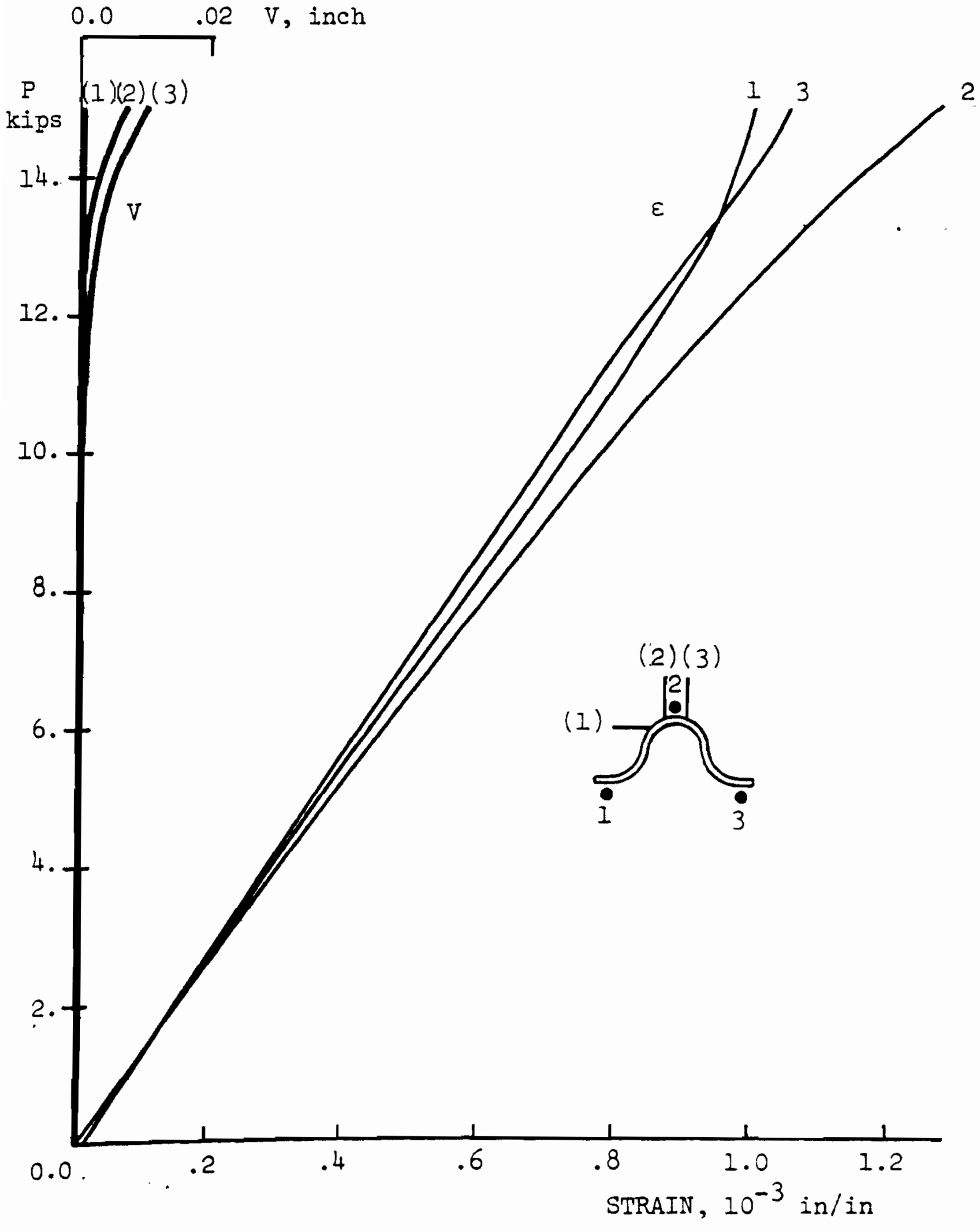

Fig. 9.56 H11 Column E2, L = 23.0".

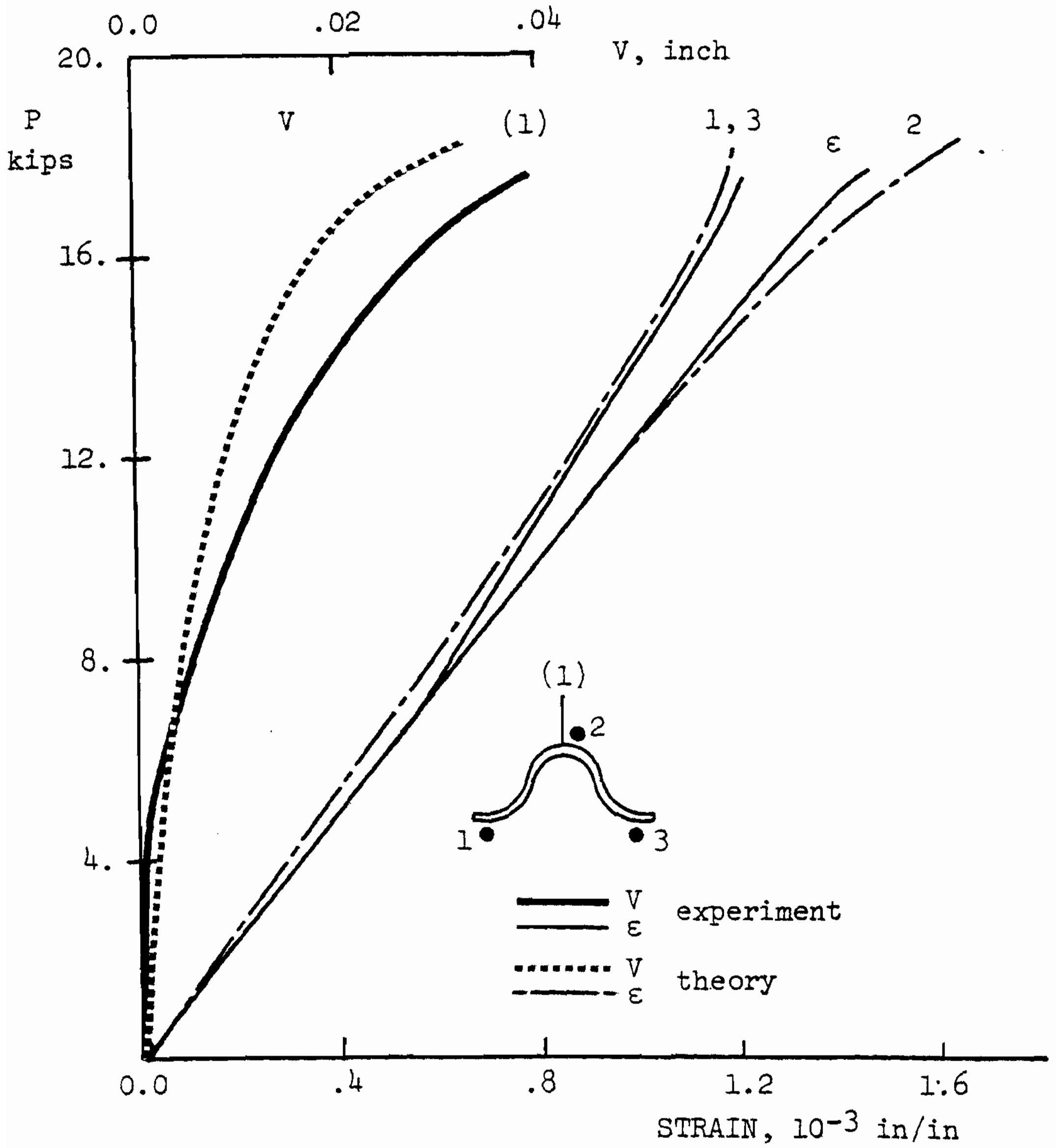

Fig. 9.57 H11 Column E3, L = 28.0"

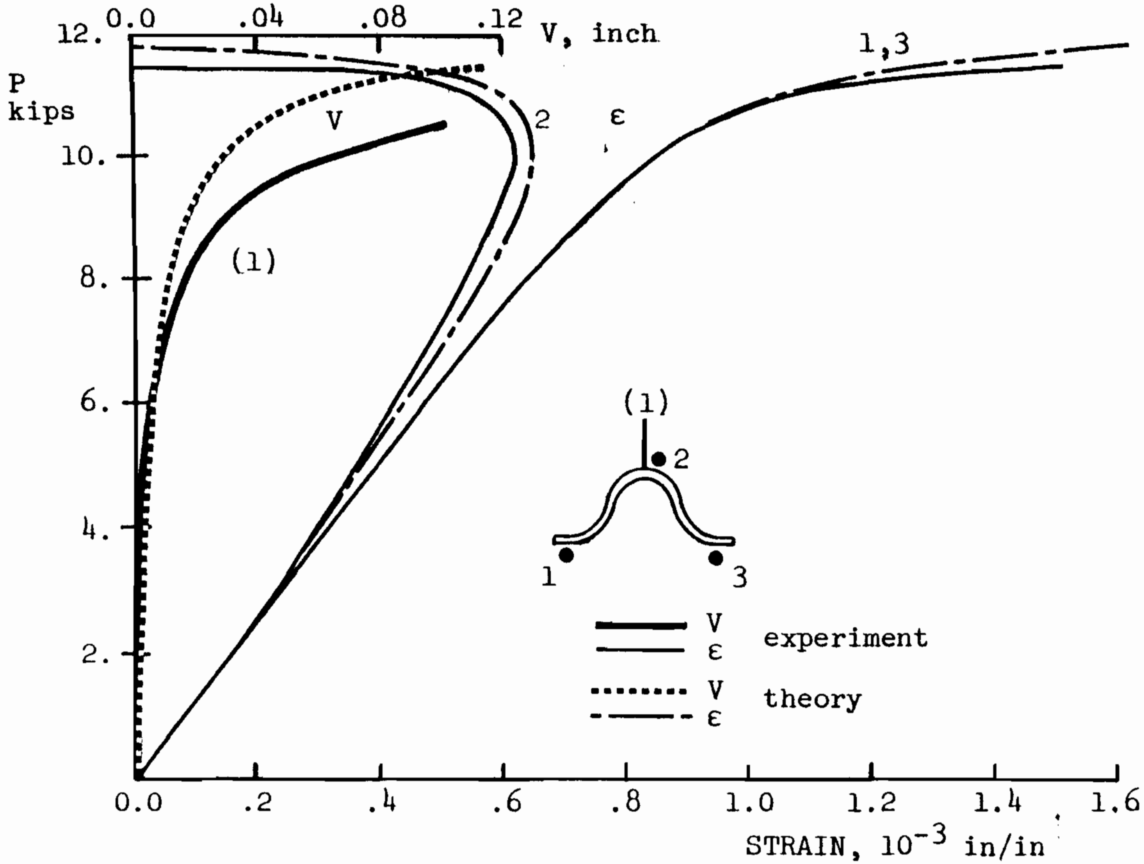

Fig. 9.58 H11 Column E4, L = 39.0"

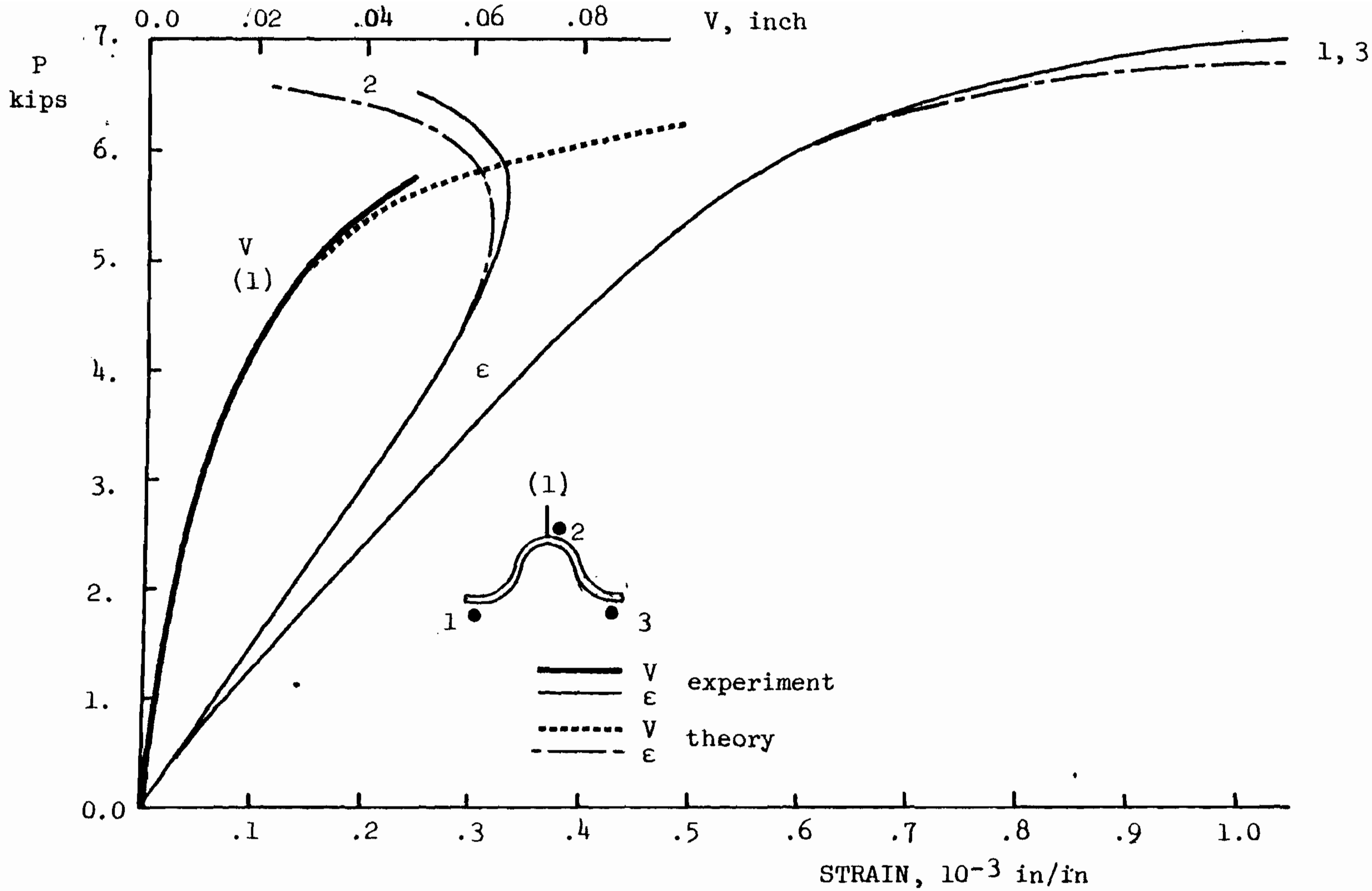

Fig. 9.59 H11 Column E5, L = 51.0"

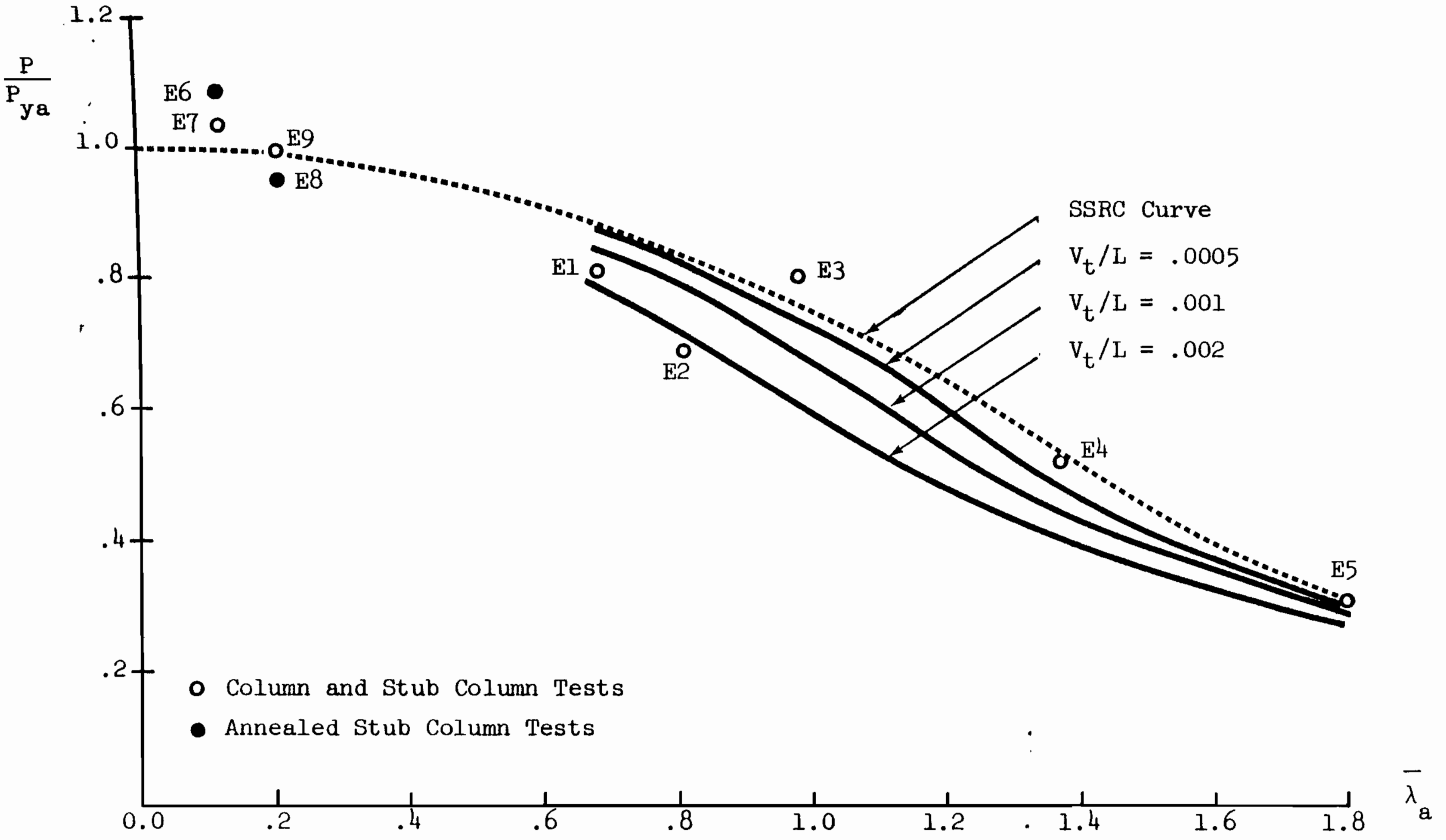

Fig. 9.60 H11 Column Tests; average yield strength

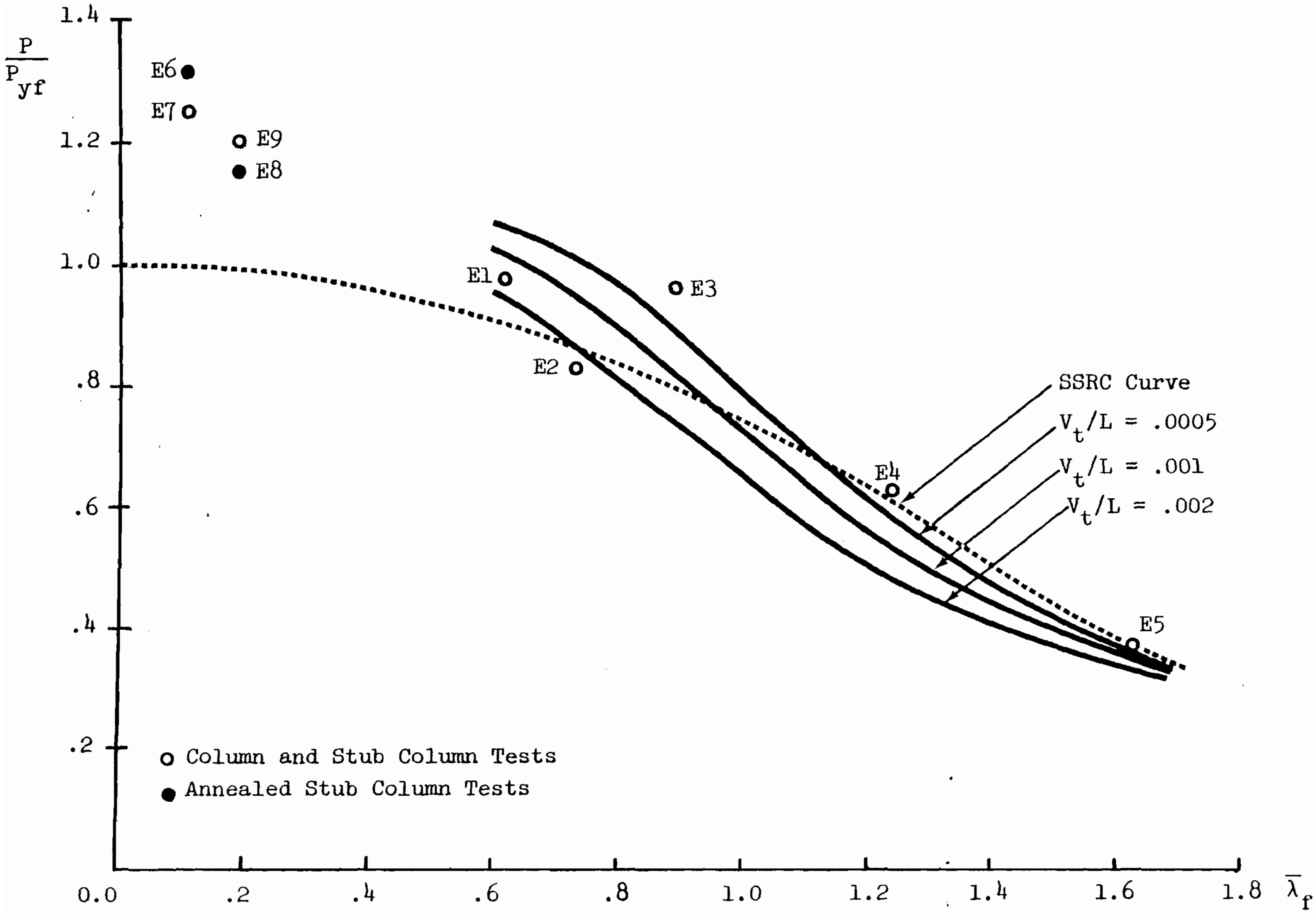

Fig. 9.61 H11 Column Tests; yield strength of flat.

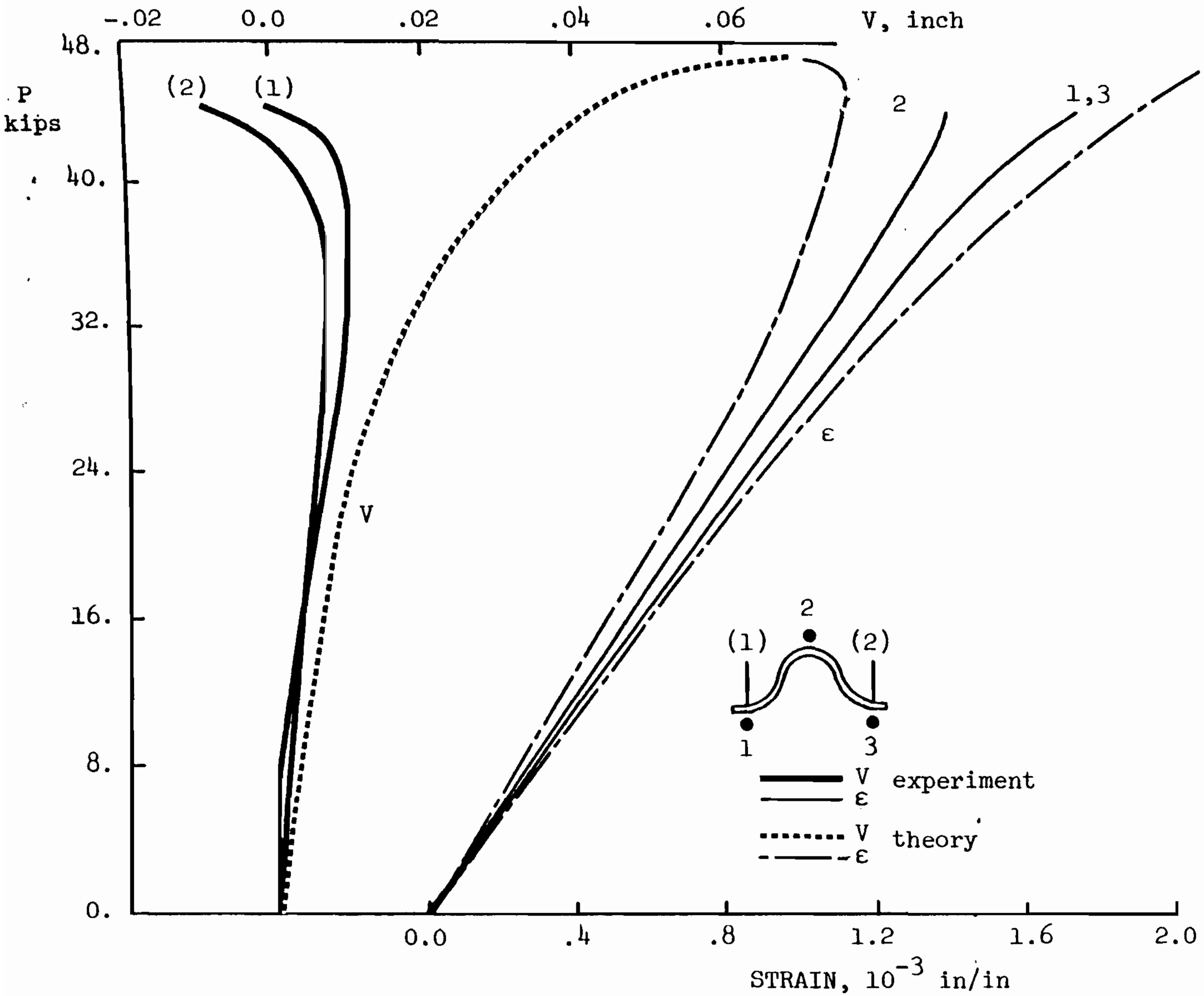

Fig. 9.62 H7 Column F1, L = 31.0".

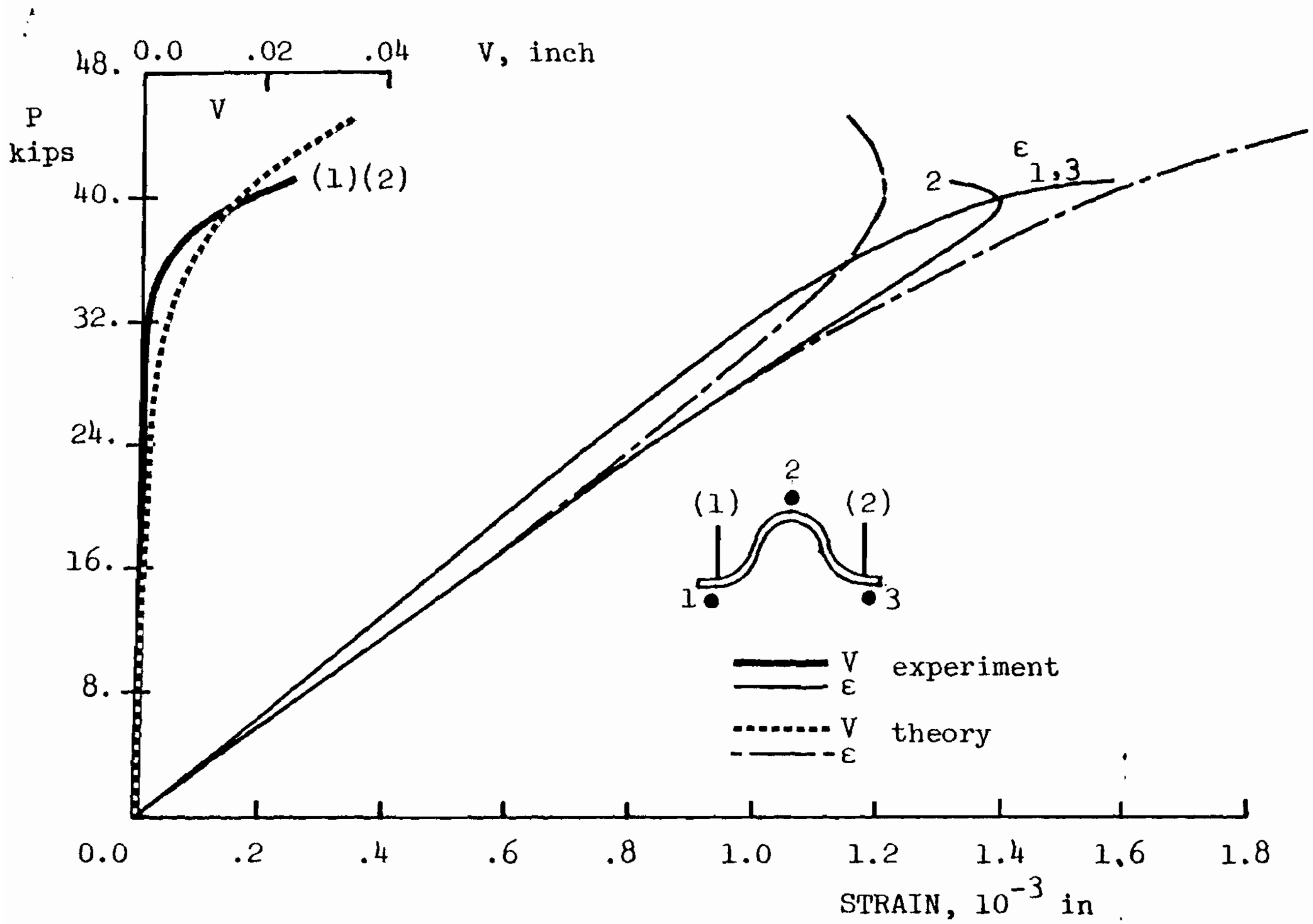

Fig. 9.63 H 7 Column F 2, L = 39.0".

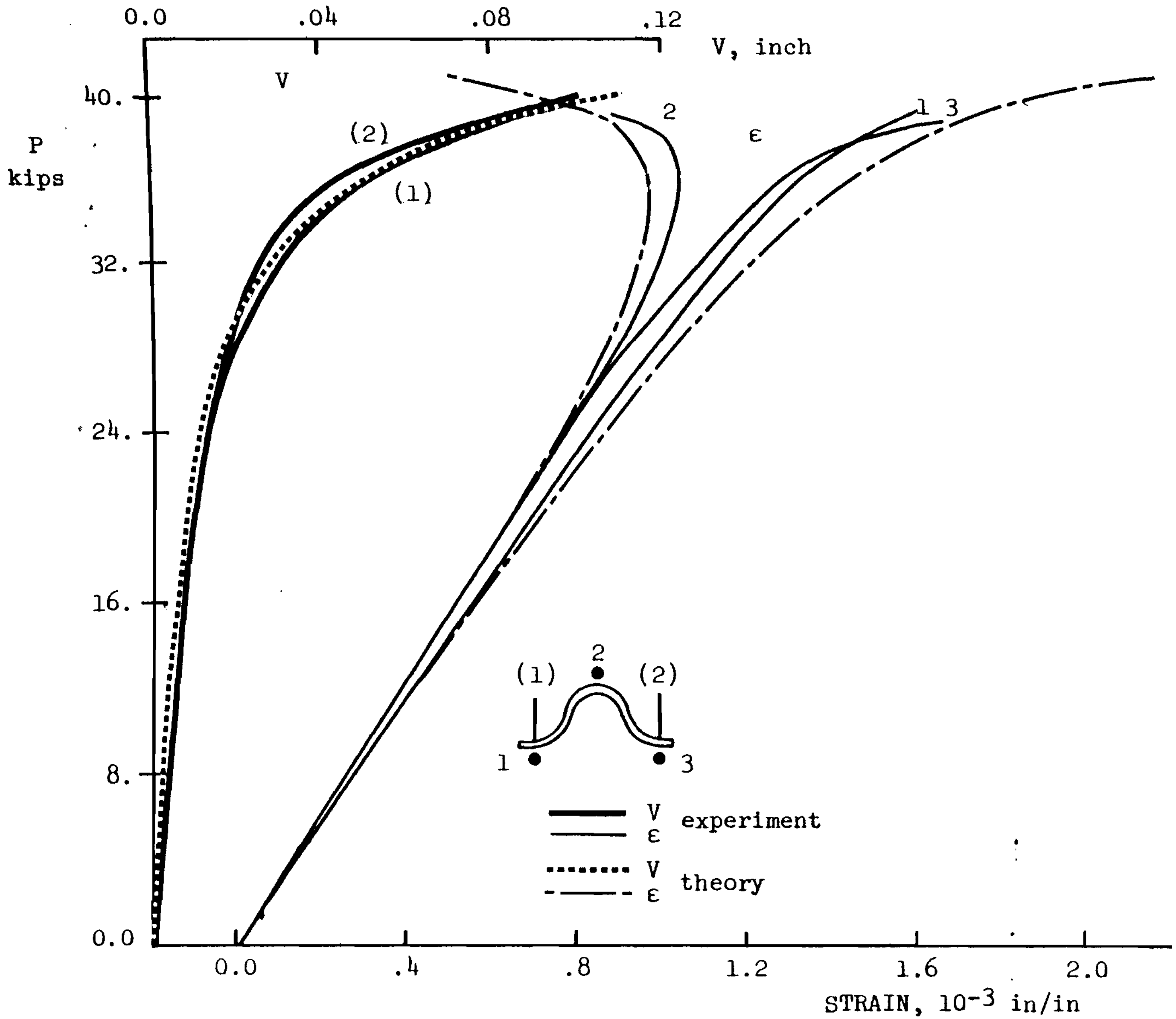

Fig. 9.64 H7 Column F3, L = 42.4"

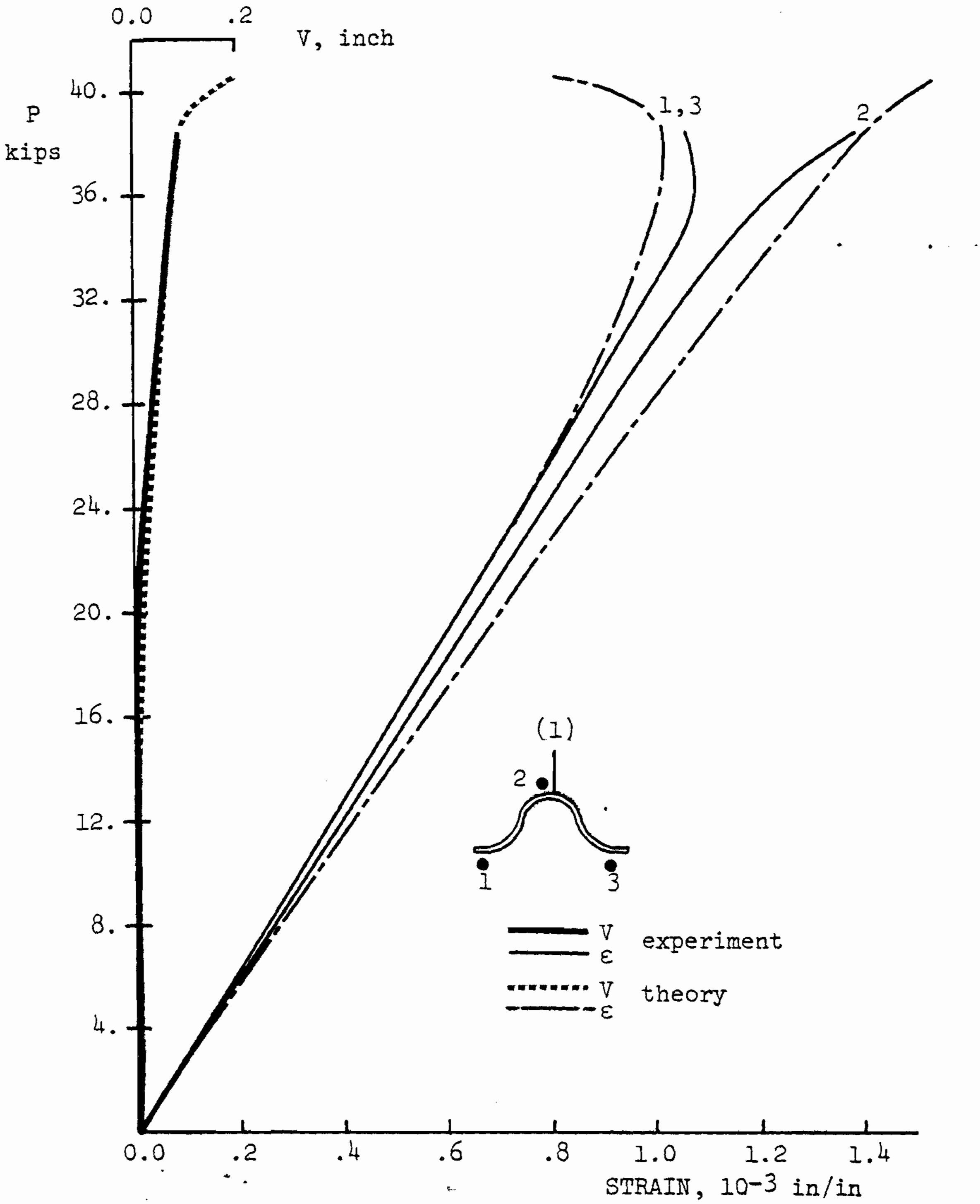

Fig. 9.65 H7 Column F4, L = 45.0"

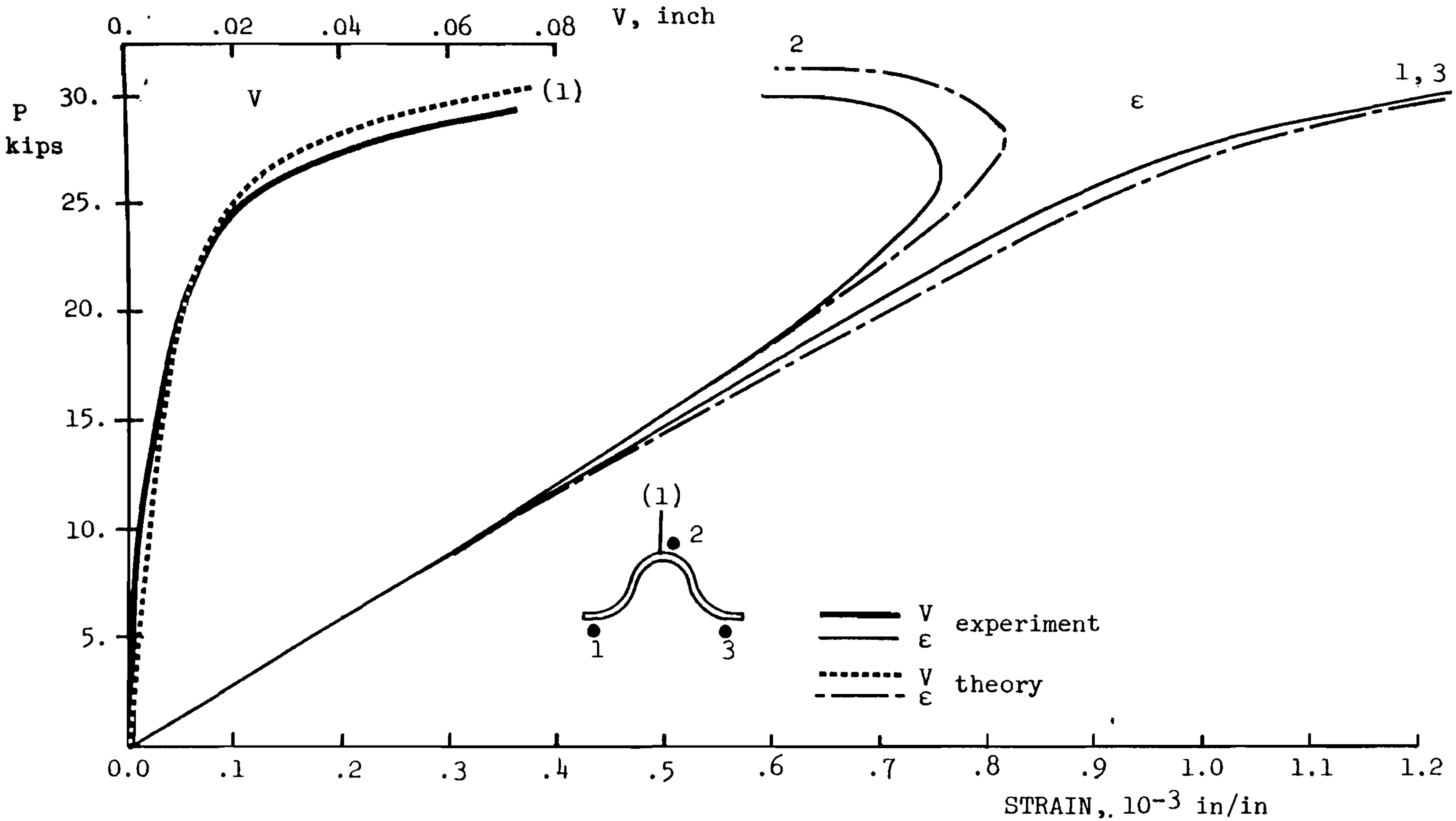

Fig. 9.66 H7 Column F5, L = 51.0"

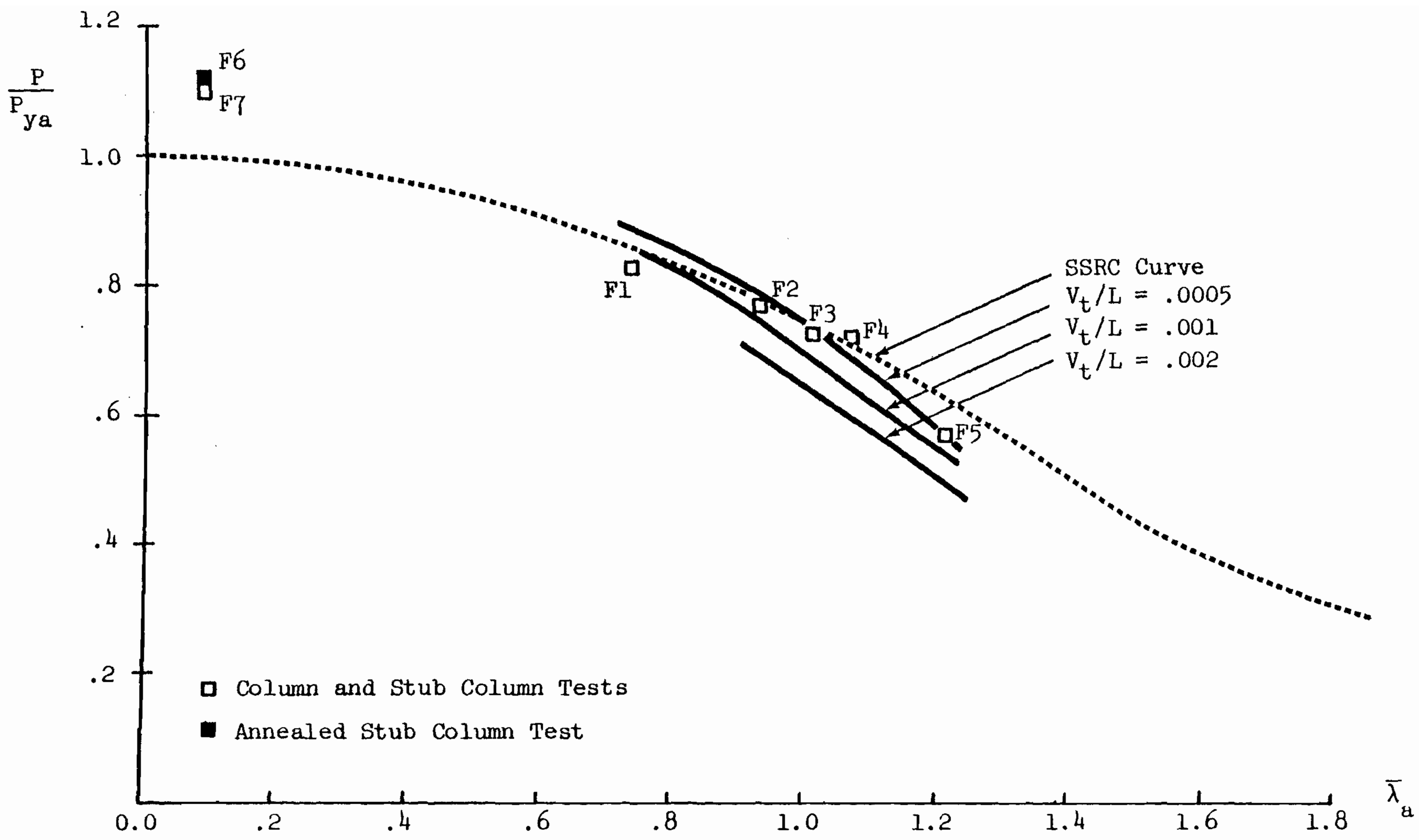

Fig. 9.67 H7 Column Tests; average yield strength

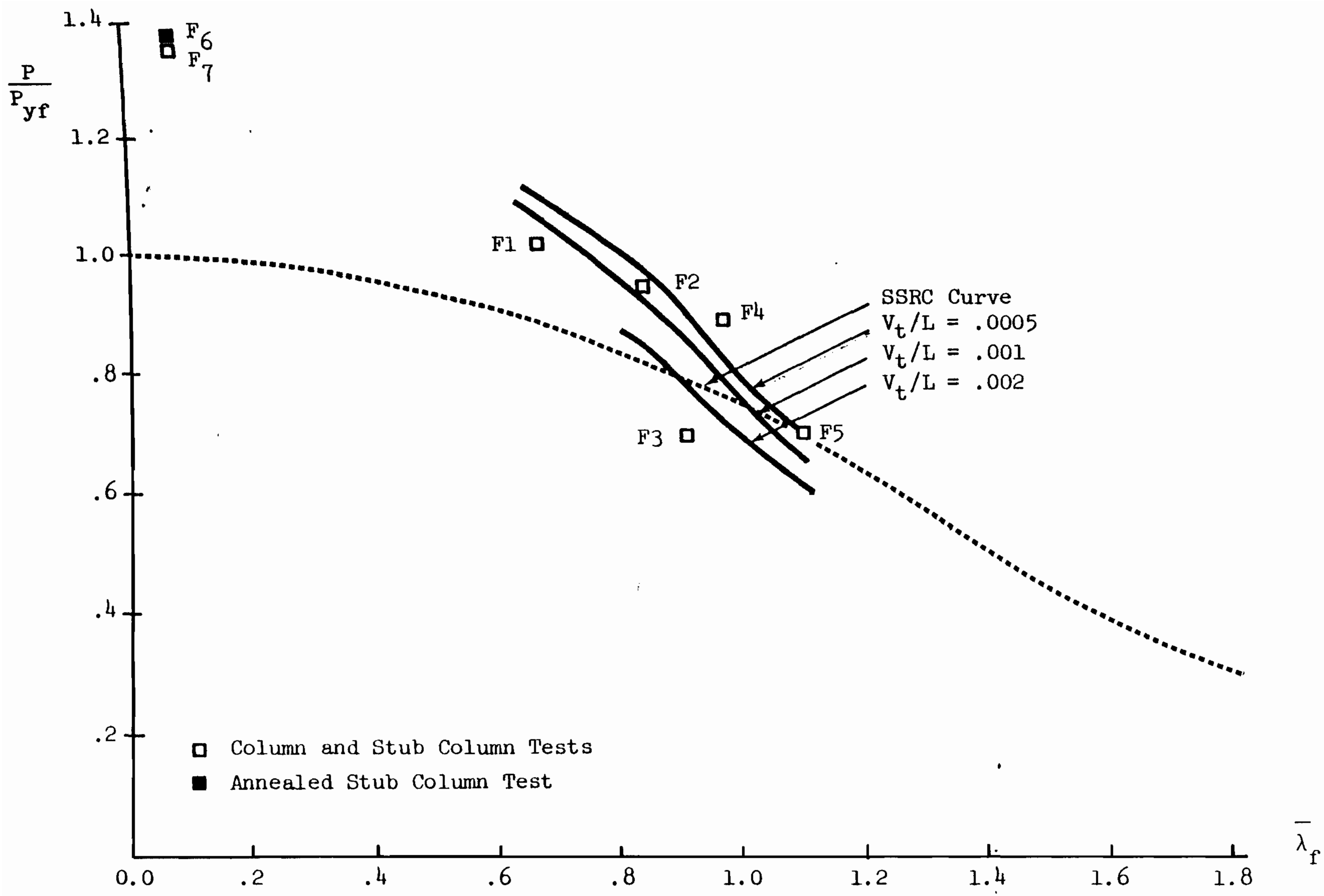

Fig. 9.68 H7 Column Tests; yield strength of flat

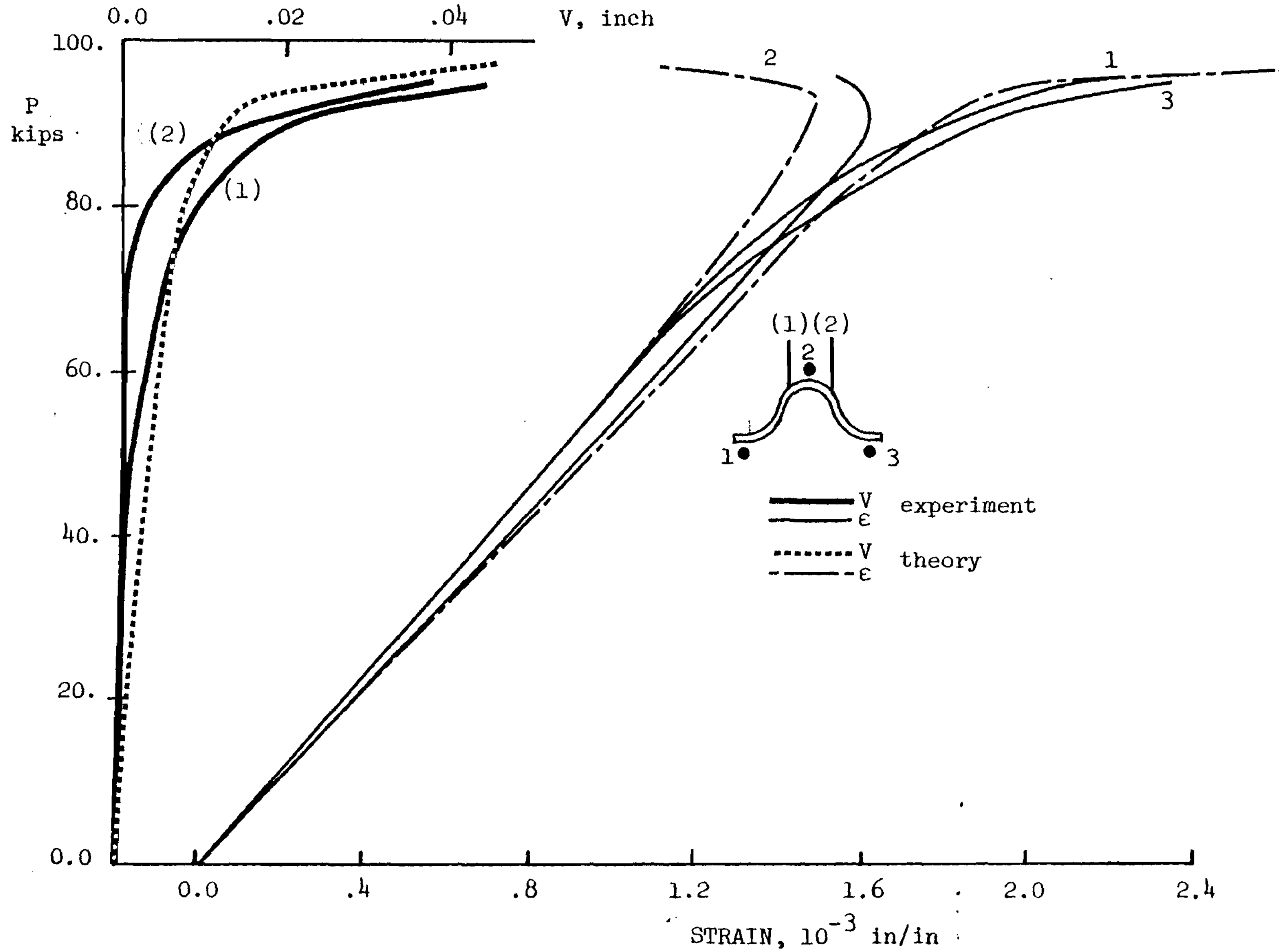

Fig. 9.69 HT Column G1, L = 27.9".

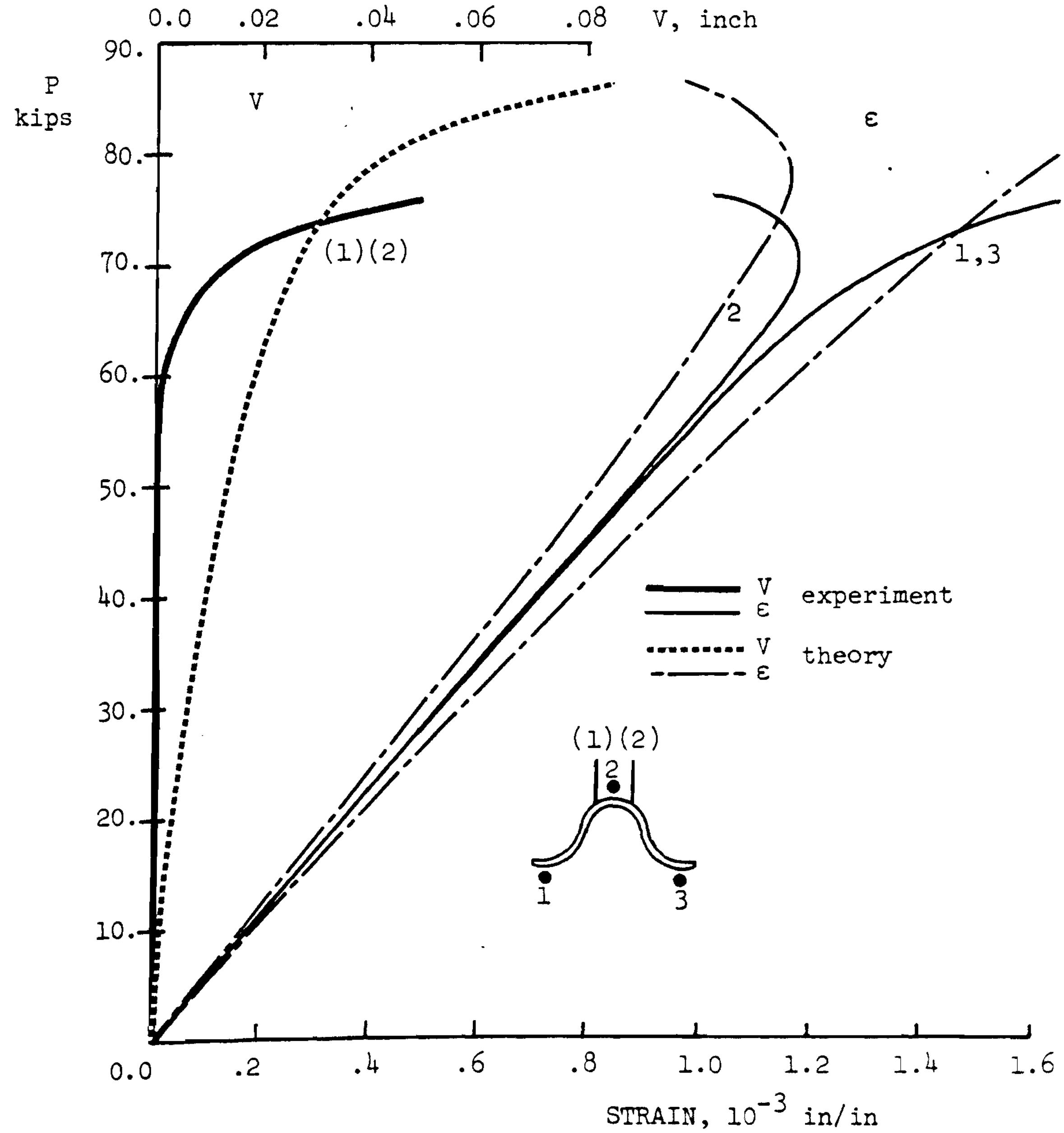

Fig. 9.70 HT Column G2, L = 39.0".

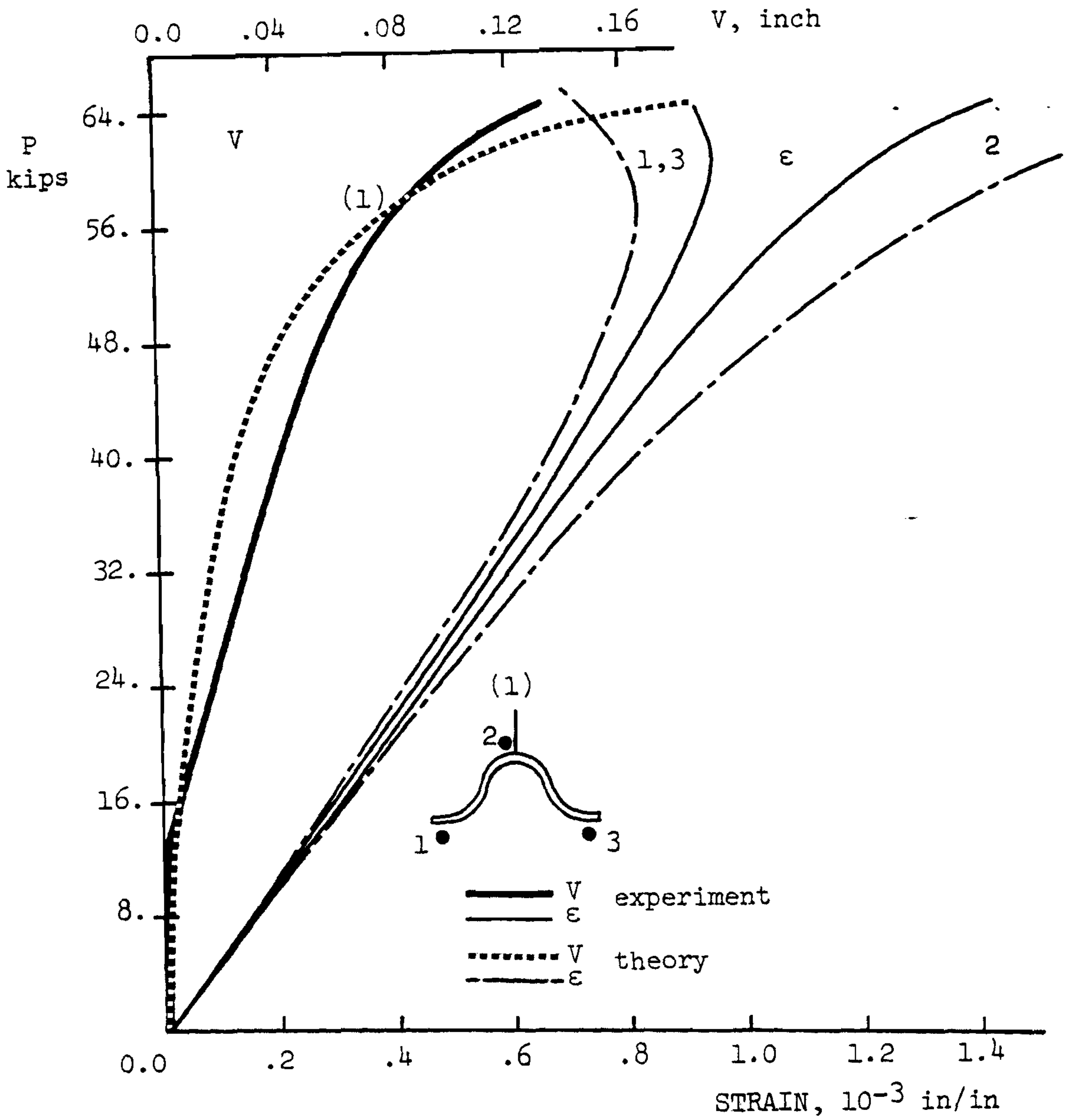

Fig. 9.71 HT Column G3, L = 51.0".

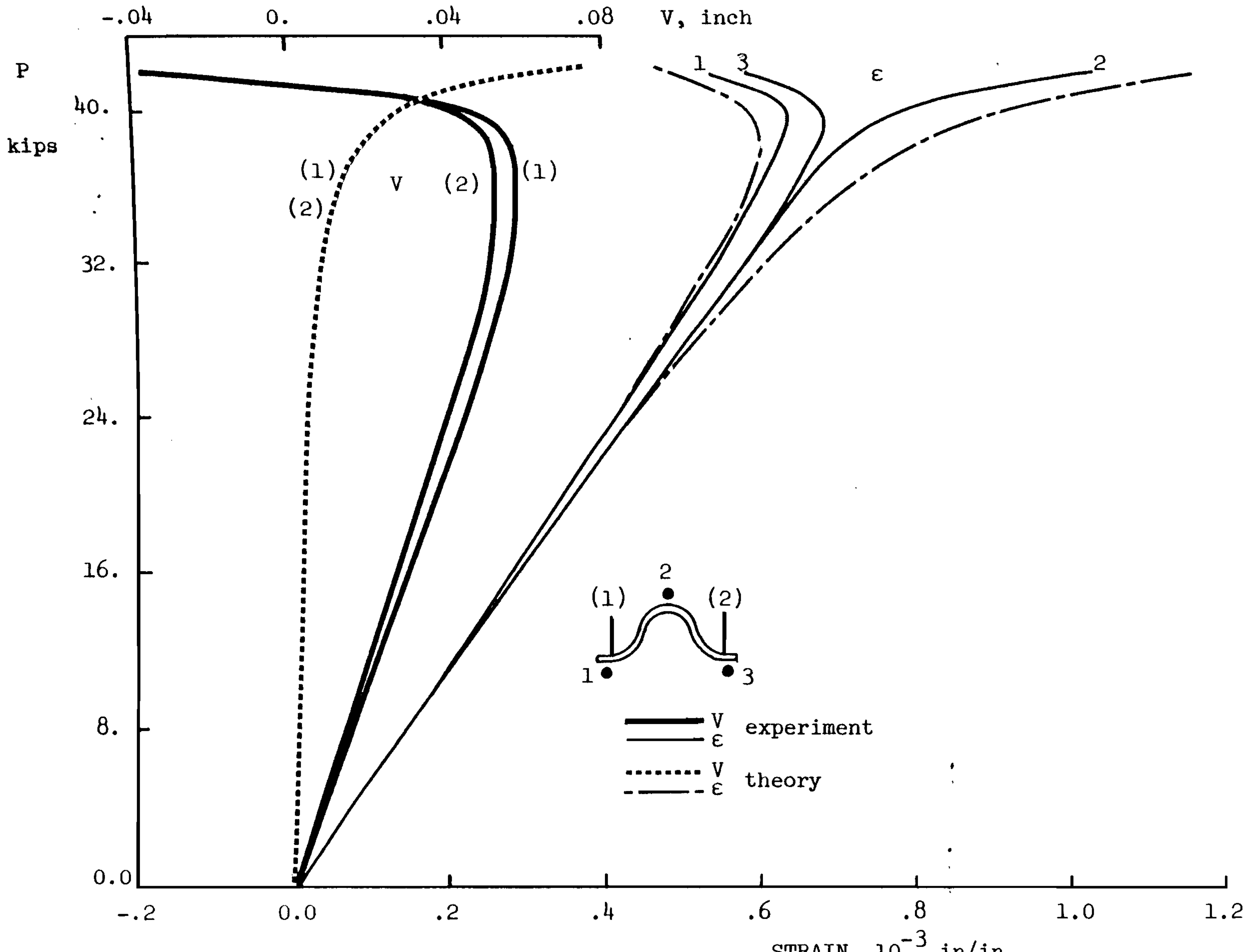

Fig. 9.72 HT Column G4, L = 65.4".

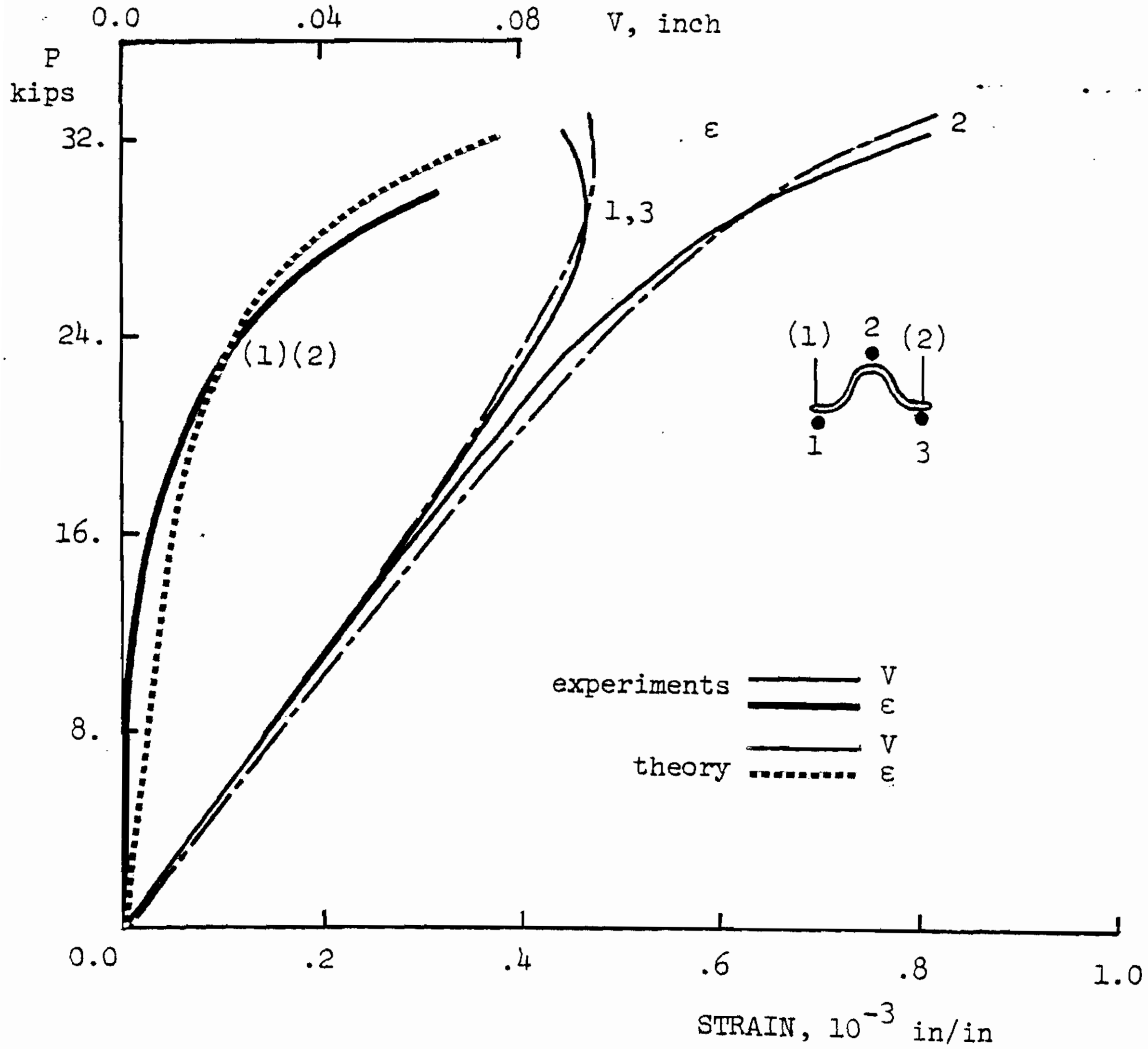

Fig. 9.73 HT Column G5 L = 71.0".

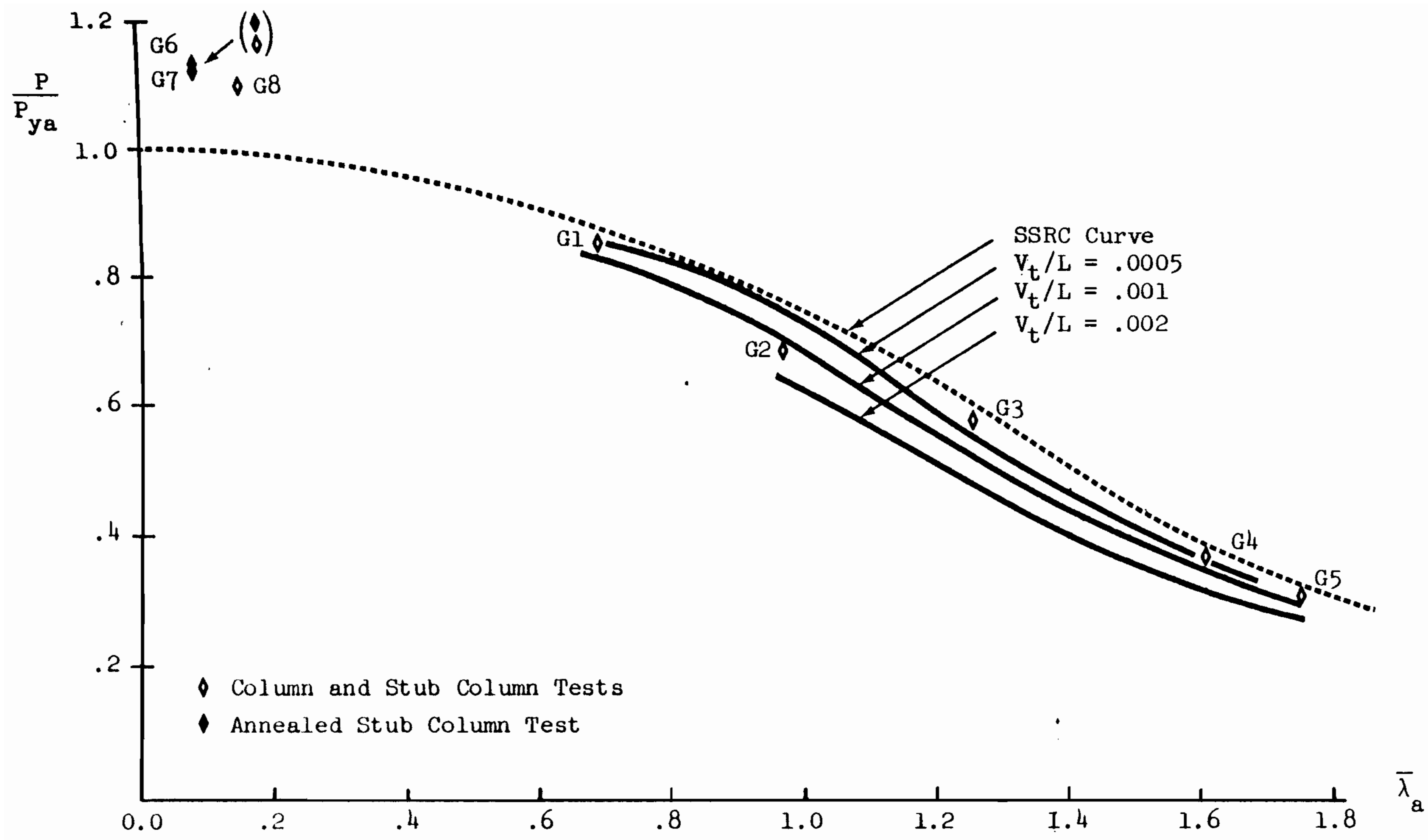

Fig. 9.74 HT Column Tests; average yield strength

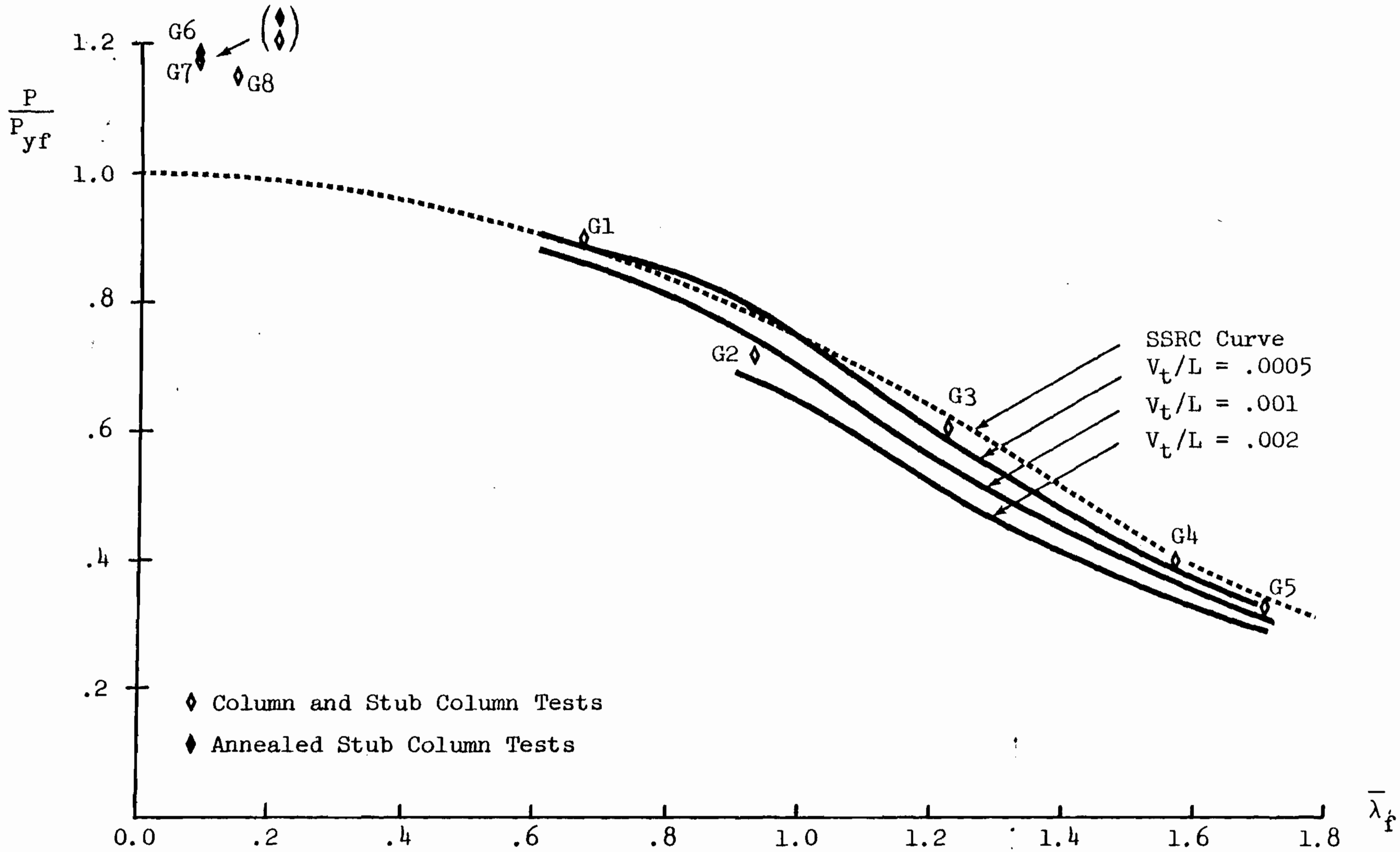

Fig. 9.75 HT Column Tests; yield strength of flat

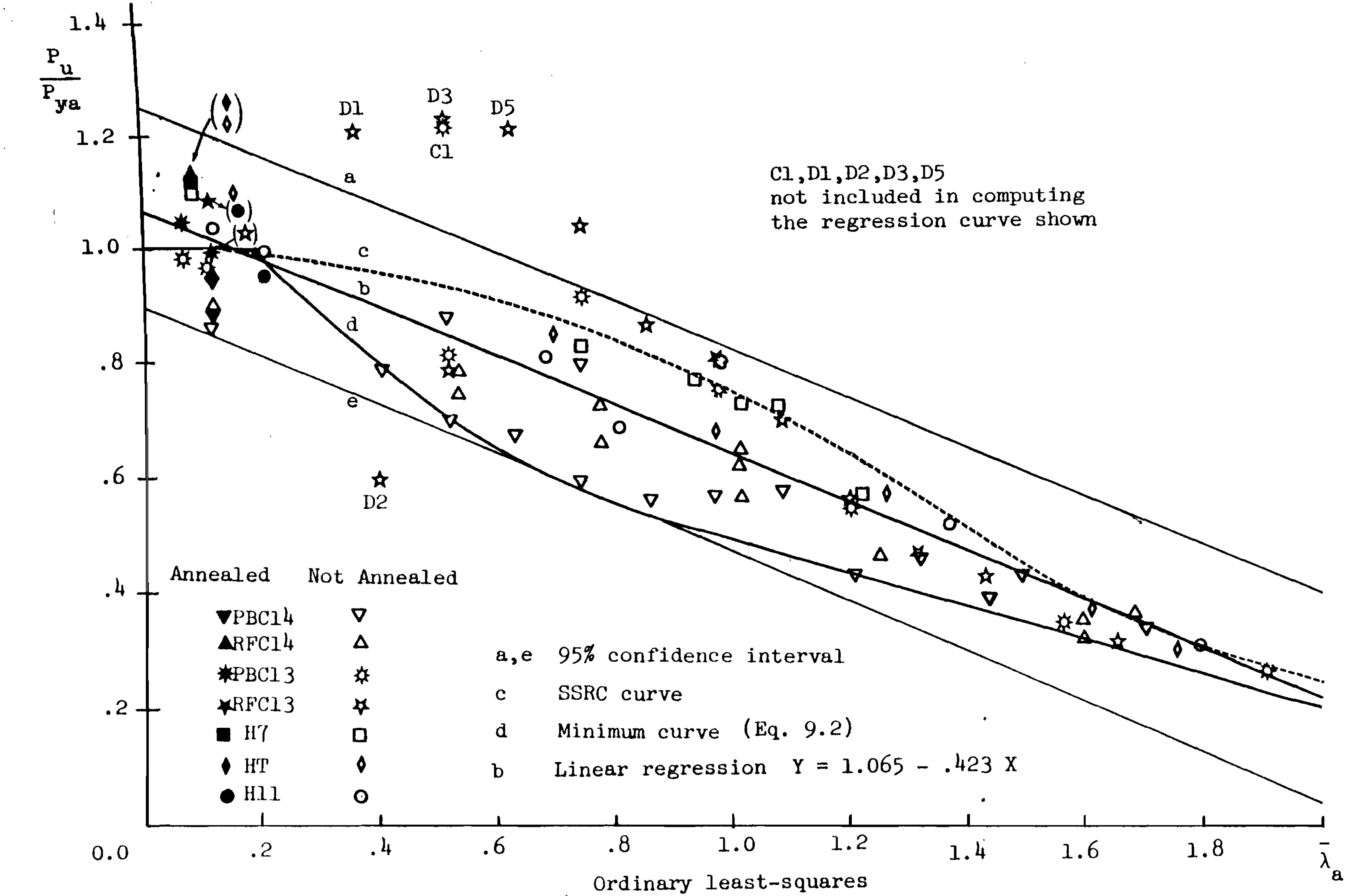

Ordinary least-squares

Fig. 9.76 Column tests; average yield strength

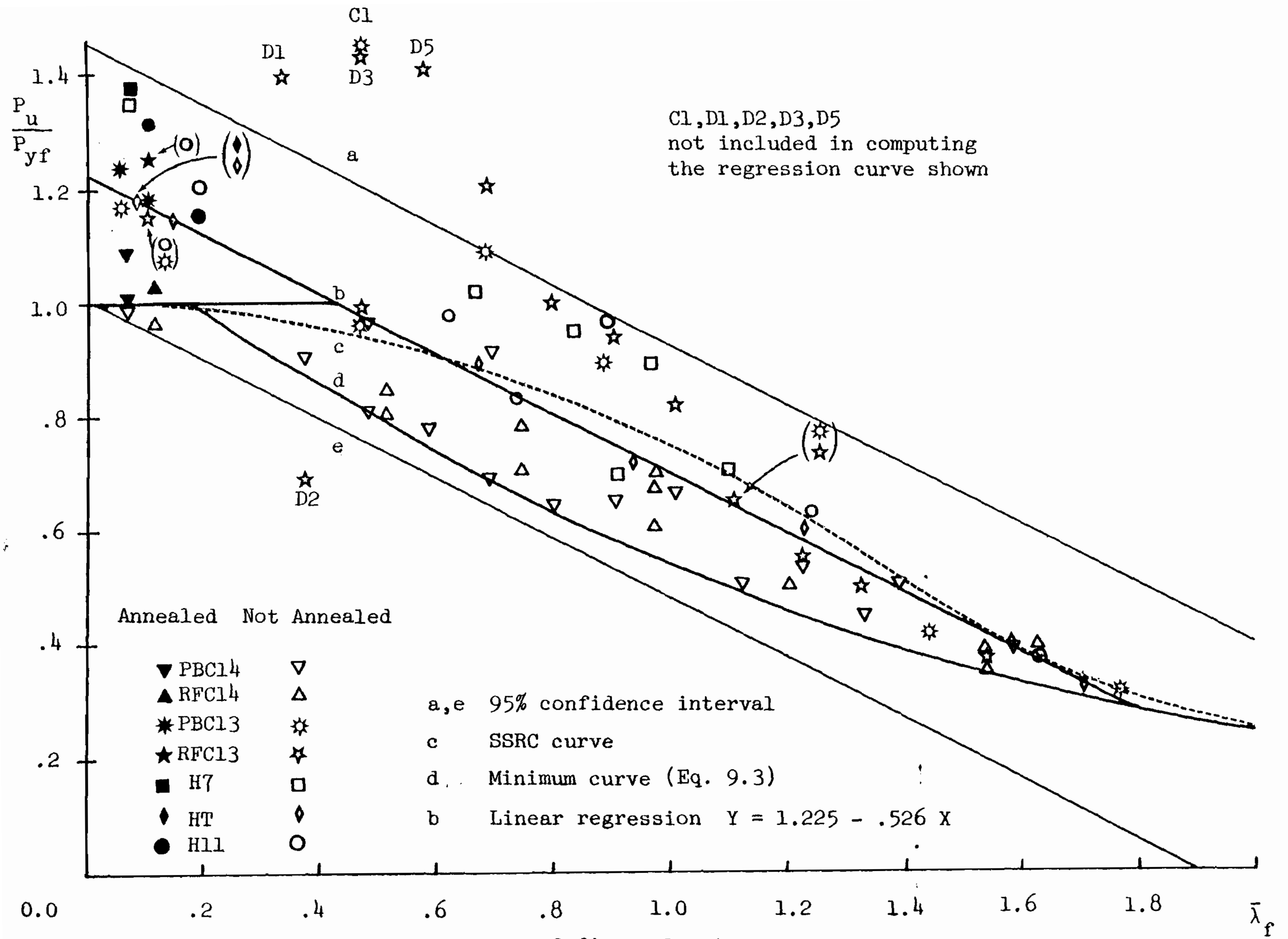

Ordinary least-squares
Fig. 9.77 Column tests; yield strength of flat

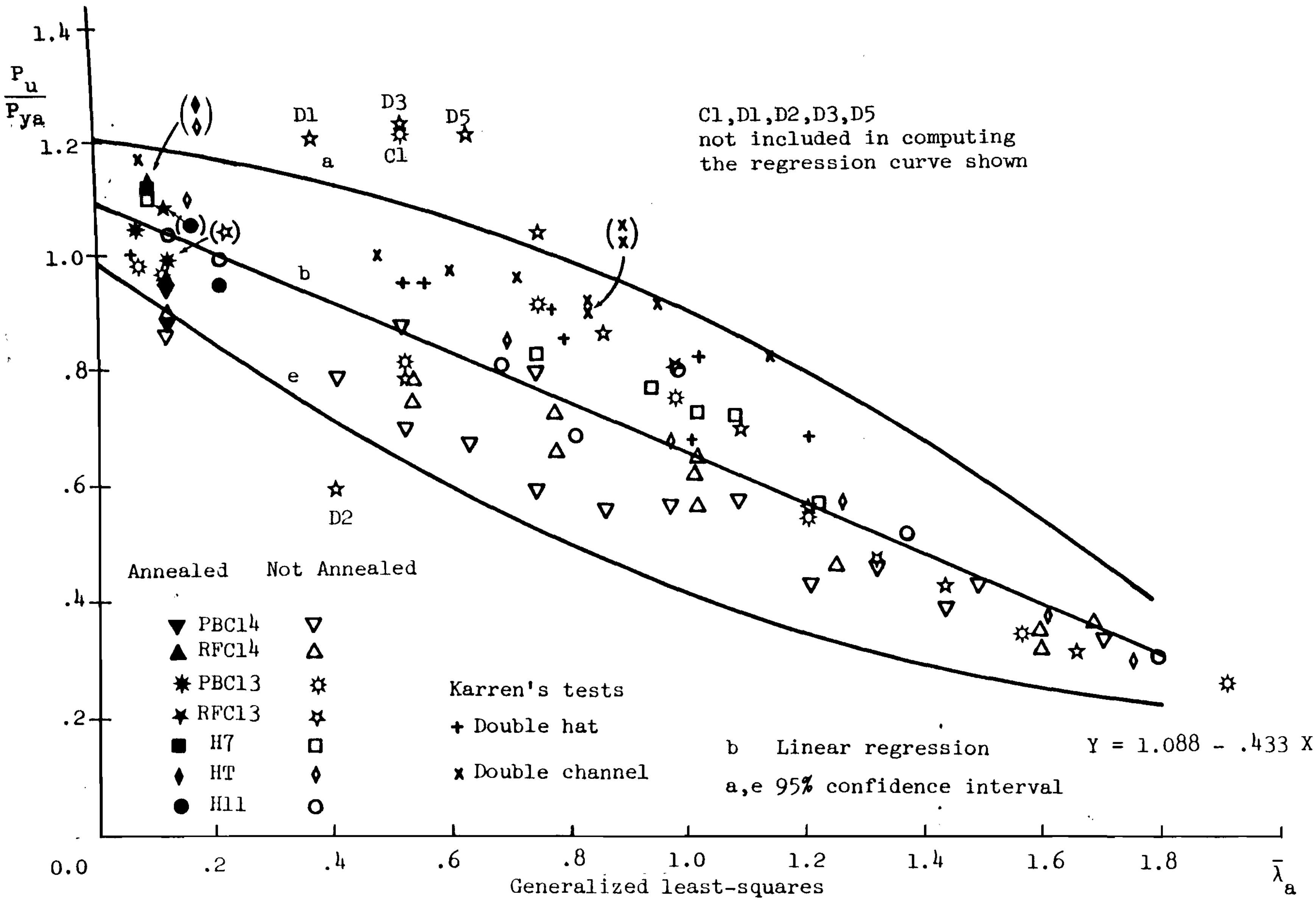

Fig. 9.78 Column tests; average yield strength

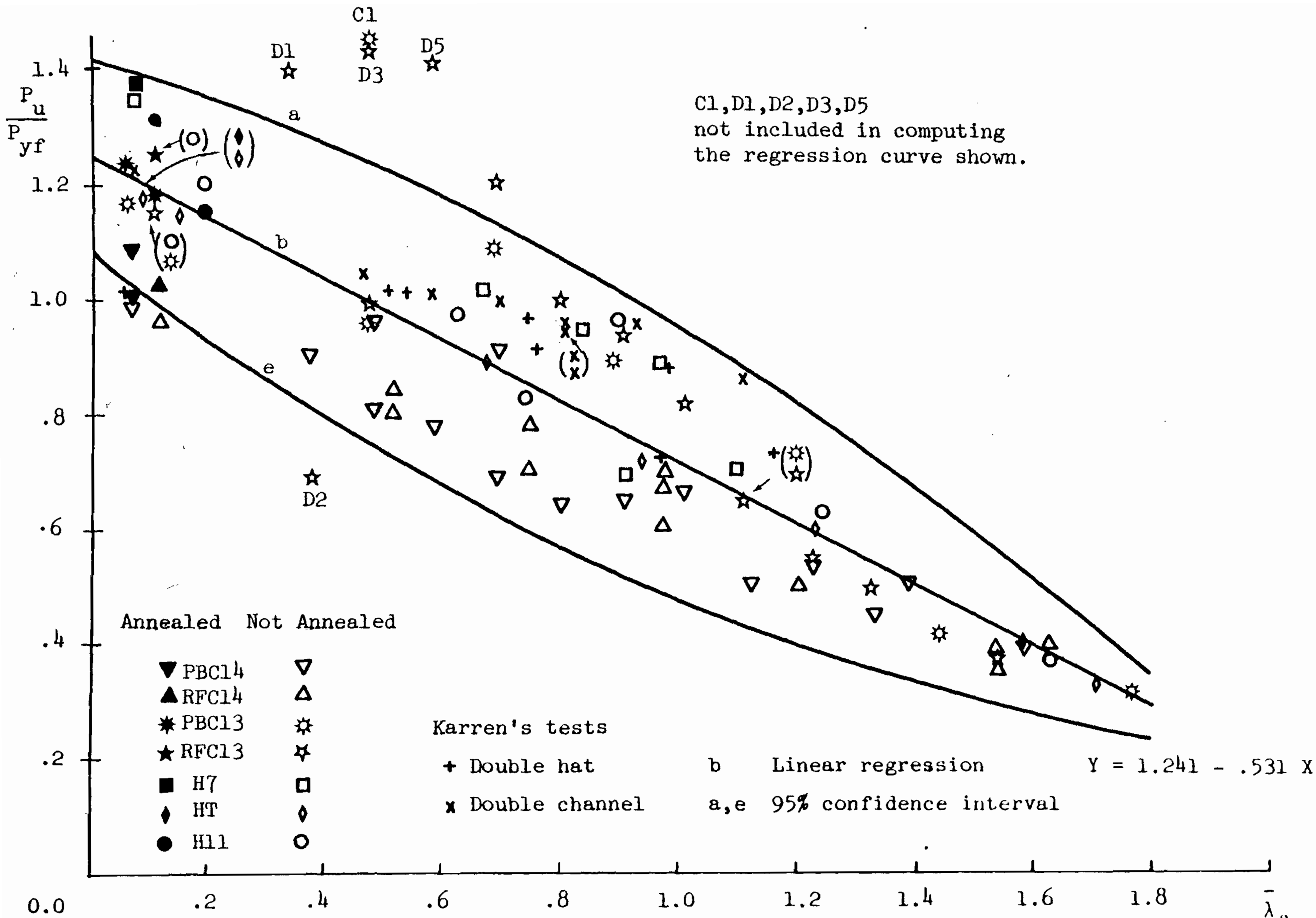

Generalized least-squares

Fig. 9.79 Column tests; yield strength of flat

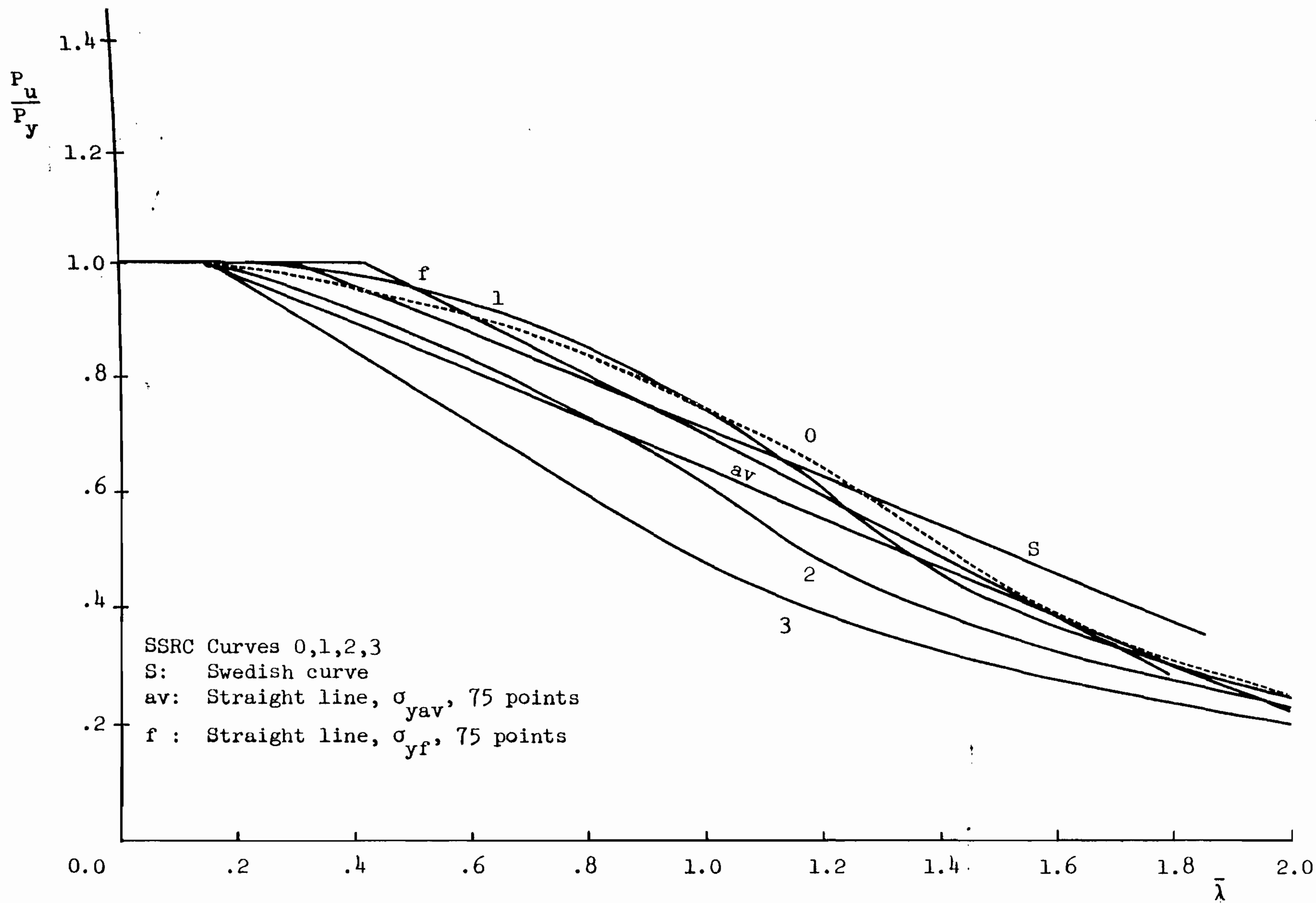

Fig. 9.80 Column Curves

CHAPTER 10

CONCLUSIONS

10.1 Contributions

This study of the strength of cold-formed steel columns contributes the following:

- Experimental data on the residual stresses due to cold-forming. Press-braked channels, roll-formed channels and hats were sectioned and the release of the longitudinal residual stresses measured with strain gages. The residual stress pattern is symmetrical about the axis of symmetry of the section. The released strains are negative (contraction) on the convex face of the section, positive on the concave face, but the average is zero. Surprisingly, there exist large residual stresses in the flat portions of a section. However, no systematic or significant difference between the residual stresses of press-braked and those of roll-formed sections is observed.

- Experimental data on the behavior and strength of cold-formed columns. Sixty pin-ended columns were loaded centrally and the strains and deflections at midheight recorded. In addition, twenty stub columns were tested under fixed end conditions. The tests span the inelastic range of flexural buckling.

- A simple theory of residual stresses due to sheet bending performed by a combination of end moments and radial pressure. It is assumed that loading brings the section to full plastification and unloading is purely elastic. Agreement is satisfactory with a more complicated theory, which assumes elasto-plastic loading and purely elastic unloading.

- A less simple theory of residual stresses due to sheet bending. Full plastification is still assumed upon loading, but unloading may be inelastic. When no radial pressure is exerted, results reduce to previously published work.

- A numerical scheme for predicting column behavior and strength. Initial and additional column deflections are assumed sinusoidal. The program accounts for variations in yield strength over the cross-section and the presence of residual stresses. Three distributions of residual stresses across the thickness are assumed: uniform, linear and "rectangular". A limited parameter study suggests the influence of residual stresses decreases as initial out-of-straightness increases. Buckling to the right or to the left of the weak axis, which is here perpendicular to the axis of symmetry of the section, produces different strengths. This computational scheme can be extended to other geometries.

- A study of the process of column centering. If alignment is monitored from midheight deflections, then introducing a small load eccentricity is equivalent to reducing the initial out-of-straightness by 5/4 the eccentricity.

- Column curves are discussed in more detail below.

10.2 Conclusions

Except for the channels of gage 14, agreement between actual and predicted column strength is satisfactory. It is thus felt that all important parameters have been accounted for, namely, initial out-of-straightness, variations in yield strength and presence of residual stresses over the cross-section.

A statistical study of the column test results is presented in Section 9.4 on page 314. Various combinations of test data are analyzed and various regression curves tried. The results that are most significant from a practical column design point of view are summarized below. For this summary, the basis will be the analyses of all the column tests of the author except 5. These 5 tests out of a total of 60 column tests will be disregarded because they were not reproducible and fell far from other similar tests results.

The following regression equations are obtained on the basis of the data described above.

- if the average yield strength of the section is used:

$$P/P_{ya} = 1.069 - .427\ \bar{\lambda}_a \qquad (10.1)$$

- if the yield strength of the flat is used:

$$P/P_{yf} = 1.225 - .525\ \bar{\lambda}_f \qquad (10.2)$$

$\bar{\lambda}_a$ and $\bar{\lambda}_f$ are defined in Table 7.2. These column curves are expressed as the ratios of the ultimate load to the yield load versus ratio of the slenderness ratio to the slenderness ratio at which Euler buckling stress equals the yield stress.

The mean and the standard deviation of the ratios of the actual column strengths to those predicted by Eq. 10.1 are given in Table 9.16 as .997 and .131, respectively. Those for Eq. 10.2 are given in Table 9.22 as .998 and .141, respectively. A graphical representation of Eq. 9.9 which is very close to Eq. 10.2 and the SSRC parabola along with the test results can be found in Fig. 9.77.

The present SSRC parabola appears seriously unconservative when used in conjunction with the average yield stress. The mean and the standard deviation of the ratios of the actual strengths to those predicted by the SSRC parabola are given in Table 9.16 as .895 and .109, respectively. These parameters become .962 and .133, respectively, as given in Table 9.22 where the yield strength of the flats is used.

When the test results of Karren are considered along with the data described above, the difference in terms of the means and the standard deviations between the results obtained using the above regression curves and the SSRC parabola becomes less significant.

As can be seen, for example, in Fig. 9.77 and as indicated by the standard deviations computed, the test data has a significant amount of scatter which should be considered in deciding upon a factor of safety or a resistance factor.

10.3 Future Work

- The influence of transverse residual stresses deserves further attention. The combination of a rectangular longitudinal residual stress distribution and its corresponding transverse component can be shown to be equivalent to a bilinear longitudinal residual stress distribution. This is the logical next step after the three models used here: uniform, linear and rectangular.

- Using the computer program developed here, a systematic study of the combined effects of residual stresses and initial deflections for various slenderness ratios and yield strengths can be done. Residual stresses may be distributed in various ways over the perimeter as well as across the thickness.

- Cold forming residual stresses need to be investigated further. A sheet bending experiment can be performed using a combination of end moments and radial pressure. Actual industrial processes can also be instrumented.

- The author's long column tests suggest a straight line to be a better basis for design than the present SSRC parabola. The present design curves for beam-columns, columns subject to torsional-flexural buckling and to local buckling are based on the SSRC parabola and thus also appear in need of revision.

REFERENCES

1. Alexander, J. M. "An Analysis of the Plastic Bending of Wide Plate and the Effect of Stretching on Transverse Residual Stresses," Proc. Instm. Mech. Engrs., Vol. 173, No. 1, 1959.

2. Alpsten, G. A. "Residual Stresses, Yield Stresses and Column Strength of Hot-Rolled and Roller Straightened Steel Shapes," Int. Colloq. on Column Strength, Paris, IABSE Proc., Nov. 1972.

3. American Iron and Steel Institute: Cold-Formed Steel Design Manual 1977 ed.

4. Bassett, M. B., and Johnson, W. "The Bending of Plate Using a Three-Roll Pyramid Type Plate Bending Machine," J. Strain An. Vol. 1, No. 5, 1966.

5. Batterman, R. H. and Johnston, B. G. "Behavior and Maximum Strength of Metal Columns," ASCE Proc. ST2, Apr. 1967.

6. Beedle, L. and Tall, L. "Basic Column Strength," ASCE Proc. ST7, July 1960.

7. Beer, H. and Schulz, G. "Bases Theoriques Des Courbes Europeennes De Flambement," Const. Metall. No. 3, 1970.

8. Bjorhovde, R. and Tall, L. "Maximum Column Strength and the Multiple Column Curve Concept," Lehigh U. Fritz Eng. Lab. Rep., No. 337.29, Oct. 1971.

9. Bjorhovde, R. "Deterministic and Probabilistic Approaches to the Strength of Columns," Ph.D. Thesis, Lehigh University Dept. of Civil Engineering, 1972.

10. Bleich, F. Buckling Strength of Metal Structures, McGraw-Hill, 1952.

11. Brozetti, J., Alpsten, G. A. and Tall, L. "Residual Stresses in a Heavy Rolled Shape 14WF730," Lehigh U. Fritz Eng. Lab. Rep. No. 337.10, Jan. 1970.

12. Bullens, D. K. Steel and its Heat Treatment. Vol. I: Principles, 5th Ed., Wiley, 1948.

13. Calladine, C. R. "Inelastic Buckling of Columns: The Effect of Imperfections," Int. J. Mech. Sci., Vol. 15, 1973.

14. Chajes, A. Principles of Structural Stability Theory, Prentice Hall, 1974.

15. Chajes, A., Britvec, S. J. and Winter, G. "Effects of Cold-Straining on Structural Sheet Steels," ASCE Proc. ST2, Vol. 89, Apr. 1963.

16. Chajes, A., Fang, P. J. and Winter, G. "Torsional-Flexural Buckling, Elastic and Inelastic, of Cold-Formed Thin-Walled Columns," Cornell Eng. Res. Bull., 66.1, Aug. 1966.

17. Chen, W. F. "Effects of Initial Curvature on Column Strength," ASCE Proc., ST12, Vol. 96, Dec. 1970b.

18. Chen, W. F. "Theory of Beam-Columns: The State of the Art Review," Int. Colloq on Stability of Structures Under Static and Dynamic Loads, SSRC, Wash. D.C., May 1977.

19. Chen, W. F. and Atsuta, T. Theory of Beam-Columns, Vol. I: In-Plane Behavior and Design, McGraw-Hill, 1976.

20. Chen, W. F. and Atsuta, T. Theory of Beam-Columns, Vol. II: Space Behavior and Design, McGraw-Hill, 1977.

21. Chen, W. F. and Ross, D. A. "Tests of Fabricated Tubular Columns," ASCE Proc. ST3, Mar. 1977.

22. Cheong Siat Moy, F. "General Analysis of Laterally Loaded Beam-Columns," ASCE Proc., ST6, Vol. 100, June 1974.

23. Chilver, A. H. and Britvec, S. J. "The Plastic Buckling of Aluminium Columns," Symp. on Al. in Struct. Eng., Al. Fed. Proc., June 1963.

24. Clark, D. S. and Varney, W. R. Physical Metallurgy for Engineers, Van Nostrand, 1952.

25. Croll, J. G. and Walker, A. C. Elements of Structural Stability, Wiley, 1972.

26. Davis, H., Troxell, G. E. and Wiskocil, C. T. The Testing and Inspection of Engineering Materials, 3rd ed., McGraw-Hill, 1964.

27. Denton, A. A. "Determination of Residual Stresses," Metal. Rev., Vol. 11, 1966a.

28. Denton, A. A. "Plane-Strain Bending with Work-Hardening," J. Strain An., Vol. 1, No. 3, 1966b.

29. Desmond, T. P. "The Behavior and Strength of Thin-Walled Compression Elements with Longitudinal Stiffeners," Cornell Struct. Eng. Rep. 369, Feb. 1968.

30. Dewolf, J. T. "Local and Overall Buckling of Cold-Formed Compression Members," Dept. of Struct. Eng. Rep. 354, Cornell U., 1973.

31. Dhalla, A. K. and Winter, G. "Steel Ductility Measurements," ASCE Proc., ST2, Feb. 1974a.

32. Dhalla, A. K. and Winter, G. "Suggested Steel Ductility Requirements," ASCE Proc., ST2, Feb. 1974b.

33. Draper, N. R. and Smith, H. Applied Regression Analysis, Wiley, 1966.

34. Duberg, J. E. and Wilder III, T. W. "Inelastic Column Behavior," NACA Rep. 1072, 1952.

35. Ellis, J. S. "Plastic Behavior of Compression Members," Eng. Inst. Canada Trans., Vol. 2, No. 2, May 1958.

36. Epstein, M., Dixon, D. and Murray, D. W. "Large Displacement Inelastic Analysis of Beam Columns," ASCE Proc. ST5, May 1978.

37. European Recommendations for the Design of Profiled Sheeting and Sections. Part I - Profiled Sheeting. Provisional Draft, Aug. 1979.

38. Frey, F. "Effet du Dressage A Froid Des Profils Laminés En Double Té Sur Leur Force Portante," IABSE Pub., Vol. 29, 1969.

39. Galambos, T. V. and Ketter, R. L. "Columns Under Combined Bending and Thrust," ASCE Proc. EM2, Apr. 1959.

40. Gilbert, R. B. and Calladine, C. R. "Interaction Between the Effects of Local and Overall Imperfections on the Buckling of Elastic Columns," J. Mech. Phys. Solids, Vol. 22, 1964.

41. Goldberger, A. S. Econometric Theory, Wiley, 1964.

42. Grumbach, M. and Prudhomme, M. "Propriétés Des Profilés A Froid," Const. Metal., No. 1, 1974.

43. Guy, A. G. Elements of Physical Metallurgy, Addison-Wesley, 1951.

44. Haijer, G. and Thürlimann, B. "On Inelastic Buckling in Steel," ASCE Proc. EM2, Apr. 1958.

45. Hanson, A. and Parr, J. G. The Engineer's Guide to Steel, Addison-Wesley, 1965.

46. Hill, R. Mathematical Theory of Plasticity, Oxford U. Press, 1950, p. 287.

47. Hlavacek, V. "Calculation of the Increase in Yield Strength Due to the Effects of Cold-Work of Forming," IABSE 8th Cong., 1968.

48. Hoff, N. J. "Buckling and Stability," 41st Wilbur Wright Memorial Lecture, J. Roy. Aero. Soc., Vol. 58, Jan. 1954.

49. Hoffman, O. and Sachs, G. Theory of Plasticity for Engineers, McGraw-Hill, 1953, p. 266.

50. Horne, M. R. "The Elasto-Plastic Theory of Compression Members," J. Mech. Phys. Solids, Vol. 4, 1956.

51. Hrenikoff, A. "Plastic Buckling of Steel Columns," IABSE Pub., Vol. 26, 1966.

52. Huber, A. W. and Beedle, L. S. "Residual Stresses and the Compressive Strength of Steel," Welding J. Sup., Dec. 1954.

53. Huber, A. W. and Ketter, R. L. "The Influence of Residual Stresses on the Carrying Capacity of Eccentrically Loaded Columns," IABSE Pub., Vol. 8, 1958.

54. Ingvarsson, L. "Cold-Forming Residual Stresses: Effect on Buckling," 3rd Int. Spec. Conf. on Cold-Formed Steel Structures, U. of Missouri-Rolla, Nov. 1975, pp. 85-119.

55. Ingvarsson, L. "Residual Stresses in Welded Box Columns," Bull. 119, Dept. of Building Statics and Struct. Eng., Roy. Inst. of Tech., Stockholm, Sweden, 1977a.

56. Ingvarsson, L. "Cold-Forming Residual Stresses and Box Columns Built Up by Two Cold-Formed Channel Sections Welded Together," Bull. 121, Dept. of Building Statics and Struct. Eng., Roy. Inst. of Tech., Stockholm, Sweden, 1977b.

57. Jezek, K. "Die Tragfähigkeit Des Exzentrisch Beanspruchten Und Des Querbelasteten Druckstabes Aus Einem Ideal Plastischen Stahl," Sitzungsber. d. Wiener Akad. d. Wiss., Math-Naturw. Kl., Abt. IIa, 143 Bd, 7 Heft, 1934.

58. Johnston, B. G. "Buckling Behavior Above the Tangent Modulus Load," ASCE Trans. Vol. 128, 1963 I.

59. Johnston, B. G. "Inelastic Buckling Gradient," ASCE Proc. EM6, Dec. 1964.

60. Johnston, B. G., ed. Guide to Stability Design Criteria for Metal Structures, 3rd ed., Wiley 1976.

61. Johnston, J. Econometric Methods, 2nd ed., McGraw-Hill, 1972.

62. Karren, K. "Corner Properties of Cold-Formed Steel Shapes," ASCE Proc., ST1, Vol. 93, Feb. 1967.

63. Karren, K. and Gohil, M. M. "Strain-Hardening and Aging in Cold-Formed Steel," ASCE Proc., ST1. Vol. 101, Jan. 1975.

64. Karren, K. and Winter, G. "Effects of Cold-Forming on Light-Gage Steel Members," ASCE Proc., ST1, Vol. 93, Feb. 1967.

65. Kato, B. and Aoki, H. "Residual Stresses in Cold-Formed Tubes," Unpublished Report.

66. Keramati, A., Gaylord, E. H. and Robinson, A. R. "Ultimate Strength of Eccentrically Loaded Columns," Int. Colloq. on Column Strength, IABSE Proc., Paris, 1972.

67. L'Hermite, R. Flambage Et Stabilité: Le Flambage Elastique Des Piéces Droites, Eyrolles, 1974.

68. L'Hermite, R. Le Flambage Elasto-Plastique Des Colonnes, Eyrolles, 1976.

69. Lin, T. H. "Inelastic Column Buckling," J. Aero. Sci., Mar. 1950.

70. Lind, N. C. and Schroff, D. K. "Utilization of Cold-Work in Cold-Formed Steel," ASCE Proc. ST1, Vol. 101, Jan. 1975.

71. Lubahn, J. D. and Sachs, G. "Bending of an Ideal Plastic Metal," ASME Trans., Feb. 1950.

72. Macadam, J. M. Discussion of "Corner Properties of Cold-Formed Steel Shapes," by Karren, K., ASCE Proc., ST1, Vol. 93, Feb. 1967a.

73. Macadam, J. M. Discussion of "Effects of Cold-Forming on Light-Gage Steel Members," by Karren, K. and Winter, G., ASCE Proc., ST1, Vol. 93, Feb. 1967b.

74. Meyer, G. E. "Residual Stresses Produced by Deformation," DMIC Rep. 243, Metal Deformation Processing, Vol. 3, Battelle Memorial Inst., June 10, 1967.

75. Newmark, N. M. "Numerical Procedure for Computing Deflections, Moments and Buckling Loads," ASCE Trans., Vol. 108, 1943.

76. Ojalvo, M. "Restrained Columns," ASCE Proc. EM5, Oct. 1960.

77. Okushima, K. and Kakino, Y. "A Study of the Residual Stresses Produced by Metal Cutting," Memoirs Fac. Eng., Kyoto U., Vol. 34, No. 2, Apr. 1972.

78. Osgood, W. R. "The Effect of Residual Stresses on Column Strength," Proc. 1st U.S. Nat. Cong. of App. Mech., 1951.

79. Pawelski, O. "Plastomechanische Grundlagen Der Kaltumformung," Zeits. f. Metallkunde, Bd. 61, H3, 1970.

80. Pekoz, T. "Torsional-Flexural Buckling of Thin-Walled Sections Under Concentric Load," Rep. 329, Dept. of Struct. Eng., Cornell U., 1967.

81. Pekoz, T. "Elastic and Inelastic Flexural Stability and Behavior of Concentrically Loaded Cold-Formed Steel Columns," Unpublished Research Proposal, Dept. of Struct. Eng., Cornell U., 1975.

82. Roark, R. R. and Young, W. C. "Formulas for Stress and Strain," 5th ed., McGraw-Hill, 1975.

83. Ross, D. A. and Chen, W. F. "Residual Stress Measurement in Fabricated Tubular Steel Columns," Lehigh U. Fritz Eng. Lab. Rep. 393.4, July 1975.

84. Schwalla, E. "Die Stabilität Zentrisch Und Exzentrisch Gedruckter Stäbe Aus Baustahl," Sitzungsber. d. Wiener Akad. d. Wiss., Math-Naturw. Kl., Abt. IIa, 137 Bd, 8 Heft, 1928.

85. Seide, P. "Accuracy of Some Numerical Methods for Column Buckling," ASCE Proc. EM5, Oct. 1975.

86. Sewell, M. J. "A Survey of Plastic Buckling," Study No. 6, Stability, Solid Mechanics Div., U. of Waterloo, 1972 (Leipholz, H. H. E., ed.).

87. Shaffer, B. W. and Ungar, E. E. "Mechanics of the Sheet Bending Process," ASME Trans., Mar. 1960.

88. Shampine, L. F. and Allen Jr., R. C. Numerical Computing: An Introduction, Saunders, 1973.

89. Shanley, F. R. "Inelastic Column Theory," J. Aero. Sci., Vol. 14, No. 5, May 1947.

90. Sherman, D. "Residual Stress Measurement in Tubular Members," ASCE Proc., ST4, Apr. 1969.

91. Sherman, D. "Residual Stresses and Tubular Compression Members," ASCE Proc. ST3, Mar. 1971.

92. Structural Stability Research Council "Determination of Residual Stresses," Tech. Memo. No. 6, 4th Draft, Sept. 1978.

93. Tall, L. "Recent Developments in the Study of Column Behavior," J. Instn. Engrs. Australia, Dec. 1964.

94. Tall, L., Beedle, L. S., Galambos, T. V., ed. Structural Steel Design, Ronald Press, 1964.

95. Tebedge, N., Alpsten, G. A. and Tall, L. "Measurements of Residual Stresses - A Comparative Study of Methods," Joint British Comm. for Stress Analysis, Conf. on the Recording and Interpretation of Eng. Measurements, Inst. Mar. Engrs., 1972.

96. Tebedge, N., Alpsten, G. and Tall, L. "Residual Stress Measurement by the Sectioning Method," Exp. Mech., Feb. 1973.

97. Theil, H. Principles of Econometrics, Wiley, 1971.

98. Thurlimann, B. "New Aspects Concerning Inelastic Instability of Steel Structures," ASCE Trans., Vol. 127, 1962 II.

99. Timoshenko, S. P. and Gere, J. M. Theory of Elastic Stability, 2nd ed., McGraw-Hill, 1961.

100. Timoshenko, S. P. and Goodier, J. N. Theory of Elasticity, 3rd ed., McGraw-Hill, 1970.

101. Uribe, J. and Winter, G. "Cold-Forming Effects of Thin-Walled Steel Members," Cornell Eng. Res. Bull. 70-1, 1970.

102. Van Vlack Elements of Materials Science, 2nd ed., Addison-Wesley, 1973.

103. Wilder III, T. W., Brooks Jr., W. A. and Mathauser, E. E. "The Effect of Initial Curvature on the Strength of an Inelastic Column," NACA TN2872, Jan. 1953.

104. Winter, G. "Design of Cold-Formed Structural Members," Structural Engineering Handbook, Section 9, McGraw-Hill, 1979 (Gaylord, Jr., E. H. and Gaylord, C. N. ed.).

105. Yanev, B. and Gjelsvik, A. "Buckling of Short Steel Columns," ASCE Proc. ST 11, Nov. 1977.

106. Young, B. W. "The Analysis of Column Buckling Behavior," Int. Colloq. on Column Strength, IABSE Proc., Paris, 1972.

107. Yu, Wei-Wen Cold-Formed Steel Structures, McGraw-Hill, 1973.

108. Zichy, J. and Moreau, G. "Stabilité Des Eléments Comprimés Formés A Froid," Const. Metall., No. 4, 1974.

APPENDIX A

COMPUTATION OF FORCES AND MOMENTS IN CHAPTER 4

<u>Case 1</u>: Derivation of Equations (4.43) and (4.42).

$$\text{Moment} = 0 = \int_a^{t_o} [-1 - p - \ln\frac{r}{a} - \frac{A}{r^2} + B(3 + \ln r^2) + C]rdr$$

$$- \int_{t_o}^{c} [1 + \ln(Dr/b)]rdr$$

$$+ \int_c^b [1 - \ln\frac{b}{r} - \frac{A}{r^2} + B(3 + \ln r^2) + C + H]rdr$$

$$= \frac{p}{2}(a^2 - t_o^2) + \frac{1}{4}(a^2 + b^2 - 2c^2) + \frac{t_o^2}{2}\ln\frac{a}{b} - c^2\ln\frac{c}{b}$$

$$+ \int_a^{t_o} [-\frac{A}{r^2} + B(3 + \ln r^2) + C]rdr - \int_{t_o}^{c} (\ln D)rdr$$

$$+ \int_c^b [-\frac{A}{r^2} + B(3 + \ln r^2) + C + H]rdr \ ,$$

but $\displaystyle\int_{t_o}^{c} (\ln D)rdr = (1 + B)(c^2 - t_o^2)\ln\frac{b}{c} + \frac{Bt_o^2}{2b^2c^2}(c^2 - b^2)(c^2 - t_o^2)$.

Also $\int_a^{t_o} [-\frac{A}{r^2} + B(3 + \ln r^2) + C]rdr = \int [p - Bt_o^2(\frac{1}{a^2} + \frac{1}{r^2})$

$+ B(2 + \ln r^2 - \ln a^2)rdr = [p - \frac{Bt_o^2}{a^2} + B(2 - \ln a^2)]\frac{1}{2}(t_o^2 - a^2) - Bt_o^2 \ln \frac{t_o}{a}$

$+ 2B \int_a^{t_o} r \ln r dr = \frac{1}{2}(t_o^2 - a^2)[p - \frac{B}{a^2}(t_o^2 - a^2)]$,

and $\int_c^b [-\frac{A}{r^2} + B(3 + \ln r^2) + C + H]rdr = \int [-Bt_o^2(\frac{1}{r^2} + \frac{1}{b^2}) + 2B(1 + \ln \frac{r}{b})]rdr$

$= B[-\frac{t_o^2}{2b^2} + 1 - \ln b](b^2 - c^2) - Bt_o^2 \ln \frac{b}{c} + 2B \int_c^b r \ln r dr$

$= B(c^2 - t_o^2)\ln \frac{b}{c} + \frac{B}{2b^2}(b^2 - c^2)(b^2 - t_o^2)$.

Summing: $0 = \frac{1}{4}(a^2 + b^2 - 2c^2) + \frac{t_o^2 p}{2} - \frac{B}{2a^2}(t_o^2 - a^2)^2 + \frac{B(b^2 - c^2)}{2b^2}(b^2 - \frac{t_o^4}{c^2})$

(4.43)

Force $= 0 = \int_a^{t_o} [-1 - p - \ln \frac{r}{a} - \frac{A}{r^2} + B(3 + \ln r^2) + C]dr$

$- \int_{t_o}^c [1 + \ln(Dr/b)]dr + \int_c^b [1 - \ln \frac{b}{r} - \frac{A}{r^2} + B(3 + \ln r^2) + C + H]dr$

$= (-p + 3B + C)(t_o - a) + t_o \ln \frac{a}{b} - 2c \ln \frac{c}{b} - \int_a^{t_o} (\frac{A}{r^2} - 2B \ln r)dr$

$- \int_{t_o}^c \ln D dr + \int_c^b [-\frac{A}{r^2} + B(3 + \ln r^2) + C + H]dr$, but $\int_a^{t_o} (\frac{A}{r^2} - 2B \ln r)dr = B(t_o - a)(2 + \frac{t_o}{a}) - 2B(t_o \ln t_o - a \ln a).$

Also $\int_{t_o}^{c} (\ln D)dr = 2(1 + B)(c - t_o)\ln\frac{b}{c} - Bt_o^2(c - t_o)(\frac{1}{c^2} - \frac{1}{b^2})$,

and $\int_c^b [-\frac{Bt_o^2}{r^2} + B(3 + 2 \ln r) - \frac{Bt_o^2}{b^2} - B(1 + \ln b^2)]dr$

$$= \frac{Bt_o^2}{r}\Big|_c^b + 2B[r \ln r - r]_c^b + [3B - \frac{Bt_o^2}{b^2} - B(1 + \ln b^2)](b - c) .$$

Summing: $\frac{p}{B} + 2 \ln\frac{bt_o}{ac} + 1 - t_o^2(\frac{1}{a^2} - \frac{1}{b^2} + \frac{1}{c^2}) = 0$ same as (4.42)

<u>Case 2</u>: Derivation of Equations (4.56) and (4.55)

Moment $= 0 = \int_a^b \sigma_\theta r dr = ① + ② + ③$

$$① = \int_a^c [-1 - p - \ln\frac{r}{a} - \frac{Bt_o^2}{r^2} + B(3 + 2 \ln r) + p - \frac{Bt_o^2}{a^2} - B(1 + 2 \ln a)]rdr$$

$$= -\frac{c^2 - a^2}{2} + B(2 - 2 \ln a - \frac{t_o^2}{a^2})\frac{c^2 - a^2}{2} - Bt_o^2\int\frac{dr}{r} - \int \ln(\frac{r}{a})rdr$$

$$+ 2B\int r \ln r dr = -\frac{c^2}{2} + \frac{a^2}{2} + B(c^2 - a^2)(1 - \ln a - \frac{t_o^2}{2a^2}) - Bt_o^2 \ln\frac{c}{a}$$

$$- \frac{c^2}{2}\ln\frac{c}{a} + \frac{c^2 - a^2}{4} + Bc^2 \ln c - Ba^2 \ln a - \frac{Bc^2}{2} + \frac{Ba^2}{2} = -\frac{c^2}{4} + \frac{a^2}{4}$$

$$- \frac{c^2}{2}\ln\frac{c}{a} + \frac{B}{2}(t_o^2 + c^2 - a^2 - \frac{c^2t_o^2}{a^2}) + B(c^2 - t_o^2)\ln\frac{c}{a}$$

$$② = \int_c^{t_o} [1 + \ln\frac{r}{b} + B(1 + 2\ln\frac{t_o}{b} - \frac{t_o^2}{b^2})]rdr$$

$$= \frac{t_o^2 - c^2}{2} + B(1 + 2\ln\frac{t_o}{b} - \frac{t_o^2}{b^2})(\frac{t_o^2 - c^2}{2}) + \frac{1}{2}t_o^2 \ln\frac{t_o}{b} - \frac{1}{2}c^2 \ln\frac{c}{b} - \frac{1}{4}(t_o^2 - c^2)$$

$$= -\frac{c^2}{4} + \frac{t_o^2}{4} - \frac{c^2}{2}\ln\frac{c}{b} + \frac{t_o^2}{2}\ln\frac{t_o}{b} + \frac{B}{2}(t_o^2 - c^2 - \frac{t_o^4}{b^2} + \frac{t_o^2 c^2}{b^2}) + B\ln\frac{t_o}{b}(t_o^2 - c^2)$$

$$③ = \int_{t_o}^{b} [1 + \ln\frac{r}{b} - \frac{Bt_o^2}{r^2} + B(3 + 2\ln r) - \frac{Bt_o^2}{b^2} - B(1 + 2\ln b)]rdr$$

$$= [1 - \frac{Bt_o^2}{b^2} + 2B(1 - \ln b)]\frac{(b^2 - t_o^2)}{2} + \frac{b^2x^2}{2}(\ln x - \frac{1}{2})\Big|_{t_o/b}^{1}$$

$$- Bt_o^2 \ln\frac{b}{t_o} + Br^2(\ln r - \frac{1}{2})\Big|_{t_o}^{b}$$

$$= \frac{b^2 - t_o^2}{2} - \frac{Bt_o^2}{2} + \frac{Bt_o^4}{2b^2} + B(b^2 - t_o^2 - b^2\ln b + t_o^2 \ln b) - Bt_o^2 \ln\frac{b}{t_o} - \frac{b^2}{4}$$

$$- \frac{t_o^2}{2}(\ln\frac{t_o}{b} - \frac{1}{2}) + Bb^2(\ln b - \frac{1}{2}) - Bt_o^2(\ln t_o - \frac{1}{2})$$

$$= \frac{b^2}{4} - \frac{t_o^2}{4} - \frac{t_o^2}{2}\ln\frac{t_o}{b} + \frac{B}{2}(b^2 - 2t_o^2 + \frac{t_o^4}{b^2})$$

$$0 = [-\frac{c^2}{4} + \frac{a^2}{4} - \frac{c^2}{2}\ln\frac{c}{a} + B\frac{(c^2 - a^2)}{2}(2 - \frac{t_o^2}{a^2} - 2\ln a) + B(\frac{a^2}{2} - \frac{c^2}{2} - t_o^2 \ln\frac{c}{a}$$

$$+ c^2 \ln c - a^2 \ln a)] + [1 - \frac{t_o^2}{4} + \frac{c^2}{4} + \frac{1}{2}t_o^2 \ln\frac{t_o}{b} - \frac{1}{2}c^2 \ln\frac{c}{b} +$$

$$+ B\frac{(t_o^2 - c^2)}{2}(1 + 2\ln\frac{t_o}{b} - \frac{t_o^2}{b^2})] + [1 - \frac{Bt_o^2}{b^2} + 2B(1 - \ln b)]\frac{(b^2 - t_o^2)}{2}$$

$$- Bt_o^2 \ln\frac{b}{t_o} - \frac{b^2}{4} - \frac{t_o^2}{2}(\ln\frac{t_o}{b} - \frac{1}{2}) + Bb^2(\ln b - \frac{1}{2}) - Bt_o^2(\ln t_o - \frac{1}{2})$$

$$0 = \frac{1}{4}(a^2 + b^2 - 2c^2) + \frac{c^2}{2}p + \frac{Bc^2t_o^2}{2}(\frac{1}{b^2} - \frac{1}{a^2}) + \frac{B}{2}(b^2 - a^2)$$

$$+ B(c^2 - t_o^2)\ln\frac{bc}{at_o} \qquad (4.56)$$

$$\text{Force} = 0 = \int_a^b \sigma_\theta dr = \int_a^c (-1 - p - \ln\frac{r}{a} - \frac{A}{r^2} + B(3 + 2\ln r) + C)dr$$

$$+ \int_c^{t_o} (1 + \ln\frac{r}{b} + D)dr + \int_{t_o}^b [1 - \ln\frac{b}{r} - \frac{A}{r^2} + B(3 + 2\ln r) + C + H]dr$$

$$= [(2B - 1)c\ln\frac{c}{a} + Bct_o^2(\frac{1}{c^2} - \frac{1}{a^2})] + [B(t_o - c)(1 + 2\ln\frac{t_o}{b} - \frac{t_o^2}{b^2})$$

$$+ t_o\ln\frac{t_o}{b} - c\ln\frac{c}{b}] + [Bt_o(\frac{t_o^2}{b^2} - 1) + (2B + 1)t_o\ln\frac{b}{t_o}]$$

$$0 = pc + Bct_o^2(-\frac{1}{a^2} + \frac{1}{b^2} + \frac{1}{c^2} - \frac{1}{t_o^2}) + 2Bc\ln\frac{bc}{at_o} \qquad \text{identical to (4.55)}$$

Case 3: Derivation of Equations (4.73a) and (4.71).

$$\text{Moment} = \int_a^b \sigma_\theta r dr = (1) - (2) - (3) + (4)$$

$$(1) = \int_a^{t_i} (1 + \ln\frac{r}{a})rdr = \frac{t_i^2}{2}\ln\frac{t_i}{a} + \frac{1}{4}(t_i^2 - a^2)$$

$$\textcircled{2} = \int_{t_i}^{t_o} \{1 + p + \ln\frac{r}{a} + \frac{Bt_o^2}{r^2} - B(3 + 2\ln r) + B[\ln(\frac{bt_o}{c})^2 + 2] - Bt_o^2(\frac{1}{c^2} - \frac{1}{b^2})\}rdr$$

$$= \frac{t_o^2}{4} - \frac{t_i^2}{4} + \frac{p}{2}t_o^2 - \frac{p}{2}t_i^2 + Bt_o^2\ln\frac{t_o}{t_i} - Bt_i^2\ln\frac{t_o}{t_i} + Bt_o^2\ln\frac{b}{c} - Bt_i^2\ln\frac{b}{c}$$

$$- \frac{Bt_o^2}{2}(\frac{t_o^2}{c^2} - \frac{t_o^2}{b^2} - \frac{t_i^2}{c^2} + \frac{t_i^2}{b^2}) + \frac{t_o^2}{2}\ln\frac{t_o}{a} - \frac{t_i^2}{2}\ln\frac{t_i}{a}$$

$$\textcircled{3} = \int_{t_o}^{c} [1 + \ln\frac{r}{b} + (B + 1)\ln(\frac{b}{c})^2 - Bt_o^2(\frac{1}{c^2} - \frac{1}{b^2})]rdr$$

$$= \frac{c^2 - t_o^2}{4} + B(c^2 - t_o^2)\ln\frac{b}{c} + (\frac{c^2}{2} - t_o^2)\ln\frac{b}{c} - \frac{t_o^2}{2}\ln\frac{t_o}{b} - \frac{Bt_o^2}{2}(1 - \frac{t_o^2}{c^2} - \frac{c^2}{b^2} + \frac{t_o^2}{b^2})$$

$$\textcircled{4} = \int_{c}^{b} [1 + \ln\frac{r}{b} - \frac{Bt_o^2}{r^2} + B(3 + 2\ln r) - \frac{Bt_o^2}{b^2} - B(1 + 2\ln b)]rdr$$

$$= \frac{b^2 - c^2}{4} + \frac{B}{2}(b^2 - c^2) - \frac{Bt_o^2}{2}(1 - \frac{c^2}{b^2} + 2\ln\frac{b}{c}) + (B + \frac{1}{2})c^2\ln\frac{b}{c}$$

$$\text{Moment} = 0 = \frac{1}{4}(-a^2 + b^2 - 2c^2 + 2t_i^2) + \frac{p}{2}t_i^2 + t_i^2\ln\frac{t_i}{a} + \frac{Bt_o^2t_i^2}{2}(\frac{1}{b^2} - \frac{1}{c^2})$$

$$+ \frac{B}{2}(b^2 - c^2) - B(t_o^2 - t_i^2)\ln(\frac{t_o b}{t_i c})$$

Multiplying by $\dfrac{2(t_i^2 - t_o^2)}{t_i^2}$ after using (4.67) and (4.72):

$$0 = (\frac{1}{t_o^2} - \frac{1}{t_i^2})[1 + p + \frac{(-a^2 + b^2 - 2c^2)}{2t_o^2} + 2\ln\frac{t_i}{a}] + \frac{1}{t_o^4}(b^2 - c^2) + (\frac{1}{b^2} - \frac{1}{c^2}) \tag{4.73a}$$

$$\text{Force} = \int_a^b \sigma_\theta dr = 0 = (1) - (2) - (3) + (4)$$

$$(1) = \int_a^{t_i} (1 + \ln\frac{r}{a})dr = t_i \ln\frac{t_i}{a}$$

$$(2) = \int_{t_i}^{t_o} [1 + p + \ln\frac{r}{a} + \frac{Bt_o^2}{r^2} - B(3 + 2\ln r) + B[\ln(\frac{bt_o}{c})^2 + 2]$$

$$- Bt_o^2(\frac{1}{c^2} - \frac{1}{b^2})]dr$$

$$= pt_o - pt_i - Bt_o^2(\frac{t_o}{c^2} - \frac{t_o}{b^2} - \frac{t_i}{c^2} + \frac{t_i}{b^2}) + 2B(t_o - t_i)\ln\frac{b}{c}$$

$$+ 2Bt_i \ln\frac{t_i}{t_o} + t_o \ln\frac{t_o}{a} - t_i \ln\frac{t_i}{a} + \frac{Bt_o^2}{t_i} - Bt_i$$

$$(3) = \int_{t_o}^{c} [1 + \ln\frac{r}{b} + (B + 1)\ln(\frac{b}{c})^2 - Bt_o^2(\frac{1}{c^2} - \frac{1}{b^2})dr$$

$$= 2B(\ln\frac{b}{c})(c - t_o) - Bt_o^2(\frac{1}{c} - \frac{c}{b^2} - \frac{t_o}{c^2} + \frac{t_o}{b^2}) + c\ln\frac{b}{c} - t_o\ln\frac{t_o}{b} - 2t_o\ln\frac{b}{c}$$

$$(4) = \int_c^b [1 + \ln\frac{r}{b} - \frac{Bt_o^2}{r^2} + B(3 + 2\ln r) - \frac{Bt_o^2}{b^2} - B(1 + 2\ln b)]dr$$

$$= (2B + 1)c\ln\frac{b}{c} + \frac{Bt_o^2}{c}(-1 + \frac{c^2}{b^2})$$

$$\text{Force} = 0 = Bt_i[\frac{p}{B} + \frac{2}{B}\ln\frac{t_i}{a} - t_o^2(\frac{1}{t_i^2} + \frac{1}{c^2} - \frac{1}{b^2} - \frac{1}{t_o^2}) + 2\ln\frac{bt_o}{ct_i}]$$

identical to (4.71)

APPENDIX B

EFFECT OF RESIDUAL STRESSES ON COLUMN STRENGTH

B.1 Elemental Force and Moment for Assumed Residual Strain Distributions

The subscript j and superscript res are dropped here.

B.1.1 Linear Strain Distribution, Straight Element (Fig. B.1)

Let the element dimensions be B*t and the residual strains at the outside and inside edges be ε_o and ε_i. The residual force is:

$$f = EBt\,(\varepsilon_o + \varepsilon_i)/2$$

The moment sign convention is such that positive moment creates less compression on the outside than the inside.

$$\varepsilon = (\varepsilon_o + \varepsilon_i)/2 + (\varepsilon_o - \varepsilon_i)\rho/t \qquad (6.22)$$

$$-\,m = EB\int_{-t/2}^{t/2} \varepsilon\rho\,d\rho = EBt^2(\varepsilon_o - \varepsilon_i)/12 \qquad (6.39a)$$

B.1.2 Linear Strain Distribution, Curved Element (Fig. B.2)

Let R be the average radius, B = 2αR the width and c the radius of the centroid of the element. From Roark and Young [1975]:

$$c = \frac{2}{3}\,\frac{\sin\alpha}{\alpha}\,\left(R - \frac{t}{2} + \frac{(R + t/2)^2}{2R}\right)$$

or

$$c = \frac{B}{2}\,\left(1 + \frac{t^2\alpha^2}{3B^2}\right)\,\frac{\sin\alpha}{\alpha^2}\,. \qquad (B.1)$$

The residual strain distribution is:

$$\varepsilon = \frac{\varepsilon_o + \varepsilon_i}{2} + \frac{\varepsilon_o - \varepsilon_i}{2}\beta \qquad \text{where } \beta = \frac{r-R}{t/2}$$

The residual force is:

$$f = 2E\int_o^{\alpha}\int_{R-t/2}^{R+t/2} \varepsilon r d\theta dr = E\int_o^{\alpha}\int_{R-t/2}^{R+t/2}[(\varepsilon_o + \varepsilon_i) + (\varepsilon_o - \varepsilon_i)\beta](\tfrac{t}{2}\beta + R)\tfrac{t}{2}\, d\theta d\beta$$

$$f = \frac{EBt}{2}(\varepsilon_o + \varepsilon_i) + \frac{Et^2\alpha}{6}(\varepsilon_o - \varepsilon_i) \tag{6.35}$$

The residual moment is:

$$-m = \int_A E\varepsilon dA(x-c) = 2E\int_{\theta=0}^{\alpha}\int_{R-t/2}^{R+t/2}\left(\frac{\varepsilon_o + \varepsilon_i}{2} + \frac{\varepsilon_o - \varepsilon_i}{2}\beta\right)(rdrd\theta)(r\cos\theta - c)$$

$$-\frac{m}{Et} = \int_{-1}^{1}\int_{\theta=0}^{\alpha}[\varepsilon_o + \varepsilon_i + (\varepsilon_o - \varepsilon_i)\beta](\tfrac{t}{2}\beta + R)[(\tfrac{t}{2}\beta + R)\cos\theta - c]d\beta d\theta$$

$$= (\varepsilon_o + \varepsilon_i)(\frac{t^2}{12}\sin\alpha + R^2\sin\alpha - Rc\alpha) + \frac{Rt\alpha}{6}(\varepsilon_o - \varepsilon_i)[\frac{2\sin\alpha}{\alpha} - \frac{c}{R}]$$

Introducing (B.1) and $R = B/2\alpha$:

$$-m = \frac{EBt^2}{12}(\varepsilon_o - \varepsilon_i)\frac{\sin\alpha}{\alpha}\left(1 - \frac{t^2\alpha^2}{3B^2}\right) \tag{6.39b}$$

B.1.3 Rectangular Strain Distribution, Straight Element (Fig. B.3)

Let $\zeta = 2\rho_n/t$. The residual force is:

$$f = EB\varepsilon_o(\tfrac{t}{2} - \rho_n) + EB\varepsilon_i(\tfrac{t}{2} + \rho_n) = \frac{EBt}{2}[(1-\zeta)\varepsilon_o + (1+\zeta)\varepsilon_i]$$

The residual moment is:

$$-m = EB\varepsilon_o(\frac{t}{2} - \rho_n)\frac{1}{2}(\frac{t}{2} + \rho_n) + EB\varepsilon_i(\frac{t}{2} + \rho_n)\frac{1}{2}(-\frac{t}{2} + \rho_n)$$

$$= \frac{EBt^2}{B}(1 + \zeta)(1 - \zeta)(\varepsilon_o - \varepsilon_i)$$

B.1.4 Rectangular Strain Distribution, Curved Element: (Fig. B.4)

Let subscripts o and i refer to the outside and inside parts, separated by the neutral axis. For each part the average radius is:

$$R_o = R + \frac{1}{2}(\frac{t}{2} + \rho_n) = R + \frac{t}{4}(1 + \zeta)$$

$$R_i = R + \frac{1}{2}(-\frac{t}{2} + \rho_n) = R - \frac{t}{4}(1 - \zeta)$$

the average width and thickness are:

$B_o = 2R_o\alpha$ $\qquad T_o = (t/2)(1 - \zeta)$

$B_i = 2R_i\alpha$ $\qquad T_i = (t/2)(1 + \zeta)$

The centroid is:

$$c_o = R_o\,\frac{\sin\alpha}{\alpha}\,(1 + \frac{T_o^2}{12R_o^2})$$

$$c_i = R_i\,\frac{\sin\alpha}{\alpha}\,(1 + \frac{T_i^2}{12R_i^2})$$

The residual force is:

$$f = E\varepsilon_o 2R_o\alpha T_o + E\varepsilon_i 2R_i\alpha T_i$$

$$= \frac{EBt}{2}[(\varepsilon_o + \varepsilon_i) - \zeta(\varepsilon_o - \varepsilon_i)] + \frac{Et\alpha^2}{4}(1 + \zeta)(1 - \zeta)(\varepsilon_o - \varepsilon_i)$$

The residual moment is:

$$+m = 2E\alpha R_o T_o \varepsilon_o \frac{\sin\alpha}{\alpha}[R(1 + \frac{t^2}{12R^2}) - R_o(1 + \frac{T_o^2}{12R_o^2})]$$

$$+ 2E\alpha R_i T_i \varepsilon_i \frac{\sin\alpha}{\alpha} [R(1 + \frac{t^2}{12R^2}) - R_i(1 + \frac{T_i^2}{12R_i^2})] \; .$$

$$-m = \frac{EBt^2}{8} (1 + \zeta)(1 - \zeta)(\varepsilon_o - \varepsilon_i) \frac{\sin\alpha}{\alpha}$$

$$+ \frac{Et^3}{12} \zeta(1 + \zeta)(1 - \zeta)(\varepsilon_o + \varepsilon_i)\sin\alpha$$

$$- \frac{Et^4}{24B} (1 + \zeta)(1 - \zeta)(\varepsilon_o - \varepsilon_i)\alpha\sin\alpha$$

B.2 Relation of Experimental Results to Assumed Rectangular Distribution

Let $\bar{m}$, $\bar{f}$ designate the moment and force resultants of the linear stresses of relaxation

$$\begin{cases} -m = +\bar{m} \\ f = -\bar{f} \end{cases}$$

B.2.1 Straight Element

$$\begin{cases} \frac{EBt^2}{12} (1 + \zeta)(1 - \zeta)(\varepsilon_o - \varepsilon_i) = \frac{EBt^2}{12} (\bar{\varepsilon}_o - \bar{\varepsilon}_i) \\ \frac{EBt}{2} [(1 - \zeta)\varepsilon_o + (1 + \zeta)\varepsilon_i] = \frac{EBt}{2} (\bar{\varepsilon}_o + \bar{\varepsilon}_i) \end{cases}$$

$$\Longrightarrow \begin{cases} \varepsilon_i = \frac{\bar{\varepsilon}_o + \bar{\varepsilon}_i}{2} - \frac{\bar{\varepsilon}_o - \bar{\varepsilon}_i}{3(1 + \zeta)} \\ \varepsilon_o = \frac{\bar{\varepsilon}_o + \bar{\varepsilon}_i}{2} + \frac{\bar{\varepsilon}_o - \bar{\varepsilon}_i}{3(1 - \zeta)} \end{cases}$$

B.2.2 Curved Element

$$\frac{EBt^2}{8}(1+\zeta)(1-\zeta)\frac{\sin\alpha}{\alpha}(\varepsilon_o-\varepsilon_i)$$

$$+\frac{Et^3}{12}\zeta(1+\zeta)(1-\zeta)(\sin\alpha)(\varepsilon_o+\varepsilon_i)$$

$$-\frac{Et^4}{24D}(1+\zeta)(1-\zeta)\alpha(\sin\alpha)(\varepsilon_o-\varepsilon_i)$$

$$=\frac{EBt^2}{12}\left(1-\frac{t^2\alpha^2}{3B^2}\right)\frac{\sin\alpha}{\alpha}(\bar{\varepsilon}_o-\bar{\varepsilon}_i)$$

$$\frac{EBt}{2}[(\varepsilon_o+\varepsilon_i)-\zeta(\varepsilon_o-\varepsilon_i)]+\frac{E\alpha t^2}{4}(1-\zeta^2)(\varepsilon_o-\varepsilon_i)$$

$$=\frac{EBt}{2}(\bar{\varepsilon}_o+\bar{\varepsilon}_i)+\frac{Et^2\alpha}{6}(\bar{\varepsilon}_o-\bar{\varepsilon}_i)$$

Let $u=\varepsilon_o+\varepsilon_i$, $w=\varepsilon_o-\varepsilon_i$, $\bar{u}=\bar{\varepsilon}_o+\bar{\varepsilon}_i$, $\bar{w}=\bar{\varepsilon}_o-\bar{\varepsilon}_i$, $\beta=t/B$ and $\psi=(1+\zeta)(1-\zeta)$.

The above equations reduce to:

$$3\psi[\alpha\beta\zeta(\alpha\beta\psi-2\zeta)+\alpha^2\beta^2-3]w=6\alpha\beta\psi\zeta\,\bar{u}+2(\alpha^2\beta^2\psi\zeta+\alpha^2\beta^2-3)\bar{w}$$

$$3\psi[\alpha\beta\zeta(\alpha\beta\psi-2\zeta)+\alpha^2\beta^2-3]u=(\alpha^2\beta^2-3)(3\lambda\bar{u}+2\zeta\bar{w}) \qquad (6.32)$$

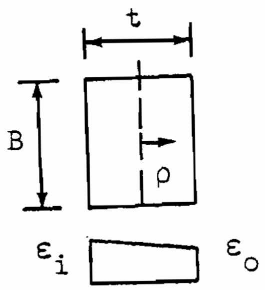

Fig. B.1

Straight Element With
Linear Strain Distribution

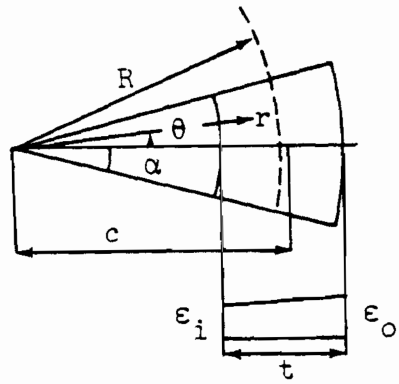

Fig. B.2

Curved Element With
Linear Strain Distribution

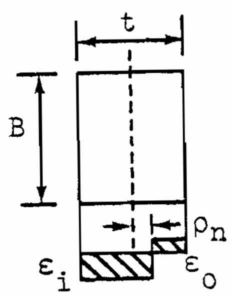

Fig. B.3

Straight Element With
Rectangular Strain Distribution

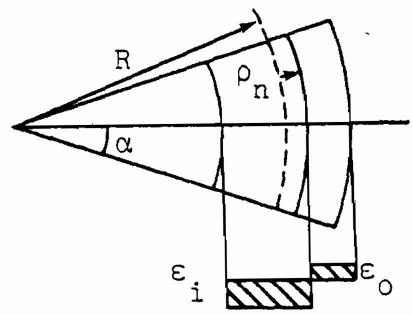

Fig. B.4

Curved Element With
Rectangular Strain Distribution

APPENDIX C

ANALYSIS OF VARIANCE

The following is taken from Draper and Smith [1966].

The linear model $\hat{Y}_i = b_o + b_1 X_i$ is fit by least-squares to the data (X_i, Y_i). An analysis of variance (ANOVA) table measures the precision of the estimate of the regression line. Let $\bar{Y}$ be the mean of the Y_i's.

The equation:

$$\Sigma(Y_i - \bar{Y})^2 = \Sigma(Y_i - \hat{Y}_i)^2 + \Sigma(\hat{Y}_i - \bar{Y})^2$$

i.e. Sum of Squares about the mean	=	Sum of Squares about regression (residual)	+	Sum of Squares due to regression

"shows that, of the variation in the Y_i's about their mean, some of the variation can be ascribed to the regression line and some, $\Sigma(Y_i - \hat{Y}_i)^2$, to the fact that the actual observations do not all lie on the regression line." Thus, a way of assessing the usefulness of the regression line as a predictor "is to see how much of the sum of squares (SS) about the mean has fallen into the SS due to regression and how much into the SS about regression. We shall be pleased if the SS due to regression is much greater than the SS about regression", i.e.

$$R^2 = \frac{\text{SS due to regression}}{\text{SS about mean}} = 1.0$$

The total variation ΣY_i^2 can be split into two parts. "The quantity $n\bar{Y}^2$ would be the sum of squares about b_o, $SS(b_o)$, if the model $\hat{Y}_i = b_o + \varepsilon_i$

were fitted (b_o = constant, ε_i = error). The remainder

$$\Sigma(Y_i - \bar{Y})^2 = \Sigma Y_i^2 - (\Sigma Y_i)^2/n$$

thus measures the extra SS removed by b_1 when the model $\hat{Y}_i = b_o + b_1 X_i + \varepsilon_i$ is used."

"The mean square about regression, s^2, provides an estimate based on n-2 degrees of freedom of the variance about the regression.

If the regression equation were estimated from an indefinitely large number of observations, the variance about the regression would represent a measure of the error with which any observed value of Y would be predicted from a given value of X using the determined equation."

The notation SS $(b_1|b_o)$ is read "the sum of squares for b_1 after allowance has been made for b_o."

APPENDIX D

ALTERNATIVE BUCKLING MODES FOR C14

It was observed in Chapter 9 that the PBC14 and RFC14 column strengths fall consistently below the predicted ones. It is therefore necessary to examine other modes of failure, namely local buckling of the plate elements, torsional and torsional-flexural buckling. The sections were chosen so these buckling modes should be irrelevant as the following calculations prove, and indeed they were not observed to occur. Since these buckling modes did not occur in the thinner sections, they need not be checked for the thicker sections.

D.1 Local Buckling

The web and the lips (stiffeners) are checked for local buckling. The flanges, being narrower than the web and being adequately stiffened so their boundary conditions are similar to those of the web, need not be checked.

D.1.1 Determination of the Critical Stress in the Inelastic Range of Buckling

The following formula is worked out in Bleich [1952] p. 343:

$$\frac{\sigma_{cr}}{\sqrt{\tau}} = K \frac{\pi^2 E}{12(1-\nu^2)(w/t)^2} \qquad \text{(D.1)}$$

where σ_{cr} = critical stress

τ = E_t/E = ratio of tangent modulus to Young's modulus E

ν = Poisson's ratio

w = plate width

t = plate thickness

K = buckling coefficient depends on boundary conditions.

The edges of the web are close to being both fixed (K = 6.97). A very conservative estimate is K = 4.0, which corresponds to simply supported edges.

$$\frac{\sigma_{cr}}{\sqrt{\tau}} = 4.0 \frac{\pi^2 \, 29500}{12(1-.09)(2.50/.073)^2} = 91. \text{ ksi}$$

Again, a very conservative estimate for the stiffener is K = .425, which corresponds to one simply supported edge, one free.

$$\frac{\sigma_{cr}}{\sqrt{\tau}} = .425 \frac{\pi^2 \, 29500}{12(1-.09)(.50/.073)^2} = 241. \text{ ksi}$$

Bleich [1952] pp. 343, 344 tabulates values of σ_{cr} corresponding to various ratios $\sigma_{cr}/\sqrt{\tau}$ for two steels with yield strength σ_y = 33 ksi and σ_y = 45 ksi.

	σ_y = 33 ksi	σ_y = 45 ksi
$\sigma_{cr}/\sqrt{\tau}$	σ_{cr}/σ_y	σ_{cr}/σ_y
90	.98	.96
250	1.00	1.00

The yield strength of the flats of the C14 sections is about 39 ksi. It can therefore be concluded that $\sigma_{cr}/\sigma_y \simeq 1.0$, i.e., local buckling will not occur before yielding. Global flexural buckling will have occurred before.

D.1.2 Effective Width of Web

The current philosophy of the AISI [1977] is to use the concept of effective width.

For the present case:

$$\text{Actual} \quad \frac{w}{t} = \frac{2.50}{.073} = 34.2 < \left(\frac{w}{t}\right)_{lim} = \frac{221}{\sqrt{\sigma_y}} = \frac{221}{\sqrt{39}} = 35.4$$

So the web is fully effective.

D.1.3 Adequacy of Stiffener (Desmond [1978])

The adequacy of the stiffener is determined by the following formula:

$$(I_s/t^4)_{ad} = 36.1 \times 10^{-6}[(w/t)\sqrt{\sigma_y} - 71.7]^3 \qquad (D.2)$$

where I_s = moment of inertia of stiffener about its own centroidal axis parallel to the stiffened element, in^4.

t = thickness of stiffener and of flange, in.

w = flat width of edge stiffened flange, in.

For the present case:

$$(I_s/t^4)_{ad} = 36.1 \times 10^{-6}[(1.20/.073)\sqrt{39} - 71.7]^3 = 1.07$$

$$\text{Actual} \quad I_s/t^4 = \frac{.5^3}{12 \times .073^3} = 26.8 > (I_s/t^4)_{ad}$$

So the stiffener is adequate.

D.1.4 Effective Width of Flange (Desmond [1978])

The effective width of an adequately stiffened flange is:

$$(w/t)_{eff} = 0.95\sqrt{\frac{E(k_w)_{a.s.}}{\sigma_y}}\left(1. - \frac{.209}{w/t}\sqrt{\frac{E(k_w)_{a.s.}}{\sigma_y}}\right) \qquad (D.3)$$

where E = modulus of elasticity, ksi

$(k_w)_{a.s.}$ = $-5D_s/w + 5.25$ when $D_s/w > 0.25$ (D.4)

= buckling coefficient for adequately stiffened flange

D_s = unstiffened flat width of the stiffener plus the corner radius.

For the present case:

$$D_s/w = .7/1.20 = .583 \quad \text{and} \quad (k_w)_{a.s.} = 2.33$$

$$(w/t)_{eff} = 0.95\sqrt{\frac{29500(2.33)}{39}}\left(1. - \frac{.209}{1.20/.073}\sqrt{\frac{29500(2.33)}{39}}\right) = 18.6$$

Actual $w/t = 1.20/.073 = 16.4 < (w/t)_{eff}$

So the flanges are adequately stiffened and fully effective.

It can be concluded that local buckling is of no concern for the C14 sections.

D.2 Torsional-Flexural Buckling (Chajes, Fang and Winter [1966], AISI [1977])

In the elastic range, the flexural, torsional and torsional-flexural buckling loads are expressed by the following formulas:

$$P_{crx} = \frac{\pi^2 EI_x}{(KL)_x^2} \tag{D.5}$$

$$P_{cry} = \frac{\pi^2 EI_y}{(KL)_y^2} \tag{D.6}$$

$$P_T = \frac{1}{r_o^2}\left(GJ + \frac{\pi^2 EC_w}{(KL)_T^2}\right) \tag{D.7}$$

$$P_{TFO} = \frac{1}{2\beta}\left(P_{crx} + P_T - \sqrt{(P_{crx} + P_T)^2 - 4\beta P_{crx}P_T}\right) \tag{D.8}$$

where P_{crx} = flexural buckling load about x

P_{cry} = flexural buckling load about y

P_T = torsional buckling load

P_{TFO} = torsional-flexural buckling load

KL = effective length

β = $1 - x_o^2/r_o^2$ = shape factor = .4017

I_x = moment of inertia about x = .712 in^4

I_y = moment of inertia about y = .219 in^4

J = St. Venant torsion constant = .000928 in^4

C_w = warping constant = .605 in^6

E = Young's modulus = 29500 ksi

G = shear modulus = 11300 ksi

x_o = distance between centroid and shear center = -1.629 in

r_o = polar radius of gyration about shear center = $\sqrt{4.435}$ in

Also A = cross-sectional area = .522 in^2

The numbers above have been worked out for the thin channels (C14).

In the inelastic range, a parabolic formula applies to the above phenomena.

For flexural buckling:

$$\sigma = \sigma_{cry} \qquad \text{for} \qquad \sigma_{cry} \leq \sigma_y/2$$

$$\sigma = \left(1.0 - \frac{\sigma_y}{4\sigma_{cry}}\right)\sigma_y \qquad \text{for} \qquad \sigma_{cry} > \sigma_y/2 \tag{D.9}$$

The same formula applies for buckling about x.

For torsional buckling:

$$\sigma = \sigma_T \qquad \text{for} \qquad \sigma_T \leq \sigma_y/2$$

$$\sigma = \left(1.0 - \frac{\sigma_y}{4\sigma_T}\right)\sigma_y \qquad \text{for} \qquad \sigma_T > \sigma_y/2 \tag{D.10}$$

For torsional-flexural buckling:

$$\sigma = \sigma_{TFO} \qquad \text{for} \qquad \sigma_{TFO} \leq \sigma_y/2$$

$$\sigma = \left(1.0 - \frac{\sigma_y}{4\sigma_{TFO}}\right)\sigma_y \qquad \text{for} \qquad \sigma_{TFO} > \sigma_y/2 \tag{D.11}$$

where σ = buckling stress

σ_{cry} = elastic flexural buckling stress about the y-axis

σ_T = elastic torsional buckling stress

σ_{TFO} = elastic torsional-flexural buckling stress

σ_y = yield stress = 39. ksi.

Table D.1 compares the buckling loads obtained from the above formulas with the actual buckling loads, P_u. The boundary conditions are such that $(KL)_y = L$, $(KL)_x = (KL)_T = L/2$. P_T, P_{TF} and P_{cry} now denote the torsional, torsional-flexural and flexural about y buckling loads, elastic or inelastic. It is seen that the flexural buckling load about the weak axis is lower than the torsional or torsional-flexural buckling loads.

D.3 Conclusion

The possibility of local buckling (web or stiffener), torsional and torsional-flexural buckling was examined in this Appendix. These buckling modes were found to occur at higher loads than the studied mode, flexural buckling about the weak axis.

It was noted in Chapter 8 that the addition of local imperfections on a column already possessing an overall imperfection has little effect on the peak load (Gilbert and Calladine [1964]). The introduction of a small eccentricity of the load reduces the initial overall imperfection.

Load eccentricity and overall imperfection affect the same buckling mode and the possibly catastrophic effect of mode coupling need not be feared.

TABLE D.1

BUCKLING LOADS FOR C14

L in	P_T kip	P_{TF} kip	P_{cry} kip	PBC14 P_u kip	RFC14 P_u kip
27.0	19.9	19.8	19.2	16.9	18.5
				20.2	19.5
33.0	19.7	19.6	18.6	16.3	
39.0	19.4	19.3	17.9	14.4	16.3
				19.3	18.0
45.0	19.1	18.9	17.1	13.5	
51.0	18.7	18.5	16.1	13.7	16.0
					15.5
					14.0
57.0	18.3	18.1	15.1	13.9	
63.0	17.9	17.6	13.9	10.4	11.5
75.0	17.0	16.5	11.2	9.50	
80.5	16.5	16.0	9.84		8.00
					8.80
84.9	16.1	15.5	8.85		9.05

APPENDIX E

INPUT FOR PROGRAM COLUMN

```
a             READ(II,205)  NT,(TITLE(I),I=1,NT)
        205   FORMAT(I2,25A1)

         NT   ≤ 25 is total number of characters in TITLE
   TITLE(I)   any title of NT characters

b             READ(II,210)  N1,N2,N3,N4,N5,NA,NB,NN,NMOD,NST,MI,
                            IRO,IWRITE,ISTUB
        210   FORMAT(14I5)

         N1   number of segments in 1st flat
         N2             —              corner
         N3             —           2nd flat
         N4             —              corner
         N5             —           last flat
         NA   number of data points for yield stress and thickness
         NB           —                 residual strain
         NN   number of points in final P-V graph
       NMOD   number of residual strain models to be considered
        NST   number of strain outputs
         MI   near maximum of P, DELV is divided by MI for a
              detailed look
        IRO   =0 if all RON(I)=0, ≠ 0 otherwise
     IWRITE   =1 if detailed output wanted, 0 otherwise
      ISTUB   =1 if stub column, 0 otherwise

c             READ(II,215)  A,B,C,R1,R2,PSI1,PSI2,FACTOR
        215   FORMAT(8D10.0)

          A   length (inch) of 1st flat
          B           —        2nd flat
          C           —        last flat
         R1   radius of 1st corner
         R2      —    2nd corner
       PSI1   angle (degrees) of 1st corner
       PSI2           —          2nd corner
     FACTOR   +1.D0 for channel, -1.D0 for hat

d             READ(II,215)  E,EN

          E   modulus of elasticity (KSI)
         EN   stop when P/PMAX=EN
```

e READ(II,215) XY(I),SIGY(I),T1(I)

- XY(I) location of data along perimeter of section, starting from axis of symmetry
- SIGY1(I) yield stress (KSI)
- T1(I) thickness (inch)

f READ(II,215) XR(I),RSO1(I),RSI1(I),RON1(I)

- XR(I) location of data
- RSO1(I) outward (+ or convex face) residual strain
- RSI1(I) inward (- or concave face) residual strain

  (RSO1, RSI1: algebraic opposite of experimentally measured elastic release)
- RON1(I) coordinate (in thickness direction w.r.t. middle surface) of neutral surface for model 3 residual strain distribution.

  For these variables, refer to sign convention.

g READ(II,210) (IS(I),I=1,NST)

- IS(I) segment number at whose outer (+) face strain is to be output

h READ(II,255) NET,MAX1,NAX1,C1,C2,F2,F3,F4

255 FORMAT(3I3,5D10.0)

- NET =0 if following 7 variables have default values. This card is then blank.

  ≠0 if following variables are input.
- MAX1 =20 by default. Maximum number of iterations for force equilibrium loop.
- NAX1 =20 by default. Maximum number of iterations for moment equilibrium loop.
- C1 =2.D-4 by default. Convergence criterion for force equilibrium.
- C2 =1.D-3 by default. Convergence criterion for moment equilibrium.
- F2 =5.5D0 by default. (PA + DL(K))/(V(I) + W)/F2
- F3 =.90D0 by default. PA = F3 * PY
- F4 =1.0D0 by default. EA + (PA - P)/(E * AE) * F4

  (F2, F3, F4: scaling factors that affect convergence)

The above parameters are used in Subroutine LOAD1.

i READ(II,210) MOD(I),I=1,NMOD),(NL(I),I=1,NMOD)

- MOD(I) Residual strain model number (1 for uniform, 2 for linear, 3 for rectangular, 4 for no strain. 4 only works for stub columns, i.e., axial straining but no lateral deflection).
- NL(I) Number of column lengths for each model.

```
j                   READ(II,285)  (NCOEF(I,J),J=1,NLI)
             285    FORMAT(20I3)
```

NCOEF(I,J) number of ratios of initial deflection/length for each model and each length.

```
k                   READ(II,260)  MOD(I),RLL(I,J),COEFF(I,J,K),
                                  DV1(I,J,K),V1(I,J,K),EC(I,J,K)
             260    FORMAT(I5,5D10.0)
```

MOD(I)	residual strain model number
RLL(I,J)	column length
COEFF(I,J,K)	ratio of initial deflection/column length
DV1(I,J,K)	deflection increment
V1(I,J,K)	first imposed deflection
EC(I,J,K)	eccentricity.

EXAMPLE
OF PARTS i, j and k OF INPUT

```
      READ(II,210)  (MOD(I),I=1,NMOD),(NL(I),I=1,NMOD)
      DO25  I=1,NMOD
      NLI=NL(I)
   25 READ(II,285)  (NCOEF(I,J),J=1,NLI)
      DO30  I=1,NMOD
      NLI=NL(I)
      DO30  J=1,NLI
      IJC=NCOEF(I,J)
      DO30  K=1,IJC
   30 READ(II,260)  MOD(I),RLL(I,J),COEFF(I,J,K),DV1(I,J,K),
                    V1(I,J,K),EC(I,J,K)
  210 FORMAT(14I5)
  260 FORMAT(I5,5D10.0)
  285 FORMAT(20I3)
```

Suppose there are NMOD=2 models of residual strains to be considered. Let these two models be MOD(1)=2 and MOD(2)=3. There is NL(1)=1 column of length RLL(1,1)=60.0D0 with MOD(1) distribution to be tested. This column is to be tested twice with NCOEF(1,1)=2 different initial deflections, COEFF(1,1)=1.D-3 and COEFF(1,2)=5.D-4.

For MOD(2)=3 distribution let there be NL(2)=2 columns of length RLL(2,1)=70.D0 and RLL(2,2)=80.0D0. Each of these is tested with the same initial deflection COEFF(2,1)=COEFF(2,2)=1.D-3. Let DV1(I,J,K) = V1(I,J,K)=1.D-3 and EC(I,J,K)=0.DO. The input looks as follows:

```
MOD(1),MOD(2),NL(1),NL(2)
NCOEF(1,1)
NCOEF(2,1),NCOEF(2,2)
MOD(1),RLL(1,1),COEFF(1,1,1),DV1(1,1,1),V1(1,1,1),EC(1,1,1)
MOD(1),RLL(1,1),COEFF(1,1,2),DV(1,1,2),V1(1,1,2),EC(1,1,2)
MOD(2),RLL(2,1),COEFF(2,1,1),DV(2,1,1),V1(2,1,1),EC(2,1,1)
MOD(2),RLL(2,2),COEFF(2,2,1),DC(2,2,1),V1(2,2,1),EC(2,2,1)
```

1st Subscript I: model number

2nd Subscript J: column number

3rd Subscript K: initial deflection number

```
FORMAT 210   2,3,1,2
       285   2
       285   1,1
       260   2,60.DO,1.D-3,1.D-3,1.D-3,0.DO
       260   2,60.DO,5.D-4,1.D-3,1.D-3,0.DO
       260   3,70.DO,1.D-3,1.D-3,1.D-3,0.DO
       260   3,80.DO,1.D-3,1.D-3,1.D-3,0.DO
```

APPENDIX F

PROGRAM COLUMN

```
C                          PROGRAM COLUMN
C
C     THE PROGRAM COLUMN COMPUTES THE LOAD VERSUS LATERAL
C     DEFLECTION CURVE OF AN INITIALLY IMPERFECT COLUMN
C     UNDER ECCENTRIC LOAD. IT IS ASSUMED THAT:
C     - THE CROSS-SECTION IS A LIPPED CHANNEL (C) OR A HAT
C       (OMEGA) SHAPE.
C     - THE COLUMN IS HINGED AT BOTH ENDS AND BENDING OCCURS
C       ABOUT THE WEAK AXIS ONLY.
C     - THE  APPLIED  LOAD REACHES ITS MAXIMUM LONG BEFORE
C       ANY LOCAL OR TORSIONAL BUCKLING OCCURS.
C     - CROSS-SECTIONAL GEOMETRY AND MATERIAL PROPERTIES DO
C       NOT VARY ALONG THE AXIS OF THE COLUMN. CONSEQUENTLY,
C       DISTORTION OF THE CROSS-SECTION WITH INCREASING LOAD
C       IS NEGLECTED.
C     - THE INITIAL DEFLECTION AND ANY ADDITIONAL DEFLECTION
C       ARE SINUSOIDAL.
C     - THE MATERIAL IS LINEARLY ELASTIC, PERFECTLY PLASTIC.
C     - PLANE SECTIONS REMAIN PLANE.
C
C     THE SIGN CONVENTION IS AS FOLLOWS:
C     - POSITIVE MOMENT PRODUCES POSITIVE LATERAL DEFLECTION
C       (TO THE RIGHT OF THE CENTROID).
C     - COMPRESSION IS POSITIVE, TENSION NEGATIVE.
C     - FOR THE THICKNESS COORDINATE, + IS RADIALLY OUTWARDS
C       - INWARDS. FLATS FOLLOW SAME SIGN CONVENTION AS
C       PREVIOUS CORNER. FOR FIRST FLAT, + IS TO THE LEFT.
C     - ANGLES ARE MEASURED COUNTERCLOCKWISE FROM THE +
C       HORIZONTAL AXIS.
C
C     FOUR DIFFERENT MODELS OF RESIDUAL STRESS DISTRIBUTION
C     ACROSS THE THICKNESS CAN BE USED:
C     - MODEL 1: UNIFORM DISTRIBUTION
C     - MODEL 2: LINEAR DISTRIBUTION
C     - MODEL 3: RECTANGULAR DISTRIBUTION
C     - MODEL 4: NO RESIDUAL STRESS.
C
      IMPLICIT REAL *8 (A-H,O-Z)
      REAL *8 L1,L2,L3,L4
      LOGICAL *1 TITLE(25)
      COMMON/A1/D(100),T(100),PHI1(100),PHI2(100),XC(100),
     1          XD(100),YI(100),PI,E,N,NN
      COMMON/A2/RSO(100),RSI(100),RON(100),EY(100),XO,AO,YO,
     1          PL,MODEL
      COMMON/A3/VSO(100),VSI(100),V(100),PF(100),E1,W,DELV,
     1          OF,OM,AEL(100),PY,IP
      COMMON/A4/U(100),ST(100,4),IS(4),NST
      DIMENSION XY(25),XR(25),RSO1(25),RSI1(25),RON1(25),
     1SIGY1(25),S(25),COEFF(4,20,8),RLL(4,20),T1(25),V1
     2(4,20,8), DV1(4,20,8),INDEX(25),MOD(4),NL(4),NCOEF
     3(4,20),   EC(4,20,8)
      II=5
      IO=6
      PI=4.D0*DATAN(1.D0)
```

```
      READ (II,205) NT,(TITLE(I),I=1,NT)
      WRITE(IO,505)    (TITLE(I),I=1,NT)
      READ (II,210)   N1,N2,N3,N4,N5,NA,NB,NN,NMOD,NST,MI,
     1IRO,IWRITE,ISTUB
      N=N1+N2+N3+N4+N5
      WRITE(IO,510) N,N1,N2,N3,N4,N5,NA,NB,NN,NMOD,NST,MI,
     1IRO,ISTUB
      READ (II,215) A,B,C,R1,R2,PSI1,PSI2,FACTOR
      WRITE(IO,515) A,B,C,R1,R2,PSI1,PSI2,FACTOR
      PSI1=PSI1*PI/180.D0
      PSI2=PSI2*PI/180.D0
      READ (II,215) E,EN
      WRITE(IO,520) E,EN
      WRITE(IO,525)
      DO 5 I=1,NA
      READ (II,215)   XY(I),SIGY1(I),T1(I)
      WRITE(IO,530) I,XY(I),SIGY1(I),T1(I)
    5 SIGY1(I)=SIGY1(I)/E
      WRITE(IO,535)
      DO 10 I=1,NB
      READ (II,215)   XR(I),RSO1(I),RSI1(I),RON1(I)
   10 WRITE(IO,540) I,XR(I),RSO1(I),RSI1(I),RON1(I)
      READ (II,210) (IS(I),I=1,NST)
   20 READ (II,255) NET,MAX1,NAX1,C1,C2,F2,F3,F4
      WRITE(IO,565)
      READ (II,210) (MOD(I),I=1,NMOD),(NL(I),I=1,NMOD)
      DO 25 I=1,NMOD
      NLI=NL(I)
   25 READ (II,285) (NCOEF(I,J),J=1,NLI)
      DO 30 I=1,NMOD
      NLI=NL(I)
      DO 30 J=1,NLI
      IJC=NCOEF(I,J)
      DO 30 K=1,IJC
      READ (II,260) MOD(I),RLL(I,J),COEFF(I,J,K),DV1(I,J,K),
     1V1(I,J,K),EC(I,J,K)
      WRITE(IO,595) MOD(I),RLL(I,J),COEFF(I,J,K),DV1(I,J,K),
     1V1(I,J,K),EC(I,J,K)
   30 CONTINUE
      IF(NST.EQ.1) WRITE(IO,545) IS(1)
      IF(NST.GT.1) WRITE(IO,550) (IS(I),I=1,NST)
      IF (NET.NE.0) WRITE(IO,555) MAX1,NAX1,C1,C2,F2,F3,F4
C
C     COMPUTE SEGMENT LENGTH
C
      DO 60 I=1,N1
   60 D(I)=A/DFLOAT(N1)
      DO 65 I=1,N2
   65 D(N1+I)=R1*PSI1/DFLOAT(N2)
      DO 70 I=1,N3
   70 D(N1+N2+I)=B/DFLOAT(N3)
      DO 75 I=1,N4
   75 D(N1+N2+N3+I)=R2*PSI2/DFLOAT(N4)
      DO 80 I=1,N5
```

```
  80   D(N1+N2+N3+N4+I)=C/DFLOAT(N5)
       U(1)=D(1)*.5D0
       DC 85 I=2,N
  85   U(I)=U(I-1)+.5D0*(D(I-1)+D(I))
C
C      INTERPOLATE CATA
C
       CALL SPCOEF (NA,XY,T1,S,INDEX)
       DO 90 I=1,N
  90   T(I)=SPLINE (NA,XY,T1,S,INDEX,U(I))
       CALL SPCOEF (NA,XY,SIGY1,S,INDEX)
       DO 95 I=1,N
  95   EY(I)=SPLINE (NA,XY,SIGY1,S,INDEX,U(I))
       CALL SPCOEF (NB,XR,RSC1,S,INDEX)
       DO 100 I=1,N
 100   RSO(I)=SPLINE (NB,XR,RSO1,S,INDEX,U(I))
       CALL SPCOEF (NB,XR,RSI1,S,INDEX)
       DO 105 I=1,N
 105   RSI(I)=SPLINE (NB,XR,RSI1,S,INDEX,U(I))
C
C      COMPUTE SQUASH LOAD
C
       PY=0.D0
       DC 110 I=1,N
 110   PY=PY+D(I)*T(I)*E*EY(I)
       PY2=2.D0*PY
C
       CALL LAYOUT (FACTOR,A,B,C,R1,R2,PSI1,PSI2)
       CALL YNERTA
       WRITE(IO,570) AO,YO,XO
       IW1=1
       IW2=1
       I=1
 115   MODEL=MOD(I)
       IF (MODEL.LT.4) GO TO 116
       CF=0.D0
       CM=0.D0
       E1=0.D0
       GO TC 157
 116   IF(MODEL.EQ.3) GO TO 125
       IF(IW1.GT.1.OR.IW2.GT.1) GO TO 155
       WRITE(IO,600)
       IW1=IW1+1
       DO 120 J=1,N
 120   WRITE(IO,605) J,D(J),T(J),XD(J),XC(J),EY(J),RSO(J),
      1RSI(J)
       GO TC 155
 125   IF(IW2.GT.1) GO TO 155
       IW2=IW2+1
       IF(IRO.EQ.0) GO TO 135
       CALL SPCOEF (NB,XR,RON1,S,INDEX)
       DO 130 IM=1,N
 130   RCN(IM)=SPLINE(NB,XR,RON1,S,INDEX,U(IM))
       GO TC 145
```

```
135   DO 140 IM=1,N
140   RON(IM)=0.D0
145   CALL ALTER
      WRITE(IO,610)
      DO 150 J=1,N
150   WRITE(IO,615) J,D(J),T(J),XD(J),XC(J),EY(J),RSO(J),
     1RSI(J),RON(J),VSO(J),VSI(J)
155   CALL RESIDU
157   WRITE(IO,620) MODEL,OF,E1,OM,PY2
      J=1
160   RL=RLL(I,J)
      K=1
165   W=RL*COEFF(I,J,K)
      V(1)=V1(I,J,K)
      DELV=DV1(I,J,K)
      ECC=EC(I,J,K)
      WRITE(IO,625) (TITLE(IL),IL=1,NT)
      WRITE(IO,630) MODEL,RL,COEFF(I,J,K),ECC
      IF (ISTUB.EQ.0) CALL
     1LOAD1(MI,NET,MAX1,NAX1,IWRITE,C1,C2,F2,F3,F4,EN,ECC)
      IF (ISTUB.EQ.1) CALL
     1LOAD2(MI,NET,MAX1,NAX1,IWRITE,C1,C2,F2,F3,F4,EN,ECC)
200   K=K+1
      IF(K.LE. NCOEF(I,J)) GO TO 165
      J=J+1
      IF(J.LE.NL(I)) GO TO 160
      I=I+1
      IF(I.LE.NMOD) GO TO 115
      STOP
205   FORMAT(I2,25A1)
210   FORMAT(14I5)
215   FORMAT(8D10.0)
255   FORMAT(3I3,5D10.0)
260   FORMAT(I5,5D10.0)
285   FORMAT(20I3)
505   FORMAT(//      10X,25A1)
510   FORMAT(//' NUMBER OF SEGMENTS IN SECTION.............',
     1'...........',I2//' NUMBER OF SEGMENTS IN FIRST FLAT'
     2,'....................',I2//' NUMBER OF SEGMENTS IN '
     3,'FIRST CORNER...................',I2//' NUMBER OF ',
     4'SEGMENTS IN SECOND FLAT....................',I2//
     5' NUMBER OF SEGMENTS IN SECOND CORNER...............',
     6 '..',I2//' NUMBER OF SEGMENTS IN LAST FLAT.........',
     7'............',I2//' NUMBER OF DATA POINTS FOR YIELD'
     8,' STRESS AND THICKNESS.',I2// 'NUMBER OF DATA POINTS'
     9,' FOR RESIDUAL STRAIN..............',I2//
     9' NUMBER OF POINTS',
     1' ON P-V GRAPH.........................',I2//' NUMBER',
     2' OF MODELS OF RESIDUAL STRAINS.................',I2
     3//' NUMBER OF STRAIN OUTPUTS.........................',
     4'.....',I2//' NEAR MAXIMUM DEFLECTION INCREMENT IS ',
     5'DIVIDED BY......',I2// ' IF IRO=0, ALL RON1(I)=0. ',
     6'IRO=......................',I2// ' IF ISTUB=1, ',
     7'THIS IS A STUB COLUMN. ISTUB=............',I2)
```

```
515  FORMAT(/ ' LENGTH OF FIRST FLAT(INCH)................',
    1'...........',1PD11.4//' LENGTH OF SECOND FLAT......',
    2'.........................',D11.4// ' LENGTH OF LAST',
    3' FLAT.................................',D11.4//
    4' RADIUS OF FIRST CORNER..................................'
    5,'..',D11.4//' RADIUS OF SECOND CORNER..............',
    6'................',D11.4//' ANGLE OF FIRST CORNER ',
    7'(DEGREE).......................',2PD11.3// ' ANGLE ',
    8'OF SECOND CORNER...............................',
    9D11.3// ' FACTOR=-1 FOR HAT SECTION, +1 FOR CHANNEL',
    1'............',1PD11.3)
520  FORMAT(/' MODULUS OF ELASTICITY (KSI)................'
    1,'..........',1PD11.4//' STOP WHEN P/PMAX =..........'
    2,'..............',D11.4)
525  FORMAT('1',12X,'LOCATION',11X,'YIELD STRESS',11X,
    1'THICKNESS'/)
530  FORMAT(5X,I2,4X,1PD11.4,10X,2PD11.3,10X,1PD11.4)
535  FORMAT(//13X,'LOCATION',14X,'OUTSIDE',14X,'INSIDE',
    113X,'NEUTRAL AXIS'/29X,' RESIDUAL STRAIN',6X,
    2'RESIDUAL STRAIN')
540  FORMAT(5X,I2,4X,1PD11.4,3(10X,D11.4))
545  FORMAT(//' STRAIN IS COMPUTED AT + FACE OF SEGMENT ',
    2'NUMBER.......',I2)
550  FORMAT(//' STRAIN IS COMPUTED AT + FACE OF SEGMENT ',
    1'NUMBER.......',I2,23(2X,I2))
555  FORMAT(/ ' MAXIMUM # OF ITERATIONS IN FORCE ',
    1'EQUILIBRIUM LOOP...',I2//' MAXIMUM # OF ITERATIONS ',
    2'IN MOMENT EQUILIBRIUM LOOP...',I2//' SCALING FACTOR',
    3' C1.....................................',1PD11.4//
    4' SCALING FACTOR C2...................................'
    5,'..',D11.4//' SCALING FACTOR F2...................',
    6'................',D11.4// ' SCALING FACTOR F3......',
    7'.............................',D11.4// ' SCALING ',
    8'FACTOR F4.....................................',D11.4)
565  FORMAT(//4X,'MODEL',4X,'COLUMN',10X,'INITIAL ',
    1'DEFLECTION',7X,'DEFLECTION',10X,'FIRST IMPOSED',11X,
    2'LOAD'/13X,'LENGTH',11X,'/ COLUMN LENGTH',9X,
    3'INCREMENT',12X,'DEFLECTION',10X,'ECCENTRICITY')
570  FORMAT(/' AREA OF HALF CROSS-SECTION...............',
    1'..........',1PD11.4// ' MOMENT OF INERTIA OF HALF ',
    2'CROSS-SECTION............',D11.4// ' ABCISSA OF ',
    3'CENTROID OF HALF CROSS-SECTION..........',D11.4)
595  FORMAT(5X,I2,4X,2PD11.4,4(10X,1PD11.4))
600  FORMAT(     '1SEGMENT',28X,'ABCISSA',8X,'ABCISSA',8X,
    1'YIELD',7X,'OUTSIDE',7X,'INSIDE'/' NUMBER',3X,'WIDTH',
    26X,'THICKNESS',9X,'OF',13X,'OF',10X,'STRAIN',6X,
    3'RESIDUAL',6X,'RESIDUAL'/36X,'MIDDLE',8X,'CENTROID',
    420X,'STRAIN',8X,'STRAIN')
605  FORMAT(1X,I2,7(3X,1PD11.4))
610  FORMAT(     '1SEGMENT',22X,'ABCISSA',5X,'ABCISSA',6X,
    1'YIELD',6X,'OUTSIDE',5X,'INSIDE',7X,'NEUTRAL',4X,
    2'OUTSIDE',5X,'INSIDE'/' NUMBER',3X,'WIDTH',3X,'THICK',
    3'NESS',6X,'OF',9X,'OF',9X,'STRAIN',5X,'RESIDUAL',4X,
    4'RESIDUAL',6X,'AXIS',6X,'MODIFIED',4X,'MODIFIED'/
```

```
     530X,'MIDDLE',6X,'CENTROID',16X,'STRAIN',6X,'STRAIN',
     618X,'RESIDUAL', 4X,'RESIDUAL'/102X,'STRAIN',6X,
     7'STRAIN')
 615  FORMAT(1X,I2,10(1X,1PD11.4))
 620  FORMAT('1'///28X,'MODEL',I2//' RESIDUAL FORCE / ',
     1'MODULUS E..........................',1PD11.4//
     2' AVERAGE CORRECTIVE STRAIN..........................'
     2,'..',D11.4//' RESIDUAL MOMENT / MODULUS E...........',
     4'...............',D11.4// ' SQUASH LOAD *2..........',
     5'............................',D11.4)
 625  FORMAT('1',' ******** RESULTS FOR ',25A1,'**********')
 630  FORMAT(/' MODEL OF RESIDUAL STRAINS USED.............'
     1,'..........',I2//' COLUMN LENGTH....................'
     2,'....................',2PD11.3//' RATIO OF INITIAL ',
     3'DEFLECTION TO LENGTH................',1PD11.4//
     4' LOAD ECCENTRICITY.................................'
     5,'..',D11.4)
      END
```

```
      SUBROUTINE SPCOEF (N,XN,FN,S,INDEX)
C     THE SUBROUTINE SPCOEF AND THE FUNCTION SPLINE ARE
C     TAKEN FROM 'NUMERICAL COMPUTING' BY SHAMPINE AND
C     ALLEN. THE SUBROUTINE SPCOEF AND THE FUNCTION SPLINE
C     CALCULATE THE NATURAL CUBIC INTERPOLATORY SPLINE FIT
C     TO THE DATA SPECIFIED BY THE ARRAY OF NODES XN, WITH
C     CORRESPONDING FUNCTION VALUES IN THE ARRAY FN. THE
C     NODES XN MUST BE DISTINCT.THE SPLINE IS DETERMINED IN
C     SPCOEF AND EVALUATED IN SPLINE.SPCOEF ARRANGES THE
C     NODES IN INCREASING ORDER AND STORES THIS ORDER IN THE
C     ARRAY INDEX. THE ARRAY ITSELF IS NOT ALTERED. SPCOEF
C     THEN CALCULATES THE ARRAY OF SECOND DERIVATIVES NEEDED
C     TO DEFINE THE SPLINE. THE ARRAYS XN, FN, S AND INDEX
C     MUST BE DIMENSIONED IN THE CALLING PROGRAM.
C
      IMPLICIT REAL *8 (A-H,O-Z)
      DIMENSION XN(N),FN(N),S(N),INDEX(N),
C
C     SPCOEF IS WRITTEN TO HANDLE PROBLEMS WITH UP TO 25
C     NODES. IF MORE NODES ARE USED, ONLY THE NEXT STATEMENT
C     NEED BE CHANGED. THE DIMENSION OF THE ARRAYS RHO AND
C     TAU MUST BE AT LEAST N.
C
     1 RHO(25),TAU(25)
      NM1=N-1
C
C     ARRANGE THE NODES XN IN INCREASING ORDER. STORE THE
C     ORDER IN THE ARRAY INDEX.
C
      DO 1 I=1,N
    1 INDEX(I)=I
      DO 3 I=1,NM1
      IP1=I+1
      DO 2 J=IP1,N
      II=INDEX(I)
      IJ=INDEX(J)
      IF(XN(II).LE.XN(IJ)) GO TO 2
      ITEMP=INDEX(I)
      INDEX(I)=INDEX(J)
      INDEX(J)=ITEMP
    2 CONTINUE
    3 CONTINUE
      NM2=N-2
C
C     CALCULATE THE ELEMENTS OF THE ARRAYS RHO AND TAU.
C
      RHO(2)=0.D0
      TAU(2)=0.D0
      DO 4 I=2,NM1
      IIM1=INDEX(I-1)
      II=INDEX(I)
      IIP1=INDEX(I+1)
      HIM1=XN(II)-XN(IIM1)
      HI=XN(IIP1)-XN(II)
```

```
      TEMP=(HIM1/HI)*(RHO(I)+2.DO)+2.DO
      RHO(I+1)=-1.DO/TEMP
      D=6.DO*((FN(IIP1)-FN(II))/HI-(FN(II)-FN(IIM1))/HIM1)
     1  /HI
    4 TAU(I+1)=(D-HIM1*TAU(I)/HI)/TEMP
C
C     COMPUTE ARRAY OF SECOND DERIVATIVES S FOR THE NATURAL
C     SPLINE.
C
      S(1)=0.DO
      S(N)=0.DO
      DO 5 I=1,NM2
      IB=N-I
    5 S(IB)=RHO(IB+1)*S(IB+1)+TAU(IB+1)
      RETURN
      END
```

```
      FUNCTION SPLINE (N,XN,FN,S,INDEX,X)
C
C     THE FUNCTICN SPLINE ACCEPTS AS INPUT THE QUANTITIES N,
C     XN, FN, S AND INDEX AS DEFINED IN THE SUBROUTINE
C     SPCOEF AND A NUMBER X AT WHICH THE SPLINE IS TO BE
C     EVALUATED. SPCOEF IS CALLED ONCE FOR EACH FIT, BUT
C     SPLINE IS CALLED ONCE FOR EACH ARGUMENT AT WHICH WE
C     REQUIRE THE VALUE OF THE FIT.
C
      IMPLICIT REAL *8 (A-H,O-Z)
      DIMENSION XN(N),FN(N),S(N),INDEX(N)
C
C     IF X<XN((INDEX(1)), APPROXIMATE FUNCTION BY THE
C     STAIGHT LINE WHICH PASSES THROUGH THE POINT
C     (XN(INDEX(1)),FN(INDEX(1))) AND WHCSE SLOPE IS HALF
C     THE SLOPE OF THE SPLINE AT THAT POINT.
C
      I1=INDEX(1)
      IF( X.GE.XN(I1)) GO TC 1
      I2=INDEX(2)
      H1=XN(I2)-XN(I1)
      SPLINE=FN(I1)+(X-XN(I1))*((FN(I2)-FN(I1))/H1-H1*S(2)/
     16.DO)*.5DO
      RETURN
C
C     IF X.GE.XN(INDEX(N)), APPROXIMATE FUNCTION BY THE
C     STRAIGHT LINE WHICH PASSES THROUGH THE POINT
C     (XN(INDEX(N)),FN(INDEX(N))) AND WHOSE SLOPE IS HALF
C     THE SLOPE OF THE SPLINE AT THAT POINT.
C
  1   IN=INDEX(N)
      IF(X.LE.XN(IN)) GO TO 2
      INM1=INDEX(N-1)
      HNM1=XN(IN)-XN(INM1)
      SPLINE=FN(IN)+(X-XN(IN))*((FN(IN)-FN(INM1))/HNM1+HNM1
     1 *S(N-1)/6.DO)*.5DO
      RETURN
C
C     FOR XN(INDEX(1)).LE.X.LE.XN(INDEX(N)) CALCULATE SPLINE
C     FIT.
  2   DO 3 I=2,N
      II=INDEX(I)
      IF(X.LE.XN(II)) GO TO 4
  3   CONTINUE
  4   L=I-1
      IL=INDEX(L)
      ILP1=INDEX(L+1)
      A=XN(ILP1)-X
      B=X-XN(IL)
      HL=XN(ILP1)-XN(IL)
      SPLINE=A*S(L)*(A*A/HL-HL)/6.DO+B*S(L+1)*(B*B/HL-HL)/
     1 6.DO+(A*FN(IL)+B*FN(ILP1))/HL
      RETURN
      END
```

```
      SUBROUTINE LAYOUT (FACTOR,  A,B,C,R1,R2,PSI1,PSI2)
C
C     LAYOUT DIVIDES THE CROSS-SECTION INTO SEGMENTS AND
C     COMPUTES THEIR GEOMETRICAL PROPERTIES. CROSS-SECTION
C     GEOMETRY AND SEGMENT LENGTHS ARE INPUT. SEGMENTS CAN
C     BE EITHER STRAIGHT OR CURVED BUT NOT CURVILINEAR.
C     SEGMENTAL LENGTH MAY BE MODIFIED BY PROGRAM TO WITHIN
C     .01 INCH TO INSURE NO CURVILINEAR SEGMENT.
C
      IMPLICIT REAL*8 (A-H,O-Z)
      REAL*8 L1,L2,L3,L4
      COMMON/A1/D(100),T(100),PHI1(100),PHI2(100),XC(100),
     1          XD(100),YI(100),PI,E,N,NN
      IO=6
      CP1 =DCOS(PSI1)
      SP1 =DSIN(PSI1)
      XCENT1=R1
      XCENT2=R1*(1.D0-CP1)+B*SP1+R2*CP1*FACTOR
      L1 = A + R1*PSI1
      L2 = L1 + B
      L3 = L2 + R2*PSI2
      L4 = L3 + C
      S=0.D0
      X=0.D0
      J=0
C
C     FIRST SEGMENT BEGINS AT ORIGIN
C
   10 J=J+1
      S=S+D(J)
      IF (DABS(S-A).GT.1.D-2) GO TO 11
      D(J)=D(J)+A-S
      S=A
   11 IF(S-A.GT.1.D-2) GO TO 12
      THETA   =PI
C     WRITE(6,105) J,X,THETA,S,D(J)
      CALL STRAIT (J,X,1.D0,THETA)
      GO TO 10
C
C     FIRST CORNER
C
   12 THETA1=PI
   13 IF (DABS(S-L1).GT.1.D-2) GO TO 14
      D(J)=D(J)+L1-S
      S=L1
   14 IF(S-L1.GT.1.D-2) GO TO 15
      THETA2=THETA1-D(J)/R1
      CALL CORNER (THETA1,THETA2,XCENT1,R1,J,1.D0,X)
      J=J+1
      S=S+D(J)
      THETA1=THETA2
      GO TO 13
C
C     SECOND FLAT
```

```
C
   15   IF (DABS(S-L2).GT.1.D-2) GO TO 16
        D(J)=D(J)+L2-S
        S=L2
   16   IF(S-L2.GT.1.D-2) GO TO 17
        THETA    =PI-PSI1
        CALL STRAIT (J,X,1.D0,THETA)
        J=J+1
        S=S+D(J)
        GO TO 15
C
C       SECOND CORNER
C
   17   IF(FACTOR.EQ.-1.D0) GO TO 18
        THETA1=PI-PSI1
        THETA2=THETA1-D(J)/R2
        GO TO 19
   18   THETA2=-PSI1
        THETA1=THETA2 + D(J)/R2
   19   IF (DABS(S-L3).GT.1.D-2) GO TO 20
        D(J)=D(J)+L3-S
        S=L3
   20   IF(S-L3.GT.1.D-2) GO TO 30
        CALL CORNER(THETA1,THETA2,XCENT2,R2,J,FACTOR,X)
        J=J+1
        S=S+D(J)
        IF(FACTOR.EQ.-1.D0)  GO TO 22
        THETA1=THETA2
        THETA2=THETA1-D(J)/R2
        GO TO 19
   22   THETA2 = THETA1
        THETA1 = THETA2 + D(J)/R2
        GO TO 19
C
C       LAST FLAT
C
   30   IF(FACTOR.EQ.1.D0) THETA    =PI-PSI1-PSI2
        IF(FACTOR.EQ.-1.D0) THETA    =-PSI1+PSI2
   32   IF (DABS(S-L4).GT.1.D-2) GO TO 35
        D(J)=D(J)+L4-S
        S=L4
   35   CONTINUE
        CALL STRAIT (J,X,FACTOR,THETA)
        J=J+1
        IF(J.GT.N) GO TO 40
        S=S+D(J)
        GO TO 32
   40   IF(DABS(S-L4).LE.1.D-2) GO TO 50
        WRITE (IO,45)
   50   RETURN
   45   FORMAT('********** ERROR IN LAYOUT **********')
        END
```

```
      SUBROUTINE YNERTA
C
C     YNERTA COMPUTES THE AREA, ABCISSA OF CENTROIC AND
C     MOMENT OF INERTIA ABOUT THE WEAK (Y) AXIS OF HALF THE
C     CROSS-SECTION.
C
      IMPLICIT REAL*8 (A-H,O-Z)
      REAL*8 L1,L2,L3,L4
      COMMON/A1/D(100),T(100),PHI1(100),PHI2(100),XC(100),
     1          XD(100),YI(100),PI,E,N,NN
      COMMON/A2/RSO(100),RSI(100),RON(100),EY(100),XO,AO,YO,
     1          RL,MODEL
      P1 = 0.D0
      AO = 0.D0
      YO    = 0.D0
      DO 10 J=1,N
      P1 = P1 + T (J)*D(J)*XC (J)
      AO = AO + T(J)*D(J)
   10 YO = YO + YI(J)
      XO = P1/AO
      DO 15 J=1,N
   15 YO=YO+(XC(J)-XO)*(XC(J)-XO)*D(J)*T(J)
      RETURN
      END
C
C
      SUBROUTINE STRAIT (J,X,FACTOR,THETA)
C
C     STRAIT COMPUTES GEOMETRIC PROPERTIES OF A STRAIGHT
C     SEGMENT
C
      IMPLICIT REAL*8 (A-H,O-Z)
      COMMON/A1/D(100),T(100),PHI1(100),PHI2(100),XC(100),
     1          XD(100),YI(100),PI,E,N,NN
      PHI1(J)= THETA
      PHI2(J)= THETA
      ST =DSIN(THETA)
      CT=DCOS(THETA)
      XC(J)=X+D(J)*ST*.5D0*FACTOR
      XD(J) = XC(J)
      YI(J)=T(J)*D(J)/12.D0*(T(J)*T(J)*CT*CT+D(J)*D(J)*ST*
     1 ST)
      X = X + D(J)*ST*FACTOR
      RETURN
      END
```

```
      SUBROUTINE CORNER (THETA1,THETA2,XCENT,R, J,FACTOR,X)
C
C     CORNER COMPUTES GEOMETRIC PROPERTIES OF A CORNER
C     SEGMENT
C
      IMPLICIT REAL*8 (A-H,O-Z)
      COMMON/A1/D(100),T(100),PHI1(100),PHI2(100),XC(100),
     1          XD(100),YI(100),PI,E,N,NN
      T12 =(THETA1-THETA2)*.5D0
      THETA    = (THETA1+THETA2)*.5D0
      PHI1(J)= THETA1
      PHI2(J)= THETA2
      ST1 =DSIN(THETA1)
      CT1 =DCOS(THETA1)
      ST2 =DSIN(THETA2)
      CT2 =DCOS(THETA2)
      ST=DSIN(THETA)
      CT=DCOS(THETA)
      S=DSIN(T12)
      C=DCOS(T12)
      RD=R+T(J)*.5D0
      XD(J)=XCENT + R*CT
      PL=S*2.D0*(RD-T(J)+RD*RD/(2.D0*R))/(3.D0*T12)
      XC(J)=XCENT+PL*CT
      Q1= T(J)/RD
      Q2= 1.D0-1.5D0*Q1+Q1*Q1-.25D0*Q1*Q1*Q1
      Q3= T12+S*C-2.D0*S*S/T12
      Q4=T(J)*T(J)*S*S*(1.D0-Q1+Q1*Q1/6.D0)/(6.D0*RD*R*T12)
      Y1=RD*RD*RD*T(J)*(Q2*Q3+Q4)
      Y2=RD*RD*RD*T(J)*Q2*(T12-S*C)
      YI(J)=Y1*CT*CT+Y2*ST*ST
      X = X + (CT2-CT1)*R*FACTOR
      RETURN
      END
```

```
      SUBROUTINE RESIDU
C
C     RESIDU COMPUTES THE EQUILIBRIUM CORRECTIONS TO THE
C     RESIDUAL FORCES. OM AND OF ARE THE FORCE AND MOMENT
C     CORRECTIONS, E1 IS THE AXIAL STRESS CORRECTION. ALL
C     QUANTITIES HAVE BEEN DIVIDED BY THE MODULUS OF
C     ELASTICITY E.
C
      IMPLICIT REAL*8 (A-H,O-Z)
      COMMON/A1/D(100),T(100),PHI1(100),PHI2(100),XC(100),
     1          XD(100),YI(100),PI,E,N,NN
      COMMON/A2/RSO(100),RSI(100),RON(100),EY(100),XO,AO,YO,
     1          RL,MODEL
      COMMON/A3/VSO(100),VSI(100),V(100),PF(100),E1,W,DELV,
     1          OF,OM,AEL(100),PY,IP
      OM = 0.D0
      OF = 0.D0
      OMP=0.D0
      IF (MODEL -2) 2,20,20
C
C     MODEL 1: UNIFORM RESIDUAL STRAIN ACROSS THICKNESS.
C
    2 DO 5 J=1,N
      OF =OF+D(J)*T(J)* .5D0*(RESTRO(J)+RESTRI(J))
    5 OM=OM-.5D0*(RESTRO(J)+RESTRI(J))*D(J)*T(J)*(XC(J)-XO)
      GO TO 60
C
C     MODEL 2: LINEAR RESIDUAL STRAIN ACROSS THICKNESS.
C     MODEL 3: TWO RECTANGULAR BLOCKS STATICALLY EQUIVALENT
C     TO MODEL 2. USER SPECIFIES NEUTRAL AXIS.
C
   20 DO 30 J=1,N
      THETA=.5*(PHI1(J)+PHI2(J))
      ALFA=(PHI1(J)-PHI2(J))*.5D0
      CT=DCOS(THETA)
      P1=  +D(J)*T(J)* .5D0*(RESTRO(J)+RESTRI(J))
      Q1=P1*(XO-XC(J))
      IF ( ALFA.NE.0.D0) GO TO 22
      P2=0.D0
      Q2=(RESTRI(J)-RESTRO(J))*D(J)*T(J)*T(J)/12.D0
      GO TO 25
   22 P2=T(J)*T(J)*ALFA*(RESTRO(J)-RESTRI(J))/6.D0
      Q =(T(J)*ALFA/D(J))**2/3.D0
      Q2=(RESTRI(J)-RESTRO(J))*D(J)*T(J)*T(J)/12.D0*(1.D0-Q)
     1*DSIN(ALFA)/ALFA
   25 OF=OF+P1+P2
      OM=OM+Q1+Q2*CT +P2*(XO-XC(J))
      OMP=OMP+Q2
   30 CONTINUE
   60 E1    = -OF / AO
      RETURN
      END
```

```
      SUBROUTINE STRAIN (RO,J,I,EA,ET)
C
C     STRAIN COMPUTES THE STRAIN AT A POINT.
C     EB = BENDING STRAIN;  ER = RESIDUAL STRAIN;
C     ET = TOTAL STRAIN; EA = AXIAL STRAIN (FROM LOAD);
C     E2 = BENDING CORRECTIVE STRAIN;
C     E1 = AXIAL CORRECTIVE STRAIN (FROM RESIDU)
C
      IMPLICIT REAL*8 (A-H,O-Z)
      COMMON/A1/D(100),T(100),PHI1(100),PHI2(100),XC(100),
     1          XD(100),YI(100),PI,E,N,NN
      COMMON/A2/RSO(100),RSI(100),RON(100),EY(100),XO,AO,YO,
     1          RL,MODEL
      COMMON/A3/VSO(100),VSI(100),V(100),PF(100),E1,W,DELV,
     1          OF,OM,AEL(100),PY,IP
      CT=DCOS((PHI1(J)+PHI2(J))*.5D0)
      EB =-PI*PI  *V(I)/(RL*RL)*(XD(J)+RO*CT-XO)
      E2=OM/YO*(XD(J)+RO*CT-XO)
      IF(MODEL.EQ.4) ET=EA +EB
      IF(MODEL.EQ.4) RETURN
      IF(MODEL-2) 1,2,3
    1 ER=.5D0*(RSO(J)+RSI(J))
      GO TO 5
    2 ER=.5D0*(RSO(J)+RSI(J))+(RSO(J)-RSI(J))*RO/T(J)
      GO TO 5
    3 IF(RO.GT.RON(J)) ER=VSO(J)
      IF(RO.LT.RON(J)) ER=VSI(J)
      IF(RO.EQ.RON(J).AND.IP.EQ.1) ER=VSO(J)
      IF(RO.EQ.RON(J).AND.IP.EQ.2) ER=VSI(J)
    5 ET=EA+EB+ER+E1+E2
      RETURN
      END
```

```
      SUBROUTINE ALTER
C
C     ALTER COMPUTES THE MAGNITUDES OF THE RECTANGULAR
C     BLOCKS OF RESIDUAL STRAINS IN MODEL 3. ALTER CAN ALSO
C     COMPUTE THE RESIDUAL FORCE AND MOMENT WHICH ARE EQUAL
C     TO THOSE OBTAINED BY RESIDU FOR MODEL 2.
C
      IMPLICIT REAL*8 (A-H,O-Z)
      COMMON/A1/D(100),T(100),PHI1(100),PHI2(100),XC(100),
     1          XD(100),YI(100),PI,E,N,NN
      COMMON/A2/RSO(100),RSI(100),RON(100),EY(100),XO,AO,YO,
     1          RL,MODEL
      COMMON/A3/VSO(100),VSI(100),V(100),PF(100),E1,W,DELV,
     1          OF,OM,AEL(100),PY,IP
      DO 20 J=1,N
      A   =(PHI1(J)-PHI2(J))*.5D0
      Z=2.D0*RON(J)/T(J)
      C=(1.D0+Z)*(1.D0-Z)
      P= RSO(J)+RSI(J)
      Q= RSO(J)-RSI(J)
      IF(A   .NE.0.D0) GO TO 5
C
C     STRAIGHT SEGMENT
C
      VSO(J)=P*.5D0+Q/(3.D0*(1.D0-Z))
      VSI(J)=P*.5D0-Q/(3.D0*(1.D0+Z))
      GO TO 10
C
C     CURVED SEGMENT
C
    5 B=T(J)/D(J)
      S=DSIN(A)
      F=(A*B)**2-3.D0
      G=3.D0*C*(A*B*Z*(A*B*C-2.D0*Z)+F)
      PV=(3.D0*C*P+2.D0*Z*Q)*F/G
      QV=(6.D0*A*B*C*Z*P+2.D0*(A*A*B*B*C*Z+F)*Q)/G
      VSO(J)=.5D0*(PV+QV)
      VSI(J)=.5D0*(PV-QV)
   10 CONTINUE
   20 CONTINUE
      RETURN
      END
```

```
      SUBROUTINE INTERN (EA,P,RM,AE,I)
C
C     INTERN COMPUTES THE INTERNAL FORCE AND MOMENT
C     FOR MODEL 1 AND 2 OF RESIDUAL STRAINS.
C
      IMPLICIT REAL*8 (A-H,O-Z)
      COMMON/A1/D(100),T(100),PHI1(100),PHI2(100),XC(100),
     1          XD(100),YI(100),PI,E,N,NN
      COMMON/A2/RSO(100),RSI(100),RON(100),EY(100),XO,AO,YO,
     1          RL,MODEL
      COMMON/A3/VSO(100),VSI(100),V(100),PF(100),E1,W,DELV,
     1          OF,OM,AEL(100),PY,IP
      AE=0.D0
      P=0.D0
      RM=0.D0
      DO 40 J=1,N
      CT=DCOS((PHI1(J)+PHI2(J))*.5D0)
      ALFA=(PHI1(J)-PHI2(J))*.5D0
      S=DSIN(ALFA)
C
C     STRAINS AT EXTREME FIBERS.
C
      CALL STRAIN ( T(J)*.5D0,J,I,   EA,ETO)
      CALL STRAIN (-T(J)*.5D0,J,I,   EA,ETI)
      IF(ETO.LE.EY(J).AND.ETI.LE.EY(J)) GO TO 10
      IF(ETO.GE. EY(J).AND.ETI.GE. EY(J)) GO TO 15
C
C     ELASTO-PLASTIC.OUTER FIBER YIELD OR INNER FIBER YIELD?
C     COMPUTE YIELD FRONT
C     TE,TP = THICKNESS OF ELASTIC AND PLASTIC SEGMENTS.
C
      IF(ETO.GT.EY(J)) F=+1.D0
      IF(ETI.GT.EY(J)) F=-1.D0
      ROY=(EY(J)-(ETO+ETI)*.5D0)*T(J)/(ETO-ETI)
      TE=T(J)*.5D0+ROY*F
      TP=T(J)*.5D0-ROY*F
      IF(F.EQ.+1.D0) ET=ETI
      IF(F.EQ.-1.D0) ET=ETO
      IF(ALFA.NE.0.D0) GO TO 7
C
C     STRAIGHT SEGMENT
C     SAE = SEGMENTAL AREA, ELASTIC
C     SEP = SEGMENTAL ELASTIC LOAD
C     SPP = SEGMENTAL PLASTIC LOAD
C     SEM1= MOMENT ABOUT CENTROID OF ELASTIC SEGMENT DUE TO
C           STRESS GRADIENT
C     SEM2= MOMENT OF ELASTIC LOAD ABOUT CENTROID OF SECTION
C     SPM = MOMENT OF PLASTIC LOAD ABOUT CENTROID OF SECTION
C
      SAE=D(J)*TE
      SEP=SAE*E*.5D0*(EY(J)+ET)
      SPP=E*EY(J)*D(J)*TP
      SEM1=-E*D(J)*TE*TE/12.D0*(EY(J)-ET)*F*CT
      SEM2=SEP*(XO-XD(J)-.5D0*(ROY-F*.5D0*T(J))*CT)
```

```
      SPM=SPP*(XO-XD(J)-.5D0*(ROY+F*.5D0*T(J))*CT)
      GO TO 9
C
C     CURVED SEGMENT
C
    7 DE=D(J)+ALFA*(ROY-F*T(J)*.5D0)
      DP=D(J)+ALFA*(ROY+F*T(J)*.5D0)
      QE=(TE*ALFA/DE)**2/3.D0
      QP=(TP*ALFA/DP)**2/3.D0
      R=D(J)/(2.D0*ALFA)
      CE=.5D0*DE*S/(ALFA*ALFA)*(1.D0+QE)-R
      CP=.5D0*DP*S/(ALFA*ALFA)*(1.D0+QP)-R
      SAE=DE*TE
      SEP=SAE*E*.5D0*(EY(J)+ET)+E*TE*TE*ALFA*(EY(J)-ET)*F/
     1 6.D0
      SPP=DP*TP*E*EY(J)
      SEM1=-E*DE*TE*TE/12.D0*(1.D0-QE)*S/ALFA*(EY(J)-ET)*F*
     1 CT
      SEM2=SEP*(XO-XD(J)-CE*CT)
      SPM=SPP*(XO-XD(J)-CP*CT)
    9 SP=SEP+SPP
      SM=SEM1+SEM2+SPM
C     WRITE(6,55) J,ROY,SEP,SPP,SPM,SAE,SEM1,SEM2
      GO TO 30
C
C     FULLY ELASTIC
C
   10 SAE=D(J)*T(J)
      SP=SAE*E*.5D0*(ETO+ETI)+E*T(J)*T(J)*ALFA*(ETO-ETI)/
     1 6.D0
      SM1=SP*(XO-XC(J ))
      IF(ALFA.NE.0.D0) GO TO 12
      S2=-E*D(J)*T(J)*T(J)/12.D0*(ETO-ETI)*CT
      GO TO 13
   12 QE=(T(J)*ALFA/D(J))**2/3.D0
      S2=-E*D(J)*T(J)*T(J)/12.D0*(1.D0-QE)*S/ALFA*(ETO-ETI)
     1 *CT
   13 SM=SM1+S2
      GO TO 30
C
C     FULLY PLASTIC
C
   15 SP= D(J)*T(J)*E*EY(J)
      SM=-SP*(XC(J)-XO)
      SAE=0.D0
   30 P=P+SP
      RM=RM+SM
      AE=AE+SAE
   40 CONTINUE
      RETURN
      END
```

```
      SUBRCUTINE INTER3 (EA,P,RM,AE,I)
C
C     INTER 3 COMPUTES THE INTERNAL FORCE AND MOMENT FOR
C     MODEL 3 OF RESIDUAL STRAINS.
C
      IMPLICIT REAL*8 (A-H,C-Z)
      CCMMCN/A1/D(100),T(100),PHI1(100),PHI2(100),XC(100),
     1          XD(100),YI(100),PI,E,N,NN
      COMMON/A2/RSC(100),RSI(100),RCN(100),EY(100),XO,AC,YC,
     1          RL,MODEL
      CCMMON/A3/VSC(100),VSI(100),V(100),PF(100),E1,W,DELV,
     1          CF,CM,AEL(100),PY,IP
      AE=0.D0
      P=0.D0
      RM=0.D0
      PI=4.D0*DATAN(1.D0)
      DC 80 J=1,N
      ALFA=(PHI1(J)-PHI2(J))*.5D0
      S=DSIN(ALFA)
      CT=DCOS(.5D0*(PHI1(J)+ PHI2(J)))
      BO=T(J)*.5D0
      BI=RCN(J)
      IP=1
C
C     STRAINS AT OUTSIDE, INSIDE EDGES AND BOTH SIDES CF
C     NEUTRAL SURFACE (FOR RESIDUAL STRAINS).
C
  5   CALL STRAIN (BO,J,I,EA,ETC)
      CALL STRAIN (BI,J,I,EA,ETI)
      IF(ETO.GE.EY(J).AND.ETI.GE.EY(J)) GC TO 40
      IF(ETC.LT.EY(J).AND.ETI.LT.EY(J)) GC TO 50
C
C     ELASTO-PLASTIC
C
      IF(BO.EQ.+T(J)*.5D0) ER=VSO(J)
      IF(BI.EQ.-T(J)*.5D0) ER=VSI(J)
C
C     LCCATION OF YIELD FRONT.
C
      POY=(EY(J)*(BO-BI)+ETC*BI-ETI*BO)/(ETO-ETI)
      IF (ETO.GE.EY(J)) F=+1.D0
      IF (ETI.GE.EY(J)) F=-1.D0
      IF(ALFA.NE.0.D0) GO TO 20
      IF(F.EQ.-1.D0) GC TO 10
C
C     STRAIGHT, OUTER SEGMENT.
C
      B1=BC
      B2=BI
      ET=ETI
      GO TC 15
C
C     STRAIGHT, INNER SEGMENT
C     SAP = SEGMENTAL AREA PLASTIC
```

```
C      SPP = SEGMENTAL PLASTIC LOAD
C      SPM = SEGMENTAL PLASTIC MOMENT
C      SAE = SEGMENTAL AREA ELASTIC
C      SEP = SEGMENTAL ELASTIC LOAD
C      Q1  = MOMENT ABOUT CENTROID OF ELASTIC SEGMENT DUE TO
C            STRESS GRADIENT.
C      SEM = TOTAL MOMENT OF ELASTIC SEGMENT ABOUT CENTROID
C            OF SECTION.
C
   10  B1=BI
       B2=BO
       ET=ETO
   15  SAP=D(J)*(B1-ROY)*F
       SPP=SAP*E*EY(J)
       SPM=SPP*(XO-XD(J)-.5D0*(B1+ROY)*CT)
       SAE=D(J)*(ROY-B2)*F
       SEP=.5D0*(EY(J)+ET)*E*SAE
       Q1=E*D(J)*(ROY-B2)*(ROY-B2)*(ET-EY(J))*F/12.D0*CT
       SEM=SEP*(XO-XD(J)-.5D0*(B2+ROY)*CT)+Q1
       GO TO 35
C
C      CURVED, OUTER SEGMENT
C      DP,TP = LENGTH, THICKNESS OF PLASTIC SEGMENT
C      DE,TE = LENGTH, THICKNESS OF ELASTIC SEGMENT
C
   20  IF(F.EQ.-1.D0) GO TO 25
       DP=D(J)+ALFA*(BO+ROY)
       DE=D(J)+ALFA*(BI+ROY)
       TP=BO-ROY
       TE=ROY-BI
       ET=ETI
       GO TO 30
C
C      CURVED, INNER SEGMENT
C      CE,CP = DISTANCES CENTROID TO OUTERMOST FIBER  OF
C      ELASTIC, PLASTIC SEGMENTS.
C
   25  DP=D(J)+ALFA*(BI+ROY)
       DE=D(J)+ALFA*(BO+ROY)
       TP=ROY-BI
       TE=BO-ROY
       ET=ETO
   30  QP=TP*ALFA/DP
       CP=DP*.5D0*(1.D0+QP*QP/3.D0)*S/(ALFA*ALFA)-D(J)/
      1  (2.D0*ALFA)
       SPP=E*EY(J)*DP*TP
       SPM=SPP*(XO-XD(J)-CP*CT)
       QE=TE*ALFA/DE
       CE=DE*.5D0*(1.D0+QE*QE/3.D0)*S/(ALFA*ALFA)-D(J)/
      1  (2.D0*ALFA)
       SAE=DE*TE
       SEP=E*SAE*.5D0*(EY(J)+ET)+E*TE*TE*ALFA*(EY(J)-ET)*F/
      1  6.D0
       Q1=E*DE*TE*TE/12.D0*(1.D0-QE*QE/3.D0)*S/ALFA*
```

```
     1  (ET-EY(J))*F*CT
      SEM=SEP*(XO-XD(J)-CE*CT)+Q1
C
C     SUM ALL SEGMENTAL VALUES
C
  35  P=P+SEP+SPP
      RM=RM+SEM+SPM
      AE=AE+SAE
      GO TO 70
C
C     FULLY PLASTIC
C
  40  TE=BO-BI
      DE=D(J)+ALFA*(BO+BI)
      SAE=0.D0
      SP=E*EY(J)*TE*DE
      Q1=0.D0
      IF(ALFA.NE.0.D0) GO TO 60
      GO TO 55
C
C     FULLY ELASTIC
C
  50  TE=BO-BI
      DE=D(J)+ALFA*(BO+BI)
      SAE=TE*DE
      SP=.5D0*(ETO+ETI)*E*SAE+E*(ETO-ETI)*TE*TE*ALFA/6.D0
      IF(ALFA.NE.0.D0) GO TO 60
      Q1=E*D(J)*TE*TE*(ETI-ETO)/12.D0*CT
  55  SM=SP*(XO-XD(J)-.5D0*(BO+BI)*CT)+Q1
      GO TO 65
  60  QE=TE*ALFA/DE
      IF(SAE.NE.0.D0)
     1Q1=E*DE*TE*TE/12.D0*(1.D0-QE*QE/3.D0)*S/ALFA*
     2  (ETI-ETO)*CT
      CE=DE*.5D0*(1.D0+QE*QE/3.D0)*S/(ALFA*ALFA)-D(J)/
     1  (2.D0*ALFA)
      SM=SP*(XO-XD(J)-CE*CT)+Q1
C
C     SUM ALL SEGMENTAL VALUES
C
  65  P=P+SP
      RM=RM+SM
      AE=AE+SAE
  70  IP=IP+1
      IF(IP.GT.2) GO TO 80
C
C     REPEAT FOR INNER SEGMENT
C
      BO=RON(J)
      BI=-T(J)*.5D0
      GO TO 5
  80  CONTINUE
      RETURN
      END
```

```
      SUBROUTINE LOAD1(MI,NET,MAX1,NAX1,IWRITE,C1,C2,F2,F3,
     1  F4,EN,ECC)
C
C     FOR EACH VALUE OF MIDHEIGHT LATERAL DEFLECTION V LOAD
C     COMPUTES THE AXIAL LOAD PF.
C     NET=0 (1 BLANK CARD) FOR DEFAULT VALUES
C     MAX1= MAXIMUM NUMBER OF ITERATIONS FOR LOAD
C     EQUILIBRIUM LOOP.
C     NAX1= MAXIMUM NUMBER OF ITERATIONS FOR MOMENT
C     EQUILIBRIUM LOOP.
C     F2,F3,F4= SCALING FACTORS THAT AFFECT CONVERGENCE
C
      IMPLICIT REAL*8 (A-H,O-Z)
      COMMON/A1/D(100),T(100),PHI1(100),PHI2(100),XC(100),
     1          XD(100),YI(100),PI,E,N,NN
      COMMON/A2/RSO(100),RSI(100),RON(100),EY(100),XO,AO,YO,
     1          RL,MODEL
      COMMON/A3/VSO(100),VSI(100),V(100),PF(100),E1,W,DELV,
     1          OF,OM,AEL(100),PY,IP
      COMMON/A4/U(100),ST(100,4),IS(4),NST
      DIMENSION DL(3),PS(3)
      IO=6
      IF(NET.NE.0) GO TO 1
      MAX1=20
      NAX1=20
      C1=2.D-4
      C2=1.D-3
      F2=5.5D0
      F3=.9D0
      F4=1.0D0
    1 IF (NST-1) 7,10,15
    7 WRITE(IO,630)
      GO TO 18
   10 WRITE(IO,640) U(IS(1))
      GO TO 18
   15 WRITE(IO,650) (U(IS(L)),L=1,NST)
      WRITE(IO,652)
   18 I=1
      MREACH=0
      PMAX=0.D0
      K=1
      MAX=0
      NAX=0
C
C     FIRST ASSUME SECTION IS ENTIRELY ELASTIC.
C
      PA= PI*PI*E*YO*V(I)/(RL*RL*(V(I)+W-ECC))
      IF(PA.GE.PY) PA= F3  *PY
   20 EA=PA/(E*AO)
   30 MAX=MAX+1
      IF(MAX.GT.MAX1) GO TO 100
      IF (MODEL.EQ.3) CALL INTER3 (EA,P,RM,AE,I)
      IF (MODEL.NE.3) CALL INTERN (EA,P,RM,AE,I)
      IF(IWRITE.EQ.1) WRITE(6,210) I,PA,EA,P,RM,AE,V(I)
```

```
C
C      DOES THE INTERNAL LOAD P EQUILIBRATE THE EXTERNAL
C      LOAD PA ?
C
       IF(DABS((P-PA)/P).LT.C1) GO TO 40
       IF(AE.LT.AO*.1DO.AND.P.LT.PA) PA=F3*PA
       IF(AE.LT.AO*.1DO.AND.P.LT.PA) GO TO 20
       IF(AE.NE.0.DO) GO TO 35
       PA=PF(I-1)
       GO TO 20
  35   EA=EA+(PA-P)/(E*AE)*F4
       GO TO 30
C
C      DOES THE INTERNAL MOMENT RM EQUILIBRATE THE EXTERNAL
C      MOMENT XM ?
C
  40   NAX=NAX+1
       IF(NAX.GT.NAX1) GO TO 100
       XM=P*(V(I)+W-ECC)
       DL(K)=RM-XM
       PS(K)=P
       IF(IWRITE.EQ.1) WRITE(6,220) K,XM,DL(K),PS(K)
       MAX=1
       IF(DABS(DL(K)/RM).LT.C2) GO TO 50
       IF(K-2) 44,45,46
C
C      SOLVE DL=RM-XM=0 BY A MODIFIED SECANT METHOD, IE FIND
C      WHERE CURVE DL-PA INTERSECTS AXIS DL=0 (REFERRED TO
C      HEREAFTER AS AXIS).FIND ANOTHER POINT ON DL-PA CURVE
C      BY ASSUMING A DIFFERENT LOAD.
C
  44   PA=PA+DL(K)/(V(I)+W-ECC)/F2
       K=K+1
       GO TO 20
  45   CONTINUE
       IF(IWRITE.EQ.1) WRITE(6,260) DL(1),PS(1)
C
C      LINE JOINING THE FIRST 2 POINTS INTERSECTS LOAD AXIS
C      AT NEW PA.
C
       PA=PS(1)-DL(1)/(DL(2)-DL(1))*(PS(2)-PS(1))
       K=K+1
       GO TO 20
  46   CONTINUE
       IF(IWRITE.EQ.1) WRITE(6,290) DL(1),PS(1),DL(2),PS(2)
C
C      KEEP THE 2 POINTS NEAREST OR ON BOTH SIDES OF AXIS
C
       IF(DL(2)*DL(3).LT.0.DO) GO TO 47
       IF(DL(1)*DL(3).LT.0.DO) GO TO 48
       IF(DABS(DL(1)).GT.DABS(DL(2)).AND.DABS(DL(1)).GT.
      1DABS(DL(3))) GO TO 47
       IF(DABS(DL(2)).GT.DABS(DL(1)).AND.DABS(DL(2)).GT.
      1DABS(DL(3))) GO TO 48
```

```
      GO TO 110
C
C     POINT 1 REJECTED: TAKE INTERSECTION OF AXIS WITH LINE
C     2-3. CONVERGENCE MAY BE DIFFICULT IF NEXT MOVE IS
C     BASED ON 2 POINTS ON BOTH SIDES OF AXIS BUT ONE MUCH
C     FURTHER AWAY FROM AXIS THAN THE OTHER. MOVE THE FAR
C     POINT CLOSER TO AXIS SO THE RATIO OF THEIR DISTANCES
C     TO AXIS IS 2. (2 WORKS BETTER THAN 1 OR 0).
C
   47 PA=PS(3)-DL(3)/(DL(2)-DL(3))*(PS(2)-PS(3))
      IF(DL(2)/DL(3).LT.-2.D0)
     1 PA=(2.D0*DL(3)*PS(2)-(DL(2)+
     2 DL(3))*PS(3))/(DL(3)-DL(2))
      IF(DL(3)/DL(2).LT.-2.D0)
     1 PA=(2.D0*DL(2)*PS(3)-(DL(3)+
     2  DL(2))*PS(2))/(DL(2)-DL(3))
      DL(1)=DL(3)
      PS(1)=PS(3)
      GO TO 20
C
C     POINT 2 REJECTED.
C
   48 PA=PS(1)-DL(1)/(DL(3)-DL(1))*(PS(3)-PS(1))
      IF(DL(1)/DL(3).LT.-2.D0)
     1 PA=(2.D0*DL(3)*PS(1)-(DL(1)+
     2  DL(3))*PS(3))/(DL(3)-DL(1))
      IF(DL(3)/DL(1).LT.-2.D0)
     1 PA=(2.D0*DL(1)*PS(3)-(DL(3)+
     2  DL(1))*PS(1))/(DL(1)-DL(3))
      DL(2)=DL(3)
      PS(2)=PS(3)
      GO TO 20
C
C     EQUILIBRIUM OBTAINED
C
   50 PF(I)=P
      PFD=2.D0*P
   58 AEL(I)=AE/A0*100.D0
      IF (NST-1) 60,70,80
   60 WRITE(IO,635) I,V(I),PFD,AEL(I)
      GO TO 90
   70 CALL DEFORM (T(IS(1))*.5D0,IS(1),I,EA,ST(I,1))
      WRITE(IO,645) I,V(I),PFD,AEL(I),ST(I,1)
      GO TO 90
   80 DO 85 J=1,NST
   85 CALL DEFORM (T(IS(J))*.5D0,IS(J),I,EA,ST(I,J))
      WRITE(6,655) I,V(I),PFD,AEL(I),(ST(I,J),J=1,NST)
C
C     INCREMENT V.
C
   90 IF(I.GT.1.AND.MREACH.EQ.0) CALLCMAX (I,MREACH,IREACH,
     1  IR1,C1,PMAX,PF)
      I=I+1
      IF(I.GT.NN) GO TO 120
```

```
      IF(PF(I-1).LT. EN  *PMAX.AND.MI.EQ.1) GO TC 120
      IF(PF(I-1).LT. EN  *PMAX.AND.MREACH.GT.2) GC TC 120
      NAX=1
      K=1
      IF(MI.EQ.1) GC TO 93
      IF(MREACH.EQ.1.OR.MREACH.EQ.2) CALL MORE (I,MREACH,
     1  IREACH,IR1,MI,DELV,V)
      IF(MREACH.EQ.1.OR.MREACH.EQ.2) GO TC 20
   93 V(I)=V(I-1) +DELV
   94 IF(DABS(AO-AE).GT.1.D-3.AND.I.GT.3) GO TC 95
      PAM= PI*PI*E*YO*V(I)/(RL*PL*(V(I)+W-ECC))
      IF (PAM.LT..90DO*PY) PA=PAM
      GO TO 20
C
C     LINEAR  EXTRAPCLATICN.
C
   95 PA=(PF(I-1)-PF(I-2))*(V(I)-V(I-2))/(V(I-1)-V(I-2))+
     1  PF(I-2)
      GO TC 20
  100 WRITE(IO,250)
      GO TO 120
  110 WRITE(IO,150)
  120 RETURN
  150 FORMAT(' NOT MONOTONIC')
  210 FORMAT(' ------------------------------------------',
     1'------------'/' I=',I2,' PA =',1PD11.4,' EA =',D11.4,
     2' P   =',D11.4,' RM =',D11.4,' AE =',D11.4,'V(I)=',
     3  D11.4)
  220 FORMAT(' K=',I2,' XM=',1PD11.4,' DL(K)=',D11.4,
     1  ' PS(K)=',D11.4)
  250 FORMAT(//'***** NO CONVERGENCE *****')
  260 FORMAT(' DL(1)=',1PD11.4,' PS(1)=',D11.4)
  290 FORMAT (' DL(1)=',1PD11.4,' PS(1)=',D11.4,' DL(2)=',
     1 D11.4,' PS(2)=',D11.4)
  630 FORMAT(/8X,' DEFLECTION',5X,'LOAD *2',5X,
     1  'ELASTIC AREA %'/)
  635 FCRMAT(3X,I2,3(3X,1PD11.4))
  640 FORMAT(/' STRAIN IS CCMPUTED AT + FACE AT THE ',
     1'FOLLOWING LOCATIONS ALONG THE PERIMETER: ',1PD11.4//
     29X, 'DEFLECTION',5X,'LCAD *2',4X,
     3'ELASTIC AREA %',3X,'STRAIN'/)
  645 FCRMAT(3X,I2,4(3X,1PD11.4))
  650 FORMAT(/' STRAIN IS CCMPUTED AT + FACE AT FOLLOWING ',
     1'LOCATIONS (1,2,3,4) ALONG PERIMETER: ',4(1PD11.4,1X))
  652 FCRMAT(/9X,'DEFLECTION',5X,'LCAD *2',4X,'ELASTIC AREA'
     1,' %',3X,'STRAIN 1',5X,'STRAIN 2',7X,'STRAIN 3',5X,
     2'STRAIN 4'/)
  655 FCRMAT(3X,I2,7(3X,1PD11.4))
      END
```

```
      SUBROUTINE LOAD2(MI,NET,MAX1,NAX1,IWRITE,C1,C2,F2,F3,
     1  F4,EN,ECC)
      IMPLICIT REAL*8 (A-H,O-Z)
      COMMON/A1/D(100),T(100),PHI1(100),PHI2(100),XC(100),
     1          XD(100),YI(100),PI,E,N,NN
      COMMON/A2/RSO(100),RSI(100),RON(100),EY(100),XO,AO,YO,
     1          RL,MODEL
      COMMON/A3/VSO(100),VSI(100),V(100),PF(100),E1,W,DELV,
     1          OF,OM,AEL(100),PY,IP
      COMMON/A4/U(100),ST(100,4),IS(4),NST
      IO=6
      EA=0.D0
      WRITE(IO,5)
      DO 2 I=1,34
      V(I)=0.D0
      EA=EA+1.D-4
      IF(MODEL.EQ.3) CALL INTER3(EA,P,RM,AE,I)
      IF(MODEL.NE.3) CALL INTERN(EA,P,RM,AE,I)
      PFD=2.D0*P
      AEL(I)=AE/AO*100.D0
      WRITE(IO,10) I,EA,PFD,AEL(I)
    2 CONTINUE
      RETURN
    5 FORMAT(/10X,'STRAIN',9X,'LOAD',6X,'ELASTIC AREA %'/)
   10 FORMAT(3X,I2,3(3X,1PD11.4))
      END
C
C
      SUBROUTINE MORE (I,MREACH,IREACH,IR1,MI,DELV,V)
C
C     FOR DETAILS, 'MORE' DECREASES THE DEFLECTION INCREMENT
C     AND INCREASES IT BACK TO ITS INITIAL VALUE ONCE THE
C     DETAILED INTERVAL PASSED.
C
      IMPLICIT REAL*8 (A-H,O-Z)
      DIMENSION V(100)
      IF(I.NE.IREACH+1) GO TO 10
      DELV=DELV/DFLOAT(MI)
      IF(MREACH.EQ.1) V(I)=V(IREACH)-DFLOAT(   MI-1)*DELV
      IF(MREACH.EQ.2) V(I)=V(IREACH)-DFLOAT(2*MI-1)*DELV
      RETURN
   10 V(I)=V(I-1)+DELV
      IF(V(I).EQ.V(IR1)) V(I)=V(I)+DELV
      IF(V(I).EQ.V(IREACH)) GO TO 20
      RETURN
   20 DELV=DELV*DFLOAT(MI)
      V(I)=V(IREACH)+DELV
      MREACH=3
      RETURN
      END
```

```
      SUBRCUTINECMAX (I,MREACH,IREACH,IR1,C1,PMAX,PF)
C
C     FINDS THE MAXIMUM LOAD
C
      IMPLICIT REAL*8 (A-H,O-Z)
      DIMENSION PF(100)
      IF(DABS(PF(I)-PF(I-1)).LT.C1*PF(I)/10.D0) GO TO 10
      IF(PF(I)-PF(I-1).LT.-C1*PF(I)/10.D0) GO TO 15
      PMAX=PF(I)
      RETURN
   10 MREACH=1
      GO TO 20
   15 MREACH=2
   20 IREACH=I
      IR1=I-1
      RETURN
      END
C
C
      SUBROUTINE DEFORM (RO,J,I,EA,EAP)
C
C     COMPUTES STRAIN IN ABSENCE OF RESIDUAL STRAINS
C     (AXIAL AND BENDING ONLY).
C
      IMPLICIT REAL*8 (A-H,O-Z)
      COMMON/A1/D(100),T(100),PHI1(100),PHI2(100),XC(100),
     1          XD(100),YI(100),PI,E,N,NN
      COMMON/A2/RSO(100),RSI(100),RON(100),EY(100),XO,AO,YO,
     1          RL,MODEL
      COMMON/A3/VSO(100),VSI(100),V(100),PF(100),E1,W,DELV,
     1          OF,OM,AEL(100),PY,IP
      CT=DCOS((PHI1(J)+PHI2(J))*.5D0)
      EB =-PI*PI  *V(I)/(RL*RL)*(XD(J)+RO*CT-XO)
      EAP=EA+EB
      RETURN
      END
```

APPENDIX G

PROGRAM SHEET BENDING

```
C                                 SHEET BENDING
C
C       SHEET BENDING WITH PLASTIC RESIDUAL STATE AT INTERIOR,
C       CONCAVE EDGE OR BOTH. D1, DL CORRESPOND TO LOGD1,
C       LOGD2 IN PAPER: 'MECHANICS OF THE SHEET BENDING
C       PROCESS' BY B.W.SHAFFER & E.E. UNGAR, J. APPLIED
C       MECHANICS,TRANS. ASME, MARCH 1960. HERE LOADS INCLUDE
C       MOMENT AND INTERNAL PRESSURE. EQUATION NUMBERS REFER
C       TO CHAPTER 4 (WAS 3) OF THESIS.
C                                 INPUT
C       NB = # OF EXTERNAL RADII
C       NP = # OF PRESSURES OR NEUTRAL AXIS LOCATIONS
C       IOPT=0 INPUT NEUTRAL AXIS, IOPT=1 INPUT PRESSURE.
C       M = # OF INTEGRATION POINTS FOR FORCE & MOMENT
C       DEFAULT 50.
C       U=1.D0 FOR TRESCA, 2.D0/DSQRT(3.D0) (DEFAULT) FOR VON
C       MISES. FOR DEFAULT, LEAVE BLANK.
C       FOR DEFAULT , LEAVE BLANK.
C       PR = RATIO OF MAXIMUM PRESSURE TO SMALLEST PRESSURE
C       RA = INTERNAL RADIUS
C       RRB(I) = EXTERNAL RADII
C       RINC(I)= RADIUS INCREMENT AT WHICH STRESSES OUTPUT
C       RCC(J) = LOCATION OF NEUTRAL AXIS (IOPT=0)
C                (STARTING FROM RA)
C                                 OUTPUT
C       P = PRESSURE
C       PM = MAXIMUM PRESSURE (RC=RA)
C       AP = P/PM
C       PRA = P AT WHICH INTERIOR YIELD ZONE REACHES CONCAVE
C       FACE.
C       RC = RADIUS OF NEUTRAL AXIS
C       TO, TI = TRANSITION RADII TO PLASTIC RESIDUAL ZONES
C       A, B, C, D1, DL, H = COEFFICIENTS OF INTEGRATION
C       CM = MOMENT
C       RY = LIMIT OF FULLY ELASTIC UNLOADING ZONES
C       TD =CT=  % OF THICKNESS IN INTERIOR THAT UNLOADS
C       PLASTICALLY.
C       TY = % OF THICKNESS AT CONCAVE EDGE THAT UNLOADS
C       PLASTICALLY.
C       R = RADIUS
C       SR, ST, SZ = RESIDUAL STRESSES IN RADIAL, TANGENTIAL
C       AND AXIAL DIRECTIONS
C       TR = ST - SR = + OR - 1 AT YIELD
C       CN, YN, ON, YT = NON-DIMENSIONALIZED RC, RY,TO, TI
C                         (SAY CN = (RC-RA)/(RB-RA) )
C       DI = % DIFFERENCE BETWEEN TO AND RY
C       NOTICE FACTOR U WITH WHICH P, OM, SR, ST, SZ ARE
C       MULTIPLIED.
C       TO OBTAIN DIMENSIONALIZED VALUES MULTIPLY BY YIELD
C       STRESS.
C       THIS PROGRAM WRITTEN FOR POSITIVE PRESSURE AND MOMENT
C       AND RC.GE.RA.
```

```
C                    MAIN
C
      IMPLICIT REAL*8 (A-H,O-Z)
      DIMENSION RRB(5),RINC(5),RCC(5,10)
      READ (5,50) NB,NP,IOPT,M,U
      READ (5,60) PR,RA,(RRB(I),I=1,NB),(RINC(I),I=1,NB)
      IF (M.EQ.0) M=50
      IF(IOPT.EQ.1) GO TO 10
      DO 5 I=1,NB
  5   READ(5,60) (RCC(I,J),J=1,NP)
  10  IF(U.EQ.0.D0) U=2.D0/DSQRT(3.D0)
      DO 40 I=1,NB
      RB = RRB(I)
      RIC=RINC(I)
      HN=((RB/RA)**2-1.D0)**2-4.D0*(RB/RA*DLOG(RB/RA))**2
      PM=DLOG(RB/RA)
      CALL PCON (RA,RB,PCR,1.D-5)
      PRA=PCR /PM
      PMM=PM*U
      WRITE (6,70) RA,RB,PMM,PRA,U
      DO 35 J=1,NP
C
C     IFLAG=1,2,3 MEANS PROBLEMS: TC NOT FOUND IN SOLVE,
C     BISECT OR CONCAV RESPECTIVELY (ALSO TI NOT FOUND IN
C     LAST CASE).
C
      IFLAG=0
      IF2=0
      IF3=0
      RY=0.D0
      IF(IOPT.EQ.0) GO TO 15
      P=DFLOAT(J-1)*PM/PP
      RC=DSQRT(RA*RB*DEXP(-P))
      GO TO 16
  15  RC=RCC(I,J)
      P=DLOG(RA*RB/(RC*RC))
  16  AP=P/PM
      THIN=P*50.D0
      CN = (RC-RA)/(RB-RA)
      CM=(RA*RA+RB*RB-2.D0*RA*RB*DEXP(-P))/4.D0-RA*RB*P/
     1  2.D0
      CMM=CM*U
      IF (CM.EQ.0.D0) GO TO 110
      IF(P.GT.1.1D0*PCR) GO TO 110
      ZETA=RA*RA*P/CM
      RY2=2.D0*(RB*RB-RA*RA)*DLOG(RB/RA)-0.5D0*ZETA*RA*RA*HN
      IF(RY2.LT.0) GO TO 110
      RY=RA*RB/(RB*RB-RA*RA)*DSQRT(RY2)
      YN = (RY-RA)/(RB-RA)
      IF(RY.GT.RC) GO TO 30
C
C     CASE 1: RY < RC
C
  20  IF(IF2.GT.1) GO TO 110
```

```
      IF (P.EQ.0.D0) CALL PSOLVE (IFLAG,RA,RB,RC,P,B,TO)
      IF (P.NE.0.D0) CALL  SOLVE (IFLAG,RA,RB,RC,P,B,TO,RY)
      IF2=IF2+1
      IF(IFLAG.EQ.1) GO TO 30
      TD=(RC-TO)/(RB-RA)*1.D2
      CN = (TO-RA)/(RB-RA)
      DI = (TO-RY)/TO*1.D2
      WRITE(6,80) AP,RC,OMM,TO,B,RY,TD,CN,YN,ON,DI,THIN
      IF(TO.LE.RA) GO TO 110
      IF(TO.GT.RC) GO TO 30
      CALL STRES1 (M,IF3,RIC,B,TO,RA,RB,RC,P,U)
      GO TO 33
C
C     CASE 2: RY > RC
C
   30 IF(IF2.GT.1) GO TO 110
      CALL BISECT(IFLAG,RA,RB,RC,P,B,TO,RY)
      IF2=IF2+1
      IF(IFLAG.EQ.2) GO TO 20
      TD=(TO-RC)/(RB-RA)*1.D2
      CN = (TO-RA)/(RB-RA)
      DI = (TO-RY)/TO*1.D2
      WRITE(6,80) AP,RC,OMM,TO,B,RY,TD,CN,YN,ON,DI,THIN
      IF(TO.LT.RC) GO TO 20
      CALL STRES2 (M,IF3,RIC,B,TO,RA,RB,RC,P,U)
C
C     CASE 3: INTERIOR AND CONCAVE EDGE UNLOAD INELASTICALLY
C
   33 IF(IF3.EQ.0) GO TO 35
      CALL CONCAV(IFLAG,RA,RB,RC,P,TO,TI)
      IF(IFLAG.EQ.3) GO TO 34
      TY=(TI-RA)/(RB-RA)*1.D2
      YT=(TI-RA)/(RB-RA)
      CN = (TO-RA)/(RB-RA)
      DI = (TO-RY)/TO*1.D2
      TD=(RC-TO)/(RB-RA)*1.D2
      WRITE(6,90) AP,RC,OMM,TO,TI,RY,TY,TD,CN,YN,ON,DI,YT
     1  THIN
      CALL STRES3 (M,RIC,TO,TI,RA,RB,RC,P,U)
      GO TO 35
C
C     CASE 4: RY.LE.RA
C
  110 TD=(RC-RA)/(RB-RA)*1.D2
      WRITE(6,150) AP,RC,CMM,TD,CN,THIN
      CALL STRES4 (M,RIC,RA,RB,RC,P,U)
      IF (IFLAG.EQ.0) GO TO 35
   34 WRITE(6,100) P,RC,OMM,RY,CN,YN
   35 CONTINUE
   40 CONTINUE
   50 FORMAT (4I5,D10.0)
   60 FORMAT(8D10.0)
   70 FORMAT(/' RA=',1PD10.3,'  RB=',D10.3,'  PM=',D10.3,
     1'  PRA=',D10.3,'  U=',D10.3)
```

```
 80  FORMAT(/'AP =',1PD10.3,'  RC=',D10.3,'  OM=',D10.3,
    1'  TC=',D10.3,'  B =',D10.3,'  RY=',D10.3,'  TD=',
    2D10.3/'  CN=',D10.3,'  YN=',D10.3,'  ON=',D10.3,
    3'  DI=',D10.3,'  PERCENT THINNING=',D10.3)
 90  FORMAT(/'AP =',1PD10.3,'  RC=',D10.3,'  OM=',D10.3,
    1'  TO=',D10.3,'  TI=',D10.3,'  RY=',D10.3,'  TY=',
    2D10.3,'  TD=',D10.3/'  CN=',D10.3,'  YN=',D10.3,
    3'  ON=',D10.3,'  DI=',D10.3,'  YT=',D10.3,
    4'  PERCENT THINNING=',D10.3)
100  FORMAT(/' AP=',1PD10.3, '  RC=',D10.3,'  OM=',D10.3,
    1'  RY=',D10.3/'  CN=',D10.3,'  YN=',D10.0/' ABOVE ',
    2'RESULTS ARE INVALID IF OBVIOUSLY CONCAVE EDGE CANNOT'
    3,'YIELD')
150  FORMAT(/' AP=',1PD10.3,'  RC=',D10.3,'  OM=',D10.3,
    1'  TD=',D10.3,'  CN=',D10.3,
    2'  PERCENT THINNING=',D10.3)
     STOP
     END
```

```
      SUBROUTINE VALUF (TO,RA,RB,RC,Q2,B,F,P)
C
C     CASE 1. SUBSTITUTES (3.42) INTO (3.43).
C     F = 0 GIVES TO
C
      IMPLICIT REAL*8 (A-H,O-Z)
    1 Q1=-1.DO+2.DO*DLOG(RC/RB)-2.DO*DLOG(TO/RA)+TO*TO*Q2
      B=P/Q1
      Q3=((TO*TO-RA*RA)/RA)**2/2.DO
      Q4=(RB*RB-RC*RC)/(2.DO*RB*RB)*(RB*RB-TO**4/(RC*RC))
      F=(RA*RA+RB*RB-2.DO*RC*RC)/4.DO+TO*TO*P/2.DO+B*(Q4-Q3)
      RETURN
      END
C
C
      SUBROUTINE VALUG (TO,RA,RB,RC,B,G,P)
C
C     CASE 2. SUBSTITUTES (3.55) INTO (3.56).
C     G = 0 GIVES TO
C
      IMPLICIT REAL*8 (A-H,O-Z)
      Q1=1.DO/(RB*RB)-1.DO/(RA*RA)
      Q2=Q1+1.DO/(RC*RC)
      Q3=(RA*RA+RB*RB-2.DO*RC*RC)/4.DO
      Q4=1.DO+2.DO*DLOG(TO*RA/(RB*RC)) -TO*TO*Q2
      B=P/Q4
      G=Q3+P*RC*RC*0.5DO+B*RC*RC*TO*TO*Q1*0.5DO+0.5DO*B*(RB*
     1 RB-RA*RA)+B*(RC*RC-TO*TO)*DLOG(RB*RC/(RA*TO))
      RETURN
      END
C
C
      SUBROUTINE VALUK (RA,RB,RC,TO,TI,P,F)
C
C     SOLVE FOR TO FROM EQUATION (3.73) THEN CALCULATES
C     RIGHT HAND SIDE OF (3.72). F=0 GIVES TI.
C
      IMPLICIT REAL *8 (A-H,O-Z)
      ALFA=1.DO/(RB*RB)-1.DO/(RC*RC)-(1.DO+P+2.DO*DLOG(TI/
     1RA))/(TI*TI)
      BETA=1.DO+P+2.DO*DLOG(TI/RA)+(RA*RA-RB*RB+2.DO*RC*RC)/
     1  (2.DO*TI*TI)
      GAMA=(-RA*RA+3.DO*RB*RB-4.DO*RC*RC)/2.DO
      TO=DSQRT((-BETA-DSQRT(BETA*BETA-4.DO*ALFA*GAMA))/
     1  (2.DO*ALFA))
      Q1=(TO/TI)**2
      Q2=1.DO/(RB*RB)-1.DO/(RC*RC)-1.0/(TI*TI)
      F=Q1*2.DO*DLOG(RA/TI)+DLOG(RB*TO*TO/(RA **3))
     2  +TO*TO*Q2-(Q1-2.DO)*P+1.DO
      RETURN
      END
```

```
      SUBROUTINE PSOLVE (IFLAG,RA,RB,RC,P,B,TO)
C
C     CASE 1. TO < RC
C     SOLVE FOR TO FOR P = 0 AND INTERIOR PLASTIC UNLOADING
C     ONLY
C
      IMPLICIT REAL*8 (A-H,O-Z)
      WRITE(6,20)
      H=RB-RA
      TO=RA
      Q2=1.D0+(H/RA)/(RB/RA)**2
 1    G=1.D0+DLOG((TO/RA)**2*RB/RA)-(TO/RA)**2*Q2
      DG=2.D0/TO-2.D0*TO*Q2/(RA*RA)
      D=-G/DG
      TO=TO+D
      IF(DABS(D/TO).LT.1.D-5) GO TO 5
      GO TO 1
 5    Q1=(TO/RB)**2*(1.D0+3.D0*H/RA+(H/RA)**2)-2.D0+(RA/TO)*
     2*2*(1.D0-H/RA-(H/RA)**2)
      B=(H/TO)**2/(2.D0*Q1)
 10   RETURN
 20   FORMAT(/' SUBROUTINE PSOLVE USED. P=0 AND TO < RC')
      END
C
C
      SUBROUTINE PCON (A,B,X,EPS)
C
C     SOLVE FOR PRESSURE AT WHICH INTERIOR YIELD ZONE
C     REACHES CONCAVE FACE (RY=RA). EQUATION (3.75)
C
      IMPLICIT REAL*8 (A-H,O-Z)
      C=B/A
      S=(C*C-1.D0)**2 - (2.D0*C*DLOG(C))**2
      Q=(C*C-1.D0)*DLOG(C) - .5D0*((C*C-1.D0)/C)**2
      Q1=S+2.D0*C*Q
      Q2=2.D0*C*Q
      Q3=(1.D0+C*C)*Q
      X=Q/S*(1.D0-C)**2
C     SOLVE Q1*X + Q2*DEXP(-X) - Q3 = 0
 5    F=Q1*X+Q2*DEXP(-X)-Q3
      G=Q1-Q2*DEXP(-X)
      D=-F/G
      IF(DABS(D/X).LT.EPS) GO TO 10
      X=X+D
      GO TO 5
 10   RETURN
      END
```

```
      SUBROUTINE SRO (A,B,C,H,RB,R,SR,ST,SZ,TR,U)
C
C     STRESSES FOR OUTSIDE ELASTIC UNLOADING REGION
C     EQUATIONS (3.32)
C
      IMPLICIT REAL*8 (A-H,O-Z)
      Q=-DLOG(RB/R)+2.D0*B*DLOG(R)+C+H
      SR=Q+A/(R*R)+B
      ST=Q+1.D0-A/(R*R)+3.D0*B
      TR=ST-SR
      SZ=.5D0+DLOG(R/RB)+.6D0*(2.D0*B*(1.D0+DLOG(R))+C+H)
      SR=U*SR
      ST=U*ST
      SZ=U*SZ
      RETURN
      END
C
C
      SUBROUTINE SRI(A,B,C,P,RA,R,SR,ST,SZ,TR,U)
C
C     STRESSES FOR  INSIDE ELASTIC UNLOADING REGION
C     EQUATIONS (3.30)
C
      IMPLICIT REAL*8 (A-H,O-Z)
      Q=-P-DLOG(R/RA)+B*2.D0*DLOG(R)+C
      SR=Q+A/(R*R)+B
      ST=Q-1.D0-A/(R*R)+3.D0*B
      TR=ST-SR
      SZ=-.5D0-P-DLOG(R/RA)+.6D0*(2.D0*B*(1.D0+DLOG(R))+C)
      SR=U*SR
      ST=U*ST
      SZ=U*SZ
      RETURN
      END
```

```
      SUBRCUTINE SPM (D1,RB,R,SR,ST,SZ,TR,U)
C
C     STRESSES FOR PLASTIC MINUS UNLOADING REGION
C     EQUATIONS (3.31)
C
      IMPLICIT REAL*8 (A-H,O-Z)
      SR = -DLOG(   R/RB)  -D1
      ST=-1.D0+SR
      TR=-1.D0
      SZ=0.5D0*(SR+ST)
      SR=U*SR
      ST=U*ST
      SZ=U*SZ
      RETURN
      END
C
C
      SUBRCUTINE SPP(D1,RB,R,SR,ST,SZ,TR,U)
C
C     STRESSES FOR PLASTIC PLUS  UNLOADING REGION
C     EQUATIONS (3.44)
C
      IMPLICIT REAL*8 (A-H,O-Z)
      SR=DLOG(R/RB) +D1
      ST=1.D0+SR
      SZ=0.5D0*(SR+ST)
      TR=1.D0
      SR=U*SR
      ST=U*ST
      SZ=U*SZ
      RETURN
      END
```

```
      SUBROUTINE SOLVE (IFLAG,RA,RB,RC,P,B,TO,RY)
C
C     CASE 1. SOLVE (3.43) AFTER SUBSTITUTING FOR B FROM
C     (3.42). SOLVE FOR TO AND B WHEN TO < RC.
C
      IMPLICIT REAL*8 (A-H,O-Z)
      WRITE(6,80)
      Q2=1.D0/(RA*RA)-1.D0/(RB*RB)+1.D0/(RC*RC)
      DO 5 I=1,16,5
      TL=RY*(1.D0-DFLOAT(I)*1.D-2)
      TR=RY*(1.D0+DFLOAT(I)*1.D-2)
      CALL VALUF (TL,RA,RB,RC,Q2,BL,FL,P)
      CALL VALUF (TR,RA,RB,RC,Q2,BR,FR,P)
      IF(FL*FR.LE.0) GO TO 7
    5 CONTINUE
      GO TO 65
    7 TM=0.5D0*(TL+TR)
      CALL VALUF (TM,RA,RB,RC,Q2,BM,FM,P)
   10 IF(FM.EQ.0) GO TO 30
      IF(DABS((TR-TL)/(RB-RA)).LE.2.D-5) GO TO 30
      IF(FL*FM.GT.0) GO TO 20
      TR=TM
      FR=FM
      TM=0.5D0*(TL+TR)
      CALL VALUF (TM,RA,RB,RC,Q2,BM,FM,P)
      GO TO 10
   20 TL=TM
      FL=FM
      TM=0.5D0*(TL+TR)
      CALL VALUF (TM,RA,RB,RC,Q2,BM,FM,P)
      GO TO 10
   30 TO=TM
      B=BM
      GO TO 100
   65 IFLAG=1
      WRITE(6,90) RY,TL,FL,TR,FR
   90 FORMAT(' PROBLEM IN SOLVE. IFLAG = 1 RY=',1PD10.3,
     2' TL=',D10.3,' FL=',D10.3,' TR=',D10.3,' FR=',D10.3)
   80 FORMAT(/' SUBROUTINE SOLVE USED. ASSUME TO < RC')
  100 RETURN
      END
```

```
      SUBROUTINE BISECT(IFLAG,RA,RB,RC,P,B,TO,RY)
C
C     CASE 2. SOLVE (3.56) AFTER SUBSTITUTING IN (3.55)
C     SOLVE FOR TO WHEN RC < TO
C
      IMPLICIT REAL*8 (A-H,O-Z)
      WRITE(6,80)
      DO 5 I=1,16,5
      TL=RY*(1.D0-DFLOAT(I)*1.D-2)
      TR=RY*(1.D0+DFLOAT(I)*1.D-2)
      CALL VALUG (TL,RA,RB,RC,BL,GL,P)
      CALL VALUG(TR,RA,RB,RC,BR,GR,P)
      IF(GL*GR.LE.0) GO TO 7
    5 CONTINUE
      GO TO 65
    7 TM=0.5D0*(TR+TL)
      CALL VALUG(TM,RA,RB,RC,BM,GM,P)
   10 IF(GM.EQ.0) GO TO 30
      IF(DABS((TR-TL)/(RB-RA)).LE.2.D-5) GO TO 30
      IF(GL*GM.GT.0) GO TO 20
      TR=TM
      GR=GM
      TM=0.5D0*(TL+TR)
      CALL VALUG(TM,RA,RB,RC,BM,GM,P)
      GO TO 10
   20 TL=TM
      GL=GM
      TM=0.5D0*(TL+TR)
      CALL VALUG(TM,RA,RB,RC,BM,GM,P)
      GO TO 10
   30 TO=TM
      B=BM
      GO TO 100
   65 IFLAG=2
      WRITE(6,90) RY,TL,GL,TR,GR
   80 FORMAT(/' SUBROUTINE BISECT USED. ASSUME RC < TO')
   90 FORMAT(' PROBLEM IN BISECT. IFLAG = 2 RY=',1PD10.3,
     2' TL=',D10.3,' GL=',D10.3,' TR=',D10.3,' GR=',D10.3)
  100 RETURN
      END
```

```
      SUBROUTINE CONCAV (IFLAG,RA,RB,RC,P,TO,TI)
C
C     SOLVES EQUATIONS (3.72) AND (3.73) FOR TI.
C     CASE: YIELDING AT CONCAVE EDGE AND INTERIOR MINUS.
C
      IMPLICIT REAL *8 (A-H,O-Z)
      WRITE(6,80)
      TL=RA
      CALL VALUK (RA,RB,RC,TO,TL,P,FL)
      IF(FL.EQ.0) GO TO 40
      DO 5 I=1,13,4
      TR=RA+(RB-RA)*1.D-2*(DFLOAT(I))
      CALL VALUK (RA,RB,RC,TO,TR,P,FR)
      IF(FL*FR.LT.0) GO TO 15
      IF(FR.EQ.0) GO TO 50
    5 CONTINUE
      GO TO 60
   15 TM=0.5D0*(TL+TR)
      CALL VALUK (RA,RB,RC,TO,TM,P,FM)
      IF(DABS(TL-TR)/(RB-RA).LT.2.D-6) GO TO 30
      IF(FM.EQ.0) GO TO 30
      IF(FL*FM.GT.0) GO TO 20
      TR=TM
      FR=FM
      GO TO 15
   20 TL=TM
      FL=FM
      GO TO 15
   30 TI=TM
      GO TO 100
   40 TI=TL
      GO TO 100
   50 TI=TR
      GO TO 100
   60 IFLAG=3
      WRITE(6,90) TL,FL,TR,FR
   80 FORMAT(/' SUBROUTINE CONCAV USED')
   90 FORMAT(' PROBLEM IN CONCAV. IFLAG=3 TL=',1PD10.3,
     2' FL=',D10.3,' TR=',D10.3,' FR=',D10.3)
  100 RETURN
      END
```

```
      SUBRCUTINE STRES1 (M,IF3,RIC,B,TO,RA,RB,RC,P,U)
C
C     CALCULATES A,C, D, H FROM EQUATIONS (3.38)-(3.43)
C     CASE TO < RC
C
      IMPLICIT REAL*8 (A-H,O-Z)
      A=B*TO*TO
      C=P-A/(RA*RA)-B*(1.D0+2.D0*DLOG(RA))
      CT=(RC-TO)/(RB-RA)*1.D2
      H=-A/(RB*RB)-B*(1.D0+2.D0*DLOG(RB))-C
      D1  =2.D0*(1.D0+B)*DLOG(RB/RC)+A*(1.D0/(RB*RB)-1.D0/
     1  (RC*RC))
      WRITE(6,80) A,C,H,D1,CT
      DO 30 K=1,100
      R=RA+RIC *DFLCAT(K-1)
      IF(R.GE.RB) GO TO 70
      IF(R.EQ.TO.OR.R.EQ.RC) GO TO 30
      IF(R.LT.TO) CALL SRI (A,B,C,P,RA,R,SR,ST,SZ,TR,U)
      IF(R.GT.TO.AND.R.LT.RC) CALLSPM(D1,RB,R,SR,ST,SZ,TR,U)
      IF(R.GT.RC) CALL SRC (A,B,C,H,RB,R,SR,ST,SZ,TR,U)
      WRITE (6,90) R,SR,ST,SZ,TR
      IF(R.GT.RA) GO TO 30
C
C     CHECK YIELD CRITERION AT CONCAVE EDGE
C
      IF(DABS(TR).GT.1.D0) IF3=1
   30 CONTINUE
   70 R=RB
      CALL SRO (A,B,C,H,RB,R,SR,ST,SZ,TR,U)
      WRITE(6,90) R,SR,ST,SZ,TR
      R=TO
      CALL SRI (A,B,C,P,RA,R,SR,ST,SZ,TR,U)
      WRITE(6,90) R,SR,ST,SZ,TR
      CALL SPM ( D1,RB,R,SR,ST,SZ,TR,U)
      WRITE (6,90) R,SR,ST,SZ,TR
      R=RC
      CALL SPM ( D1,RB,R,SR,ST,SZ,TR,U)
      WRITE(6,90) R,SR,ST,SZ,TR
      CALL SRC (A,B,C,H,RB,R,SR,ST,SZ,TR,U)
      WRITE(6,90) R,SR,ST,SZ,TR
      MI=M*(TO-RA)/(RB-RA)
      MM=M*(RC-TO)/(RB-RA)
      MC=M*(RB-RC)/(RB-RA)
      RFI=0.D0
      RMI=0.D0
      RFM=0.D0
      RMM=0.D0
      RFO=0.D0
      RMO=0.D0
      DRI=(TO-RA)/DFLOAT(MI)
      DO 5 I=1,MI
      R=RA+(DFLOAT(I)-0.5D0)*DRI
      CALL SRI (A,B,C,P,RA,R,SR,ST,SZ,TR,U)
      RFI=RFI+SZ*R*DRI
```

```
      RMI=RMI+SZ*R*R*DRI
5     CONTINUE
      IF(MM.EQ.0) GO TO 12
      DRM=(RC-TO)/DFLOAT(MM)
      DO 10 I=1,MM
      R=TO+(DFLOAT(I)-0.5D0)*DRM
      CALL SPM (D1,RB,R,SR,ST,SZ,TR,U)
      RFM=RFM+SZ*R*DRM
      RMM=RMM+SZ*R*R*DRM
10    CONTINUE
12    DRO=(RB-RC)/DFLOAT(MO)
      DO 15 I=1,MO
      R=RC+(DFLOAT(I)-0.5D0)*DRO
      CALL SRO (A,B,C,H,RB,R,SR,ST,SZ,TR,U)
      RFO=RFO+SZ*R*DRO
      RMO=RMO+SZ*R*R*DRO
15    CONTINUE
      Q=(RB**4-RA**4)/2.D0-(RB**3-RA**3)*(RA+RB)/3.D0
      RF=RFI+RFM+RFO
      RM=RMI+RMM+RMO
      RAS=2.D0*RF/(RA*RA-RB*RB)
      RBS=(RB-RA)*RM/Q
      WRITE(6,20) RF,RM,RAS,RBS
      RETURN
20    FORMAT(/' Z RESIDUAL FORCE=',1PD10.3,9X,
     1'Z RESIDUAL MOMENT=',D10.3/' AXIAL RELAXATION STRESS='
     2,D10.3,'  BENDING RELAXATION STRESS=',D10.3)
80    FORMAT( ' A =',1PD10.3,'  C =',D10.3,'  H =',D10.3,
     1'  D1=',D10.3,'  CT=',D10.3/T5,'R',T17,'SR',T29,'ST',
     2T41,'SZ',T53,'TR')
90    FORMAT(/1X,5(1PD10.3,2X))
      END
```

```
      SUBROUTINE STRES2 (M,IF3,RIC,B,TO,RA,RB,RC,P,U)
C
C     CALCULATES A, C, D, H FROM EQUATIONS (3,50)-(3.52) AND
C     (3.54). CASE RC < TO.
C
      IMPLICIT REAL*8 (A-H,O-Z)
      A=B*TO*TO
      C=P-A/(RA*RA)-B*(1.D0+2.D0*DLOG(RA))
      CT=(RC-TO)/(RB-RA)*1.D2
      H=-A/(RB*RB)-B*(1.D0+2.D0*DLOG(RB))-C
      D1=B*(1.D0+2.D0*DLOG(TO/RB)-(TO/RB)**2)
      WRITE(6,80) A,C,H,D1,CT
      DO 30 K=1,100
      R=RA+RIC *DFLOAT(K-1)
      IF(R.GE.RB) GO TO 70
      IF(R.EQ.TO.OR.R.EQ.RC) GO TO 30
      IF(R.LT.RC) CALL SRI (A,B,C,P,RA,R,SR,ST,SZ,TR,U)
      IF(R.GT.RC.AND.R.LT.TO) CALLSPP(D1,RB,R,SR,ST,SZ,TR,U)
      IF(R.GT.TO) CALL SRO (A,B,C,H,RB,R,SR,ST,SZ,TR,U)
      WRITE (6,90) R,SR,ST,SZ,TR
      IF(R.GT.RA) GO TO 30
C
C     CHECK YIELD CRITERION AT CONCAVE EDGE
C
      IF(DABS(TR).GT.1.D0) IF3=1
   30 CONTINUE
   70 R=RB
      CALL SRO (A,B,C,H,RB,R,SR,ST,SZ,TR,U)
      WRITE(6,90) R,SR,ST,SZ,TR
      R=RC
      CALL SRI (A,B,C,P,RA,R,SR,ST,SZ,TR,U)
      WRITE(6,90) R,SR,ST,SZ,TR
      CALL SPP ( D1,RB,R,SR,ST,SZ,TR,U)
      WRITE(6,90) R,SR,ST,SZ,TR
      R=TO
      CALL SPP ( D1,RB,R,SR,ST,SZ,TR,U)
      WRITE (6,90) R,SR,ST,SZ,TR
      CALL SRO (A,B,C,H,RB,R,SR,ST,SZ,TR,U)
      WRITE(6,90) R,SR,ST,SZ,TR
      MI=M*(RC-RA)/(RB-RA)
      MP=M*(TO-RC)/(RB-RA)
      MO=M*(RB-TO)/(RB-RA)
      RFI=0.D0
      RMI=0.D0
      RFP=0.D0
      RMP=0.D0
      RFO=0.D0
      RMO=0.D0
      DRI=(RC-RA)/DFLOAT(MI)
      DO 5 I=1,MI
      R=RA+(DFLOAT(I)-0.5D0)*DRI
      CALL SRI(A,B,C,P,RA,R,SR,ST,SZ,TR,U)
      RFI=RFI+SZ*R*DRI
      RMI=RMI+SZ*R*R*DRI
```

```
5     CONTINUE
      IF(MP.EQ.0) GO TO 12
      DRP=(TO-RC)/DFLOAT(MP)
      DO 10 I=1,MP
      R=RC+(DFLOAT(I)-0.5D0)*DRP
      CALL SPP (D1,RB,R,SR,ST,SZ,TR,U)
      RFP=RFP+SZ*R*DRP
      RMP=RMP+SZ*R*R*DRP
10    CONTINUE
12    DRO=(RB-TO)/DFLOAT(MO)
      DO 15 I=1,MO
      R=TO+(DFLOAT(I)-0.5D0)*DRO
      CALL SRO (A,B,C,H,RB,R,SR,ST,SZ,TR,U)
      RFO=RFO+SZ*R*DRO
      RMO=RMO+SZ*R*R*DRO
15    CONTINUE
      Q=(RB**4-RA**4)/2.D0-(RB**3-RA**3)*(RA+RB)/3.D0
      RF=RFI+RFP+RFO
      RM=RMI+RMP+RMO
      RAS=2.D0*RF/(RA*RA-RB*RB)
      RBS=(RB-RA)*RM/Q
      WRITE(6,20) RF,RM,RAS,RBS
      RETURN
20    FORMAT(/' Z RESIDUAL FORCE=',1PD10.3,9X,
     1'Z RESIDUAL MOMENT=',D10.3/' AXIAL RELAXATION STRESS='
     2,D10.3,'  BENDING RELAXATION STRESS=',D10.3)
80    FORMAT( ' A =',1PD10.3,'  C =',D10.3,'  H =',D10.3,
     1'  D1=',D10.3,'  CT=',D10.3/T5,'R',T17,'SR',T29,'ST',
     2T41,'SZ',T53,'TR')
90    FORMAT(/1X,5(1PD10.3,2X))
      END
```

```
      SUBROUTINE STRES3 (M,RIC,TO,TI,RA,RB,RC,P,U)
C
C     CALCULATES A, C, D, H FROM EQUATIONS (3.65)-(3.70)
C     RESIDUAL PLASTIC STATE AT CONCAVE EDGE AND INTERIOR
C     TO < RC
C
      IMPLICIT REAL*8 (A-H,O-Z)
      B=TI*TI/(TI*TI-TO*TO)
      A=B*TO*TO
      Q1=1.DO/(RC*RC)-1.DO/(RB*RB)
      Q2=1.DO/(TI*TI)-1.DO/(RB*RB)
      D1=(B+1.DO)*2.DO*DLOG(RB/RC)-B*TO*TO*Q1
      C=2.DO*DLOG(TI/RA)-B*(TO/TI)**2-B*(1.DO+2.DO*DLOG(TI))
     1  +P
      H=B*2.DO*DLOG(TI/RB)-2.DO*DLOG(TI/RA)+B*TO*TO*Q2-P
      DL=DLOG(RB/RA)
      WRITE(6,80) A,B,C,D1,DL,H
      DO 30 K=1,100
      R=RA+RIC *DFLOAT(K-1)
      IF(R.GE.RB) GO TO 70
      IF(R.EQ.TO.OR.R.EQ.RC.OR.R.EQ.TI) GO TO 30
      IF(R.LT.TI) CALL SPP(DL,RB,R,SR,ST,SZ,TR,U)
      IF(R.GT.TI.AND.R.LT.TO) CALL SRI(A,B,C,P,RA,R,SR,ST,
     1  SZ,TR,U)
      IF(R.GT.TO.AND.R.LT.RC) CALLSPM(D1,RB,R,SR,ST,SZ,TR,U)
      IF(R.GT.RC) CALL SRO(A,B,C,H,RB,R,SR,ST,SZ,TR,U)
      WRITE(6,90) R,SR,ST,SZ,TR
   30 CONTINUE
   70 R=RB
      CALL SRO (A,B,C,H,RB,R,SR,ST,SZ,TR,U)
      WRITE(6,90) R,SR,ST,SZ,TR
      R=TI
      CALL SPP(DL,RB,R,SR,ST,SZ,TR,U)
      WRITE(6,90) R,SR,ST,SZ,TR
      CALL SRI (A,B,C,P,RA,R,SR,ST,SZ,TR,U)
      WRITE(6,90) R,SR,ST,SZ,TR
      R=TO
      CALL SRI (A,B,C,P,RA,R,SR,ST,SZ,TR,U)
      WRITE(6,90) R,SR,ST,SZ,TR
      CALL SPM(D1,RB,R,SR,ST,SZ,TR,U)
      WRITE(6,90) R,SR,ST,SZ,TR
      R=RC
      CALL SPM(D1,RB,R,SR,ST,SZ,TR,U)
      WRITE(6,90) R,SR,ST,SZ,TR
      CALL SRO (A,B,C,H,RB,R,SR,ST,SZ,TR,U)
      WRITE(6,90) R,SR,ST,SZ,TR
      MP=M*(TI-RA)/(RB-RA)
      MI=M*(TO-TI)/(RB-RA)
      MM=M*(RC-TO)/(RB-RA)
      MC=M*(RB-RC)/ (RB-RA)
      RFP=0.DO
      RMP=0.DO
      RFI=0.DO
      RMI=0.DO
```

```
      RFM=0.D0
      RMM=0.D0
      RFO=0.D0
      RMO=0.D0
      IF(MP.EQ.0) GO TO 4
      DRP=(TI-RA)/DFLOAT(MP)
      DO 3 I=1,MP
      R=RA+(DFLOAT(I)-0.5D0)*DRP
      CALL SPP (DL,RB,R,SR,ST,SZ,TR,U)
      RFP=RFP+SZ*R*DRP
      RMP=RMP+SZ*R*R*DRP
3     CONTINUE
4     DRI=(TO-TI)/DFLOAT(MI)
      DO 5 I=1,MI
      R=TI+(DFLOAT(I)-0.5D0)*DRI
      CALL SRI(A,B,C,P,RA,R,SR,ST,SZ,TR,U)
      RFI=RFI+SZ*R*DRI
      RMI=RMI+SZ*R*R*DRI
5     CONTINUE
      IF(MM.EQ.0) GO TO 11
      DRM=(RC-TO)/DFLOAT(MM)
      DO 10 I=1,MM
      R=TO+(DFLOAT(I)-0.5D0) *DRM
      CALL SPM (D1,RB,R,SR,ST,SZ,TR,U)
      RFM=RFM+SZ*R*DRM
      RMM=RMM+SZ*R*R*DRM
10    CONTINUE
11    DRO=(RB-RC)/DFLOAT(MO)
      DO 15 I=1,MO
      R=RC+(DFLOAT(I)-0.5D0)*DRO
      CALL SRO (A,B,C,H,RB,R,SR,ST,SZ,TR,U)
      RFO=RFO+SZ*R*DRO
      RMO=RMO+SZ*R*R*DRO
15    CONTINUE
      Q=(RB**4-RA**4)/2.D0-(RB**3-RA**3)*(RA+RB)/3.D0
      RF=RFP+RFI+RFM+RFO
      RM=RMP+RMI+RMM+RMO
      RAS=2.D0*RF/(RA*RA-RB*RB)
      RBS=(RB-RA)*RM/Q
      WRITE(6,20) RF,RM,RAS,RBS
      RETURN
20    FORMAT(/' Z RESIDUAL FORCE=',1PD10.3,9X,
     1'Z RESIDUAL MOMENT=',D10.3/' AXIAL RELAXATION STRESS='
     2,D10.3,' BENDING RELAXATION STRESS=',D10.3)
80    FORMAT(' A =',1PD10.3,'  B =',D10.3,'  C =',D10.3,
     1'  D1=',D10.3,'  DL=',D10.3,'  H =',D10.3/T5,'R',T17,
     2'SR',T29,'ST',T41,'SZ',T53,'TR')
90    FORMAT(/1X,5(1PD10.3,2X))
      END
```

```
      SUBROUTINE STRES4 (M,RIC,RA,RB,RC,P,U)
C
C     CALCULATE STRESSES FOR CASE RY.LE.RA
C     EQUATIONS (3.81)-(3.83)
C
      IMPLICIT REAL*8 (A-H,O-Z)
      H=0.D0
      D1=-DLOG(RA/RB)
      BC=2.D0*DLOG(RB/RC)
      E=(RB*RB-RC*RC)
      Q1=(RA*RA+RB*RB-2.D0*RC*RC)*E/2.D0 - RB*RB*RC*RC*P*BC
      B=Q1/((RB*RC*BC)**2-E*E)
      A=(P+B*BC)*(RB*RC)**2/E
      C=-A/(RB*RB)-B*(1.D0+2.D0*DLOG(RB))
      WRITE(6,80) A,B,C,D1,H
      DO 10 K=1,100
      R=RA+RIC *DFLOAT(K-1)
      IF(R.GE.RB) GO TO 70
      IF(R.EQ.RC) GO TO 10
      IF(R.LT.RC) CALL SPM (D1,RB,R,SR,ST,SZ,TR,U)
      IF(R.GT.RC) CALL SRO (A,B,C,H,RB,R,SR,ST,SZ,TR,U)
      WRITE(6,90) R,SR,ST,SZ,TR
   10 CONTINUE
   70 R=RB
      CALL SRO (A,B,C,H,RB,R,SR,ST,SZ,TR,U)
      WRITE(6,90) R,SR,ST,SZ,TR
      R=RC
      CALL SPM (D1,RB,R,SR,ST,SZ,TR,U)
      WRITE(6,90) R,SR,ST,SZ,TR
      CALL SRO (A,B,C,H,RB,R,SR,ST,SZ,TR,U)
      WRITE(6,90) R,SR,ST,SZ,TR
      MM=M*(RC-RA)/(RB-RA)
      MO=M*(RB-RC)/(RB-RA)
      RFM=0.D0
      RMM=0.D0
      RFO=0.D0
      RMO=0.D0
      IF(MM.EQ.0) GO TO 16
      DRM=(RC-RA)/DFLOAT(MM)
      DO 15 I=1,MM
      R=RA+(DFLOAT(I)-0.5D0)*DRM
      CALL SPM(D1,RB,R,SR,ST,SZ,TR,U)
      RFM=RFM+SZ*R*DRM
      RMM=RMM+SZ*R*R*DRM
   15 CONTINUE
   16 DRO=(RB-RC)/DFLOAT(MO)
      DO 20 I=1,MO
      R=RC+(DFLOAT(I)-0.5D0)*DRO
      CALL SRO (A,B,C,H,RB,R,SR,ST,SZ,TR,U)
      RFO=RFO+SZ*R*DRO
      RMO=RMO+SZ*R*R*DRO
   20 CONTINUE
      Q=(RB**4-RA**4)/2.D0-(RB**3-RA**3)*(RA+RB)/3.D0
      RF=RFM+RFO
```

```
      RM=RMM+RMO
      RAS=2.D0*RF/(RA*RA-RB*RB)
      RBS=(RB-RA)*RM/Q
      WRITE(6,25) RF,RM,RAS,RBS
      RETURN
25    FORMAT(/' Z RESIDUAL FORCE=',1PD10.3,9X,
     1'Z RESIDUAL MOMENT=',D10.3/' AXIAL RELAXATION STRESS='
     2,D10.3,'  BENDING RELAXATION STRESS=',D10.3)
80    FORMAT(' A =',1PD10.3,'  B =',D10.3,'  C =',D10.3,
     1'  D1=',D10.3,'  H =',D10.3,'  STRES4 USED'/T5,'R',
     2T17,'SR',T29,'ST',T41,'SZ',T53,'TR')
90    FORMAT(/1X,5(1PD10.3,2X))
      END
```